

A STUDY OF PDZ PROTEIN EXPRESSION DURING  
THE HUMAN PAPILLOMAVIRUS LIFE CYCLE

by

CLAIRE DEBORAH JAMES

A thesis submitted to the  
UNIVERSITY OF BIRMINGHAM  
for the degree of  
DOCTOR OF PHILOSOPHY

School of Cancer Sciences  
College of Medical and Dental Sciences  
University of Birmingham

April 2015

UNIVERSITY OF  
BIRMINGHAM

**University of Birmingham Research Archive**

**e-theses repository**

This unpublished thesis/dissertation is copyright of the author and/or third parties. The intellectual property rights of the author or third parties in respect of this work are as defined by The Copyright Designs and Patents Act 1988 or as modified by any successor legislation.

Any use made of information contained in this thesis/dissertation must be in accordance with that legislation and must be properly acknowledged. Further distribution or reproduction in any format is prohibited without the permission of the copyright holder.

## ABSTRACT

The E6 protein of oncogenic  $\alpha$ -human papillomaviruses encodes a conserved C-terminal PDZ binding motif (PBM). Conservation of an overlapping kinase recognition site has shown that phosphorylation negatively regulates the E6:PDZ interaction. Many E6 PDZ targets are associated with signalling complexes that regulate cell proliferation and polarity. This study used primary keratinocyte-based models of HPV16 and 18 life cycles to investigate the expression of PDZ targets and the functional role of PBM phosphorylation.

The data indicate that changes in total levels of major E6 PDZ targets are not associated with E6-PBM activity. Interestingly, transcription profiles of E6-PBM targets *DLG1*, *PATJ* and *PTPN13* are dramatically changed in the presence of HPV16 and 18, whilst others remain unaffected. Further analysis of transcriptional changes of *DLG1* revealed upregulation of specific alternatively spliced isoforms, including a novel isoform containing an exon previously thought to be intronic.

This investigation revealed that phosphorylation of the PBM is linked to oncoprotein stability, presenting a potential regulatory mechanism of E6 PDZ interactions during the virus life cycle.

Together, these data offer interesting new perspectives on interactions between oncogenic HPV types and PDZ domain-containing targets and indicate that deregulation of their function by the virus may occur through multiple mechanisms.

## ACKNOWLEDGEMENTS

I would like to express my appreciation to Dr Sally Roberts for her supervision during this project, and to the members of the Roberts lab, Margaret, Claire, Pete and Elizabeth, for their advice and support. I am especially grateful to Dr Sarah Leonard for her guidance throughout this project. Furthermore, this studentship was made possible by funding from the MRC and Wellcome Trust.

Special thanks are extended to the School of Cancers Sciences, to my colleagues in the lab and office for their encouragement and camaraderie. Thanks also to those in Suffolk and Birmingham, whose friendship has been and continues to be invaluable. I am especially thankful to Corisande Ladies, Aliesha, Annika and Kate, who provided much inspiration and entertainment over the last four years.

Lastly, but by no means least, I am hugely grateful for my family, who have always been unquestioningly encouraging and loving.

## TABLE OF CONTENTS

CHAPTER 1: INTRODUCTION.....	1
1.1 Papillomaviruses.....	1
1.2 Benign HPV infection.....	2
1.3 HPV infection and cancer.....	4
1.3.1 Anogenital cancers.....	5
1.3.2 Non-genital cancers.....	9
1.4 The HPV life cycle.....	12
1.4.1 HPV E6 and E7 in the HPV life cycle.....	16
1.4.2 HPV oncogenesis.....	24
1.5 Epithelial polarity.....	28
1.5.1 Polarity complexes.....	29
1.5.2 The PDZ domain.....	31
1.5.3 Alternative splicing.....	34
1.5.4 PDZ domain containing proteins in cancer.....	35
1.5.5 Virus interactions with PDZ domain containing proteins.....	37
1.5.6 PDZ domain containing proteins in viral oncogenesis.....	42
1.6 High-risk HPV E6 and cellular PDZ proteins.....	47
1.6.1 The E6 PBM in viral life cycle.....	48
1.6.2 The E6 PBM in viral oncogenesis.....	49
1.6.3 PDZ targets of high-risk E6.....	50
1.7 Hypothesis and Aims.....	55
CHAPTER 2: MATERIALS AND METHODS.....	56
2.1 Cell culture.....	56
2.1.1 Culture of cell lines.....	56
2.1.2 Cell counting.....	58
2.1.3 Mycoplasma testing.....	58
2.1.4 Generation and maintenance of HPV genome-containing cell lines.....	58
2.1.5 Treatment and manipulation of cells.....	65
2.2 Molecular biology.....	68
2.2.1 RNA analysis.....	68
2.2.2 DNA analysis.....	77
2.2.3 Bacterial culture.....	82
2.2.4 Protein analysis.....	85
2.3 Immunocytochemical techniques.....	87
2.3.1 Immunofluorescence.....	87
2.4 Computational methods.....	88
2.4.1 Protein and nucleotide sequence alignment.....	88
2.4.2 Protein motif prediction.....	89
2.4.3 Nucleotide motif analysis.....	89
2.4.4 Densitometry analysis.....	90
2.5 List of suppliers.....	92
CHAPTER 3: THE INVESTIGATION OF PDZ PROTEIN EXPRESSION DURING THE HPV LIFE CYCLE.....	94
3.1 Introduction.....	94

3.2 Hypothesis and Aims.....	100
3.3 Results .....	101
3.3.1 Generation of cell-based models of the HPV16 and HPV18 life cycle.....	101
3.3.2 Transcription of E6 PDZ targets in keratinocytes containing high-risk $\alpha$ -papillomavirus genomes.....	102
3.3.3 Analysis of PDZ protein expression during the HPV life cycle .....	109
3.3.4 Proteasomal inhibition of primary keratinocytes.....	119
3.4 Discussion .....	122
3.4.1 Transcriptional upregulation in the presence of HPV genomes.....	122
3.4.2 Protein distribution in HPV genome containing cells.....	124
3.4.3 Future directions.....	130
CHAPTER 4: IDENTIFICATION AND CHARACTERISATION OF A NOVEL	
ISOFORM OF DLG1 .....	132
4.1 Introduction .....	132
4.1.1 DLG1 protein structure .....	132
4.1.2 DLG1 expression .....	139
4.3 Hypothesis and objectives .....	141
4.4 Results .....	142
4.4.1 Identification of a novel insertion in <i>DLG1</i> in mRNA.....	142
4.4.2 Investigation into protein expression of the novel DLG1 isoform .....	146
4.4.3 Investigation of DLG1 isoform expression .....	150
4.5 Discussion .....	157
4.5.1 Identification of a novel insertion.....	157
4.5.2 Consequences of I6 inclusion on DLG1 function.....	159
4.5.3 Differential expression of DLG1 isoforms .....	163
4.5.4 Future directions.....	165
CHAPTER 5: REGULATION OF THE HUMAN PAPILLOMAVIRUS E6 PDZ	
BINDING MOTIF DURING THE VIRUS LIFE CYCLE.....	167
5.1 Introduction .....	167
5.1.1 Cellular PDZ interactions .....	167
5.1.2 Viral PBM regulation .....	169
5.3 Hypothesis and objectives .....	174
5.4 Results .....	175
5.4.1 Computational screening predicts phosphorylation of $\alpha$ -HPV E6 PBMs.....	175
5.4.2 Investigation into the effect of PBM phosphorylation upon E6.....	176
5.4.3 14-3-3z.....	181
5.5 Discussion .....	182
CHAPTER 6: FINAL DISCUSSION .....	
6.1 Overview of findings .....	187
6.2 Future directions .....	189
6.3 Final statement.....	190
REFERENCES.....	192
APPENDIX I: PUBLICATIONS	
APPENDIX II: PRIMER OPTIMISATION AND SEQUENCE ALIGNMENTS	
APPENDIX III: CELL CULTURE REAGENTS AND STOCK SOLUTIONS	

## LIST OF FIGURES

Page numbers represent the preceding page

### Chapter 1

Figure 1.1: Human papillomavirus classification	1
Figure 1.2: Stages of cervical intraepithelial neoplasia	5
Figure 1.3: HPV genome organisation	11
Figure 1.4: Epithelial differentiation and the HPV life cycle	17
Figure 1.5: E7 acting upon the cell cycle	18
Figure 1.6: Structure of E6	19
Figure 1.7: E6 interacts with a number of cellular proteins	19
Figure 1.8: HPV oncoprotein cooperation in cervical carcinogenesis	29
Figure 1.9: E6 and E7 affect a number of cellular targets in carcinogenesis	29
Figure 1.10: Epithelial polarity and junction complexes	29
Figure 1.11: The PDZ domain structure	31
Figure 1.12: PDZ domain containing protein domain structure	33
Figure 1.13: Patterns of alternative splicing	33
Figure 1.14: Differential expression of PDZ proteins in tumour progression	35
Figure 1.15: Viral proteins target common cellular PDZ proteins	41
Figure 1.16: C-terminal alignment of high- and low-risk HPV E6 proteins	53

### Chapter 2

Figure 2.1: Transfection of primary keratinocytes with HPV genomes	59
Figure 2.2: Organotypic raft culture	63

### Chapter 3

Figure 3.1: C-terminal alignment of high- and low-risk $\alpha$ -HPV E6 proteins	97
Figure 3.2: Generation of HPV16 and HPV18 genome containing primary keratinocyte cell lines	103
Figure 3.3: Confirmation of episomal genomes in HPV18 genomes with modified PDZ binding activity	103
Figure 3.4: Quantification of selected E6-PDZ target transcription in HPV16 and HPV18 genome containing keratinocytes	108
Figure 3.5: Quantification of MAGI-1, MAGI-2 and MAGI-3 transcription in HPV16 and HPV18 genome-containing keratinocytes	109
Figure 3.6: Cumulative qRT-PCR analysis PDZ targets of E6 expression in HPV genome containing HFKs	109
Figure 3.7: Quantification of E6-PDZ target transcription in HPV16 and HPV18 genome containing keratinocytes following cell propagation	111
Figure 3.8: Quantification of E6-PDZ target transcription in HPV18 genome containing keratinocytes	113
Figure 3.9: Confirmation of successful enrichment of protein from subcellular fractions	113

Figure 3.10: DLG1 protein expression in keratinocytes replicating HPV genomes	113
Figure 3.11: DLG1 protein distribution in keratinocytes	113
Figure 3.12: DLG1 protein in differentiated keratinocytes containing HPV18 genomes	115
Figure 3.13: Immunofluorescence of DLG1 in differentiated keratinocytes	115
Figure 3.14: SCRIB protein levels in HPV genome containing keratinocytes	115
Figure 3.15: Distribution of SCRIB in monolayer keratinocytes	115
Figure 3.16: SCRIB protein in differentiated keratinocytes containing HPV18 genomes	115
Figure 3.17: SCRIB distribution in differentiated keratinocytes	115
Figure 3.18: CASK protein level and distribution in monolayer grown keratinocytes	117
Figure 3.19: PATJ protein levels in HPV genome containing keratinocytes	117
Figure 3.20: Distribution of PATJ in monolayer keratinocytes	117
Figure 3.21: PARD3 protein levels and distribution in primary keratinocytes	117
Figure 3.22: MAGI-1 protein levels and distribution in primary keratinocytes	119
Figure 3.23: MUPP1 protein levels and distribution in primary keratinocytes	119
Figure 3.24: ZO-1 protein levels in HPV genome containing keratinocytes	119
Figure 3.25: ZO-1 protein in differentiated keratinocyte culture	119
Figure 3.26: Distribution of ZO-1 in monolayer keratinocytes	119
Figure 3.27: ZO-1 distribution in differentiated keratinocytes	119
Figure 3.28: ZO-2 protein levels in HPV genome containing keratinocytes	121
Figure 3.29: Distribution of ZO-2 protein in monolayer keratinocytes	121
Figure 3.30: ZO-2 protein in differentiated keratinocytes	121
Figure 3.31: NHERF1 protein levels in HPV genome containing keratinocytes	121
Figure 3.32: Distribution of NHERF1 protein in monolayer keratinocytes	121
Figure 3.33: NHERF1 protein in differentiated keratinocytes	121
Figure 3.34: NHERF1 distribution in differentiated keratinocytes	121
Figure 3.35: PTPN13 protein levels in HPV genome containing keratinocytes	121
Figure 3.36: Distribution of PTPN13 in monolayer keratinocytes	121
Figure 3.37: PTPN13 protein in differentiated keratinocytes	121
Figure 3.38: Proteasomal inhibition of primary keratinocytes	121
Figure 3.39: DLG1 protein levels in keratinocytes under proteasomal inhibition	121
Figure 3.40: SCRIB protein in keratinocytes under conditions of proteasomal inhibition	121
Figure 3.41: NHERF1 and PTPN13 protein levels in keratinocytes under proteasomal inhibition	121
Figure 3.42: Summary of PDZ protein expression in the presence of high-risk $\alpha$ -HPV genomes	133
 Chapter 4	
Figure 4.1: Domain structure of DLG1 isoform	135
Figure 4.2: Regions of alternative splicing of DLG1	135
Figure 4.3: <i>DLG1</i> HOOK domain corresponding primers and probes	145
Figure 4.4: Amplification of the DLG1 HOOK region	147
Figure 4.5: Sequencing across exon junctions	147
Figure 4.6: Amplification of the <i>DLG1</i> N-terminus	147
Figure 4.7 <i>In silico</i> translation of nucleotide sequence	149

Figure 4.8: Cross-reaction of subcellular fractions with HRP-conjugated secondary antibody	151
Figure 4.9: Detection of DLG1 protein in cellular compartments of HeLa and HPV18 genome containing keratinocytes	153
Figure 4.10: Detection of DLG1 $\alpha$ protein	153
Figure 4.11: <i>DLG1</i> isoform expression in primary keratinocytes containing $\alpha$ -HPV genomes	153
Figure 4.12: Expression of <i>DLG1</i> in differentiating keratinocytes containing HPV18	157
Figure 4.13: <i>DLG1</i> isoform expression in keratinocytes containing HPV18 genomes	157
Figure 4.14: <i>DLG1</i> isoform expression in keratinocytes containing episomal and integrated forms of the HPV18 genome	157
Figure 4.15: <i>DLG1</i> isoform expression in normal tissue	157
Figure 4.16: <i>DLG1</i> isoform expression in cancer cell lines	159
Figure 4.17: <i>DLG1</i> isoform expression in head and neck cancer derived cell lines	159
Figure 4.18: Predicted protein structure of I6-containing DLG1	167

## Chapter 5

Figure 5.1: Alignment of E6 C-terminal sequences	171
Figure 5.2: The HPV18 E6 PDZ binding motif	176
Figure 5.3: Computational screen of E6 C-terminal sequences	179
Figure 5.4: Phosphorylation of E6 in HPV18 positive cells	179
Figure 5.5: Distribution of phosphorylated E6 in monolayer-grown cells	181
Figure 5.6: The effect of PKA inhibition upon HPV18 E6 protein	183
Figure 5.7: HPV oncoprotein expression in HeLa expressing mPKI	183
Figure 5.8: HPV oncoprotein expression in primary cells expressing mPKI	183
Figure 5.9: E6 protein in HPV18 genome containing HFKs	183
Figure 5.10: 14-3-3 $\zeta$ protein expression in HPV genome containing keratinocytes	183
Figure 5.11: The consequences of E6 phosphorylation	189

## LIST OF TABLES

Tables are found alongside the text

### Chapter 1

Table 1.1: Biological properties associated with different HPV genus.....	2
Table 1.2: HPV types associated with human disease.....	5
Table 1.3: IARC classification of HPV carcinogenic risk.....	6
Table 1.4: High-risk HPV ORFs.....	14
Table 1.5: Protein partners of E6.....	21
Table 1.6: Cell polarity and adhesion complex components.....	30
Table 1.7: Classes of PDZ-binding motif.....	32
Table 1.8: PDZ proteins in human disease.....	36
Table 1.9: Virus interactions with PDZ proteins.....	41
Table 1.10: PDZ targets of high-risk HPV E6 proteins.....	54

### Chapter 2

Table 2.1: Cell lines.....	57
Table 2.2: qRTPCR primers.....	72
Table 2.3: <i>DLG1</i> primers.....	75
Table 2.4: Restriction enzymes used to assess HPV genome status.....	79
Table 2.5: Primary antibodies used in western blotting and immunofluorescence.....	90
Table 2.6: Secondary antibodies used in western blotting and immunofluorescence.....	91

### Chapter 3

Table 3.1: PDZ proteins associated with high-risk HPV E6 proteins.....	99
Table 3.2: Affymetrix microarray analysis of E6 PDZ target expression in HPV16 and HPV18 genome containing keratinocytes.....	103
Table 3.3: Summary of PDZ target qRTPCR analysis.....	107
Table 3.4: Comparison of microarray and qRTPCR analyses.....	108
Table 3.5: Summary of PDZ protein analysis.....	121

### Chapter 4

Table 4.1: Insertions in <i>DLG1</i> variants.....	134
Table 4.2: <i>DLG1</i> primer and array probe positions.....	143
Table 4.3: Exon and intron comparison to consensus splice nucleotide sequence.....	145
Table 4.4: Potential protein interactions with I2-I6 sequence.....	147
Table 4.5: <i>DLG1</i> Antibodies.....	148
Table 4.6: Microarray and qRTPCR analysis of <i>DLG1</i> expression.....	152

### Chapter 5

Table 5.1: Examples of PBM phosphorylation.....	168
Table 5.2: Consequences of cellular PBM Phosphorylation.....	172

## LIST OF ABBREVIATIONS

Standard international (SI) units are used throughout this thesis.

AIG - Anchorage independent growth	E6AP - E6-associated protein
AKAP - A-kinase anchor protein	E6BP - E6-binding protein
AMPA - $\alpha$ -amino-3-hydroxy-5-methyl-4-isoxazole propionic acid	EB - Ezrin binding
AMPA - AMPA receptor	EBV - Epstein-Barr virus
ANOVA - Analysis of variants	ECL - Enhanced chemiluminescence
AP-1 - Activator protein-1	ECM - Extracellular matrix
APC - Adenomatous polyposis coli protein	EDTA - Ethylene diamine tetraacetic acid
APS - Ammonium persulphate	EGF - Epidermal growth factor
ATM - Ataxia telangiectasia mutated protein	EMT - Epithelial-mesenchymal transition
ATP - Adenine triphosphate	EV - Epidermodysplasia verruciformis
B2M - $\beta$ 2-Microglobulin	FBS - Foetal bovine serum
BCC - Basal cell carcinoma	FCS - Foetal calf serum
BPV - Bovine papillomavirus	FERM - 4.1, ezrin, radixin, moesin
BrdU - 5-bromo-2-deoxyuridine	FK - Forskolin
BSA - Bovine serum albumin	GAPDH - Glyceraldehyde 3-phosphate dehydrogenase
CAL - Conductance regulator-associated ligand	GEF - Guanine nucleotide exchange factor
cAMP - Cyclic adenosine monophosphate	GFP - Green fluorescent protein
CAMK - $Ca^{2+}$ /Calmodulin dependant protein kinase	GK - Guanylate kinase
CARD - Caspase activation and recruitment domain	GKAP - Guanylate kinase associated protein
CASK - Calcium/calmodulin-dependent serine protein kinase	GMP - Guanosine monophosphate
CEM - Complete E media	GPCR - G-protein coupled receptor
cDNA - Complementary DNA	GRB2 - Growth factor receptor-bound protein 2
CDK - Cyclin-dependent protein kinase	GRID2IP - Glutamate receptor ionotropic, delta 2 interacting protein
CIN - Cervical intraepithelial neoplasia	GRIP - Glutamate receptor interacting protein
CK2 - Casein kinase 2	GRB2 - Growth factor receptor-bound protein 2
CMV - Cytomegalovirus	GRK5 - G protein coupled receptor kinase 5
Co-IP - co-Immunoprecipitation	GukH - GKHolder protein
CR - Conserved region	Gy - Gray
crPV - Cottontail rabbit papillomavirus	H89 - Dihydrochloride
DABCO - 1,4-diazabicyclo{2,2,2}octane	Hr - Hour
DAPI - 4',6'-diamino-2-phenylindole	H and E - Haematoxylin and Eosin
DbcAMP - Dibutyl cyclic adenosine monophosphate	HAT - Histone acetyltransferase
DLG - Discs large	HBSS - Hank's balanced salt solution
DMEM - Dulbeccos modified medium	HBV - Hepatitis B virus
DMSO - Dimethyl sulphoxide	HCV - Hepatitis C virus
DNA - Deoxyribonucleic acid	HDAC - Histone deacetylase
dNTP - Deoxynucleotide tri-phosphate	HFK - Human foreskin keratinocyte
DTT - Dithiothreitol	HIER - Heat-induced epitope retrieval
DV - Dengue virus	

HINGS - Heat-inactivated goat serum	NET - Neuroepithelioma transforming gene
HIV - Human immunodeficiency virus	NHERF1 - Na <sup>+</sup> /H <sup>+</sup> exchange regulatory factor 1
HMAST - Microtubule associated protein kinase	NMDA - N-methyl-D-aspartate
HNSCC - Head and neck squamous cell carcinoma	NMDAR - NMDA receptor
HPV - Human papillomavirus	NMSC - Non-melanoma skin cancer
HRP - Horseradish peroxidase	NR2B - NMDAR subtype 2B
HTK - Human tonsil keratinocyte	NS - Non-structural protein
HTLV - Human T-lymphotrophic virus	OC - Open circle
IBMX - 3-Isobutyl-1-methylxanthine	OPC - Oropharyngeal carcinoma
IARC - International agency for research on cancer	ORF - Open reading frame
IgG - Immunoglobulin G	P - Passage
IL - Interleukin	PAGE - Polyacrylamide gel electrophoresis
IP - Immunoprecipitation	PAK1 - p21 activated kinase 1;
IRF - Interferon response factor	PALS1 - Pals associated with lin-7
JNK - Jun N-terminal kinase	PARD -Partitioning defective
K18 - Keratin 18	PATJ - Pals-1 associated tight junction protein
Kb - Kilobase	PBK – PDZ binding kinase
kDa - Kilodalton	PBM - PDZ-Binding domain motif
Kir 2.3 - Potassium inwardly rectifying channel	PBS - Phosphate buffered saline
KSHV - Kaposi's sarcoma herpes virus	PBST - Phosphate buffered saline-Tween20
L27 - Lin2-7	PCR - Polymerase chain reaction
LB - Luria-Bertani	PDGF - Platelet derived growth factor receptor
LncRNA - Long non-coding RNA	PDZ - PSD/DLG/ZO
LRP - Lipoprotein receptor related protein	PH - Pleckstrin homology
mAmp - Milliamp	PI3K - Phosphatidylinositol 3-kinase
NFκB – Nuclear factor κ-light chain enhancer of activated B cells	PICK1 - Protein interacting with C kinase 1
NMSC - Non-melanoma skin cancer	PIP2 - 4,5-Bisphosphate
MAGI - Membrane associated guanylate kinase homology with an inverted domain	PKA - Protein kinase A
MAGUK - Membrane-associated guanylate kinase	PKC - Protein kinase C
MAPK - Mitogen-activated protein kinase	PKI – Protein kinase A inhibitor
MC - Methycellulose	PSD - Post-synaptic density protein
MCC - Mutated in colorectal cancer	PSF - Protein associated splicing factor
MCM7 - Minichromosome maintenance complex component 7	PTEN- Phosphatase and tensin homologue
MCV - Merkel cell polyomavirus	PTP - Protein tyrosine phosphatase
MDCK - Madin-Darby Canine Kidney	PTPN - Protein tyrosine phosphatase non-receptor
MG132 - z-Leu-Leu-Leu-CHO	PVDF - Polyvinylidene fluoride
MG115 - z-Leu-Leu-Nva-H	qRTPCR - Quantitative RT PCR
MLV - Murine leukemia virus	Rb - Retinoblastoma
MUPP - Multiple PDZ protein	rhPV - Rhesus papillomavirus
	RNA - Ribonucleic acid
	RNase - Ribonuclease
	RT - Reverse transcription

RTPCR - Reverse transcription  
polymerase chain reaction  
SAP97 - Synapse-associated protein 97  
SARS - Severe acute respiratory  
syndrome  
SC - Supercoiled  
SCC - Squamous cell carcinoma  
SCC - Saline sodium citrate  
SCRIB - Scribble protein  
SDS - Sodium dodecyl sulphate  
SFM - Serum free media  
SH3 - Src Homology 3  
SI - Standard international  
SIV - Simian immunodeficiency virus  
SP-1 - Stimulating protein-1  
SRPK - Serine-arginine protein kinase  
SRSF - Serine/arginine rich splicing  
factor  
T3 - Tri-iodo-L-thyronine  
TCR - T-cell receptor  
TE - Tris-EDTA  
TEMED -  
N,N,N',N'Tetramethylethylene-diamine  
TBE - Tris/Borate/EDTA  
TBEV - Tick borne encephalitis virus  
TBS - Tris-buffered saline  
TBST - Tris-buffered saline-Tween20  
TI - Trypsin inhibitor  
TIP - Tax interacting protein  
TJ - Tight junction  
 $T_m$  - Primer melting temperature  
TNF - Tumour necrosis factor  
TNFR - Tumour necrosis factor  
receptor  
UTB - Urea, Tris,  $\beta$ -mercaptoethanol  
UTR - Untranslated region  
UV - Ultraviolet  
V - Volts  
VLP - Virus like particle  
VP - Viral protein  
WHO - World Health Organisation  
WT - Wild type  
ZA - Zonula adherens  
ZO - Zona occludens protein  
ZONAB - ZO-1 associated nucleic acid  
binding protein

## CHAPTER 1: INTRODUCTION

### 1.1 Papillomaviruses

Papillomaviruses were first discovered in 1907, when the Italian scientist Giesepe Ciuffo inoculated himself with the cell-free extract of warts to prove that the growths were caused by a transmissible agent (Ciuffo, 1907). More than twenty years later, while Francis Peyton Rous was investigating transmissible agents causing tumours in chickens, virologists Richard Shope and E. Weston Hurst were studying warts taken from wild cottontail rabbits. In the soluble extracts of these warts, they found a transmissible agent, the cottontail rabbit papillomavirus (CRPV), that was capable of inducing benign growths when introduced to uninfected rabbits (Shope and Hurst, 1933). The pair passed on tissue to the aforementioned Rous, who used it to infect a domestic species of rabbit. These rabbits failed to form warts, which would have been evidence of normal successful viral replication, but instead developed aggressive skin carcinomas (Rous and Beard, 1935). Rous went on to establish retroviruses as cancer-causing agents in chickens, but it would be more than 30 years until human papillomaviruses (HPVs) were linked to human cancers and accepted as a human tumour virus.

Papillomaviruses, named for the *papilla* (buds in Latin) that infected cells form, are a highly diverse group of small, double-stranded DNA viruses. Their diversity is reflected in the wide range of hosts that they infect, which includes reptiles, birds and mammals (Herbst *et al.*, 2009; Chen *et al.*, 1982; Schulz *et al.*, 2009; Bernard *et al.*, 2010). There are more than 300 known papillomaviruses, 170 of which are officially human-specific, with other types pending classification (Bernard *et al.*, 2010; de Villiers, 2013; van Doorslaer *et al.*, 2013). The viruses are classified by the nucleotide sequence encoding the conserved L1 open reading frame (ORF); this is the most conserved gene within the genome. Members of the same

papillomavirus genus are denoted by Greek letters (i.e.  $\alpha$ ,  $\beta$ ,  $\gamma$ ,  $\mu$ ) and share more than 60% nucleotide sequence identity in the L1 ORF (Bernard *et al.*, 2010; de Villiers, 2013; de Villiers *et al.*, 2004). These are sub-divided into HPV types, which are numbered (e.g. HPV16, HPV18; both  $\alpha$ -papillomaviruses) and defined by an L1 region containing DNA sequence that differs by more than 10% to the closest known type (Figure 1.1, Table 1.1). Virus variants are further classified (e.g. HPV16 114/B, HPV16 114/K), by containing a less than 2% difference in the L1 region (Bernard *et al.*, 2010; de Villiers, 2013; de Villiers *et al.*, 2004).

**Table 1.1: Biological properties associated with different HPV genus**

Genus	Biological Properties	Examples
Alpha-papillomavirus	Mucosal and cutaneous lesions in humans and primates Many high-risk types under this genus	HPV6, HPV11, HPV16, HPV18
Beta-papillomavirus	Cutaneous lesions in humans Predominantly latent infection, re-activated in immunosuppressed conditions Close association with Epidermodysplasia verruciformis (EV)	HPV8 HPV12
Gamma-papillomavirus	Cutaneous lesions in humans	HPV60
Nu-papillomavirus	Benign and malignant cutaneous lesions	HPV41
Mu-papillomavirus	Cutaneous lesions	HPV1

The major human-tropic genus are mentioned here. Adapted from de Villiers *et al.*, 2004.

HPVs infect cutaneous or mucosal epithelial (Table 1.1), causing a variety of lesions; from benign plantar, flat and common warts and genital warts, to cervical neoplasia and cancer (Table 1.2). As such, HPV types can be classified as high- or low-risk, according to their capacity to promote malignant growth.

## 1.2 Benign HPV infection

A number of HPV types cause benign growths in mucosal and cornified epithelia. Infection with low-risk types of HPV can cause condylomata acuminata (genital warts) or

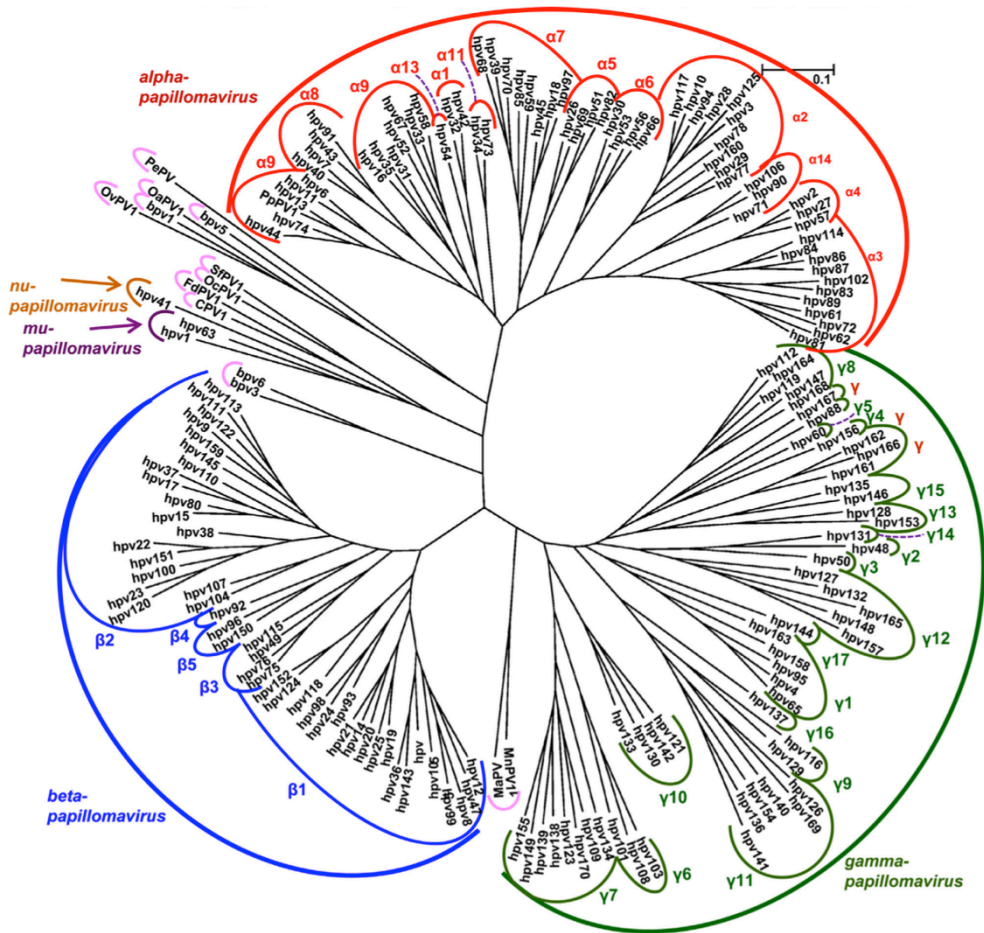


**Figure 1.1: Human papillomavirus classification**

Classification of papillomavirus types is based on the DNA sequence of the L1 gene; HPV types differ by more than 10% in the DNA sequence of the L1, whereas HPV variants differ by less than 2% in L1 sequence. Members of the same genus share >60% nucleotide sequence identity in the L1. HPVs are contained within evolutionary groups. The outermost semicircular symbols indicate papillomavirus genera, e.g. alpha-papillomavirus. The number at the inner semicircular symbol refers to papillomavirus species e.g. HPV16. The HPV types that infect the cervix come from the Alpha group which contains over 60 members. HPV types from the Beta, Gamma, Mu and Nu groups primarily infect cutaneous sites. Adapted from de Villiers, 2004.

verrucae (skin warts). Genital warts are the most prevalent sexually-transmitted infection worldwide (Baseman and Koutsky, 2005), with the HPV types 6 or 11 found in 100% of cases and co-infection with high-risk types associated with 25% of cases (Lacey, 2005; Brown *et al.*, 1999; Greer *et al.*, 1995). Genital warts are highly infectious, with a transmission rate of about 65% and an incubation period of between 3 weeks and 8 months, with the majority developing warts at around 2–3 months (Oriol, 1971). After regression, it has been suggested that asymptomatic infection persists for life (Stanley, 2010).

Verrucae, caused by HPV infection of cornified epithelium, are most common in children and adolescents, the majority of whom clear the growths spontaneously (Williams *et al.*, 1993). The many and varied types of warts are classified based upon the site of infection and pathology (Table 1.2). Painful and unsightly warts can be treated by removal, but there is still a requirement for the immune system in disease clearance (Sterling *et al.*, 2001).

Although infection with low-risk viruses is largely benign, immunocompromised individuals can experience more damaging effects. Patients with the rare heritable disease, epidermodysplasia verruciformis (EV), are susceptible to  $\beta$ -HPV infection and are at risk of developing non-melanoma skin cancer (NMSC); 30-60% of the patients develop carcinoma (Akgül *et al.*, 2006). EV patients exhibit an inability to control HPV infection, resulting in the development of scaly growths, particularly on the hands and feet. This is attributed to a defect in the immune system's ability to reject the HPV-positive keratinocytes (Majewski and Jabłońska, 1995; Majewski and Jablonska, 2002; Baadsgaard *et al.*, 1990). This is reinforced by the fact that  $\beta$ -HPVs are ubiquitous in the general population and EV-like conditions develop in HIV infected individuals as well as other immunosuppressive conditions (Majewski and Jabłońska, 1995). In addition, genetic screening has revealed that loss of function mutations in the *EVER1* and *EVER2* genes,

which encode zinc-transporting proteins, are responsible in a majority of cases (Ramos *et al.*, 1999; 2000; 2002). It has been suggested that the *EVER* genes affect the virus life cycle by limiting the accessibility of  $Zn^{2+}$  ions to the viral zinc binding proteins E6 and E7, and that somatic mutations remove this anti-HPV activity (Lazarczyk *et al.*, 2008). It is also thought that the loss of *EVER* gene function impairs T-cell activation and proliferation, by impairing regulation of lymphocyte  $Zn^{2+}$  concentration, thus impairing immunity against HPV in EV patients (Lazarczyk *et al.*, 2012). UV light is also influential in the development of EV associated squamous cell carcinoma (SCC); although warts develop on all body sites, carcinomas occur exclusively on sites exposed to the sun (Majewski and Jabłońska, 1995). Thus, the pathology of EV demonstrates the interplay between multiple factors, genetic and environmental in HPV mediated carcinogenesis.

### 1.3 HPV infection and cancer

It was not until the late 1980s that papillomaviruses were established as the etiological agent of cervical cancer in humans, and now HPVs are associated with more human cancers than any other virus (WHO). Infection with high-risk HPV is responsible for 4.8% of the world's cancer burden, causing over 610,000 cases per year worldwide (de Martel *et al.*, 2012; Forman *et al.*, 2012). The discovery was made by Nobel laureate Harald zur Hausen, who was studying the genital condylomata-causing virus in women (Hausen *et al.*, 1974). HPV has subsequently been shown as the causative agent in a number cancers of the anogenital tract, as well as important factors in the development of NMSC and in carcinomas of the oral and oropharyngeal mucosa (Parkin and Bray, 2006; Lowy and Schiller, 2012). To date, twelve HPV types have been defined by the World Health Organisation (WHO) as 'high-risk' with respect to causing cancer (IARC Group 1), and a

further ten types are recognised as ‘probably’ and ‘possibly’ cancer-causing (IARC Group 2A and 2B, Table 1.3, Bouvard *et al.*, 2009).

**Table 1.2: HPV types associated with human disease**

<b>Disease</b>	<b>Most frequently associated HPV types</b>	
Common warts	HPV2, 4, 7; occasionally other types in immunosuppressed (e.g. HPV 75, 76, 77)	
Flat plane warts	HPV3, 10, occasionally types 26–29 and 41	
Plantar warts	HPV1, 2, 4	
Epidermodysplasia verruciformis (EV)	Plane warts	HPV3, 10
	Scale-like plaques	HPV5, 8; less commonly 9, 12, 14, 15, 17, 19, 20, 21–25, 36–39, 47, 49
	Squamous cell carcinomas of sun-exposed skin	HPV5, 8, less commonly 14, 17, 20 and 47
	External warts	HPV6, 11, 40, 42, 43, 44, 54, 61, 72, 81, 89
Anogenital Warts	Buschke–Lowenstein tumour	HPV6
	Bowenoid papulosis	HPV16, 55
Anogenital cancers and precancers	IARC Group 1: Carcinogenic	HPV16, 18, 31, 33, 35, 39, 45, 51, 52, 56, 58, 59, 66
	IARC Group 2A: Probably carcinogenic	HPV68
	IARC Group 2B: Possibly carcinogenic	HPV26, 53, 64, 65, 66, 67, 69, 70, 73, 82
Oral Lesions	Oral papillomas	HPV2, 6, 7, 11, 16, 18, 32, 57
	Laryngeal papillomas	HPV6, 11
	Focal hyperplasia (Heck's disease)	HPV13, 32
	Oropharyngeal carcinoma	Predominantly HPV16

Adapted from Cubie, 2013.

### 1.3.1 Anogenital cancers

Altogether, there are more than 530,000 new cases and 275,000 deaths from cervical cancer per year (Ferlay *et al.*, 2012). In identifying HPV as a cause of cervical cancer, Harald zur

Hausen determined the presence of HPV16 and 18 DNA in cancer tissue; together these  $\alpha$ -HPVs contribute to more than 70% of cervical cancer cases worldwide (Li *et al.*, 2011). HPV-induced cancer of the cervix is the most characterized; stages of cervical neoplasia are clinically categorized by cytological and histological examination; pre-malignant phases are termed cervical intraepithelial neoplasia (CIN) and are graded 1 to 3 (Woodman *et al.*, 2007). These pre-malignant changes represent a spectrum ranging from mild dysplasia (CIN1), moderate dysplasia (CIN2), to severe dysplasia and carcinoma (CIN3) (Figure 1.2). These progressively malignant changes are associated with the increased expression of HPV encoded oncoproteins E6 and E7, which together provide the primary transforming activity of high-risk HPVs (Section 1.4.2). The most common HPV types found in cervical cancers are HPVs 16, 18, 58, 52, 31 and 33 (Clifford *et al.*, 2006). In the cervix, HPV-driven cancers arise from squamous cells and adenomatous glandular cells. Squamous cell carcinomas (SCC) account for 80% of cervical cancer cases, of which 62% are HPV16 associated (de Sanjose *et al.*, 2010; Walboomers *et al.*, 1999). By contrast, adenocarcinomas are less frequent and are more commonly associated with HPV18 (de Sanjose *et al.*, 2010; Green *et al.*, 2003).

**Table 1.3: IARC classification of HPV carcinogenic risk**

IARC Group	HPV types
Group 1 - carcinogenic	16, 18, 31, 33, 35, 39, 45, 51, 52, 56, 58, 59
Group 2A - probably carcinogenic	68
Group 2B - possibly carcinogenic	26, 53, 66, 67, 70, 73, 5, 8, 6, 11

Adapted from Bouvard *et al.*, 2009.

Other anogenital malignancies associated with high-risk HPV include penile and vulvo-vaginal cancers, where 40% of incidences are attributed to HPV, and anal carcinomas, where 90% of incidences are attributed to HPV (Parkin and Bray, 2006; Ferlay *et al.*, 2012). The high proportion of HPV associated with anogenital cancers indicates the necessity for

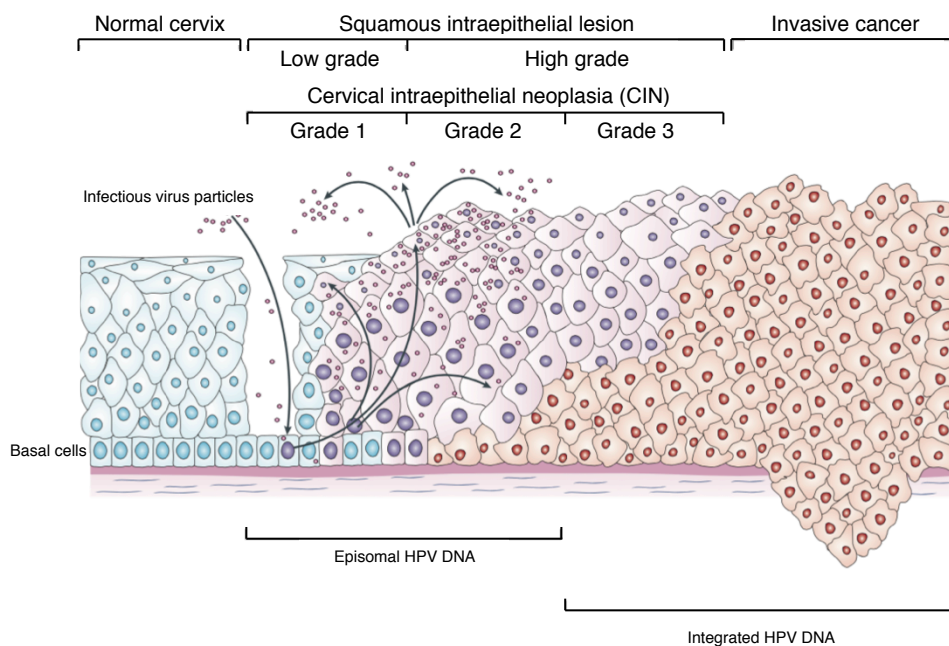


### Figure 1.2: Stages of cervical intraepithelial neoplasia

HPV is thought to access basal cells via micro-abrasions in the cervical epithelium. Following infection, viral DNA replicates and exists as episomes (purple nuclei). In the upper layers of epithelium, the viral genome is replicated further, and progeny virions form in the nucleus. Low-grade intraepithelial lesions support productive viral replication. An unknown number of high-risk HPV infections progress to high-grade cervical intraepithelial neoplasia (CIN). These pre-malignant changes represent a spectrum of histological abnormalities ranging from CIN1 (mild dysplasia), CIN2 (moderate dysplasia), to CIN3 (severe dysplasia/carcinoma *in situ*). The progression of untreated lesions to microinvasive and invasive cancer is associated with the integration of the HPV genome into the host chromosomes (red nuclei). Adapted from Woodman *et al.* 2007.

viral infection in cancer development. However, not all infections with HPV lead to invasive disease; it has been suggested that 80 to 90% of HPV infections persist for 12 to 18 months and are cleared by the immune system (Bodily and Laimins, 2011; Stanley, 2012). As with EV, a number of co-factors have been reported to aid the development of high-risk HPV-driven anogenital carcinoma, including hormones, smoking and immunosuppression (Green *et al.*, 2003; Kjellberg *et al.*, 2000; Coutlee *et al.*, 2012; Hildesheim *et al.*, 1990; Harper *et al.*, 1994). Smoking has been shown to be the most significant cofactor in cervical cancer development; current smokers are twice as likely as non-smokers to be diagnosed with CIN (Collins *et al.*, 2010; Kjellberg *et al.*, 2000). Chemical carcinogens found in cigarette smoke are thought to influence carcinogenesis by causing DNA damage and impairing the immune system; there is no evidence to suggest that HPV infection is prolonged by the effects of smoking (Collins *et al.*, 2010; Castellsagué and Muñoz, 2003). As with low-risk types, immunosuppressed patients are susceptible to the development of HPV-driven cancers. For example, HPV infection is more common and more likely to persist in HIV-positive compared to HIV-negative women (Clifford *et al.*, 2006). Whilst the exact mechanisms are unclear, co-factors are proposed to influence progression to carcinogenesis *via* suppression of the immune system, increased viral persistence, and/or inducing DNA damage.

#### *1.3.1.1 Screening and vaccination*

Rates of cervical cancer have fallen in developed countries over the last few decades, thanks to the implementation of screening programs, which allow the early detection and treatment of pre-cancerous cervical lesions (Feldman, 2014). In the UK, the Papanicolaou (Pap) test of exfoliated cervical cells was introduced nationally in 1988, since which mortality rates of cervical cancer have decreased by 80% (Peto *et al.*, 2004). Despite the

decrease in SCC rates, the rates of adenocarcinoma have been reported to increase, which is attributed to cervical screening being less efficient at the detection of adenocarcinoma; the disease presents minor cytological abnormalities compared to SCC and so screening is less likely to identify and interrupt disease progression (Clifford *et al.*, 2003; Muñoz *et al.*, 2003; Feldman, 2014; Woodman *et al.*, 2007; 2001).

A recent development in the protection against cervical carcinoma has been achieved in the licensing of two prophylactic vaccines against HPV infection: the quadrivalent vaccine Gardasil<sup>®</sup>, which protects against HPV types 16, 18, 6 and 11 and the bivalent vaccine Cervarix<sup>®</sup>, which protects against HPV16 and 18. Both vaccines show a level of cross-protection against infection with other HPV types, including types HPV31 and HPV45 (Bonanni *et al.*, 2009; Toft *et al.*, 2014). Cervical cancer screening is an expensive preventative health care measure; in England, it costs the NHS around £175 million a year, including treatment (<http://www.cancerscreening.nhs.uk/>). A vaccination program may alleviate some of this cost, but screening will still be required for those who are missed by the vaccination program, and to catch cancers induced by the high-risk HPV types not targeted by the vaccines (Villa, 2011). As the incidence of cervical cancer decreases in the developed world due to a better understanding and improved screening protocols, it remains constant in the developing world where screening and treatment are difficult and expensive to implement (Forouzanfar *et al.*, 2011; Parkin and Bray, 2006). The HPV-associated cancer burden is disproportionately spread geographically; more than 76% of cervical cancers occur in developing countries, where there is a 80% lower chance of successful treatment, compared to women living in more developed countries (Baseman and Koutsky, 2005; Parkin *et al.*, 2001; de Martel *et al.*, 2012). As in the case of screening programs, poor infrastructure and high costs make implementation of vaccination in

developing countries unfeasible, and so better methods of prevention are still required in countries where disease burden is greatest (de Martel *et al.*, 2012).

Interestingly, vaccine development is being explored as a treatment against HPV-positive tumour cells; using peptide sequences corresponding to E6 and E7 to induce an immune response against these proteins and thus against E6 and E7-expressing tumor cells. This is currently under development, but has been effective in inducing a response from lymphocytes during a study of HPV-positive vulvar intraepithelial neoplasia (VIN) patients (Le Buanec *et al.*, 1999; Wieking *et al.*, 2012; Wang *et al.*, 2000).

### 1.3.2 Non-genital cancers

#### 1.3.2.1 *Non-melanoma skin cancer*

NMSC is the most prevalent malignancy in the Caucasian population worldwide (Alam and Ratner, 2001). The term includes both basal cell carcinomas (BCCs) and squamous cell carcinomas (SCCs); the former being more common and contributing to 80% of NMSC (Rubin *et al.*, 2005). Ultraviolet (UV) irradiation is a well characterised risk factor in the development of NMSC and molecular studies have identified HPV as a co-factor also; HPV DNA has been identified in 30% to 50% of NMSCs in the non-immunosuppressed population (Meyer *et al.*, 2001; Berkhout *et al.*, 1995; Pfister, 2003). A number of HPV types have been associated with NMSC; notably types 5, 8, 14, 17, 20 and 47 (Harper *et al.*, 2013; Jemal *et al.*, 2013). Unlike in anogenital cancers, the number of copies of HPV genomes per cell in NMSCs is low; only 1 in 20-50,000 cells contain HPV DNA (Pfister, 2003; Weissenborn *et al.*, 2005). Both the requirement for UV radiation in carcinogenesis and the low viral DNA copy number suggests that HPVs promote the initiation and progression of NMSCs, but are not essential for the maintenance of a malignant phenotype (Majewski and Jabłońska, 1995). The influence of HPV in promoting NMSC has not been fully elucidated;

in contrast to mucosal HPVs, the E6 and E7 oncoproteins of cutaneous HPVs have weak or no transforming properties *in vitro* (Akgül *et al.*, 2005). However, E6 and E7 from HPV49 have been shown to efficiently deregulate p53 and Rb pathways in a similar fashion to their mucosal equivalents (Cornet *et al.*, 2012). Furthermore, current thinking suggests that the E6 and E7 proteins of cutaneous HPV types inhibit the normal DNA damage repair response or UV-induced apoptosis (Muschik *et al.*, 2011; Jackson and Storey, 2000; Underbrink *et al.*, 2008; Viarisio *et al.*, 2011). According to this hypothesis, infected cells are less able to efficiently repair any genetic errors induced by UV radiation, leading to the accumulation of mutations, changes in cellular phenotype and the development of cancer (Hanahan and Weinberg, 2011). The E6 proteins of HPV5 and 18 prevent the translocation of apoptosis-inducing factors to the nucleus (Leverrier *et al.*, 2007) and HPV38 E6 has been shown to interact with the histone acetyltransferase (HAT) p300 to inhibit p53 acetylation, and thus inhibit p53-mediated growth arrest and apoptosis (Muench *et al.*, 2009; Muschik *et al.*, 2011). Similarly, E6 proteins of HPV types 5, 10 and 77 have been shown to prevent UV-induced apoptosis, by abrogating the anti-apoptotic functions of Bak (Underbrink *et al.*, 2008; Holloway *et al.*, 2014; Simmonds and Storey, 2008). As with other HPV infections, the immune status of the host is an important co-factor in the development of NMSC; organ-transplant recipients have a 10-fold increased risk of BCC and up to a 100-fold increased risk of SCC (Pfister, 2003). The immunomodulatory functions of E6 and E7 have been suggested to play a role in NMSC progression; it is argued that the secretion of anti-inflammatory cytokines by just a few HPV-positive cells can impair the cancer cell elimination by the host immune system (Harwood and Proby, 2002; Pfister, 2003).

### 1.3.2.2 Oropharyngeal cancers

Oropharyngeal carcinoma (OPC) is one of the many cancers associated with smoking and alcohol consumption, and results in more than 300,000 deaths per year worldwide (Blot *et al.*, 1988; Ang and Sturgis, 2012; Canova *et al.*, 2010). Since HPV DNA has been found to be more prevalent in OPC tumour than in adjacent normal tissue, the virus is considered an etiological agent for disease (D'Souza *et al.*, 2007). In both the USA and Europe, the incidence of HPV-related OPC has been increasing since the early 1990s, although the proportion of OPC caused by HPV varies widely; in North America 40 to 80% of OPCs are associated with HPV, whereas in Europe the proportion varies from 20 to 90% (Kreimer *et al.*, 2005a; Hansson *et al.*, 2005; Applebaum *et al.*, 2007; Pintos *et al.*, 2008; Smith *et al.*, 2004; Tachezy *et al.*, 2009; Termine *et al.*, 2008; Du *et al.*, 2011; Attner *et al.*, 2009; Mehanna *et al.*, 2012; Chaturvedi *et al.*, 2008). Unlike in cervical carcinomas, HPV16 is more commonly found than HPV18, with 60% of HPV associated OPC in the USA containing HPV16 genomes (Kreimer *et al.*, 2005b; Marur *et al.*, 2010; Herrero *et al.*, 2003). Perhaps counter-intuitively, patients with HPV-positive OPC have a better prognosis than those without; presence of HPV is associated with better tumor control and survival outcomes following radiotherapy, chemotherapy and combined radiation with cisplatin (Lassen *et al.*, 2011; Fakhry *et al.*, 2008; Posner *et al.*, 2011; Ang *et al.*, 2010; Rischin *et al.*, 2010). The mechanism for this is not known, although HPV-positive tumours are on average smaller than HPV-negative carcinomas at diagnosis and it has been suggested that the virus promotes sensitivity to therapy. Furthermore, HPV-mediation of OPC development has been suggested to follow a similar pathway as anogenital cancers (Oh *et al.*, 2013). Ongoing studies aim to identify driver mutations and predictive biomarkers of this disease in order to improve treatment outcome (Ang and Sturgis, 2012).

#### 1.4 The HPV life cycle

Compared to many other viruses, the HPV genome is small, comprising of 8 kb double-stranded DNA and encoding 8 open reading frames (ORFs, Figure 1.3, Table 1.4). These ORFs encode 6 early proteins, E1, E2, E4, E5, E6 and E7, and 2 late structural proteins, L1 and L2, which form the icosahedral capsid of the virus (Buck *et al.*, 2013; Finnen *et al.*, 2003). With the exception of the helicase E1, these ORFs do not encode enzymatic functions, and so viral replication requires cellular machinery. As such, the papillomavirus life cycle is closely tied to the biology of keratinocytes.

Whether or not a productive HPV life cycle is completed depends upon the nature of the epithelial site where infection occurs. A specific population of cells in the cervix (at the squamo-columnar junction) have been identified as having the potential of developing HPV-related CIN, while cells located elsewhere do not (Herfs *et al.*, 2012). As previously indicated, HPV infection can also depend upon the presence of external factors such as hormones and cytokines (Gariglio *et al.*, 2009; de Jong *et al.*, 2004).

Initial HPV infection occurs *via* micro-abrasions in the epithelium, enabling viral access to the basal lamina (Kines *et al.*, 2009). Viral entry into basal keratinocytes is mediated by L1 and L2; L1 interacts with heparin sulphate molecules, as well as laminin, on the surface of the basal lamina (Combata *et al.*, 2001; Giroglou *et al.*, 2001; Finnen *et al.*, 2003; Johnson *et al.*, 2009; Culp *et al.*, 2006; Joyce *et al.*, 1999). L1 binding induces structural changes in the virion capsid, exposing L2 for cleavage by furin and thus facilitating virus interaction with a secondary receptor on the keratinocyte surface and subsequent internalization of virus (Richards *et al.*, 2006; Johnson *et al.*, 2009; Kines *et al.*, 2009; Surviladze *et al.*, 2012). The mechanism of virus internalisation has not been fully resolved for all HPV types and findings are disparate. Most recently, it has been suggested that entry of HPV types 16, 18

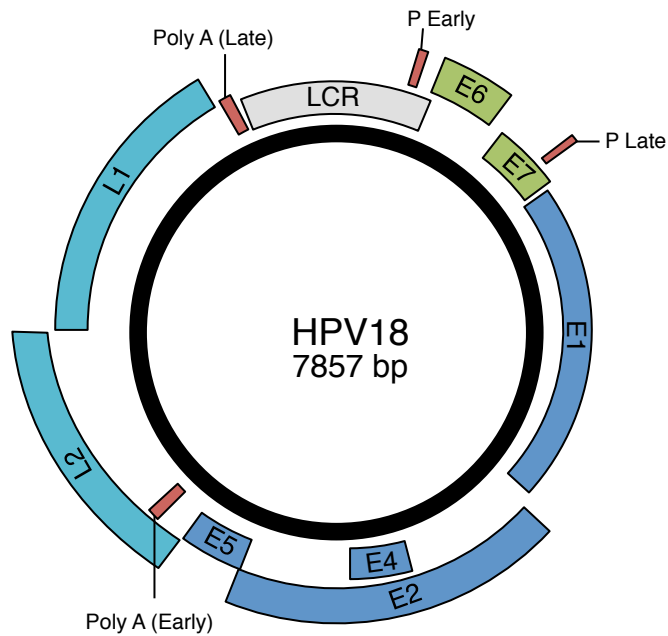


### Figure 1.3: HPV genome organisation

The HPV genome has a circular double stranded DNA genome, encoding 8 ORFs. Splicing of mRNA creates a number of gene products. Viral genes are transcribed in a clockwise direction to produce 6 early, non structural proteins (E1, E2, E4, E5, E6 and E7), and 2 late transcripts encoding structural proteins (L1 and L2, light blue). The major oncoproteins E6 and E7 are highlighted in green, and the transcriptional control region (long control region; LCR, highlighted in grey). The LCR contains a DNA replication origin and functions as the regulator for the DNA replication. This region contains binding sites for cellular transcription factors (e.g. SP1, AP1, Oct1), and for the viral E2 protein, which control viral gene expression. The HPV genome contains two promoter elements (P Early and P Late, indicated in red) which regulate the expression of differentially-spliced mRNAs. The genome also contains two polyadenylation sites, (Poly A Early and Late, indicated in red).

Adapted from Kajitani *et al.* 2012 and Doorbar *et al.* 2012 .

and 31 are all independent of clatherin, caveolin, and dynamin, but require actin polymerization and the tetraspanin CD151 (Spoden *et al.*, 2013).

Following internalisation, the viral capsid disassembles in the endosome compartment and L2 mediates relocation of the viral genome from the endosomal compartment to the nucleus, where genomes are replicated and maintained at a low copy number in basal cells (Richards *et al.*, 2006; Day *et al.*, 2003; Pyeon *et al.*, 2009; Parish *et al.*, 2006; McBride, 2008).

The initial round of viral DNA replication occurs independently of the cell cycle, and results in amplification of the viral genome to around 50–100 copies per cell (Moody and Laimins, 2010). Here, the viral transcription factor E2 is important for the initiation of viral replication and segregation of viral genomes into infected daughter cells (Lehman and Botchan, 1998; Sanders and Stenlund, 2000; Mohr *et al.*, 1990). There are multiple E2 binding sites in the viral LCR, which enable E2 to recruit the helicase E1 along with cellular transcriptional machinery to position it at the viral origin of replication and promote HPV gene transcription (Stubenrauch *et al.*, 1996; Mohr *et al.*, 1990; Sanders and Stenlund, 2000). At this stage, HPV genes are transcribed from the early promoter (Figure 1.3). E2 also acts to tether HPV genomes to mitotic chromosomes *via* interaction with Brd4 and is able to activate or repress cellular gene transcription, depending on the context of the binding sites and nature of the associated cellular factors (Bernard *et al.*, 1989; Dostatni *et al.*, 1991; Dong *et al.*, 1994; You *et al.*, 2004).

Following the initial replication stage, known as establishment, the infected cell leaves the basal compartment and migrates upwards in the epithelia. During a normal, uninfected, life cycle, basal keratinocytes divide and migrate upwards, differentiating as they do so (Figure 1.4). Basal cells divide asymmetrically; one daughter cell migrates, leaving a basal layer of dividing epithelial stem cells (Figure 1.4). However, entering the differentiation program requires exit from the cell cycle and poses an obstacle to HPV genome replication, which

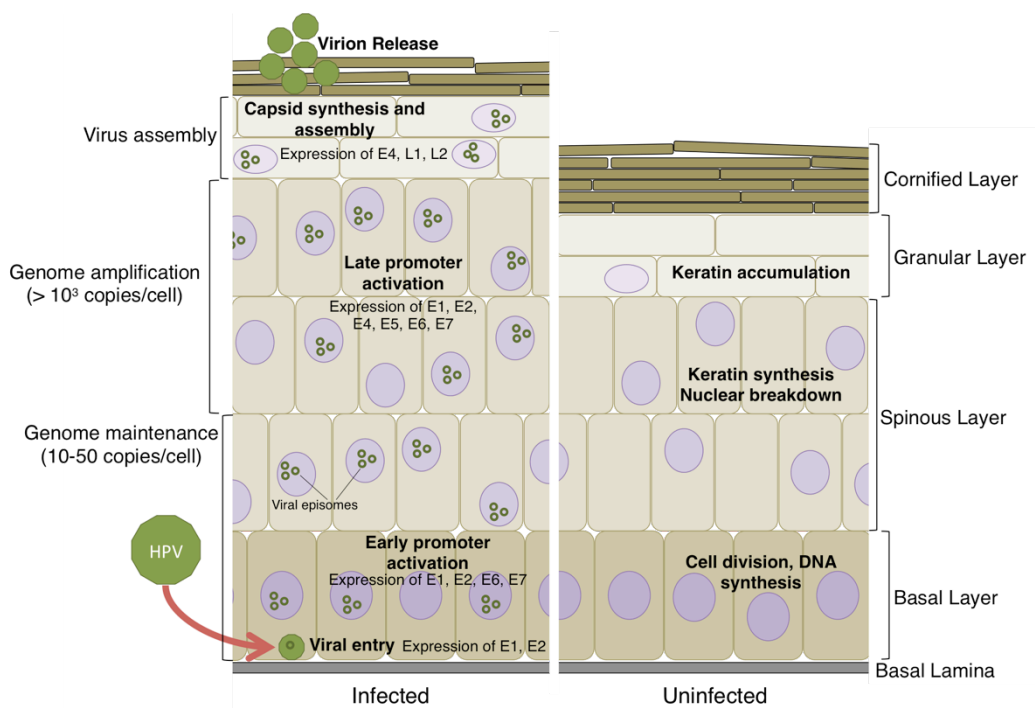


**Figure 1.4: Epithelial differentiation and the HPV life cycle**

The right-hand side depicts the structure of uninfected differentiated epithelia and the main characteristics of each cell layer. Basal cells in the cervical epithelium rest on the basal lamina, which is supported by the dermis. Basal cells divide asymmetrically, and a daughter cell migrates upwards as differentiation occurs, in which cells exit the cell cycle and progressively accumulate cytoplasmic keratin. The left-hand side depicts the HPV infectious cycle. Initially, HPV infects basal cells via microabrasions in epithelia. Infected basal cells form the reservoir of virus. In these cells, the early genes E1, E2, E5, E6 and E7 are expressed and the viral DNA establishes as episomes within the nuclei of cells. As cells migrate upwards, the viral episomes are maintained at a copy number of 100-1000 genomes per cells. The late productive life cycle occurs in upper layers of the epithelia, where the viral genome is amplified, and the late genes L1 and L2, and E4 are expressed. Virions are assembled and released from cornified keratinocytes as they slough off, and are able to produce a new infection.

depends upon host replication substrates and machinery. To overcome this, HPV expresses the early proteins E6 and E7. The combined actions of these proteins reactivates cellular DNA synthesis in non-dividing cells, inhibits apoptosis, and uncouples the differentiation program of the infected keratinocyte from the cell cycle (Section 1.4.1).

**Table 1.4: High-risk HPV ORFs**

HPV ORF	Function(s)	Target Factors
<b>E6</b>	Reactivation of cellular replication mechanisms Proliferation, immortalisation, inhibition of apoptosis Maintenance of viral genome Co-operates with E7 to immortalise primary keratinocytes	p53, ADA3, p300/CBP, E6AP, SP1, c-myc, NFX1-91, TERT, FAK, FADD, Caspase 8, BAX, BAK, IRF3, PDZ domain proteins
<b>E7</b>	Reactivation of cellular replication mechanisms Proliferation, immortalisation, inhibition of apoptosis Maintenance of viral genome Binds retinoblastoma protein (pRb), deregulates the G <sub>1</sub> /S checkpoint Co-operates with E6 to immortalise primary keratinocytes	RB, p107, p130, HDAC, E2F6, p21, p27, CDK/cyclin, ATM, ATR, gamma-tubulin
<b>E4</b>	Interacts with cytoskeletal proteins, allows viral assembly	Cytokeratin 8/18
<b>E5</b>	Weak transforming activity Upregulates growth factor receptors	EGFR, PDGFR, V-ATPase, MHC1, TRAIL receptor, FAS receptor
<b>E1</b>	Replication of viral genome: Helicase, ATPase, ATP-binding protein	RPA, topoisomerase, polymerase alpha-primase
<b>E2</b>	Viral genome replication, transcription and maintenance: Acts as a transcription factor, facilitates initiation of HPV DNA replication, important for genome encapsidation	Brd4, ChIR1 HPV E1
<b>L1</b>	Major capsid function	-
<b>L2</b>	Minor capsid function	-

Adapted from Stanley, 2001 and Kajitani *et al.*, 2012.

Next follows a phase where viral gene expression is minimal and, importantly, the expression of the oncogenes E6 and E7 is tightly control by E2 (Gammoh *et al.*, 2009). As infected keratinocytes enter the differentiating compartment of the epithelia, there is an expansion in viral gene expression, including abundant expression of E6 and E7 (Chow *et al.*, 1987)Figure 1.4). Transcription occurs from the differentiation-dependent late

promoter (P late) located within the E7 ORF, and terminates at the late polyadenylation site (Figure 1.3), amplifying viral genomes to more than 1000 copies per cell (Lambert, 1991; Bedell *et al.*, 1991). This promoter drives the expression of E1, E2, E4 and E5 proteins as well as the late proteins L1 and L2 (Hummel *et al.*, 1992; Ozburn and Meyers, 1998; 1997), Figure 1.4). Both E1<sup>E4</sup> (a fusion protein comprising the first amino acids of E1 and the E4 ORF) and E5 proteins contribute to this differentiation-dependent phase of the viral life cycle (Wilson *et al.*, 2005; Peh *et al.*, 2004). Cleavage of E1 by cellular caspases and activation of the ATM (ataxia telangiectasia mutated protein)-mediated DNA damage pathway are necessary for viral genome amplification as cells enter G2 (Moody *et al.*, 2007; Moody and Laimins, 2009). It is suggested that the subsequent induction of the homologous recombination pathway recruits cellular DNA repair factors to facilitate HPV DNA replication, thus enabling the virus to replicate in an S phase independent manner, in the differentiating compartment of stratified epithelia (Gillespie *et al.*, 2012).

Little is known about the actions of E5 during the HPV life cycle, although it has been shown to downregulate MHC class I expression to promote viral immune evasion, as well as activating epidermal growth factor (EGF) signal cascades to induce keratinocyte proliferation (Petti *et al.*, 1991; Belleudi *et al.*, 2011; Pim *et al.*, 1992; Crusius *et al.*, 1998; Straight *et al.*, 1993). The sequences of the high-risk HPV E5 proteins are conserved, and it has been shown to have weak transforming properties (Bouvard *et al.*, 1994a; Straight *et al.*, 1993; Stöppler *et al.*, 1996). The E5 protein has also been shown to form pore structures, thought to allow the maturation of endosomes during viral entry and/or release (Wetherill *et al.*, 2012). Similarly, the function of E4 in the upper layers of the epithelia has not been fully elucidated although it is abundantly expressed (Figure 1.4). The E4 protein is translated from spliced transcripts which includes the first 5 amino acids of E1 to generate E1<sup>E4</sup> fusion proteins (Chow *et al.*, 1987). Several studies have shown that E4 is able to

arrest transition of the cell cycle from G2 to M, and inhibit entry into S phase as well as inhibiting cellular DNA replication (Knight *et al.*, 2004; Davy *et al.*, 2009; Peh *et al.*, 2004). However Knight *et al.* (2011) showed that G2 arrest was not associated with viral genome amplification. Together, the functions of E4 produce an environment which is suitable for viral DNA replication without competition from the host, as well as optimising viral genome amplification and the expression of capsid proteins (Wilson *et al.*, 2007; 2005; Nakahara *et al.*, 2005).

In the final stages of the viral life cycle, the L1 and L2 proteins encapsulate viral genomes to form infectious virus particles (Figure 1.4). Virus capsids are assembled in the nucleus from 360 molecules of L1 and variable number of L2 molecules, arranged into 72 pentameric units to form an icosahedral structure, stabilized by intermolecular disulphide bonds between L1 proteins (Buck *et al.*, 2008; Finnen *et al.*, 2003). Infectious virions are released during the natural sloughing of keratinocytes, a process which may be facilitated by E4-mediated disruption of the keratin cytoskeleton (Roberts *et al.*, 1997; Doorbar *et al.*, 1991). The entire life cycle takes 2-3 weeks *in vivo*; the time taken for a basal keratinocyte to migrate up the epithelial layers and differentiate (Figure 1.4).

#### 1.4.1 HPV E6 and E7 in the HPV life cycle

The E6 and E7 proteins of both high and low-risk viruses are translated from a bicistronic E6E7 mRNA (Tang *et al.*, 2006). Together they target a number of cellular factors, including those involved in cell cycle regulation, gene expression, DNA replication and cell signalling, culminating in the uncoupling of keratinocyte differentiation from division to promote an environment favorable for viral replication.

#### 1.4.1.1 HPV E7

The functions of E7 induce cellular DNA synthesis, bypass cellular growth arrest, prevent cellular senescence and modulate immune responses.

The interaction of E7 with the retinoblastoma protein (pRb) family is a well-characterised example of E7 acting upon the cell cycle (Figure 1.5). The interaction occurs *via* a conserved LXCXE motif at the N-terminus of high-risk HPV E7 proteins (Münger *et al.*, 1989b). The pRb family of proteins, consisting of p105, p107 and p130, regulate the transition of the cell cycle from G1 to S phase by acting upon the activity of the transcription factor family E2F (Dyson *et al.*, 1989). In quiescent cells, pRb is hypophosphorylated, which promotes its ability to bind to E2F (Neuman *et al.*, 1994; Hiebert *et al.*, 1992; Morkel *et al.*, 1997). The pRb:E2F heterodimer prevents binding of the transcription factor to the promoter region of genes required for G1 to S phase transition, thus repressing transcription of E2F-responsive genes (Jones *et al.*, 1997; DeGregori and Johnson, 2006; Zwicker *et al.*, 1996). In the presence of mitogenic signals, pRb is progressively phosphorylated during G1 by active CDK:cyclin complexes CyclinD1:CDK4, CyclinD1:CDK6 and CDK2:cyclin2, which causes the complex to dissociate thus allowing transcription of E2F-responsive genes. These genes are required in nucleotide synthesis, DNA replication and progression of the cell cycle into S phase. For example, cyclin A is transcribed, which binds to CDK2 to activate the kinase, allowing the phosphorylation of target proteins to activate S phase specific processes, including DNA replication (Jeffrey *et al.*, 1995; Harper *et al.*, 1993). HPV E7 mimics the phosphorylation of pRb, disrupts the pRb:E2F complex and causes proteasomal degradation of pRb (Figure 1.5, Dyson *et al.*, 1989; Huh *et al.*, 2007). This enables the constitutive expression of E2F-responsive genes; inducing infected cells to enter S phase despite absence of mitogenic signals (Cheng *et al.*, 1995; Chellappan *et al.*, 1992).

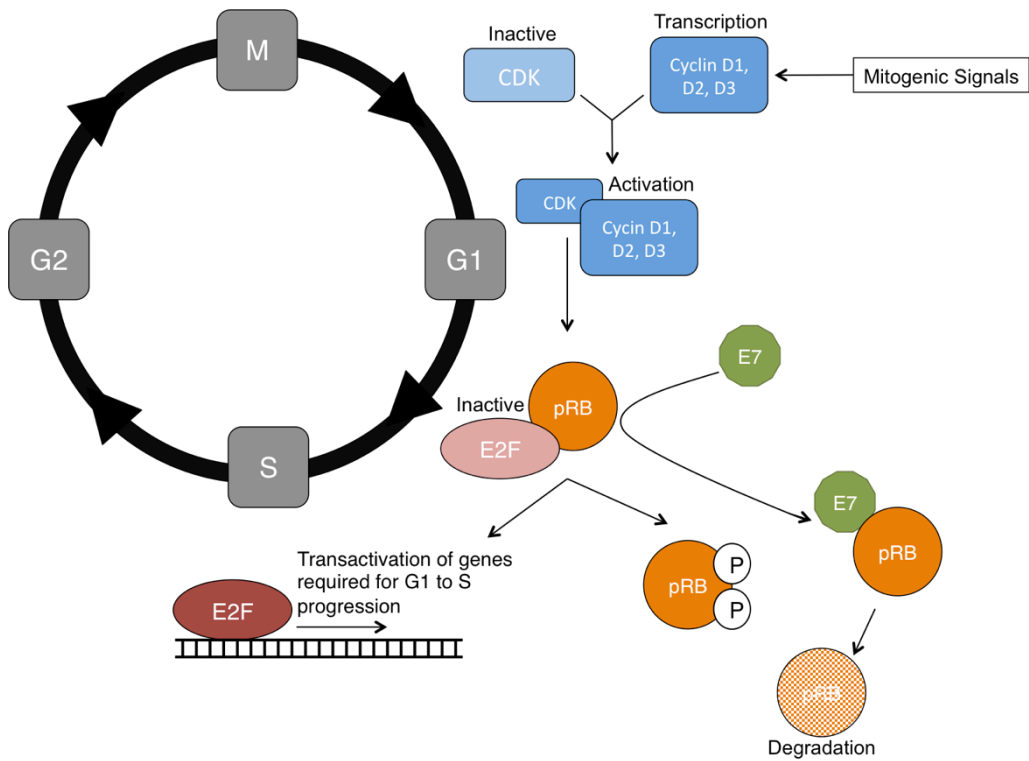


**Figure 1.5: E7 acting upon the cell cycle**

E2F transcription factors form heterodimeric complexes with members of the pRb family and regulate the transcription of several genes during the cell cycle. In quiescent cells, pRb is present in a hypophosphorylated form and associates with E2F molecules, thereby inhibiting their transcriptional activity. When quiescent cells are exposed to mitogenic signals, genes encoding the G1 specific D-type cyclins (D1, D2 and D3) are activated. Subsequently, cyclins associate with a cyclin-dependant kinase, CDK4 or 6, transport into the nucleus and phosphorylate pRb in mid-G1 phase. Phosphorylation of pRb releases active E2F complexes and progression into S phase. E7 binding to pRb mimics its phosphorylation, promoting its proteasomal degradation. Thus, E7 expressing cells can enter S phase in the absence of a mitogenic signals.

High-risk  $\alpha$ -HPV E7 affects CDK2 *via* a number of mechanisms to promote cell cycle progression from G<sub>1</sub> to S phase. E7 binds to the CDK2 inhibitors p21 and p27, preventing their inhibitory activity, and E7 expression induces increased CDC25 transcription; the phosphatase dephosphorylates and consequently activates CDK2 (Zerfass-Thome *et al.*, 1996; Funk *et al.*, 1997; Jones and Münger, 1997; Nguyen *et al.*, 2002). Similarly, E7 upregulates the transcription of cyclin E to promote cell cycle progression and increases transcription of the senescence inhibitor protein DEK (Wise-Draper *et al.*, 2005). Moreover, E7 affects S phase-specific gene expression by interacting with transcription factors; E7 binds to E2F to act as a transcriptional activator (Hwang *et al.*, 2002).

The viral protein is able to modulate transcription directly *via* the zinc finger domain. This domain allows E7 to bind and recruit chromatin modifiers such as histone deacetylases (HDACs) to repress the activity of specific promoters, including E2F responsive ones (Brehm *et al.*, 1998; Longworth *et al.*, 2005; Longworth and Laimins, 2004a). Furthermore, E7 is able to facilitate the removal of HDAC at other promoters, in order to activate transcription of growth-promoting genes (Brehm *et al.*, 1999). This interaction is important in S phase promotion but has also been shown to influence the maintenance of episomal genomes (Longworth *et al.*, 2005; Longworth and Laimins, 2004b).

The transcriptional upregulation of interleukin-8 (IL-8) induced by E7 not only prevents cellular senescence, but also enables infected cells to evade immune detection (Walker *et al.*, 2011). Furthermore, E7 expression has recently been shown to increase the levels IL-18 binding protein (IL-8BP), an antagonist of the proinflammatory cytokine IL-18 (Richards *et al.*, 2014). This enables infected keratinocytes to evade immune detection by interfering with IL-18-mediated lymphocyte activation (Richards *et al.*, 2014). The multifarious nature of E7 can also be seen in the inhibition of tumour necrosis factor  $\alpha$  (TNF $\alpha$ )-mediated cell cycle arrest by the oncoprotein, where the proteins ability to interrupt translation also

inhibits TNF $\alpha$ -mediated differentiation and apoptosis and aids immune evasion (Basile *et al.*, 2001; Thompson *et al.*, 2001; Boccardo *et al.*, 2010). All of which enables the virus to evade detection as well as promote cell survival despite the activation of apoptotic signals.

During the viral life cycle, E7 expression and activity is regulated by E2; HPV16 E2 protein directly binds to E7 to inhibit degradation of pRb (Gammoh *et al.*, 2009). Disruption of the cell cycle by E7 induces p53-dependent apoptosis and stabilises p53; degradation of pRb leads to an increase p53 protein and would trigger apoptotic pathways and end viral propagation, were it not for the functions of E6 (Demers *et al.*, 1994).

#### 1.4.1.2 HPV E6

Full-length E6 protein is transcribed from the bicistronic E6E7 mRNA to produce a protein of approximately 150 amino acids in length, which resides in the cytoplasm and nucleus of infected cells (Howie *et al.*, 2009; Tao *et al.*, 2003). It has been suggested that E6 forms a dimer in high concentrations of salt and protein but remains predominantly monomeric under physiological conditions (Lipari *et al.*, 2001). Like E7, E6 contains two zinc finger motifs (Figure 1.6) and the protein is known to interact with a number of cellular targets, *via* which it affects a range of cellular processes, including apoptosis, cellular differentiation, cell-cell adhesion, polarity and proliferation (Figure 1.7, Barbosa *et al.*, 1989; Grossman and Laimins, 1989).

The association between HPV E6 proteins and the cellular ubiquitin ligase E6AP occurs *via* an LXLL motif within the oncoprotein and allows E6 to promote the proteasomal degradation of a number of targets, as well as increasing E6 stability (Huibregtse *et al.*, 1993b; Tomaić *et al.*, 2009; Daniels *et al.*, 1998b). One of the most well known targets is the DNA damage response protein, p53, which ordinarily is not targeted for degradation *via* E6AP (Camus *et al.*, 2003). However, E6 binding both E6AP and p53 facilitates

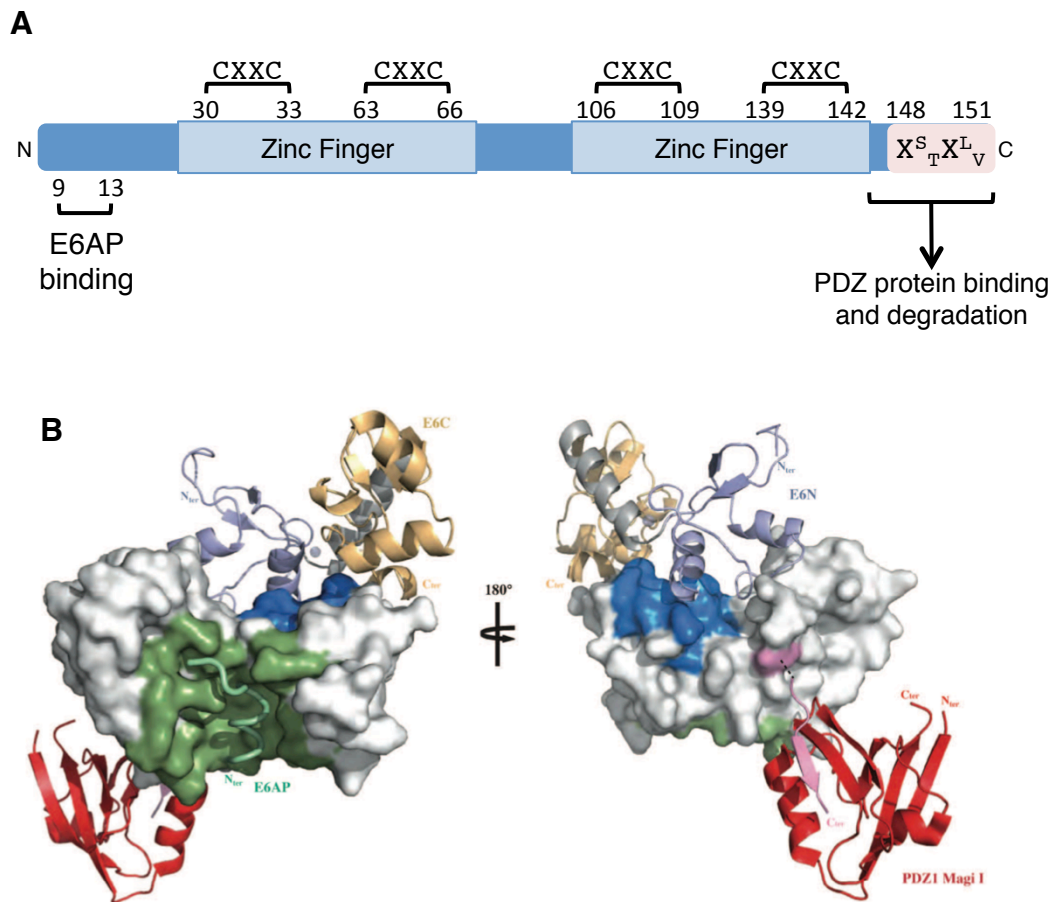


**Figure 1.6: Structure of E6**

- (A) Schematic of HPV E6 protein domain structure. E6 proteins are approximately 150 amino acids in length and contain two zinc-finger domains and a C terminus PDZ binding motif (PBM, highlighted in pink). Numbers correlate to the amino acid sequence of HPV18 E6.
- (B) The 3D structure of E6 from Zanier *et al.* 2013, shows that the PBM (pink) is disordered in NMR structural studies and adopts a  $\beta$ -strand confirmation upon binding to the PDZ domain of MAGI-1 (red ribbon structure). The right-hand image shows the protein rotated by 180 degrees relative to the left-hand image. Region in green indicates E6AP binding (LXXLL) motif, with the interacting helix of E6AP shown (green). Blue indicates region of E6 involved in self-association, with a ribbon structure indicating a second E6 molecule. The white region indicates residues which are potentially available to interact with p53.

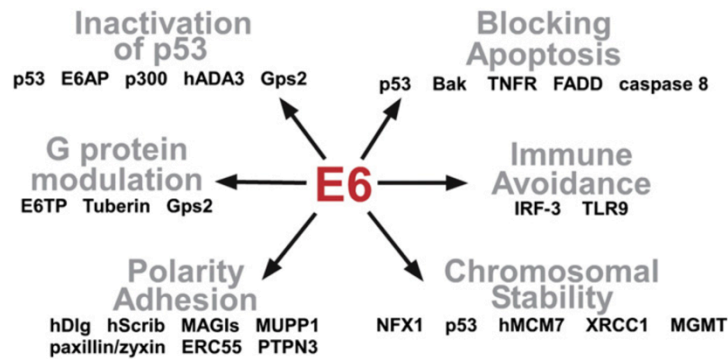


**Figure 1.7: E6 interacts with a number of cellular proteins**

From Howie *et al.* 2009. E6 alters numerous cellular pathways through the binding of proteins. The interactions predominantly function to promote cell-cycle progression for the propagation of virus, but promote transformation of infected cells when the protein is deregulated, aiding the progression of cancer and highlighting the role of E6 as a viral oncoprotein.

Examples of proteins involved are indicated below the affected pathways.

ubiquitination and subsequent degradation of the cellular tumour suppressor (Huibregtse *et al.*, 1993a; Werness *et al.*, 1990; Crook *et al.*, 1991; Muench *et al.*, 2010). Interestingly, the association between HPV16 E6 and E6AP is stronger than between E6AP and HPV18 E6, and drives the degradation of p53 more efficiently than HPV18 E6 (Scheffner *et al.*, 1990). E6 proteins also disrupt the function of p53 directly; binding to the protein interferes with the DNA-binding activity and blocks transcription of p53-dependent genes (Lechner and Laimins, 1994). E6 further disrupts p53 activity by binding to the histone acetyltransferases p300 and CREB binding protein (CBP), inhibiting p53 acetylation, which would otherwise stabilize the cellular protein, and increasing E6 stability (Patel *et al.*, 1999; Zimmermann *et al.*, 1999). A decrease in p53 provides the infected cell with resistance to apoptosis; E6-expressing cells are able to continue promoting cell proliferation without disruption. In this respect, the HPV oncoproteins E6 and E7 act synergistically; where E7 puts the cell at risk of p53-mediated apoptosis, E6 intervenes removing p53 and allowing the cell to continue providing substrates for DNA synthesis and viral propagation (Figure 1.8). Moreover, loss or abrogation of E6-directed p53 degradation impairs the ability of HPV16 to maintain genomes and silencing E6 in the context of HPV18 negatively affects viral genome amplification (Park and Androphy, 2002; Wang *et al.*, 2009c; 2009b; 2009a; Kho *et al.*, 2013). Similarly, HPV11 encoding a non-functional E6 were unable to maintain episomal genomes, indicating the importance of HPV E6 in viral replication (Oh *et al.*, 2004).

HPV E6 is also able to affect p53-independent apoptotic pathways to prevent virally induced cell-death. This was first observed in transgenic mouse models expressing HPV16 E6 and E7 in the mouse eye lens; expression of E7 alone induced apoptosis, which was partially rescued by knocking down p53 (Pan and Griep, 1994; Griep *et al.*, 1993). Although both high and low-risk HPV E6 proteins promote the degradation of pro-apoptotic factor Bak, only high-risk E6 has been shown to bind to procaspase 8, an event which induces

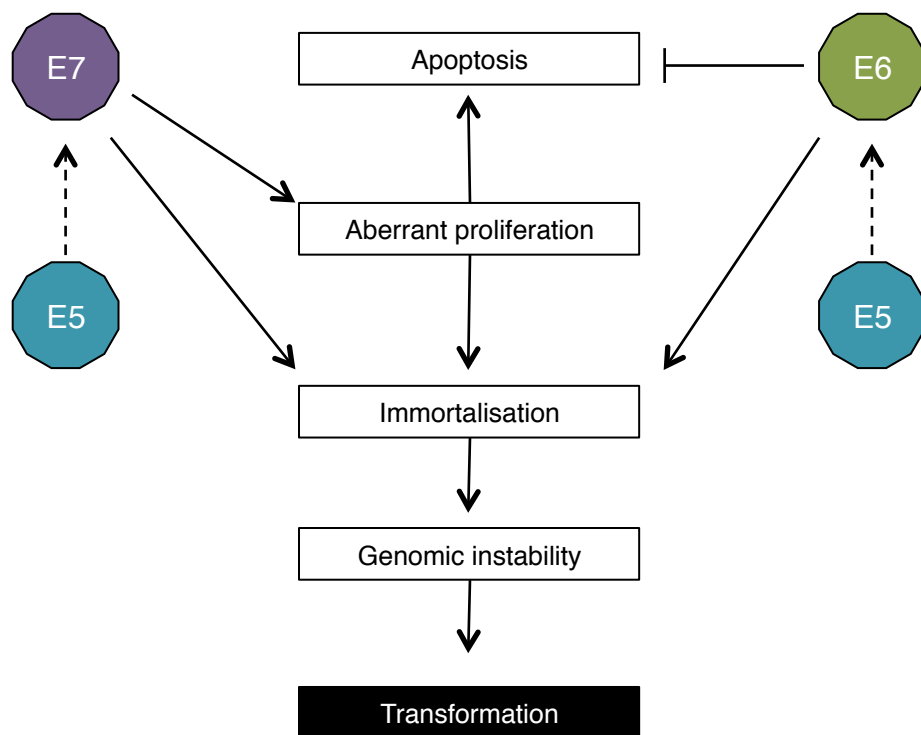


**Figure 1.8: HPV oncoprotein cooperation in cervical carcinogenesis**

The ability of E6 and E7 to target cellular regulators of proliferation, apoptosis, immortalization and genomic stability collectively bestows cells with a growth advantage and an increased propensity for transformation and malignant progression. The viral proteins work synergistically; the induction of hyperproliferation by the E7 protein triggers cellular apoptotic pathways, which is blocked by the actions of the E6 protein. Cells are therefore immortalized via the cooperative actions of E6 and E7, although these functions are potentiated by the actions of E5. Adapted from Moody and Laimins 2010.

conformational changes that interrupt downstream signalling and the cells response to pro-apoptotic stimuli (Thomas and Banks, 1999; 1998; Underbrink *et al.*, 2008; Tungteakkhun and Duerksen-Hughes, 2008; Filippova *et al.*, 2004).

**Table 1.5: Protein partners of E6**

<b>Function</b>	<b>E6 Binding partner</b>
E3 ubiquitin ligase	E6AP
Mediators of apoptosis	p53, Bak, c-myc, procaspase-8, FADD, TNFR1
Transcriptional regulation	CBP/p300, NF $\kappa$ B
Immune regulation	IRF3
Chromosomal stability	Mcm7, hTERT
Epithelial differentiation and organisation	E6-BP, fibulin-1, zyxin, Notch pathway
Cell polarity, adhesion and proliferation	PDZ proteins*

Adapted from Howie *et al.*, 2009; Vande Pol and Klingelutz, 2013. \*Cell polarity proteins are discussed in more detail in Section 1.6

During HPV infection, keratinocyte differentiation must be tightly controlled in order to balance the promotion of viral genome amplification in the spinous layer of epithelia with keratinocyte differentiation in the granular and cornified layers (Figure 1.4). High-risk E6 proteins modulate keratinocyte differentiation and it is likely that these functions of E6 are temporally regulated (Alfandari *et al.*, 1999; Sherman *et al.*, 1997). In cell culture and mouse models, E6 has been shown to enhance the activity of the Wnt signalling pathway, which is involved in cell proliferation, in an E6AP dependent manner (Lichtig *et al.*, 2010; Bonilla-Delgado *et al.*, 2012). Moreover, E6 activates the mTOR receptor tyrosine kinase cascade by enhancing phosphorylation of the kinase mTOR which activates downstream signalling pathways, culminating in the stimulation of protein synthesis (Spangle and Münger, 2010; Spangle *et al.*, 2012). The oncoprotein also acts on the Notch pathway, which is central to epithelial differentiation; cutaneous HPV E6 proteins are able to downregulate the pathway by binding to MAML1 protein, and E6 proteins have been shown to repress pathway

components transcriptionally (Brimer *et al.*, 2012; Meyers *et al.*, 2013; Henken *et al.*, 2012; Tan *et al.*, 2012). However, HPV has been shown to potentiate the Notch pathway in keratinocytes via transcription factor NFX-123 (Vliet-Gregg *et al.*, 2013; 2015). Interestingly, a recent study indicated that NF $\kappa$ B activation by E6 is cell context specific; whereas E6-mediated activation of the pathway in ectocervical cells increased proliferation, it inhibited growth in cells derived from the endocervix (Vandermark *et al.*, 2012). Further complexity is added by the addition of a temporal aspect; it is likely that E6 differentially modulates Notch signalling during the viral life cycle, repressing and enhancing signalling in the spinous and upper layers respectively (Brimer *et al.*, 2012; James *et al.*, 2006; Nees *et al.*, 2001; Yuan *et al.*, 2005; Havard *et al.*, 2005; D'Costa *et al.*, 2012; Vandermark *et al.*, 2012). In addition, the C-terminus of high-risk  $\alpha$ -HPV E6 proteins contains a conserved motif that is able to interact with a number of PDZ-domain containing proteins involved in differentiation and the regulation of epithelial polarity. The relationship between high-risk HPV E6 and these polarity proteins is discussed in more depth in Section 1.5.4.

By interacting with transcription factors, such as p300/CBP and c-myc, E6 is able to influence the regulation of gene transcription (Crook *et al.*, 1991; Desaintes *et al.*, 1992; Ronco *et al.*, 1998; Patel *et al.*, 1999). By activating c-myc, high-risk HPV E6 is able to regulate the expression of hTERT a telomerase complex which prevents telomeric DNA loss during repeated cell replication cycles (Oh *et al.*, 2001; Kiyono *et al.*, 1998). This is beneficial to the viral life cycle as it extends the replicative potential of infected cells, however chronic activation leads to an immortal phenotype, promotes chromosomal instability and mutation accumulation, all of which are oncogenic phenotypes (Figure 1.5). Furthermore, the expression of HPV16 E6 causes downregulation of a number of genes involved in keratinocyte differentiation, including IFN-responsive genes, including IFN $\alpha$  and IFN $\beta$  (Nees *et al.*, 2001; Vandermark *et al.*, 2012). The same study observed an

upregulation in expression of proliferation promoting genes, including IL-8 and NFκB pathway components, in the presence of E6 alone (Nees *et al.*, 2001). Moreover, it has recently been observed that expression of high-risk E6 alone is sufficient to cause transcriptional upregulation of *APOBEC3B*, which encodes a DNA deaminase (Vieira *et al.*, 2014). It has been suggested that this is an effect of E6-mediated p53 abrogation, rather than a direct interaction with cellular DNA, but it must be noted that E6 is able to effect gene expression more directly. For example, E6 proteins have been shown to bind and target the HAT ADA3 for degradation; as such, interaction with chromatin remodeling machinery is a mechanism by which E6 can alter host gene expression (Kumar *et al.*, 2002). The effect of E6 upon transcription contributes to the proteins ability to delay cell differentiation and promote a favourable environment for viral genome replication.

Another feature of high-risk HPV E6 proteins is their ability to regulate cellular microRNA (miRNA) expression (Martinez *et al.*, 2008; Wang *et al.*, 2009c; Wald *et al.*, 2011; McKenna *et al.*, 2014; Yablonska *et al.*, 2013). For example, HPV16 E6 downregulates miR34a, which targets cell cycle control genes (Wang *et al.*, 2009c). The mechanism by which E6 regulates miRNAs is not known, but it has been suggested to that the reduction in p53 and the increase in E2F activity when E6 and E7 are present plays a role (Yablonska *et al.*, 2013).

#### 1.4.1.2.1 Spliced forms of E6

Variations of the E6 protein, denoted E6\*I and E6\*II, are produced *via* alternative splicing (Smotkin and Wettstein, 1986). The splice site is highly conserved, and causes expression of the first 42 or 44 amino acids of HPV16 or HPV18 E6 respectively followed by a variable sequence (Comerford *et al.*, 1995). The functions of E6 spliced variants remain unclear, although interactions with both E6AP and full-length E6 have been observed (Pim *et al.*, 1997). The overexpression of HPV18 E6\*I promotes the proteasome-dependent degradation of junctional proteins DLG1, MAGI-1 and PATJ which are also targets of

full-length E6 (Pim *et al.*, 2009; Storrs and Silverstein, 2007). Moreover, both HPV16 and HPV18 E6\*I have been shown to target the HAT TIP60 for degradation (Jha *et al.*, 2010). Conversely, the kinase AKT has been identified as a target of E6\*I, but is not targeted by the full-length protein (Pim *et al.*, 2009).

The actions of E6\*I appear to antagonize some functions of the full-length protein. For example, *in vitro* HPV18 E6\*I is able to inhibit E6-mediated p53 degradation and stabilize procaspase 8 (Pim *et al.*, 1997; Tungteakkhun *et al.*, 2010; Pim and Banks, 1999). It has been suggested that the antagonistic functions of E6\* controls the activity of full-length E6 during the virus life cycle by preventing complete removal of cellular p53 (Mantovani and Banks, 2001). Interestingly, the full-length and E6\*I versions bind to different regions of procaspase 8 (Tungteakkhun *et al.*, 2010; Filippova *et al.*, 2007).

#### 1.4.2 HPV oncogenesis

HPVs are well adapted to their host; in most instances the virus manages to proliferate and is maintained in the host population without causing any apparent disease (Woodman *et al.*, 2007; Liaw *et al.*, 1999; Wallin *et al.*, 1999). However, malignant growth can be a side effect of infection, with the time from initial exposure to invasive growth spanning a period of 15-30 years (Woodman *et al.*, 2007; Bekkers *et al.*, 2004). The progression of infected cells from neoplastic lesions to invasive cancer is associated with failure of the immune system to clear persistent infection and the integration of the HPV genomes into host chromosomes (Cricca *et al.*, 2006; Andersson *et al.*, 2005; Peitsaro *et al.*, 2002; Berumen *et al.*, 1995; Fuchs *et al.*, 1989; Cooper and McGee, 1992; Das *et al.*, 1992; Hausen, 2002; Collins *et al.*, 2009). Although integrated HPV genomes are present in the majority of cervical cancers and the frequency of integration increases with severity of cervical neoplasia, it should also be noted that integration of viral genomes is an early event (Wentzensen *et al.*, 2004; Xu *et al.*, 2013; Collins *et al.*, 2009). While no integration hotspots

have been confirmed, it has been suggested that preferential integration occurs at a site near the c-myc gene and that genomes integrate at naturally occurring regions of host genomic instability, known as fragile sites (Ziegert *et al.*, 2003; Ferber *et al.*, 2003; Akagi *et al.*, 2014). Integration of the genome is influential in HPV oncogenesis; in epithelial cell culture, integration of HPV16 genomes is associated with a selective growth advantage and an increased proliferative capacity (Jeon *et al.*, 1995; Jeon and Lambert, 1995). HPV genome transcription is regulated by the viral E2 protein, which represses early gene expression and regulates copy number (Bouvard *et al.*, 1994b). Integration disrupts the viral genome, often interrupting E1 and E2 expression and thus removing the regulatory influence of E2 over the expression of early viral genes (Pett and Coleman, 2007). This was demonstrated in culture, when reintroduction of E2 into HPV18-positive cancer cells containing integrated genomes caused cellular senescence (Goodwin and DiMaio, 2000; Francis *et al.*, 2000). Furthermore, the expression of E6 and E7 oncoproteins is retained in cancers, and the transcripts expressed from integrated genomes are more stable than from episomes (DeFilippis *et al.*, 2003; Hausen, 1999; Schwartz, 2013; Jeon *et al.*, 1995; Jeon and Lambert, 1995). Replication of integrated genomes also results in the activation of host DNA repair and recombination systems, which increases the likelihood of acquiring cellular mutations, increased genomic instability and, eventually, malignant progression (Kadaja *et al.*, 2009). It has also been suggested that the coexistence of episomal genomes with integrated copies may be important in carcinogenesis; Kadaja *et al.* (2009) propose that expression of HPV E1 and E2 from episomal genomes can initiate DNA replication from integrated viral origins, resulting in the induction of chromosomal abnormalities as well as viral gene transcription, leading to genomic instability. Thus, there is a significant role for HPV genome integration in the transformation of infected cells to cervical cancer, and the viral oncoproteins E6 and E7 are important in maintaining a transformed phenotype.

#### 1.4.2.1 HPV E6 and E7 in oncogenesis

There is a wealth of evidence demonstrating the ability of HPV oncoproteins E6 and E7 to drive immortalisation of cells. Expression of the E6 protein from high-risk HPV types 16, 18, and 31 have been shown to extend keratinocyte lifespan (Münger *et al.*, 1989a; Hudson *et al.*, 1990; Sedman *et al.*, 1991; Woodworth *et al.*, 1989). Expression of high-risk HPV E7 immortalises human primary keratinocytes in culture at low frequency, but is unable to immortalise mammary cells alone (Hawley-Nelson *et al.*, 1989). Moreover, mouse models of cervical cancer have shown that E6 and E7 are able to induce dysplasia independently, with E7 expression generating a more invasive phenotype than E6 (Riley *et al.*, 2003). Mice expressing E6 under the control of a keratin promoter develop epithelial hyperplasia (Herber *et al.*, 1996; Song and Pitot, 1999). In this transgenic mouse model, expression of E7 alone is sufficient to induce high-grade cervical dysplasia and invasive cervical malignancies (Arbeit *et al.*, 1996). Similarly, expression of HPV16 E7 in transgenic embryonic mouse lens led to induction of hyperplastic growth (Howes *et al.*, 1994; Pan and Griep, 1994). When E6 was induced alongside E7 in this system, an increased susceptibility to tumour development was observed (Howes *et al.*, 1994; Pan and Griep, 1994; 1995). In raft culture, expressing both E6 and E7 induced cellular changes are comparable to changes seen in the development of CIN (McCance *et al.*, 1988). Although the oncoproteins have transformative properties alone, concurrent expression produced larger and more extensive cancers, highlighting the cooperative nature of E6 and E7 in driving tumour development (Riley *et al.*, 2003).

Despite the ability of high-risk E6 and E7 to immortalise primary cells efficiently, HPV immortalised cells are not tumorigenic in nude mouse models (Hawley-Nelson *et al.*, 1989; Münger *et al.*, 1989a; Kaur and McDougall, 1988). In order to develop tumourigenic capabilities, HPV-immortalised cells require the coexpression of additional oncogenes,

such as v-ras, or extensive passaging in tissue culture (Durst *et al.*, 1989; Pei *et al.*, 1998; Hurlin *et al.*, 1991). Transgenic mice expressing high-risk E6 and E7 in epithelial cells develop squamous carcinomas when treated with oestrogen, highlighting hormone levels as a cofactor in cervical cancer development (Arbeit *et al.*, 1996). Furthermore, murine experiments have suggested that, during the development of HPV-associated cancers, E6 contributes to the later stages of oncogenesis, whereas the functions of E7 contribute to the early stages (Song *et al.*, 2000; Simonson *et al.*, 2005).

The same functions that promote cell growth during the HPV life cycle, when deregulated, allow E6 and E7 to drive cell proliferation and survival, as well as promoting genetic instability and immune evasion, all of which contribute to HPV-driven oncogenesis (Figure 1.8). For example, the activation of hTERT by E6 leads to an immortal phenotype, promotes chromosomal instability and mutation accumulation (Oh *et al.*, 2001). Furthermore, there is a strong correlation between the ability of HPV E6 to activate hTERT and the ability of the HPV type with association cancer (van Doorslaer and Burk, 2012). Interestingly, whilst low-risk HPV E6 proteins are able to associate with E6AP as well as high-risk types, this does not result in p53 degradation, indicating that this interaction plays an important role in E6-driven transformation (Brimer *et al.*, 2007; Lechner and Laimins, 1994). Similarly, low-risk HPV E7 proteins associate with pRb, but are less efficient than high-risk proteins at activating E2F responsive genes (Longworth and Laimins, 2004a). Moreover, only high-risk HPV E7 proteins have been identified as able to bind to HDACs *via* conserved sequences, indicating that this mechanism of controlling gene transcription is significant to the contribution of E7 to transformation (Figure 1.9).

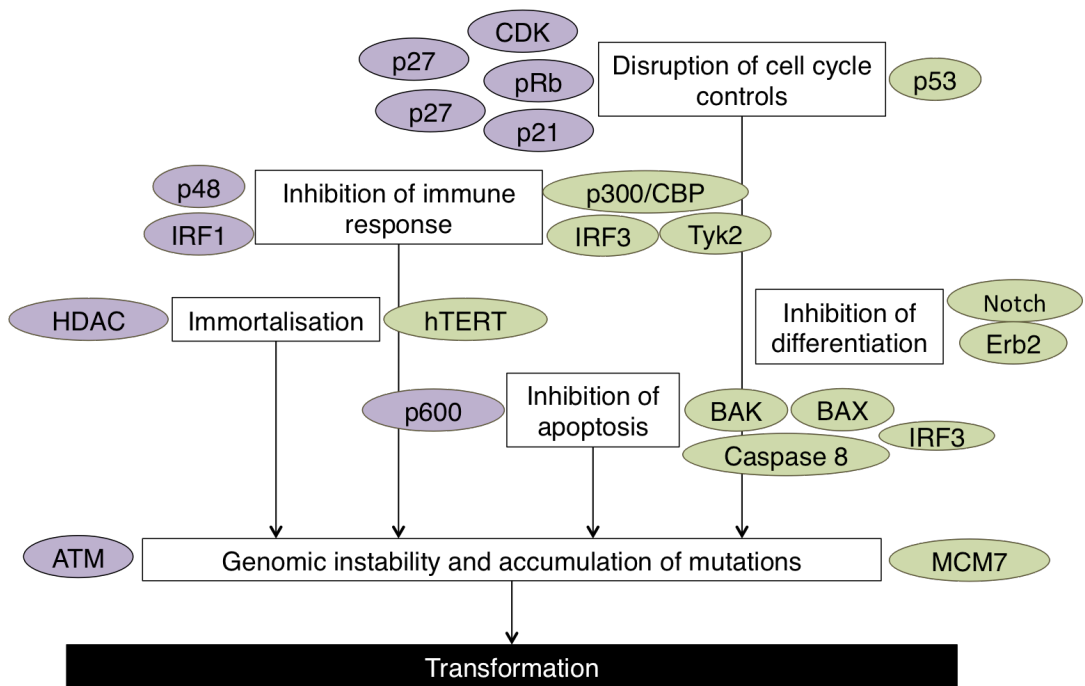


**Figure 1.9: E6 and E7 affect a number of cellular targets in carcinogenesis**

By targeting cellular proteins, E6 and E7 are able to affect a number of cellular processes (boxed) culminating in transformation of E6 and E7 expressing cells. Factors targeted by E7 are indicated in purple, at the left-hand side of the cellular processes and factors affected by E6 are indicated in green at the right-hand side. Adapted from Yugawa and Kiyono, 2009.

#### 1.4.2.2 HPV E5 in oncogenesis

Although E6 and E7 provide the primary functions in HPV driven oncogenesis, the functions of E5 have also been shown to contribute to tumour progression (Stöppler *et al.*, 1996). E5 promotion of cell proliferation has been observed in tissue culture when expressed with E6 and E7, and to a lesser extent when expressed alone (Petti *et al.*, 1991; Valle and Banks, 1995; Bouvard *et al.*, 1994a). In transgenic mice expressing HPV16 E5 in the skin, epithelial hyperproliferation is observed, eventually leading to tumour formation and oestrogen treatment of mice induces cervical cancers when E5 is expressed (Maufort *et al.*, 2010; 2007). It is suggested that the protein provides a supporting role in tumour progression and the involvement of this protein during the HPV life cycle and oncogenesis has yet to be fully elucidated.

#### 1.5 Epithelial polarity

Epithelial tissues comprise the foundation of the majority of human organs, and 90% of cancers are epithelia-derived carcinomas (Tanos and Rodriguez-Boulan, 2008). Epithelia line the cavities of the body and are specialised to perform secretion, absorption, protection and sensory functions. These functions depend largely upon the establishment of tissue polarity and integrity of cell-cell attachments, which enable cells to form a sheet-like structure, and to distinguish between the surfaces of epithelial sheets (Figure 1.10).

Individually, all cell types exhibit polarity, in that structures and membrane domains are organised assymmetrically. Such cell shape is fundamental during the development of an organism, in defining tissue architecture and maintaining tissue homeostasis. The deregulation of mechanisms regulating cell polarity can lead to developmental disorders, tissue degeneration or cancer (Humbert *et al.*, 2003).

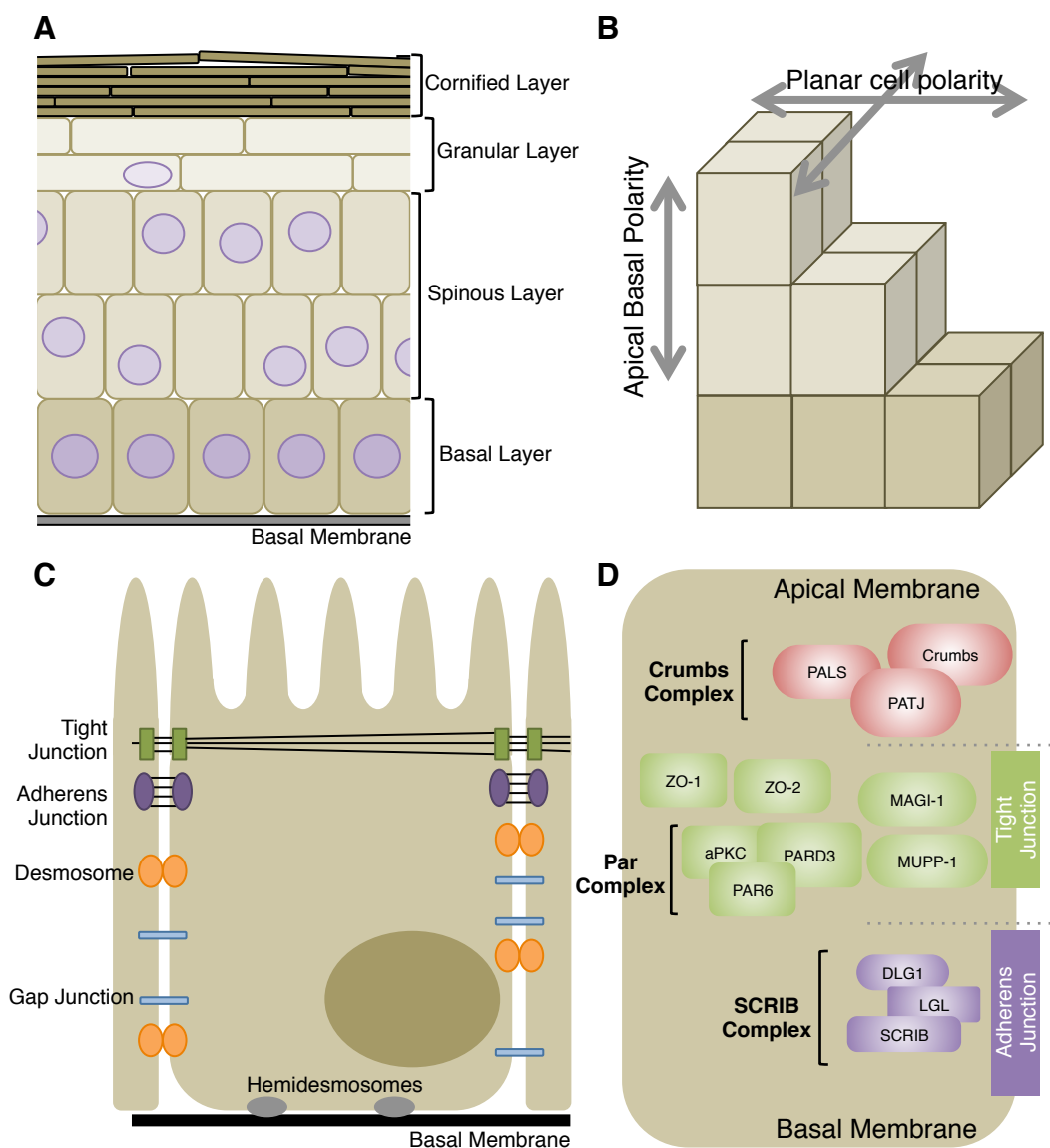


**Figure 1.10: Epithelial polarity and junction complexes**

- (A) Epithelial differentiation, as depicted in Figure 1.4. Basal cells rest on the basal lamina, which is supported by the dermis, and divide asymmetrically. A daughter cell migrates upwards as differentiation occurs, in which cells exit the cell cycle and progressively accumulate cytoplasmic keratin.
- (B) Cells themselves are polar and epithelia also exhibits planar and apical-basal polarity, allowing the trafficking of molecules and specialized functions on different faces of the tissue.
- (C) There are three main complexes involved in the organization of epithelial cell-cell junctions. Tight junctions coordinate the zona occludens, a belt-like structure which ties planes of epithelia together.
- (D) The Crumbs complex (red) consists of PATJ, PALS and Crumbs proteins. Tight-junctions (green) involve the Par complex, made up of PAR3, PAR6 and atypical PKC, as well as associated tight junction PDZ-domain containing proteins MAGI-1, MUPP1, ZO-1 and ZO-2. Adherens junctions (purple) contain the Scribble complex, made up of SCRIB, DLG1 and LGL.

As a tissue, epithelial polarity requires the vertical organisation of individual cells, such that specialized structures (e.g. adherens junctions) are orientated along the apical-basolateral axis, known as apical-basolateral polarity (ABP), as well as the positioning of cells within the plane of epithelial tissues, known as planar cell polarity (PCP, Figure 1.10 B). Furthermore, epithelial polarity is retained during cell division *via* asymmetrical replication; in basal cells, orientation of the mitotic spindle enables division to occur in parallel to or perpendicular to the epithelial sheet (Lechler and Fuchs, 2005). Division of basal cells within the plane of the epithelium functions to expand cell number, whereas division perpendicular to the plane produces stratified epithelia (Kim *et al.*, 2009).

The correct regulation of both apico-basal polarity (ABP) and planar cell polarity (PCP) is accomplished *via* the precise localisation of polarity proteins and other molecules such as lipids (Knust and Bossinger, 2002; Wodarz and Näthke, 2007). Central to ABP regulation are the Scribble, Par (Partitioning defective) and Crumbs protein complexes (Yamanaka and Ohno, 2008; Assémat *et al.*, 2008, Table 1.6). These complexes link cell polarity with the regulation of cell–cell contact *via* junctional complexes, as well as with regulation of cell proliferation, migration and apoptosis. The main junctional complexes involved in epithelial organisation and integrity are the tight junctions (TJs) and the adherens junctions (AJs), formed at the apical and basolateral domains of a cell, respectively (Table 1.6, Figure 1.10).

### 1.5.1 Polarity complexes

In order to distinguish between the outer and inner surfaces of epithelial sheets, the membrane of epithelial cells is segregated into apical and basolateral domains with an asymmetric distribution of trafficking machinery and membrane proteins (St Johnston and Ahringer, 2010). Within a cell, the apical and basolateral regions are separated by the zonula adherens (ZA), a belt-like structure circling the apical side of the cell (Figure 1.10 C). The

apical and basolateral membrane regions are defined by the distinct lipid components, creating distinct functions, and polarity is further determined and regulated by a number of interacting protein complexes forming scaffolds, signalling complexes and trafficking systems (Figure 1.10).

**Table 1.6: Cell polarity and adhesion complex components**

	Complex	Components	Function
<b>Cell polarity complexes</b>	Scribble	SCRIB, DLG1 and LGL	Apical-Basal polarity
	Crumbs	CRB, PALS1 and PATJ	Apical plasma membrane establishment
	Par	PARD3, PAR6, CDC42 and aPKC	Apical-Lateral polarity
<b>Cell adhesion complexes</b>	Adherens junctions	Cadherins, catenins, nectins and afadins	Adherens junction
	Tight junctions	ZO-1, ZO-2, ZO-3, Occludin, Claudin and JAM	Tight junction

The Scribble complex was first identified in *Drosophila melanogaster* and consists of Scribble (SCRIB), Discs large (DLG1) and Lethal giant larvae (LGL1) proteins. In epithelial cells, the Scribble complex is located at the basolateral region and is required for membrane organisation and maintenance (Figure 1.10, (Woods *et al.*, 1996; Yates *et al.*, 2013; Humbert *et al.*, 2012). The Crumbs complex was also identified in *Drosophila*. The complex consists of Crumbs, Pals1 (Protein associated with Lin seven 1) and Pals1-associated tight junction (PATJ), also known as INADL) proteins (Figure 1.10 D). The partitioning defective (Par) complex was initially identified in *Caenorhabditis elegans*, and in humans consists of the proteins PARD3, PAR6 and an atypical protein kinase C (aPKC, Figure 1.10 D, (Kemphues *et al.*, 1988). The Par complex is localised to the apical region of epithelial cells and, together with Crumbs, regulates the maintenance of the apical membrane. The complexes do not exist in isolation; Par and Crumbs act in a mutually antagonistic fashion

with the Scribble complex (Bilder *et al.*, 2003). In the Par complex, aPKC negatively regulates LGL in the Scribble complex by phosphorylation, which prevents the protein's apical localisation (Betschinger *et al.*, 2003). Conversely, the kinase is required for the stabilization of the Crumbs complex, possibly *via* PAR6 binding or directly by phosphorylation of Crumbs proteins (Sotillos *et al.*, 2004).

Both the polarity and junctional complexes of epithelia involve proteins containing the PDZ (PSD/DLG/ZO) interaction domain, forming polarity complexes and defining the polarity required for epithelial functions.

### 1.5.2 The PDZ domain

PDZ domains are one of the most widely distributed protein-protein interaction domains; the human genome encodes over 320 PDZ-domain containing proteins (Fan and Zhang, 2002). The PDZ domain is an evolutionarily conserved domain of approximately 90 amino acids folded into six  $\beta$ -sheets and two  $\alpha$ -helices (Figure 1.11). A groove between the second  $\beta$ -strand and the second  $\alpha$ -helix forms a hydrophobic pocket that interacts with specific C-terminal sequence motifs of target proteins (Songyang *et al.*, 1997; Niethammer *et al.*, 1998). The structure of the PDZ domain does not change upon ligand binding; the PDZ binding motif (PBM) peptide serves as an extra  $\beta$ -strand and participates in the extensive hydrogen-bonding pattern with main chain PDZ domain residues (Doyle *et al.*, 1996). Crystal structures of PDZ domains in complex with peptides reveal that a loop at the end of the binding groove, which contains a conserved motif (R/K-X-X-X-G-L-G-F), is involved in positioning the target peptide within the binding groove (Figure 1.11). In the PBM:PDZ complex, the terminal COOH of the PBM is coordinated by a network of hydrogen bonds to main-chain amide groups in this loop (Tochio *et al.*, 1999; Daniels *et al.*, 1998a). When bound to the PDZ domain groove, the side chain of the terminal and -3

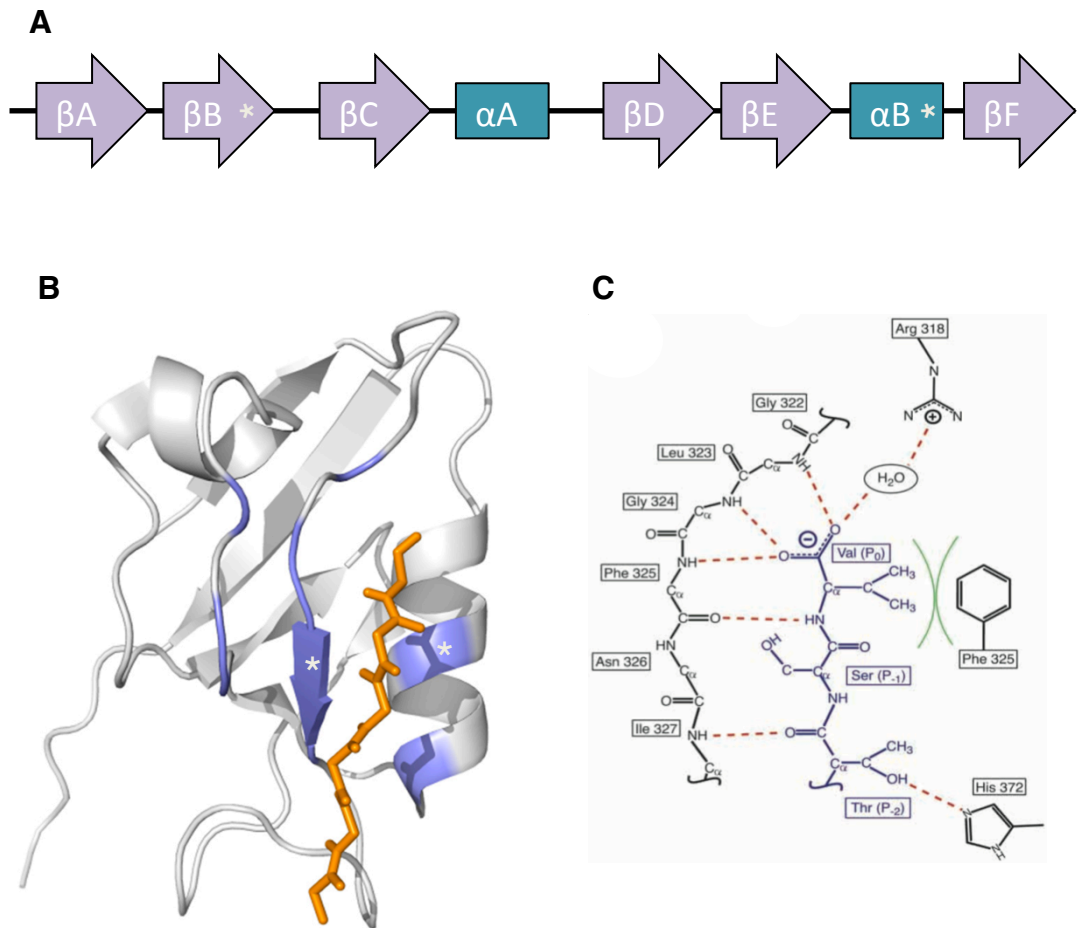


**Figure 1.11: The PDZ domain structure**

The secondary (A) and tertiary (B) protein structure of the PDZ domain. A groove between the second  $\beta$ -strand ( $\beta B$ ) and the second  $\alpha$ -helix (indicated with \*) forms a hydrophobic pocket that interacts with specific target proteins. The ten core domain binding sites are highlighted in blue and the bound peptide (orange). A schematic of the bond formation between residues in the PDZ binding groove and peptide is shown in C. Residues in the binding pocket are shown in black and the peptide is shown in blue. Hydrogen bonds are indicated by red dotted lines, and hydrophobic packing is indicated by green arcs. Adapted from Subbaiah *et al.* 2011, Hui *et al.* 2013 and Harris and Lim, 2001.

residues of the PBM peptide point towards the base of the peptide-binding groove. As such, interactions with these residues provide much of the PBM binding specificity (Songyang *et al.*, 1997; Doyle *et al.*, 1996). For example, the preference of the first PDZ domain of NHERF1 for a C-terminal PBM leucine is attributed to its large hydrophobic pocket (Karthikeyan *et al.*, 2001). In some cases, recognition of the PBM involves residues outside of the four amino acid consensus motif, enabling specificity of interactions unique to individual PDZ domains (Niethammer *et al.*, 1998). In terms of PBM sequence, there are three classes, with different C-terminal consensus sequences (Table 1.7). Although PDZ domains are mainly known for their ability to bind to the short C-terminal peptides of their target proteins, they have also been shown to recognize internal sequences that form a beta hairpin fold, other PDZ domains, and membrane phospholipids (Zimmermann *et al.*, 2002; Zhang *et al.*, 2009; Wong *et al.*, 2003; Hillier *et al.*, 1999; Brenman *et al.*, 1998; Gee *et al.*, 1998; Penkert *et al.*, 2004). Lipid binding further enables PDZ proteins to locate to specific membrane domains lipid rafts. For example, Syntenin-1 binding to phosphoinositide containing lipids localises the PDZ protein to the cell membrane and phosphatase and tensin homologue (PTEN) binding to membrane lipids aids the clustering of the Par complex proteins to cell membrane junctions (Feng *et al.*, 2008).

**Table 1.7: Classes of PDZ-binding motif**

Class	Consensus	Position	Example
<b>Class I</b>	X- <sup>S</sup> /T-X- <sup>L</sup> /V	C-terminal	DLG4 binding shaker type K <sup>+</sup> channel (Kim <i>et al.</i> , 1995)
<b>Class II</b>	X-Y-X- <sup>V</sup> /Y	C-terminal	CASK binding Neurexin (Songyang <i>et al.</i> , 1997)
<b>Class III</b>	X-X-C	C-terminal	SITAC binding L6 antigen (Borrell-Pagès <i>et al.</i> , 2000)

Adapted from Harris and Lim, 2001.

As a protein-protein interaction module, PDZ-domain containing proteins often comprise more than one PDZ domain and/or more than one type of interaction module (Figure 1.12). DLG1 encodes three PDZ domains alongside an SH3, L27 and GUK domains, all

of which are involved in protein-protein interactions and, by contrast, MUPP1 consists solely of 13 PDZ domains (Figure 1.12). The presence of modular domains within a single protein allows PDZ proteins to form interactions with many partner proteins simultaneously and act as a scaffold; organising large protein complexes at specific sub-cellular locations (Giallourakis *et al.*, 2006).

Cell-cell junction complexes comprise a number of PDZ domain containing proteins (Figure 1.10). These proteins form complexes at the cell membrane and form interactions with junctional complexes in adjacent cells, providing integrity and connecting extracellular space to intracellular components, allowing communication *via* signalling between the two (Figure 1.10, Laura *et al.*, 2002; Balda and Anderson, 1993; Stucke *et al.*, 2007; Yates *et al.*, 2013). For example PATJ is essential for TJ formation, it is important for localisation of PARD3 to the junction complex, and also in localising PARD3 to the leading edge of migrating cells (Lemmers, 2002). The expression of PATJ in turn is regulated by fellow PDZ protein MUPP1, indicating the wide-ranging effects and diverse roles of PDZ domain containing proteins (Assémat *et al.*, 2013). PDZ domain containing proteins are also involved in the destination and recycling of target proteins; for example, DLG4 is crucial for endocytic recycling of NMDA receptors and  $\beta$ 2-adrenergic receptors at the synapse and in muscle cells, affecting the cells response to signals such as adrenaline (Lavezzari *et al.*, 2003; Xiang *et al.*, 2002). As well as acting at the cell membrane, PDZ-containing proteins have been implicated in targeting proteins to intracellular organelles and protein trafficking around the cell. The PDZ interactor with cellular kinase 1 (PICK1) protein targets PKC to mitochondria (Wang *et al.*, 2003), thus affecting the access of the kinase to target proteins and downstream signalling.

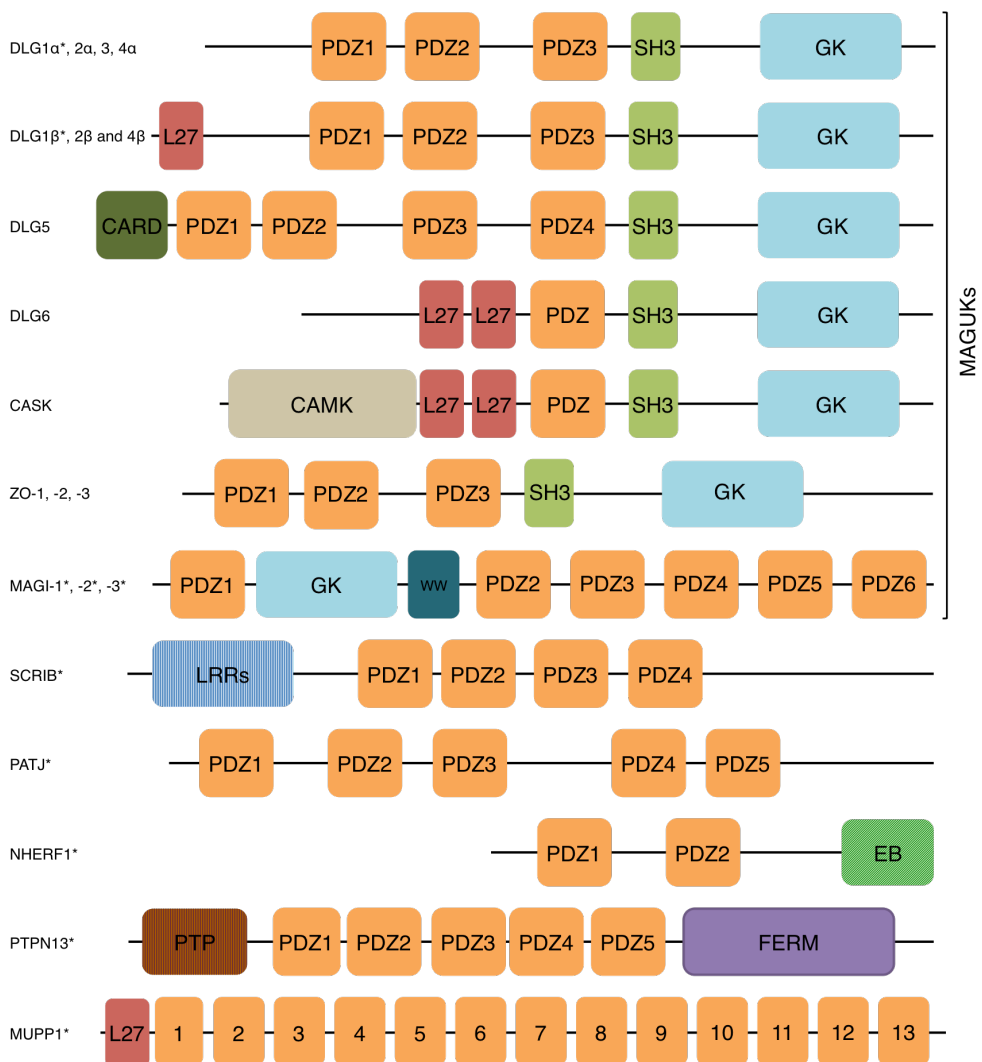


**Figure 1.12: PDZ domain containing protein domain structure**

Schematic to show the organization of several human PDZ domain containing proteins. MAGUK family proteins grouped at the top, contain an inactive guanylate kinase domain. Known PDZ targets of high-risk HPV E6 proteins are indicated by a star (\*).

SH3, Src Homology 3; PDZ, PSD/DLG/ZO; GK, Guanylate kinase; L27, Lin2-7; CARD, caspase activation and recruitment domain; CAMK, Ca<sup>2+</sup>/Calmodulin dependant protein kinase; ww, tryptophan fold; LRR, Leucine rich repeat; EB, Ezrin binding; PTP, Protein tyrosine phosphatase; FERM, 4.1/Ezrin/Radixin/Moesin.

Thus, there is a huge range and number of interactions that PDZ proteins can form and yet they are able direct interactions with many target proteins in a specific fashion, enabling PDZ domain containing proteins to perform roles in organizing multimeric signalling complexes, forming cell-cell interactions and organizing junctional complexes (Figure 1.10).

### 1.5.3 Alternative splicing

PDZ protein diversity is further extended *via* alternative processing of mRNA (Figure 1.13). Alternative splicing generates a variety of protein isoforms expressed from a single gene. Notable examples of PDZ protein splicing include the ErbB2 interacting protein (ERBIN), which has 7 known mRNA variants, including some with a truncated PDZ domain, and the Enigma homolog protein, which has more than 100 predicted variants (Yamazaki *et al.*, 2010; Favre *et al.*, 2001). Differential expression of spliced variants may depend upon cellular context; in the case of PDZ proteins, alternative splicing has been shown to generate isoforms specific to cell context and to developmental stages (Sierralta and Mendoza, 2004). Both MAGI-1 and MAGI-3 encode three spliced variants that differ in the C-terminal sequence and are expressed in a tissue specific fashion; two of the MAGI-1 isoforms are brain specific (Dobrosotskaya *et al.*, 1997; Hirao *et al.*, 2000; Laura *et al.*, 2002). Furthermore, expression of alternative exons not only defines tissue specificity variant, but also cellular localisation; in a cellular context one MAGI-1 isoform (MAGI-1c) is predominantly nuclear, whereas the other two are absent from the nucleus (MAGI-1a and b), when expressed exogenously (Laura *et al.*, 2002). Different spliced isoforms may have different roles or interacting partners in different tissues; whilst all of the PARD3 isoforms associate with tight junctions in epithelial cells, they are differentially expressed in epithelial and haematopoietic cells and have different binding affinities with other Par complex components, PAR6 and aPKC (Gao *et al.*, 2002; Zhou *et al.*, 2008).

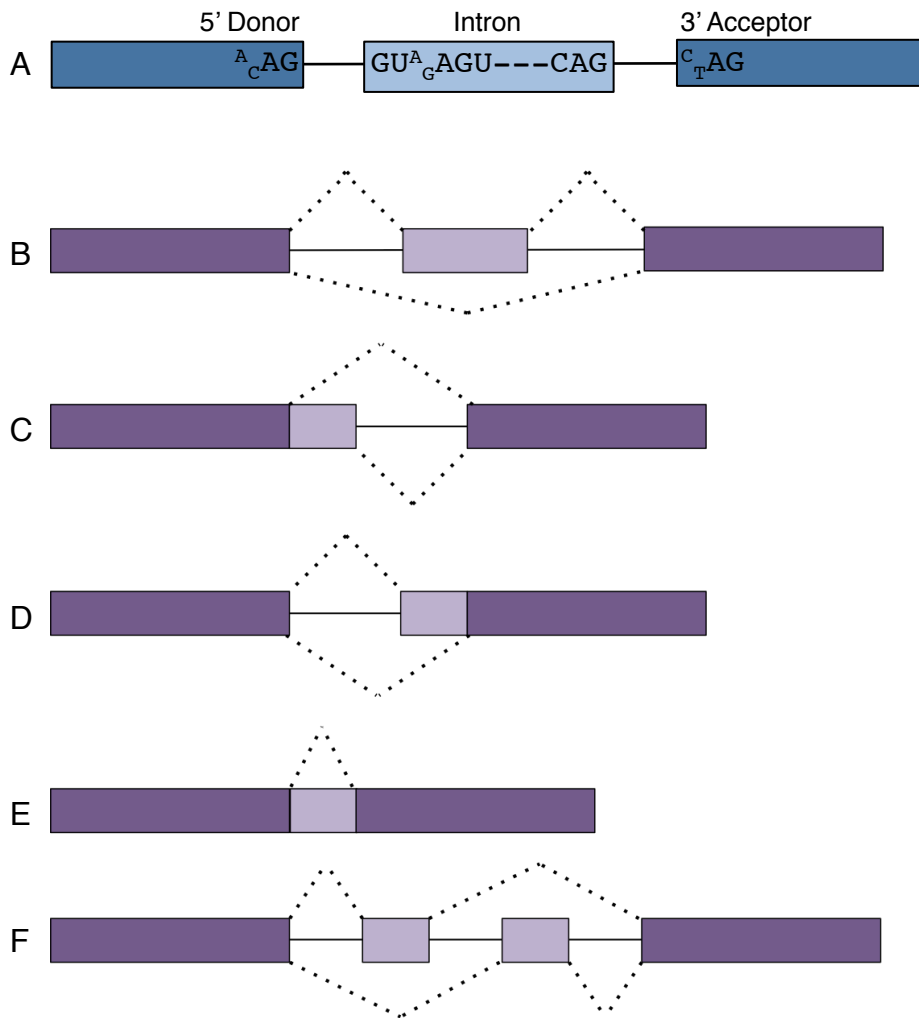


**Figure 1.13: Patterns of alternative splicing**

The inclusion or exclusion of exons can occur in many splicing patterns. Consensus splice site sequence (A) derived from Srebrow *et al.* 2006, Ghinga *et al.* 2008 and Harris and Senapathy, 1990. Solid rectangles represent exons, and dotted lines the pattern of inclusion. Intron retention (B), alternative 5' splice site selection (C), alternative 3' splice-site selection (D), cassette-exon inclusion or skipping (E) and mutually exclusive exon inclusion (F).

Deregulation of PDZ protein expression can lead to inappropriate isoform expression and promotion of carcinogenesis, for example spliced variants of DLG2 have been identified as transcriptionally upregulated in kidney cancer precursor growths (Zubakov *et al.*, 2006). With such diversity in form and function, PDZ domain containing proteins have significant oncogenic potential when deregulated at a transcriptional, translational or post-translational level. Alternative splicing of DLG1 will be discussed in more depth in Chapter 4.

#### 1.5.4 PDZ domain containing proteins in cancer

Epithelial cancers are characterized by epithelial-mesenchymal transition (EMT, Huber *et al.*, 2005). EMT is caused by a loss of ABP and cell–cell adhesion; cell-to-cell junctions become disrupted so that neighboring cells begin to dissociate from each other, no longer forming tight junctions or the interface that characterises their function (Moreno-Bueno *et al.*, 2008; Huber *et al.*, 2005). Since cell polarity is crucial for tissue integrity and homeostasis, it is logical that loss results in tissue disorganisation and facilitates both initiation and progression of cancer (Figure 1.14). Deregulation of epithelial polarity leads to abnormal cellular trafficking, signalling and migration, all of which contribute to the development of carcinomas and progression to an invasive phenotype (Tanos and Rodriguez-Boulan, 2008; Hanahan and Weinberg, 2011). As PDZ proteins have extensive roles in cell polarity and signalling, their deregulation has been implicated in a number of human diseases (Table 1.8).

In the Scribble complex, a reduction in DLG1 protein expression has been described in the later stages of a number epithelial cancers, including cervical and colon (Watson *et al.*, 2002; Cavatorta *et al.*, 2004; Lin *et al.*, 2004). Furthermore, mutations in the *DLG1* gene which are suggested to affect the binding of DLG1 to adenomatous polyposis coli (APC) and PTEN proteins, are associated with mammary carcinomas (Navarro *et al.*, 2005; Fuja *et al.*, 2004).

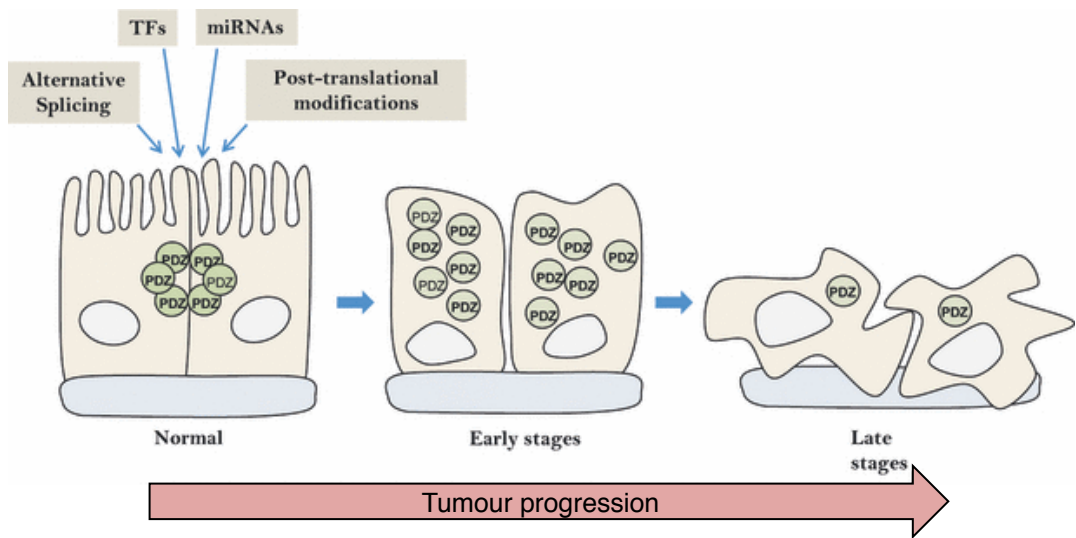


**Figure 1.14: Differential expression of PDZ proteins in tumour progression**

The localization and abundance of PDZ proteins is regulated in normal tissues by transcriptional, post-transcriptional and post-translational mechanisms. Several tumours exhibit mislocalisation of PDZ proteins, with gradual loss of the protein at cell–cell contacts, and increased protein in the cytoplasm during early stages of tumorigenesis. Downregulation of polarity proteins is usually associated with a more invasive phenotype, and late stages of carcinogenesis. The light blue area represents the basal membrane. TFs, transcription factors. From Facciuto *et al.* 2012.

**Table 1.8: PDZ proteins in human disease**

<b>PDZ Protein</b>	<b>Function</b>	<b>Disease associations</b>
DLG1 (SAP97)	Cell polarity, proliferation, migration and adhesion, cell division, synapse formation	Breast, cervical and colon cancers, schizophrenia, Chron's disease
DLG2 (PSD93)	Cell polarity, proliferation, synapse formation	Retinoblastoma
DLG3 (SAP102)	Cell polarity, proliferation, synapse formation	Schizophrenia
DLG4 (PSD95)	Receptor clustering	Schizophrenia, Alzheimer's, epilepsy
DLG5	Cell polarity, proliferation, invasion and migration, cell division	Breast and prostate cancer, Crohn's disease, inflammatory bowel disease
DLG6 (MPP4)	Cell polarity, proliferation, synapse formation	Retinopathies
PALS1 (MPP5)	Cell polarity, proliferation, synapse formation	Prostate cancer
SCRIB	Cell polarity and integrity, proliferation, apoptotic signalling	Breast, colon, endometrial and prostate cancers
PTPN13 (FAP-1)	Fas-associated phosphatase, cell growth signalling, apoptotic signalling	Pancreatic, ovarian and colon cancers, autoimmune thyroid disease
PARD3 (PAR3)	Cell polarity, asymmetrical cell division	Esophageal and breast cancers, glioblastomas
PAR6	Cell polarity, asymmetrical cell division	Breast cancer
CASK	Cell polarity and migration, synapse formation	Renal failure, cerebellar hypoplasia, idiopathic ataxia
ZO-1	Cell polarity and migration	Breast and liver cancer, kidney disease, cardiopathies
ZO-2	Cell polarity and migration	Breast cancer, kidney disease, Pancreatic adenocarcinoma
ZO-3	Cell polarity and migration	Kidney disease
MAGI-1	Cell polarity, synapse formation, apoptosis	Leukemia, hepatocellular carcinoma
MAGI-2	Cell polarity, synapse formation, apoptosis	Hepatocellular carcinoma
MAGI-3	Cell polarity, synapse formation, apoptosis	Hepatocellular carcinoma
MUPP1 (MPP1)	Cell polarity, proliferation	Retinopathies, inflammatory bowel disease
NHERF1	Regulation of GPCRs, cytoskeletal anchoring	Hypouricemia

Adapted from Facciuto *et al.*, 2012. Commonly used alternative protein names in brackets.

Similarly, loss of SCRIB has been demonstrated in breast carcinomas, and loss of MAGI-1 is observed in colon and liver carcinomas (Navarro *et al.*, 2005). In Madin-Darby canine kidney (MDCK) cells, expression of MAGI-1 suppresses cell invasion by recruiting PTEN to cell–cell contacts (Kotelevets *et al.*, 2005). In the Par complex, PAR6 has been shown to be overexpressed in breast cancer, and is thought to activate growth signalling cascades and promote cell proliferation independently of growth factor signalling (Aranda *et al.*, 2008; Nolan *et al.*, 2008). Downregulation of PARD3 has been implicated in oesophageal cancer, breast cancers and glioblastomas (Zen *et al.*, 2009; Tokes *et al.*, 2012; Rothenberg *et al.*, 2010), this is suggested to be due to the disassembly of the Par complex that occurs when PARD3 is decreased (Tokes *et al.*, 2012).

Furthermore, colon cancers exhibit a loss of the non-junctional PDZ protein PTPN13, whilst protein levels are increased in aggressive breast cancers (Wang *et al.*, 2004; Glondou-Lassis *et al.*, 2010). This apparent dissimilarity reiterates the fact that the role of PTPN13 (and indeed PDZ proteins) is cell context specific; often it is not clear whether to define PDZ proteins as an oncogene or a tumour suppressor, as their roles depend upon cellular localisation and tissue type (Roberts *et al.*, 2012). A change in abundance and localisation of PDZ proteins disturb the balance of protein function and has severe consequences, namely carcinogenesis.

#### 1.5.5 Virus interactions with PDZ domain containing proteins

A number of human viruses encode proteins containing PDZ-binding motifs (Table 1.9). Given that viral genomes are limited in size, the inclusion of a PBM indicates that the ability to interact with cellular PDZ proteins plays an important role in viral propagation. Computational screening has identified a C-terminal PBM in over 99% of Influenza A virus NS1 proteins (Obenauer *et al.*, 2006). The importance of this PBM to the virulence of

Influenza A was demonstrated by studies showing that deletion or masking of the motif attenuated the virus (Soubies *et al.*, 2010a; Cauthen *et al.*, 2007; Li *et al.*, 2006). Removal of the PBM decreases efficacy of influenza H1N1 virus transmission, as well as virus replication, and increases interferon expression in infected cells (Kim *et al.*, 2014; Soubies *et al.*, 2013; Thomas *et al.*, 2011). Moreover, switching the PBM for the sequence of an avian-specific strain increased virus virulence (Jackson *et al.*, 2008; Zielecki *et al.*, 2010). The NS1 PBM of the human strain H5N1 has been shown to interact with the PDZ domains of MAGI-1, MAGI-2, MAGI-3, DLG1 and SCRIB (Golebiewski *et al.*, 2011; Liu *et al.*, 2010). Despite the homology of the MAGI proteins, the strength of NS1 binding to each is not equal, indicating that viral PBM interactions are highly specific, and are determined by both the PDZ domain and the PBM sequences (Liu *et al.*, 2010; Thomas *et al.*, 2011). The swine-specific strain H6N6 NS1 alters the subcellular localisation of polarity regulator MAGI-1 and H5N1 NS1 colocalises with DLG1 and SCRIB, disrupts cellular tight junctions and produces a similar phenotype to cells in which DLG1 and SCRIB have been knocked down (Golebiewski *et al.*, 2011). It has been suggested that such disruption of cell junctions may benefit viral dissemination within the host, and/or spread to other hosts (Golebiewski *et al.*, 2011; Liu *et al.*, 2010). Furthermore, targeting SCRIB abrogates the pro-apoptotic function of the protein and may therefore protect infected cells from viral induction of apoptotic pathways, thus supporting viral propagation (Liu *et al.*, 2010; Thomas *et al.*, 2011). The PBM has also been suggested to aid viral immune evasion, by downregulating the cellular interferon response (Soubies *et al.*, 2010b; 2013; Kumar *et al.*, 2012).

Propagation of the RNA viruses tick borne encephalitis virus (TBEV) and dengue virus (DV) is dependent upon two virally-encoded PBMs within the NS5 proteins; mutations in the PBM negatively affect viral replication (Melik *et al.*, 2012; Ellencrona *et al.*, 2009). Interestingly, both viruses target the PDZ protein ZO-1, but *via* different approaches;

where TBEV NS5 is stabilised at the cell membrane by the interaction, DV NS5 colocalises with ZO-1 in the nucleus (Ellencrona *et al.*, 2009). The viruses have also been shown to interact with IL-16, a chemotactic cytokine which contains a PDZ domain (Werme *et al.*, 2008). A number of PDZ proteins have been identified as able to interact with TBEV NS5 protein with varying affinities; the viral factor binds strongly to ZO-2, and less strongly to TIP2, CASK (calcium/calmodulin-dependent serine protein kinase) and GRIP2 (glutamate receptor interacting protein 2, Werme *et al.*, 2008). Furthermore, TBEV NS5 has a high affinity for SCRIB, an interaction which has been suggested to be important in viral protein localisation and in preventing the host anti-viral interferon response, *via* the JAK-STAT pathway (Werme *et al.*, 2008).

Expression of the core protein of fellow flavivirus hepatitis C virus (HCV) leads to a decrease in DLG1 protein and mislocalisation of SCRIB from cell-cell contacts in liver and kidney epithelial cells (Awad *et al.*, 2013). A redistribution of PDZ proteins E-cadherin, claudin and ZO-1 has also been observed in HCV infected cells, which leads to disruption of cell polarity and aids the cell-cell transmission of virus (Mee *et al.*, 2010).

Interaction with cellular PDZ-domain containing proteins has been reported to promote the entry of human immunodeficiency virus 1 (HIV-1); knockdown of the cytoskeletal protein PDZD8 inhibits HIV-1 infection and negatively affects viral capsid stability (Henning *et al.*, 2010; Guth and Sodroski, 2014). The PDZ protein Syntenin-1 has been implicated in HIV-1 entry; Gordón-Alonso *et al.* (2012) suggest that the PDZ protein is recruited to the membrane by HIV-1 protein Env and clusters HIV-1 entry receptors on the cell membrane. Furthermore, overexpression of PDZD8 enhances infection by HIV-1 and related retroviruses murine leukemia virus (MLV), simian immunodeficiency virus (SIV, Henning *et al.*, 2011; 2010). HIV also acts upon the tight junction proteins ZO1,

occludin and claudin, disrupting their localisation and epithelial integrity, as well as downregulating their expression at a transcriptional level (Nazli *et al.*, 2010).

Rhinovirus also appears to affect tight junction proteins at a transcriptional level; ZO-1, claudin, occludin and E-cadherin gene expression is decreased by rhinovirus in cultured epithelia (Yeo and Jang, 2010). This may be the cause of the loss of ZO-1 from tight junctions observed in Rhinovirus infected cells (Sajjan *et al.*, 2008). It is not yet clear which viral factors are responsible for this, but it is suggested that the function promotes viral transmission (Yeo and Jang, 2010). Similarly, the consequences of PDZ binding during the infectious cycle of Hepatitis B virus (HBV) have yet to be fully characterized, although it has been suggested that PTPN3 suppresses the expression of viral genes and HBV core protein has been shown to interact with TIP-2 (Razanskas and Sasnauskas, 2010).

SARS coronavirus E protein interacts with Crumbs complex protein PALS1 and Syntenin-1 (Teoh *et al.*, 2010; Jimenez-Guardeño *et al.*, 2014). The former interaction has been shown to effect epithelial polarity and tight junction formation (Teoh *et al.*, 2010). SARS E protein is crucial to viral virulence and the PBM is a determinant of virus pathogenicity; deletion of the PBM had no effect on viral growth in cell culture but attenuated viral infection of mice, where less lung damage and no mortality occurred in mice infected with a PBM-deletion virus compared to wild-type virus (Jimenez-Guardeño *et al.*, 2014; DeDiego *et al.*, 2007; 2008).

Rabies pathogenicity is associated with the ability of the envelope G protein to interact with PDZ proteins PTEN, PTPN4 and MAST2 (Prehaud *et al.*, 2010; Terrien *et al.*, 2012). Both attenuated and virulent strains of Rabies exhibit an affinity for PDZ proteins, but it has been suggested that virulence is not associated solely with the ability to bind PDZ proteins generally, but rather the ability to bind and target proteins specifically (Prehaud *et al.*, 2010).

Intriguingly, the F11 protein of vaccinia virus encodes both a C-terminal PBM and a central PDZ-like domain (Handa *et al.*, 2013). Removal of the PBM results in the production of less infectious virus, and the PDZ domain has been shown to act as a scaffold protein and enhance viral spread (Handa *et al.*, 2013).

**Table 1.9: Virus interactions with PDZ proteins**

Virus/viral protein	Interacting PDZ protein	Reference
Adenovirus E4ORF1	DLG1, MAGI-1, MUPP1, ZO-2 Tight junction disruption, loss of cell polarity	Glaunsinger <i>et al.</i> , 2000; Lee <i>et al.</i> , 1997
Influenza A NS1	Interactions with DLG1, SCRIB, MAGI-1, -2, -3 and PDLIM2 Mislocalisation of ZO-1	Golebiewski <i>et al.</i> , 2011; Liu <i>et al.</i> , 2010
Rotavirus NSP4 VP8	Localisation of ZO-1 disrupted TJ formation blocked	Tafazoli <i>et al.</i> , 2001; Nava <i>et al.</i> , 2004
Hepatitis B core protein	TIP-2	Razanskas and Sasnauskas, 2010
SARS coronavirus envelope protein E	PALS1, Syntenin-1	Jimenez-Guardeño <i>et al.</i> , 2014; Teoh <i>et al.</i> , 2010)
Rhinovirus	ZO-1 and E-cadherin mRNA and protein downregulation	Yeo and Jang, 2010; Sajjan <i>et al.</i> , 2008
Tick borne encephalitis virus NS5	SCRIB, TIP2, CASK, ZO-1	Melik <i>et al.</i> , 2012; Werme <i>et al.</i> , 2008; Ellenrona <i>et al.</i> , 2009)
HTLV-1 Tax	DLG1 and MAGI-3 mislocalisation, pro-IL16	Suzuki <i>et al.</i> , 1999; Rousset <i>et al.</i> , 1998; Wilson <i>et al.</i> , 2003; Ohashi <i>et al.</i> , 2004
*High-risk $\alpha$ -HPV E6	DLG1, SCRIB, MAGI-1, -2, -3, PTPN13, NHERF1, etc.	Kiyono <i>et al.</i> , 1997; Kranjec and Banks, 2011; Thomas <i>et al.</i> , 2002; Spanos <i>et al.</i> , 2008b; Accardi <i>et al.</i> , 2011; Nakagawa and Huibregtse, 2000
rhPV1 E7	PARD3	Tomaic <i>et al.</i> , 2009
CRPV	DLG1	Du <i>et al.</i> , 2005
HIV-1 gp120	Inhibit localisation of ZO-1, occludin and claudin to TJs	Nazli <i>et al.</i> , 2010
Rabies G protein	DLG1, PTPN13, MUPP1	Prehaud <i>et al.</i> , 2010

Adapted from Banks *et al.*, 2012; Javier, 2008. \*A comprehensive list of PDZ targets of HPV E6 is shown in Table 1.10.

A number of human viruses encode PBMs, which have been implicated in viral entry, propagation and immune evasion. They appear to do so *via* common PDZ targets proteins,

namely DLG1, SCRIB and MAGI-1, -2 and -3, which is highly suggestive of the important roles that these proteins play in cellular polarity, proliferation, immune evasion and apoptosis, the interruption of which are fundamental in viral replication.

#### 1.5.6 PDZ domain containing proteins in viral oncogenesis

The oncogenic viruses HTLV-1 and adenovirus 9, as well as tumourigenic papillomaviruses rhPV1 (rhesus papillomavirus), CRPV (cottontail rabbit papillomavirus) and HPVs have also been shown to affect PDZ domain containing proteins, and this function has been linked to the oncogenic potential of the virus as well as their infectious cycles (Figure 1.15, Weiss *et al.*, 1997; Rousset *et al.*, 1998).

##### 1.5.6.1 HTLV-1 Tax

Mutational studies have demonstrated the importance of the Tax PBM in viral persistence and to the induction of proliferation in infected cells (Xie *et al.*, 2006). These studies also revealed the PBM is not essential to HTLV-1 mediated immortalisation, although its presence enhances the ability of HTLV-1 to transform rodent cells and enables Tax to transform mouse lymphocytes in cooperation with NFκB (Hirata *et al.*, 2004; Xie *et al.*, 2006). In human cells, the Tax PBM is also required for Tax-induced proliferation of T-cells (Xie *et al.*, 2006; Higuchi *et al.*, 2007). *In vitro* assays show that the protein kinase CK2 phosphorylates Tax within the PBM, at threonine 351, suggesting that phosphorylation of the PBM can regulate viral protein binding to PDZ proteins (Bidoia *et al.*, 2010).

Yeast two-hybrid screening experiments identified a number of PDZ domain containing Tax-interacting proteins, including DLG4, TIP-1, TIP-2 and PAR6 (Rousset *et al.*, 1998). Additionally, in cell culture, overexpressed Tax was shown to interact with MAGI-3 whereas the PBM mutant protein did not (Ohashi *et al.*, 2004). The interaction results in altered localisation of the viral protein from the nucleus to the cytoplasm and increased

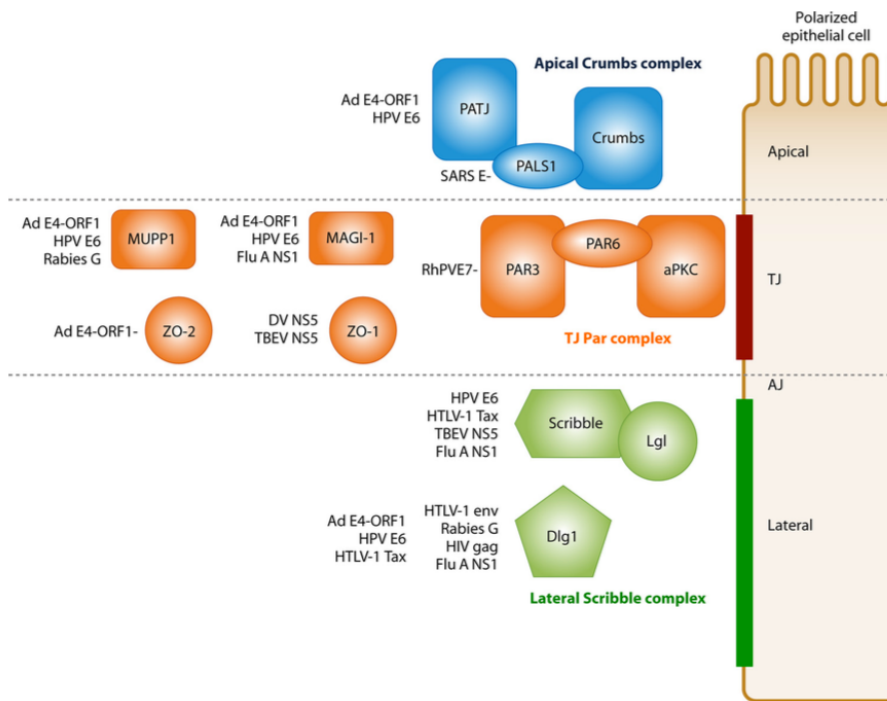


**Figure 1.15: Viral proteins target common cellular PDZ proteins**

A number of PDZ proteins involved in the formation and maintenance of cell polarity are commonly targeted by viruses. The oncoproteins Tax, E4ORF1 and E6, from oncogenic viruses HTLV-1, adenovirus and HPV respectively, specifically target a number of PDZ substrates.

From Javier and Rice, 2011.

Flu A, influenza A virus; AJ, adherens junction; TJ, tight junction

Tax stability (Ohashi *et al.*, 2004). MAGI-3 is involved in cell polarity and in cell survival signalling; the ability of Tax to target such pathways is suggested to promote viral replication, as well as promoting aberrant growth and transformation of infected cells (Ohashi *et al.*, 2004). Tax was also identified as interacting with PDZ domain containing protein Erbin during screening experiments (Ress and Moelling, 2006). This interaction was confirmed by immunoprecipitation of endogenous Erbin in epithelial cells with Tax protein encoding an intact PBM, but not when the PBM was absent (Song *et al.*, 2009). The first PDZ domain of the T-cell specific interleukin-16 precursor (Pro-IL16) binds to the Tax PBM in both human T-cells and immortalized monkey fibroblasts, where both proteins colocalise in the nucleus (Wilson *et al.*, 2003). The presence of an intact PBM enables Tax-expressing cells to overcome pro IL-16-driven cell cycle arrest, suggesting a role for the interaction in overcoming the growth inhibitory activity of pro IL-16 and promoting cell cycle progression (Wilson *et al.*, 2003). Such progression is favourable for viral propagation and is likely to contribute to the overproliferative phenotype of transformed cells.

The first target of HTLV-1 Tax to be identified was DLG1 (Lee *et al.*, 1997). Expression of wild-type but not PBM-mutant Tax protein hampers DLG1 inhibition of S phase progression in mouse fibroblasts (Suzuki *et al.*, 1999). Furthermore, Tax causes a redistribution in DLG1 protein from the soluble to the insoluble compartment of T-cells in a PBM dependent manner (Hirata *et al.*, 2004). Sequestering of DLG1 has been suggested to be a mechanism of DLG1 inactivation by Tax (Tsubata *et al.*, 2005; Ishioka *et al.*, 2006). However, depletion of DLG1 does not complement transformation in the absence of the Tax PBM, although it does augment transformation by wild-type virus, altogether suggesting that HTLV-1 transformation does not depend on the Tax PBM binding and inactivating DLG1 (Tsubata *et al.*, 2005; Ishioka *et al.*, 2006). Yeast two-hybrid

screening experiments revealed that HTLV-1 Tax binds to fellow Scribble complex member SCRIB (Arpin-Andre and Mesnard, 2007). This interaction was confirmed *in vivo* by the detection of a Tax and SCRIB complex in infected human T-cells, where Tax caused SCRIB mislocalisation (Aoyagi *et al.*, 2010). Both DLG1 and SCRIB block T-cell receptor (TCR)-induced activation *via* NFAT a key regulator of T-cell activation and differentiation (Round *et al.*, 2007b; Xavier *et al.*, 2004). In wild-type Tax expressing T-cells, this activity of SCRIB was inhibited, whereas inhibition still occurred when the Tax PBM was mutated (Arpin-Andre and Mesnard, 2007). DLG1 is important in the formation and organisation of the immunological synapse (Cullinan *et al.*, 2002). HTLV-1 infected T-cells fail to establish proper apical-basal polarity (Barnard *et al.*, 2005). Together, this suggests that the interaction between Tax and DLG1 or SCRIB disrupts T-cell polarity, migration, and signalling as well as immune synapse formation, resulting in the stimulation of cell proliferation and prohibition of immune activation by the virus, thus aiding HTLV-1 persistence (Ludford-Menting *et al.*, 2005; Rebeaud *et al.*, 2007; Rincon and Davis, 2007; Round *et al.*, 2005; 2007b).

Interestingly, the association between the Tax oncoprotein and the PDZ domain containing ubiquitin E3 ligase PDLIM2 does not occur between the viral PBM and the PDLIM2 PDZ domain (Fu *et al.*, 2010). Instead, Tax binds to PDLIM2 *via* multiple regions in Tax and an  $\alpha$ -helical motif in PDLIM2, unlike the multiple PDZ targets which have been identified to interact *via* the PBM of the viral protein (Fu *et al.*, 2010). The interaction causes transport of the viral protein to the nucleus and subsequent proteasome-mediated degradation, thereby suppressing Tax's transforming activity (Yan *et al.*, 2009b).

### 1.5.6.2 Adenovirus E4ORF

Adenovirus type 9 causes benign eye infections in humans, but is capable of causing mammary tumours in rats in the presence of high levels of oestrogen and of transforming cells in culture (Graham *et al.*, 1984; Horwitz, 2001). Adenovirus 9-induced transformation is driven by the viral factor E4ORF1 and, more specifically, the PBM at the C-terminus of E4ORF1 has been shown to be crucial in this oncogenesis (Weiss and Javier, 1997). Furthermore, expression of the E4ORF1 causes tight junction defects in epithelial cells in a PBM-dependent manner, but does not affect the structure of adherens junctions (Latorre *et al.*, 2005).

DLG1 was the first identified target of E4ORF1, shown to interact *via* PDZ domains 1 and 2 (Lee *et al.*, 1997). Subsequently, it was demonstrated that E4ORF1 was able to bind to the cellular PDZ proteins MUPP1, PATJ, MAGI-1, and ZO-2 (Glaunsinger *et al.*, 2000; Lee *et al.*, 2000; Latorre *et al.*, 2005; Glaunsinger *et al.*, 2001). Interestingly, there are differences in PDZ protein binding between the monomeric and trimeric forms of the E4ORF1 protein; where monomeric E4ORF1 interacts with MAGI-1, PATJ, MUPP1 and ZO-2, the trimer only binds to DLG1 (Chung *et al.*, 2008). E4ORF1 expression causes the sequestering of MUPP1, PATJ, MAGI-1, and ZO-2 away from tight junctions into cytoplasmic membrane vesicles, disrupting cell adhesion and polarity (Glaunsinger *et al.*, 2000; Lee *et al.*, 2000; Glaunsinger *et al.*, 2001; Latorre *et al.*, 2005). E4ORF1 trimers promote DLG1 translocation to the plasma membrane, which may contribute to the junctional defects observed in adenovirus infected cells (Laprise *et al.*, 2004; Stucke *et al.*, 2007). However, E4ORF1 monomers exert a gain-of-function upon DLG1, as the interaction constitutively activates the PI3K signalling pathway *via* the PDZ protein (Frese *et al.*, 2003). The association of the E4ORF1 with DLG1 facilitates adenovirus activation of the phosphatidylinositol 3-kinase (PI3K) signalling cascade *via* oncogene RAS, which

culminates in an increase in cellular metabolism and thus increases cellular substrates available for viral replication (Kong *et al.*, 2014; Frese *et al.*, 2006; Kumar *et al.*, 2014). This interaction also induces anchorage independent growth (AIG), a characteristic of transformed cells (Frese *et al.*, 2003; 2006).

It has been suggested that both Tax and E4ORF interfere with the interaction between DLG1 and the cellular tumor suppressor adenomatous polyposis coli protein (APC) by competing for binding to the same PDZ domain (Javier and Rice, 2011; Frese *et al.*, 2006). The APC:DLG1 interaction has growth-inhibitory consequences; viral protein binding DLG1 would prevent APC binding and thus lead to an increase in cell proliferation, due to increased growth promoting signalling (Ishidate *et al.*, 2000; Matsumine *et al.*, 1996; Javier, 2008).

#### 1.5.6.3 Papillomavirus oncoproteins

Both animal and human PVs are able to target PDZ proteins. The E6 protein of CRPV has also been shown to interact with cellular DLG1, underlining a commonality in viral PDZ protein targeting (Du *et al.*, 2005). Although expression of CRPV E6 is able to immortalise rabbit keratinocytes, the protein does not bind cellular p53 (Muench *et al.*, 2010). Furthermore, CRPV is able to induce skin cancer in rabbits without additional co-factors (Ganzenmueller *et al.*, 2008; Jeckel *et al.*, 2002; Muench *et al.*, 2010). Together this suggests that DLG1 binding may contribute to CRPV E6 mediated immortalization, in the absence of this tumorigenic interaction.

Interestingly, the oncogenic rhesus papillomavirus type 1 (RhPV1) E7 oncoprotein, but not the E6 protein, contains a C-terminal PBM, *via* which it interacts with the polarity protein PARD3 (Tomaic *et al.*, 2009). RhPV1 drives mucosal neoplasia in rhesus macaques, in an

analogous fashion to high-risk HPVs, again indicating a potential carcinogenic role for the E6 PBM.

The  $\beta$ -papillomaviruses do not encode an E6 PBM, but do encode a conserved C-terminal hydrophobic motif (YXDW). In HPV5, this motif interacts with the adhesion protein  $\beta_1$ -integrin and disrupts normal signalling (Du *et al.*, 2005). Furthermore, the  $\beta$ -papillomavirus HPV8 encodes an alternative mechanism to regulate the PDZ protein Syntenin-2 by influencing transcription (Lazic *et al.*, 2012). Both HPV5 and HPV8 are associated with the development of skin cancer, and a level of control over adhesion proteins may be important to the cancer-causing capability of viruses as well as functioning during normal papillomavirus life cycle.

The commonality in viral PDZ targets further highlights oncogenic potential of the proteins as well as their importance in cellular proliferation (Figure 1.15). Viral PBMs function to promote a favourable cellular environment for viral replication, but are also important in driving oncogenesis. By activating cellular proliferation and anti-apoptotic pathways, PBMs contribute to transformation of infected cells which, when combined with additional mutations and carcinogenic environmental influences, can lead to cancerous growth.

#### 1.6 High-risk HPV E6 and cellular PDZ proteins

Like Tax and E4ORF1, the E6 oncoproteins of high-risk HPVs encode a C-terminal PBM (Figure 1.16). To date, more than 15 PDZ domain containing proteins have been shown to interact with high-risk HPV E6 oncoproteins. The proteins identified encompass a variety of roles in cell polarity, tissue integrity, scaffold formation, signalling and intracellular trafficking (Table 1.10). The biological consequences of HPV E6 PBM binding PDZ

proteins are varied, and have been investigated in cell-based models of papillomavirus oncogenesis and life cycle.

#### 1.6.1 The E6 PBM in viral life cycle

The E6 protein functions to decouple keratinocyte differentiation from proliferation (Section 1.4.1.2). The interaction of the E6 PBM with a subset of cellular PDZ proteins is influential in the life cycle of high-risk HPVs, where E6 is expressed at physiological levels. The motif may contribute to the overall function of E6 by promoting disruption of cell polarity and enabling proliferation in cells that would otherwise differentiate.

Studies in mice have revealed that the E6 PBM promotes DNA replication; in mouse epithelia the interaction between E6 and PDZ proteins correlates with the induction of suprabasal DNA synthesis by the oncoprotein (Nguyen *et al.*, 2003). Deletion of the PBM in the context of whole HPV genomes has shown that the motif contributes to HPV-driven keratinocyte proliferation; where stratified cells containing HPV18 or HPV31 genomes exhibited a thicker spinous layer, PBM mutant genome containing cells exhibited a morphology that resembled normal keratinocytes (Lee and Laimins, 2004; Delury *et al.*, 2013). In addition, the HPV31 E6 PBM is necessary for the induction of keratinocyte proliferation in both undifferentiated and stratified cell culture and keratinocyte growth is lessened in cells containing a HPV18 E6 PBM mutant compared to cells containing the wild-type genome or to normal keratinocytes (Lee and Laimins, 2004; Delury *et al.*, 2013). Similarly, in both undifferentiated and stratified primary keratinocytes, Choi *et al.* (2013) demonstrated that the PBM of HPV16 E6 is required for the increased growth seen in cells expressing E6 as well as in cells containing both E6 and E7 oncoproteins.

Deletion within the context of the whole HPV genome affects the viral genome; the loss of the E6 PBM of HPV16, HPV18 and HPV31 reduces the capacity of the virus to maintain episomes (Nicolaidis *et al.*, 2011; Delury *et al.*, 2013; Lee and Laimins, 2004; Brimer and

Vande Pol, 2014). Indeed, the PBM is essential to viral propagation; its absence results in a lack of genome amplification and late protein expression (Delury *et al.*, 2013).

It has been suggested that removal of the PBM destabilizes the E6 protein; Nicolaides *et al.*, (2011) demonstrated an enhanced proteasomal degradation rate of HPV16 E6 in the absence of a PBM, as well as an increase in the levels of E6 protein when the PDZ target SCRIB was overexpressed. However, deletion of the HPV18 and HPV31 E6 PBM does not affect E6 stability in primary keratinocytes (Lee and Laimins, 2004; Delury *et al.*, 2013). Furthermore, phosphorylation of the E6 PBM has been implicated in E6 stability, suggesting a more complex interplay (Boon and Banks, 2012b).

The PBM has been implicated in protecting cells from TNF-induced apoptosis; HPV16 E6 activates nuclear factor kappa B (NF $\kappa$ B) in human airway epithelial cells and subsequently inhibits downstream apoptotic signalling in a PBM dependent manner (James *et al.*, 2006). A number of known PDZ targets of E6 have roles in apoptotic signalling, including PTPN13 and SCRIB, and it may be that these interactions have anti-apoptotic consequences, but it is likely that such activation also promotes epithelial proliferation and thus viral replication (Nakagawa and Huibregtse, 2000; Spanos *et al.*, 2008b; James *et al.*, 2006).

Thus there is evidence that the PBM function contributes to E6-mediated promotion of viral propagation. Such functions are also influential in the transformation of infected cells, under conditions where E6 is deregulated.

### 1.6.2 The E6 PBM in viral oncogenesis

The E6 PBM is found exclusively in the high-risk type HPVs (Figure 1.16), and in culture this PBM is required for E6-mediated transformation of rodent cells (Kiyono *et al.*, 1997; Spanos *et al.*, 2008a). In primary human tonsil keratinocytes (HTKs) containing HPV16,

		Consensus motif	
		$X^S_T X^L_V$	
<b>Group 1</b>			
HPV 16	CMSCC	RSSRTRRRE <b>ET</b> QL	
HPV 18	CHSCCNRARQE	RLQRRRRE <b>ET</b> QV	
HPV 31	CIVCW	RRPRTE <b>ET</b> QV	
HPV 33	CAACW	RS RRRE <b>ET</b> AL	
HPV 35	CMSCW	KPTRRE <b>ET</b> EV	
HPV 39	CRRCWTTKRED	RRLTRRE <b>ET</b> QV	
HPV 45	CNTCCDQARQE	RLRRRRRE <b>ET</b> QV	
HPV 51	CANCW Q	RTRQRN <b>AT</b> QV	
HPV 52	CSECW	RPRPV <b>ET</b> QV	
HPV 56	CLGCW RQ	TSREPRE <b>ST</b> V	
HPV 58	CAVCW	RPRRR <b>Q</b> TV	
HPV 59	CRGCRTRARHLRQQRQAR <b>SE</b> TV		
<b>Group 2A</b>			
HPV 68	CRHCWTSKRED	RRRTR <b>Q</b> ETQV	
<b>Group 2B</b>			
HPV 26	CTNCW	RPRR <b>Q</b> ETQV	
HPV 30	CLQCW	RHTT <b>ST</b> ETAV	
HPV 34	CRQCW	RPS <b>AT</b> TV	
HPV 53	CLTCW	RHTT <b>AT</b> ESAV	
HPV 66	CLQCW	RHTSR <b>Q</b> ATES <b>ST</b> V	
HPV 67	CSVCW	RP <b>Q</b> RT <b>Q</b> TV	
HPV 69	CTNCW	RPRRE <b>AT</b> ETQV	
HPV 70	CRHCWTSNRED	RRRIRRE <b>ET</b> QV	
HPV 73	CTRCW	RPS <b>AT</b> TV	
HPV 82	CANCRTAA	R <b>Q</b> R <b>SE</b> ETQV	
HPV 85	CRRCMTRA QE	QQGSRRRE <b>ET</b> QV	
HPV 97	CNSCYNQSRQE	RLSRRRE <b>ET</b> QV	
<b>Group 3</b>			
HPV 6	CLHCWTT <b>CM</b> ED	ML <b>P</b>	
HPV 11	CLHCWTT <b>CM</b> ED	LL <b>P</b>	
HPV 8	CR <b>LC</b> KHLYHDW		

**Figure 1.16: C-terminal alignment of high- and low-risk HPV E6 proteins**

E6 protein To date, twelve HPV types have been defined by the WHO as high-risk with respect to causing cancer - these are designated as IARC Group 1- and a further ten types are recognised as ‘possibly’ (Group 2A) and ‘probably’ cancer-causing (Group 2B). HPV6 and 11 are included as examples of low risk virus. HPV8 is associated cutaneous SCC, and has been shown to effect the transcription of PDZ protein Syntenin-2.

The canonical PBM sequence ( $X^S_T X^L_V$ ) is shown above the highlighted region, which indicates the E6 PBM sequence. Phospho acceptor sites within the PBM are highlighted in bold. Adapted from Delury *et al.* 2013.

PBM deletion depleted the efficiency of HPV-driven immortalisation of cells, and removed the ability of HPV16 E6 to induce AIG (Spanos *et al.*, 2008a). Similarly, the expression of HPV18 E6 in human keratinocytes led to disrupted cell-cell junctions and promotion of a fibroblast-like morphology, phenotypes which are characteristics of EMT and these were reduced when the PBM was deleted (Watson *et al.*, 2003).

As in cell culture, E6 is able to induce epithelial hyperplasia in transgenic mice independently of interactions with p53 (Song *et al.*, 2000; Kiyono *et al.*, 1997). In concordance with this, mouse models expressing HPV16 E6 under a keratin promoter have demonstrated that the PBM is key to the development of hyperplasia of the skin, the cervix and the eye, although the E6 PBM is not required for the immortalisation of other keratinocytes (Nguyen *et al.*, 2003; 2005; Shai *et al.*, 2010). Furthermore, murine studies have shown that the E6 PBM promoted greater invasive properties and tumour size, and that the cooperation of E6 and E7 in driving tumour growth was shown to be dependent upon the E6 PDZ binding function (Nguyen *et al.*, 2003; Simonson *et al.*, 2005).

A number of PDZ proteins have been identified to interact with the high-risk HPV E6 PBM (Table 1.10), and have been investigated in systems that resemble a cancer-like cellular environment, highlighting interactions that may be crucial in promoting the HPV life cycle.

### 1.6.3 PDZ targets of high-risk E6

As with other oncogenic viruses, the PDZ proteins DLG1 and SCRIB are common targets of both high-risk HPV types 16 and 18 (Kiyono *et al.*, 1997; Nakagawa and Huibregtse, 2000). Furthermore, the different HPV types display differing affinities for targets; despite the PBM differing by a single amino acid, HPV16 preferentially binds SCRIB over DLG1, and HPV18 DLG1 over SCRIB, these affinities can be altered within the context of whole E6 by switching the PBM sequences (Pim *et al.*, 2000; Thomas *et al.*, 2001). In addition,

DLG4 has been shown to be a stronger target for HPV18 than for HPV16, whilst GOPC was found to bind more strongly to HPV16 E6 than HPV18 (Handa *et al.*, 2007; Kranjec and Banks, 2011; Jeong *et al.*, 2007).

The binding of PDZ proteins themselves are formed in a select fashion; despite the presence of more than one PDZ domain per cellular protein, only one domain is thought to interact with E6. Specificity is determined by the sequence of the viral PBM, sequence upstream of the PBM and the target PDZ domain (Thomas *et al.*, 2001; 2002). The first two PDZ domains of DLG1 (PDZ1 and PDZ2) are important for HPV18 E6 binding (ETQV) and the threonine residue of the PBM is essential for the interaction; substitutions with either neutral or acidic residues abolishes binding and subsequent ubiquitin ligase recruitment (Gardioli *et al.*, 1999). Structural analysis confirmed this, and indicated that the arginine residues proximal to the PBM form additional contacts with PDZ2 to strengthen the interaction (Liu *et al.*, 2007). Similarly, the structure of MAGI-1 PDZ1 bound to HPV16 E6 confirmed that residues located inside and outside the binding groove contribute to binding, notably lysine 499 of the junctional protein is important in the specificity of the E6 interaction (Fournane *et al.*, 2011). E6 PDZ targeting is also specific to cellular location; in the case of DLG1 and MAGI-1, HPV18 E6 preferentially induces the degradation of the cytoplasmic and nuclear forms (Massimi *et al.*, 2004; Kranjec and Banks, 2011; Narayan *et al.*, 2009).

Although hundreds of PDZ domains exist in a human keratinocyte, HPV E6 has been shown to associate with seventeen (Table 1.10). Recent screening studies have identified an additional number of PDZ targets which have yet to be confirmed *in vivo* (Belotti *et al.*, 2013). The identified targets of the E6 PBM comprise a range of cellular proteins involved in epithelial cell polarity, tissue integrity and proliferation (Table 1.10). PDZ targets of E6 have been identified from the Scribble, Par and Crumbs polarity complexes (Figure 1.15),

as have a number of cellular PDZ proteins involved in cell signalling. Specific E6 PDZ targets are discussed in more detail in Chapter 3.

#### 1.6.3.1 Kinase recognition of HPV E6 PBM

The PBM of high-risk HPV types lies in close proximity to a canonical serine/threonine-specific kinase recognition site (Figure 1.16). X-ray crystal structures predict that phosphorylation of the PBM would sterically hinder the ability of E6 to fit within the PDZ binding groove (Ainsworth *et al.*, 2008; Charbonnier *et al.*, 2011; Liu *et al.*, 2007). *In vitro* experiments have shown that HPV18 E6 PBM phosphorylation reduces DLG1 binding and activation of the PKA pathway in cell culture decreases degradation of DLG1 by E6, which suggests that phosphorylation of the PBM negatively affects E6 PDZ binding ability (Kühne *et al.*, 2000). Furthermore, *in vitro* protein kinase A (PKA) phosphorylates the E6 PBM of high-risk HPV types 16 and 18, and a site proximal to the PBM of HPV31 (Boon *et al.*, 2014). Moreover, different E6 proteins exhibit different susceptibilities to phosphorylation. HPV18 E6 shows a higher susceptibility to PKA phosphorylation than HPV16, and HPV31 is only weakly phosphorylated by PKA (Kühne *et al.*, 2000; Boon *et al.*, 2014). The kinase AKT (also known as protein kinase B, PKB) is a serine/threonine kinase family member which has been also shown to act upon both HPV16, 58 and 31 E6 PBMs *in vitro* (Boon *et al.*, 2014). It is therefore likely that other kinases recognize these sites, and perhaps recognize certain E6 PBMs better than others.

Investigations by the Roberts lab have indicated that E6 PBM phosphorylation may function to regulate interactions with PDZ proteins during the virus life cycle (Delury *et al.*, 2013). By reversibly interrupting PDZ binding, it is hypothesized that phosphorylation may provide a mechanism of regulating PDZ-PBM interactions during the viral life cycle and during epithelial differentiation. In addition to interrupting PDZ interactions,

phosphorylation has been shown to introduce a novel interaction; phosphorylation of the HPV18 E6 PBM facilitates binding of the phospho-tyrosine binding scaffold protein 14-3-3 $\zeta$  (Boon and Banks, 2012b). This indicates that E6 PBM function depends on the phosphorylation status, mediating interactions with either PDZ domain containing substrates or 14-3-3 family members.

Table 1.10: PDZ targets of high-risk HPV E6 proteins

PDZ protein (Gene Symbol)	Alternative Name(s)	Cellular Functions	Effect of Interaction with E6	References
<u>DLG1</u>	SAP97	Cell polarity, cell proliferation, migration and adhesion	Degradation, mislocalisation	Kiyono <i>et al.</i> , 1997 Gardiol <i>et al.</i> , 1999
<u>SCRIB</u>	Scribble, Vartul, LAP4	Cell polarity and integrity, proliferation, apoptotic signalling	Degradation	Nakagawa and Huibregtse, 2000
<u>INADL</u>	PATJ	Tight junction formation, cell polarity	Degradation E6* also able to target	Latorre <i>et al.</i> , 2005; Storrs and Silverstein, 2007
SLC9A3R1	<u>NHERF1</u> , EBP50	GPCR regulation, cytoskeleton anchoring	Degradation	Accardi <i>et al.</i> , 2011
<u>PTPN13</u>	FAP-1, PTPL-1, PTP-BAS, PTPBL	Fas-associated phosphatase, cell growth signalling, apoptotic signalling	Degradation	Spanos <i>et al.</i> , 2008b
MPDZ	<u>MUPP1</u>	Receptor clustering, scaffold protein	Degradation	Lee <i>et al.</i> , 2000
<u>MAGI-1</u>	AIP3, WWP3	Cell polarity, invasiveness, synapse formation, apoptosis	Degradation	Glaunsinger <i>et al.</i> , 2000
<u>MAGI-2</u>	AIP1	Cell polarity, invasiveness, synapse formation, apoptosis	Degradation	Thomas <i>et al.</i> , 2002
<u>MAGI-3</u>	-	Cell polarity, invasiveness, synapse formation, apoptosis	Degradation	Thomas <i>et al.</i> , 2002
<u>DLG4</u>	PSD95, SAP90, TIP15	Receptor clustering	Degradation	Handa <i>et al.</i> , 2007
<u>PTPN3</u>	PTPH1	Phosphatase, cell growth signalling, apoptotic signalling	Degradation	Jing <i>et al.</i> , 2007; Töpffer <i>et al.</i> , 2007
TAX1BP3	<u>TIP-1</u>	Wnt pathway inhibitor	-	Hampson <i>et al.</i> , 2004
GIPC1	Synectin, <u>TIP-2</u>	Cell surface receptor expression and trafficking, TGF $\beta$ signalling	Degradation	Favre-Bonvin <i>et al.</i> , 2005
<u>GOPC</u>	CAL	Intracellular trafficking	Degradation	Jeong <i>et al.</i> , 2007
<u>PARD3</u>	PAR3	Cell polarity, asymmetrical cell division	Mislocalisation	Facciuto <i>et al.</i> , 2014
SDCBP2	<u>Syntenin-2</u>	Cell adhesion, growth factor signalling	Decreased transcription	Lazic <i>et al.</i> , 2012
<u>PDZRN3</u>	LNx3	E3 ubiquitin ligase	Degradation	Thomas and Banks, 2014

E6\* is a truncated isoform of E6. Underlined symbols indicate nomenclature used in this thesis.

## 1.7 Hypothesis and Aims

The E6 PBM is a conserved feature of high-risk  $\alpha$ -HPV types and a number of cellular PDZ proteins have been identified as interacting with this motif. In many cases, the E6:PDZ interaction leads to proteasome-mediated degradation of the cellular protein. However, the effect of HPV genome replication upon PDZ protein expression has not been fully characterized. Moreover, the physiologically relevant targets and the consequences of the E6:PDZ interaction remains unclear. Furthermore, the PBM overlaps with a kinase recognition site, which may function to regulate PDZ interactions during the viral life cycle. Given the large number of cellular PDZ domain containing proteins and the specificity of PDZ:PBM binding, it is likely that E6 targets specific proteins at certain subcellular locations and at specific times during the HPV life cycle. Thus, this thesis aims to investigate PDZ protein expression in a primary keratinocyte model of the HPV life cycle.

1. To investigate PDZ domain containing protein expression during the life cycle of high-risk HPV types 16 and 18 (*Chapter 3*).

2. To characterize the expression of E6 PDZ target DLG1 in epithelia and during the HPV16 and 18 life cycles (*Chapter 4*).

3. To determine the effect of PKA phosphorylation upon the HPV18 E6 PDZ binding domain motif (*Chapter 5*).

## CHAPTER 2: MATERIALS AND METHODS

Unless otherwise stated, materials and chemicals were obtained from commercial sources (Section 2.5). For cell culture reagents and stock solution recipes, see Appendix III.

### 2.1 Cell culture

Media and solutions were prepared as described below, or purchased from indicated suppliers. All culture procedures were performed under sterile conditions in a Holton Laminair S2000 1.2 microbiological safety cabinet (Thermo Fisher Scientific, UK). Culture media components were filter sterilised using 0.22 µm hydrophilic polyvinylidene fluoride (PVDF) membrane filters. Cells were cultured in sterile dishes (BD Biosciences, UK) in the appropriate growth medium, and were incubated in a cell culture incubator at 37°C and with 5% CO<sub>2</sub> in air.

#### 2.1.1 Culture of cell lines

The cancer-derived cell lines HeLa, Caski, HEK293T, H1299 and SiHa were all cultured in Dulbecco's modified eagle medium (DMEM, Sigma-Aldrich, UK) supplemented with 4 mM L-glutamine (Gibco, UK) and either 10% v/v foetal bovine serum (FBS, Gibco) or foetal calf serum (FCS, Gibco, see Table 2.1). The HPV-negative cervical cancer cell line C33A was cultured in RPMI-1640 (Roswell Park Memorial Institute) medium (Sigma-Aldrich) supplemented with 10% v/v FCS and 4 mM L-glutamine (Gibco). The head and neck cancer derived cell lines Vu40T, Vu147, SCC040 and SCC154 were cultured in DMEM supplemented with 10% v/v FBS, 1% v/v penicillin streptomycin (PenStrep, Sigma-Aldrich) and 4 mM L-glutamine. Primary cervical epithelial cells, Cx129 were cultured in serum-free media (SFM, Sigma-Aldrich). For subculture, cells were first washed with 5 mL sterile phosphate-buffered saline (PBS, Sigma-Aldrich) and then incubated with

1 mL TrypLE (Life Technologies, UK) until cells were no longer adherent. The TrypLE was quenched with media and the entire suspension transferred to a sterile tube for centrifugation at  $10000 \times g$  for 5 min. The cell pellet was resuspended in the appropriate culture media, cells were counted and cells were seeded at the desired density into 10 cm dishes with 10 ml of warmed medium.

**Table 2.1: Cell lines**

<b>Cell Line</b>	<b>Tissue of origin</b>	<b>Media requirements</b>	<b>HPV status</b>
<b>HeLa</b>	Cervical adenocarcinoma	DMEM, 10% v/v FBS, 4mM L-glutamine	HPV18 integrated
<b>Caski</b>	Cervical carcinoma	DMEM, 10% v/v FCS, 4mM L-glutamine	HPV16 positive
<b>SiHa</b>	Cervical carcinoma	DMEM, 10% v/v FBS, 4mM L-glutamine	HPV16 positive
<b>SCC154</b>	Oropharyngeal SCC	DMEM, 10% v/v FBS, 4mM L-glutamine, 1% v/v PenStrep	Positive
<b>Vu147</b>	HNSCC	DMEM, 10% v/v FBS, 4mM L-glutamine, 1% v/v PenStrep	Positive
<b>H1299</b>	Lung carcinoma	DMEM, 10% v/v FCS, 4mM L-glutamine	Negative
<b>Cx129</b>	Primary cervical epithelia	SFM	Negative
<b>C33A</b>	HPV negative cervical epithelia	RPMI-1640, 10% v/v FCS, 4mM L-glutamine	Negative
<b>HEK293T</b>	Adenovirus transformed embryonic kidney	DMEM, 10% v/v FCS, 4mM L-glutamine	Negative
<b>SCC040</b>	Oropharyngeal SCC	DMEM, 10% v/v FBS, 4mM L-glutamine, 1% v/v PenStrep	Negative
<b>Vu40T</b>	HNSCC	DMEM, 10% v/v FBS, 4mM L-glutamine, 1% v/v PenStrep	Negative

For storage of stocks in liquid nitrogen, two million cells were counted, pelleted and resuspended in cryopreservation media consisting of media (DMEM or SFM as

appropriate), supplemented with 20% (v/v) FCS or FBS and 10% (v/v) dimethyl sulphoxide (DMSO, Sigma-Aldrich).

### 2.1.2 Cell counting

During cell harvest, disposable Glasstic™ slides (Hycor Biomedical Ltd., UK) were used to determine cell concentration in culture. Ten microlitres of cell suspension was pipetted into a well on the Glasstic™ slide. Using an inverted light microscope, all live (bright spherical) cells contained within three large squares of the Glasstic™ grid were counted. This number was divided by three to obtain an average count of cell number, which was multiplied by  $10^4$  to calculate the number of cells per ml of culture medium. Typically, cells were then made up to a density of  $2 \times 10^6$  cells per ml.

### 2.1.3 Mycoplasma testing

All cell lines were periodically tested using the MycoAlert mycoplasma detection kit (Lonza, UK), as per the manufacturer's instructions and were found to be consistently negative for mycoplasma.

### 2.1.4 Generation and maintenance of HPV genome-containing cell lines

#### *2.1.4.1 Maintenance of primary foreskin keratinocytes prior to transfection*

Normal primary human foreskin keratinocytes (HFks) were isolated from neonate foreskin by Dr Sally Roberts following the protocol described by Meyers and Laimins (1994). Foreskin tissues were obtained from circumcisions (carried out by Dr Joseph Spitzer) with informed parental written consent (Regional Ethics Committee approval number 06/Q1702/45, Roberts). Also, HFks were purchased from Lonza (Clonetics). Throughout this thesis, the donor number assigned to cells derived from the same background is consistent (Donor 1-4). HFks were cultured on collagen-coated tissue culture dishes in

serum-free keratinocyte growth medium (Invitrogen, UK) and media was replaced every two days. Cells were grown to 80% confluency, at which point they were passaged by removal of media followed by a wash with sterile PBS and the addition of 1 ml of 0.05% trypsin/EDTA (Gibco). This was incubated for 5 minutes at 37°C, in a similar procedure as described for cell lines. Trypsin was inactivated by the addition of 1 ml trypsin inhibitor (TI; 0.25 mg/ml soyabean trypsin inhibitor in Dulbecco's PBS without calcium or magnesium, pH 7.2, Invitrogen). Cells were then transferred to a 15 ml conical tube and pelleted by centrifugation at  $10000 \times g$  for 5 minutes at room temperature. The supernatant was subsequently removed and the pellet resuspended in SFM. Typically, a 10 cm tissue culture dish was seeded with  $2 \times 10^5$  cells in 10 ml SFM.

#### *2.1.4.2 Cryopreservation of HFKs*

Cells were frozen at a density of between 1 and  $2 \times 10^6$  cells per vial. Freezing media consists of SFM supplemented with 10% (v/v) FCS and 10% (v/v) DMSO. HPV genome-containing HFKs were frozen in E-medium supplemented with 10% (v/v) Hyclone™ FCS (Thermo Fisher Scientific) and 20% (v/v) glycerol (Thermo Fisher Scientific).

#### *2.1.4.3 Generation of HPV genome-containing HFKs*

Generation of HFK cell lines was undertaken according to the methods described by Wilson and Laimins, (2005, see Figure 2.1). In preparation, HFKs were seeded into uncoated 5 cm tissue culture dishes and allowed to grow. Once the cells reached 50-60% confluency, recircularised HPV genomes (Section 2.2.3.6) were co-transfected into HFKs alongside *pCDNA3.1* (Invitrogen), a plasmid that carries the neomycin resistance gene. Control transfections carried out in parallel include; the *pCDNA3.1* (Neo) alone, E green fluorescent protein (EGFPc1; Clontech, France) reporter expression vector, and a no plasmid vector DNA. For each transfection, 94 µl of SFM was dispensed into a

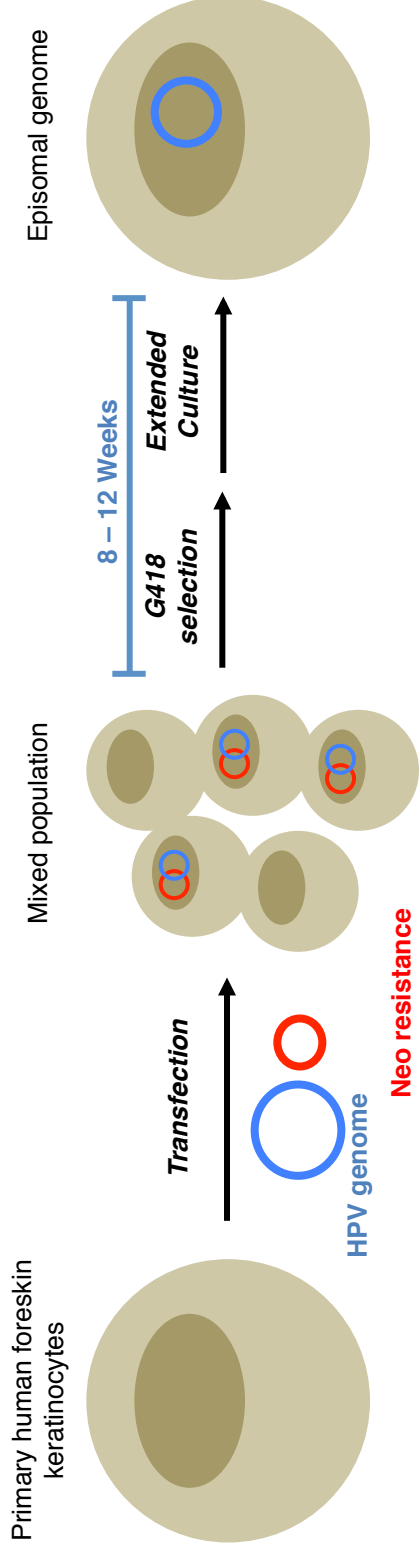


**Figure 2.1: Transfection of primary keratinocytes with HPV genomes**

Primary foreskin keratinocytes were grown to 50-60% confluency in 5 cm tissue culture dishes. For transfection with recirculised HPV genomes, media was replaced with serum-free media. Genomes were co-transfected into cells alongside a neomycin resistance plasmid using Fugene6 transfection reagent. After incubation at 37°C, 5% CO<sub>2</sub> for 48 h, transfected keratinocytes were re-plated onto 10 cm tissue culture dishes previously seeded with 2×10<sup>6</sup>  $\gamma$ -irradiated J2-3T3 fibroblasts and cultured in complete E medium. A G418 selection process was applied over the next 8 days; addition of selection-containing media and 1×10<sup>6</sup> irradiated J2-3T3 cells was alternated by day. This selection period began two replenishments with CEM containing 100  $\mu$ g/ml G418 followed by two replenishments of 200  $\mu$ g/ml G418. Following the last day of G418 treatment, media was replaced with normal CEM and 2×10<sup>6</sup> irradiated J2-3T3 cells were added.

Once colonies reached approximately 2 cm in diameter, typically 1 month after completion of the selection process, the cells were pooled and transferred onto a single dish pre-seeded with  $\gamma$ -irradiated J2-3T3 cells. Upon reaching 80% confluence, HF<sup>+</sup>Ks were passaged onto five 10 cm tissue culture dishes.

polypropylene conical tube (BD Biosciences), followed by the addition of 6  $\mu\text{l}$  FuGene 6 Transfection Reagent (Roche, UK). In a separate tube, 100  $\mu\text{l}$  of SFM, 1  $\mu\text{g}$  of HPV genomic plasmid DNA and 1  $\mu\text{g}$  of neomycin resistance plasmid were mixed. The contents of two tubes were combined and then incubated at room temperature for 30 min. Media from the HFKs was replaced with SFM media (Gibco), and the transfection mixture was added to the dish dropwise, rocked gently to mix and incubated at 37°C and 5%  $\text{CO}_2$  for 24 hrs.

Transfection efficiency was measured by observation of the GFP control transfection, using a Zeiss Axiovert 100 microscope, with GFP-expressing cells typically representing 5% of the total population. Transfected keratinocytes were then removed from the dish by trypsin treatment and re-plated onto 10 cm tissue culture dishes previously seeded with  $2 \times 10^6$   $\gamma$ -irradiated J2-3T3 fibroblasts in complete E medium (CEM, Section 2.1.4.5). Over the next 8 days the HFKs underwent a selection process, with the alternate addition of selection-containing media and  $1 \times 10^6$  irradiated J2-3T3 cells. The selection period began with the replacement of CEM with CEM containing 100  $\mu\text{g}/\text{ml}$  G418 (PAA Laboratories, UK). After two replenishments with 100  $\mu\text{g}/\text{ml}$  G418 CEM (typically 4 days), selection was increased to 200  $\mu\text{g}/\text{ml}$  G418 for two replenishments (typically 4 days). Following the last day of G418 treatment, media was replaced with normal CEM and  $2 \times 10^6$  irradiated J2-3T3 cells were added. In the event that cells reached 80% confluence during the selection process, the dish was split equally onto two dishes previously seeded with  $2 \times 10^6$  irradiated J2-3T3 fibroblasts in the presence of normal CEM and the selection process was resumed the following day.

Once colonies reached approximately 2 cm in diameter, typically observed 1 month after completion of the selection process, the dishes were pooled and transferred onto a single dish pre-seeded with  $\gamma$ -irradiated J2-3T3 cells. Upon reaching 80% confluence, HFKs were

passed onto five 10 cm tissue culture dishes. Once 70-80% confluence was reached, cell pellets were harvested by trypsin treatment, washed with ice-cold saline and prepared for RNA, DNA and protein analysis, as well as samples cryopreserved in liquid nitrogen.

#### *2.1.4.4 Maintenance of HFKs following transfection of HPV genomes*

Genome-containing HFKs were cultured on a feeder layer of  $2 \times 10^6$  irradiated J2-3T3 fibroblast feeder cells in CEM. CEM consists of Dulbecco's modified eagle media (DMEM, 60% v/v, Gibco), Ham's F12 (32% v/v, Gibco), the antibiotics penicillin and streptomycin (2% v/v PenStrep, Gibco), hydrocortisone (0.1% v/v, Sigma-Aldrich), Hyclone™ FCS, (10% v/v, Thermo Fisher Scientific), mouse epidermal growth factor (EGF, 0.5% v/v, BD Biosciences), L-glutamine (2% v/v, Gibco), cholera toxin A (0.1% v/v, MP Biomedicals, USA), insulin (0.2% v/v, Sigma-Aldrich), transferrin (0.2% v/v, Sigma-Aldrich), tri-iodo-L-thyronine (T3, 4 nM, Sigma-Aldrich) and adenine (36  $\mu$ M, Sigma-Aldrich). The media was replaced every two days and the cells grown to a confluency of no greater than 80% prior to passaging. Irradiated J2-3T3 cells were seeded onto 10 cm dish containing 10 ml E-medium at least 2 h, or 24 h, prior to addition of HFKs. HFKs were passaged by first removing the J2-3T3 feeder layer, using 0.5 mM EDTA (ethylene diamine tetraacetic acid) in PBS. Once the feeder cells were detached, a transfer pipette was used to aspirate the EDTA and the dish was washed twice with 5 ml of sterile PBS. HFKs were then removed with 2 ml TrypLE and incubated at 37°C for 5-10 minutes with regular checks for cell detachment. The TrypLE was quenched with CEM and dishes washed with 10 ml media, all of which was transferred to a sterile conical tube.. HFKs were pelleted by centrifugation at  $538 \times g$  for 5 minutes at room temperature. The supernatant was removed and the cells resuspended in warmed CEM. HFKs were counted and seeded out at a density of  $2 \times 10^5$  cells per dish onto  $2 \times 10^6$  irradiated J2-3T3 cells. The

plates were gently rocked several times to ensure thorough mixing and the cells incubated at 37°C and 5% CO<sub>2</sub>. The media was replaced every 2 days, with cells taking typically 5-7 days to reach a confluency of 80%. At each passage, aliquots of 5×10<sup>5</sup> cells were pelleted by centrifugation, washed with phosphate buffered saline (PBS) and stored at -80°C for further analysis. The establishment and maintenance of HPV episomes was confirmed by blot analysis of total DNA (Section 2.2.2.3).

Cell lines containing the HPV16 114/B, HPV16 114/K (Kanda *et al.*, 1988; Roden *et al.*, 1996) or HPV18 (Wilson *et al.*, 2007) episomal genomes were cultured alongside untransfected HFKs derived from the same donor.

#### 2.1.4.5 Maintenance and irradiation of J2-3T3 fibroblasts

Following transfection of primary keratinocytes with HPV genomes, cells were cultivated with a feeder layer of irradiated NIH J2-3T3 mouse fibroblasts. J2-3T3 cells were cultured in DMEM supplemented with L-glutamine (2% v/v) and newborn calf serum (10% v/v, Gibco) and were grown to a confluency of no greater than 90% before passaging. For subculture, 3T3 cells were first washed with 5 mL sterile PBS and then incubated with 1 mL TrypLE until cells were no longer adherent (typically 5 min). Trypsin was quenched and cells washed off of the dish with medium. The suspension transferred to a sterile tube for centrifugation at 10000 × *g* for 5 min. Cells were resuspended in culture media, counted and seeded into 10 cm dishes with 10 ml of prewarmed medium. J2-3T3 cells were grown to no more than passage 25 and then replaced with earlier passage J2-3T3 cells. When J2-3T3 cells were required as feeder cells, they were harvested by trypsinisation and resuspended in CEM at 2×10<sup>6</sup> cells/ml. Cells were irradiated with 50 Grays of a Caesium-137 source and were stored in CEM at 4°C for up to 5 days.

For cryopreservation,  $2 \times 10^6$  J2-3T3 cells were resuspended in 1 ml DMEM supplemented with 20% (v/v) newborn calf serum, and 10% (v/v) DMSO.

#### 2.1.4.6 Organotypic raft culture

Organotypic raft cultures were prepared as described by Wilson and Laimins (2005). Each collagen plug was prepared in 3 cm dishes using 2.4 ml Rat-tail collagen (BD Biosciences, UK) diluted to 4mg/ml with 0.02 M acetic acid. Per plug,  $2 \times 10^6$  3T3-J2 cells were reconstituted in 0.3 ml  $10 \times$  filtered DME and 0.3 ml  $10 \times$  filtered reconstitution buffer (0.05 M NaOH, 260 mM NaHCO<sub>3</sub>, 200 mM Hepes; all Sigma-Aldrich). To this, the acetic acid and collagen were added and mixed using an ice-cold strippette. The pH of plug mixture was adjusted by addition of 1 M NaOH dropwise, before the addition of 3 ml per 3 cm dish. Plugs were incubated overnight at 37°C 5% CO<sub>2</sub>. Typically,  $2 \times 10^6$  untransfected or genome-containing HFKs were grown on a collagen plug pre-seeded with  $2 \times 10^6$  J2-3T3 fibroblasts in a 3 cm tissue culture dish. Media was replaced daily, and cells were allowed to expand on the plugs until the media turned yellow (24-48 hr), after which the collagen plug was carefully lifted and placed on top of a wire mesh platform (known as a grid), and placed in a 10 cm tissue culture dish. This was then filled CEM lacking EGF, in order to create an air/liquid interface (see Figure 2.2). Rafts were grown for 13 days; the media was replaced every 2 days. Six hours before fixing, 20  $\mu$ M of the thymidine analogue 5-Bromo-2'-deoxyuridine (BrdU, BD Biosciences) was added to media. BrdU is incorporated into the newly synthesized DNA of replicating cells, and thus it allows the detection of replicating cells. In preparation for downstream immunofluorescent analysis (Section 2.3), rafts were fixed by flooding the raft-containing dish with 4% (w/v) paraformaldehyde in DMEM. Rafts were paraffin embedded and sections (4 microns) were prepared for staining by Propath Ltd, UK.

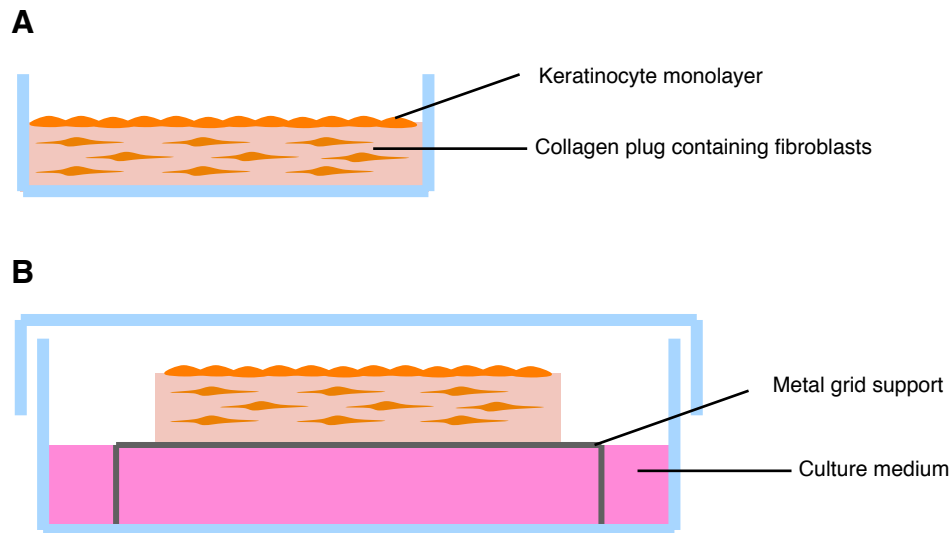


### Figure 2.2: Organotypic raft culture

- (A) Schematic of the organotypic raft culture system. HFKs containing HPV genomes are seeded onto collagen plugs containing fibroblasts in a 3 cm tissue culture dish and cultured in complete E media.
- (B) When HFKs reach confluence, indicated by media turning yellow, the collagen plugs are lifted onto stainless steel support grids. This is cultured with E media supplemented with L-glutamine, forming an air-liquid interface at the raft grid. This induces differentiation of the HFKs, leading to the production of a stratified epithelium.

The metal grids were prepared by cutting squares of wire mesh approximately 4 x 4 cm and bending two opposite edges down evenly. Use of a spirit level confirmed the creation of a level surface. Grids were then sterilized by incubation for 2 hours in concentrated (24 M) sulphuric acid (Thermo Fisher Scientific). For safety, this took place in a glass beaker in a fume cupboard. The grids were rinsed by placement of the beaker under cold running water overnight, after which they were dried on paper, placed in a Pyrex beaker and autoclaved.

#### *2.1.4.7 Protein extraction from raft cultures*

Protein was extracted from raft cultures by peeling off the stratified HFks from the collagen layer followed by homogenization in 1 ml of UTB lysis buffer (8 M urea, 50 mM Tris-HCl pH 8, 0.15 M  $\beta$ -mercaptoethanol, Sigma-Aldrich) supplemented with protease and phosphatase inhibitors (Sigma-Aldrich) in a glass Dounce homogeniser. Lysate was incubated for 30 minutes on ice before being transferred by transfer pipette into a pre-cooled microcentrifuge tube. This was centrifuged at  $16000 \times g$  for 15 minutes at 4°C. The supernatant was subsequently removed and designated as the 'soluble fraction'. The pellet was thus designated the 'insoluble fraction', and was solubilised in 250  $\mu$ l of Laemmli buffer (BioRad, UK) supplemented with 5% (v/v)  $\beta$ -mercaptoethanol. The soluble fraction was aliquoted at a 1:1 ratio into Laemmli buffer supplemented with 5% (v/v)  $\beta$ -mercaptoethanol, heated at 95°C for 5 minutes prior to storage at -20°C and/or SDS-PAGE and subsequent analysis.

#### *2.1.4.8 RNA extraction from raft cultures*

Similar to the extraction of protein, RNA extraction from raft culture began with removal of the HFks from the collagen layer using sterile forceps. This was then placed into a 15 ml collection tube and homogenized in 100  $\mu$ l of RNA Stat-60 (AMS Biotechnology, UK)

using a glass Dounce homogenizer. HFKs were incubated for 5 minutes at room temperature in the RNA Stat-60, which is a monophasic solution containing phenol and guanidinium thiocyanate. Once 200  $\mu\text{l}$  of chloroform was added and the sample shaken vigorously for 15 seconds, the homogenate separated into two phases, the aqueous and the organic. After centrifugation at  $12000 \times g$  for 5 minutes at  $4^{\circ}\text{C}$ , the total RNA in the aqueous phase was transferred to a fresh collection tube, leaving any DNA and proteins in the organic phase. Addition of 500  $\mu\text{l}$  isopropanol and incubation at room temperature for 5 minutes allowed precipitation of the RNA from the aqueous phase. This was centrifuged at  $12000 \times g$  for 10 minutes at  $4^{\circ}\text{C}$  and the pellet washed by resuspension in 1 ml 75% (v/v) ethanol and centrifugation at  $7500 \times g$  for 5 minutes at  $4^{\circ}\text{C}$ . Once the pellet had been dried briefly, it was resuspended in 40  $\mu\text{l}$  of nuclease-free water.

## 2.1.5 Treatment and manipulation of cells

### 2.1.5.1 Subcellular fractionation

Subcellular fractionation was carried out on HeLa cells and HFKs using the ProteoExtract® subcellular proteome extraction kit (EMD Millipore, USA), and was optimised for use on untransfected and genome-containing HFKs grown in monolayer. All buffers were supplemented with protease and phosphatase inhibitors, and Buffer III was also supplemented with the endonuclease benzonase®. Firstly, supporting 3T3-J2 fibroblasts were first removed and cells washed with ice-cold PBS. Cells were then washed with 1 mL Wash Buffer before incubation in 500  $\mu\text{l}$  extraction Buffer I with gentle agitation at  $4^{\circ}\text{C}$  for 15 min. All traces of the buffer were removed and transferred into a pre-cooled microcentrifuge tube and designated fraction 1 (F1), representing the cytoplasmic fraction of cell contents. Next, 500  $\mu\text{l}$  extraction Buffer II was added to the dish of cells and incubated at  $4^{\circ}\text{C}$  for 30 minutes with gentle agitation. The buffer was then

transferred to a pre-cooled microcentrifuge tube and designated fraction 2 (F2), the membrane fraction. A final incubation in 250  $\mu$ l extraction Buffer III at 4°C for 10 minutes with gentle agitation was transferred to a pre-cooled 1.5 ml microcentrifuge tube and designated fraction 3 (F3), the nuclear fraction. The remaining fraction, the cytoskeletal fraction, was resuspended in 250  $\mu$ l extraction Buffer IV, transferred to a pre-cooled 1.5 ml microcentrifuge tube and designated fraction 4 (F4). For subsequent SDS-PAGE and subsequent protein analysis, 10  $\mu$ l of each fraction was aliquotted into 10  $\mu$ l Laemmli buffer supplemented with 5% (v/v)  $\beta$  mercaptoethanol, and treated as a western blot (Section 2.2.4.2).

#### *2.1.5.2 Proteasome inhibition*

Untransfected or HPV genome-containing HFks were seeded into a 6 cm dishes containing  $2 \times 10^5$  irradiated J2-3T3 fibroblasts as a feeder layer. HFks were allowed to grow for 48 h before the addition of the proteasome inhibitor MG132 (z-Leu-Leu-Leu-CHO), which was dissolved in DMSO and applied at a final concentration of 40  $\mu$ M in cell culture medium. As a control, vehicle (DMSO) treated cells were cultured and harvested alongside MG132 treated cells. Cells were harvested at 4 and 6 h post-treatment; feeder cells were removed and cells pelleted by trypsinisation, as described previously. Cell pellets were washed by resuspension in ice-cold saline and centrifuged for  $10000 \times g$  for 5 minutes at 4°C, before being lysed in UTB buffer and subject to downstream western blot analysis (Section 2.2.4.2).

#### *2.1.5.3 Protein kinase A activation and inhibition*

As for MG132 treatment, in preparation for treatment with protein kinase A (PKA) inhibitors or activators, untransfected or HPV genome-containing keratinocytes were

seeded into a 6 cm dishes containing a feeder layer of  $2 \times 10^5$  irradiated J2-3T3 fibroblasts. HeLa cells were seeded at a density of  $2 \times 10^5$  cells/dish. Cells were allowed to attach for 24 h before the addition of specific PKA activating or inhibiting compounds. The PKA activators forskolin (FK) and 3-isobutyl-1-methylxanthine (IBMX, both Sigma-Aldrich) were dissolved in DMSO and used in combination at the final concentrations of 50  $\mu\text{M}$  and 1 mM in culture medium, respectively. The more specific PKA activator PKI and cyclic AMP (cAMP) analogue, dibutyl cAMP (dbcAMP, EMD Millipore) was dissolved in Hank's balanced salt solution (HBSS) and diluted in culture medium to a final concentration of 1 mM. The PKA inhibitor H89 (Sigma-Aldrich, UK) was dissolved in DMSO and added to the culture medium at a final concentration of 10  $\mu\text{M}$ . Exogenous expression of the PKI peptide was induced by transfection with mPKI plasmid (Section 2.1.5.4, gift from M. Diskar). Vehicle treated cells were cultured and harvested alongside those treated with activators or inhibitors. Cells were harvested at various time points up to 96 hr; feeder cells were removed and washed off before cells were harvested by trypsinisation, washed in saline and lysed in UTB for western blot analysis as described in Section 2.2.4.2.

#### *2.1.5.4 Transfection of cells*

HeLa, C33A and HFks were cultured overnight in serum free medium prior to transfection. Cells were transfected at 80% confluency with 3-5  $\mu\text{g}$  DNA in Xtremegene<sup>TM</sup> transfection reagent (Roche), at a ratio of 2  $\mu\text{l}$  per 1  $\mu\text{g}$  of DNA, in 500  $\mu\text{l}$  Optimem (Invitrogen). Reagent, DNA and Optimem were incubated together for 30 minutes at room temperature before dropwise addition to cells. Cells were then incubated at 37°C with 5% CO<sub>2</sub> for 48 hours before harvesting. Transfection with plasmid expressing the peptide PKA inhibitor mPKI was confirmed by observation of GFP expression, using a

Zeiss Axiovert 100 microscope. Cells were washed with ice-cold saline before downstream protein analysis (Section 2.2.4).

## 2.2 Molecular biology

### 2.2.1 RNA analysis

#### *2.2.1.1 RNA isolation from cultured cells*

Total RNA was extracted from  $1 \times 10^6$  cells using an RNeasy Mini kit (QIAGEN, UK) and treated with DNase (Promega), according to manufacturer's instructions. Cultured cells were centrifuged and collected as a cell pellet at the time of passage. The pellet was then washed by resuspension in 500  $\mu$ l PBS and centrifuged for 5 minutes at  $16000 \times g$ . The supernatant was discarded and cells resuspended in 750  $\mu$ l lysis buffer containing guanidinium thiocyanate, a strong denaturant which lyses cell membranes and rapidly inactivates ribonucleases (Chomczynski and Sacchi, 1987). This was mixed thoroughly by pipetting; any vortex mixing was avoided throughout the preparation in order to prevent shearing of RNA. One volume (750  $\mu$ l) of 70% ethanol was added to the pellet lysate, and the mixture passed at least 5 times through a 0.9 mm (20 gauge) needle attached to a sterile plastic syringe (BD Biosciences). Lysate was then transferred to a silica filter cartridge inserted into a 1.5 ml collection tube. Centrifugation for 30 seconds at  $16000 \times g$  in a microcentrifuge 5415 R, refrigerated benchtop centrifuge (Eppendorf, UK), allowed the mix to be drawn through the filter and the RNA to bind the silica matrix. The bound RNA was then washed by the addition of 700  $\mu$ l wash buffer RW1 and centrifuged for 30 seconds at  $16000 \times g$ . The flow through was discarded. Two sequential washes with 500  $\mu$ l wash buffer RPE followed; first for 30 seconds at  $16000 \times g$  and the second for 2 minutes at  $16000 \times g$ , to remove any traces of salts remaining from previous buffer washes. The

flow through was discarded each time. The filter cartridge was then transferred to a clean collection tube and centrifuged for 2 minutes at  $16000 \times g$ , in order to remove any last traces of ethanol from the wash solutions. The cartridge was placed into a sterile 1.5 ml collection tube and RNA eluted by the application of 30  $\mu$ l RNase-free water to the filter, incubation at room temperature for 1 minute, followed by centrifugation for 2 minutes at  $16000 \times g$ . To ensure maximum RNA yield, a second application of 30  $\mu$ l RNase-free water and a final centrifugation for 1 minute at  $16000 \times g$  followed.

#### 2.2.1.2 RNA extraction from tissue

In order to extract RNA, tissue samples were first homogenised in 1 mL RNA stat-60 (AMS Biotechnology) per mg of tissue, using a glass Dounce homogeniser. This was incubated for 5 minutes at room temperature in the RNA Stat-60, and 200  $\mu$ l of chloroform added per 1 ml of RNA stat-60. The sample was shaken vigorously for 15 seconds and incubated for 5 minutes at room temperature. After centrifugation at  $12,000 \times g$  for 15 minutes at  $4^{\circ}\text{C}$ , the total RNA in the aqueous phase was transferred to a pre-cooled collection tube, leaving any DNA and proteins in the organic phase. To this, 500  $\mu$ l isopropanol was added, and incubated at room temperature for 5 minutes to allow the precipitation of the RNA from the aqueous phase. This was centrifuged at  $12000 \times g$  for 10 minutes at  $4^{\circ}\text{C}$  and the pellet washed by resuspension in 1 ml 75% (v/v) ethanol and centrifugation at  $7500 \times g$  for 5 minutes at  $4^{\circ}\text{C}$ . Once the pellet had been dried briefly, it was resuspended in 40 $\mu$ l of nuclease-free water.

#### 2.2.1.3 DNase treatment of RNA

RNA was treated with DNase in order to degrade any contaminating DNA. One microgram of eluted RNA was mixed with 1  $\mu$ l of  $10\times$  DNase buffer (Promega, UK; 100 mM Tris-HCl, 25 mM  $\text{MgCl}_2$ , 1 mM  $\text{CaCl}_2$ ), 1  $\mu$ l DNase I (2000 units/ml, Promega) and

water to a final volume of 10  $\mu\text{l}$ . This was incubated at 37°C for 30 min, after which the reaction was inactivated by the addition of 1  $\mu\text{l}$  stop solution and incubation at 65°C for 10 min. This was stored at -20°C for short term, or at -80°C for longer term.

#### 2.2.1.4 Spectrophotometry of nucleic acids

RNA and DNA samples were quantified using a NanoDrop ND-1000 Spectrophotometer (Thermo Fisher Scientific). The sample pedestal was first cleaned with 2  $\mu\text{l}$  nuclease-free water and then calibrated with 1  $\mu\text{l}$  elution solution, to provide a reference measurement of background light absorbance against which sample light absorbance could be compared. One  $\mu\text{l}$  of each sample was pipetted onto the sample pedestal and its absorbance measured at 280 nm. The ND-1000 Spectrophotometer v 3.2 software (Thermo Fisher Scientific) calculated the concentration (ng/ $\mu\text{l}$ ) using a modified form of the Beer-Lambert equation and the wavelength-dependant molar absorptivity (or extinction) coefficient to correlate measured light with sample concentration:

$$c = \frac{(A \times e)}{b}$$

Where:  $c$  = nucleic acid concentration (ng/ $\mu\text{l}$ )

$A$  = Absorbance (absorbance units, AU)

$e$  = extinction coefficient (ng-cm/ $\mu\text{l}$ )

$b$  = light path length (cm)

#### 2.2.1.5 Reverse transcription

RNA from cultured cells was reverse transcribed using the Promega MLV reverse transcription (RT) system to produce complementary DNA (cDNA). One microgram of RNA was preincubated with random hexodeoxynucleotide (100 mM) or oligodT (100 mM) primers at 72°C for 10 minutes in a reaction volume made up to 12  $\mu\text{l}$  with sterile distilled

water. This was then cooled on ice, to denature any secondary RNA structures that would interfere with primer annealing. To this mixture, 5  $\mu$ l of 5 $\times$  reaction buffer, deoxynucleotides (10 mM, Promega), 1  $\mu$ l Moloney murine leukemia virus reverse transcriptase (MLV RT, 20 units/ $\mu$ l, Promega), 1  $\mu$ l RNase inhibitor (40 units/ $\mu$ l, Promega) and nuclease-free water, were added to a final volume of 25  $\mu$ l (Thermo Fisher Scientific). Reactions were incubated in a heat block at 37°C for 1 hour, after which the enzyme was denatured by incubation at 70°C for 10 min. To confirm the absence of genomic DNA during downstream applications, concurrent reactions were performed in the absence of reverse transcriptase.

#### 2.2.1.6 Oligonucleotide primer design

Oligonucleotide primers were designed using primer 3 software ([www.primer3.com](http://www.primer3.com)) and previously published genomic and mRNA transcript sequences available from the NCBI Genbank database (<http://www.ncbi.nlm.nih.gov/genbank/>). The following formula was used to calculate the melting temperature ( $T_m$ ) of designed primers:

$$T_m = \%GC \times 0.41 + 64.9 - \left(\frac{600}{n}\right)$$

where:  $T_m$  = melting temperature of primers

$\%GC$  = percentage of G and C bases in primer

$n$  = total number of bases in primer

Primer sets (forward and reverse pairs) were designed to have similar GC content and total number of base pairs (bp) to produce complementary primers with similar annealing temperatures, at around 60°C (

Table 2.2). Basic local alignment search tool (BLAST) searches (<http://www.ncbi.nlm.nih.gov/BLAST/>) were performed in all cases to ensure that primers were not complementary to other regions of the genome and bound specifically to

the target sequences. Following oligonucleotide synthesis (Alta Bioscience, Birmingham UK), optimum conditions for each primer set were determined by performing parallel reverse transcription polymerase chain reactions (RTPCR) at different temperatures based around the calculated  $T_m$  (

Table 2.2).

**Table 2.2: qRTPCR primers**

<b>Target protein</b>	<b>Forward primer sequence (5'-3')</b>	<b>Reverse primer sequence (5'-3')</b>	<b>Amplified Fragment (bp)</b>	<b><math>T_m</math> (°C)</b>
<b>SCRIB</b>	CCTGCCAGCTCCAGCACCAC	CGGCTGGGGTGGGGCAGTTA	147	59
<b>INADL</b>	AGATCGGAGTTTTGCAGAGG T	TCGAAGCAATGTTCTTGACCCA	100	59
<b>NHERF1</b>	TCACCAATGGGGAGATACAG	GTCTTGGGAATTCAGCTCCT	126	59
<b>PTPN13</b>	ATGAAACCTGTGCTAGGGAT TATA	CGACCTCCCAGGCTCAAGTAG	286	60
<b>MAGI-1</b>	GACTGTGAAGGAGTTCTTGG	TCGTGATCACTTTCCCACTG	125	59
<b>MAGI-2</b>	TTCAAGGGACAGCACAAACC	GGAAGAACAGCAGACTTTGC	146	59
<b>MAGI-3</b>	CCACAAACTGCAGCAAGTGA	AATGCTCCACTCTCTTCCAG	150	59
<b>B2M</b>	GCCTGCCGTGTGAACCATGT	GCAGCCTCCTAGAGCTACC	296	59
<b>DLG1<math>\alpha</math></b>	CAGTCGAGGAGGCAATACTA	AGCGTGAAGGTTCTGGCTCA	103	59
<b>DLG1<math>\beta</math></b>	CGGAAGCAAGATACCCAGAG	AATTGGTTCAGACGGCTTTG	113	59
<b>DLG1 HOOK region</b>	GCCCATTCCTAGCGCATGAA CTCC	GCCATTCTGGTGGATGGCAGAG	98	59

$T_m$  indicates annealing temperature used in PCR reactions, having calculated predicted  $T_m$  and carried out reactions at several temperatures to obtain an optimal  $T_m$ . B2M –  $\beta$ 2-microglobulin.

#### 2.2.1.7 Reaction conditions for RTPCR

RTPCR reactions were set up on ice using filter pipette tips (StarLab, UK). Each 25  $\mu$ l RTPCR reaction contained; 5  $\mu$ l cDNA, 12.5  $\mu$ l hotstart GoTaq mastermix (Promega) and 0.1 nM of forward and reverse primers, with nuclease-free water made up to the final volume. Reactions were performed in a 2720 Thermocycler (Applied Biosystems, UK),

beginning with 10 minutes at 95°C, in order to activate the polymerase. This was followed by 40 cycles of denaturation at 95°C for 30 seconds, annealing for 50 seconds) and an extension step at 72°C for 1 minute.

Table 2.2 details the primer sequences and optimal annealing temperatures. Amplified DNA fragments of expected length were visualized by 1% (w/v) agarose gel electrophoresis and ethidium bromide staining.

#### *2.2.1.8 Agarose gel electrophoresis*

DNA from PCR, as well as plasmid DNA, was visualised using agarose gel electrophoresis. Fragments were resolved on a 1-2% (v/w) agarose gel, prepared by heating 1.5-3 g of molecular grade agarose (BioLine) in 150 ml 0.5× TBE buffer (0.1 nM Tris-HCl, 0.1 nM Boric acid, 100 mM EDTA). Ethidium bromide was added to a final concentration of 0.5 µg/ml prior to cooling and the entire solution poured into a Mini Sub Gel GT Electrophoresis Tank (BioRad). Once set, this was submerged in 0.5× TBE buffer. DNA samples were combined with 5 µl loading buffer (30% v/v glycerol, 0.3% w/v bromophenol blue, 0.1% xylene cyanol FF, 10× TBE) and loaded onto the gel, alongside a lane containing 2 µl DNA marker (1kb plus, Invitrogen). A potential of 100 V was applied across the gel for approximately 1 hr. Ethidium bromide is an intercalating agent that fluoresces when exposed to ultraviolet (UV) light, allowing the visualization of DNA, using a Gene Flash UV light box (Syngene Bio Imaging, UK).

For the resolution of genomic DNA prior to Southern blot analysis, 0.8% (w/v) agarose gels were prepared as described and cast in Fisherband horizontal gel electrophoresis tanks (Thermo Fisher Scientific), run at 50 V overnight.

#### *2.2.1.9 Purification of cDNA from agarose gels*

cDNA was isolated from agarose gels and purified using the QIAquick Gel Extraction Kit (QIAGEN), as per the manufacturer's instructions. Each DNA band (approximately 100 mg of gel) was excised from the gel using a sterile scalpel and placed in a sterile microcentrifuge tube. Once weighed, three volumes (typically 300  $\mu$ l) of QG buffer was added and the gel dissolved by incubation at 50°C with occasional agitation. Once the gel had completely dissolved (approximately 15 min), 1 volume (typically 100  $\mu$ l) isopropanol was added and mixed by inversion of the tube several times, aiming to precipitate the DNA. The solution was transferred to a QIAquick Spin column placed in a fresh microcentrifuge tube and drawn through the column by centrifugation at 16000  $\times g$  for 1 minute, allowing cDNA to bind to the filter cartridge. The flow-through was discarded, and any traces of agarose were washed away by the addition of 500  $\mu$ l QG buffer and centrifugation at 16000  $\times g$  for 1 minute. To remove salts and ethidium bromide, a second wash was performed by the addition of 750  $\mu$ l PE buffer and centrifugation at 16000  $\times g$  for 1 minute. The flow-through was discarded after each wash stage. The filter column was again centrifuged at 16000  $\times g$  for 1 minute to remove any remaining PE buffer before being transferred into a sterile microcentrifuge tube. Thirty microlitres of sterile, nuclease-free water was added to the centre of the filter and the column incubated for 1 minutes at room temperature. The column was then centrifuged at 16000  $\times g$  for 1 minutes to elute the DNA. This addition of water was repeated for a second time, and DNA concentration measured using a NanoDrop spectrophotometer before storage at -20°C.

#### *2.2.1.10 DNA sequencing*

RTPCR products were sequenced in order to confirm that the intended genes of interest had been amplified. Sequencing was performed by the Functional Genomics facility

(Department of Biosciences, University of Birmingham, UK). In preparation, 10 ng of RTPCR product and 5 picomoles forward or reverse primer was made up to a final volume of 10 µl with nuclease-free water. Returned chromatograms were viewed using FinchTV software (GeoSpiza Inc.) and the EMBL-EBI Clustal-Omega facility (<http://www.ebi.ac.uk/Tools/msa/clustalo/>) used to align sequencing results to published sequences and confirm homology.

**Table 2.3: *DLG1* primers**

<b>Primer name</b>	<b>Sequence (5'-3')</b>	<b>Region of <i>DLG1</i></b>
<b>DLG1 F1</b>	CCCAGAGAGCATTCACCC	α N terminus
<b>DLG1 F2</b>	CAGAGATTGAGAATGTCC	Nts 428-446
<b>DLG1 F3</b>	CTCGACCAGTGATCATATTG	Nts 2140-2160
<b>DLG1 F4</b>	CTGGAACAGGAGTTACTG	Nts 2577-2596
<b>DLG1 R1</b>	GCCTGAAAGAGGTTGCTCTG	GUK domain
<b>DLG1 I2<sub>Fwd</sub></b>	GAGATCCCTGACGACATGGG	Insertion 2
<b>DLG1 I5<sub>Rev</sub></b>	TTCACATATCGCTGGCATTAGAA	Insertion 5
<b>DLG1 GUK<sub>Rev</sub></b>	CCTGTCTTTCATAGGTCCCA	GUK domain

#### 2.2.1.11 *Quantitative* RTPCR (*q*RTPCR)

qRTPCR reactions were performed to determine the level of expression of particular genes of interest, using SYBR green chemistry. SYBR Green I is an asymmetrical cyanine dye which intercalates into the minor groove of double-stranded DNA (dsDNA) and produces a complex that emits a green fluorescent signal (524 nm) upon excitation with blue light (485 nm) (Zipper *et al.*, 2004). The intensity of the fluorescent signal is proportional to the amount of SYBR-bound DNA present and so measurement of the fluorescent signal can be used to quantify DNA. During the qPCR reaction, the fluorescent signal is measured at every cycle of PCR and immediately following the product extension phase. During the reaction, the number of copies of the gene increases exponentially as described by the following equation (Livak and Schmittgen, 2001):

$$X_n = X_0 \times (1 + E_x)^n$$

Where:  $X_n$  = number of molecules of gene of interest at cycle  $n$

$X_0$  = initial number of molecules of gene of interest

$E_x$  = efficiency of amplification of gene of interest

$n$  = number of completed cycles

The values obtained for the genes of interest were referenced to the values of expression of the housekeeping gene  $\beta 2$ -microglobulin, as an internal control to account for difference in cell number and initial RNA load (Schmittgen and Zakrajsek, 2000). Prior to analysis of gene expression, several housekeeping genes of choice were compared by qRT-PCR for consistency of expression across cDNA samples. The result of gene expression quantification was then given as a ratio of the levels of mRNA transcripts of the gene of interest in an experimental sample (HPV genome-containing keratinocytes) to a defined control sample (untransfected HFK).

Each qRT-PCR reaction contained 40 ng cDNA template, 12.5  $\mu$ l SYBR green mastermix (Applied Biosystems) and 0.1  $\mu$ M forward and reverse primer, made up to a total volume of 25  $\mu$ l with nuclease-free water. Reactions were set up in triplicate on ice in 96-well reaction plates (Applied Biosystems) and analysed using the ABI Prism 7700 Sequence Detection System (Applied Biosystems). Samples were initially subjected to a denaturation step at 95°C for 10 minutes, followed by 40 cycles of denaturation at 95°C for 20 seconds, annealing for 45 seconds and an extension step at 72°C for 1 minute. Primers specific to the housekeeping gene  $\beta 2$ -microglobulin were included on each qRT-PCR plate, to account for loading variability.

#### 2.2.1.12 Comparative Ct method (ddCt) for relative quantitation of gene expression

The delta-delta (dd)Ct method enables relative quantitation of transcripts without the need for standard curves when looking at expression levels of a target gene relative to an endogenous control (e.g  $\beta 2$ -microglobulin, Livak and Schmittgen, 2001). This method was

used to measure the amount of target gene transcripts in different samples. Firstly, the difference (dCt) between the Ct values of the target gene and the endogenous gene was calculated for each sample studied (dCt = target Ct - endogenous Ct). The sample selected as the baseline sample for expression of the target gene is referred to as the reference sample. Here, untransfected, non-HPV containing keratinocytes were used as the reference sample, to which gene expression in the HPV-containing keratinocytes were normalised, unless otherwise stated. The difference between the dCt values of each sample and its reference sample was calculated, generating a ddCt value (ddCt = reference dCt - target dCt). The ddCt for each sample was then converted to an absolute value using the following equation:

$$\text{fold change in expression level} = 2^{-\text{ddCt}}$$

*Where: dCt = target Ct - endogenous Ct*

*ddCt = reference dCt - target dCt*

## 2.2.2 DNA analysis

### 2.2.2.1 DNA extraction

DNA was extracted from cells using a standard phenol-chloroform method:  $2 \times 10^6$  cells were resuspended in lysis buffer (10 mM Tris-HCl pH 7.4, 10 mM EDTA; 400mM NaCl; all Sigma-Aldrich), treated with RNase A at a final concentration of 50  $\mu\text{g}/\text{ml}$  for 30 minute at 37°C, and digested overnight by proteinase K (50  $\mu\text{g}/\text{ml}$  final concentration, Sigma-Aldrich) at 37°C with 0.2% (w/v) SDS. The resulting digestion was passed through a blunt 0.8 gauge needle 10 times to shear the DNA. The DNA was extracted firstly by washing twice with 2 volumes of phenol:chloroform:isoamylalcohol (25:24:1, Sigma-Aldrich), mixing thoroughly and centrifuging at  $16000 \times g$  and washing once with 2

volumes of chloroform:isoamyl alcohol (24:1). Following each wash, the liquid phase was transferred to a fresh 15 ml conical tube. DNA was precipitated by incubation in two volumes of 100% ethanol, with 0.3 M sodium acetate (pH 5.2), overnight at -20°C. Tubes were centrifuged for 30 minutes at 4°C, the pellet was washed with ice-cold 70% ethanol and centrifuged for 15 minutes at 4°C. The resulting pellet was dried and resuspended in 100 µl TE buffer (10 mM Tris-HCl, 1 mM EDTA, pH 8). DNA concentration was measured, as previously described, using a NanoDrop ND-1000 Spectrophotometer.

#### 2.2.2.2 DNA digestion

Restriction enzyme digestions were typically performed upon 2-10 µg of plasmid DNA, using enzymes purchased from New England Biolabs (NEB, UK). Enzymes, DNA and the appropriate buffer were incubated in a total volume of 20-50 µl at 37°C overnight. After incubation, enzymes were heat-inactivated by incubation at 65°C for 10 minutes followed by cooling on ice for 2 minutes. Digestion with multiple restriction enzymes were carried out by selecting the appropriate buffer for the activity of both restriction enzymes, according to the manufacturer's guidelines.

#### 2.2.2.3 Preparation of DNA for Southern analysis

For the analysis of HPV genomes, 5 µg of genomic DNA extracted from cells was subjected to restriction enzyme digest (Table 2.4). All digestions also included the enzyme *DpnI* (NEB) to remove residual input DNA. Digested genomic DNA was analysed by electrophoresis using a 0.8% (w/v) agarose gel. To enable quantification of genome copy numbers, copy number standards were generated by digestion of pGEMII-HPV18 with *EcoRI* (NEB) to release the HPV18 genome from the vector and the equivalent 5 and 50 genome copies/cell were run alongside samples as standards. In the case of HPV16 copy number standards were generated by digestion of pUC-HPV16 with *BamHI* (NEB).

**Table 2.4: Restriction enzymes used to assess HPV genome status**

HPV genome	Restriction Enzyme	
	Linearises genome	Non-cutter
HPV16	<i>HindIII</i>	<i>BamHI</i>
HPV18	<i>EcoRI</i>	<i>BglII</i>

#### 2.2.2.4 Transfer of DNA from agarose gel to nylon membrane

Prior to blotting, the agarose gel was washed twice in 250 mM HCl for 20 minutes (the depurination stage), and twice in 400 mM NaOH for 30 minutes (denaturation and neutralization stages), all at room temperature. To set up the transfer of DNA from the agarose gel to a Gene Screen Plus nylon membrane (Perkin Elmer, UK), a tray was filled with 1 L of 400 mM NaOH and a glass plate rested on top. Three sheets of 24 × 33 cm Whatman<sup>TM</sup> 3MM paper were soaked in 400 mM NaOH, laid across the glass plate with both ends submerged in the NaOH reservoir, and all the bubbles removed. The washed agarose gel was placed on top of this paper wick, with the loading wells facing downwards. A 20 × 22.5 cm sheet of Gene Screen Plus nylon membrane (Perkin Elmer) pre-soaked in NaOH was placed on top. Four layers of 21 × 23.5 cm Whatman<sup>TM</sup> soaked in 0.4 M NaOH were placed onto the membrane and the bubbles removed. On top of this, two stacks of absorbent paper towels were placed, to reach approximately 10 cm in height and covering the filter paper layers, with no gaps between the stacks. A glass plate was placed in top of the towels, and a weight centered on top. The filter paper layer was separated from the wick via plastic wrap placed between the top and bottom filter paper layers. This set up was left overnight for DNA to transfer by capillary action.

Upon disassembly, the position of the loading wells was marked onto the membrane with a pencil, and the DNA crosslinked to the membrane using a UV crosslinker 90 (Stratalinker, Stratagene, UK) on auto-crosslink mode. Following rinsing in 2× saline-sodium citrate (SSC; 300 mM NaCl, 30 mM sodium citrate, pH 7.0), the membrane was stored at -20°C in plastic wrap.

#### *2.2.2.5 Preparation of radiolabelled DNA probe*

In preparation for generation of a HPV18 DNA probe, the pGEMII-HPV18 vector was linearised by *EcoRI* digestion. To generate a HPV16 DNA probe, the pUC-HPV16 vector was linearised by digestion with *BamHI*. Probe DNA was separated from the vector backbone by agarose gel electrophoresis, and purified as previously described. Fifty nanograms of DNA was subsequently diluted into 45 µl of TE buffer and the DNA denatured by heating to 95°C for 5 minutes, followed by incubation on ice slurry for 2 minutes. The denatured DNA was then used as a template for radiolabelled probe generation using the Ready To Go DNA labelling beads-dCTP kit (Amersham Biosciences, UK), according to manufacturer's instructions. Following re-suspension of the labelling beads with the denatured linear DNA, 50 µCi of [ $\alpha$ -<sup>32</sup>P] dCTP (Perkin Elmer) was added and the mixture left to incubate at 37°C for 30 minutes. The labelled probe was purified using an Illustra Probe Quant G-50 microcolumn (Amersham Biosciences), a radiolabelled probe purification kit, following manufacturer's instructions.

#### *2.2.2.6 Hybridisation of radiolabelled probe to DNA*

To prepare the hybridisation buffer, a 2× hybridisation buffer (5× SSC; 750 mM NaCl, 1.5 M sodium citrate, pH 7.0), 10× Denhart's (0.2% w/v ficoll 400, 0.2% w/v polyvinylpyrrolilone, 0.2% w/v BSA fraction V, and 20% w/v dextran sulphate, all Sigma-Aldrich), was diluted with deionized formamide (Sigma-Aldrich) at a 1:1 ratio, and SDS

added to a final concentration of 0.1% (w/v). A 200  $\mu$ l aliquot of 10 mg/ml salmon sperm DNA (Invitrogen) was denatured by heating to 95°C for 5 minutes, cooled on ice slurry for 2 minutes, and subsequently diluted into 10 ml of 1 $\times$  hybridisation buffer; this constituted the pre-hybridisation buffer. The nylon membrane onto which the DNA was immobilised was then defrosted and placed onto a damp square of gauze. Together, the gauze and membrane were rolled and carefully placed into a glass hybridisation canister (Hybaid, UK). The pre-hybridisation buffer was added and the canister incubated in a hybridisation oven (Hybaid), rotating at 42°C for 1 hr, during which hybridisation buffer containing the radiolabelled DNA probe was prepared. A 200  $\mu$ l aliquot of (10 mg/ml) salmon sperm DNA was added to the radiolabelled probe, followed by denaturation 95°C for 5 minutes and cooling on ice slurry for 2 minutes. This was added to 10 ml 1 $\times$  hybridisation buffer. Once the pre-hybridisation buffer was removed, the hybridisation buffer containing the probe was added to the canister and this was incubated overnight, rotating at 42°C.

#### 2.2.2.7 Stringency washes

Following removal from the hybridisation canister, the nylon membrane was rinsed in Buffer I (2 $\times$  SSC, 0.1% w/v SDS), using a sponge to firmly wipe the surface of the membrane to remove excess, unbound probe. The membrane was then washed twice for 15 minutes in the same buffer, with gentle agitation. Two successive 15 minute washes in Buffer II (0.5 $\times$  SSC, 0.1% w/v SDS) followed, and then two 15 minute washes in Buffer III (0.1 $\times$  SSC, 0.1% w/v SDS), both with gentle agitation at room temperature. Following this, the membrane was then washed in Buffer IV (0.1 $\times$  SSC, 1% w/v SDS) at 65°C for 30 min. The membrane was then wrapped in plastic wrap and exposed to autoradiography film (GE Healthcare), in a cassette containing an intensifying screen. In order to slow the  $\beta$ -particles, this was stored at -20°C. Films were typically developed after 24 h and another

after 1 week exposure times, using a Compact ×4 automatic processor (Xograph Healthcare, UK).

### 2.2.3 Bacterial culture

#### 2.2.3.1 *Bacterial growth*

The DH5 $\alpha$  strain of *Escherichia coli* (*E. coli*) was used as a bacterial host for the amplification of plasmid vectors. Bacteria were grown on Agar plates consisting of 5% w/v agar in Luria-Bertani (LB) medium (1% w/v bacto-tryptone, 0.5% w/v bacto-yeast extract, 1% w/v NaCl, all Sigma-Aldrich), which was sterilized by autoclaving. To make up ampicillin plates, the agar medium was melted, cooled to approximately 50°C and ampicillin (Sigma-Aldrich) added to a final concentration of 100  $\mu\text{g}/\text{ml}$ . This was then dispensed into petri dishes in 25 ml aliquots and left in a sterile environment to dry. Excess plates were sealed and stored at 4°C prior to use.

#### 2.2.3.2 *Bacterial transformation*

The chemically competent DH5 $\alpha$  strain was used to amplify plasmids. To do so, *E. coli* was first thawed on ice and 30-50  $\mu\text{l}$  of cells pipetted into a pre-cooled tube. To this, 1-2  $\mu\text{g}$  of plasmid DNA containing ampicillin resistance gene, was added directly into the thawed cells and incubated on ice for 30 min. The *E. coli* were heat shocked at 42°C for 45 seconds, followed by a 2 minute incubation on ice and the addition of 500  $\mu\text{l}$  LB media (1% w/v bacto-tryptone, 0.5% w/v bacto-yeast extract, 1% w/v NaCl). This was incubated at 37°C shaking at 200 rpm for 1 hr. From this, 50-200  $\mu\text{l}$  of transformed cells were plated onto ampicillin agar plates and incubated overnight at 37°C.

A starter culture of transformed cells was prepared by inoculating 6 ml LB media supplemented with 100  $\mu\text{g}/\text{ml}$  antibiotic, with a single bacterial colony and incubating

overnight in a shaker at 37°C. Glycerol stocks were also prepared from the starter culture by the addition of 500 µl of sterile 80% (v/v) glycerol solution to a 500 µl aliquot of bacteria. To amplify bacteria, the 6 ml preparation was added to 200 ml of ampicillin-supplemented LB and grown overnight in a 2 L conical flask, shaking at 200 rpm at 37°C.

#### 2.2.3.3 Storage of *E.coli*

Bacteria were grown from glycerol stocks by streaking out the bacteria across the surface of an agar plate with a sterile fine loop, which was then incubated overnight at 37°C. Transformed bacteria were stored on agar plates for short periods of time at 4°C, or for longer periods of time, stored as a glycerol stock at -80°C. Untransformed stocks of *E.coli* were stored at -80°C.

#### 2.2.3.4 Purification of plasmid DNA

Following incubation overnight in 200 ml LB supplemented with antibiotic, the overnight culture was pelleted by centrifugation at 13,000 rpm in a Sorvall GS3 rotor at 4°C for 20 min. Amplified plasmid DNA was extracted using the QIAprep Spin MaxiPrep Kit (Qiagen), following manufacturer's instructions. The purification procedure involved lysis of bacterial cells using alkaline lysis buffer, adsorption of plasmid DNA onto a silica filter in the presence of high salt buffer, followed by washing and elution of plasmid DNA from that filter.

Plasmid DNA was precipitated by the addition of 0.7 volumes of isopropanol (Thermo Fisher Scientific) and the sample was then centrifuged at  $3000 \times g$  in a Sorvall SS-34 rotor for 40 minutes at 4°C. The pellet was then washed with 5 ml 70% (v/v) ethanol and centrifuged for a further 15 minutes at 4°C. DNA was air-dried and resuspended in 50 µl of  $1 \times$  Tris-EDTA (TE) buffer for storage at 4°C (short term) or -20°C (long term). The concentration of DNA was determined by spectrophotometry (Nanodrop).

### 2.2.3.5 Plasmid vectors

The pGEMII-HPV18 plasmid contains the total HPV18 genome (accession number: NC 001357) cloned into the pGEMII vector at the *EcoRI* restriction site at residue 2440. The pUC-HPV16 plasmid contains the total HPV16 genome cloned into the pUC vector at the *BamHI* restriction site. The HPV18 genome containing plasmid was a gift from Frank Stubenrauch, University of Tübingen, and the HPV16 114/K (HPV16K) and 114/B (HPV16B) containing plasmids were both provided by Ethel de Villiers, the German Cancer Research Centre, Heidelberg.

### 2.2.3.6 Preparation of HPV genomes for transfection

To extract the HPV18 genome from the bacterial vector, 10 µg of pGEMII-HPV18 wild type or mutant genomes were digested with *EcoRI*. Similarly, the HPV16 genome was extracted from the pUC-HPV16 genome by digestion with *BamHI*; both digestions occurred in a total volume of 50 µl and were incubated overnight at 37°C. Digested HPV genomes were recircularised in 900 µl total volume ligation reaction mix with T4 DNA ligase containing 400 units/ml (NEB), to encourage self-ligation of the HPV genomes. This was incubated overnight at 16°C. HPV DNA was then precipitated by the addition of 2 volumes of isopropyl alcohol and 1/5 volume of 5 M NaCl, followed by vortexing and subsequent incubation at -20°C overnight. DNA was pelleted by centrifugation at 16,100 × *g* for 30 minutes at 4°C, the supernatant removed and the pellet washed with 70% ethanol (pre-cooled to -20°C), prior to centrifugation at 16,100 × *g* for a further 15 minutes at 4°C. The supernatant was subsequently removed and the DNA pellet resuspended in 12 µl of 1× TE buffer. The DNA concentrations were then estimated by running a 1 µl aliquot on an agarose gel alongside 1 µl of DNA marker (1 µg/ml, 1kb plus ladder, Invitrogen)

## 2.2.4 Protein analysis

### 2.2.4.1 Protein extraction and preparation

Cells were harvested by trypsinisation, washed twice with PBS and finally with ice-cold saline. Pelleted cells were lysed in RIPA (50 mM Tris-HCl pH 7.5, 150 mM NaCl, 1% v/v SDS, 2% sodium deoxycholate, 1% v/v Triton-x-100), UTB or NP40 (200 mM Tris-HCl pH 7.5, 150 mM NaCl, 0.5% v/v NP40, Sigma-Aldrich) lysis buffers, as appropriate and incubated on ice for 20 minutes and then sonicated for ten seconds at 2 watts. This was then centrifuged at 4°C for 20 minutes at  $16000 \times g$ , to remove the insoluble fraction. The amount of protein was quantified by Bradford assay. Bradford reagent (Biorad) was diluted 1:4 in distilled water, and standards of bovine serum albumin (BSA) at 4, 8, 12, 16 and 20  $\mu\text{g}/\text{mL}$  set up. The standard curve was set up and absorbance measured using an Eppendorf Biophotometer (Eppendorf).

Prior to loading, the protein of samples were heated to 95°C in an equal volume of 2 $\times$  Laemmli buffer (Sigma-Aldrich) supplemented with 5% (v/v)  $\beta$ -mercaptoethanol, for 5 min, cooled on ice and spun quickly to collect the contents of the tube.

### 2.2.4.2 Sodium dodecyl sulphate polyacrylamide gel electrophoresis (SDS-PAGE)

Sodium dodecyl sulphate polyacrylamide gel electrophoresis (SDS-PAGE) gels were set up in two phases using the mini-Protean 3 Bio-rad apparatus. A 10 or 12% resolving gel containing 30:1 acrylamide:bisacrylamide (Bio-rad), 390 mM Tris-HCl pH 8.8, 0.1% w/v SDS (Sigma-Aldrich), 0.06% w/v N,N,N',N'- tetramethylethylenediamine (TEMED, Sigma-Aldrich) and 0.1% w/v ammonium persulphate (APS, Sigma-Aldrich) was made. A layer of isopropanol was applied to the top to give a uniform surface. Once this had set, the isopropanol was removed and a stacking gel containing 3% acrylamide, 125 mM Tris-HCl pH 6.8, 0.1% w/v SDS, 0.1% w/v TEMED and 0.1% w/v APS was poured on top of

the resolving gel, a comb was placed in the stacking gel and allowed to set for 30 min. Protein lysates were added to equal volumes of loading buffer (5% v/v  $\beta$ -mercaptoethanol in Laemmli buffer), heated at 95°C for 5 min, cooled on ice and centrifuged quickly to collect. Samples were then loaded into each SDS-PAGE gel well alongside a lane containing 7  $\mu$ l of ColorPlus Prestained protein ladder (NEB), and separated by electrophoresis at 100V for 1 hr. Gels were run using Mini Protean® 3 Cell (BioRad) tanks, containing 1 $\times$  running buffer consisting of 25 mM Tris-HCl pH 7.5, 2 mM glycine (Thermo Fisher Scientific) and 10% SDS.

#### *2.2.4.3 Electrophoretic protein transfer*

Two pieces of sponge, two pieces of Whatman™ chromatography paper (Sigma-Aldrich) and one piece of BioTrace NT membrane (VWR International, UK), cut to gel size, were soaked in transfer buffer (25 mM Tris-HCl pH 7.5, 2 mM glycine, 20% v/v methanol in distilled water). The ‘transfer sandwich’ was set up in (BioRad), ensuring air bubbles were pushed out between each layer, in the following order: sponge, filter paper, gel, BioTrace NT membrane, filter paper, sponge. The transfer module was then placed into the transfer tank (BioRad) and filled with transfer buffer. Protein was then transferred from the gel to the BioTrace NT membrane at 350 mA for 3 hr.

#### *2.2.4.4 Protein visualisation*

Successful transfer was assessed by Ponceau S stain (0.1% w/v Ponceau S, 5% acetic acid), which was then rinsed off in phosphate- or Tris-HCl-buffered saline (PBS or TBS) as appropriate. Non-specific protein binding was blocked by incubating the membrane for 1 h at room temperature in 2-5% (w/v) non-fat milk (Marvel, Premier Foods) or 2% (w/v) BSA (Sigma-Aldrich) dissolved in PBS or TBS. The membrane was incubated overnight at 4°C in primary antibody, diluted in the appropriate milk/BSA PBS/TBS solution (see

Table 2.5). To assess for equal loading, the levels of housekeeping genes  $\beta$ -actin or GAPDH were determined using a mouse anti- $\beta$ -actin monoclonal antibody, or mouse anti-GAPDH antibody, respectively. After three 15 minute washes in TBS or PBS with 0.1% (v/v) Tween-20, the membrane was incubated for 1 h in HRP-conjugated secondary IgG (Table 2.6) and then washed as before, with the last wash in TBS or PBS without Tween. Antibody-protein complexes were detected using the enhanced chemiluminescence (ECL) kit (Amersham Biosciences). 1 ml of each ECL reagent was mixed in a universal tube immediately prior to use. The membrane was incubated in the ECL mixture for 1 minutes before being wrapped carefully in plastic wrap and placed into an autoradiography cassette, containing X-ray film (Hyperfilm™, Amersham Biosciences) and developed for between 30 seconds to 1 hr, using a Compact  $\times 4$  automatic processor (Xograph Healthcare) at various exposure times (typically 30 seconds, 5 minutes and 30 minutes).

#### *2.2.4.5 Generation of DLG1 $\alpha$ specific antibody*

An immunogenic peptide was selected from the N-terminus sequence unique to DLG1 $\alpha$ . This peptide (KGSSDELQAEPEPSR) was inoculated into rabbits by a commercial company (Generon, UK). The subsequent antibody (DLG1 $\alpha$  1524) recognised the peptide in ELISA based assay (performed by Generon). Rabbit serum extracted before exposure to immunogen (pre-immune) was taken for use as a control for non-specific binding.

### 2.3 Immunocytochemical techniques

#### 2.3.1 Immunofluorescence

A heat-induced epitope retrieval (HIER) technique using an EDTA buffer was applied to paraffin-embedded and formalin-fixed samples, in order to unmask the antigens in the

formalin-fixed sections and thus enhance the staining intensity of antibodies (Watson *et al.*, 2002). Firstly, 4 nm raft sections were incubated for 5 minutes in Histo-Clear™ (National Diagnostics, UK), to clear the paraffin. This was followed by hydration for 15 minutes in 100% ethanol (IMS). Slides were then rinsed three times in water, incubated for 10 minutes in 0.3% (v/v) hydrogen peroxide, and washed three times in water again. The sections were immersed overnight in EDTA buffer (1 mM EDTA NaOH pH 8, 0.1% v/v Tween) heated to 65°C and continually agitated on a stirrer.

Retrieved raft sections were blocked in 5% v/v heat-inactivated goat serum (HINGS) with 0.1% w/v BSA in PBS, for 1 h at room temperature. During the staining procedure, incubations took place in a humidified chamber, in order to prevent the evaporation of solutions. Primary antibody was made up in blocking buffer, applied to raft sections and incubated overnight at 4°C. Excess antibody was removed by washing slides in agitated PBS for 10 min, three times. The appropriate secondary fluorophore-conjugated antibody (Molecular probes®, Life Technologies), made up in the same blocking buffer, was applied to each slide, incubated for an hour at 37°C and washed in agitated PBS as before. The final wash contained 1 µl of 4',6-diamidino-2-phenylindole (DAPI, Sigma-Aldrich), a blue (461 nm) fluorescent stain that binds strongly to A-T rich regions of DNA, highlighting the nuclei of cells. Slides were mounted onto coverslips in 80% (v/v) glycerol in PBS containing 2% 4-Diazabicyclo-2,2,2-octane (DABCO, Sigma-Aldrich) and visualized on a Nikon Eclipse E600 microscope (Nikon, USA). Images were captured using a Leica DC200 camera and software. Slides were stored at -20°C.

## 2.4 Computational methods

### 2.4.1 Protein and nucleotide sequence alignment

Protein and nucleotide sequences were obtained from NCBI and Ensembl databases (<http://www.ncbi.nlm.nih.gov>, Altschul *et al.*, 1990 and <http://www.ensembl.org/index.html>, Flicek *et al.*, 2014), and sequence alignments were performed using ClustalW software (<http://www.ebi.ac.uk/Tools/msa/clustalw2/>, Larkin *et al.*, 2007). Nucleotide sequences resulting from sequencing reactions were aligned using the NCBI basic local alignment search tool (BLAST, <http://blast.st-va.ncbi.nlm.nih.gov/Blast.cgi>, Altschul *et al.*, 1990), which finds regions of similarity between sequences, and compares sequences to sequence databases and calculates the statistical significance of matches (Altschul *et al.*, 1990; Johnson *et al.*, 2008).

### 2.4.2 Protein motif prediction

Protein sequences were analysed for hypothetical secondary structure motifs using the programs Scansite ([www.scansite3.mit.edu](http://www.scansite3.mit.edu), Obenauer *et al.*, 2003), and Prosite (<http://prosite.expasy.org>, Sigrist *et al.*, 2010). These sites scan an input amino acid sequence and, using a database of consensus sequences, provide a prediction and probability score for the presence of secondary structure motifs found within that sequence.

### 2.4.3 Nucleotide motif analysis

Splice site analysis was performed using nucleotide sequences from DLG1 variants, and from sequencing data. Analysis was performed on more than one platform; the Maximum Entropy ([http://genes.mit.edu/burgelab/maxent/Xmaxentscan\\_scoreseq.html](http://genes.mit.edu/burgelab/maxent/Xmaxentscan_scoreseq.html), Yeo and Burge, 2004) program and the Human Splicing Finder (HSF, <http://www.umd.be/HSF/>, Desmet *et al.*, 2009), which are designed to predict the effects of mutations on splicing

signals or to identify splicing motifs in any human sequence. Results were also compared to known splice site recognition motifs (Harris and Senapathy, 1990; Srebrow and Kornblihtt, 2006; Ghigna *et al.*, 2008).

#### 2.4.4 Densitometry analysis

Western blot films were scanned in and .tif images analysed using ImageJ software (Schneider *et al.*, 2012). Once quantified, the area values for absorbance peaks were transferred to Microsoft Excel, where normalising and comparison calculations took place and graphs created.

**Table 2.5: Primary antibodies used in western blotting and immunofluorescence**

Category	Protein detected	Size (kDa)	Supplier/No.	Animal	Dilution for WB	Dilution for IF
PDZ Proteins	DLG1	135	NAG	Rabbit	1/1000	1/500
			Santa Cruz 2D11	Mouse	1/1000	1/30
			Santa Cruz H-60	Rabbit	1/500	-
			NT- Gift from L. Banks	Rabbit	1/500	-
			I2 specific, Roberts Lab	Rabbit	1/200	-
			I3 specific	Rabbit	1/200	-
	INADL	196	Gift from R. Javier	Rabbit	1/200	-
	NHERF1	50	BD Biosciences	Mouse	1/500	1/500
	PTPN13	250	Santa Cruz	Rabbit	1/300	1/50
	SCRIB	210	Santa Cruz	Goat	1/2000	1/100
	MAGI-1	120,130, 170	Sigma	Rabbit	1/500	-
	MUPP-1	219	Gift from R. Javier	Rabbit	1/500	-
	PARD3	151	Sigma	Rabbit	1/500	-
CASK	105	Cell Signaling Technology	Rabbit	1/400	1/50	
ZO-2	134	Cell Signaling Technology	Rabbit	1/500	1/100	

	ZO-1	240	BD Biosciences	Mouse	1/1000	1/100
<b>Housekeeping Genes</b>	p53	53	Gift from R. Grand	Mouse	1/100	1/10
	$\beta$ -actin	42	Sigma	Mouse	1/50000	-
	GAPDH	37	Santa Cruz	Mouse	1/3000	-
	Keratin 18	46	Sigma CK5	Mouse	1/1000	-
	E-Cadherin	120/80	BD Biosciences	Mouse	1/1000	-
	GRB2	25	Cell Signaling Technology	Rabbit	1/1000	-
	HPV18 E6	17	Santa Cruz	Mouse	1/100*	-
<b>HPV proteins</b>	Phosphorylated HPV18 E6	17	Gift from L. Banks	Rabbit	1/200*	-
	HPV18 E7	17	Abcam	Mouse	1/1000	-
	HPV18 E4	12	R424	Rabbit	1/5000	1/1000
	HPV18 E4	12	1D11	Mouse	-	1/10
	<b>Signalling Proteins</b>	14-3-3 $\zeta$	30	Santa Cruz	Rabbit	1/1000

Antibodies were diluted in 2% w/v Milk (Marvel) PBS, \* indicates requirement for 2% w/v BSA PBS.

**Table 2.6: Secondary antibodies used in western blotting and immunofluorescence**

Category	Protein detected	Isotype	Supplier	Animal	Dilution for WB	Dilution for IF
<b>Secondary Antibodies (HRP conjugated)</b>	Anti-mouse HRP	-	Sigma	Goat	1/3000	-
	Swine anti-rabbit HRP	-	Sigma	Swine	1/2000	-
	Rabbit anti-Goat HRP	-	Sigma	Rabbit	1/2000	-
<b>Secondary Antibodies (Fluorophore conjugated)</b>	AlexaFluor® 488 anti-mouse	IgG	Invitrogen	Goat	-	1/3000
	AlexaFluor® 594 anti-goat	IgG2a	Invitrogen	Rabbit	-	1/3000
	AlexaFluor® 594 anti-rabbit	IgG	Invitrogen	Rabbit	-	1/3000

Antibodies were diluted in 5% v/v heat-inactivated goat serum (HINGS) with 0.1% w/v BSA in PBS

## 2.5 List of suppliers

Abcam, 330 Cambridge Science Park, Cambridge, CB4 0FL, UK

Agilent Technologies, 5301 Stevens Creek Blvd, Santa Clara, CA 95051, USA

Alta Biosciences, University of Birmingham, Edgbaston, Birmingham, B15 2TT, UK

Amersham Pharmacia Biotech UK Ltd, Amersham Place, Little Chalfont, Bucks, HP7 9NA, UK

AMS Biotechnology Limited, 184 Park Drive, Milton Park, Abingdon, OX14 4SE, UK

Applied Biosystems, Lingley House, 120 Birchwood Boulevard, Birchwood, WA3 7QH, UK

BD Biosciences, Edmund Halley Road, Oxford Science Park, OX4 4DQ, UK

BioRad Laboratories Ltd., Maxted Road, Hemel Hempstead, Hertfordshire, HP2 7DX, UK

Cell Signaling Technology Inc., 3 Trask Lane, Danvers, MA 01923, USA

Clonetics Biowhittaker, 8830 Biggs Ford Rd, Walkersville, MD 21793-8415, USA

DAKO UK Ltd, Cambridge House, St Thomas Place, Ely, CB7 4EX, UK

EMD Millipore Headquarters, 290 Concord Road, Billerica, MA 01821, USA

Eppendorf UK Ltd, Endurance House, Chivers Way, Histon, Cambridge, CB24 9ZR, UK

GE Healthcare, Pollards Wood, Nightingales Lane, Chalfont St Giles, Bucks, HP8 4SP, UK

Genron Ltd., 12 Rawcliffe House, Howarth Road, Maidenhead, Berkshire, SL6 1AP

Gibco-Invitrogen, 3 Fountain Drive, Inchinnan Business Park, Paisley, PA4 9RF, UK

Hycor Biomedical Ltd., Douglas House, Bush Loan, Penicuik, Midlothian, EH26 0PL, UK

Hybaid Ltd, Solaar House, 19 Mercers Row, Cambridge, CB5 8BZ, UK

Invitrogen, 1600 Faraday Avenue, Carlsbad, CA 92008, USA

Life Technologies, 3 Fountain Drive, Inchinnan Business Park, Paisley, PA4 9RF, UK

MP Biomedicals Inc., 1263 S. Chillicothe Road, Aurora, OH 44202, USA

National Diagnostics, Unit 4 Fleet Business Park, Itlings Lane, Hessle, Yorkshire HU13 9LX

New England Biolabs, 240 County Road, Ipswich, MA 01938-2723, USA

Nikon Inc, 1300 Walt Whitman Road, Melville, NY 11747-3064, USAPAA Laboratories Ltd, Termate Close, Houndstone Business Park, Yeovil, BA22 8YG, UK

Perkin Elmer Ltd, Post Office Lane, Beaconsfield, Buckinghamshire, HP9 1QA, UK

Promega, Delta House, Chilworth Research Centre, Southampton, SO16 7NS, UK

Propath, Willow Court, Netherwood Road, Hereford, HR2 6JU, UK

Qiagen, QIAGEN House, Fleming Way, Crawley, West Sussex, RH10 9NQ, UK

Roche Diagnostics, Bell Lane, Lewes, East Sussex, BN7 1LG, UK

SantaCruz Biotechnology Inc., Bergheimer Str. 89-2, 69115 Heidelberg, Germany

Sigma-Aldrich Company Ltd., Fancy Road, Poole, Dorset, BH12 4QH, UK

Starlab (UK) Ltd., 5 Tanners Drive, Blakelands, Milton Keynes, MK14 5BU, UK

Stratagene, 11011 N. Torrey Pines Road, La Jolla, CA 92037, USA

Syngene (UK), Beacon House, Nuffield Road, Cambridge, CB4 1TF, UK

Takara Bio Europe (Clontech), 2 Avenue du President Kennedy, 78100 Saint-Germain-en-Laye, France

Thermo Fisher Scientific Ltd, Bishop Meadow Road, Loughborough, LE11 5RG, UK

Vector Laboratories Ltd., 3 Accent Park, Bakewell Road, Orton Southgate, PE2 6XS, UK

VWR International Ltd., Hunter Boulevard, Magna Park, Lutterworth, LE17 4XN, UK

Xograph Healthcare, Xograph House, Ebley Road, Stonehouse, Gloucestershire, GL10 2LU, UK

Zeiss, 15 - 20 Woodfield Road, Welwyn Garden City, Hertfordshire, AL7 1JQ, UK

## CHAPTER 3: THE INVESTIGATION OF PDZ PROTEIN EXPRESSION DURING THE HPV LIFE CYCLE

### 3.1 Introduction

The E6 PBM is a highly conserved feature of high-risk  $\alpha$ -papillomaviruses types, which is a strong indication that a PDZ targeting function is important in the life cycle of this group of viruses (Figure 3.1). This concept was reinforced by the discovery of a PDZ binding motif in the E7 protein of fellow papillomavirus RhPV and the identification of a mode of PDZ targeting by HPV8 (Tomaic *et al.*, 2009; Lazic *et al.*, 2012). The human genome encodes over 300 PDZ domain-containing proteins and to date seventeen of these have been identified as targets of high-risk E6 proteins (Table 3.1), with several more suggested from high-throughput screening experiments (Belotti *et al.*, 2013). The identified PDZ substrates of E6 comprise a number of proteins involved in a range of functions, including defining cell polarity, cell-cell attachment, and organising cell signalling pathways associated with these functions (Figure 1.10, Table 3.1).

The first proteins shown to interact with the E6 PBM were the Scribble complex components DLG1 and SCRIB (Kiyono *et al.*, 1997; Nakagawa and Huibregtse, 2000). The second PDZ domain of DLG1 is required for HPV16 E6 binding, whereas HPV18 E6 is able to bind all three DLG1 PDZ domains independently (Gardiol *et al.*, 1999; Kiyono *et al.*, 1997). Moreover, of the four PDZ domains encoded by SCRIB, HPV binds to only one (PDZ3); indicating a specificity in HPV PDZ targeting, even within a protein (Nakagawa and Huibregtse, 2000). It was further discovered that the co-expression of HPV16 or HPV18 E6 alongside the PDZ proteins induced their degradation by the proteasome, and that E6\*, a spliced isoform of E6 which lacks a PBM, is able to target endogenous DLG1, and to a lesser extent SCRIB, for degradation (Gardiol *et al.*, 1999; Nakagawa and

		Consensus motif	
		$X^S_T X^L_V$	
<b>Group 1</b>			
HPV 16	CMSCC	RSSRTRRETQ	L
HPV 18	CHSCCNRARQE	RLQRRRETQ	V
HPV 31	CIVCW	RRPRRETQ	V
HPV 33	CAACW RS	RRRETAL	
HPV 35	CMSCW	KPTRRETEV	
HPV 39	CRRCWTTKRED	RRLTRRETQ	V
HPV 45	CNTCCDQARQE	RLRRRRETQ	V
HPV 51	CANCW Q	RTRQRNATQ	V
HPV 52	CSECW	RPRPVTQ	V
HPV 56	CLGCW RQ	TSREPRESTV	
HPV 58	CAVCW	RPRRRQTQ	V
HPV 59	CRGCRTRARHLRQQRQARSETV		
<b>Group 2A</b>			
HPV 68	CRHCWTSKRED	RRRTRQETQ	V
<b>Group 2B</b>			
HPV 26	CTNCW	RPRRQTETQ	V
HPV 30	CLQCW	RHTTSTETAV	
HPV 34	CRQCW	RPSATVV	
HPV 53	CLTCW	RHTTATESAV	
HPV 66	CLQCW	RHTSRQATESTV	
HPV 67	CSVCW	RPQRTQTQ	V
HPV 69	CTNCW	RPRREATETQ	V
HPV 70	CRHCWTSNRED	RRRIRRETQ	V
HPV 73	CTRCW	RPSATVV	
HPV 82	CANCR TAA	RQRSETQ	V
HPV 85	CRRCMTRA QE	QQGSRRETQ	V
HPV 97	CNSCYNQSRQE	RLSRRRETQ	V
HPV 8	CRLCKHLYHDW		
<b>Group 3</b>			
HPV 6	CLHCWTTMED	MLP	
HPV 11	CLHCWTTMED	LLP	

**Figure 3.1: C-terminal alignment of high- and low-risk  $\alpha$ -HPV E6 proteins**

To date, twelve HPV types have been defined by the WHO as high-risk with respect to causing cancer - these are designated as IARC Group 1- and a further ten types are recognised as ‘probably’ (Group 2A) and ‘possibly’ cancer-causing (Group 2B). HPV6 and 11 are included as examples of low risk virus. HPV8 is a  $\beta$ -papillomavirus associated with cutaneous SCC, and has been shown to effect the transcription of PDZ protein Syntenin-2.

The canonical PBM sequence ( $X^S_T X^L_V$ ) is shown above the highlighted region, which indicates the E6 PBM sequence.

Huibregtse, 2000; Pim *et al.*, 2009). It has been suggested that SCRIB degradation by E6 is dependent upon the oncoprotein binding to the cellular ubiquitin ligase E6AP, and that this is not the case for DLG1; E6-mediated degradation of DLG1 still occurs in the absence of E6AP (Pim *et al.*, 2000; Nakagawa and Huibregtse, 2000; Grm and Banks, 2004; Massimi *et al.*, 2008). However, studies also demonstrated only a modest rescue of DLG1 and SCRIB in HPV-positive cancer cell lines where E6AP is silenced, suggesting that other cellular ligases may be recruited, the identity of which remain elusive (Kranjec and Banks, 2011; Massimi *et al.*, 2008). Furthermore, E6AP was initially identified as important in the E6-mediated degradation of DLG4 in co-expression studies, but this was not observed in HPV-positive cancer cell lines, indicating that the different cellular conditions may contribute to the mechanism of E6-mediated PDZ protein degradation (Handa *et al.*, 2007; Kranjec and Banks, 2011). Although co-expression studies have demonstrated E6-mediated DLG1 degradation, endogenous levels of DLG1 and SCRIB protein remain unaltered in primary human keratinocytes expressing HPV16 E6 and E7 (Choi *et al.*, 2013; Lee *et al.*, 2000; Lee and Laimins, 2004). In addition, no change in abundance or subcellular localisation of these PDZ proteins was observed in HPV31 genome containing HFKs (Lee and Laimins, 2004). Furthermore, in mice expressing HPV16 E6 under the K14 promoter, no change was observed in DLG1 or SCRIB protein levels or distribution compared to the equivalent skin of non-transgenic mouse (Simonson *et al.*, 2005). These discrepancies between *in vitro* and *in vivo* experimental results highlight differences between the experimental models and the requirement to validate these targets in a relevant model of the HPV life cycle.

The Par complex includes PDZ proteins PARD3 and PAR6, and the complex associates with MUPP1 and the MAGUK family members MAGI-1, -2 and -3 (Figure 1.10). MUPP1 has been identified as a target of HPV18 E6, leading to degradation of the PDZ protein

(Lee *et al.*, 2000). In addition, MAGI-1, -2 and -3 have all been shown to be targeted for degradation by HPV16 and HPV18 *in vitro* (Glaunsinger *et al.*, 2000; Thomas *et al.*, 2002). Moreover, E6 mediated degradation was demonstrated in the HPV16 and 18 positive cancer cell lines Caski and HeLa, where the oncoprotein was shown to target membrane bound and nuclear pools of MAGI-1 (Kranjec and Banks, 2011).

Conversely, the recently shown interaction between HPV18 E6 and PARD3 does not lead to degradation of the PDZ protein (Facciuto *et al.*, 2014). Instead, it was observed that HPV18 E6 redistributes the protein; a loss of PARD3 from the apical domain cell junctions and an increase in cytoplasmic and nuclear protein was observed when the viral protein was expressed (Facciuto *et al.*, 2014). In addition, cellular protein TIP-1 was identified as interacting with HPV16 E6, but no degradation of the protein was seen during co-expression of the two proteins (Hampson *et al.*, 2004). It was also observed that knockdown of endogenous E6 in Caski and HeLa did not affect TIP-1 protein levels (Kranjec and Banks, 2011), reiterating that not all known E6 PDZ interactions promote PDZ protein degradation.

The Crumbs complex protein PATJ associates with both HPV16 and HPV18 E6, via its fourth and fifth PDZ domains (Storrs and Silverstein, 2007). The resulting PATJ degradation does not require E6AP, and was the first example of a PDZ substrate degraded by E6\* and thus revealed an alternative method of E6 association with PDZ proteins (Storrs and Silverstein, 2007).

The signalling proteins PTPN13, PTPN3 and NHERF1 have also been identified as targets of high-risk HPV E6 proteins. Jing *et al.* and Töpffer *et al.* showed that both HPV16 and HPV18 target the protein tyrosine phosphatase PTPN3, and that resulting degradation of the phosphatase is dependent upon both E6AP and proteasome. However, silencing of E6 in HeLa and Caski cervical cancer cell lines does not rescue PTPN3 protein levels and, as

PTPN13 decreases in these conditions, it was suggested that E6 and E7 stabilises PTPN13 in the cancer cell lines (Kranjec *et al.*, 2014). In primary keratinocytes, expression of HPV16 E6 using retroviral vectors induced the PBM-dependent degradation of PTPN13, and expression of both HPV16 and HPV18 E6 led to the proteasomal degradation of NHERF1 (Spanos *et al.*, 2008b; Accardi *et al.*, 2011). In the latter experiments, HPV16 E7 activation of CDKs promoted NHERF1 phosphorylation and E6 preferentially targeted these phosphorylated forms for proteasome-mediated degradation in a PBM-dependent manner (Accardi *et al.*, 2011). These findings suggest a cooperative mechanism of action on the PDZ protein NHERF1.

More recently, immunoprecipitation and yeast two hybrid screening experiments have identified interactions between the HPV16 E6 PBM and the known interacting proteins DLG1, SCRIB, MAGI-1, MAGI-3, MUPP1 and PTPN3 as well as highlighting potential novel targets SNTA1, SNTB1, SNX27, CASK and LIN7C (Belotti *et al.*, 2013). Similar methods were used to identify TIP-2, a known target of HTLV-1 Tax, as an interacting protein of HPV18 E6 (Favre-Bonvin *et al.*, 2005; Rousset *et al.*, 1998), and GOPC as able to interact with both HPV16 and HPV18 E6 PBM sequences (Jeong *et al.*, 2007). Most recently, PDZRN3 has been identified as a target for proteasomal degradation by both HPV16 and HPV18 E6 (Thomas and Banks, 2014). Silencing of E6 in the HPV18 positive HeLa cells rescued PDZRN3 protein levels (Thomas and Banks, 2014).

High-risk HPV E6 proteins exhibit differing specificities for cellular PDZ proteins. (Kranjec and Banks, 2011). For example, both HPV16 and HPV18 E6 proteins are able to target DLG1 and SCRIB, but exhibit different preferences in binding the PDZ proteins; HPV16 E6 preferentially binds SCRIB over DLG1 and *vice versa* for HPV18 (Thomas *et al.*, 2005, ). The PBM of these two oncoproteins only differs by a single amino acid and, notably, the specificity for DLG1 and SCRIB can be switched within the context of the

whole E6 protein by switching the last residue (Thomas *et al.*, 2005). In the same study, HPV18 exhibited a stronger affinity for MAGI-1 than HPV16 (Thomas *et al.*, 2005). Similarly, GOPC was found to bind more strongly to HPV16 E6 than HPV18 and DLG4 has been shown to be a stronger target for HPV18 than for HPV16 (Handa *et al.*, 2007; Kranjec and Banks, 2011). PDZ targeting by E6 is also specific to subcellular localisation; the cytoplasmic and nuclear pools of both DLG1 and MAGI-1 are preferentially targeted by HPV18 for degradation over protein at cell-cell contacts (Massimi *et al.*, 2004; Kranjec and Banks, 2011; Narayan *et al.*, 2009).

Interestingly, Lazic *et al.* revealed that expression of the skin-cancer associated HPV8 E6 significantly downregulated syntenin-2 transcription, with HPV16 E6 also producing a decrease in syntenin-2 mRNA, but to a lesser extent (Lazic *et al.*, 2012). This study suggests alternative mechanisms by which HPVs modify PDZ protein expression, a field that requires further investigation.

While the E6 PDZ interaction is highly specific, it has been suggested that, at high enough concentrations, the E6 PBM may recognize any class I PDZ domain (Zhang *et al.*, 2007). Thus, analyses in overexpression conditions are more analogous to the interactions during HPV-driven oncogenesis (Zhang *et al.*, 2007). In terms of interactions with cellular targets, it is unclear which are the important PDZ targets in driving HPV propagation and, indeed, they may vary at different stages of the HPV life cycle.

Table 3.1: PDZ proteins associated with high-risk HPV E6 proteins

PDZ protein (Gene Symbol)	Alternative Name(s)	Cellular Functions	Effect of Interaction with E6	References
<u>DLG1</u>	SAP97	Cell polarity, proliferation, migration and adhesion	Degradation, Mislocalisation	Kiyono <i>et al.</i> , 1997 Gardiol <i>et al.</i> , 1999
<u>SCRIB</u>	Scribble, Vartul, LAP4	Cell polarity and integrity, proliferation, apoptotic signalling	Degradation	Nakagawa and Huijbregtse, 2000
<u>INADL</u>	PATJ	Tight junction formation, cell polarity	Degradation	Latorre <i>et al.</i> , 2005; Storrs and Silverstein, 2007
SLC9A3R1	<u>NHERF1</u> , EBP50	GPCR regulation, cytoskeleton anchoring	Degradation	Accardi <i>et al.</i> , 2011
<u>PTPN13</u>	FAP-1, PTPL-1, PTP-BAS, PTPBL	Fas-associated phosphatase, cell growth signalling, apoptotic signalling	Degradation	Spanos <i>et al.</i> , 2008b
MPDZ	<u>MUPP1</u>	Receptor clustering, scaffold protein	Degradation	Lee <i>et al.</i> , 2000
<u>MAGI-1</u>	AIP3, WWP3	Cell polarity, invasiveness, synapse formation, apoptosis	Degradation	Glaunsinger <i>et al.</i> , 2000
<u>MAGI-2</u>	AIP1	Cell polarity, invasiveness, synapse formation, apoptosis	Degradation	Thomas <i>et al.</i> , 2002
<u>MAGI-3</u>	-	Cell polarity, invasiveness, synapse formation, apoptosis	Degradation	Thomas <i>et al.</i> , 2002
<u>DLG4</u>	PSD95, SAP90, TIP15	Receptor clustering	Degradation	Handa <i>et al.</i> , 2007
<u>PTPN3</u>	PTPH1	Phosphatase, cell growth signalling, apoptotic signalling	Degradation	Jing <i>et al.</i> , 2007; Töpffer <i>et al.</i> , 2007
TAX1BP3	<u>TIP-1</u>	Wnt pathway inhibitor	-	Hampson <i>et al.</i> , 2004
GIPC1	Synectin, <u>TIP-2</u>	Cell surface receptor expression and trafficking, TGF $\beta$ signalling	Degradation	Favre-Bonvin <i>et al.</i> , 2005
GOPC	CAL	Intracellular trafficking	Degradation	Jeong <i>et al.</i> , 2007
<u>PARD3</u>	PAR3	Cell polarity, assymetrical cell division	Mislocalisation	Facciuto <i>et al.</i> , 2014
SDCBP2	<u>Syntenin-2</u>	Cell adhesion, growth factor signalling	Decreased transcription	Lazic <i>et al.</i> , 2012
PDZRN3	<u>LNX3</u>	E3 ubiquitin ligase	Degradation	Thomas and Banks, 2014

### 3.2 Hypothesis and Aims

Studies to date have demonstrated that the high-risk HPV E6 PBM interacts with PDZ targets, yet the function of the E6 PBM in the context of the viral life cycle, where E6 is expressed at physiological levels, remains to be investigated. This study aims to investigate within the context of a physiologically relevant model of the HPV16 and HPV18 life cycle to identify relevant PDZ protein targets of the E6 PBM.

Thus, using a primary human foreskin keratinocyte (HFK) model of the HPV life cycle, the experiments described in this chapter aimed to:

- i. Investigate the effect of HPV16 or HPV18 replication on transcription of E6 PDZ targets.
- ii. Determine the abundance and distribution of E6 PDZ targets in HPV genome containing cells.

### 3.3 Results

#### 3.3.1 Generation of cell-based models of the HPV16 and HPV18 life cycle

In order to study the life cycle of high-risk HPVs, primary human keratinocyte cell lines containing HPV16 and 18 genomes were generated in two donor backgrounds. Two separate HPV16 genome variants were utilised, 114/B (HPV16B) and 114/K (HPV16K). Variants are defined by having a less than 2% difference in the L1 ORF nucleotide sequence compared to the reference genome (Chen *et al.*, 2011; Chan *et al.*, 1995). Both HPV16B and HPV16K were originally derived from productive cervical lesions, and differ by a single amino acid; L1 asparagine 379 in HPV16K is replaced by a histidine residue in HPV16B (Kirnbauer *et al.*, 1993). Early passage (p2) primary foreskin keratinocytes were co-transfected with the recircularised viral genomes and a neomycin resistance plasmid (see Section 2.1.4.4). Following drug selection and growth of cells, the presence of viral DNA was confirmed by Southern blot analysis (Section 2.2.2). Analysis of early passages of HPV16 and HPV18 genome containing keratinocytes confirmed the presence of HPV genomes in the two donors (Figure 3.2). These genomes migrate as supercoiled (SC) and open circle (OC) forms when digested with non-cutting restriction enzymes (HPV16, *HindIII*; HPV18, *BglII*), indicating that the HPV genome has established as episomes in these cells (Figure 3.2).

In a previous study by the Roberts group, HPV18 genomes were generated in which the *E6* gene sequence was mutated to encode an E6 protein lacking the four amino acid C-terminal PDZ binding motif ( $\Delta$ PDZ). At the same time, HPV18 genomes were generated with a mutation which abrogates PKA recognition of a sequence (RRXS) that overlaps with the PBM ( $\Delta$ PKA) (Figure 3.3, Delury *et al.*, 2013). Since loss of the E6 PBM function is known to affect the episomal genome maintenance upon increased population doubling

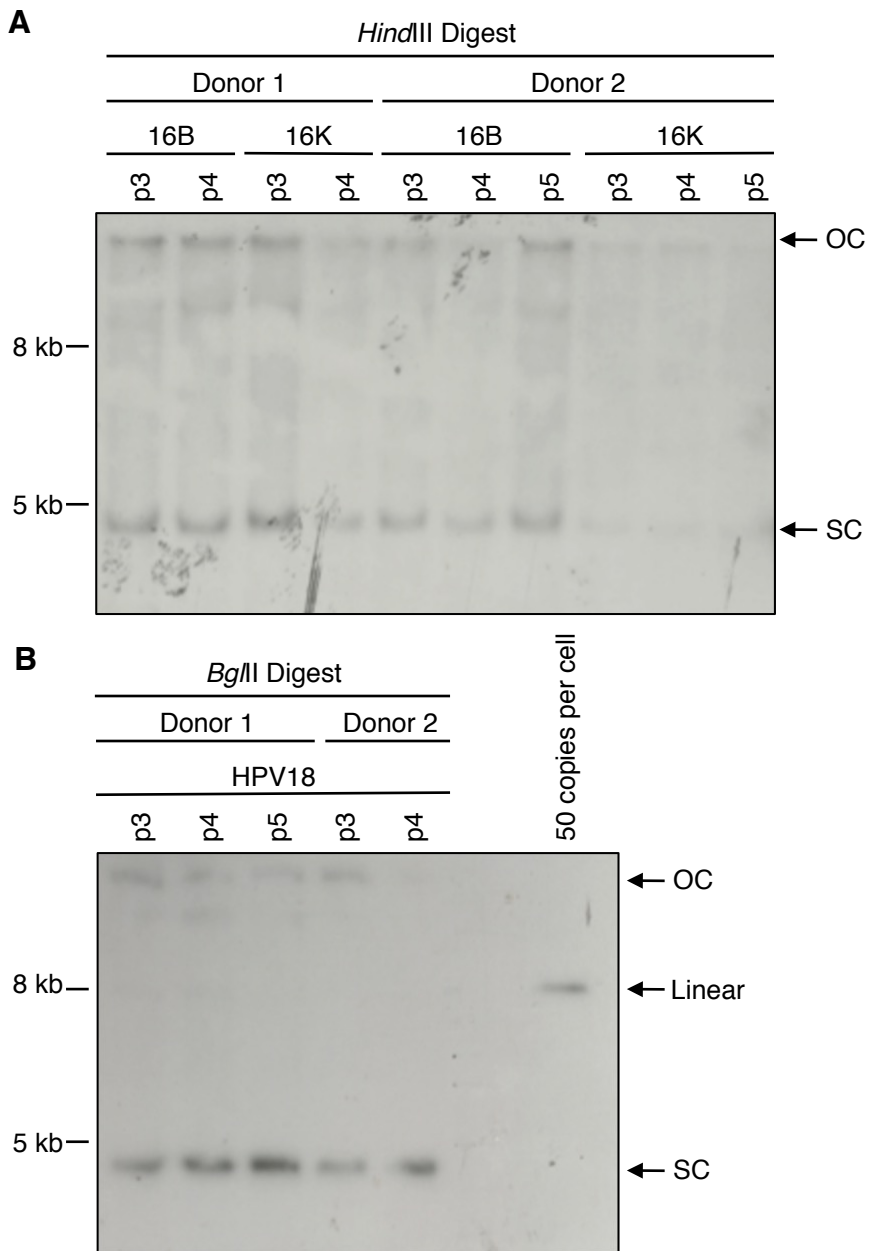


**Figure 3.2: Generation of HPV16 and HPV18 genome containing primary keratinocyte cell lines**

Southern blot analysis of total DNA isolated from two donor lines transfected with HPV16B, HPV16K (A) or HPV18 (B) genomes. DNA was digested with *Hind*III (HPV16B and HPV16K) or *Bgl*II (HPV18), which do not cut within the HPV genome. The addition of *Dpn*I digests residual input DNA. Radiolabelled genomic HPV16 (A) or HPV18 (B) DNA was used as a probe. Episomal genomes migrate as open circle (OC) and supercoiled (SC) forms.

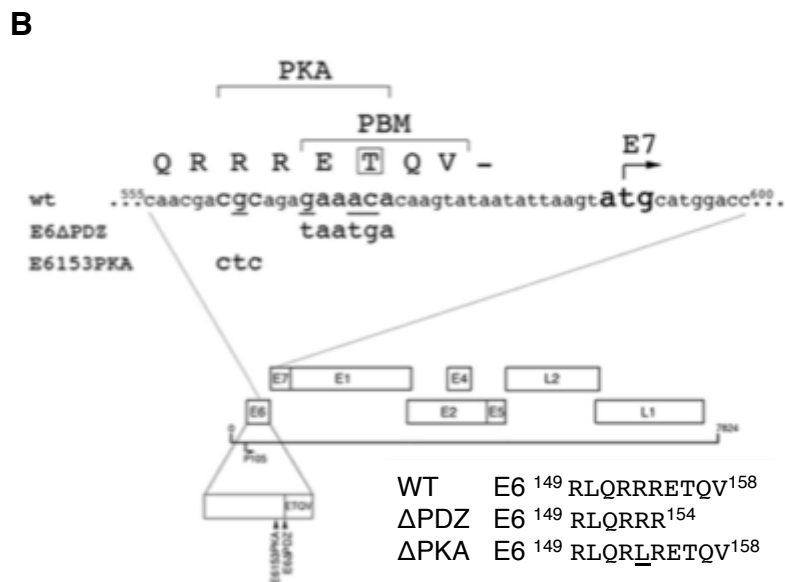
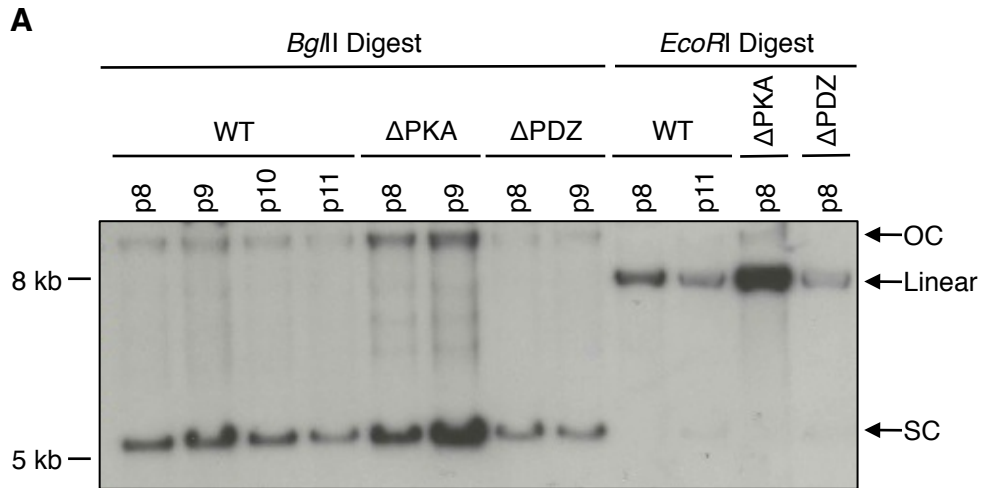


**Figure 3.3: Confirmation of episomal genomes in HPV18 genomes with modified PDZ binding activity**

- (A) Southern blot of keratinocytes containing HPV18 wild-type,  $\Delta$ PKA and  $\Delta$ PDZ genomes. Total DNA was extracted and digested with *Eco*RI or *Bgl*II, alongside *Dpn*I. HPV18 genomes are linearised by digestion with *Eco*RI, but remain uncut by *Bgl*II. Radiolabelled genomic HPV18 DNA was used as a probe. Episomal genomes migrate as open circle (OC) and supercoiled (SC) forms.
- (B) Schematic of mutations within the HPV18 mutation taken from Delury *et al.* 2013. The  $\Delta$ PDZ mutation encodes a deletion of the E6 PBM (ETQV), whereas the  $\Delta$ PKA mutation abrogates the PKA recognition site which overlaps with the PBM (RRX<sup>S</sup><sub>7</sub>).

(Delury *et al.*, 2013), the presence of viral episomes in early passages of the cell lines containing these genomes was also confirmed by Southern blot analysis (Figure 3.3). In the cell lines used, both mutant HPV genomes migrated as open circle and supercoiled forms, indicating replication of unintegrated episomes (Figure 3.3).

When grown in monolayer culture, these HPV16 and HPV18 genome containing cell lines, recapitulate the non-virus producing stages of the virus life cycle.

### 3.3.2 Transcription of E6 PDZ targets in keratinocytes containing high-risk $\alpha$ -papillomavirus genomes

The primary cell lines described above formed the basis for the following systematic analysis of PDZ protein expression. Although many studies have reported alterations in PDZ protein levels where high-risk HPV E6 is expressed, few have reported upon the transcriptional activity of the genes encoding this group of cellular proteins in the presence of HPV. It has been shown that the high-risk  $\beta$ -papillomavirus HPV8 E6 protein inhibits the transcription of the PDZ protein syntenin-2, leading to the downregulation of protein expression (Lazic *et al.*, 2012). Although the same study identified a low level of transcriptional inhibition of syntenin-2 by HPV16, there has been no in-depth analysis of PDZ protein gene expression in cells replicating HPV genomes. Therefore, this study aimed to investigate the transcription of known E6 PDZ targets using the cell-based models of the HPV16 or HPV18 life cycle.

Prior to this study, a microarray gene analysis (Affymetrix) had been performed on monolayer cultures of HPV16 and HPV18 containing keratinocytes prepared in a different donor keratinocyte background to those used in this thesis (Leonard *et al.*, unpublished data). Scrutiny of the array data for the expression of known E6 PDZ targets showed an

increase in the transcription of selected targets in the presence of both high-risk types when compared to transcription in untransfected HFKs of the same donor (Table 3.2).

**Table 3.2: Affymetrix microarray analysis of E6 PDZ target expression in HPV16 and HPV18 genome containing keratinocytes**

Protein	Gene Symbol	Probe Set ID	Chromosomal Location	Fold change in expression		
				HPV16B	HPV16K	HPV18
<b>DLG1</b>	DLG1	230229_at	3q29	11.67	10.01	7.50
<b>SCRIB</b>	SCRIB	212556_at	8q24.3	1.57	1.12	2.01
<b>PATJ</b>	INADL	214705_at	1p31.3	4.47	4.04	2.58
<b>PTPN13</b>	PTPN13	243792_x_at	4q21.3	4.22	7.45	4.40
<b>MAGI-2</b>	MAGI2	207702_s_at	7q21	3.66	-1.28	2.30
<b>MAGI-3</b>	MAGI3	226770_at	1p12-p11.2	2.13	1.71	1.57
<b>PTPN3</b>	PTPN3	203997_at	9q31	1.24	1.04	1.26
<b>TIP-1</b>	TAX1BP3	209154_at	17p13	-1.75	-1.55	-1.78
<b>TIP-2</b>	GIPC1	207525_s_at	19p13.1	1.23	-1.17	1.17
<b>NHERF1</b>	SLC9A3R1	201349_at	17q25.1	-1.23	1.24	-1.08
<b>p53</b>	TP53	210609_s_at	17p13	-1.67	-1.21	-2.33
<b>Syntenin-2</b>	SDCBP2	233565_s_at	20p13	1.18	-1.73	-2.01

In the case of genes encoding the E6 PDZ targets *MAGI-1*, *MUPP1*, *DLG4*, *PARD3* and *GOPC*, cellular transcript levels were below the detectable limit of the microarray probes, and these genes were consequently omitted from further analysis. Of the remaining E6 targets, transcripts were present. The level of *SCRIB*, *MAGI-2*, *MAGI-3*, *MPDZ* (*MUPP1*) *PTPN3*, *TAX1BP3* (*TIP-1*) and *GIPC1* (*TIP-2*) transcripts were not influenced (by more than ~2.5 fold) by HPV16 or HPV18 genome replication. In contrast, transcript levels of *DLG1*, *PATJ* and *PTPN13* showed an upregulation of greater than 2.5-fold in the cells containing both high-risk genotypes (Table 3.2). The level of increase of both *DLG1* and *PATJ* transcripts was much greater in the presence of HPV16 than HPV18. *DLG1* transcription increased by 11.67-fold (HPV16) and 7.5-fold (HPV18) and *PATJ*

transcription was upregulated by 4.47-fold (HPV16) and 2.58-fold (HPV18). *PTPN13* transcription increased equally by just over 4-fold between the two HPV genotypes (Table 3.2). The level of transcription of *TP53*, another protein target of high-risk  $\alpha$ -HPV types was unaffected in keratinocytes containing HPV16 or 18 genomes (Table 3.2).

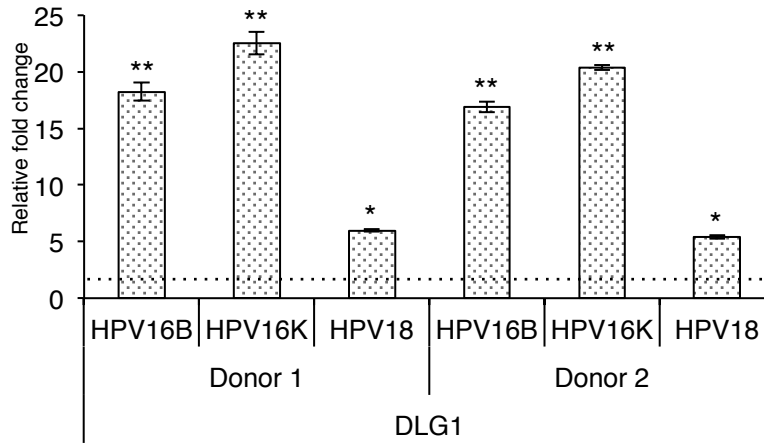
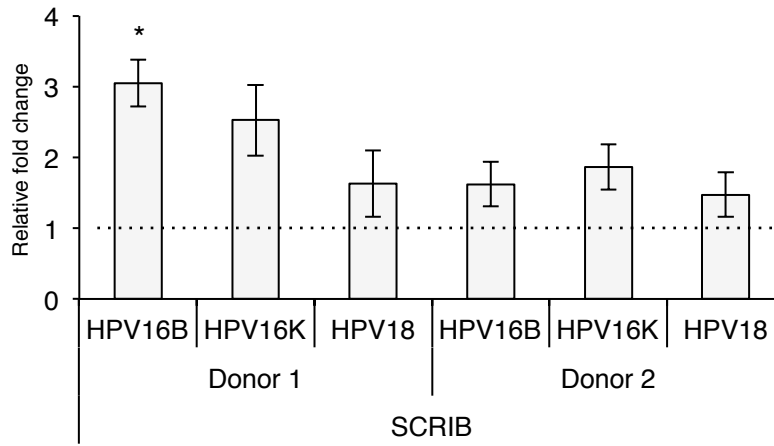
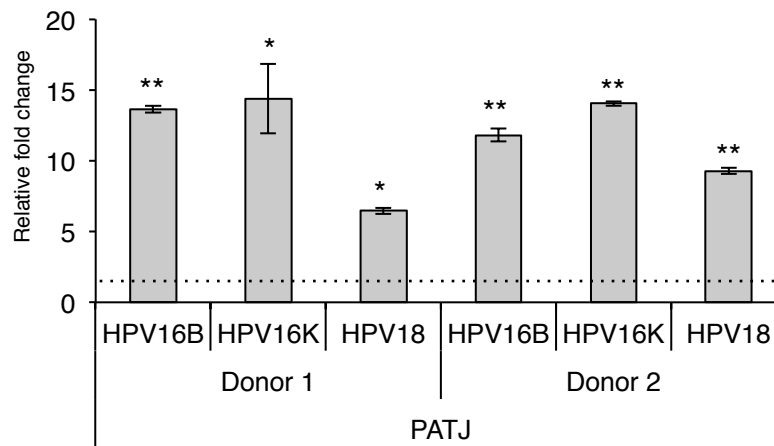
A similar profile of gene transcription was seen in a second cell line containing the HPV16K variant, indicating that transcriptional changes are not variant specific (Table 3.2). Next, qRTPCR analysis was used for verification of the microarray data. Because of the changes in transcription seen in the microarray analysis, the E6 PDZ targets *DLG1*, *PATJ* and *PTPN13* were selected for further validation, alongside the known target *SCRIB*, whose transcription remained unaffected. As well as the analysis of *DLG1*, *SCRIB*, *PATJ* and *PTPN13*, a primer set was included for the PDZ protein NHERF1, gene symbol *SLCR9A3R1*, which had recently been identified as a novel target of HPV16 and HPV18 E6 proteins (Accardi *et al.*, 2011). By including *NHERF1* in qRTPCR validation, the expression of the PDZ protein could be investigated in a model system where whole HPV genomes were present. The microarray analysis indicated that high-risk HPV replication does not affect *NHERF1* transcription; the fold change detected in the microarray was below 2.5 in both HPV16 and HPV18 containing keratinocytes compared to untransfected primary cells (Table 3.2). This data is in agreement with the findings of Accardi *et al.*, who showed that there was no change in *NHERF1* transcription following co-expression of E6 and E7 in primary keratinocytes.

Oligonucleotide primer sets for each PDZ target were designed to correspond to the region of the gene recognized by the probe used in the microarray analysis (see Section 2.2.1.2, Table 2.2). Each primer set was initially optimized by performing PCR at a range of different annealing temperatures, using DNase treated cDNA transcribed from the same RNA utilized in the microarray (Appendix II). Gene expression quantification by qRTPCR

was carried out on RNA isolated from HPV16 and HPV18 genome containing keratinocytes in the two donor backgrounds, each harvested at passage 3 (P3) and transcribed using oligodT primers (see Section 2.2.1.1). Changes in transcript levels were calculated relative to untransfected cells of the same donor. Figure 3.4 shows levels in individual donors, each repeated three times, and the data is summarized in Table 3.3 where the fold change in transcription is given as the mean change averaged across the two donors.

In this analysis, *DLG1* transcripts were elevated in both HPV16 and HPV18 genome containing cells in both donor backgrounds (Figure 3.4 A). Where HPV16 was present, *DLG1* expression was increased by ~18-fold (HPV16B) over untransfected, and in HPV18 genome containing keratinocytes, *DLG1* transcription was increased by more than 5-fold (Figure 3.4 A). By contrast, transcription of the fellow Scribble complex protein *SCRIB* remained largely unaffected in cells containing the high-risk HPV genomes (Figure 3.4 B). However, one donor exhibited a significant 3-fold increase of *SCRIB* transcripts in cells containing the HPV16B variant, but this was not consistently upheld in the other donor background, or in the presence of the HPV16K variant (Figure 3.4 B). Other than this, analysis of keratinocytes transfected with the two different variants HPV16 genomes (HPV16B and HPV16K) showed consistent effects upon the gene expression of the selected PDZ proteins; where there was an increase in cells containing the variant 16B (*DLG1*, *PATJ*, *NHERF1* and *PTPN13*), the same trend occurred in the presence of HPV16K (Figure 3.4, summarized in Table 3.3). This analysis indicates that transcriptional changes are not variant specific.

Levels of *PATJ* transcripts were elevated in HPV16 and HPV18 genome containing cells, exhibiting an 11 to 14-fold and 6 to 9-fold increase in transcripts respectively (Figure 3.4

**A****B****C**

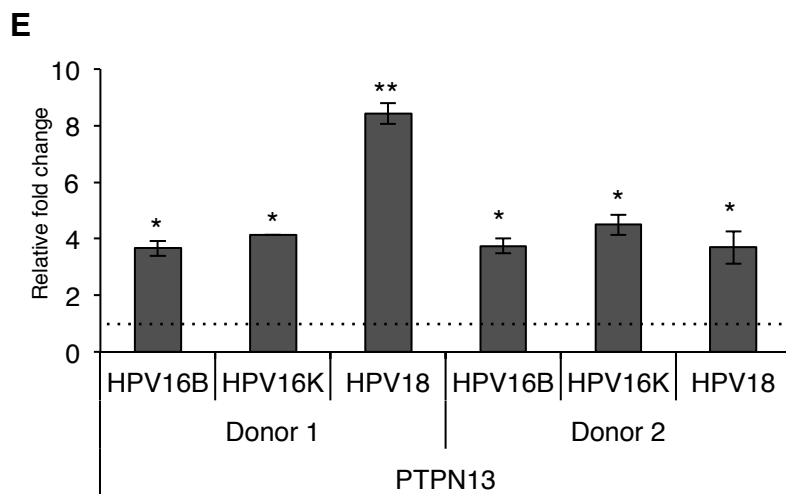
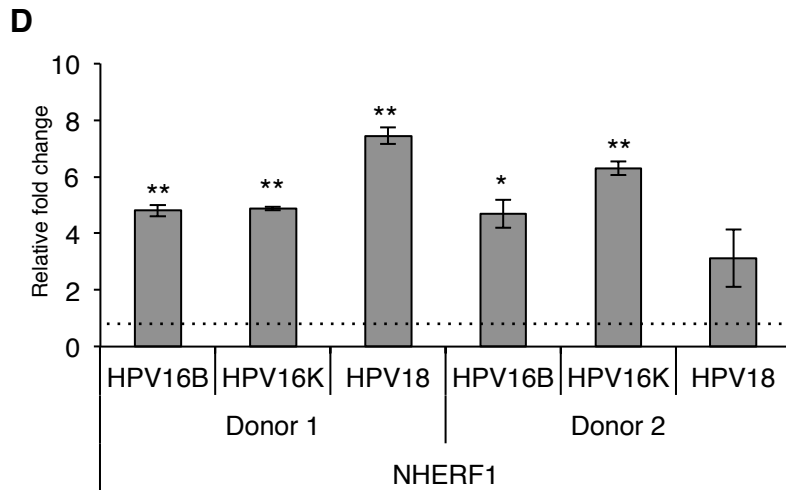


**Figure 3.4: Quantification of selected E6-PDZ target transcription in HPV16 and HPV18 genome containing keratinocytes**

Transcription analysis of *DLG1* (A), *SCRIB* (B), *PATJ* (C), *NHERF1* (D) and *PTPN13* (E) genes in two donor keratinocyte backgrounds. mRNA was extracted from primary foreskin keratinocytes following establishment of stable lines containing HPV16 or HPV18 genomes, alongside untransfected keratinocytes at passage 3 (P3). This was transcribed to cDNA using oligodT primers and levels were measured by qRT-PCR.  $\Delta\Delta\text{Ct}$  values were calculated relative to the housekeeping gene  $\beta 2$ -microglobulin, which was normalised to transcript levels in untransfected keratinocytes ( $\Delta\Delta\text{Ct}$ ) derived from the same donor background (indicated by dotted line). Error bars show  $\pm\text{SEM}$  of three experimental repeats, statistical significance indicated by \* ( $p < 0.05$ ) and \*\* ( $p < 0.01$ ).

C). Like the *DLG1* gene, transcription of *PATJ* was increased to a greater extent by HPV16 genome replication than by replication of HPV18 in monolayer keratinocytes.

Transcription of the signalling protein *NHERF1* was increased by 3 to 4-fold in keratinocytes containing the HPV16 variants (Figure 3.4 D). The level of upregulation of *NHERF1* transcription in HPV18 positive cells was only significant in one donor, where a more than 7-fold increase was observed (Figure 3.4 D). This analysis differs from published work, which demonstrated no change in *NHERF1* mRNA expression in HFks expressing HPV16 E6 and/or E7 (Accardi *et al.*, 2011).

Like *DLG1* and *PATJ*, *PTPN13* transcription was significantly upregulated in the presence of both HPV16 and HPV18; there was a ~4-fold increase in *PTPN13* mRNA in HPV16 containing cells, and an ~8- (Donor 1) and ~3- (Donor 2) fold increase in cells replicating HPV18 (Figure 3.4 E).

Transcriptional analysis was extended to the E6 PBM targets *MAGI-1*, -2 and -3, which encode junctional complex components. *MAGI-1* transcription was unchanged in HPV16 genome containing cells, although transcript levels were decreased in HPV18 genome containing cells to approximately half the levels of untransfected, in both donor keratinocytes (Figure 3.5 A). By contrast, a more than 3-fold increase in *MAGI-2* transcription was observed in the presence of both HPV types analysed and the transcription of *MAGI-3* remains unchanged by high-risk HPV replication (Figure 3.5 B and C).

Cumulatively, when averaged across donor keratinocyte backgrounds, there is a significant increase in the transcription of selected E6 targets in both HPV16 and HPV18 genome containing cells (Figure 3.6). The targets *DLG1*, *PATJ*, *MAGI-2*, *NHERF1* and *PTPN13* are increased transcriptionally in the presence of both high-risk  $\alpha$ -HPV genotypes, although to different extents. The largest increase in transcription was seen for the *DLG1*

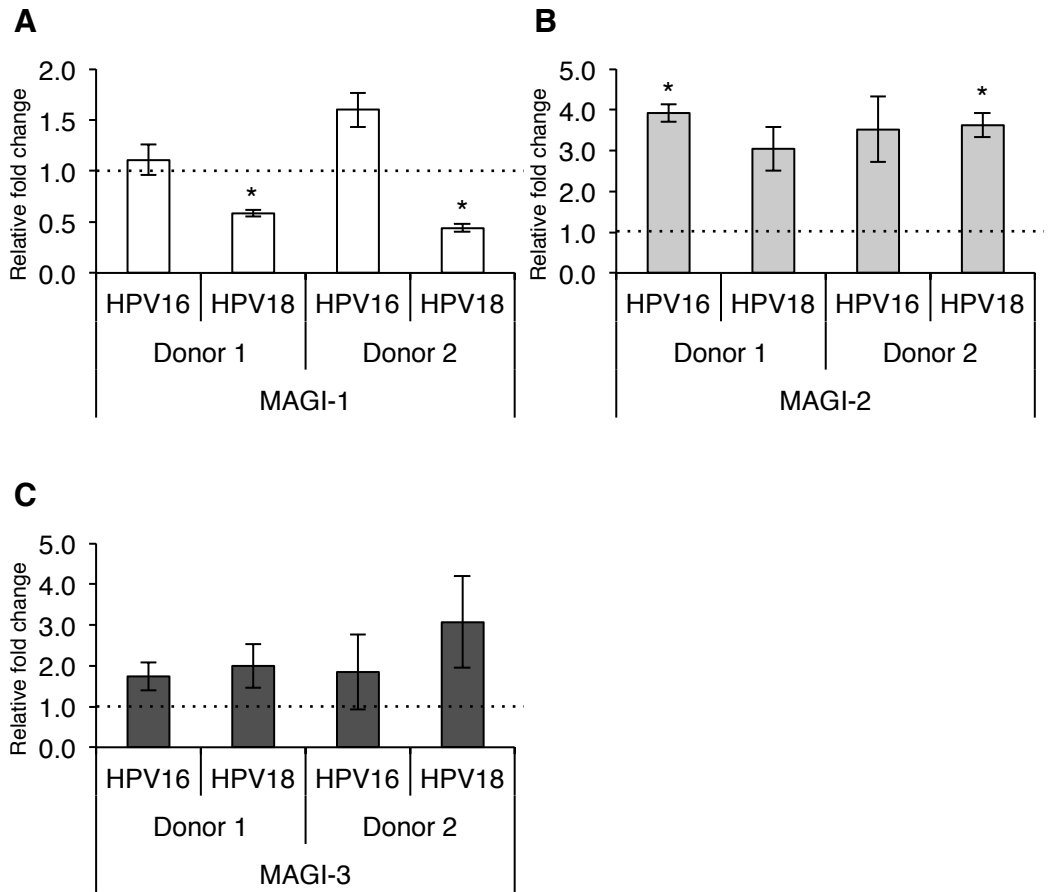


**Figure 3.5: Quantification of *MAGI-1*, *MAGI-2* and *MAGI-3* transcription in HPV16 and HPV18 genome-containing keratinocytes**

Transcription analysis of *MAGI-1* (A), *MAGI-2* (B) and *MAGI-3* (C) genes. mRNA was extracted from primary foreskin keratinocytes following establishment of stable lines containing HPV16 or HPV18 genomes, alongside untransfected keratinocytes at passage 3 (P3). The mRNA was transcribed to cDNA and levels were measured by qRT-PCR.  $\Delta\Delta\text{Ct}$  values were first calculated relative to the housekeeping gene  $\beta 2$ -microglobulin, and then to untransfected keratinocytes ( $\Delta\Delta\text{Ct}$ ) derived from the same donor background (indicated by dotted line). Error bars show  $\pm\text{SEM}$  of three experimental repeats, statistical significance indicated by \* ( $p < 0.05$ ) and \*\* ( $p < 0.01$ ).

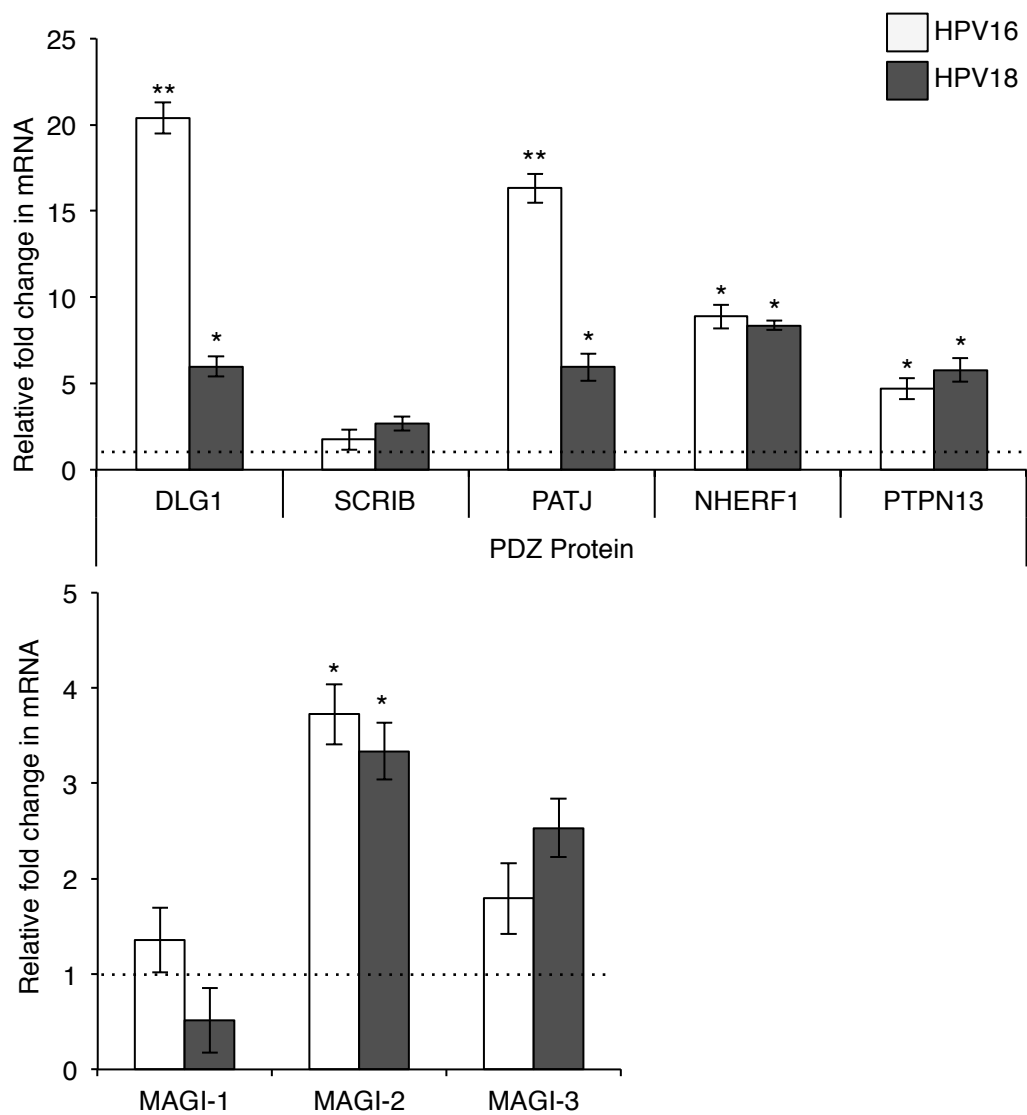


**Figure 3.6: Cumulative qRTPCR analysis PDZ targets of E6 expression in HPV genome containing HFKs**

Transcription of E6 PDZ targets in HPV16 and HPV18 genome containing keratinocytes as measured by qRTPCR, in two donor backgrounds. Transcription of DLG1, SCRIB, PATJ, NHERF1, PTPN13, MAGI-1, MAGI-2 and MAGI-3 were averaged following normalization to untransfected HFKs (dotted line). Error bars show  $\pm$  SEM of three repeats in two donors. \*\*indicates  $p < 0.01$ , \* indicates  $p < 0.05$ .

gene in HPV16 positive cells (20-fold), with a similarly large (16-fold) increase in *PATJ* transcription in the same cells. In both HPV16 and HPV18 positive keratinocytes, the transcription of these targets, and of *NHERF1* and *PTPN13*, was increased in HPV18 containing keratinocytes. Notably, the transcription of both *SCRIB* and *MAGI-3* remained unaffected by both HPV genotypes (Figure 3.6). Interestingly, *MAGI-1* transcription decreases in the presence of HPV18, whilst remaining unaffected by HPV16 (Figure 3.6).

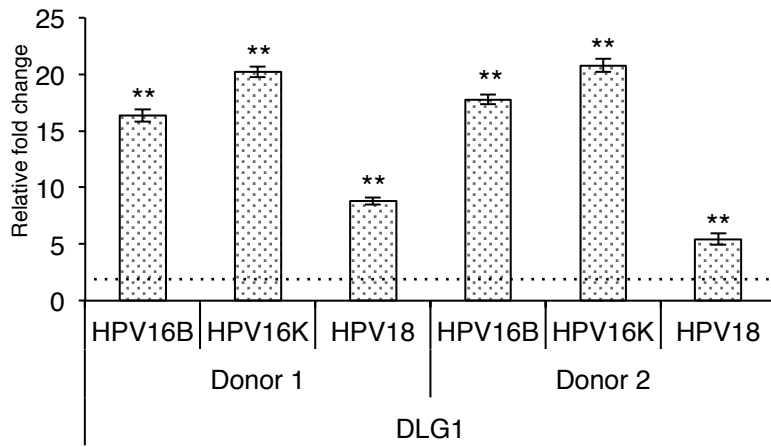
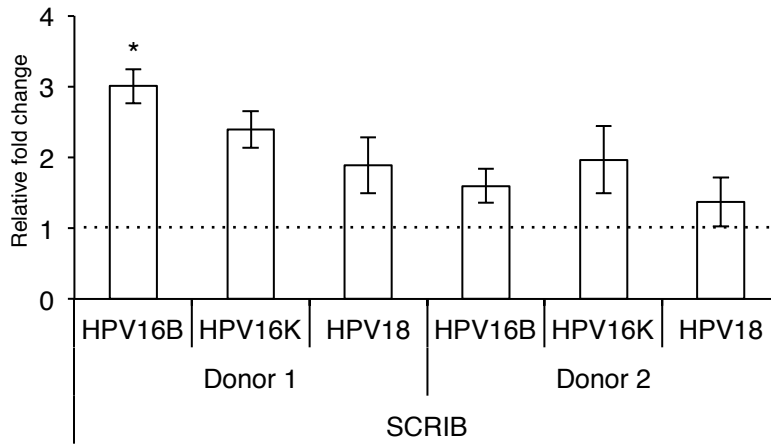
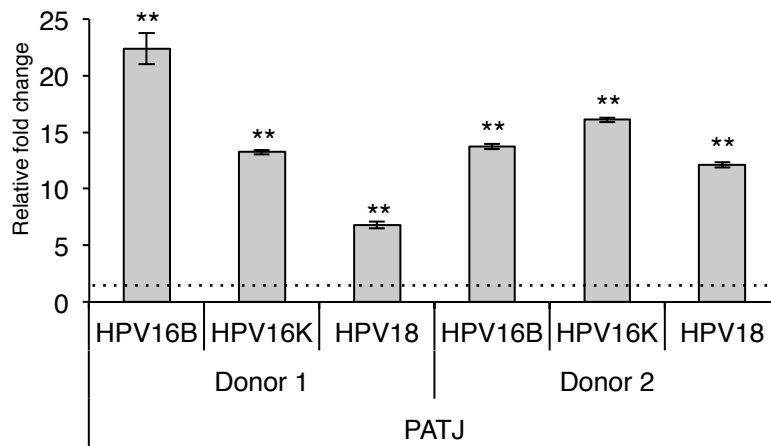
To establish whether the increase in transcription of selected PDZ targets is maintained upon cell propagation, qRT-PCR was performed on RNA extracted from the cells after a further five population doublings (P4). The profile of change in the level of transcripts in comparison to the untransfected cells remained the same as found in cells grown to P3 (Figure 3.7, summarized in Table 3.4). The expression of *PATJ*, *NHERF1* and *PTPN13* remained elevated across the population doublings analysed, with *PATJ* showing a trend towards a further increase in mRNA transcripts in the later passage.

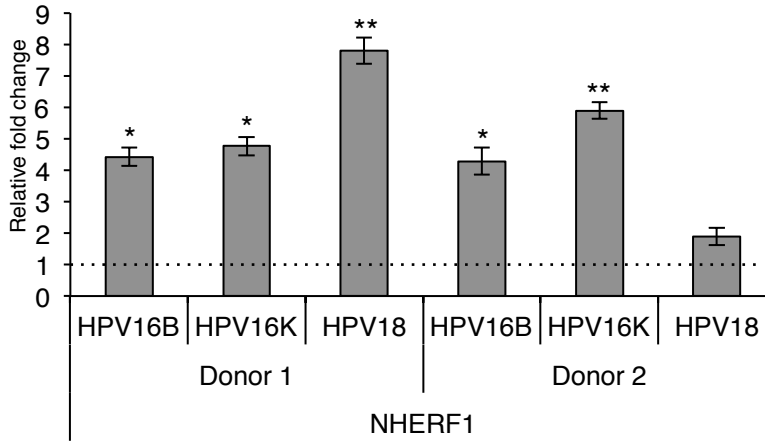
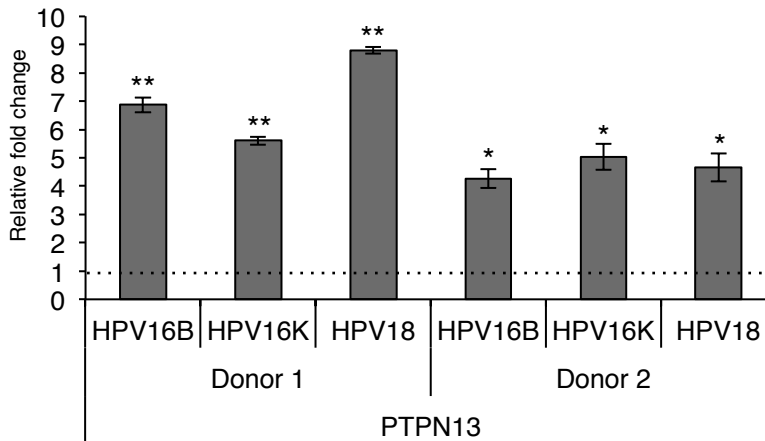
**Table 3.3: Summary of PDZ target qRT-PCR analysis**

Gene	Fold change in expression					
	HPV16B		HPV16K		HPV18	
	p3	p4	p3	p4	p3	p4
<b>DLG1</b>	17.56	17.05	21.45	20.47	5.70	7.12
<b>SCRIB</b>	2.39	2.30	2.39	2.18	1.55	1.63
<b>PATJ</b>	12.73	18.06	14.21	14.67	7.87	9.46
<b>NHERF1</b>	4.74	4.35	5.58	5.33	5.29	4.84
<b>PTPN13</b>	3.70	5.57	4.31	5.31	6.06	6.72
<b>MAGI-1</b>	-	2.82	-	1.35	-	0.51
<b>MAGI-2</b>	-	3.66	-	3.72	-	3.34
<b>MAGI-3</b>	-	2.13	-	1.79	-	2.53

Average of two donors. Fold change calculated relative to levels of transcription in HFKs derived from the same donor.

To investigate the contribution of the E6 PBM binding function with respect to PDZ target gene expression, qRT-PCR gene expression analysis was carried out on monolayer

**A****B****C**

**D****E**

**Figure 3.7: Quantification of E6-PDZ target transcription in HPV16 and HPV18 genome containing keratinocytes following cell propagation**

Transcription analysis of *DLG1* (A), *SCRIB* (B), *PATJ* (C), *NHERF1* (D) and *PTPN13* (E) genes. mRNA was extracted from primary foreskin keratinocytes following passage (p4) of stable lines containing HPV16 or HPV18 genomes in two donor backgrounds. mRNA levels were measured in HPV16 and HPV18 positive keratinocytes, alongside untransfected cells, by qRT-PCR.  $\Delta\text{Ct}$  values were first calculated relative to the housekeeping gene  $\beta$ 2-microglobulin, and then to untransfected keratinocytes ( $\Delta\Delta\text{Ct}$ ) derived from the same donor background (indicated by dotted line). Error bars show  $\pm$ SEM of three experimental repeats, statistical significance indicated by \* ( $p < 0.05$ ) and \*\* ( $p < 0.01$ ).

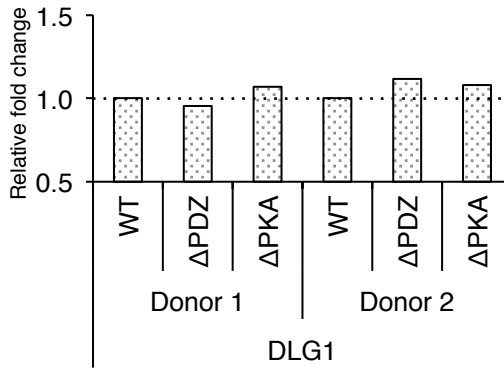
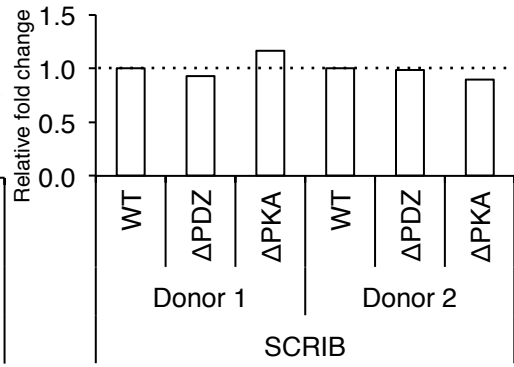
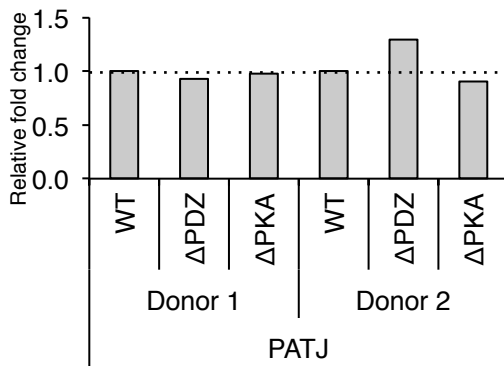
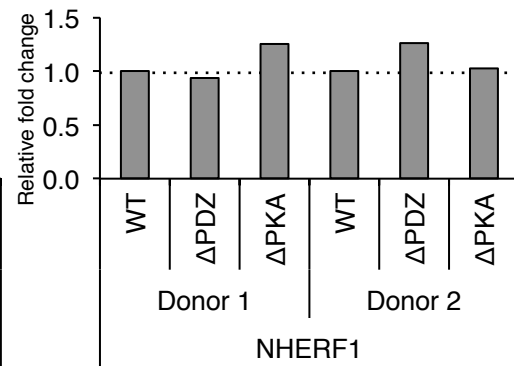
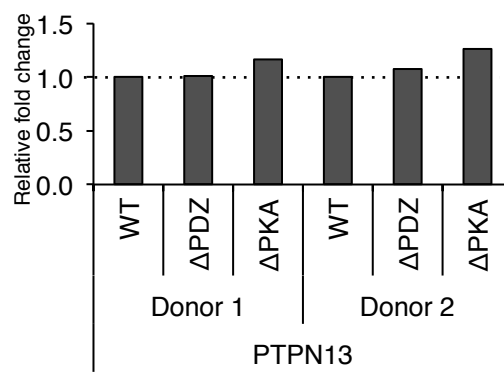
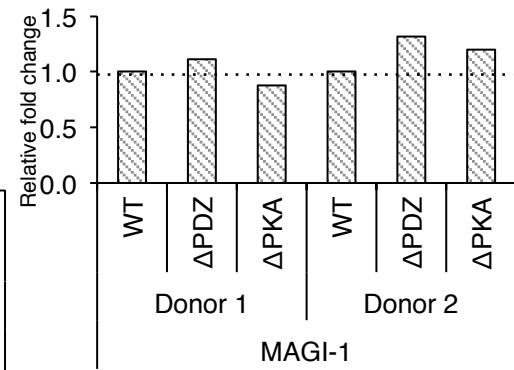
keratinocytes containing wild-type HPV18 genomes (WT), or the genomes containing a PBM deletion ( $\Delta$ PDZ) or the PKA unresponsive genome  $\Delta$ PKA. In this analysis, gene expression in two donors was carried out and calculated relative to transcript levels in wild-type genome containing keratinocytes of the same donor background (Figure 3.8). There were no significant changes in the transcription of *DLG1*, *SCRIB*, *PATJ*, *NHERF1*, *PTPN13*, *MAGI-1*, *MAGI-2* or *MAGI-3* in both mutant lines (Figure 3.8). These data indicate that changes in PBM activity are not linked to the transcriptional change observed for selected PDZ proteins.

In summary, the upregulation of selected PDZ targets in HPV16 and HPV18 observed in microarray analysis was confirmed by qRT-PCR (Table 3.4). The two donor cell lines exhibited a consistent trend towards increased gene expression in the presence of both high-risk HPV genomes, which was calculated as significant compared to HFK gene expression. Notably, in the presence of both viral genotypes, transcripts of *DLG1* were substantially increased and *SCRIB* transcript levels remained largely unchanged.

**Table 3.4: Comparison of microarray and qRT-PCR analyses**

Gene	Average fold change in expression					
	HPV16B		HPV16K		HPV18	
	Microarray	qRT-PCR	Microarray	qRT-PCR	Microarray	qRT-PCR
<b>DLG1</b>	11.67	17.56	10.01	21.45	7.50	5.70
<b>SCRIB</b>	1.57	2.39	1.12	2.39	2.01	1.55
<b>PATJ</b>	4.47	12.73	4.04	14.21	2.58	7.87
<b>NHERF1</b>	1.54	4.74	1.97	5.58	1.86	5.29
<b>PTPN13</b>	4.22	3.70	7.45	4.31	4.40	6.06
MAGI-1	2.82	-	3.53	1.35	3.63	0.51
<b>MAGI-2</b>	3.66	-	-1.28	3.72	2.58	3.34
<b>MAGI-3</b>	2.13	-	1.71	1.79	1.57	2.53

MAGI-1 transcripts below detectable level of microarray probe. qRT-PCR shows average of 2 donors.

**A****B****C****D****E****F**

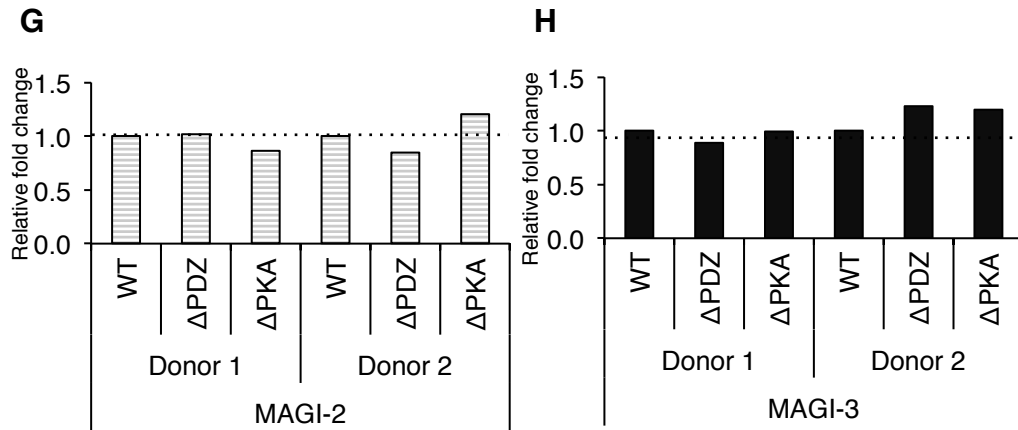


**Figure 3.8: Quantification of E6-PDZ target transcription in HPV18 genome containing keratinocytes**

Transcription of *DLG1* (A), *SCRIB* (B), *PATJ* (C), *NHERF1* (D) and *PTPN13* (E) genes in primary keratinocytes replicating HPV18 genomes. mRNA extracted from HPV18 encoding wild-type (WT), ΔPDZ or ΔPKA E6 proteins. Expression levels in keratinocytes containing mutant (ΔPDZ and ΔPKA) genomes were calculated relative to mRNA levels in WT genome containing keratinocytes (dotted line) derived from the same donor background. Transcription analysis of *DLG1* (A), *SCRIB* (B), *PATJ* (C), *NHERF1* (D) and *PTPN13* (E) genes. Graphs show results from three technical repeats.

### 3.3.3 Analysis of PDZ protein expression during the HPV life cycle

Given that the transcription of known E6 PDZ targets were altered in the presence of high-risk  $\alpha$ -HPV genotypes, the next step was to investigate protein expression in the HPV life cycle model. In this study, seven identified targets of high-risk HPV E6 proteins (DLG1, SCRIB, PATJ, MAGI-1, MUPP1, NHERF1 and PTPN13) were investigated. This was performed alongside analysis of putative targets, suggested by recent screening experiments (Belotti *et al.*, 2013, CASK, ZO-1 and ZO-2). These proteins are representative of proteins involved in the Scribble, Crumbs and Par epithelial junctional complexes, as well as in cellular signalling and scaffold organisation (Figure 1.10).

For the initial PDZ protein analysis, HPV16 or HPV18 genome containing keratinocytes were cultured until they reached 70% confluency (to ensure they remained in an undifferentiated state) and were then harvested and solubilised in a lysis buffer containing 8 M urea, and the protein extracts subjected to western blot analysis (see Section 2.1.4.4). PDZ protein expression was also examined in the HPV18 mutant genome containing keratinocytes,  $\Delta$ PDZ and  $\Delta$ PKA, and compared to wild-type HPV18 positive cells in order to assess whether any changes in protein expression were dependent upon the activity of the E6 PBM.

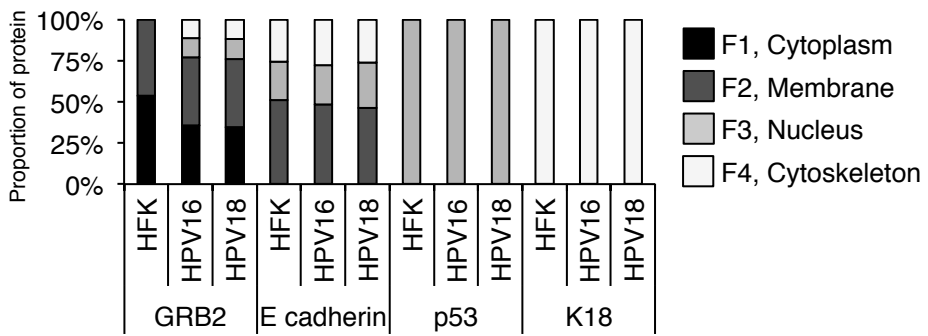
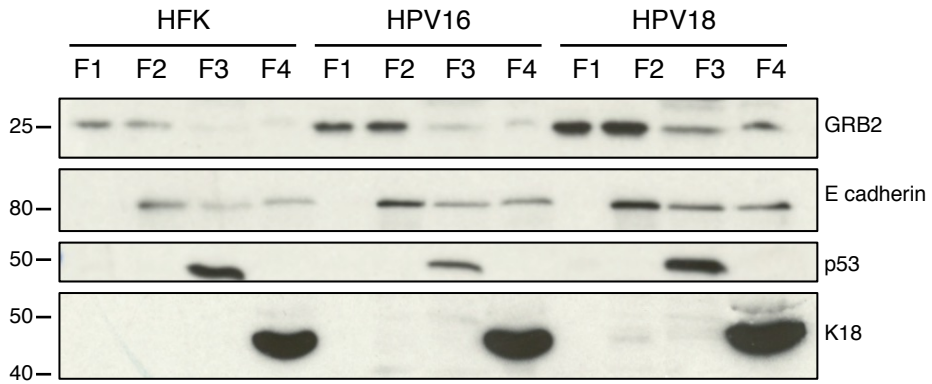
Since it has been shown that specific cellular pools of some PDZ proteins are preferentially degraded by E6 (Massimi *et al.*, 2004; Simonson *et al.*, 2005; Kühne *et al.*, 2000; Narayan *et al.*, 2009; Kranjec and Banks, 2011; Latorre *et al.*, 2005), the subcellular localisation of PDZ proteins was examined in the life cycle model by fractionation of the monolayer-grown cells. This process used a series of lysis buffers to sequentially extract the following cellular compartments; the cytoplasm, the membrane, the nucleus and the cytoskeleton. The resulting protein extracts was subjected to western blot analysis, alongside analysis of host cell marker proteins in order to show enrichment of each of cellular fractions; growth

factor receptor-bound protein 2 (GRB2) in the cytoplasm, E-cadherin in the membrane, p53 in the nucleus and keratin 18 (K18) in the cytoskeleton (Figure 3.9). As can be seen in Figure 3.9 A, the fractionation process successfully enriched for the various cellular compartments of monolayer-grown keratinocytes. Each marker was found predominantly in the expected fraction; both p53 and K18 are exclusively detected in the nucleus and cytoskeleton respectively. GRB2 was enriched in the cytoplasmic and membrane fractions and E-cadherin was predominantly detected in the membrane fraction with some protein present in the nuclear and cytoskeletal fractions (Figure 3.9). The enrichment of these proteins was consistent across the cell lines; the presence of HPV16 or 18 genomes does not affect their localisation, and thus the distribution of these proteins is a suitable indicator for successful subcellular fractionation.

To investigate changes in PDZ protein expression during the productive phase of the virus life cycle, the HPV18 genome containing cells (WT and  $\Delta$ PDZ) were stratified by growth in organotypic raft culture for 13 days (see Section 2.1). The differentiated structures were solubilized in urea lysis buffer and the protein extracts subjected to western blot analysis. Further analysis of sections of raft structures allowed the analysis of PDZ protein localisation during the HPV life cycle by immunofluorescent staining for PDZ targets.

Thus, the following analysis examined known and indicated targets of high-risk HPV E6 proteins, proteins involved in the epithelial junction complexes, Scribble, Par and Crumbs, each of which contain known targets of E6, as well as PDZ-proteins involved in cellular signalling.

**A**



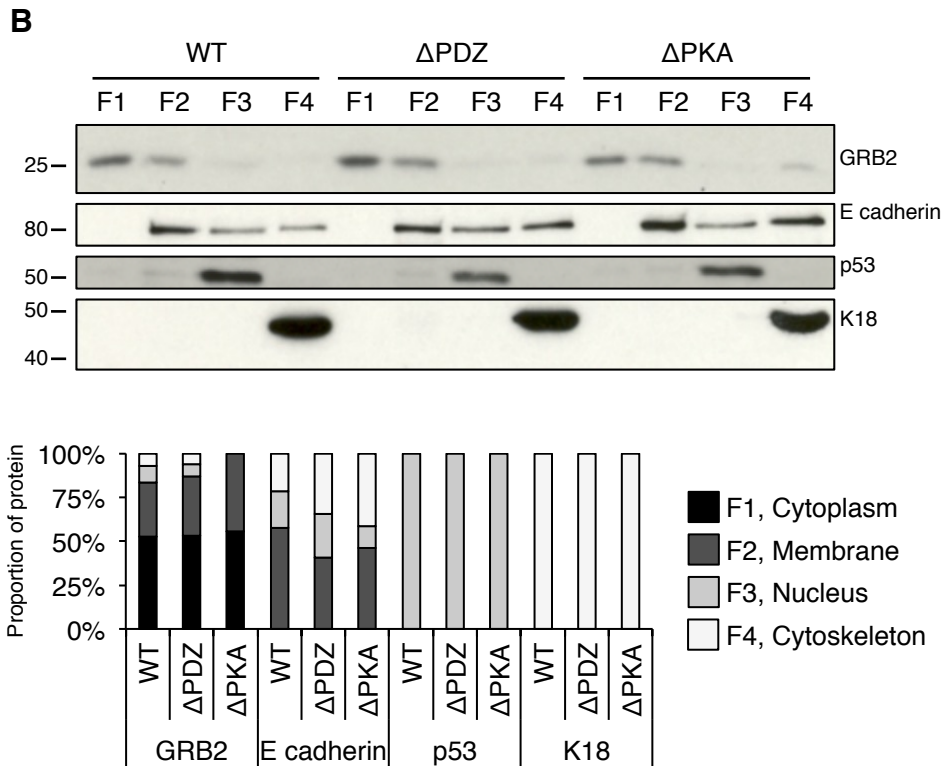


**Figure 3.9: Confirmation of successful enrichment of protein from subcellular fractions**

Subcellular fractionation was carried out on monolayer-grown keratinocytes at 70% confluency. Protein from subcellular fractions was extracted by treatment with sequential lysis buffers. Successful enrichment was confirmed by western blot analysis; detection of the marker proteins GRB2, E-cadherin, p53 and K18 indicate enrichment of the cytoplasmic, membrane, nuclear and cytoskeletal fractions, respectively. The cell lines containing HPV16 and HPV18 (A) and HPV18 PBM mutants (B) were subject to fractionation in parallel. Western blots were quantified by densitometry using ImageJ software. Figures representative of three experimental repeats carried out on cells derived from two donor backgrounds.

### 3.3.3.1 The Scribble complex

#### 3.3.3.1.1 DLG1

Despite the increase in transcription of the *DLG1* gene, there was no change in DLG1 protein levels in HPV18 genome containing keratinocytes (Figure 3.10 A). Moreover, deletion of the E6 PDZ binding function ( $\Delta$ PDZ) did not impact upon DLG1 protein levels (Figure 3.10 B). Furthermore, altering the E6 sequence to encode a constitutively active PBM, *via* removal of the PKA recognition site ( $\Delta$ PKA), also had no effect upon the level of DLG1 protein (Figure 3.10 B). In the HPV18-positive cancer cell line HeLa, there was a 70% decrease in DLG1 protein levels, compared to normal keratinocytes (Figure 3.10 A), indicating differences between the life cycle model and a late stage carcinogenesis cell line. In HPV16 genome containing cells, there was a subtle trend towards a decrease in DLG1 protein; in two donors DLG1 protein was 0.7 and 0.8 times the level of untransfected cells (Figure 3.10 A). Taken together, no extensive change in protein levels was observed in these cells.

Subcellular fractionation of monolayer grown cells detected the majority of DLG1 in the nucleus of primary keratinocytes (Roberts *et al.*, 2007), although the protein was also strongly detected in the membrane and weakly detected in the cytoskeleton and cytoplasm (Figure 3.11 A). Subcellular distribution of DLG1 protein remained unaffected by the presence of HPV16 or HPV18 genomes (Figure 3.11 A), and changes in the activity of the E6 PBM did not affect the distribution of DLG1 between subcellular pools (Figure 3.11 B). The distribution of DLG1 was verified using two antibodies specific for DLG1, a mouse monoclonal antibody (2D11) and a polyclonal antibody (NAG, Watson *et al.*, 2002), which were raised to different N-terminal regions of DLG1.

During epithelial differentiation, the subcellular localisation of DLG1 changes (Roberts *et al.*, 2007), and so analysis of DLG1 was applied to differentiating keratinocytes. To

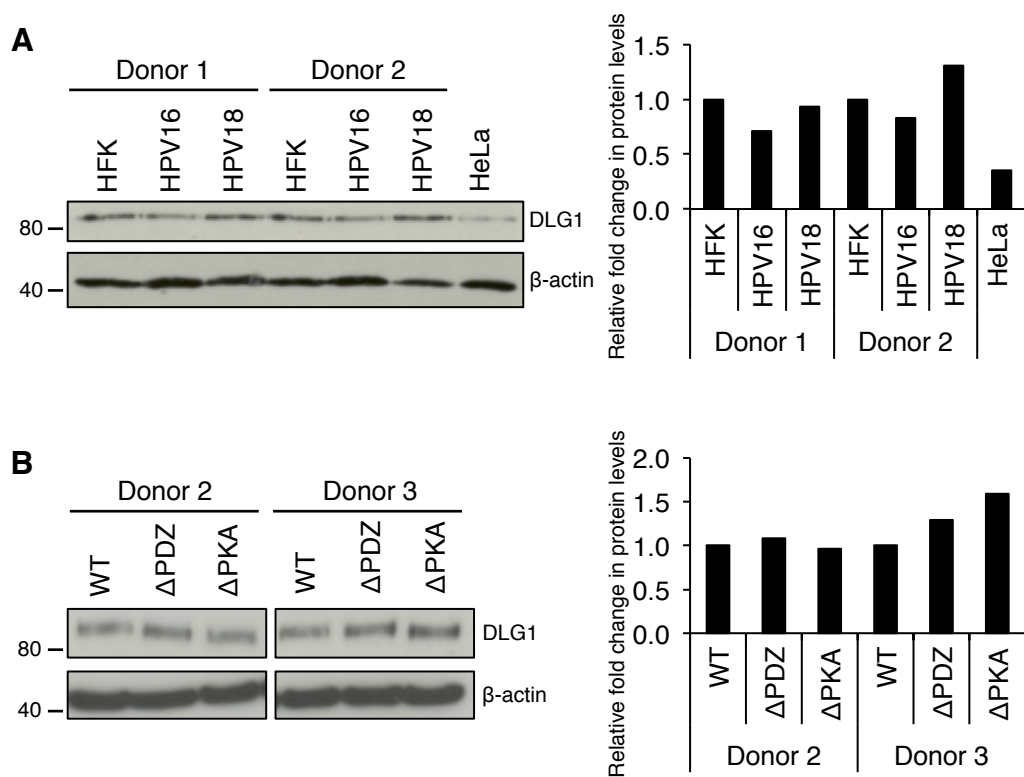


**Figure 3.10: DLG1 protein expression in keratinocytes replicating HPV genomes**

DLG1 protein levels in keratinocytes containing HPV16 and 18 genomes (A) and mutant HPV18 genomes (B). Protein was extracted from cells grown in monolayer culture to 70% confluency, quantified by Bradford assay and separated by SDS-PAGE. Membranes were probed with mouse monoclonal antibody raised against DLG1 (2D11), and  $\beta$ -actin as a loading control. Figures representative of two repeats. Western blots were quantified by densitometry using ImageJ software. Graphs show relative levels, first normalised to  $\beta$ -actin and then to HFK (A) or WT (B) levels. Representative of two experimental repeats. Markers show molecular weight in kDa.

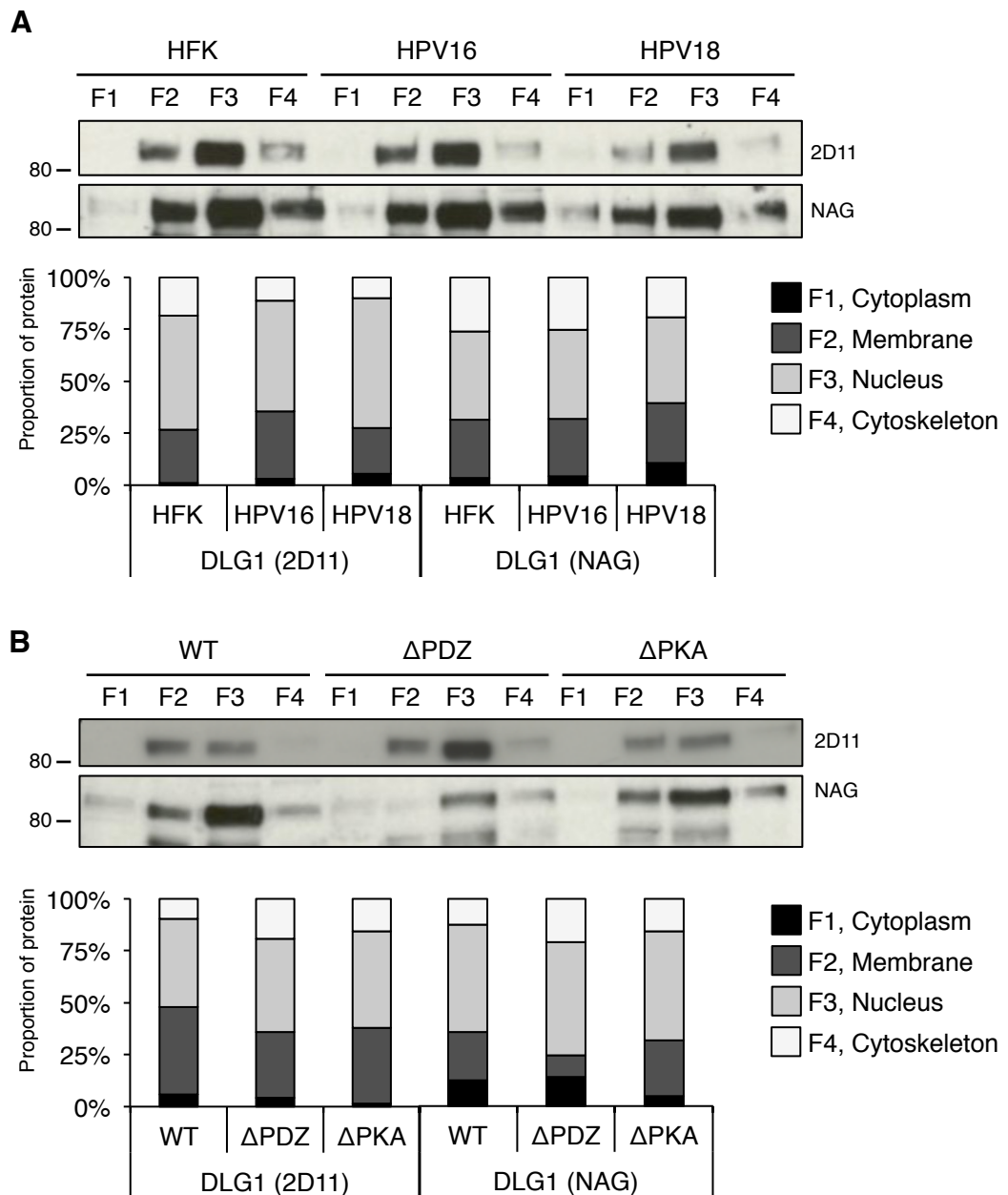


**Figure 3.11: DLG1 protein distribution in keratinocytes**

Distribution of DLG1 in keratinocytes containing HPV16 and 18 genomes (A) and mutant HPV18 genomes (B) grown in monolayer culture. Subcellular fractionation was carried out on keratinocytes at 70% confluency. The cytoplasmic, membrane, nuclear and cytoskeletal fractions were extracted by treatment with sequential lysis buffers, an equal amounts separated by SDS-PAGE. Membranes were probed with mouse monoclonal (2D11) or rabbit polyclonal (NAG) antibody raised against DLG1, Western blots were quantified by densitometry using ImageJ software. Figures representative of three experimental repeats carried out on cells derived from two donor backgrounds.

determine if HPV affects DLG1 during stratification, HPV18 genome containing keratinocytes were grown in organotypic raft culture and protein was extracted in urea lysis buffer (Section 2.1). Detection of DLG1 with the mouse monoclonal antibody 2D11 indicated a decrease in DLG1 protein where the E6 PDZ binding function was removed, compared to cells containing the wild-type HPV18 genome (Figure 3.12). However, detection with the NAG antibody indicated no change in DLG1 protein levels in differentiated keratinocytes irrespective of E6 PBM function (Figure 3.12).

Both the 2D11 and NAG antibodies were utilized in analysis of DLG1 localization in stratified keratinocytes by immunofluorescence (Figure 3.13). Using both antibodies, immunofluorescent staining of raft cultures showed DLG1 located predominantly at the cell junctions in the upper layers of HFks, with a more cytoplasmic form detected in the basal layer (Figure 3.13). In HPV18 containing keratinocytes, the cell-cell location of DLG1 occurred earlier in the stratification of HPV18 genome containing cells, although this was more obvious when using 2D11 to detect DLG1 compared to NAG (Figure 3.13).

#### 3.3.3.1.2 SCRIB

While levels of SCRIB protein in keratinocytes containing HPV16 were comparable to HFks, in HPV18 positive cells SCRIB protein increased by approximately 40%, and this was consistent between both donors (Figure 3.14 A). In contrast, the polarity protein is depleted by 20% in the HPV18 DNA-positive cervical cancer cell line HeLa, compared to primary foreskin keratinocytes (Figure 3.14). Interestingly, the observed change on SCRIB expression is unrelated to the HPV18 PDZ binding function, as removal of the PBM ( $\Delta$ PDZ) or altering the PKA recognition site ( $\Delta$ PKA) does not restore the SCRIB protein levels to the level found in primary keratinocytes (Figure 3.14 B).

The localisation of SCRIB, in HPV16 and HPV18 positive keratinocytes as well as in normal cells, was predominantly cytoplasmic, nuclear and cytoskeletal (Figure 3.15 A). A

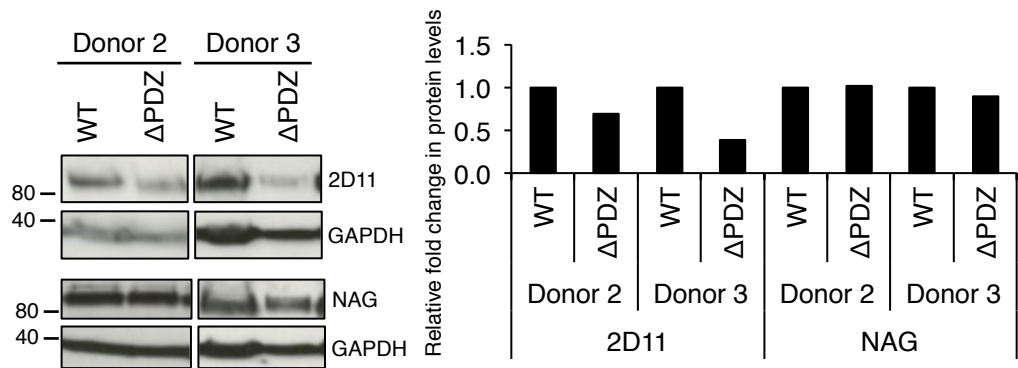


**Figure 3.12: DLG1 protein in differentiated keratinocytes containing HPV18 genomes**

Keratinocytes containing wild-type (WT) HPV18 genomes or HPV18 encoding an E6 without a PBM ( $\Delta$ PDZ) were grown in organotypic raft culture. After 13 days, the raft was harvested, homogenised and lysed in order to extract protein. Protein was separated by SDS-PAGE and membranes were probed with mouse monoclonal (2D11) or rabbit polyclonal (NAG) antibody raised against DLG1, alongside GAPDH as a loading control. Western blots were quantified by densitometry using ImageJ software. Graphs show relative levels, first normalised to GAPDH and then to WT levels. Figures representative of two technical repeats.

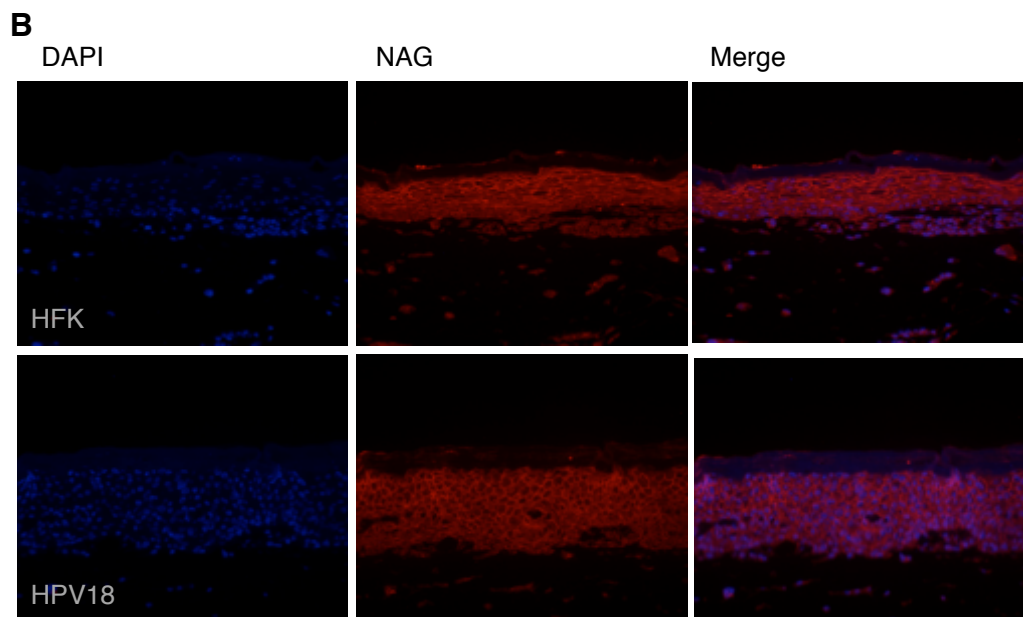
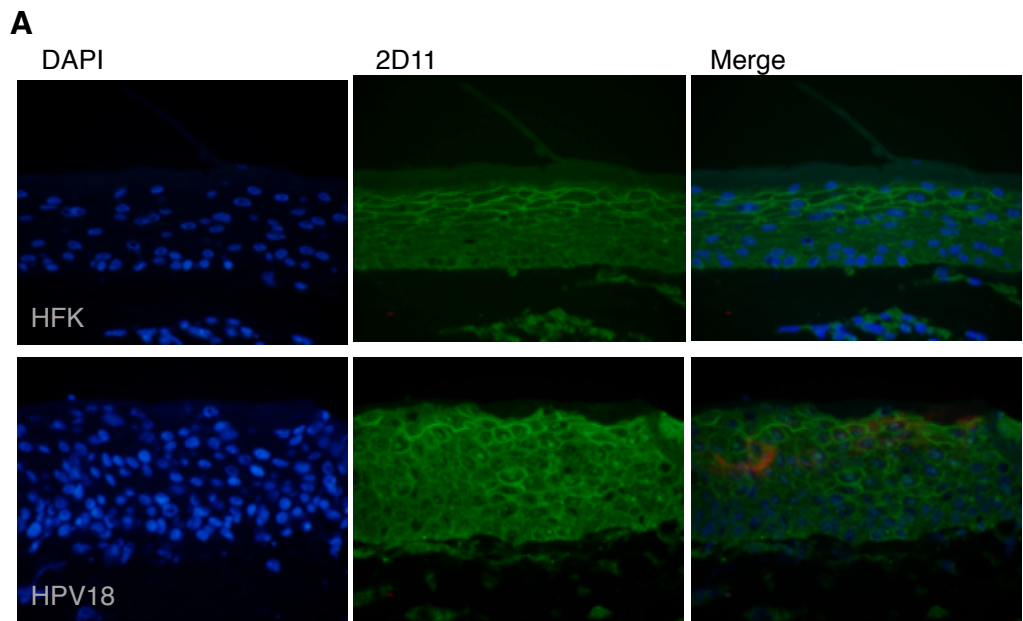


**Figure 3.13: Immunofluorescence of DLG1 in differentiated keratinocytes**  
 Immunofluorescent staining of keratinocytes grown in organotypic raft culture. Raft cultures were grown for 13 days, harvested and paraformaldehyde fixed. Individual sections were cut and stained for DLG1 using 2D11 (A, green) or NAG (B, red) antibodies. The nucleus stain DAPI (blue) was also used. Images were taken at 40x magnification.

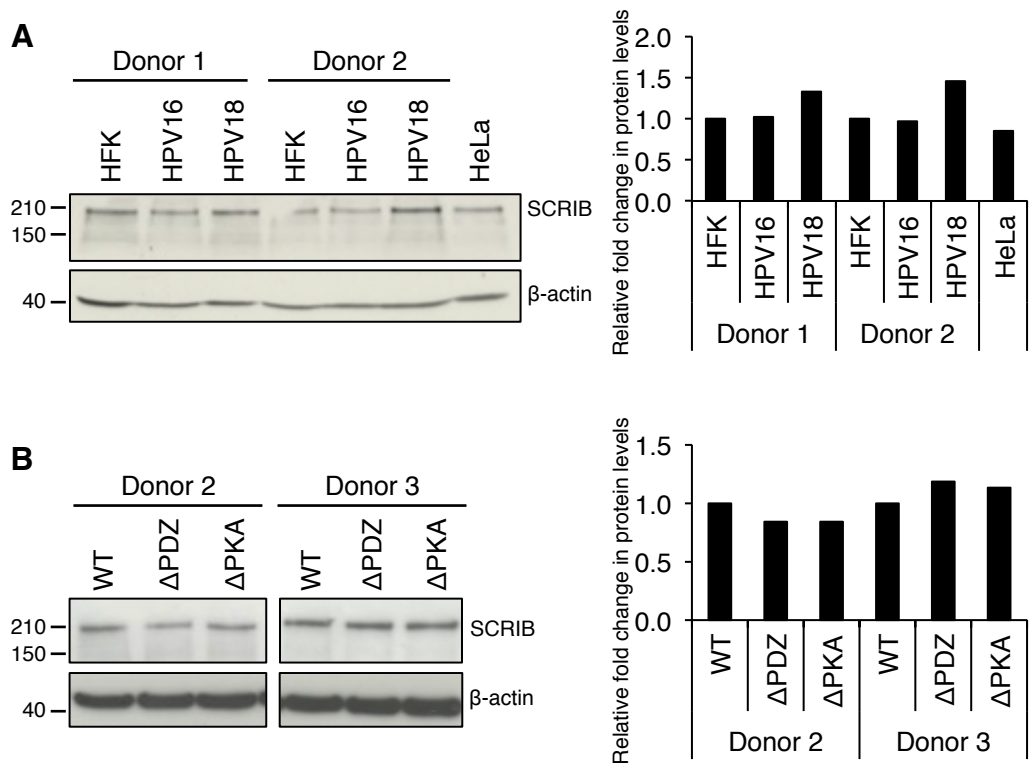


**Figure 3.14: SCRIB protein levels in HPV genome containing keratinocytes**  
 SCRIB protein levels in keratinocytes containing WT HPV16 and 18 genomes (A) and mutant HPV18 genomes (B) grown in monolayer culture. Protein was extracted from cells grown in monolayer culture to 70% confluency, quantified by Bradford assay and separated by SDS-PAGE. Membranes were probed with goat polyclonal antibody raised against SCRIB, and  $\beta$ -actin as a loading control. Representative of two repeats. Western blots were quantified by densitometry using ImageJ software. Graphs show relative levels, first normalised to  $\beta$ -actin and then to HFK (A) or WT (B) levels.

subtle change in protein levels was observed in HPV16 genome containing cells, indicating an increase in SCRIB at the cytoskeleton and a decrease in the nuclear fraction, but this was not consistently observed. This distribution is maintained in the presence of HPV18 genomes encoding E6 proteins with modified PBM binding activity (Figure 3.15 B).

Following differentiation of the HPV18 genome containing cells in organotypic raft culture, SCRIB protein levels decrease upon abrogation of PDZ binding (Figure 3.16). This was trend seen in two donors; in one case there was an almost 50% decrease in protein in the presence of  $\Delta$ PDZ genomes compared to wild-type HPV18 genomes (Figure 3.16). Like DLG1, immunofluorescent staining of differentiated keratinocytes indicated that SCRIB protein becomes increasingly at the cell periphery as keratinocytes migrate upwards, with basal cells exhibiting a predominantly nuclear pattern of SCRIB expression (Figure 3.17). Compared to untransfected keratinocytes, stratified cells containing HPV18 genomes exhibited a more obvious junctional location of SCRIB protein, which occurred in the mid layers of the epithelia (Figure 3.17).

In summary, DLG1 and SCRIB exhibited no marked alterations in protein level or subcellular distribution in the presence of HPV16 or HPV18 genomes in monolayer grown primary human keratinocytes. An increase in SCRIB protein in the presence of HPV18 was not restored by removal of the PBM, although in differentiating cells, the levels of both proteins decreased in cells containing HPV18 genomes expressing E6 without a PBM. In differentiated culture, the location of SCRIB and DLG1 at the periphery of cells in the upper layers is altered in the presence of HPV18 and expression is increased in the mid-layers.

#### 3.3.3.1.3 CASK

CASK is known to interact with DLG1 in epithelia (Nix *et al.*, 2000), and has been observed by the Roberts lab to co-immunoprecipitate with DLG1 in human keratinocytes

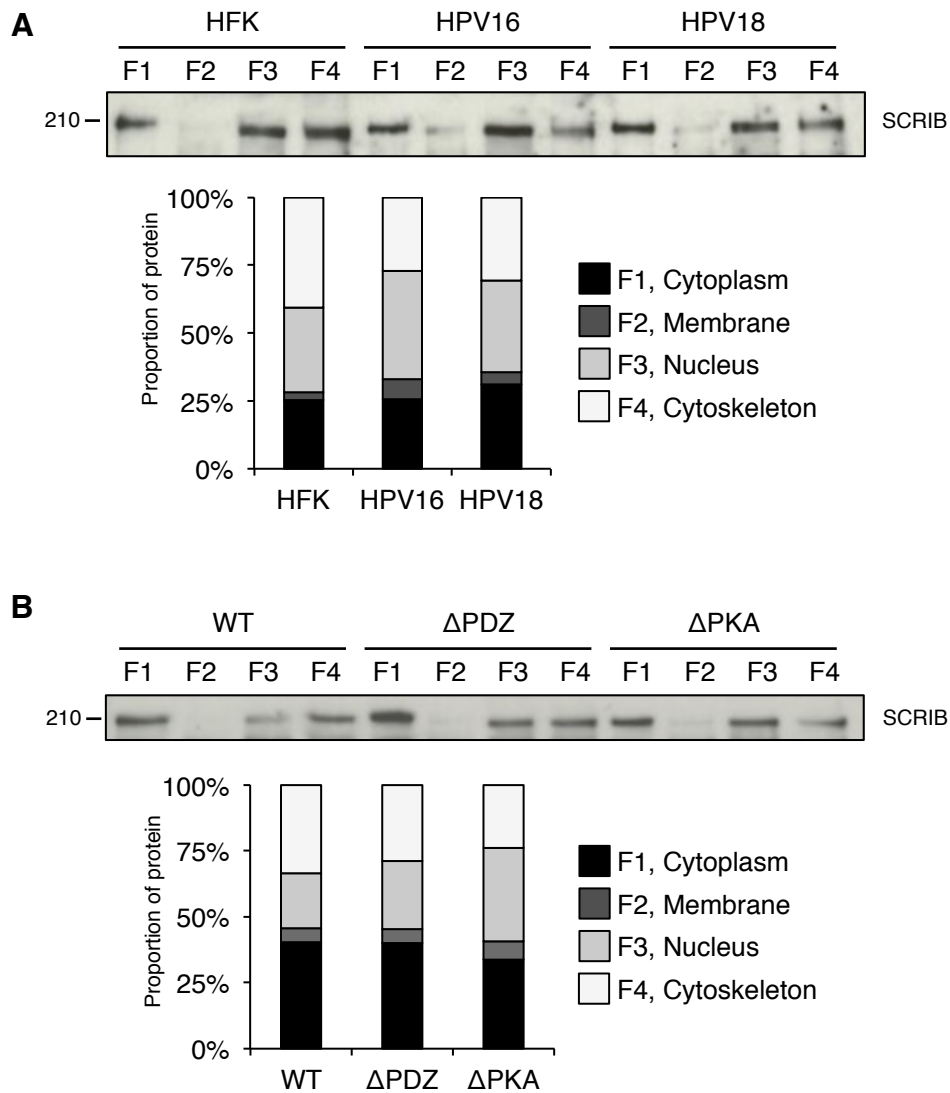


**Figure 3.15: Distribution of SCRIB in monolayer keratinocytes**

Distribution of SCRIB in keratinocytes containing HPV16 and 18 genomes (A) and mutant HPV18 genomes (B) grown in monolayer culture. Subcellular fractionation was carried out on keratinocytes at 70% confluency. The cytoplasmic, membrane, nuclear and cytoskeletal fractions were extracted by treatment with sequential lysis buffers, an equal amounts separated by SDS-PAGE. Membranes were probed with goat polyclonal antibody raised against SCRIB, Western blots were quantified by densitometry using ImageJ software. Representative of two donors, each repeated three times.

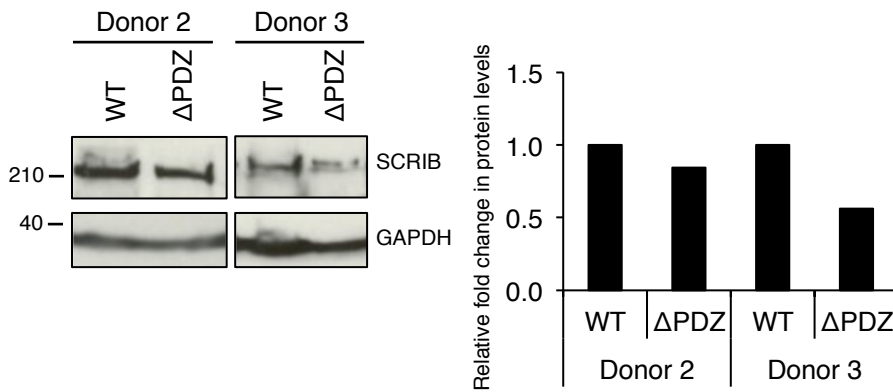


**Figure 3.16: SCRIB protein in differentiated keratinocytes containing HPV18 genomes**

Keratinocytes containing wild-type (WT) HPV18 genomes or HPV18 encoding an E6 without a PBM ( $\Delta$ PDZ) were grown in organotypic raft culture. After 13 days, the raft was harvested, homogenised and lysed in order to extract protein. Protein was separated by SDS-PAGE and membranes were probed with goat polyclonal antibody raised against SCRIB, alongside GAPDH as a loading control. Western blots were quantified by densitometry using ImageJ software. Graphs show relative levels, first normalised to GAPDH and then to WT levels. Representative of two technical repeats.

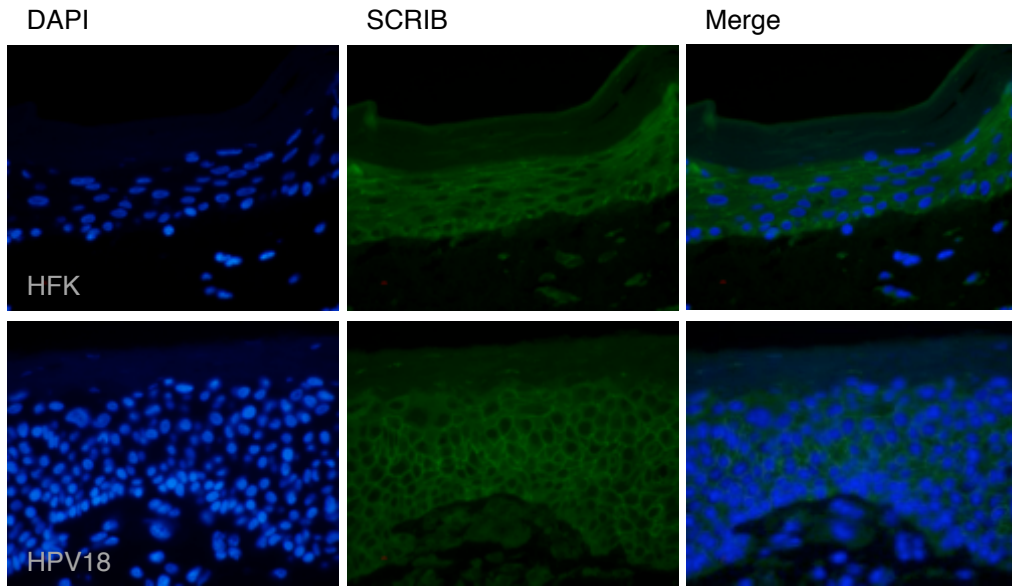


**Figure 3.17: SCRIB distribution in differentiated keratinocytes**

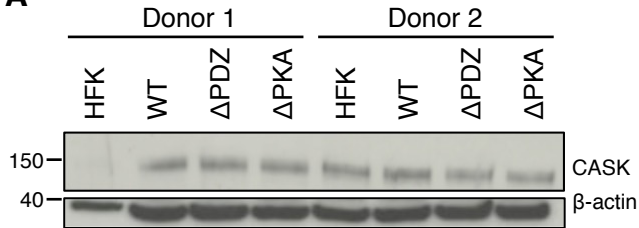
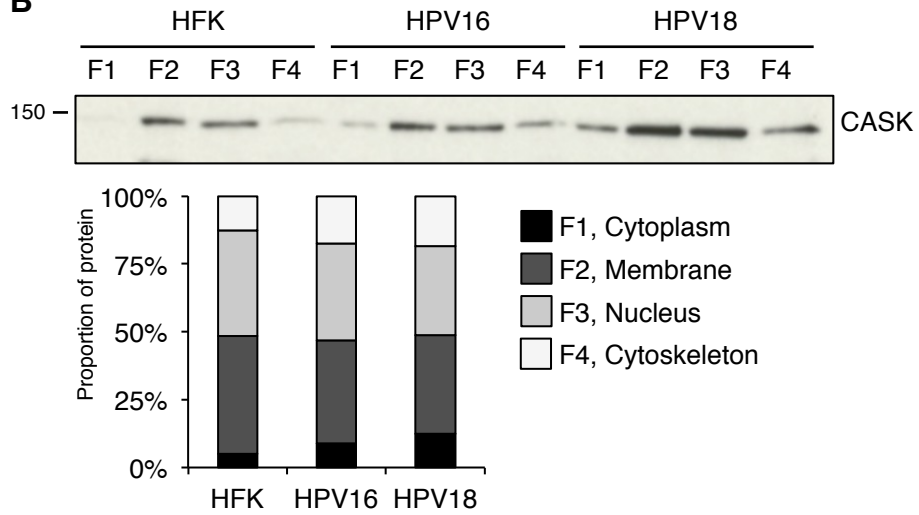
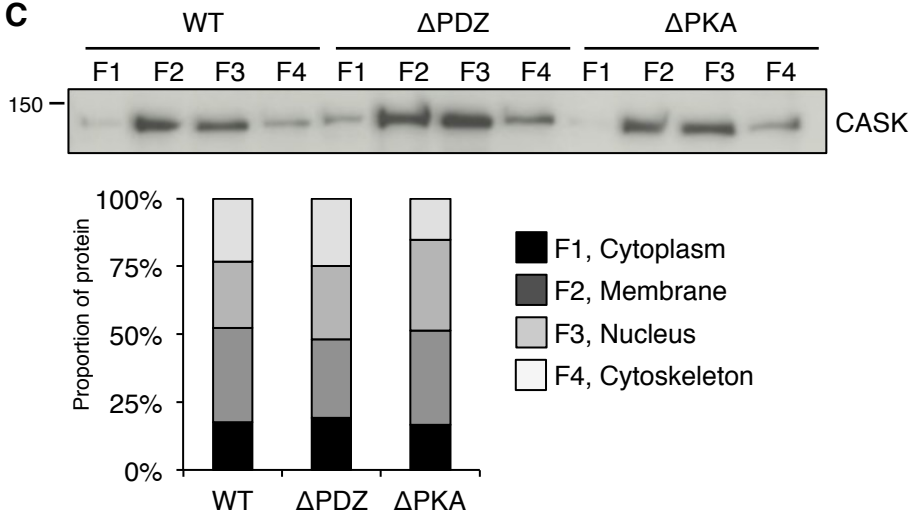
Immunofluorescent staining of keratinocytes grown in organotypic raft culture. Raft cultures were grown for 13 days, harvested and paraformaldehyde fixed. Individual sections were cut and stained for SCRIB (green) and the nucleus stained with DAPI (blue). Images were taken at 40x magnification.

(S Roberts, personal communication). Furthermore, the protein sequence exhibits 25% sequence homology to DLG1 and is suggested to associate with the HPV16 PBM in yeast-two hybrid screening experiments (Belotti *et al.*, 2013). To assess whether CASK protein expression was affected by HPV16 or HPV18, lysates isolated from monolayer cultures were western blotted for CASK protein. There was no alteration in the CASK protein levels in keratinocytes containing HPV18 (Figure 3.18 A). Furthermore, removal or alteration of the HPV18 PDZ binding ability did not produce any effect upon CASK protein (Figure 3.18 A). Next, the distribution of CASK was analysed (Figure 3.18 B and C). CASK was detected predominantly in the membrane and the nucleus in untransfected keratinocytes, with a small amount present in the cytoplasmic and cytoskeleton fractions of the cell (Figure 3.18 B and C). This subcellular distribution was not perturbed by the presence of HPV16 or HPV18, nor by alteration in the activity of the E6 PBM (Figure 3.18).

### 3.3.3.2 *Crumbs complex*

#### 3.3.3.2.1 *PATJ*

In this analysis, the levels of PATJ protein remained constant in HPV16 and HPV18 positive keratinocytes, compared to untransfected cells. Protein levels remained the same in the cancer cell line HeLa as primary keratinocytes (Figure 3.19 A). Furthermore, perturbing the PDZ binding function of E6 had no effect on protein levels compared to wild-type HPV18 genome containing cells (Figure 3.19 B). (Storrs and Silverstein, 2007) demonstrated that the truncated spliced form of E6, E6\*, was able to induce PATJ degradation, indicating that the effects of E6 on this oncoprotein is PBM independent (Storrs and Silverstein, 2007). However, this analysis did not find any overwhelming change in PATJ in monolayer grown keratinocytes (Figure 3.20). The expression of adenovirus E4-

**A****B****C**

**Figure 3.18: CASK protein level and distribution in monolayer grown keratinocytes**

- (A) Total protein was extracted from monolayer grown keratinocytes containing WT,  $\Delta$ PDZ or  $\Delta$ PKA HPV18 genomes, alongside HFKs and separated by SDS PAGE. Representative of two repeats.
- (B) Distribution of CASK in keratinocytes containing HPV16 and 18 genomes
- (C) Distribution of CASK protein in keratinocytes containing HPV18 WT and mutant genomes

Cells for B and C were grown in monolayer culture. Subcellular fractionation was carried out on keratinocytes at 70% confluency. The cytoplasmic, membrane, nuclear and cytoskeletal fractions were extracted by treatment with sequential lysis buffers, an equal amounts separated by SDS-PAGE.

In all cases, membranes were probed with rabbit polyclonal antibody raised against CASK. Western blots were quantified by densitometry using ImageJ software. Markers show molecular weight in kDa. Representative of two donors, each repeated three times.

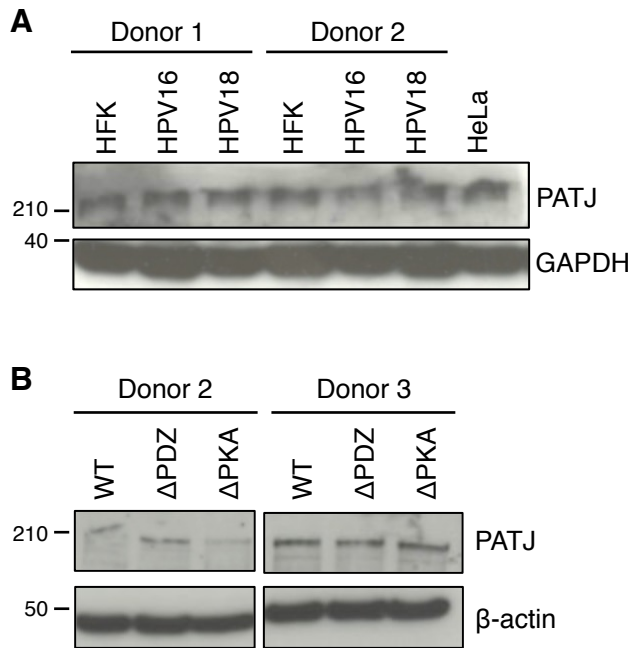


**Figure 3.19: PATJ protein levels in HPV genome containing keratinocytes**

PATJ protein levels in keratinocytes containing WT HPV16 and 18 genomes (A) and mutant HPV18 genomes (B) grown in monolayer culture. Protein was extracted from cells grown in monolayer culture to 70% confluency, quantified by Bradford assay and separated by SDS-PAGE. Membranes were probed with rabbit polyclonal antibody raised against PATJ, and  $\beta$ -actin as a loading control. Representative of two repeats. Western blots were quantified by densitometry using ImageJ software. Markers show molecular weight in kDa.

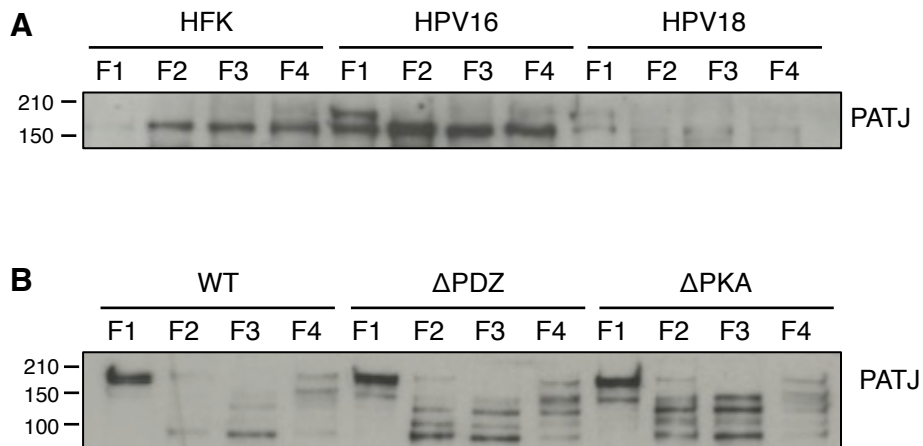


**Figure 3.20: Distribution of PATJ in monolayer keratinocytes**

Distribution of PATJ in keratinocytes containing HPV16 and 18 genomes (A) and mutant HPV18 genomes (B) grown in monolayer culture. Representative of two donors and three repeats. Subcellular fractionation was carried out on keratinocytes at 70% confluency. The cytoplasmic, membrane, nuclear and cytoskeletal fractions were extracted by treatment with sequential lysis buffers, an equal amounts separated by SDS-PAGE. Membranes were probed with rabbit polyclonal antibody raised against PATJ. Markers show molecular weight in kDa.

ORF1 has been shown to cause mislocalisation of PATJ (Latorre *et al.*, 2005), but it is not known whether expression of E6 similarly affects the localisation of PATJ protein. Thus, the distribution of PATJ was investigated in monolayer keratinocytes containing HPV genomes (Figure 3.20). During this analysis multiple bands were detected in all the fractions isolated (Figure 3.20). Five isoforms of PATJ have been identified, with molecular weights ranging between 125 to 196 kDa (Roh *et al.*, 2002; Philipp and Flockerzi, 1997; Soejima *et al.*, 2001). It may be that the bands detected by this western blot analysis correspond to PATJ variants; however, the results were inconsistent and therefore inconclusive.

### *3.3.3.3 The Par complex and other tight junction components*

#### *3.3.3.3.1 PARD3*

Western blot detection of PARD3 revealed an increase in the level of protein, in both monolayer and differentiated keratinocytes replicating HPV18 (Figure 3.21 A and D). In organotypic raft culture, a decrease in PARD3 was observed in the cells containing the HPV18  $\Delta$ PDZ mutant genomes, suggesting a role for the E6 PBM in stability of the PDZ protein, although this was not the case in cells grown monolayer culture (Figure 3.21 A and D). In HeLa cells, the level of PARD3 was similar to HFK (Figure 3.21 A). A recent study has shown that HPV18 E6 causes a PBM-dependent change in PARD3 localisation, but not proteins levels (Facciuto *et al.*, 2014). However, analysis of subcellular distribution showed no alteration in distribution of PARD3 in the viral genome containing cells; PARD3 remained predominantly nuclear and cytoskeletal, with some cytoplasmic forms (Figure 3.21 B and C). PARD3 exists as several isoforms, ranging from 100 to 200 kDa (Jan *et al.*, 2013). Interestingly, PARD3 was detected as a doublet in protein from both HFK and HeLa cells, whereas only a single form of PARD3 was detected in HPV genome

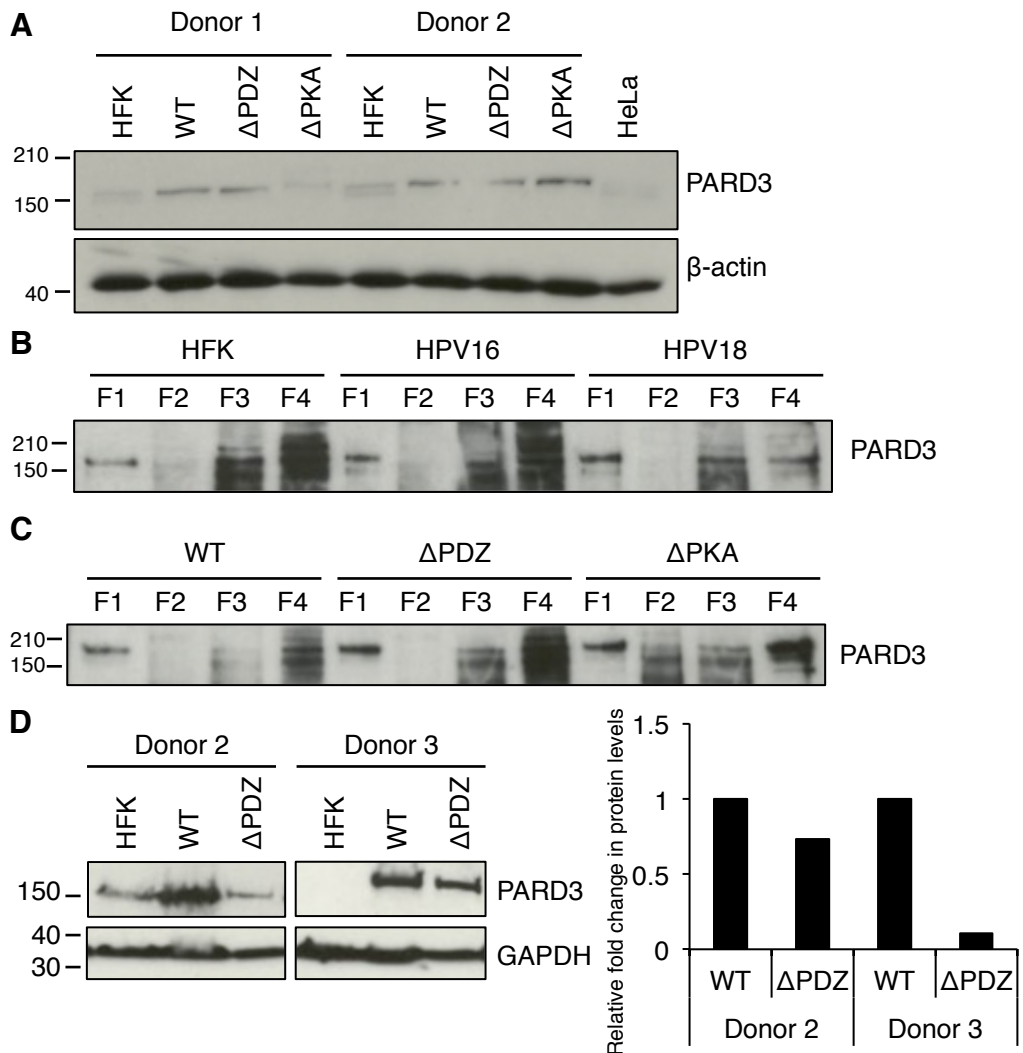


**Figure 3.21: PARD3 protein levels and distribution in primary keratinocytes**

(A) Total protein in monolayer grown keratinocytes, representative of two experimental repeats.

(B) Subcellular distribution in untransfected, HPV16- and HPV18-containing keratinocytes grown in monolayer.

(C) Subcellular distribution in HPV18 mutant genome containing cells grown in monolayer.

F1, cytoplasmic; F2, membrane; F3, Nuclear; F4, cytoskeletal. Blots representative of three repeats in two donors.

(D) Total protein levels in keratinocytes grown in organotypic raft culture, representative of two technical repeats. Densitometry shows quantification of protein in WT and  $\Delta$ PDZ genome containing cells.

All blots probed with rabbit polyclonal antibody raised against PARD3. Markers show molecular weight in kDa.

replicating cells (Figure 3.21 A). Similarly, PARD3 was detected as multiple bands in fractionation analysis, which made quantification difficult but indicated that more PARD3 variants were present in the nucleus and cytoskeleton in all keratinocytes investigated.

#### 3.3.3.3.2 *MAGI-1*

Although MAGI-1 was difficult to detect by western blotting, there is a slight increase in protein levels in undifferentiated HPV18 genome containing keratinocytes, but this was not reinforced in analysis of differentiated cells (Figure 3.22). Upon subcellular differentiation fractionation, the protein exhibited a membrane, nuclear and cytoskeleton distribution in all the primary cells analysed and this trend was largely unaffected by replication of the two high-risk genomes (Figure 3.22).

#### 3.3.3.3.3 *MUPP1*

MUPP1 protein levels were increased in HPV18 genome containing cells, and this increase was independent of the activity of the E6 PBM (Figure 3.23 A). MUPP1 protein was detected mainly in nuclear and cytoskeletal fractions, with minor expression in the cytoplasm and membrane (Figure 3.23 B and C). The distribution was largely unaffected by the viral genomes (Figure 3.23 D).

#### 3.3.3.3.4 *ZO-1*

Although no change in ZO-1 protein levels was observed in the presence of HPV16 genomes, levels of ZO-1 protein increased in HPV18 genome containing cells (Figure 3.24 A). This increase may be related to E6 PBM activity; in monolayer cells, a subtle decrease was observed when ZO-1 protein was quantified in cells containing genomes where the E6 PDZ binding function is deleted ( $\Delta$ PDZ or  $\Delta$ PKA, Figure 3.24 B). A subtle effect of the E6 PBM on ZO-1 levels is also observed in raft cultures of E6 $\Delta$ PDZ cells (Figure 3.25). However, the observed increase in protein does reflect a change in the distribution of ZO-1 (Figure 3.26). Fractionation indicated that ZO-1 resides mainly in the nucleus and

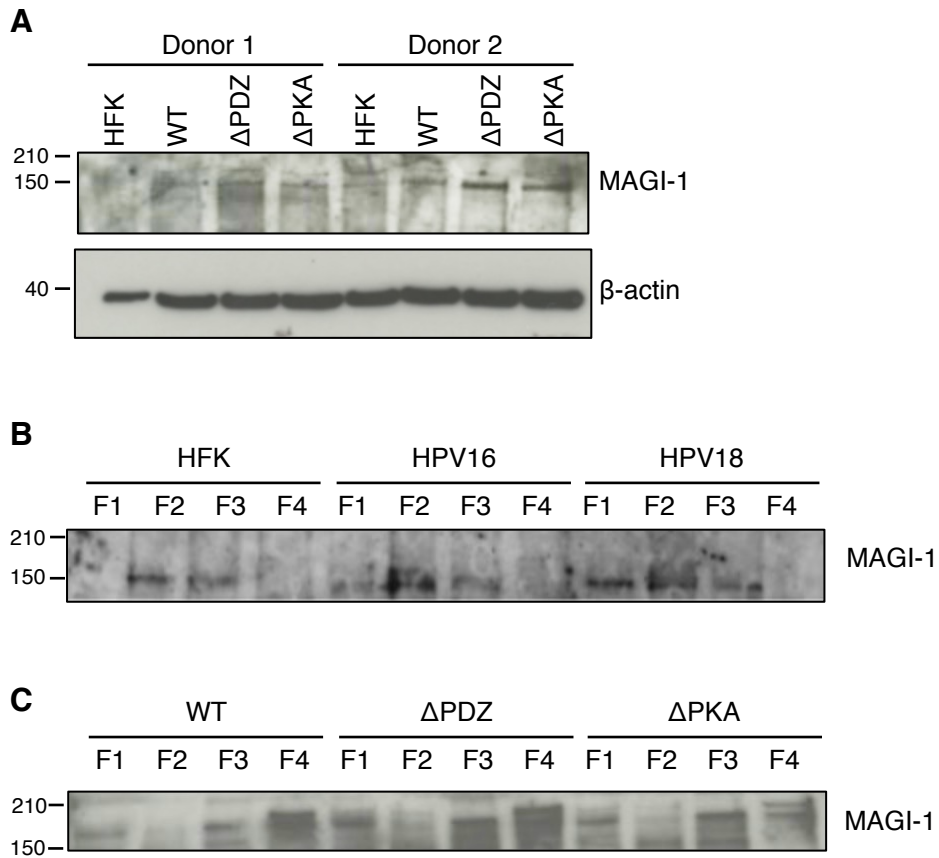


**Figure 3.22: MAGI-1 protein levels and distribution in primary keratinocytes**

(A) Total MAGI-1 protein in monolayer grown keratinocytes. Representative of two repeats.

(B) Subcellular distribution of MAGI-1 in untransfected, HPV16- and HPV18-containing keratinocytes.

(C) Subcellular distribution of MAGI-1 in HPV18 mutant genome containing cells. F1, cytoplasmic; F2, membrane; F3, Nuclear; F4, cytoskeletal.

B and C representative of three repeats in two donors. Cells grown to 70% confluency before protein extraction, and blots probed with rabbit polyclonal antibody raised against MAGI-1. Markers show molecular weight in kDa.

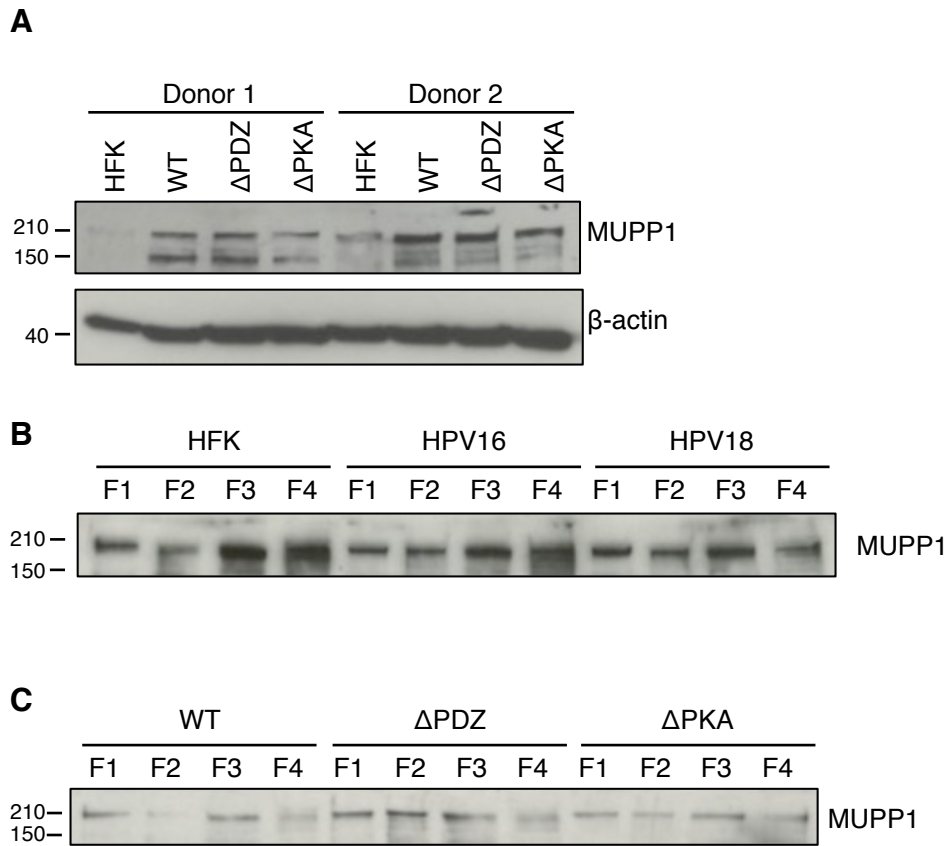


**Figure 3.23: MUPP1 protein levels and distribution in primary keratinocytes**

(A) MUPP-1 protein in monolayer grown keratinocytes. Representative of two repeats.

(B) MUPP1 subcellular distribution in untransfected, HPV16- and HPV18-containing keratinocytes

(C) Subcellular distribution of MUPP1 in HPV18 mutant genome containing cells. F1, cytoplasmic; F2, membrane; F3, Nuclear; F4, cytoskeletal. Markers show molecular weight in kDa.

B and C representative of three repeats in two donors. Cells grown to 70% confluency before protein extraction, and blots probed with rabbit polyclonal antibody raised against MAGI-1. Markers show molecular weight in kDa.

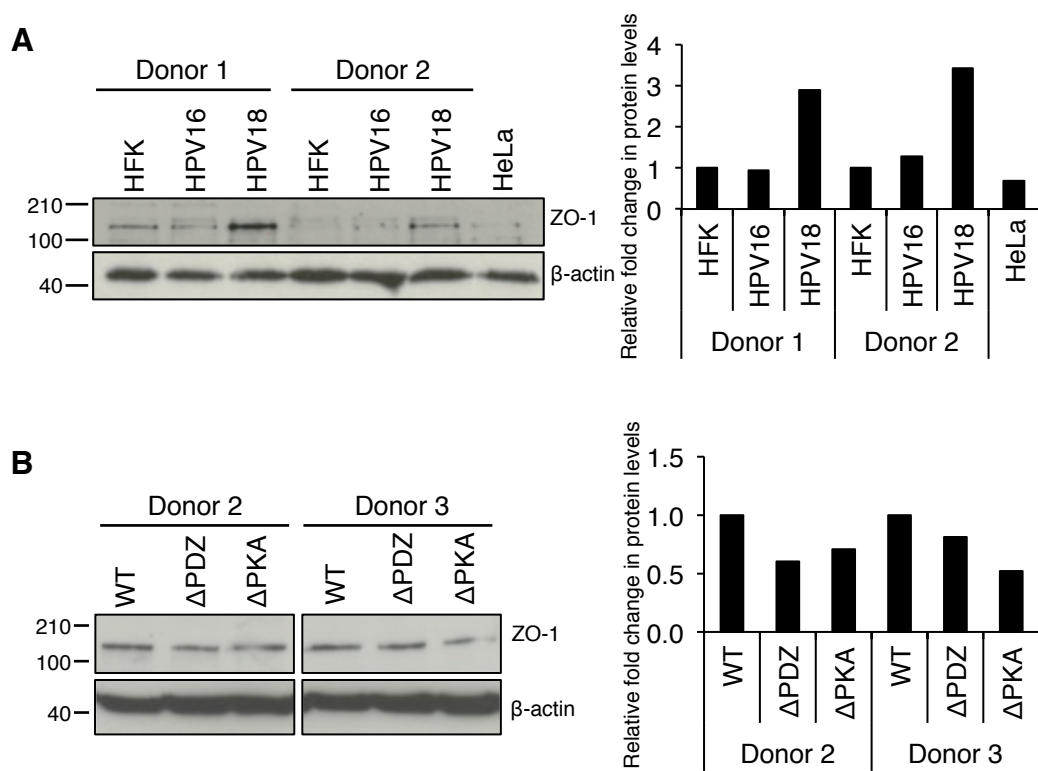


**Figure 3.24: ZO-1 protein levels in HPV genome containing keratinocytes**

Total ZO-1 protein in keratinocytes containing HPV16 and 18 genomes (A) and in keratinocytes containing mutant HPV18 genomes (B). Protein was extracted from cells grown in monolayer culture to 70% confluency, quantified by Bradford assay and separated by SDS-PAGE. Membranes were probed with mouse monoclonal antibody raised against ZO-1, and  $\beta$ -actin as a loading control. Representative of two repeats. Western blots were quantified by densitometry using ImageJ software. Graphs show relative levels, first normalised to  $\beta$ -actin and then to HFK (A) or WT (B) levels.

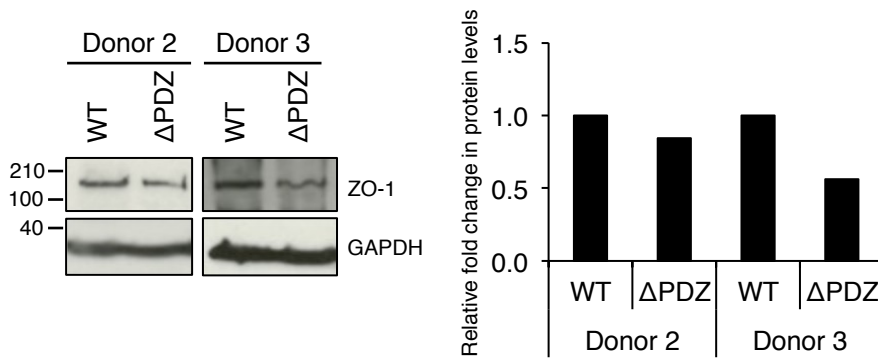


**Figure 3.25: ZO-1 protein in differentiated keratinocyte culture**

Total ZO-1 protein in keratinocytes grown in organotypic raft culture. Cells containing wild-type HPV18 (WT) genomes or genomes encoding E6 where the PBM is deleted ( $\Delta$ PDZ) were stratified for 13 days and total protein extracted in urea buffer. Separated protein was probed for ZO-1, alongside GAPDH as a loading control. Representative of two technical repeats. Western blots was quantified using ImageJ and fold change calculated relative to to WT levels.

associated with the cytoskeleton of keratinocytes, and that this situation is unperturbed by mutation of the HPV18 E6 PBM (Figure 3.26 B). A number of ZO-1 variants become apparent in subcellular fractionation analysis, and the distribution of these may be altered by the presence of HPV genomes, for example, the lower band detected in the cytoskeletal fraction is absent where HPV18 genomes are able to constitutively bind to PDZ proteins (Figure 3.26 B). However, as with PATJ and MAGI-1, this makes a conclusion difficult.

The distribution of ZO-1 was assessed in sections of differentiated keratinocytes, where expression was most apparent at the periphery of cells residing in the upper layers (Figure 3.27). However, in the presence of HPV18 genomes, expression of ZO-1 was more evenly spread across the layers of cells and the protein concentrates at regions of the membrane (Figure 3.27). Alteration of PBM activity restored the HFk phenotype in part; protein was located at the cell membrane in the upper layers of differentiated cells in the presence of  $\Delta$ PDZ genomes, suggesting that the effect of HPV18 upon ZO-1 is PBM-dependent (Figure 3.27).

#### 3.3.3.3.5 ZO-2

Similarly to ZO-1, ZO-2 protein levels are slightly increased in keratinocytes in the presence of HPV18 genomes compared to untransfected cells, but the change is not PBM dependent (Figure 3.28). In raft cultures, the level of ZO-2 in  $\Delta$ PDZ genome containing cells was less than cells containing wild-type genomes (Figure 3.28 B). More apparent is the decrease in ZO-2 in the presence of HPV16 genomes (Figure 3.28 A). In cultured epithelial cells, HPV16 E6 expression has been shown to cause ZO-2 relocalisation to the nucleus and cytoplasm from cell borders (Hernandez-Monge *et al.*, 2013). In this study of ZO-2 cellular distribution, in viral genome containing cells, ZO-2 was detected consistently in the membrane, nuclear and cytoskeletal fraction (Figure 3.29). An increase in ZO-2 protein was observed in the nuclear fraction of cells containing PBM-deletion mutants, and in

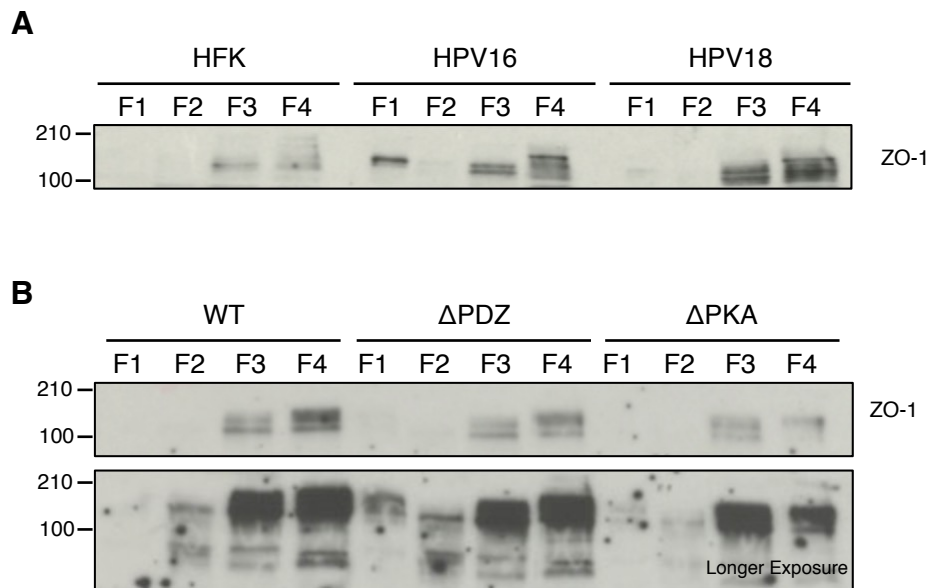


**Figure 3.26: Distribution of ZO-1 in monolayer keratinocytes**

Distribution of ZO-1 in keratinocytes containing HPV16 and 18 genomes (A) and mutant HPV18 genomes (B) grown in monolayer culture. Representative of two donors and three repeats. Subcellular fractionation was carried out on keratinocytes at 70% confluency. The cytoplasmic (F1), membrane (F2), nuclear (F3) and cytoskeletal (F4) fractions were extracted by treatment with sequential lysis buffers, an equal amounts separated by SDS-PAGE. Membranes were probed with mouse monoclonal antibody raised against ZO-1. Representative of three repeats of two donors.

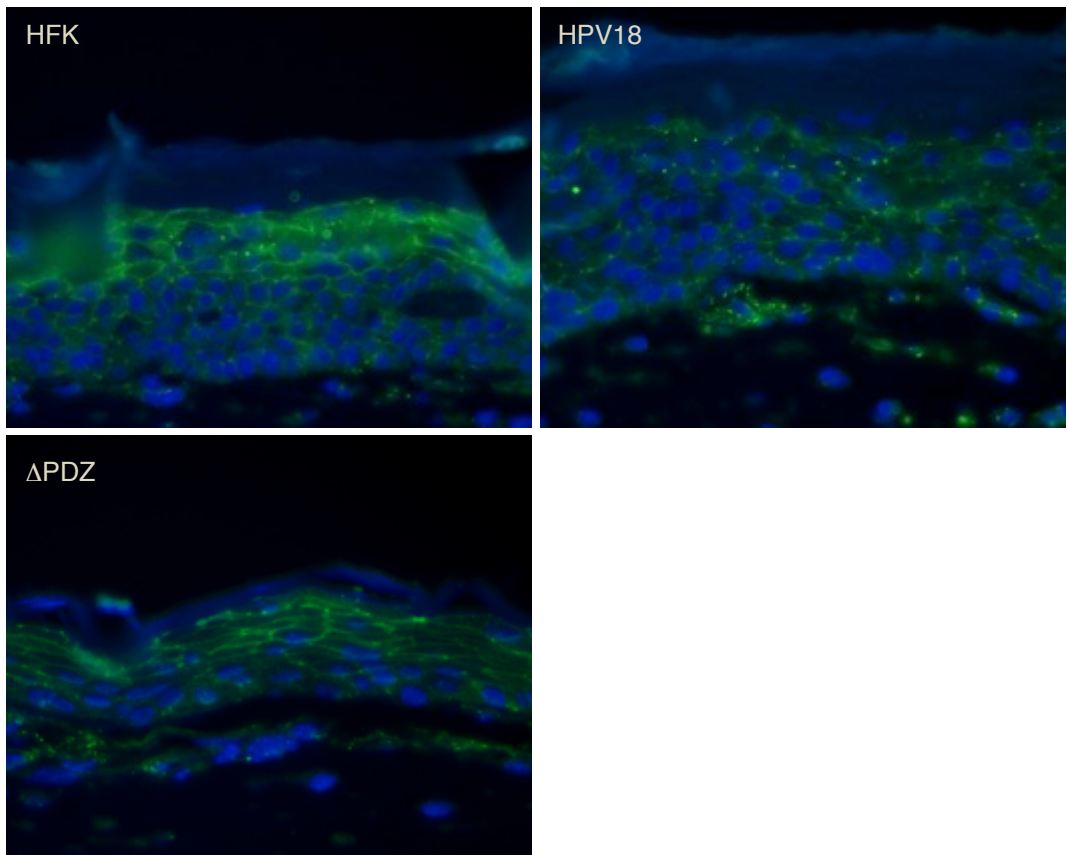


**Figure 3.27: ZO-1 distribution in differentiated keratinocytes**

Immunofluorescent staining of keratinocytes grown in organotypic raft culture. Raft cultures were grown for 13 days, harvested and paraformaldehyde fixed. Individual sections were cut and stained for ZO-1 (green) and the nucleus stained with DAPI (blue). Images were taken at 40x magnification.

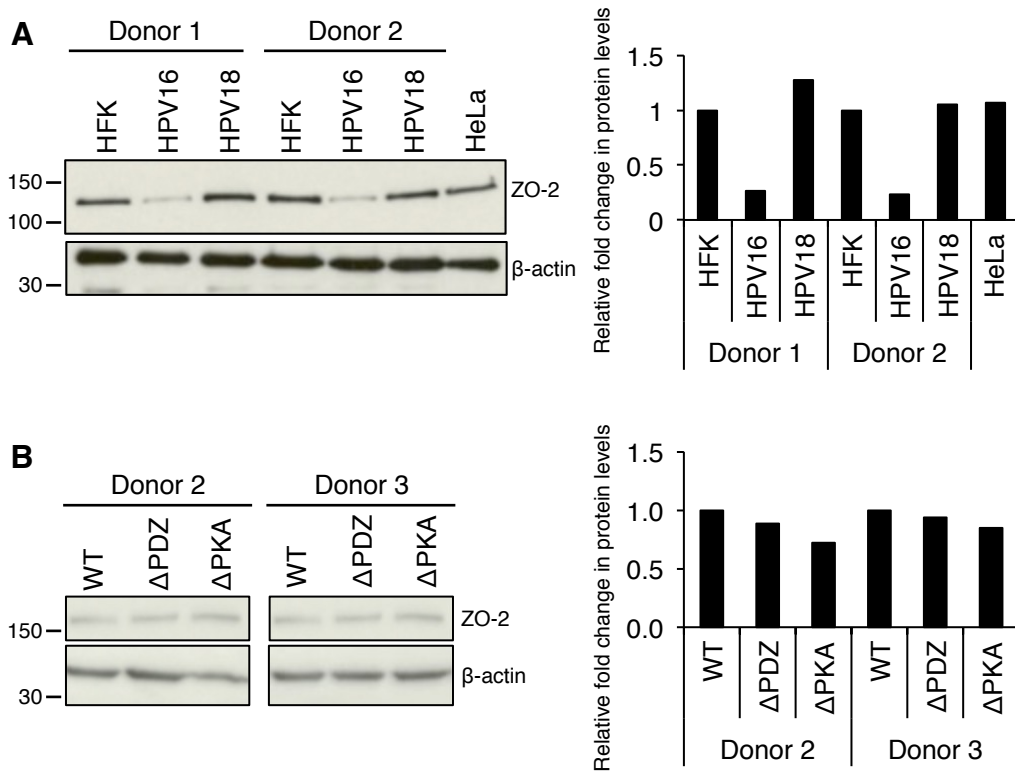


**Figure 3.28: ZO-2 protein levels in HPV genome containing keratinocytes**

ZO-2 protein levels in keratinocytes containing WT HPV16 and 18 genomes (A) and mutant HPV18 genomes (B) grown in monolayer culture. Protein was extracted from cells grown in monolayer culture to 70% confluency, quantified by Bradford assay and separated by SDS-PAGE. Membranes were probed with rabbit polyclonal antibody raised against ZO-2, and  $\beta$ -actin as a loading control. Representative of two repeats. Western blots were quantified by densitometry using ImageJ software. Graphs show relative levels, first normalised to  $\beta$ -actin and then to HFK (A) or WT (B) levels.

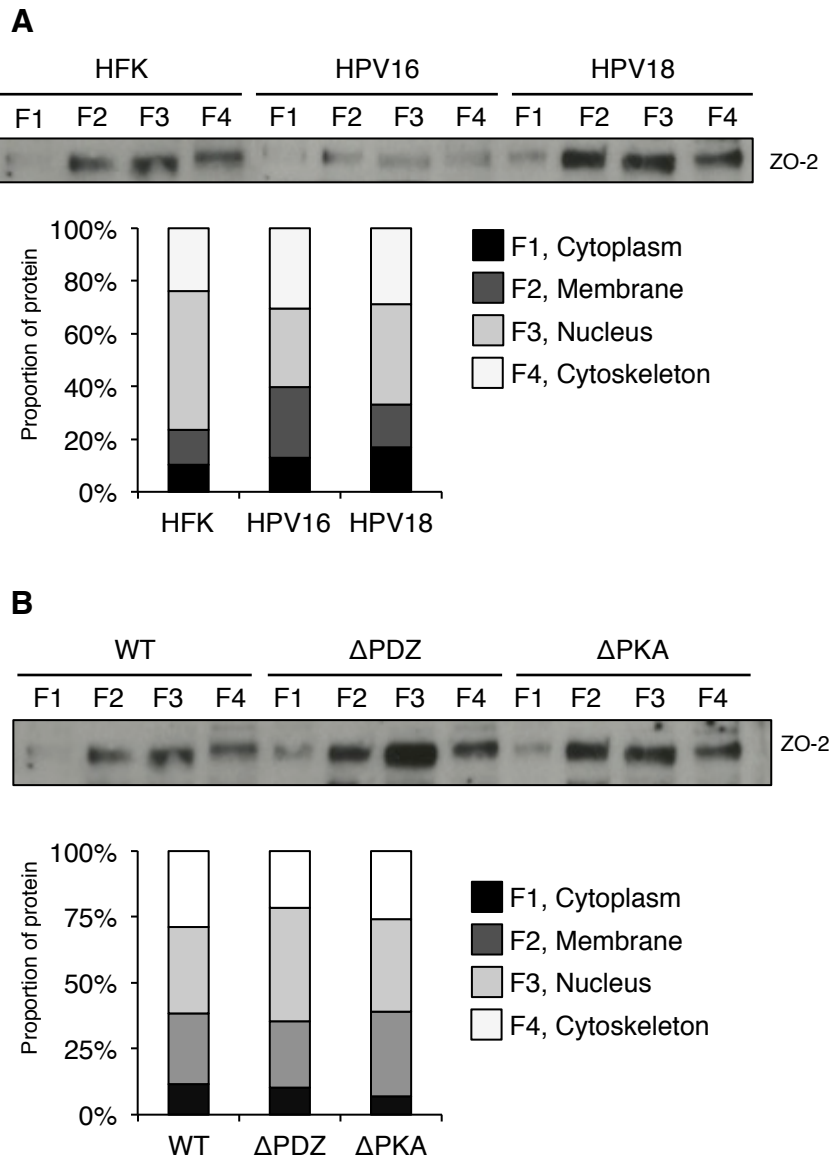


**Figure 3.29: Distribution of ZO-2 protein in monolayer keratinocytes**

Distribution of ZO-2 in keratinocytes containing HPV16 and 18 genomes (A) and mutant HPV18 genomes (B) grown in monolayer culture. Representative of two donors and three repeats. Subcellular fractionation was carried out on keratinocytes at 70% confluency. The cytoplasmic, membrane, nuclear and cytoskeletal fractions were extracted by treatment with sequential lysis buffers, an equal amounts separated by SDS-PAGE. Membranes were probed with rabbit polyclonal antibody raised against ZO-2. Western blots were quantified by densitometry using ImageJ software.

HFks, indicating a PBM-dependent effect upon ZO-2 distribution by HPV. However, analysis of differentiated cells revealed no change in ZO-2 protein levels in the presence of HPV18 (Figure 3.30).

#### *3.3.3.4 Signalling proteins*

##### *3.3.3.4.1 NHERF1*

The expression of NHERF1 protein is unaffected by the presence of HPV16 or HPV18 episomes. Similarly, levels of the cellular PDZ protein are not affected by the activity of the E6 PBM (Figure 3.31). Investigation of the subcellular distribution of NHERF1 revealed that the pattern of NHERF1 expression is unaltered by viral genome replication (Figure 3.32). During Western blot analysis, several forms of NHERF1 migrating at different molecular weights were identified (Figure 3.32). These are likely to correspond to hypo and hyper-phosphorylated forms of the protein (He *et al.*, 2001). NHERF1 protein was predominantly detected in the cytoplasm, but was also present at the membrane and nuclear fractions (Figure 3.32). A potential hypophosphorylated form of NHERF1 is predominantly detected in the cytoskeletal compartment, detected as a faster migrating polypeptide (Figure 3.32 He *et al.*, 2001). Although high-risk viruses had no effect to report upon NHERF1 protein levels in monolayer culture or differentiated cells compared to untransfected cells, levels of NHERF1 protein increased (by 2-fold) in cells upon loss of E6 PBM activity (Figure 3.33). Further investigation by immunofluorescent staining of differentiated culture sections revealed that, whereas low levels of NHERF1 protein was detected throughout differentiated HFks, in the presence of HPV18 NHERF1 levels remained low in the basal layer but expression was increased in the mid and upper layers (Figure 3.34). A similar phenotype was observed in the absence of the E6 PBM, although the protein is more obviously not at the cell membranes in these sections (Figure 3.34).

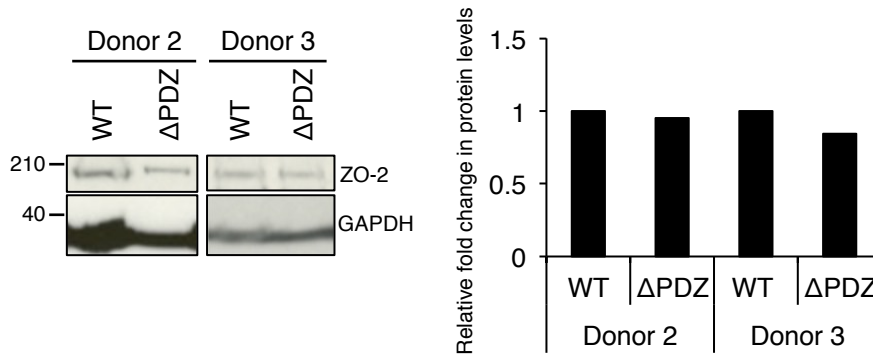


**Figure 3.30: ZO-2 protein in differentiated keratinocytes**

Total ZO-2 protein in keratinocytes grown in organotypic raft culture. Cells containing wild-type HPV18 (WT) genomes or genomes encoding E6 where the PBM is deleted ( $\Delta$ PDZ) were stratified for 13 days and total protein extracted in urea buffer. Separated protein was probed for ZO-2, alongside GAPDH as a loading control. Representative of two technical repeats. Western blots was quantified using ImageJ and fold change calculated relative to to WT levels.

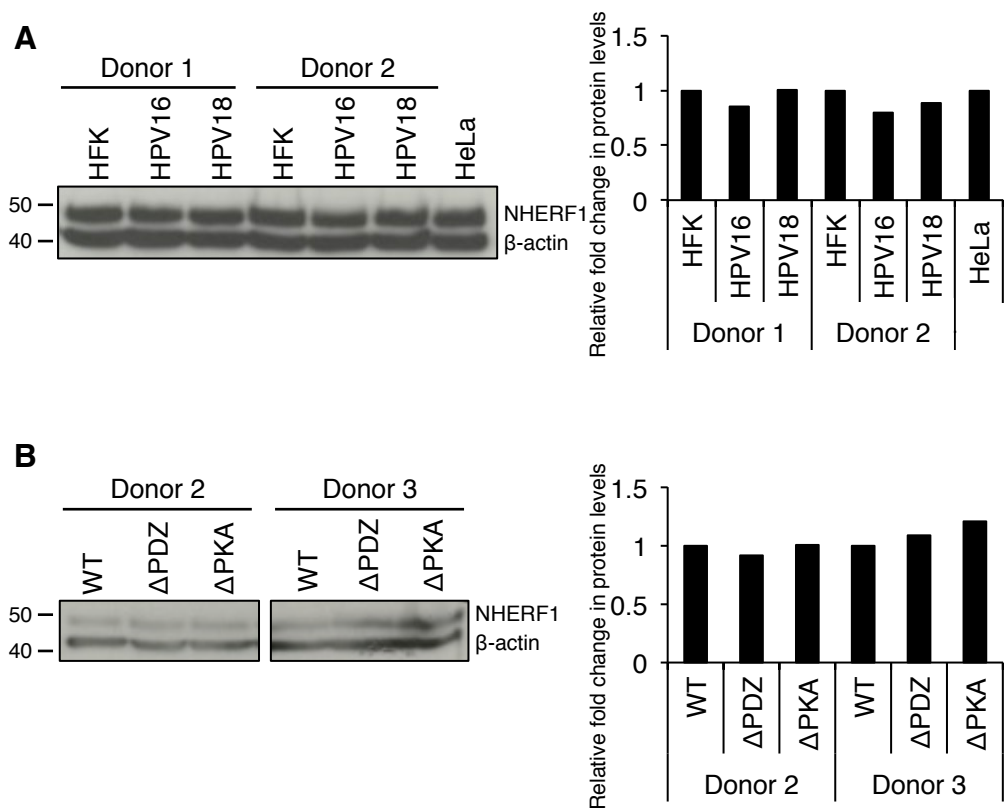


**Figure 3.31: NHERF1 protein levels in HPV genome containing keratinocytes**

NHERF1 protein levels in keratinocytes containing WT HPV16 and 18 genomes (A) and mutant HPV18 genomes (B) grown in monolayer culture. Protein was extracted from cells grown in monolayer culture to 70% confluency, quantified by Bradford assay and separated by SDS-PAGE. Membranes were probed with mouse polyclonal antibody raised against NHERF1, and  $\beta$ -actin as a loading control. Representative of two repeats. Western blots were quantified by densitometry using ImageJ software. Graphs show relative levels, first normalised to  $\beta$ -actin and then to HFK (A) or WT (B) levels.

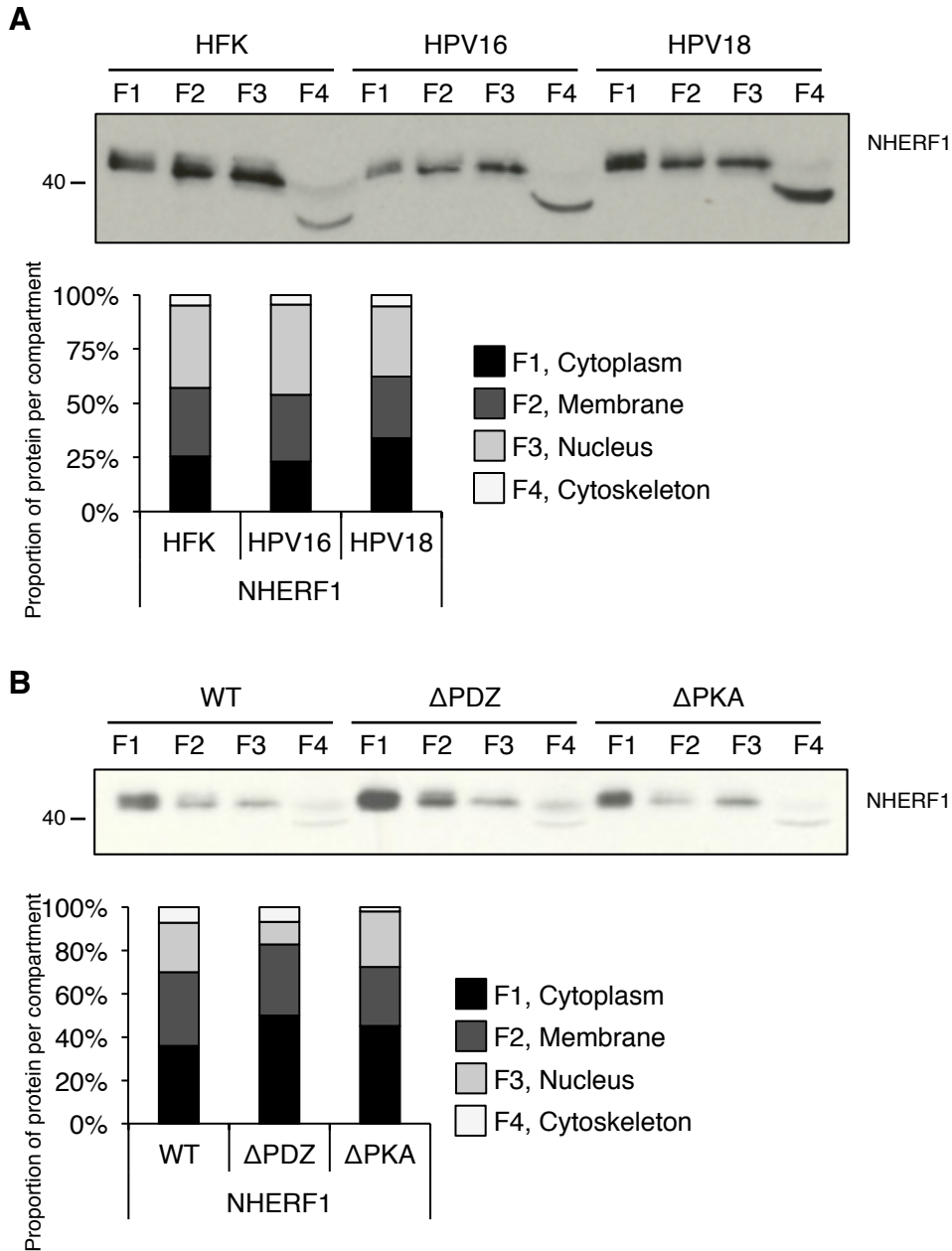


**Figure 3.32: Distribution of NHERF1 protein in monolayer keratinocytes**

Distribution of NHERF1 in keratinocytes containing HPV16 and 18 genomes (A) and mutant HPV18 genomes (B) grown in monolayer culture. Representative of two donors and three repeats. Subcellular fractionation was carried out on keratinocytes at 70% confluency. The cytoplasmic (F1), membrane (F2), nuclear (F3) and cytoskeletal (F4) fractions were extracted by treatment with sequential lysis buffers, an equal amounts separated by SDS-PAGE. Membranes were probed with mouse monoclonal antibody raised against NHERF1. Western blots were quantified by densitometry using ImageJ software, quantifying the top band only.

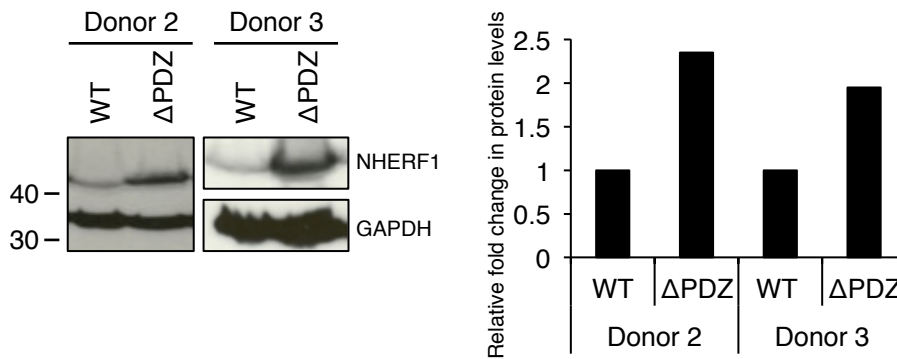


**Figure 3.33: NHERF1 protein in differentiated keratinocytes**

Total NHERF1 protein in keratinocytes grown in organotypic raft culture. Cells containing wild-type HPV18 (WT) genomes or genomes encoding E6 where the PBM is deleted ( $\Delta$ PDZ) were stratified for 13 days and total protein extracted in urea buffer. NHERF1 was detected alongside GAPDH as a loading control. Representative of two technical repeats. Western blots was quantified using ImageJ and fold change calculated relative to WT levels.

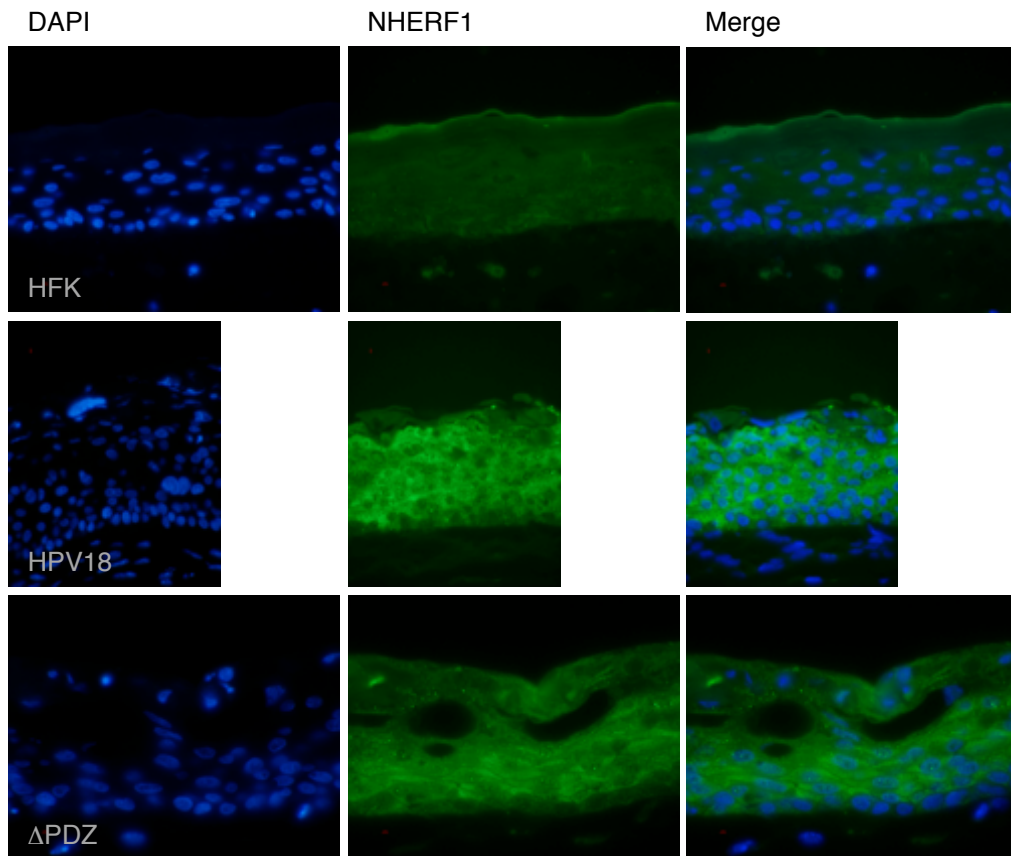


**Figure 3.34: NHERF1 distribution in differentiated keratinocytes**

Immunofluorescent staining of keratinocytes grown in organotypic raft culture. Raft cultures were grown for 13 days, harvested and paraformaldehyde fixed. Individual sections were cut and stained for NHERF1 (green) and the nucleus stained with DAPI (blue). Images were taken at 40x magnification.

#### 3.3.3.4.2 *PTPN13*

There was no change in PTPN13 protein levels in undifferentiated keratinocytes containing HPV16 or HPV18 genomes, compared to levels in the untransfected HFKs (Figure 3.35 A). Furthermore, the protein is not perturbed in HeLa compared to normal primary keratinocytes (Figure 3.35 A). Abrogation of the HPV18 E6 PBM did not affect cellular levels of PTPN13 protein; equivalent levels of PTPN13 were observed in cells containing WT,  $\Delta$ PDZ and  $\Delta$ PKA genomes (Figure 3.35 B). Although an increase in PTPN13 in the membrane fraction can be observed in HPV16 genome containing keratinocytes, the number of potential variants detected made the analysis in genome containing cells unclear (Figure 3.36). In monolayer, alteration of the E6 PBM led to a higher proportion of PTPN13 detected in the nucleus and, in differentiated keratinocytes removal of the PBM caused an increase in PTPN13 protein compared to wild-type HPV18 genome containing cells (Figure 3.37).

#### 3.3.4 Proteasomal inhibition of primary keratinocytes

In the context of cells containing the complete HPV genome, where E6 is expressed from its natural promoter, no decrease in PDZ protein levels has been observed, compared to control keratinocytes. A number of PDZ proteins, including DLG1, SCRIB, PTPN13 and NHERF1, have been identified as targets of high-risk  $\alpha$ -HPVs for proteasome-mediated degradation, in a PBM dependent manner. Therefore, to assess the expression of these proteins in response to inhibition of the proteasome in the viral genome containing cells, cells were treated with MG132 for 4 or 6 hours, alongside cells treated with the vehicle DMSO. Protein was harvested in urea lysis buffer and subjected to western blot analysis as described in Section 2.2.4.

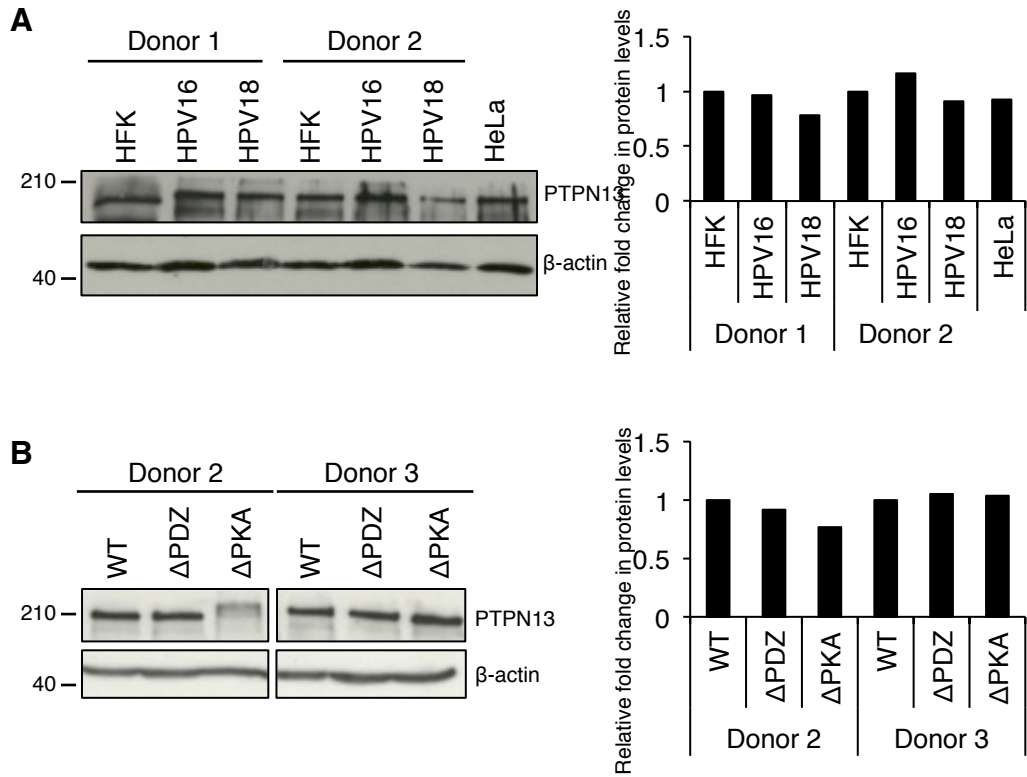


**Figure 3.35: PTPN13 protein levels in HPV genome containing keratinocytes**

PTPN13 protein levels in keratinocytes containing WT HPV16 and 18 genomes (A) and mutant HPV18 genomes (B) grown in monolayer culture. Protein was extracted from cells grown in monolayer culture to 70% confluency, quantified by Bradford assay and separated by SDS-PAGE. Membranes were probed with rabbit polyclonal antibody raised against PTPN13, and  $\beta$ -actin as a loading control. Representative of two repeats. Western blots were quantified by densitometry using ImageJ software. Graphs show relative levels, first normalised to  $\beta$ -actin and then to HFK (A) or WT (B) levels.

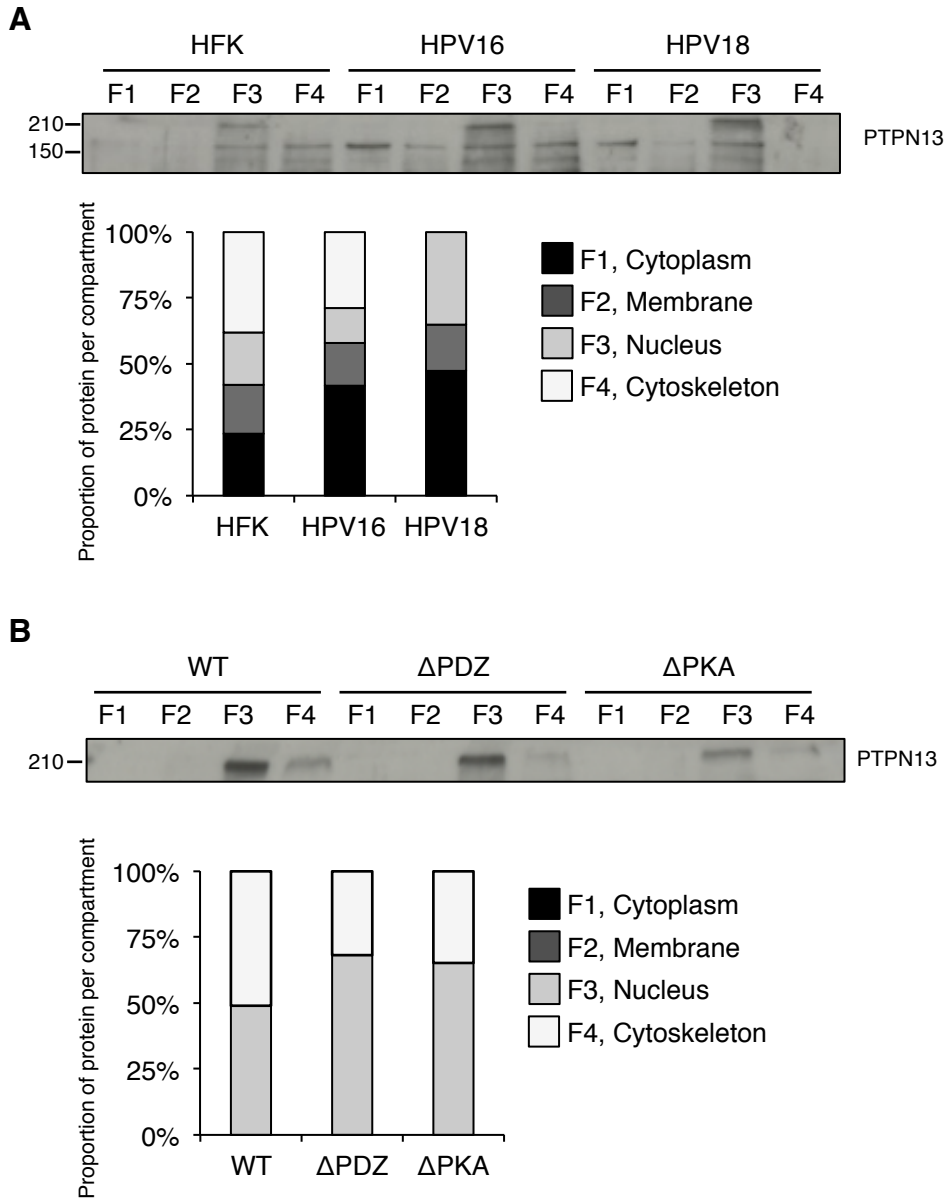


**Figure 3.36: Distribution of PTPN13 in monolayer keratinocytes**

Distribution of PTPN13 in keratinocytes containing HPV16 and 18 genomes (A) and mutant HPV18 genomes (B) grown in monolayer culture. Representative of two donors and three repeats. Subcellular fractionation was carried out on keratinocytes at 70% confluency. The cytoplasmic, membrane, nuclear and cytoskeletal fractions were extracted by treatment with sequential lysis buffers, an equal amounts separated by SDS-PAGE. Membranes were probed with rabbit polyclonal antibody raised against PTPN13 and Western blots were quantified by densitometry using ImageJ software.

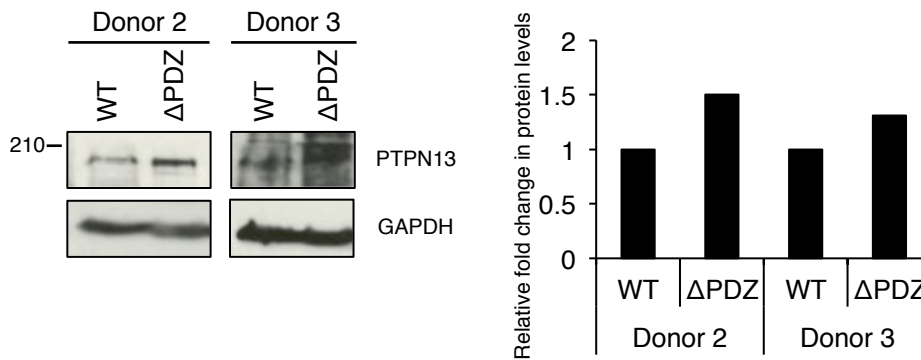


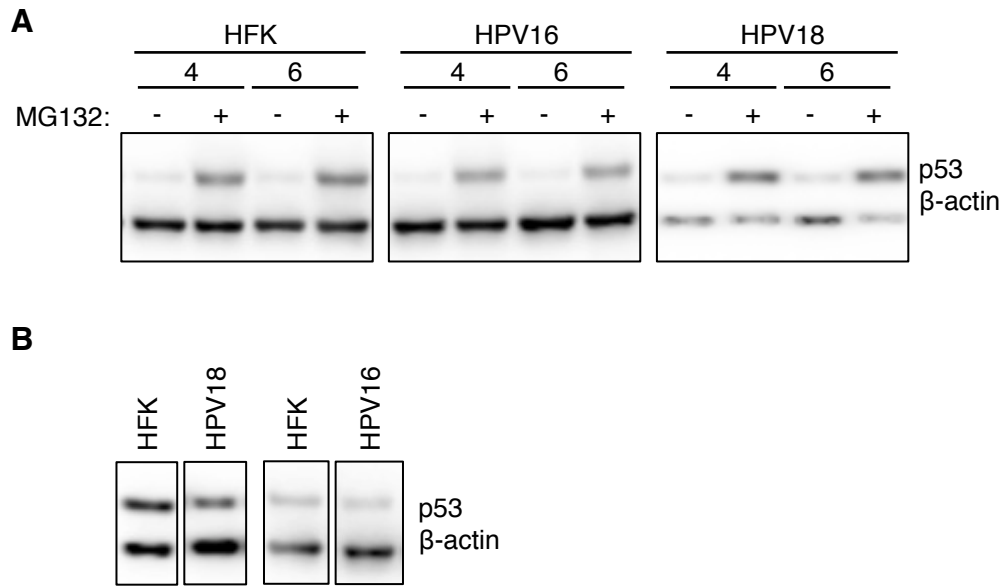
**Figure 3.37: PTPN13 protein in differentiated keratinocytes**

Total PTPN13 protein in keratinocytes grown in organotypic raft culture. Cells containing wild-type HPV18 (WT) genomes or genomes encoding E6 where the PBM is deleted ( $\Delta$ PDZ) were stratified for 13 days and total protein extracted in urea buffer. Separated protein was probed for PTPN13, alongside GAPDH to indicate equal loading. Representative of two technical repeats. Western blots were quantified using ImageJ and fold change calculated relative to WT levels.

Since p53 is a known target of proteasomal degradation, both in the presence and absence of the E6 oncoprotein, the lysates were immunoblotted for p53. As expected, an increase in p53 was observed in both HFK and HPV positive cells upon addition of MG132, confirming that proteasomal inhibition was successful (Figure 3.38 A). A decrease in p53 protein was observed when comparing HPV positive cells to untransfected control cells (Figure 3.38 B).

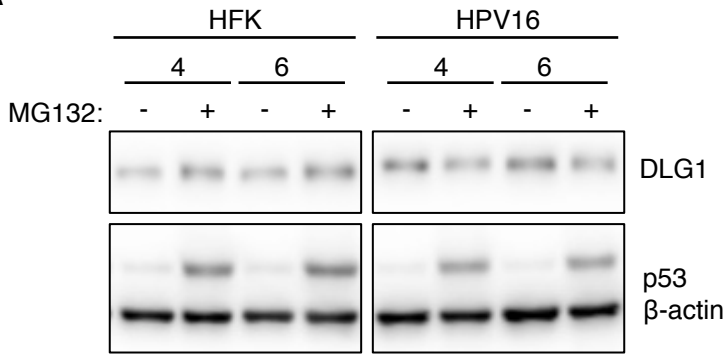
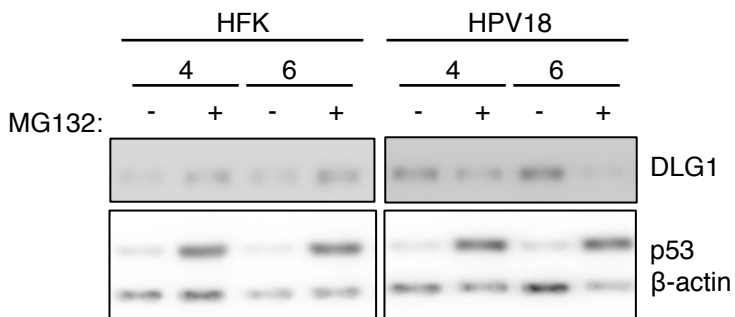
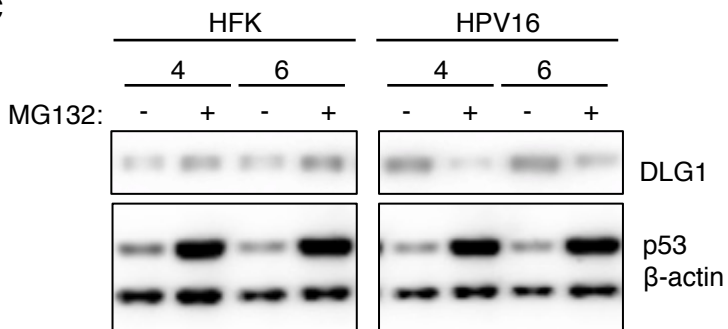
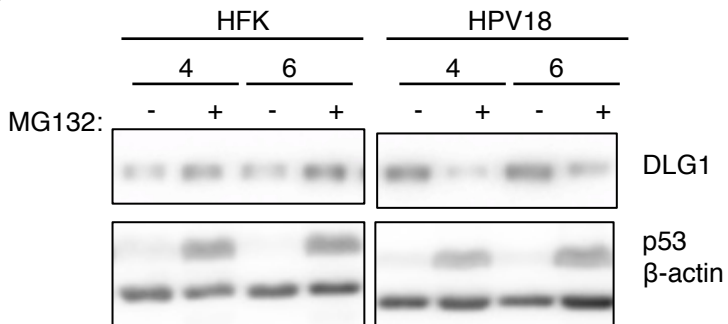
In HFKs under conditions of proteasomal inhibition, DLG1 protein accumulated following 4 and 6 hours of inhibition, confirming that the protein is targeted for proteasomal degradation (Mantovani *et al.*, 2001, Figure 3.39). By contrast, there was a marked decrease in the level of DLG1 protein in viral genome containing untransfected keratinocytes treated with proteasomal inhibitor, compared to equivalent cells treated with vehicle (Figure 3.39 A and B). As a junction complex protein, it was expected that DLG1 levels would be increased in cells harvested at a higher density. However, a similar pattern was observed in cells harvested at a higher confluency (90% vs. 70%); levels of DLG1 decreased following proteasomal inhibition (Figure 3.39 C and D). Intriguingly, a similar profile was observed for SCRIB, albeit the effect was less marked and was not specific to keratinocytes containing viral genomes (Figure 3.40). This response to proteasomal inhibition was not consistent between all PDZ proteins tested, because both NHERF1 and PTPN13 levels increased upon proteasomal inhibition, irrespective of the presence of HPV genomes (Figure 3.41). Moreover, the change in PTPN13 levels in response to MG132 in cells containing HPV16 genomes is not striking (Figure 3.41).

The interaction between high-risk HPV E6 with NHERF1, SCRIB and DLG1 has been shown to result in proteasomal degradation of the PDZ proteins (Gardioli *et al.*, 1999; Massimi *et al.*, 2008; Accardi *et al.*, 2011; Nakagawa and Huibregtse, 2000). However, treatment of primary keratinocytes with proteasomal inhibitor revealed that the presence of



**Figure 3.38: PDZ protein levels in keratinocytes under proteasomal inhibition**

- (A) Monolayer-grown keratinocytes containing HPV16 or HPV18 genomes were treated alongside HFK with vehicle (DMSO, -) or the proteasomal inhibitor MG132 (+), for 4 or 6 hours before protein was extracted using a urea buffer. Equal amounts of protein were separated by SDS-PAGE and p53 levels detected alongside  $\beta$ -actin loading control.
- (B) Comparison of untreated controls run on the same gels. Equal amounts of protein were separated by SDS-PAGE and p53 levels detected alongside  $\beta$ -actin loading control. Representative of three repeats in cells derived from one donor background.

**A****B****C****D**

**Figure 3.39: DLG1 protein levels in keratinocytes under proteasomal inhibition**

DLG1 protein analysis of keratinocytes treated with vehicle (DMSO, -) or proteasomal inhibitor MG132 (+) for four or six hours before harvesting. Keratinocytes containing HPV16 (A and C) or HPV18 (B and D) genomes were grown alongside untransfected cells to 70% (A and B) or 90% (C and D) confluency before treatment. DLG1 was detected using a mouse monoclonal antibody (2D11). Representative of three repeats in cells derived from one donor background.

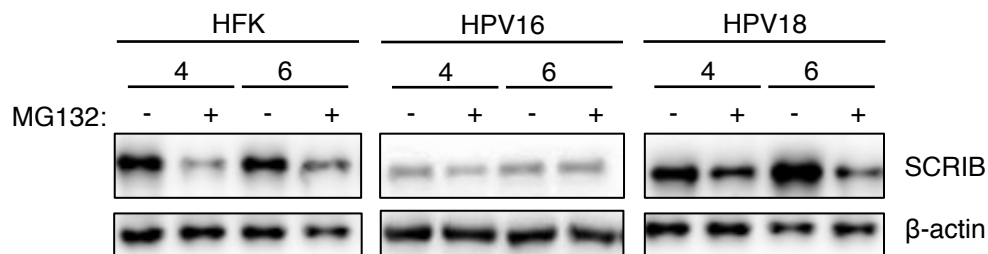


**Figure 3.40: SCRIB protein in keratinocytes under conditions of proteasomal inhibition**

SCRIB protein analysis of keratinocytes treated with vehicle (DMSO, -) or proteasomal inhibitor MG132 (+) for four or six hours before harvesting. Keratinocytes containing HPV16 or HPV18 genomes were grown alongside untransfected cells to 70% confluency before treatment. SCRIB was detected using a goat polyclonal antibody. Representative of three repeats in cells derived from one donor background.

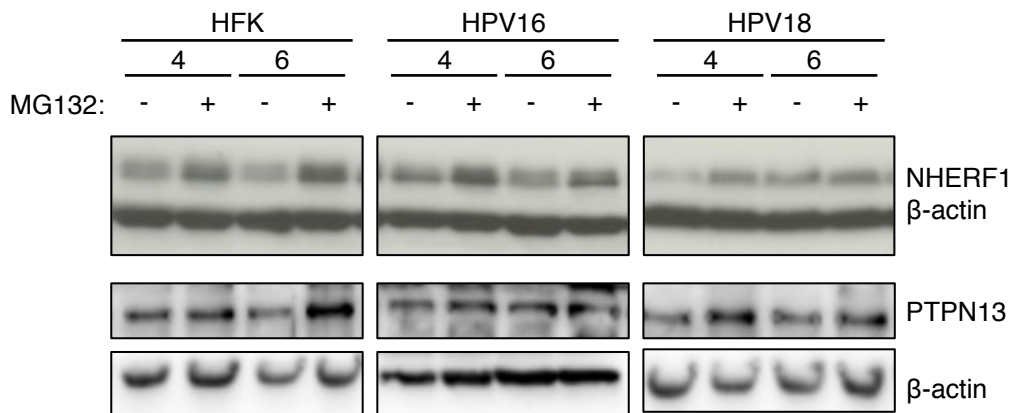


**Figure 3.41: NHERF1 and PTPN13 protein levels in keratinocytes under proteasomal inhibition**

NHERF1 and PTPN13 Protein analysis of keratinocytes treated with vehicle (DMSO, -) or proteasomal inhibitor MG132 (+) for four or six hours before harvesting. HFKs and HPV16 or 18 genome containing keratinocytes were grown to 70% confluency and harvested in urea buffer. Detection of  $\beta$ -actin was included as a loading control. Representative of three repeats in cells derived from one donor background.

HPV genomes does not affect the proteasome-mediated degradation of E6 PDZ targets SCRIB, PTPN13 and NHERF1. Moreover, proteasome inhibition of primary keratinocytes containing high-risk HPVs had an unexpected effect upon DLG1.

**Table 3.5: Summary of PDZ protein analysis**

PDZ target	Compared to untransfected keratinocytes			Compared to HPV18 wild-type		
	HPV16	HPV18	HeLa	Monolayer culture	Differentiated culture	
				$\Delta$ PDZ	$\Delta$ PKA	$\Delta$ PDZ
DLG1	(-)	NC	-	NC	NC	-
SCRIB	NC	+	NC	NC	NC	(-)
CASK	NT	NT	NT	NC	NC	NT
MAGI-1	NT	(+)	NT			
MUPP1	NT	+	NT	NC	NC	NT
PARD3	NT	+	NC	NC	NC	-
PATJ	NC	NC	NC	NC	NC	NC
ZO-1	NC	+	NC	(-)	(-)	(-)
ZO-2	-	NC	NC	-	NC	(-)
NHERF1	NC	NC	NC	NC	NC	+
PTPN13	NC	NC	NC	NC	NC	+

+, increase; -, decrease; NC, No change; NT, not tested. Bracketed values indicate subtle changes

### 3.4 Discussion

#### 3.4.1 Transcriptional upregulation in the presence of HPV genomes

Primary keratinocyte cell lines containing HPV16 or HPV18 were established and subjected to analysis of PDZ protein expression. The viral genomes in these lines exist as episomes and in monolayer the cell model is comparable to basal infected cells. Both microarray and qRTPCR analyses revealed that the polarity proteins *DLG1* (Scribble complex), *MAGI-2* (tight junctions) and *PATJ* (Crumbs complex), as well as the signalling proteins *NHERF1* and *PTPN13*, were upregulated at a transcriptional level in HPV16 and HPV18 genome containing cells. This was in contrast to the other PDZ proteins investigated, *SCRIB* (Scribble complex) and *MAGI-3* (tight-junctions), whose transcription was unaffected. The values of fold change were consistently higher than microarray values when quantified by qRTPCR, but the trend in transcriptional change was comparable. Differences in values between qRTPCR and microarray quantification may reflect the different donor backgrounds utilized, as well as being an indication of the sensitivity of each technique (Git *et al.*, 2010). In the case of *NHERF1* expression, only qRTPCR showed a significant increase in transcription. The difference in *NHERF1* gene expression compared to work by Accardi *et al.* may be attributable to the presence of whole HPV16 genomes in this study; the presence of other viral factors may, directly or via cellular processes, affect the transcription of E6 PDZ targets. Similarly, in identifying *PTPN13* as a HPV16 E6 target, Spanos *et al.* demonstrated that the presence of HPV16 E6 does not affect *PTPN13* mRNA levels in primary keratinocytes, whereas this thesis presents an upregulation of the PDZ protein in high-risk HPV genome containing keratinocytes. Together with our data, this suggests that a protein other than E6 acts to increase the transcription of *PTPN13* during viral genome replication.

A previous study by Lazic *et al.* demonstrated that HPV8 and HPV16 E6 protein expression induced a decrease in syntenin-2 transcript levels, but the transcription of other known PDZ targets, including DLG1, SCRIB, MAGI-1, MAGI-3, DLG4 and MUPP1 were unaffected, indicating that the effect of E6 upon PDZ protein transcription is specific. Such specificity was also observed in this study; the targets SCRIB and MAGI-3 remain transcriptionally unaffected, whilst MAGI-1 transcription was decreased by HPV18 only.

By using a PBM deletion mutant, this study ruled out any effects of the motif upon transcriptional upregulation; altering the PDZ binding activity of HPV18 revealed upregulation consistent results with WT HPV18 containing cells. Thus, the study in this thesis is the first in-depth study to indicate that high-risk  $\alpha$ -HPVs are able to modulate PDZ protein expression, independently of the E6 PBM.

A potential viral candidate in causing the observed PDZ gene upregulation is the HPV protein E2. The N-terminal domain of E2 can regulate transcription from adjacent promoters and HPV16 has been shown to increase or decrease transcription of cellular genes depending upon the level of E2 protein (Bouvard *et al.*, 1994a). A study by Gauson *et al.* identified more than 40 genes, that were downregulated and more than 30 genes, including the PDZ domain containing protein SNTB1, that were upregulated in cells expressing HPV16 E2. Thus, it is conceivable that E2 acts to upregulate selected PDZ targets of E6 in primary keratinocytes. Recently, E6 has been shown to be influential in inducing upregulation of transcription of the cytosine deaminase *APOBEC3B* (Vieira *et al.*, 2014). Both the transfection of high-risk HPV genomes and the expression of E6 alone induced increased transcription and further experiments showed that this was a characteristic of high-risk E6 proteins (Vieira *et al.*, 2014). The authors propose that de-repression of gene transcription occurs via the inactivation of p53 by E6. Similarly, HPV16

E6 has been shown to transcriptionally upregulate components of the NFκB pathway in cervical cells and induce upregulation of involucrin gene transcription (Gyongyosi *et al.*, 2012; Nees *et al.*, 2001). Work by Vliet-Gregg *et al.* indicated that E6 can induce the transcriptional upregulation of NOTCH1 when expressed alongside the transcription factor NFX1-123. Thus, there is a precedent for E6 alone causing a change in gene transcription.

### 3.4.2 Protein distribution in HPV genome containing cells

#### 3.4.2.1 Comparison to HeLa

This study shows a downregulation of the junctional proteins DLG1, SCRIB, ZO-1 and PARD3 in the HPV18 positive cancer cell line HeLa, compared to keratinocytes, which corresponds with data from the Banks lab (Kühne *et al.*, 2000). HeLa express relatively high levels of HPV18 E6, and are thus more able to deregulate PDZ proteins than keratinocytes. However, the changes cannot solely be attributed to HPV18 E6, there are likely many consequences of continuous cell culture, including the accumulation of somatic mutations. The levels of NHERF1 protein in HeLa were equivalent to the levels in keratinocytes, which differs from the analysis by Accardi *et al.*, who described an increase in NHERF1 protein in HeLa. This may be due to the different primary keratinocytes used as a comparison, but also highlights the variations seen in extensively cultured cells (Castillo *et al.*, 2014).

#### 3.4.2.2 Tight junction proteins

The presence of high-risk HPV genomes in monolayer grown keratinocytes had no or an undetectable effect upon the levels or distribution of PTPN13 or PATJ proteins, or fellow PDZ domain containing proteins CASK PARD3, MAGI-1 and MUPP1. This latter group (CASK, PARD3, MAGI-1 and MUPP1), along with PATJ, registered no change in protein

levels in differentiated keratinocytes replicating high-risk HPV genomes, despite studies which have shown protein interaction (CASK, MAGI-1, MUPP1), redistribution (PARD3) and E6AP independent degradation (PATJ. Facciuto *et al.*, 2014; Glaunsinger *et al.*, 2000; Belotti *et al.*, 2013; Lee *et al.*, 2000; Storrs and Silverstein, 2007). Additionally, it has been shown that E6 can preferentially target PDZ proteins at particular cellular locations, and also that E6 is able induce cellular redistribution of PDZ proteins, something that this study does not replicate (Narayan *et al.*, 2009; Massimi *et al.*, 2004; Facciuto *et al.*, 2014). In monolayer, the distribution of known and putative E6 targets remained the same in HPV16 and HPV18 positive and negative keratinocytes. These disparities reflect the differences between high throughput and overexpression assays and our primary cell model of HPV replication. It is likely that the E6 interactions that promote cancerous growth differ from those that are formed during the HPV life cycle, where E6 expression is tightly regulated.

This study also encountered difficulties in detecting MAGI-1, PATJ and MUPP1 proteins, preventing the drawing of concrete conclusions. Optimisation of these reagents would enable further studies to investigate the abundance and distribution of these proteins in a cell-based model of HPV replication

HPV16 expression leads to an upregulation of ZO-2 in mouse epithelium and a change in distribution in MDCK cells (Hernandez-Monge *et al.*, 2013). Here, we show a decrease in ZO-2 protein in the presence of HPV16 genomes, whilst there was no effect in HPV18 genome containing cells. The levels of fellow tight-junction protein ZO-1 were increased in HPV18 genome containing cells. Initially, it may seem unexpected for the interaction between E6 and ZO-1 results in an increase in the PDZ protein, but it may be that PBM binding has a stabilising effect, much like that observed by Nicolaides *et al.* The stability of E6 is aided by interaction with SCRIB, and it is possible that such a stabilising effect can be

reciprocated (Nicolaidis *et al.*, 2011). It is interesting to note that HPV16 downregulated ZO-2 whilst HPV18 upregulated ZO-1, indicating that targeting of one of these tight-junction components alone is sufficient for viral purposes. Furthermore the interaction between ZO-1 and HPV18 E6 is likely to be dependent upon PBM activity, as removal of the PBM in monolayer relieved some of the increase in protein level seen in WT genome containing cells and analysis of raft cultures revealed that the change in protein distribution from the periphery of HFKs to more focussed regions of the membrane of HPV18 genome containing cells was restored in part by deletion of the PBM.

#### 3.4.2.3 *The Scribble complex*

The two components of the Scribble complex analysed are the main identified targets of high-risk  $\alpha$ -papillomaviruses. These proteins are targeted for proteasomal degradation by HPV16 and HPV18 E6 oncoproteins, with HPV16 preferentially targeting SCRIB, and HPV18 targeting DLG1 (Thomas *et al.*, 2005). It is interesting that, despite the different affinities of HPV16 and HPV18 E6 for DLG1 protein, both viruses genomes induced an increased *DLG1* transcript levels, whereas neither had an effect upon *SCRIB* gene expression. Surprisingly, this upregulation did not correspond to an observed increase in DLG1 protein in the HPV16 and HPV18 genome containing keratinocytes, and this was validated using two detection antibodies. A more in depth analysis of DLG1 expression in HPV genome containing cells is provided in Chapter 4.

Numerous over and co-expression studies have demonstrated the degradation of DLG1 mediated by high-risk HPV E6 proteins (Lee and Laimins, 2004; Thomas *et al.*, 2005; Gardiol *et al.*, 1999). However, it has also been shown that endogenous DLG1 is not as readily targeted (Delury *et al.*, 2013; Choi *et al.*, 2013). Moreover, in primary tonsil keratinocytes, there was no change in DLG1 protein when overexpressing HPV16 E6

(Spanos *et al.*, 2008b). The maintenance of the DLG1 protein distribution in HPV positive and negative primary cells observed in this study agrees with data from other high-risk HPV types; HPV31 genome containing keratinocytes demonstrate the same localisation of cellular DLG1 than untransfected keratinocytes (Lee and Laimins, 2004; Choi *et al.*, 2013).

Although both HPV types are known to target SCRIB, it is a preferential target of the HPV16 E6 PBM (Thomas and Banks, 2005). Thus, it was surprising that there was no change in SCRIB protein levels in HPV16 genome containing cells, but an increase in protein occurred in the presence of HPV18 genomes. Furthermore, transcription of this PDZ protein remained unchanged in HPV16 and HPV18 replicating cells. It was also unexpected that membrane protein SCRIB was not detected in membrane fraction in monolayer cells. However, the observation was reinforced by the subsequent detection of SCRIB in the nucleus of basal cells and at the cytoskeleton in the upper layers of differentiated keratinocytes. Simonson *et al.* suggest that any differences observed in the distribution of DLG1 and SCRIB are subtle, and observe no change in differentiated culture. Work from the same group suggest that HPV31 does not induce dramatic changes in the subcellular distribution of DLG1 when transfected into primary keratinocytes; only a subtle reduction in cytoplasmic DLG1 protein was detected (Simonson *et al.*, 2005; Lee and Laimins, 2004).

In differentiated cells replicating HPV18 genomes, the levels of Scribble complex associated proteins DLG1, SCRIB and CASK, and the tight junction proteins ZO-1 and ZO-2 were influenced by the activity of the E6 PBM; a lower level of these proteins was detected in protein extracted from raft cultures containing genomes encoding the E6 PBM than those encoding a PBM deletion. However, examination of total protein from stratified cells does not indicate which pools of PDZ protein are affected. Furthermore, analysis of protein from differentiated culture can be problematic as the raft growth is inconsistent;

keratinocytes replicating HPV18 genomes that do not encode an E6 PBM grow more slowly than cells containing wild-type HPV18 genomes (Delury *et al.*, 2013).

Observing sections of differentiated rafts to identify protein location during stratification of epithelial cells containing HPV genomes enables observation of protein localisation during the full viral life cycle. Perhaps the susceptibility of PDZ proteins to E6-mediated degradation depends upon the location of the PDZ target in question; PDZ proteins could be more resistant to E6-induced degradation when they are already incorporated into cytoskeletal structures around membrane regions of cell–cell contacts. In this study no HPV-related changes in DLG1 and SCRIB protein levels were observed in monolayer grown cells or in the basal layer of stratified cells. However, observation of organotypic raft culture showed an increased detection of these Scribble complex proteins in the mid layer of the cultured epithelia, indicating that interactions between HPV E6 and PDZ proteins occur specifically during stages of the HPV life cycle. Furthermore, although no changes in NHERF1 abundance or distribution were observed in monolayer culture, differentiated cells containing HPV18 exhibited an increase in the protein levels. However, as this does not correlate with any observed increase in protein extracted from stratified cells, this requires more thorough investigation, perhaps utilizing confocal techniques to more accurately detect changes in protein abundance and distribution.

Inhibition of the proteasome revealed that the observed increases in PDZ protein gene transcription, and any downstream increase in translation, was not countered by proteasomal degradation; no increase in DLG1 protein was observed in HPV genome containing cells treated with proteasome inhibitor. This is also true of PTPN13 and PATJ; the increase in transcript levels in HPV genome containing keratinocytes did not correspond to a change in protein levels in these cells. Counter-intuitively, in HPV16 and HPV18 genome containing cells, a decrease in DLG1 protein levels was seen in conditions

of proteasome inhibition. It is unclear what occurs to induce this, but the decrease in protein may be due to non-specific effects of MG132 on these primary cells.

Taken together, no extensive change in protein levels was observed in these cells. This was surprising as DLG1 is a well characterized target of high-risk HPV E6, for proteasome degradation (Gardiol *et al.*, 1999; Thomas *et al.*, 2005). However, the observed effects of HPV genomes on PDZ targets appears to concentrate on proteins involved in tight junction formation and signalling (Figure 3.42). Protein levels of the tight-junction proteins ZO-1 and ZO-2 were altered by HPV genomes and mRNA of the tight-junction associated MAGI-1 was decreased. Both NHERF1 and PTPN13, which were upregulated transcriptionally in the presence of HPV genomes, have roles in tight-junction organisation and signalling; NHERF1 has been shown to function in tight junction organization, specifically in ZO-1 and occluding localization and PTPN13 is suggested to function in junction formation *via* ephrin (Castellani *et al.*, 2012; Sotelo *et al.*, 2014; Vermeer *et al.*, 2012). Disruption of epithelial polarity and tight junctions has been linked to activation of growth factor signalling and the release of pro-stimulatory transcription factors (Vermeer *et al.*, 2003; Balda and Matter, 2003; Betanzos *et al.*, 2004). Indeed, ZO-2 associates with the AP-1 components fos and jun at tight junctions, and our observed decrease of the PDZ protein in HPV16 positive cells may reveal a mechanism to release the pro-growth transcription factor (Betanzos *et al.*, 2004). In addition, ZO-2 blocks cell cycle progression by acting upon cyclin D1; the PDZ protein downregulates protein synthesis, increases proteasomal degradation and downregulates cyclin D1 transcription via interaction with the TF Myc, (Tapia *et al.*, 2009; Huerta *et al.*, 2007; González-Mariscal *et al.*, 2009). This culminates in the suppression of epithelial cell proliferation, which is counter to HPV

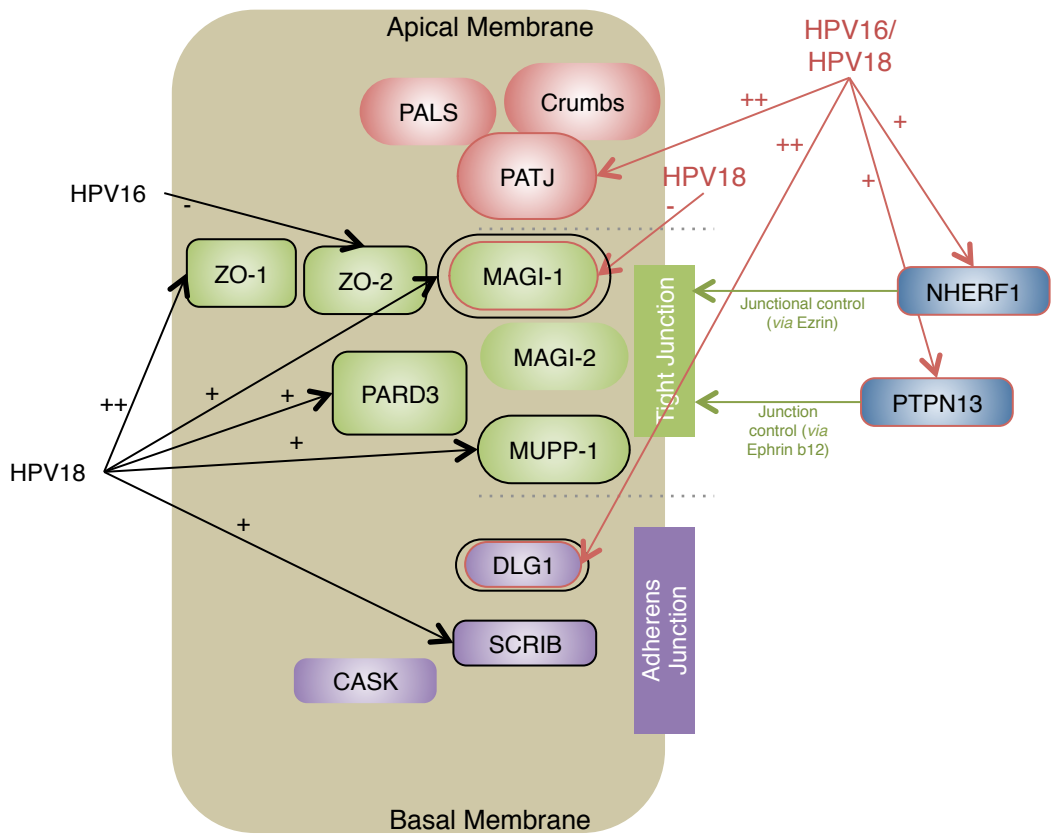


**Figure 3.42: Summary of PDZ protein expression in the presence of high-risk  $\alpha$ -HPV genomes**

The effects of HPV genomes upon keratinocytes concentrates on the tight junctions.

Red outline and arrows indicate a change in transcription and a black outline indicates a change in protein level in the presence of HPV. The number on the line indicates HPV type.

proliferation. Thus it is conceivable that, by decreasing ZO-2, HPV16 E6 promotes progression of the cell cycle.

The TJ protein ZO-1 interacts with the transcription factor ZONAB (ZO-1 associated nucleic acid binding protein), which is involved in the regulation of epithelial cell proliferation (Balda and Matter, 2000; 2003). Perhaps an increase in this protein by HPV18 functions to promote the PDZ:TF interaction with the aim of promoting cell proliferation. Furthermore, it is conceivable that this release of TFs and propagation of growth signalling by deregulated E6, promotes an uncontrollable growth that transforms infected cells and promotes cancer development.

By interrupting the junctions, HPV propagation may be favoured by promoting cell growth signalling. However, too much disruption of junction complexes may lead to dissociation of the epithelia and a halt in differentiation, which would also interrupt viral replication. Thus targeting of junctional proteins is selective, and does not result in the complete degradation of proteins involved.

### 3.4.3 Future directions

Protein analysis of keratinocytes does not validate existing data that shows E6-mediated degradation of PDZ targets. This is not to say that interactions between E6 and PDZ proteins do not occur during the HPV life cycle, PARD3 is an example of an E6 target which is not degraded as a result of the interaction (Facciuto *et al.*, 2014). However the effect of E6 upon PDZ proteins during the HPV life cycle is subtle, and it is still unclear which is the major target at a protein level. The PBM of high-risk HPV E6 proteins contributes to episomal maintenance, and it has been suggested that the stabilizing effect of PBM PDZ interactions contributes to this (Nicolaidis *et al.*, 2011). E6 mediated degradation may be an artifact of E6 overexpression and the deregulation of viral

oncoproteins that occurs in cancer, as such it would be of interest to investigate these proteins in cells where the HPV genome has integrated, which occurs in primary keratinocytes following serial culture.

This study identifies a number of targets of the HPV E6 PBM, which are upregulated at a transcriptional level in the presence of viral genomes. This does not, however, correspond to an increase in protein levels. However, this study was limited to investigating one method of protein degradation; it may be that E6 targets these proteins for degradation via the lysosomal pathway. It is possible that a viral factor decreases the mRNA stability, before translation occurs. Alternatively, the upregulated transcripts may encode less stable proteins or not translate as efficiently that other variants. As such, the pattern of DLG1 expression investigated in more depth in Chapter 4.

Further investigation may also identify viral factors and cellular pathways involved in the observed changes in PDZ target transcription. This could begin with expression analysis of cells containing single viral gene products (such as E2), before dissection of mechanisms of action.

## CHAPTER 4: IDENTIFICATION AND CHARACTERISATION OF A NOVEL ISOFORM OF DLG1

### 4.1 Introduction

#### 4.1.1 DLG1 protein structure

Like other members of the MAGUK family of proteins, DLG1 is composed of modular interaction domains that enable a variety of protein-protein interactions. The protein consists of 3 PDZ domains, an Src Homology 3 (SH3) domain and a guanylate kinase (GK) domain (Figure 4.1). Two isoforms of DLG1 have been identified, one containing an N-terminal L27 motif, referred to as DLG1 $\beta$ , and another without this L27 motif termed DLG1 $\alpha$ . These isoforms correlate to *Drosophila* DLGS97 and DLGA, respectively (Figure 4.2, Albornoz *et al.*, 2008; Mendoza *et al.*, 2003). Further diversity in DLG1 is introduced by the inclusion of short amino acid sequences designated insertions (I1-I5), produced by splicing alternative exons in the *DLG1* gene. This splicing occurs in two main regions of DLG1, one at the N-terminus and another in the C-terminal HOOK region that lies between the SH3 and GK domains (Figure 4.2). Five alternatively spliced insertions have been defined to date, I1A and I1B at the N-terminal region, and I2, I3, I4 and I5 within the HOOK domain, each of which results in the inclusion of a short (10-30) amino acid sequence (Table 4.1). These insertions influence DLG1 localisation as well as potentially altering binding partner preferences of DLG1 (McLaughlin *et al.*, 2002).

The N-terminal L27 motif of DLG1 facilitates dimerization via interaction with the L27 domains of other proteins as well as other DLG1 molecules (Lin *et al.*, 2013). The region remains largely unstructured until association with other L27 motifs, when the motifs together form an ordered helical structure and become a compact four-helix bundle

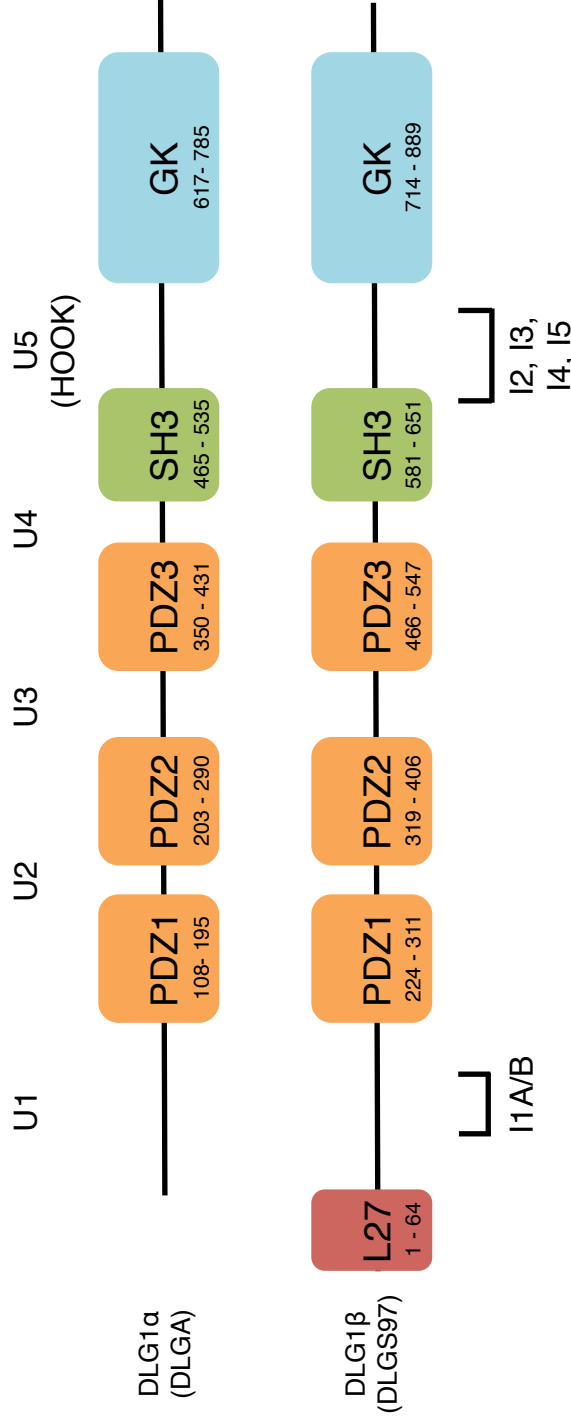
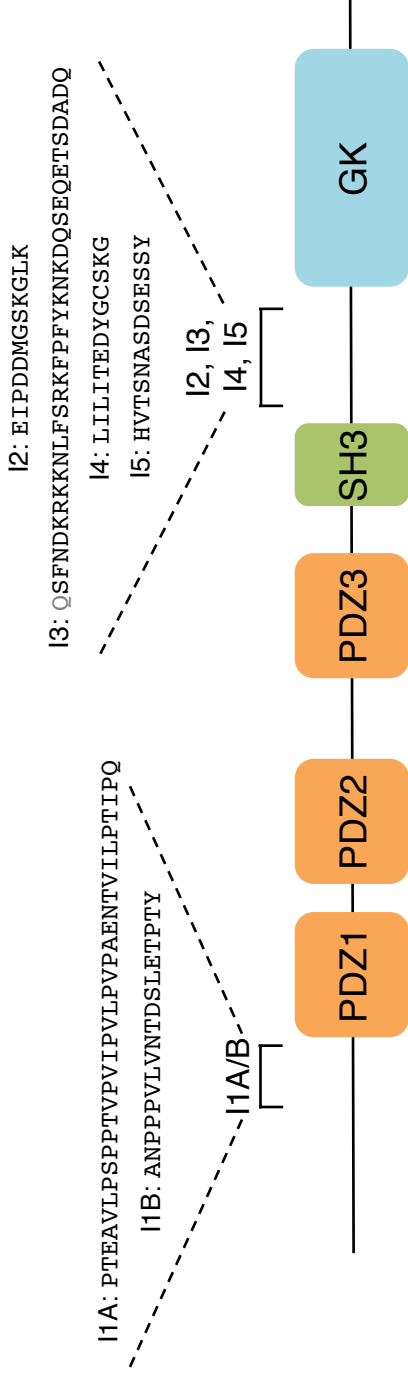


**Figure 4.1: Domain structure of DLG1 isoforms**

Adapted from Roberts *et al.* 2012. Two human DLG1 isoforms (accession numbers U13896 and U13897) were originally identified, encoding proteins of 926 and 904 amino acids respectively. Both the DLG1 $\alpha$  and DLG1 $\beta$  isoforms encode 3 PDZ domains, an SH3 and a C-terminal GUK domain. In addition, the DLG1 $\beta$  isoform encodes an N-terminal L27 region, which is involved in DLG1 homomultimerization and mediates interactions with other DLG1 binding proteins. Regions of alternative mRNA splicing at the N-terminus (I1A/I1B) and in the HOOK region (I2, I3, I4 and I5) are shown. Splicing further diversifies the isoforms of DLG1 expressed. The five unstructured regions (U1-U5) are indicated. U5 is also known as the HOOK region.



N Terminus;  
DLG1 $\alpha$  or  $\beta$

DLG1 $\alpha$ : MNYIFGNNTLLYSRGRGNTSSSHGSAGPKQKHWAKKGSSDELQAEPEPSRWQQIVAFFTRRHSFIDCISVATSSTQ

DLG1 $\beta$ :

MPVRKQDTQRALHLLLEEYRSKLSQTEDRQLRSSIERVINIFOSNLFQALIDIQEFFYEVTVLLDNPKCIDRSKPSSEPIQPVNTWEISSL  
PSSVTSETLLPSSLSPSVEKYRYQDEDTPPQEHISPOITNEVIGPELVHVSEKNLSEIENVHGFVSHSHISPIK

**Figure 4.2: Regions of alternative splicing of DLG1**

Adapted from Roberts *et al.* 2012. Both the DLG1 $\alpha$  and DLG1 $\beta$  isoforms encode 3 PDZ domains, an SH3 and a C-terminal GUK domain. In addition, the DLG1 $\beta$  isoform encodes an N-terminal L27 region, sequence indicated in red. Regions of alternative mRNA splicing at the N-terminus (11A/11B) and in the HOOK region (12, 13, 14 and 15) are shown.

(Doerks *et al.*, 2000). In non-neuronal cells, the L27 domain of DLG1 facilitates interactions with the first L27 domain of fellow MAGUK protein, calcium/calmodulin-dependent serine protein kinase (CASK) and stabilises a more extended form of DLG1 (Jeyifous *et al.*, 2009; Lee *et al.*, 2002; Waites *et al.*, 2009). Moreover, this interaction with CASK is important for localization of the  $\beta$  isoform of DLG1 to the baso-lateral membrane of epithelia (Lozovatsky *et al.*, 2009). Similarly, this region in the  $\beta$  isoform has been shown to mediate membrane localization via association with DLG2 (Hanada *et al.*, 2003). In neuronal cells, the presence of the  $\alpha$  and  $\beta$  isoforms affects the trafficking of specific receptors at the synapse; the  $\beta$  isoform associates with AMPA receptors primarily at post-synaptic regions and the  $\alpha$  form at perisynaptic regions (Waites *et al.*, 2009). In the fly, both the DlgA and DlgS97 isoforms are present at larval neuromuscular junctions (Mendoza *et al.*, 2003). Recently, DlgA and DlgS97 were shown to be differentially expressed in the fly; whereas DlgA is required for adult viability, specific loss of DlgS97 leads to perturbation of circadian activity and courtship (Mendoza-Topaz *et al.*, 2008). It has also been observed that DlgA is predominant in epithelia whereas the DlgS97 is mainly expressed in the *Drosophila* neuronal system (Mendoza *et al.*, 2003; Lee *et al.*, 2002).

DLG1 encodes three PDZ domains, which influence DLG1 localisation and interact with a wide range of cellular proteins. For example, DLG1 binds to the tumour suppressor adenomatous polyposis coli (APC) protein, *via* PDZ1 and PDZ2, forming a complex which inhibits cell cycle progression in response to epithelial cell-cell contact, indicating a role for DLG1 in controlling progression of cells from G0/G1 to S phase (Ishidate *et al.*, 2000; Zhang *et al.*, 2011; Makino *et al.*, 1997). The PDZ domains of DLG1 are known to interact with different transmembrane proteins; for example PDZ1 interacts with the AMPA receptor subunit GluR1, PDZ2 with the NR2B subunit of NMDA receptor and PDZ3

with neuroligin (Kornau *et al.*, 1995; Leonard *et al.*, 1998; Cai *et al.*, 2002; Wang *et al.*, 2005). Binding of PDZ domains 1 and 2 of DLG1 to the Rho-GEF NET1 (neuroepithelioma transforming gene 1) leads to the relocalisation of both proteins to the nucleus (Garcia-Mata *et al.*, 2007; Carr *et al.*, 2009).

**Table 4.1: Insertions in DLG1 variants**

Insertion	Exon No.	Amino acid sequence	Present in variants
1A	6	PTEAVLPSPTVPVIVLPVPAENTVILPTIPQ	1, 2, 6 and 7
1B	7	ANPPPVLVNTDSLETPTY	1, 2, 3, 4, 6, 7, 8 and 9
2	21	EIPDDMGSKGLK	1, 3, 5, 6, 7, 8 and 9
3	20 A/B	(Q)SFNPKRKKNLFSRKFPFYKNKDQSEQETSADADQ	2 and 4
4	23	LILITDEYGCSKG	7 and 9
5	22	HVTSNASDSESSY	1, 2, 3, 4, 7, 8 and 9

Brackets indicate alternative inclusion of residue at the beginning of I3

Mammalian SH3 domains bind to proline rich regions of target protein and DLG1 is no exception; DLG1 SH3 and GK domains form an interaction with the synaptic protein GKHolder (GukH), enabling proper localisation of fellow junctional protein SCRIB (Newman and Prehoda, 2009). DLG1 SH3 interactions have been shown to facilitate the organization of protein complexes. DLG1 protein colocalizes with E-cadherin at the sites of cell-cell contacts in mammary epithelial cells (Reuver and Garner, 1997; Wu *et al.*, 1998; Reuver and Garner, 1998). In these cells, depletion of DLG1 altered the integrity of adherens junctions or tight junctions (Laprise *et al.*, 2004; Stucke *et al.*, 2007). Furthermore, in *Drosophila* Dlg, loss of the SH3 and GK domains leads to a dissociation of septate junctions, reinforcing the importance of DLG1 domains in facilitating the protein interactions that form cell-cell contacts (Woods *et al.*, 1996; Hough *et al.*, 1997).

In all MAGUK proteins, the GK domain is catalytically inactive, despite sharing a strong structural similarity with cellular soluble guanylate kinases (Kuhlendahl *et al.*, 1998; Olsen and Bredt, 2003). Studies in *C. elegans* have shown that the GK domain is important for cell viability (Lockwood *et al.*, 2008), suggesting that, though inactive, the domain contributes to DLG1 function. Investigation in human cells have revealed that the GK domain forms a number of interactions with cellular proteins, including guanylate kinase associated protein (GKAP), microtubule-associated protein 1A (MAP1A), guanylate kinase associated kinesin (GAKIN), kinesin superfamily protein 13B (KIF13B), brain-enriched guanylate kinase-associated protein (BEGAIN), SPA-1-like protein (SPAL), and leucine glycine asparagine repeat protein (LGN) (Zhu *et al.*, 2011; Sans *et al.*, 2005; Deguchi *et al.*, 1998; Saadaoui *et al.*, 2014; Brenman *et al.*, 1998; Yamada *et al.*, 2007; Kim *et al.*, 1997). These protein-protein interactions facilitate the attachment of DLG1 to cytoskeletal factors, microtubules and actin-based transport machinery, as well as aiding the organization of signal transduction complexes. The GK domain has also been shown to associate with protein kinase C (PKC) and is required for the localization of DLG1 to the synapse (Thomas *et al.*, 2000; O'Neill *et al.*, 2011). Recently, the DLG1 GK domain has been shown to bind to phosphorylated threonine or serine residues of fellow Scribble complex protein LGL and regulator of asymmetric cell division LGN (Zhu *et al.*, 2014; 2011). DLG1 binding to phosphorylated LGL has been indicated as a regulatory mechanism in Scribble complex formation and binding to phosphorylated LGN has been suggested to be important in localizing DLG1 to the midbody along with LGN during cytokinesis (Zhu *et al.*, 2011; 2014). Furthermore, a nuclear export signal has been identified in the GK domain (KRKK), removal of which restricts DLG1 to the cytoplasm (Kohu *et al.*, 2002). Since a number of DLG1 interacting proteins, including protein 4.1 and ErbB4, exist in the nucleus, it has been speculated that

DLG1 translocates with these proteins, to function in the nucleus as a transcription factor, splicing factor or scaffolding protein (Kohu *et al.*, 2002; Lue *et al.*, 1994; Huang *et al.*, 2000). Post-translational modifications of DLG1 have been reported. Commonly, phosphorylation is related to the control of DLG1 subcellular localization. In *D. melanogaster*, phosphorylation of Dlg PDZ1 by CAMKII decreases the synaptic localisation of the protein (Koh *et al.*, 1999). In human cells, phosphorylation of DLG1 by the MAPK p38 $\gamma$  promotes dissociation from GKAP, releasing the protein from the cytoskeleton (Sabio *et al.*, 2005). Furthermore, stress conditions induce phosphorylation of DLG1 by JNK (Jun N-terminal kinase), which leads to the accumulation of DLG1 at cell-cell contacts (Massimi *et al.*, 2006). DLG1 interacts with the mitotic kinase PBK (PDZ binding kinase) and both proteins are phosphorylated during mitosis (Gaudet *et al.*, 2000). The differential phosphorylation of DLG1 during S phase and mitosis is likely to affect the interactions that DLG1 can form and thus function to control the protein interactions during the cell cycle (Gaudet *et al.*, 2000). Furthermore, DLG1 is differentially phosphorylated during the cell cycle by CDK1 and 2, enhancing nuclear localisation of the protein (Narayan *et al.*, 2009; 2008).

#### 4.1.1.1 DLG1 Insertions

Extensive alternative processing of the *DLG1* gene further diversifies DLG1 protein interactions and functions, and this occurs both in *Drosophila* and in humans (McLaughlin *et al.*, 2002). Splice variants differ in the use of alternative exons, which have been identified in a region at the N-terminus and in the C-terminal HOOK region, between the SH3 and GK domains (Figure 4.2). These insertions have been found in different combinations in different variants of DLG1 protein and they affect DLG1 localisation as well as promoting interactions with cellular factors (Table 4.1).

The N-terminal alternatively spliced region of DLG1 comprises the proline rich insertions I1A and I1B, which are able to moderate oligomerisation, forming interactions with other DLG1 molecules and with other cellular proteins (Nix *et al.*, 2000; Wu *et al.*, 2000). Immunoprecipitation of DLG1 and the pro-proliferative tyrosine kinase Lck in T-cells demonstrated that the SH2 domain of the kinase interacts with DLG1 I1A and I1B (Hanada *et al.*, 1997). More recently, it has been shown that the I1A-containing DLG1 isoform is phosphorylated in response to T-cell receptor (TCR) stimulation and that this event is mediated by Lck (Crocetti *et al.*, 2014). It has been suggested that this interaction allows DLG1 to couple TCR activation to the release of cytotoxic granules via Lck (Round *et al.*, 2007a; Crocetti *et al.*, 2014; Hanada *et al.*, 1997).

The amino acid sequences of insertions I1A and I1B are involved in DLG1 self-association (McLaughlin *et al.*, 2002; Hanada *et al.*, 2000; 1997). Furthermore, I1A has been shown to influence the activity and surface expression of the voltage-gated potassium channel Kv1.5; presence of the insertion enables DLG1 to stimulate Kv1.5-mediated current (Godreau *et al.*, 2003; McLaughlin *et al.*, 2002). The stimulatory function of I1A containing isoforms may be due to the ability of the protein to organise synaptic channels and facilitate interactions with accessory proteins (Hibino *et al.*, 2000; DeMarco and Strehler, 2001).

The inclusion of insertions affects DLG1 function, for example McLaughlin *et al.* suggest that isoforms containing I1A and I1B are involved predominantly in DLG1 signalling functions, whereas isoforms without these insertions are predominantly involved in scaffolding. This is perhaps most clearly observed in T-cells where the two expressed forms of DLG1 differ by the inclusion or exclusion of I1B. Both forms facilitate cytotoxic granule release but the I1B-containing form is unable to coordinate p38 activation and proinflammatory cytokine production (Crocetti *et al.*, 2014).

Nuclear functions of DLG1 are perhaps mediated by the I2 isoform. Inclusion of I2 in DLG1 is associated with relocation of the protein to the nucleus and it has been suggested that the I2-form is involved in chromatin reorganization (McLaughlin *et al.*, 2002). During epithelial differentiation, I2-containing forms of DLG1 translocate from the nucleus to the cytoplasm, suggesting that the nuclear I2-mediated functions are not necessary for differentiated keratinocytes (Roberts *et al.*, 2007).

The alternatively spliced I3 is associated with DLG1 localisation to the cell membrane and has been shown to interact with the membrane-bound proteins  $\beta$ 1-Adrenergic GPCR, A-kinase anchor protein 5 (AKAP5) and protein 4.1 (Lue *et al.*, 1996; Nooh *et al.*, 2013; Gardner *et al.*, 2007). The I3 containing isoform of DLG1 promotes the recycling of  $\beta$ 1-Adrenergic receptor by DLG1 and provides a weak binding site for CAMKII; in the absence of I3, CAMKII is able to bind upstream of I2, indicating that this interaction is important for more than one DLG1 isoform (Paarmann *et al.*, 2002). Phosphorylation of I3 by CAMKII disrupts binding of the PKA organizing protein AKAP5 to the insertion sequence (Nikandrova *et al.*, 2010; Schlueter *et al.*, 2006). Protein 4.1 binding to I3 facilitates DLG1 recruitment to the neuronal synapse, association with the actin cytoskeleton within dendritic spines and association to membranes in both polarized and non-polarized cells (Hanada *et al.*, 2003; Lue *et al.*, 1994; Rumbaugh *et al.*, 2003; Nooh *et al.*, 2013). The HOOK region also contains a calmodulin binding site, a region which is also able to compete for binding to DLG1 I3 in homodimerisation (Paarmann *et al.*, 2002).

The combinations of insertions included in DLG1 are also dependent upon the tissue in which they are expressed. I3 is predominantly expressed in cardiac tissue whereas the I2-containing form appears to be restricted to neurons and liver (Mori *et al.*, 1998; McLaughlin *et al.*, 2002; Godreau *et al.*, 2003). However, both insertions have been detected in epithelia,

although the expression of each changes during epithelial differentiation (Godreau *et al.*, 2003; McLaughlin *et al.*, 2002; Roberts *et al.*, 2007).

Although the first 65 amino acids of DLG1 direct the recruitment of DLG1 to sites of cell-cell contact, and the presence of I3 affects the efficiency of this localization, DLG1 mutants without PDZ domains show a nuclear localization. Insertions and domains all influence DLG1 localisation and function (Wu *et al.*, 1998). This is in part due to the fact that the interactions formed by DLG1 involve more than one domain interface; for example, binding of the SH3 increases affinity of DLG1 to CAMKII and promotes calmodulin and protein 4.1 binding to the HOOK domain (Gardoni *et al.*, 2003; Mauceri *et al.*, 2007).

#### 4.1.2 DLG1 expression

DLG1 mRNA is transcribed from chromosome 3 and consists of 24 described exons (Figure 4.3). Transcription of the *DLG1* gene is repressed by the snail family of transcription factors and a number of transcription factor binding sites have been identified in the 5' untranslated region (UTR) of *DLG1*, including AP-1, AP-2 NFκB and SP-1 (Cavatorta *et al.*, 2008). The *DLG1* gene contains 50 distinct introns which could be transcribed to produce 33 different mRNAs (Thierry-Mieg and Thierry-Mieg, 2006). It has been suggested that there are 11 potential alternative promoters and 16 alternative polyadenylation sites (Cavatorta *et al.*, 2008; Thierry-Mieg and Thierry-Mieg, 2006). Two different 5' UTRs have been identified by the Gardiol lab (Cavatorta *et al.*, 2011). These UTRs are generated by alternative splicing within the 5' region of DLG1 mRNA and is a region which mediates *DLG1* transcriptional control, influences mRNA stability, localization and translational efficiency (Cavatorta *et al.*, 2011). It is therefore reasonable to

assume that the inclusion of different 5' regions affects DLG1 protein abundance (Cavatorta *et al.*, 2011).

Thus, DLG1 is a multi-functional protein, able to form a range of interactions and perform cell context and subcellular-specific roles. DLG1 was the first identified PDZ target of high-risk  $\alpha$ -HPVs and the ability of the E6 oncoprotein to target the protein for ubiquitin mediated degradation is well documented (Kiyono *et al.*, 1997; Gardiol *et al.*, 2006; Narayan *et al.*, 2009; Thomas *et al.*, 2005). The virus has been shown to target specific subcellular pools of DLG1, exhibiting a preference for nuclear, phosphorylated forms of the protein (Narayan *et al.*, 2009; Massimi *et al.*, 2004).

### 4.3 Hypothesis and objectives

A number of forms of the DLG1 protein have been identified, with diversity introduced via short, alternatively spliced insertions and expression of alternative N-terminal sequences (Figure 4.1 and 4.2). The expression of DLG1 isoforms is tissue and cell context specific, and likely affects DLG1 localisation and function within a cell. Moreover, many studies of DLG1 have focussed on the  $\beta$  isoform and little is understood of DLG1 $\alpha$  expression. DLG1 is a major target of high-risk HPV E6 oncoproteins and this study has identified an increase in DLG1 transcription in the presence of HPV genomes. Thus, this investigation aims to characterize *DLG1* expression in epithelia under a number of conditions, in the presence of high-risk HPVs, in normal tissue and in cancer tissue.

The experiments outlined in this chapter aim to:

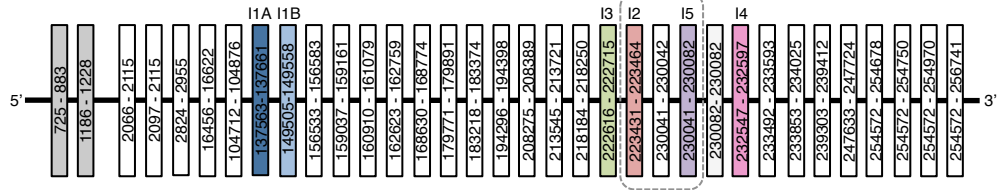
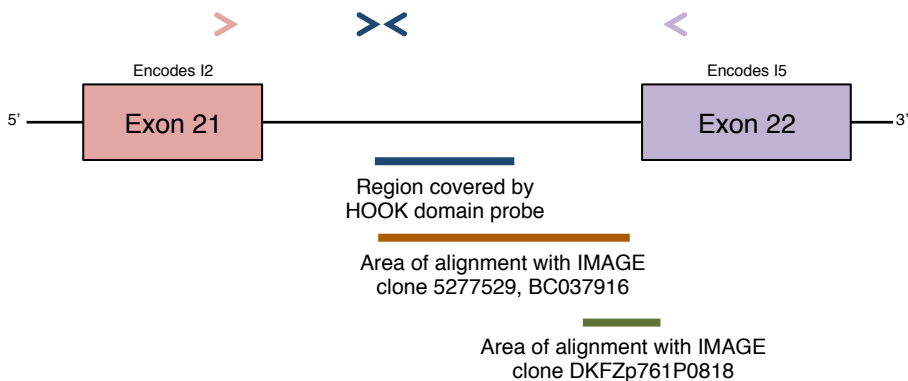
- i. Characterise *DLG1* expression during the HPV life cycle
- ii. Investigate novel *DLG1* isoform in the context of mRNA and protein
- iii. Characterise *DLG1* isoform expression in cancer cell lines and normal tissue

## 4.4 Results

### 4.4.1 Identification of a novel insertion in *DLG1* in mRNA

Previously in this thesis, an investigation into the expression of DLG1 during the HPV life cycle was carried out (Chapter 3). During this, it was noted that mRNA expression of the *DLG1* gene was increased in the presence of high-risk HPV genomes (Chapter 3, Section 3.3.2). Since DLG1 exists as two main isoforms and is further diversified by the inclusion of spliced insertions, it was deemed important to characterise the expression of *DLG1* in these  $\alpha$ -HPV genome containing cells and to determine which of the isoforms were being upregulated in the genome containing cells. Microarray and subsequent qRTPCR analysis had identified that the increased level of *DLG1* expression occurred in transcripts containing a region in the HOOK domain. The primers used in qRTPCR analysis were designed according to the nucleotide sequence of the Affymetrix probe (230229\_at), both of which covered the HOOK domain region of *DLG1* (Figure 4.3, Table 4.2). It was surprising that, upon examination of the probe position and primer sequences (Table 4.2), the region under analysis in the Affymetrix array corresponded to was in fact a region of the *DLG1* gene previously described as intronic, between known exons 21 and 22. Exon 21 encodes DLG1 insertion I2 and exon 22 encodes I5 (Figure 4.3, Table 4.2). Furthermore, Affymetrix included this probe because of the previous identification of two cDNA clones from hypothalamus- and brain-derived libraries, containing sequence overlapping with this region (Strausberg *et al.*, 2002; Wiemann *et al.*, 2003, Figure 4.3).

To further examine the sequence of this HPV-upregulated ‘intronic’ region of DLG1, PCR primers were designed to the flanking exons of I2 and I5 (I2<sub>Fwd</sub> and I5<sub>Rev</sub>, Figure 4.4) and used in combination with the HOOK region primers (HOOK<sub>Fwd</sub> and HOOK<sub>Rev</sub>, Figure 4.4), previously used in qRTPCR (Chapter 3), to amplify from cDNA generated from

**A***DLG1* Gene**B****Figure 4.3: *DLG1* HOOK domain corresponding primers and probes**

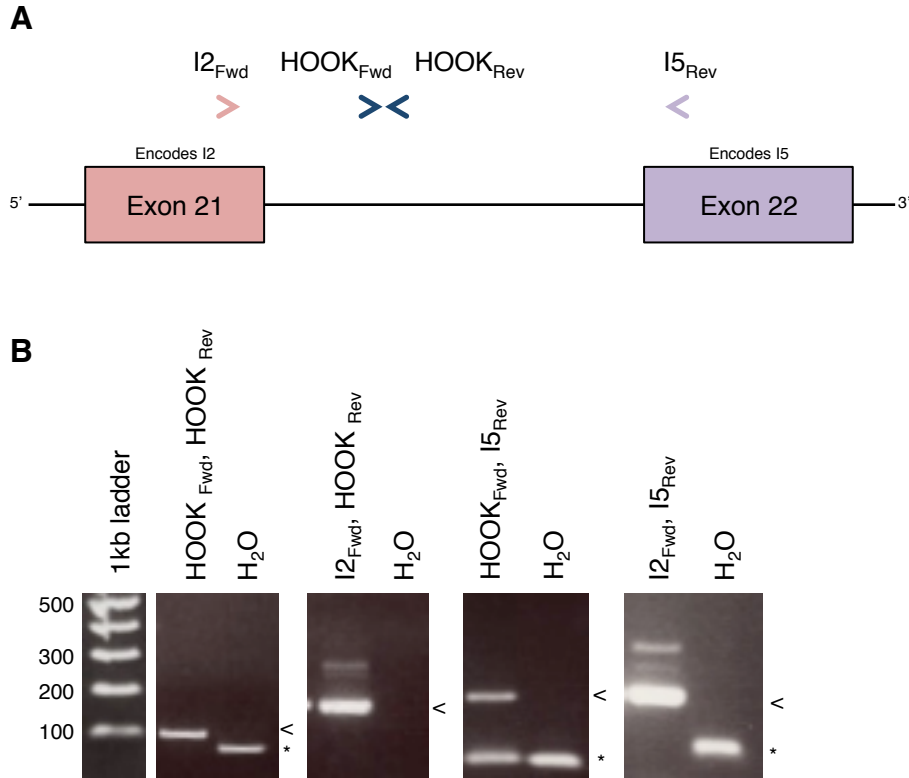
- (A) Schematic of the *DLG1* gene showing the 23 exons, and the exon start and finish nucleotide numbers, according to NCBI. The exons coding for insertions I1A, I1B and I2-I5 are shown. The region included in the dashed line is the region of focus in B.
- (B) Exon 21 and 22 encode I2 and I5, respectively. It is between these exons where the microarray probe (blue line) and the HOOK domain primers (blue arrows) anneal. This region overlaps with the known cDNA IMAGE clone, derived from human hypothalamus, BC037916 (Strausberg *et al.* 2002), corresponding to nucleotides 231928 to 233005 of *DLG1* (orange line). Also in this region is an area of alignment with IMAGE clone DKFZp761P0818 derived from amygdala (Wiemann *et al.* 2003, green line). Further primers were designed to known exonic sequence in Exons 21 and 22, indicated by the pink and purple arrows.

DNase-treated polyA selected RNA that had been isolated from HPV16 genome positive keratinocytes. A control reaction containing water was included. The PCR products were separated by ethidium bromide agarose gel electrophoresis and the lower band observed in both the cDNA and water control indicated amplification of primer dimers (Figure 4.4). The amplified bands were excised; the single band amplified by the HOOK primers and the single product amplified by the HOOK<sub>Fwd</sub> in combination with the I5<sub>Rev</sub> (Figure 4.4). In the case of the HOOK<sub>Fwd</sub> I5<sub>Rev</sub> and I2<sub>Fwd</sub> I5<sub>Rev</sub> combinations the brightest and the fainter bands was excised (a total of 2 and 3 bands cut out, respectively), but in both cases the fainter bands were unsuccessful in sequencing reactions (Figure 4.4).

**Table 4.2: DLG1 primer and array probe positions**

<b>Primer Name</b>	<b>Sequence (5'-3')</b>	<b>Position in <i>DLG1</i></b>
I5 <sub>Rev</sub>	CCTGTCTTTTCATAGGTCCCA	230051-230071
I2 <sub>Fwd</sub>	GAGATCCCTGACGACATGGG	223464-223484
HOOK <sub>Fwd</sub>	GCCCATTCCTAGCGCATGAACTC C	228817-228841
HOOK <sub>Rev</sub>	GCCATTCTGGTGGATGGCAGAG	228908-228930
Affymetix probe 230229_at		227651-228736

Sequencing of excised bands from the I2<sub>Fwd</sub> I5<sub>Rev</sub> combination of primers revealed the established I2-I5 junction. Successful sequencing of excised bands from I2<sub>Fwd</sub> HOOK<sub>Rev</sub> combination and the HOOK<sub>Fwd</sub> I5<sub>Rev</sub> combination revealed the presence of 208 nucleotides between exon 21 and 22, which has not been shown previously to be transcribed (Figure 4.5, sequence data Appendix II). The 208 nucleotides corresponded to *DLG1* gene sequence in a region of the gene between exons encoding I2 and I5, sequence previously thought to be intronic (Figure 4.4). Further sequencing reactions confirmed the presence of this intronic sequence in mRNA containing I2 and I5, with sequence data covering the splice junctions (Figure 4.5). Thus, the region amplified by the HOOK region primers, and

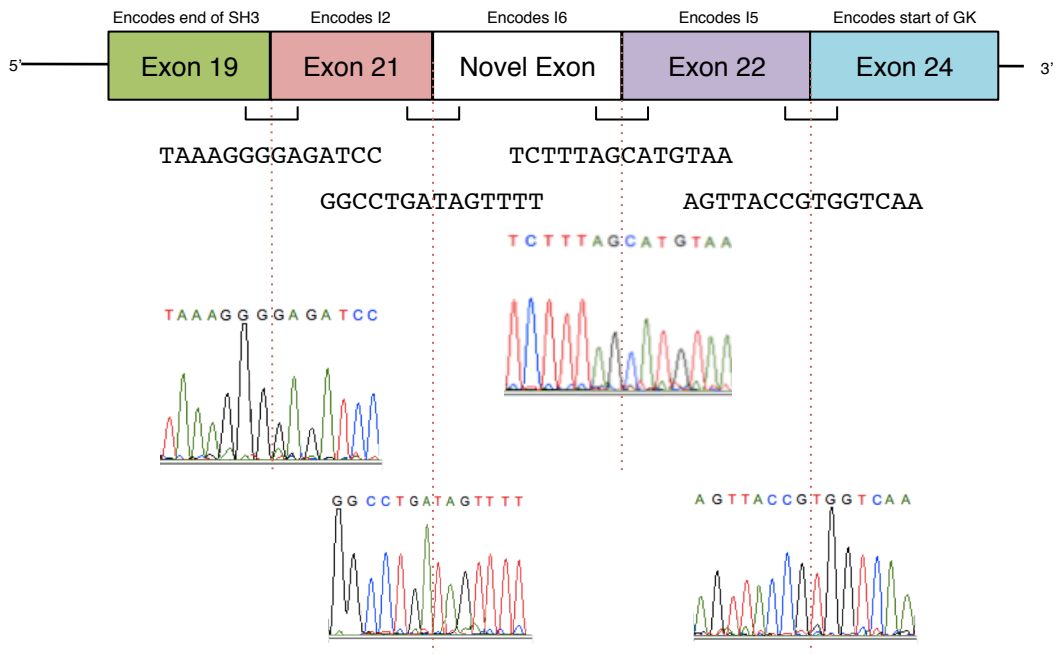


**Figure 4.4: Amplification of the DLG1 HOOK region**

- (A) Schematic of the primers positioned with respect to the *DLG1* gene (Boxes indicate exons and the line intronic regions). Primers indicated by arrows, with names above. Pink,  $I2_{Fwd}$ ; Blue  $HOOK_{Fwd}$  and  $HOOK_{Rev}$  and purple  $I5_{Rev}$ .
- (B) The PCR products amplified using primer combinations were separated by agarose gel electrophoresis and visualised using ethidium bromide. cDNA was transcribed using oligodT primers from DNase-treated RNA extracted from from HPV16-genome containing keratinocytes. PCR containing water was included as a control. Bands indicated by the arrow were excised and sequenced using the above primers. Primer dimers indicated by \*. Fainter bands were not successfully sequenced. Ladder shown is 1  $\mu$ g of 1kb plus (Invitrogen). Expected molecular weights of amplified fragments (Left to right) are 98, 149, 222 and 274 bp.

**A**

5' **AGGGAGATCCCTGACGACATGGGATCAAAGGCCTGA**tagttttacc  
 agtttgccattcctagcgcacgaactccattgctgcataatcattatc  
 gatgcttgacatgtctgttttgtgttttcatttttagccattctggtgga  
 tggcagagacactctttgtggttataatttgcatttcctgacaagtaa  
 ttaacttgaacacttttctatatgtttattggttatttgactgtcttct  
 ttag**CATGTA**ACTTCTAATGCCAGCGATAGTGAAAGTAGTTAC 3'

**B**

**Figure 4.5: Sequencing across exon junctions**

- (A) Purified amplified *DLG1* fragments were subject to sequencing reactions to reveal sequence indicated. Pink corresponds to exon 21 and purple to exon 22. Exons are indicated in capitals and intronic sequence in lower case.
- (B) Sequencing results corresponded to *DLG1* sequence and covered the splice sites of exons 19, 21, the novel exon, 22 and 24. The schematic indicates *DLG1* mRNA with the order of the exons and the nucleotide sequence of splice junctions and the corresponding image of sequencing peaks below. Red dotted line indicates splice junction

covered by the Affymetrix microarray probe 229130\_at, is a region that is expressed and is upregulated in the presence of HPV genomes. In keeping with DLG1 insertion terminology, this exon was termed I6.

As the data indicated a novel insertion in the HOOK region, flanked by I2 and I5, the next stage was to characterise the transcripts containing the I6 insertion in more detail. PCR amplification was performed using a combination of forward primers specific to the N-terminus of either DLG1 $\alpha$  or DLG1 $\beta$  isoforms, alongside a reverse primer within the novel insertion I6 (Figure 4.6). Both combinations of primers amplified fragments and more than 6 bands were visible from each reaction. Successful sequencing was achieved of one excised band (~1000 bp), amplified by the DLG1 $\alpha$ <sub>Fwd</sub> and HOOK<sub>Rev</sub> combination (Figure 4.6). Sequencing of this purified fragment revealed the presence DLG1 $\alpha$  specific N-terminus along with the first two PDZ domains (Figure 4.6, Appendix II). Thus, this data indicates that the I6 insertion is present in  $\alpha$  forms of DLG1.

However, it cannot be ruled out that that I6 is present in DLG1 $\beta$  transcripts; more than 6 amplified bands were visible, which were not successful in sequencing reactions. The bands may be a result of non-specific amplifications due to the increased PCR extension time (1.5 min) and number of amplification cycles (50); increased cycling increases the opportunity for nonspecific amplification and errors (Bustin and Nolan, 2004; Bell and DeMarini, 1991). This is something that requires further investigation.

Thus, this study has identified a novel insertion in an established region of extensive *DLG1* alternative splicing. It is likely that mRNAs containing this insertion (I6) also encode the  $\alpha$  form of the DLG1 N-terminus. Furthermore, I6 is upregulated in the presence of both high-risk HPV16 and 18 genomes (Chapter 3, Figure 3.4). The rest of this chapter aims to investigate potential consequences of the inclusion of the I6 sequence in DLG1 mRNA.

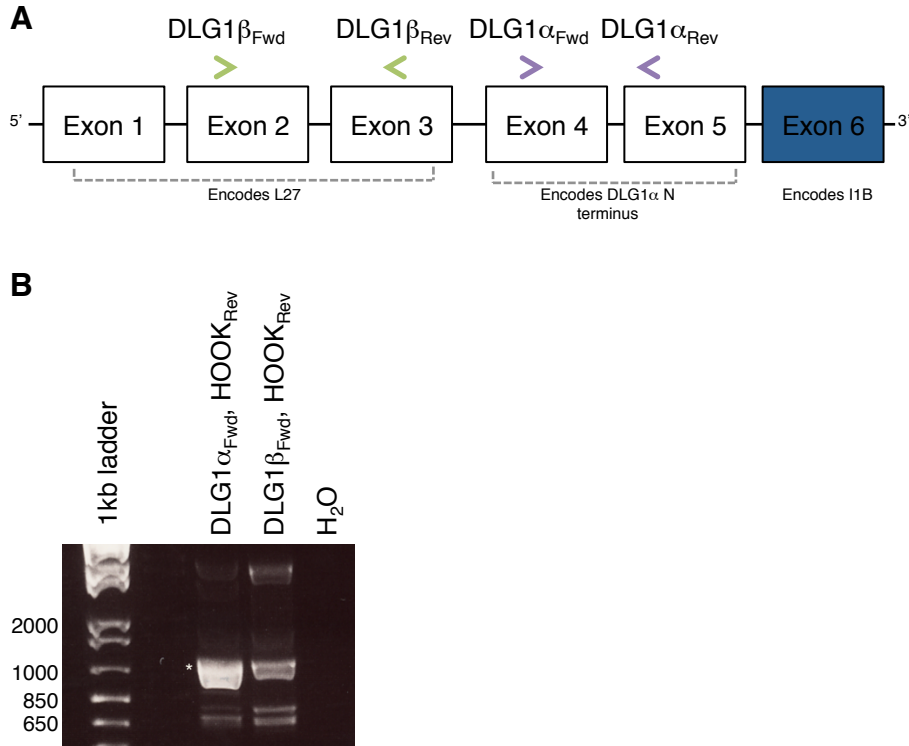


**Figure 4.6: Amplification of the *DLG1* N-terminus**

- (A) Schematic of the primers positioned with respect to the *DLG1* N-terminus (Boxes indicate exons and the line intronic regions). Primers indicated by arrows, with names above. Green,  $DLG1\beta_{Fwd}$  and  $DLG1\beta_{Rev}$ ; Purple  $DLG1\alpha_{Fwd}$  and  $DLG1\alpha_{Rev}$ .
- (B) Agarose gel electrophoresis separated PCR products. cDNA was transcribed using oligodT primers upon DNase-treated RNA extracted from from HPV16-genome containing keratinocytes, or water as a control. Bands were excised and sequenced. Star (\*) indicates successfully sequenced band.

## 4.4.1.1 Splice site analysis of novel insertion

The analysis of *DLG1* transcription in the genome containing keratinocytes identified an isoform of DLG1 that contained a previously unknown insertion. To examine the splice donor and acceptor regions of this novel exon and compare them to the consensus sequences, splice site analysis was carried out upon the *DLG1* gene sequence between exons 21 and 22. Splice site analysis was also carried out on the known DLG1 spliced insertions that result in the  $\alpha$  or  $\beta$  N-terminus and in the inclusion of I1A I1B, I2, I3, I4 and I5. A computational splice site analysis programme designed to predict the effects of mutations on splicing signals or to identify splicing motifs in any human sequence, was used alongside knowledge of known splice site recognition motifs (Table 4.3). The consensus sequences included the nucleotides at the 5' end of the donor exon (<sup>A</sup>/<sub>c</sub>AG) and 3' of the acceptor exon (<sup>c</sup>/<sub>T</sub>AG), as well as intronic sequence proximal to the exons, i.e. 3' of the donor and 5' of the acceptor exons, with the consensus nucleotides GU<sup>A</sup>/<sub>c</sub>AGU and CAG, respectively (Table 4.3).

**Table 4.3: Exon and intron comparison to consensus splice nucleotide sequence**

5'Exon-3'Exon	5' Donor	Intron (5'-3')	3' Acceptor
<b>Consensus</b>	----- <sup>A</sup> cAG	GU <sup>A</sup> <sub>c</sub> AGU----CAG	<sup>c</sup> TAG-----
<b><math>\alpha</math> N-terminus-I1B</b>	CTCCACCCAG	GTAACA---AAG	GCAAATCCTCC
<b><math>\beta</math> N-terminus-I1B</b>	ACCAATAAAG	GTAGGA---AAG	GCAAATCCTCC
<b>I1A-I1B</b>	CATACCACAG	GTTTTT---AAG	GCAAATCCTCC
<b>I2-I5</b>	GGGCCTGAAG	GTAAGT---CAG	CATGTAACTTC
<b>I3-I5</b>	GATGCTGACC	GTAAGT---CAG	AGCATGTAACT
<b>I2-I6</b>	AAAGGCCTGA	GTAAGT---CAG	TAGTTTTACCA
<b>I6-I5</b>	TTTATTTTTC	CTTAAA---CAG	CATGTAACTTC
<b>I5-GK</b>	AGTAGTTACC	GTAAGT---TAG	CGTGGTCAAGA
<b>I5-I4</b>	AGTAGTTACC	GTAAGT---AAG	TAATCTTGATT

Consensus derived from Srebrow and Kornblihtt, 2006; Ghigna *et al.*, 2008; Harris and Senapathy, 1990. Full sequences of exons are listed in Appendix II.

Examination of the known DLG1 exons encoding the insertions revealed that the exons corresponding to the  $\alpha$  (exon 5) and  $\beta$  (exon 3) N-terminus, and to I1A (exon 6) and I2 (exon 21), all contain a consensus 5' AG dinucleotide. However, the exons encoding I3, I5 and the new insertion I6 contain a 5' cytosine that does not conform to the consensus sequence (Table 4.3). Similarly, the canonical 3'  $^c$ /T<sub>T</sub>AG acceptor nucleotides were present in exons encoding I5 and I6 but not in the other exons analysed (Table 4.3).

Although there are consensus sequences, these are not strictly adhered to by all the exons of DLG1. The intronic sequence is as important as the donor and acceptor sequences in splicing, as it contains the branchpoint adenosine and regions of spliceosome recognition (Williams, 2002; Harris and Senapathy, 1990). Screening of the *DLG1* gene sequence showed conservation of a 5' GT in all the introns analysed, apart from between I6 and I5, where a cytosine replaced the guanosine (Table 4.3). The 3' intronic AG dinucleotide was conserved in all the sequences included in the screening analysis (Table 4.3). The non-adherence to consensus sequence may indicate obscure or 'weak' splice sites, where the inclusion of exons requires additional specific factors, which may be cell or condition specific.

#### 4.4.2 Investigation into protein expression of the novel DLG1 isoform

##### 4.4.2.1 *In silico* screening suggests interacting proteins for novel insertion

In order to investigate the potential roles for the novel DLG1 sequence, the nucleotide sequence was translated *in silico* using the ExPasy resource and the resulting amino acid sequence of the insert I6 and upstream I2 was screened for potential protein-protein interactions using ScanSite software. An amino acid sequence of 20 residues was predicted, followed by a stop codon (Figure 4.7). In the context of the whole DLG1 protein, inclusion of this sequence would produce a truncated protein containing the three

## A

Frame 1  
ST<sup>OP</sup>FYQFAHS<sup>STOP</sup>R<sup>MET</sup>NSHCCISLS<sup>MET</sup>LDSVLCFHFSSHGGQRHSLWL<sup>STOP</sup>FAFP<sup>STOP</sup>QVINLNTFLYVYWLFDCLL

Frame 2  
SFTSLPIPSA<sup>STOP</sup>PTPIAAAYHYRCLTCLFCVFIILAILVDGRD<sup>STOP</sup>TLCGYNLHFPDKA<sup>STOP</sup>L<sup>STOP</sup>T<sup>STOP</sup>TLFY<sup>MET</sup>FIGYLTVFF

Frame 3  
VLPVCPFLAHELPLLLHIIIDA<sup>STOP</sup>HVCVFSF<sup>STOP</sup>PF<sup>MET</sup>W<sup>MET</sup>AE<sup>MET</sup>TLFVVIICISLTSN<sup>STOP</sup>LEHFSICLLVI<sup>STOP</sup>SLSS

## B

REI<sup>STOP</sup>PDDMGSKGLI<sup>STOP</sup>VLPVCPFLAHELPLLLHIIIDA<sup>STOP</sup>HVCVFSF<sup>STOP</sup>PF<sup>MET</sup>W<sup>MET</sup>AE<sup>MET</sup>TLFVVIICISLTSN<sup>STOP</sup>LEHFSICLL  
I<sup>STOP</sup>LSSLACNF<sup>STOP</sup>CQR<sup>STOP</sup>STOP<sup>STOP</sup>K<sup>STOP</sup>L

### Figure 4.7 *In silico* translation of nucleotide sequence

- (A) Translation of the nucleotide sequence of the novel insertion into amino acid sequence. The sequence was translated in three frames.
- (B) Translation of sequenced fragment including exons 21 (I2, pink) and 23 (I5, purple) at either side. The novel insertion is designated I6. Non-translated sequence is indicated in grey. The final lysine of I2 is excluded in the I2-I6 variant.

PDZ domains, followed by the SH3 domain, I2 and a novel sequence of 21 amino acids; the truncated protein however would lack the GK domain (Figure 4.7). Furthermore, the final lysine of I2 is not included, instead an isoleucine takes its place. Similar alternative inclusion of single amino acids in insertions has been observed with the glutamine residue at the beginning of DLG1 I3 (McLaughlin *et al.*, 2002). The predicted molecular mass of the novel isoform is 60 kDa, compared to the full-length protein of 120 kDa.

**Table 4.4: Potential protein interactions with I2-I6 sequence**

Motif Group	Motif	Gene	Sequence target	Score
Kinase binding site group	Erk D-domain	MAPK1	DMGSKGLI <u>V</u> LPVCP <u>P</u> F	0.868
			GSKGLI <u>V</u> L <u>P</u> VCP <u>P</u> FLA	0.798
			KGLI <u>V</u> LP <u>V</u> CP <u>P</u> FLAHE	0.726
Src homology group (SH3)	Cbl-associated protein CSH3	SORBS1	LIVLPV <u>C</u> P <u>P</u> FLA <u>H</u> ELP	0.909
	Cortactin SH3	HCLS1	LIVLPV <u>C</u> P <u>P</u> FLA <u>H</u> ELP	0.760
	PLCg SH3	PLCG1	LIVLPV <u>C</u> P <u>P</u> FLA <u>H</u> ELP	0.687
	Src SH3	SRC	SKGLI <u>V</u> LP <u>V</u> CP <u>P</u> FLA <u>H</u>	0.658
	P85 SH3 mode 1	PI3KR1	SKGLI <u>V</u> LP <u>V</u> CP <u>P</u> FLA <u>H</u>	0.665

Target residues underlined. The SH3 domain binds proline residues, the Erk D-domain consensus sequence is  $\phi$ -X- $\phi$ -P, where  $\phi$  indicates a hydrophobic residue.

The translated protein sequence of I2-I6 was analysed for secondary structure motifs to predict protein interacting domains, with a score to indicate the probability of an interaction, where 0 indicates an unfavourable interaction and 1 a highly favourable interaction (Table 4.4). Two protein binding motifs were highlighted *via* the screen: the kinase binding site group and the SH3 group (Table 4.4). Five protein families were suggested to bind the central proline of the novel insertion via an SH3 domain, including regulatory subunits of the kinases PI3K and PKC $\gamma$  (Table 4.4). The mitogen-associated kinase MAPK1 was also predicted to bind to three residues within the insertion, an isoleucine, leucine and a valine, all predicted to bind with a score of over 0.7 (Table 4.4).

These residues stand in the place of ‘X’ in the Erk D (docking)-domain binding consensus sequence ( $\phi$ -X- $\phi$ -P, Table 4.4, Sheridan *et al.*, 2008; Fernandes and Allbritton, 2009).

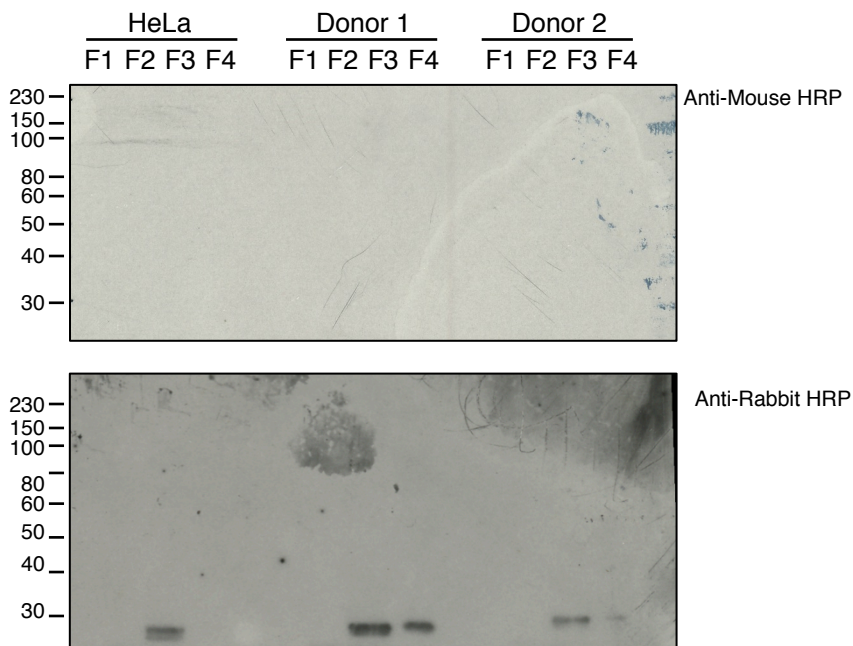
#### 4.4.2.2 DLG1 isoform expression analysis using antibodies

In order to identify whether a truncated form of DLG1 is expressed, several antibodies against DLG1 were used to detect protein extracted from cellular fractions of HPV16 and HPV18 genome containing keratinocytes, as well as from the HPV18 positive cancer cell line HeLa. These antibodies were a selection of commercial and non-commercial antibodies raised to different regions of DLG1 (Table 4.5). Control blots incubated with either secondary anti-mouse or anti-rabbit IgG antibody were carried out to highlight any non-specific binding (Figure 4.8). In these control blots, a non-specific band can be seen at 30 kDa in both the nucleus and cytoskeleton, when incubated with the anti-rabbit IgG horseradish peroxidase (HRP) -conjugated secondary antibody whereas no bands were detected in blots incubated with the anti-mouse IgG secondary antibody, which was conjugated to HRP (Figure 4.8).

**Table 4.5: DLG1 Antibodies**

Antibody name	Source	Animal origin	Region of DLG1	Reference
2D11	Santa Cruz	Mouse	1-229 DLG1 $\beta$	-
H-60	Santa Cruz	Rabbit	49-108 DLG1 $\beta$	-
NAG	S. Roberts	Rabbit	1-200 DLG1 $\beta$	Roberts <i>et al.</i> , 2007; McLaughlin <i>et al.</i> , 2002
NT	L. Banks	Rabbit		-
DLG1 $\alpha$	S. Roberts	Rabbit	DLG1 $\alpha$ N-terminus: KGSSDELQAEPEPSR	Designed during this thesis

The predicted molecular mass of the truncated form of DLG1 was 60 kDa. The mouse monoclonal antibody 2D11 and the rabbit polyclonal antibody H60 were both raised to the N-terminus of DLG $\beta$ . As expected, both antibodies detected DLG1 migrating at



F1, Cytoplasm F2, Membrane F3, Nucleus F4, Cytoskeleton

**Figure 4.8: Cross-reaction of subcellular fractions with HRP-conjugated secondary antibody**

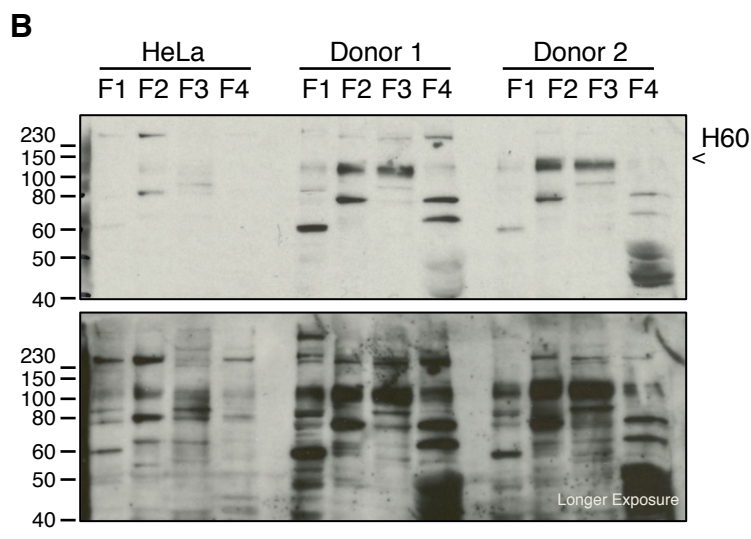
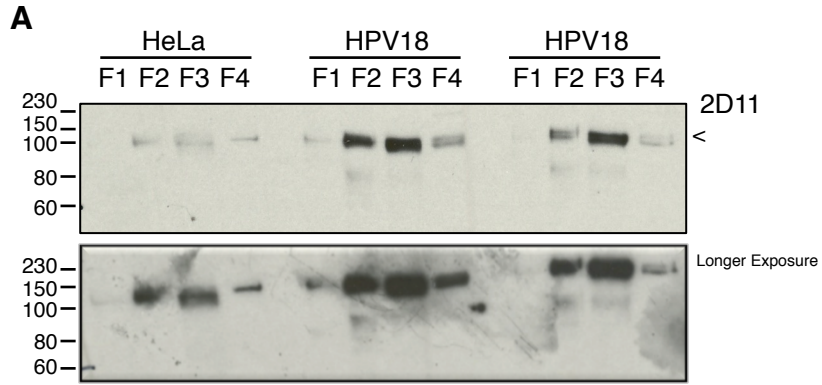
HeLa and HPV18 genome containing keratinocytes were cultured in monolayer to 70% confluency and subjected to subcellular fractionation. The cytoplasmic (F1), membrane (F2), nuclear (F3) and cytoskeletal (F4) fractions were then separated by SDS-PAGE and probed with anti-mouse (top panel) or anti-rabbit (top panel) HRP-conjugated secondary antibody. Molecular weight markers show kDa.

approximately 120 kDa in both HeLa cells and in the genome containing keratinocytes (Figure 4.9 A). As noted previously, the majority of DLG1 was located in the nucleus. (Figure 4.9 A). Detection with 2D11 revealed no smaller bands, but the H60 antibody identified a number of small bands in the cytoplasmic fraction including several between 60-80 kDa in both donors and to a lesser extent in HeLa.

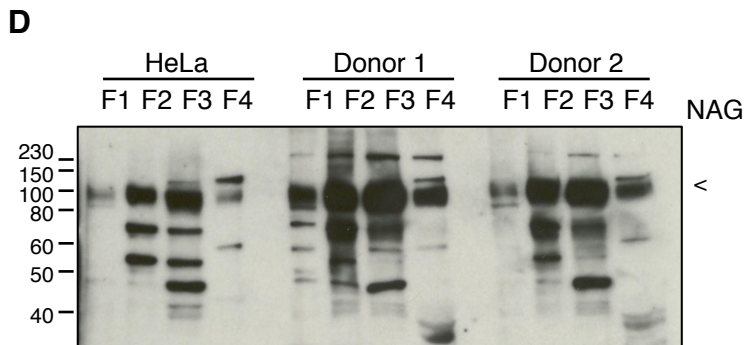
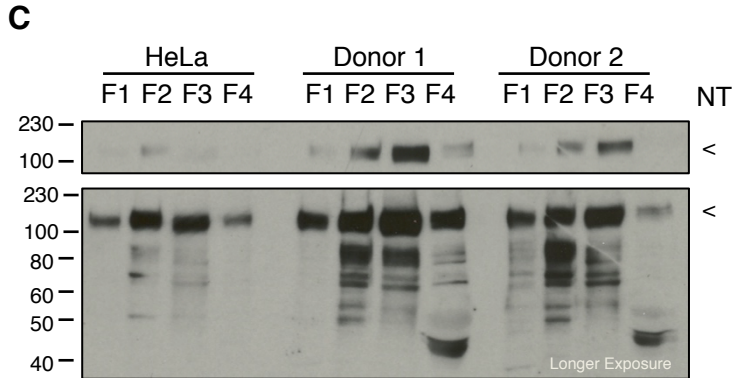
Likewise, the NT antibody detected full-length DLG protein plus an array of faster migrating proteins, but the profile differed from the one recognized by H60. NT detects several bands between 40 and 80 kDa in the membrane and cytoskeleton and at 80 kDa in the cytoplasmic fraction, all of which are stronger in the keratinocytes containing HPV genomes than in HeLa cells (Figure 4.9 B).

The N-terminal NAG antibody NAG is raised to a region of DLG1 encompassing the insertions I1A and I1B (McLaughlin-Drubin and Meyers, 2004; Lue *et al.*, 1994). As with H60 and NT, the NAG antibody detected full length DLG1 and a number of smaller species (Figure 4.9 D). In particular, protein detected at approximately 65 kDa in the membrane and nuclear fractions are more prominent in genome containing cells than in HeLa (Figure 4.9 D).

Thus, protein analysis with a number of DLG1-specific antibodies suggested the existence of smaller (less than 120 kDa) species, including a form of approximately 60 kDa. However, the analysis of the I6 containing transcripts indicated a  $\alpha$  isoform although it cannot be ruled out that  $\beta$  forms contain the I6 insertion too, and none of the existing antibodies recognised this isoform of DLG1. In order to assess the expression of DLG1 $\alpha$ , an immunogenic peptide was designed from the N-terminus sequence unique to DLG1 $\alpha$  by a commercial company (Generon, Figure 4.2). The peptide (KGSSDELQAEPEPSR) was used as an immunogen in rabbits and the subsequent



F1, Cytoplasm F2, Membrane F3, Nucleus F4, Cytoskeleton



F1, Cytoplasm F2, Membrane F3, Nucleus F4, Cytoskeleton

**Figure 4.9: Detection of DLG1 protein in cellular compartments of HeLa and HPV18 genome containing keratinocytes**

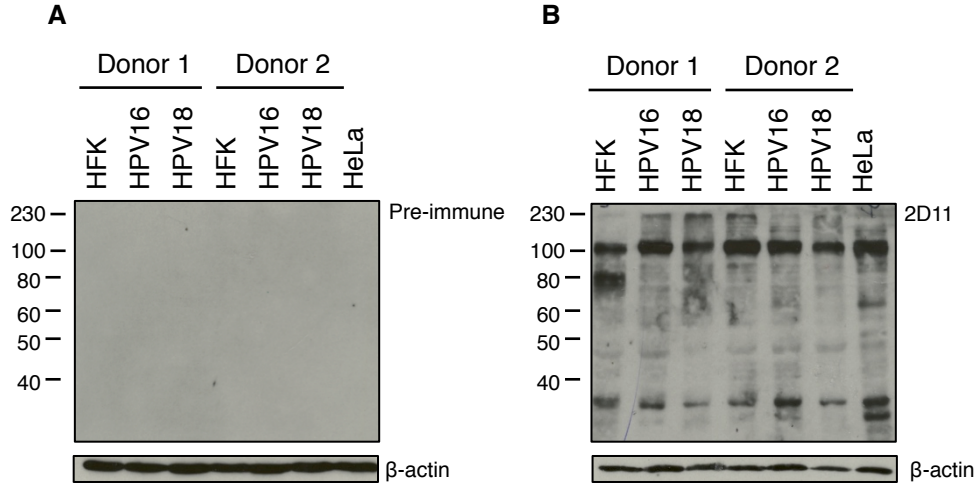
The cytoplasmic (F1), membrane (F2), nuclear (F3) and cytoskeletal (F4) fractions were sequentially extracted from monolayer grown HeLa and HPV18 genome containing keratinocytes derived from two donor backgrounds, separated by SDS-PAGE and detected using various antibodies against regions of DLG1. Both 2D11 (A) and H-60 (B) are specific to the N-terminal region of DLG1 $\beta$ . The NT-antibody (C) detects.....The N-terminal antibody NAG (D) was developed in-house by the Roberts lab.

In each case, the bands corresponding to full-length DLG1 protein (100-120kDa) is indicated by the arrow head. Molecular weight marker indicates kDa.

antibody (DLG1 $\alpha$  1524) recognised the peptide in ELISA based assay (performed by Generon). The antibody was then tested upon protein extracted from keratinocytes containing HPV16 and HPV18 by western blotting. Rabbit serum extracted before exposure to immunogen (pre-immune) was used as a control for non-specific binding. No non-specific bands were detected using the pre-immune serum (Figure 4.10 A). In parallel experiments on the same lysates the 2D11 antibody confirmed the presence of full-length DLG1 migrating at approximately 120 kDa (Figure 4.10 B). The full-length protein was present in primary cells and in the genome containing keratinocytes when using the DLG1 $\alpha$  antibody and a number of additional bands were detected in all lysates (Figure 4.10 C). Furthermore, in keratinocytes the bands detected by the DLG1 $\alpha$  specific antibody migrated slightly faster than in HeLa, indicating differences in phosphorylation of the  $\alpha$  forms between HeLa and other cells (Figure 4.10 C). Upon longer exposure, a profile of faster migrating bands were visible including several bands between 50 and 60 kDa, suggesting the presence of truncated forms of the proteins. However, there was no obvious change in the level of these smaller species between primary cells and those containing HPV genomes (Figure 4.10 C), which would be expected if the bands corresponded to the I6-containing form of DLG1 upregulated by HPV.

#### 4.4.3 Investigation of DLG1 isoform expression

Chapter 3 details the expression of the HOOK domain containing transcripts of DLG1 in keratinocytes containing high-risk HPV genomes. Having identified that this corresponded to a region of *DLG1*, which was previously not known to be expressed, here expression analysis was extended to characterise the expression of *DLG1* transcripts containing this novel insertion. In addition, the expression of the two main isoforms, DLG1 $\alpha$  and DLG1 $\beta$  was also characterised because studies in Chapter 4 (Section 4.3.2) suggested that



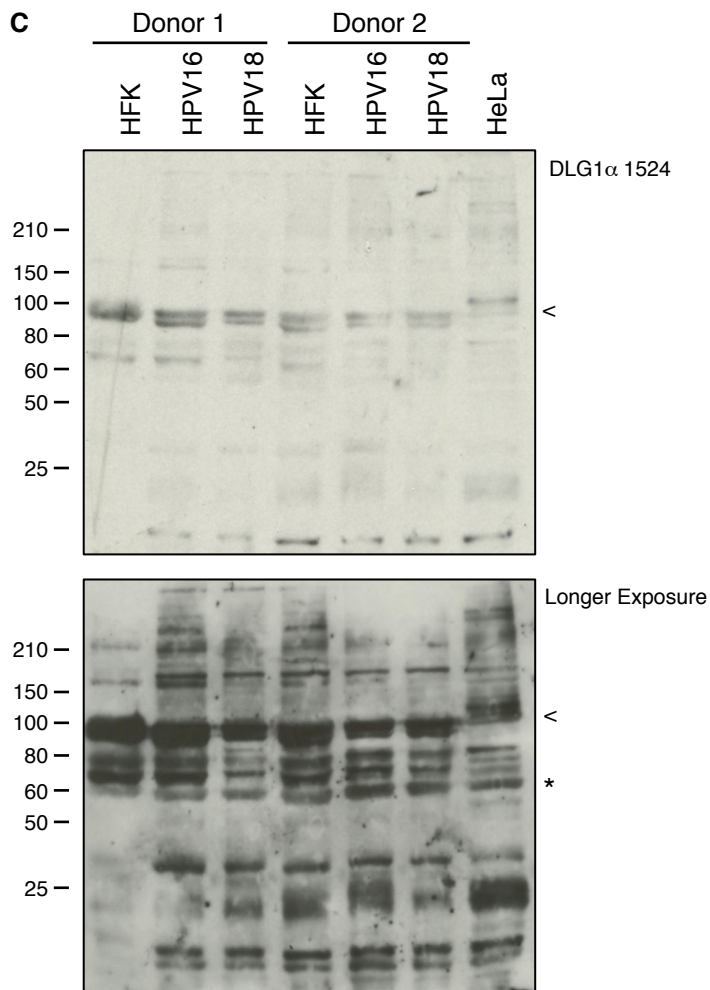


**Figure 4.10: Detection of DLG1 $\alpha$  protein**

Total protein was extracted from untransfected HFKs as well as HFKs containing HPV16 and HPV18 genomes from two donor backgrounds and from HeLa cells. All cells were grown in monolayer culture, harvested at 70% confluency and lysed in urea buffer. Protein was separated by SDS-PAGE and probed with pre-immune serum (A), commercial DLG1 antibody (2D11, B) and DLG1 $\alpha$  1524 (C).

In each case, the bands corresponding to full-length DLG1 protein (100-120kDa) is indicated by the arrow head and loading control ( $\beta$ -actin) is positioned beneath. Molecular weight marker indicates kDa.

the novel insertion was expressed primarily as part of the  $\alpha$  isoform. Moreover, our current knowledge of DLG1 is focussed on the  $\beta$  isoform and little is understood of DLG1 $\alpha$  expression. In qRTPCR analysis, primers were utilised that corresponded specifically to the DLG1 $\alpha$  N-terminus, to the DLG1 $\beta$  L27 domain or to the HOOK domain I6 insertion (see Section 2.2.1.2, Table 2.2). cDNA was transcribed from DNase treated RNA using oligodT primers before being subjected to qRTPCR. Gene expression was calculated relative to the number of transcripts of the internal control  $\beta$ 2microglobulin (B2M), before comparison to external control (*e.g.* untransfected keratinocytes), to generate ddCt fold change.

#### 4.4.3.1 *DLG1 isoform expression in keratinocytes containing high-risk HPV genomes*

As previously described, a screen of *DLG1* expression levels in keratinocytes containing high-risk HPV genomes was carried out by microarray, and was validated using qRTPCR (Chapter 3). The microarray included two probes corresponding to different regions of DLG1, the aforementioned HOOK region, and a probe that aligned to the N-terminus of the DLG1 $\beta$  isoform (Figure 4.11). Microarray analysis showed an increase in DLG1 transcripts containing the HOOK domain in monolayer-grown keratinocytes containing either HPV16 (11-fold) or HPV18 (7.5-fold) compared to untransfected keratinocytes from the same donor background (Table 4.6). Conversely, microarray analysis of DLG1 $\beta$  transcripts was not above the limit of 2.5 fold (Table 4.6). Gene expression analysis by qRTPCR verified the trend seen by microarray; in two donors a 18-20-fold increase in the *DLG1* I6 insertion was observed in the presence of HPV16 genomes, and a 5-6-fold increase in HOOK transcripts was detected in HPV18 genome containing cells (Figure 4.11). Although there was no microarray probe corresponding to DLG1 $\alpha$  transcripts, the use of specific primers to this isoform in qRTPCR demonstrated that DLG1 $\alpha$  transcripts

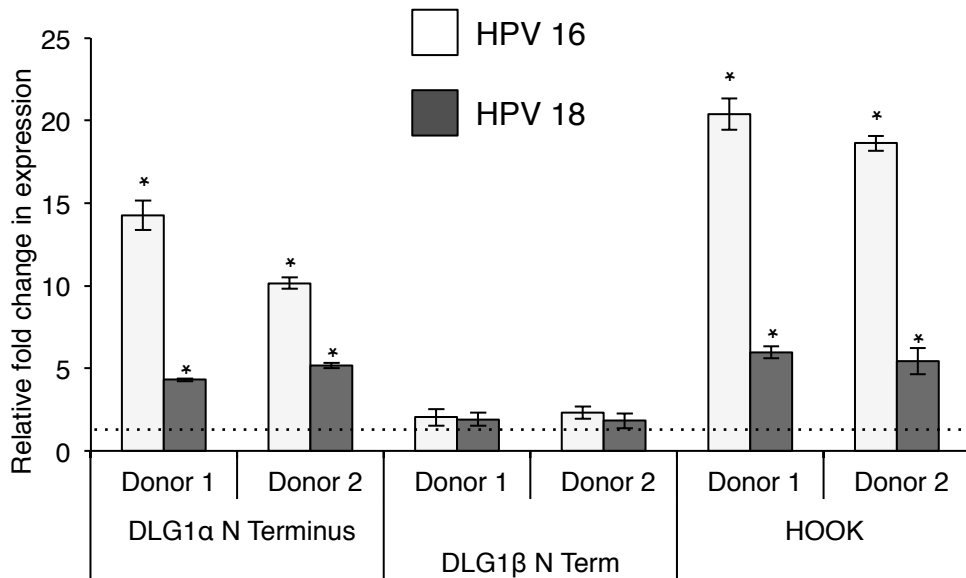


**Figure 4.11: *DLG1* isoform expression in primary keratinocytes containing  $\alpha$ -HPV genomes**

RNA was extracted from primary keratinocytes containing HPV16 or HPV18 genomes, alongside untransfected HFKs, from two donor backgrounds. Following DNase treatment and translation using oligodT primers, cDNA was subjected to SYBR green qPCR, using primers specific to the DLG1 $\alpha$  or DLG1 $\beta$  N-terminus, and to the I6-containing HOOK region.

Transcript levels were normalised to an internal B2M control and then to transcript levels in HFKs of the same donor background (indicated by dotted line). Error bars  $\pm$ SEM of three experimental repeats and star (\*) indicates a p value of  $<0.05$ .

were increased in both HPV16 and HPV18 genome containing keratinocytes, by more than ~10- and ~4-fold respectively (Figure 4.11).

**Table 4.6: Microarray and qRTPCR analysis of *DLG1* expression.**

Region of <i>DLG1</i>	HPV16		HPV18	
	Microarray	qRTPCR	Microarray	qRTPCR
DLG1 $\alpha$ N-terminus	-	12.20	-	4.73
DLG1 $\beta$ N-terminus	1.70	1.97	2.02	2.48
HOOK Region	11.67	17.56	7.50	5.7

Microarray and qRTPCR analysis of *DLG1* expression. Fold change relative to HFKs and average from 2 donor backgrounds.

Both DLG1 $\alpha$  and I6-containing transcripts were elevated to greater levels in keratinocytes containing HPV16 genomes than cells containing HPV18, and this was consistent in two donor keratinocyte backgrounds (Figure 4.11). Data is summarised in Table 4.6.

#### 4.4.3.2 *DLG1* isoform expression during the productive life cycle

To establish whether the *DLG1* isoforms are affected upon activation of the productive virus life cycle, HPV18 genome containing keratinocytes were grown in semi-solid media (1.5% methylcellulose), which stimulates differentiation and activates productive viral events including viral genome amplification (Wilson and Laimins, 2005). Total cellular RNA was extracted from cells harvested at 0, 24 and 48 h and *DLG1* isoform transcripts analysed using the primers in RT-PCR analysis. Transcript level quantification at 24 and 48 h was normalised to 0 h. DLG1 $\alpha$  and DLG1 $\beta$  exhibited a ~3-fold increase in transcripts after 24 h and transcript levels remained elevated at 48 h (Figure 4.12). *DLG1* transcripts containing the novel HOOK region insertion demonstrated a 2-fold increase after 24 h growth in methylcellulose and remained at this levels at 48 h (Figure 4.12).

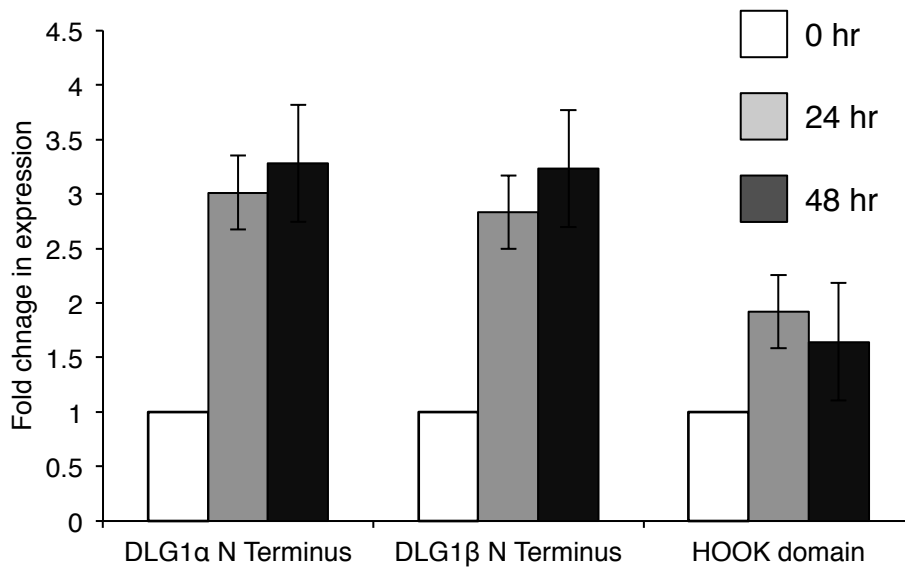


**Figure 4.12: Expression of *DLG1* in differentiating keratinocytes containing HPV18**

Primary keratinocytes containing HPV18 genomes cultured in semi-solid media (methylcellulose) and harvested at 24 and 48 h. Total RNA was extracted and transcribed to cDNA using oligodT primers, following treatment with DNase. Three primer sets utilized in SYBR green qPCR, to measure transcript levels of DLG1α, DLG1β and the I6-containing HOOK region. Fold change in expression was calculated relative to the internal control B2M, and then to corresponding 0 h timepoint. Error bars show  $\pm$ SEM of three technical repeats.

#### 4.4.3.3 Investigating HPV regulation of DLG1 isoform expression

Although changes in E6 PBM activity are unlikely to have an effect upon the transcription of DLG1 isoforms, the change in E6 PBM activity is associated with alterations in proliferation of the genome containing cells (Delury *et al.*, 2013), which may be reflected by changes in DLG1 isoform expression. Therefore, qRT-PCR analysis was carried out upon monolayer keratinocytes containing HPV18 WT genomes or cells harbouring the  $\Delta$ PDZ and  $\Delta$ PKA genomes. The data showed that transcript levels of DLG1 isoforms - DLG1 $\alpha$ , DLG1 $\beta$  and HOOK (I6) - were unchanged in the presence of genomes that have alteration on E6 PBM activity compared to the WT cells (Figure 4.13). At this stage of the study, it is not understood how the virus regulates DLG1 isoform expression.

The studies to date have focussed on cells harbouring the viral episomes, which replicate as low copy extra-chromosomal plasmids. It may be that this effect on DLG1 is specific to this stage of virus replication and if so it would be expected to change if the episomes were lost and the viral genomes integrated into the host chromosomal DNA. To examine this, the expression of the different DLG1 isoforms was assessed in monolayer keratinocytes containing HPV18 genomes at early (P8, viral genomes are episomes) and late (P21, viral episomes are lost and viral DNA integrated) passages (E. Marsh, personal communication). When compared to episomal genome containing keratinocytes, the levels of DLG1 $\beta$  transcripts remain unchanged (Figure 4.14). Although the trend indicates that DLG1 $\alpha$  and HOOK domain containing transcripts were decreased in cells containing integrated HPV18; this is based upon three technical repeats in one donor and therefore requires further experimental repeats across multiple donors (Figure 4.14).

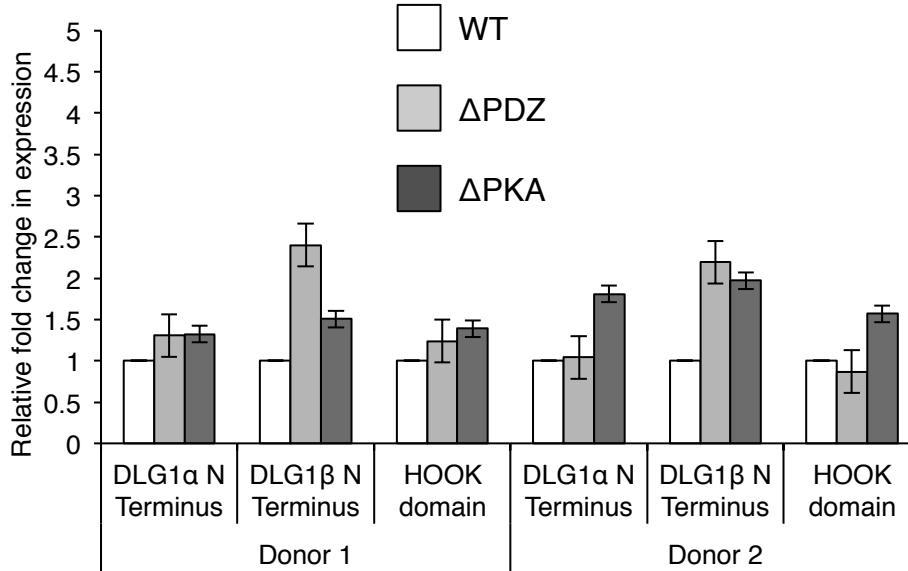


**Figure 4.13: *DLG1* isoform expression in keratinocytes containing HPV18 genomes**

RNA extracted from primary keratinocytes containing HPV18 WT,  $\Delta$ PDZ or  $\Delta$ PKA genomes was DNase treated and reverse transcribed using oligodT primers. The transcript levels of DLG1 $\alpha$ , DLG1 $\beta$  and the I6-containing HOOK region were measured by SYBR green qPCR, values were normalised to internal control (B2M) and then to levels of cells containing WT HPV18 genomes. Error bars show SEM of three technical repeats in two donors.

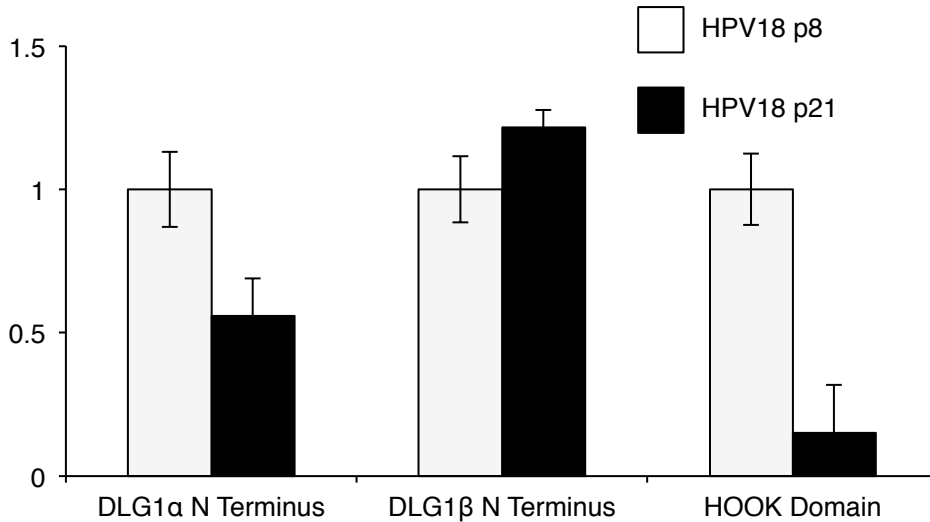


**Figure 4.14: *DLG1* isoform expression in keratinocytes containing episomal and integrated forms of the HPV18 genome**

RNA extracted from primary keratinocytes containing HPV18 genomes was DNase treated and reverse transcribed using oligodT primers. The transcript levels of DLG1 $\alpha$ , DLG1 $\beta$  and the I6-containing HOOK region were measured by SYBR green qPCR, values were normalised to internal control (B2M) and then to levels of cells containing episomal genomes. Error bars  $\pm$ SEM of three technical repeats.

#### 4.4.3.4 *DLG1 isoform expression in normal tissue*

DLG1 is expressed in a range of tissue types and isoforms are likely to be expressed in a tissue specific pattern (McLaughlin *et al.*, 2002; Mori *et al.*, 1998; Godreau *et al.*, 2003). Thus, the expression of *DLG1* isoforms DLG1 $\alpha$ , DLG1 $\beta$  and HOOK region-containing transcripts were investigated in normal tissues of the brain, skin, kidney and liver and in normal immune cells (T-cells). For comparison of transcript levels, fold change was calculated relative to DLG $\alpha$  transcripts. In all the tissues analysed, DLG1 $\beta$  transcripts were more abundant than DLG1 $\alpha$  or the HOOK region (I6) containing transcripts. Expression of DLG1 $\beta$  in kidney and skin was more than 7-fold higher and the level of DLG1 $\beta$  transcript in the liver was 4-fold higher than DLG1 $\alpha$  (Figure 4.15). In brain tissue, the difference in expression between the  $\alpha$  and  $\beta$  isoforms was the largest of the tissues analysed; expression of DLG1 $\beta$  was 11.9-fold higher than DLG1 $\alpha$  (Figure 4.15). The expression of HOOK domain containing transcripts varied in the tissue analysed. In brain and liver the transcripts were less abundant than DLG1 $\alpha$  transcripts, whilst in kidney tissue HOOK domain containing transcript levels were more than 3-fold higher than the DLG1 $\alpha$ -containing transcripts (Figure 4.15). HOOK domain containing transcripts were expressed equally with DLG1 $\alpha$  in skin (Figure 4.15). Analysis of *DLG1* expression in T-cells revealed equal levels of expression of the three transcripts assessed (Figure 4.15).

#### 4.4.3.5 *DLG1 isoform expression in cancer cell lines*

Analysis of *DLG2* expression has shown transcriptional upregulation of specific spliced variants in kidney cancer precursor growths (Zubakov *et al.*, 2006). Furthermore, several studies have demonstrated differential expression of DLG1 in cancers (Watson *et al.*, 2002; Frese *et al.*, 2006; Cavatorta *et al.*, 2004). To investigate the expression of DLG1 isoforms

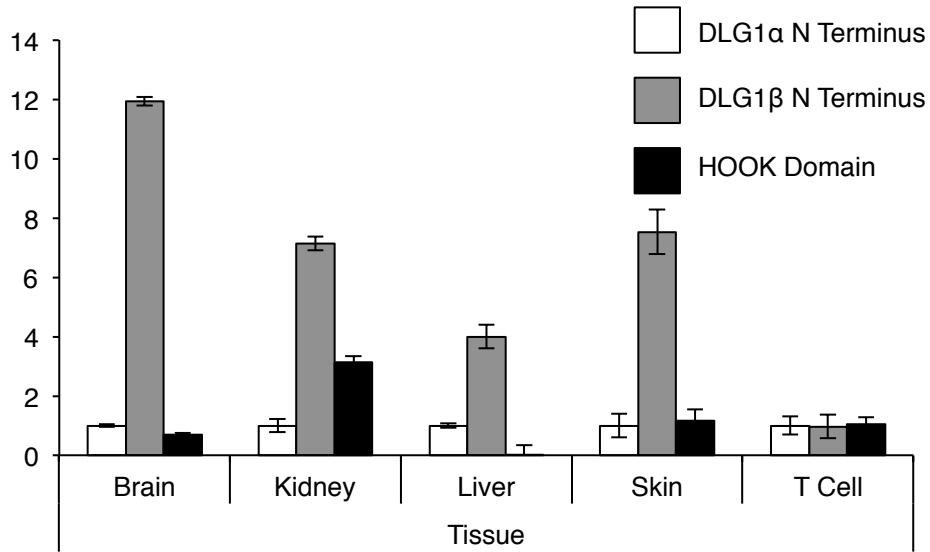


**Figure 4.15: *DLG1* isoform expression in normal tissue**

Total RNA was extracted from human brain, kidney, liver and skin tissue samples, as well as from T-cells. Following DNase treatment and reverse transcription using oligodT primers, the levels of DLG1 $\alpha$ , DLG1 $\beta$  and the I6-containing HOOK region transcripts were measured by SYBR green qPCR, values were normalised to internal control (B2M) and then to the levels of DLG1 $\alpha$  transcripts. Error bars  $\pm$ SEM of three technical repeats.

during growth of cancer cells, qRT-PCR analysis was applied to epithelial cancer cell lines. These cervical cancer-derived cell lines comprise the HPV18 positive line HeLa, the HPV16 positive cell lines SiHa and Caski and the HPV negative cervical cancer cell line, C33A. The fold change in *DLG1* expression in these cells was calculated relative to the primary cervical keratinocytes (Cx129), which were isolated from uterine cervical tissue removed for a non-cancerous condition and therefore are considered non malignant. None of the cervical cancer cell lines analysed exhibited a change in *DLG1* isoform expression levels; with the exception of the HPV16 positive cell line Caski, which demonstrated a 4.9-fold increase in DLG1 $\alpha$  transcripts (Figure 4.16). A trend towards a decrease in transcript levels was observed in the HPV negative cell line C33A, but this was not statistically significant (Figure 4.16). Expression of both DLG1 $\beta$  and HOOK domain containing transcripts remained unchanged in HeLa, SiHa and Caski (Figure 4.16).

Since high-risk HPVs have also been etiologically linked to the development of head and neck cancers (Gillison and Shah, 2001), *DLG1* expression analysis was extended to HPV positive and HPV negative head and neck cancer derived cell lines. Four HNSCC cells lines were examined; SCC040 and Vu40T, which are both HPV negative, and the HPV16 positive cell lines SCC154 and Vu147 (Steenbergen *et al.*, 1995; Rampias *et al.*, 2009). Transcript levels in HPV positive cells were normalised to their HPV negative counterpart. All DLG1 transcripts detected were less abundant in SCC154 (HPV16+) compared to the SCC040 (HPV-), whereas DLG1 $\alpha$  and HOOK domain containing transcripts are increased nearly 2-fold in the HPV positive Vu147 compared to Vu40T (Figure 4.17). The abundance of DLG1 $\beta$  was equal in Vu147 to Vu40T cells (Figure 4.17).

In summary, transcription of DLG $\beta$  is unaffected by HPV, whereas  $\alpha$  is upregulated along with the I6-containing isoform in episomal genome containing cells. The DLG1 $\alpha$ , DLG1 $\beta$

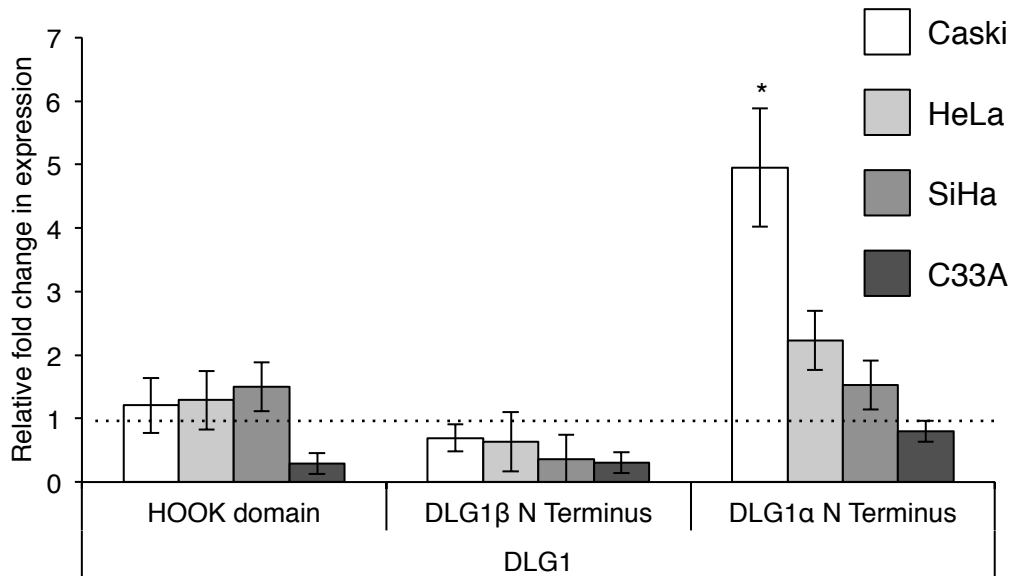


**Figure 4.16: *DLG1* isoform expression in cancer cell lines**

Transcriptional analysis performed the HPV positive cervical cancer cell lines HeLa (HPV18), SiHa (HPV16) and Caski (HPV16), and the HPV negative cervical carcinoma-derived cell line, C33A. The levels of *DLG1α*, *DLG1β* and HOOK region containing transcripts were measured by SYBR green qRT-PCR, using DNase treated RNA transcribed to cDNA with oligodT primers.

Expression levels were calculated relative to internal control (B2M), and then to non-cancerous cervical epithelial cells (Cx129 cells, indicated by dotted line). Error bars  $\pm$ SEM of three experimental repeats, \* denotes  $p < 0.05$ .

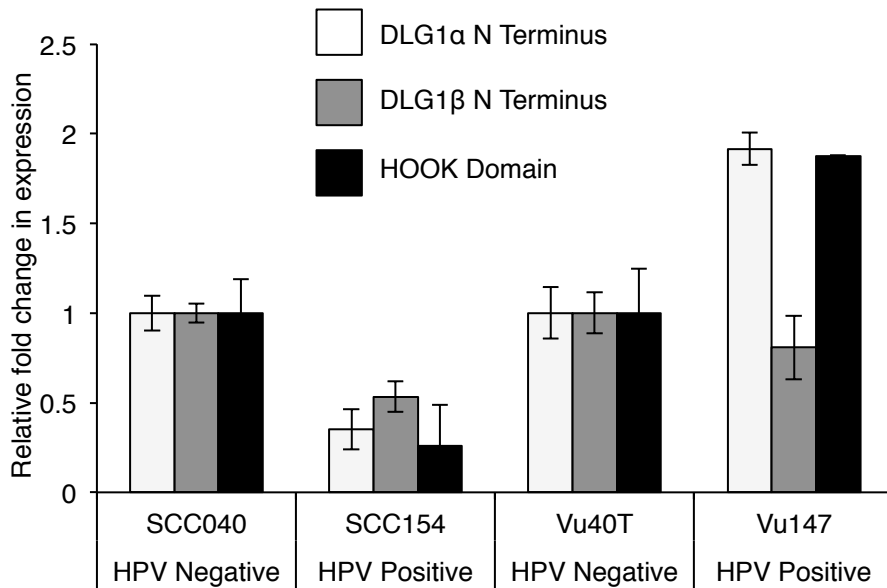


**Figure 4.17: *DLG1* isoform expression in head and neck cancer derived cell lines**

Transcriptional analysis performed on HPV negative (SCC040 and Vu40T) and HPV16 positive (SCC154 and Vu147) HNSCC derived cell lines. RNA was extracted, treated with DNase and transcribed to cDNA using oligodT primers. SYBR green qPCR was then carried out using three primer sets, to measure the levels of DLG1α, DLG1β and HOOK region transcripts. Relative expression levels were calculated relative to the internal control B2M, and then to the corresponding HPV negative cell line. Error bars show ±SEM of three technical repeats.

and I6-containing transcripts were detected in a range of cell types and, although the  $\beta$  form appears to be the predominant form in normal tissue, the observed change in the ratio between the two main isoforms in certain cancer derived cell lines indicates that perturbing the balance of DLG1 isoforms may play a role in cancer development.

## 4.5 Discussion

### 4.5.1 Identification of a novel insertion

DLG1 encodes five known insertions, occurring in two regions of the protein (McLaughlin *et al.*, 2002). This study has identified a new exon in the *DLG1* gene, which is inserted into an area of DLG1 where alternative splicing has already been identified (the HOOK region). The new insertion has been named I6. DLG1 transcripts containing the I6 insertion were detected in normal human liver, kidney, brain, skin and immune cells indicating that I6 is important in DLG1 function in normal tissue.

Interestingly, in primary human foreskin keratinocytes, transcripts containing I6 were upregulated by both high-risk viruses analysed, although the increase was greater in the presence of HPV16. The levels of these I6 containing transcripts were further increased upon activation of the productive virus life cycle. Together, these data indicate that I6-containing variants of DLG1 are important in the replication of the viral genome. Indeed when the expression of I6-containing transcripts was examined in cells containing integrated  $\alpha$ -HPV genome containing cells, the levels were decreased compared to cells containing episomal genomes, perhaps suggesting that the inclusion of I6 is required for the maintenance of episomal genomes.

It may be that the increased inclusion of I6 in DLG1 is a function of the complete HPV genome. As integration disrupts the viral genome, and this data revealed a decrease in I6 upregulation upon integration, it follows that viral factors are perhaps involved in the upregulation of the I6 spliced variant. The viral E2 protein has been shown to affect the transcription and splicing of a number of human genes, particularly those implicated in cancer development and in cell motility (Gauson *et al.*, 2014; Bouvard *et al.*, 1994a). Investigation by (Gauson *et al.*, 2014) identified 522 genes with differentially spliced exons

in the presence of HPV16 E2. Although the mechanism of this is not known, E2 is known to bind to host transcription factors and may be able to bind and recruit splicing factors also (Johansson *et al.*, 2012). Furthermore, E2 transcriptionally upregulates splicing factors, for example the factor SRSF1 (Mole *et al.*, 2009). It is feasible that an increase in this factor increases splicing in the DLG1 HOOK region and promotes the inclusion of I6 in E2-expressing cells. In addition, work in the Roberts lab has recently identified relationships between HPV and splicing regulators (Prescott *et al.*, 2014). As the virus is able to manipulate splicing machinery, it may be that such manipulations cause or lead to the alternative splicing in the HOOK domain and inclusion of I6. Furthermore, splice site analysis revealed that the I6 exon did not completely adhere to the established consensus sequence; the acceptor sequence conformed to consensus but the 5' donor was a weak match. This reflects a requirement for additional specific factors in splicing, a process which may be facilitated by the virus.

The question remains as to why this variant is upregulated in the presence the high-risk viruses. Perhaps the ability of the virus to target DLG1 protein via the PBM is a mechanism of control to counter virally induced overexpression of the protein, or perhaps upregulation of DLG1 containing I6 is a consequence of viral interactions with cellular splicing and transcription machinery. Investigation into the functional consequences of the variant should help to answer this.

As both the HOOK domain and  $\alpha$  isoform were upregulated in HPV genome containing keratinocytes and were both downregulated upon integration of HPV18 genomes, it can be inferred that I6 is included in  $\alpha$  N-terminus containing isoforms. Amplification using forward primers corresponding to DLG1 $\alpha$  in combination with the reverse primer within the identified I6 insertion amplified a number of bands within the predicted size range of the mRNA (~1500 bp). Although sequencing of amplified fragments confirmed the

presence of the DLG1 $\alpha$  5' sequence, further analysis is required to eliminate the possibility of an I6-containing DLG1 $\beta$  isoform. Cloning the entire cDNA would not only confirm this, but also allow endogenous expression of the variant and thus in depth analysis of the functional consequences of I6 inclusion.

#### 4.5.2 Consequences of I6 inclusion on DLG1 function

Translation of I6-containing transcripts is predicted to produce a truncated form of DLG1 protein (Figure 4.18). There is a precedence for alternative splicing as a mechanism of generating PDZ protein diversity; notably alternative splicing of the related PDZ protein CASK results in the inclusion of a 40 residue loop within the GK domain and ERBIN is predicted to encode a variant with a truncated PDZ domain, which has yet to be characterised (Favre *et al.*, 2001). Given the specificity of DLG1 isoform interactions in T-cells, where I1A-containing but not I1B-containing proteins are able to facilitate release of granules (Crocetti *et al.*, 2014), and the tissue-specific nature of DLG1 expression, where I3 is predominantly in mammalian cardiac tissue whereas the I2-containing form appears to be restricted to neurons and liver (Mori *et al.*, 1998; McLaughlin *et al.*, 2002; Godreau *et al.*, 2003), it is probable that I6 expression is tissue and cell dependent (Godreau *et al.*, 2003; Lue *et al.*, 1994).

The predicted truncated protein would lack the GK domain. Without the GK domain, DLG1 can no longer form associations with the cytoskeleton (Wu *et al.*, 2000; Manneville *et al.*, 2010). Furthermore, absence of the GK domain would remove the ability of DLG to bind to phosphorylated proteins LGN and LGL, thus affecting Scribble complex regulation. The GK domain is involved in localising DLG1 to the midbody of the cell during asymmetrical cell division. It has been observed that truncation of the *Drosophila* Dlg C-terminus negatively affects the ability of neuronal cells to divide asymmetrically but did

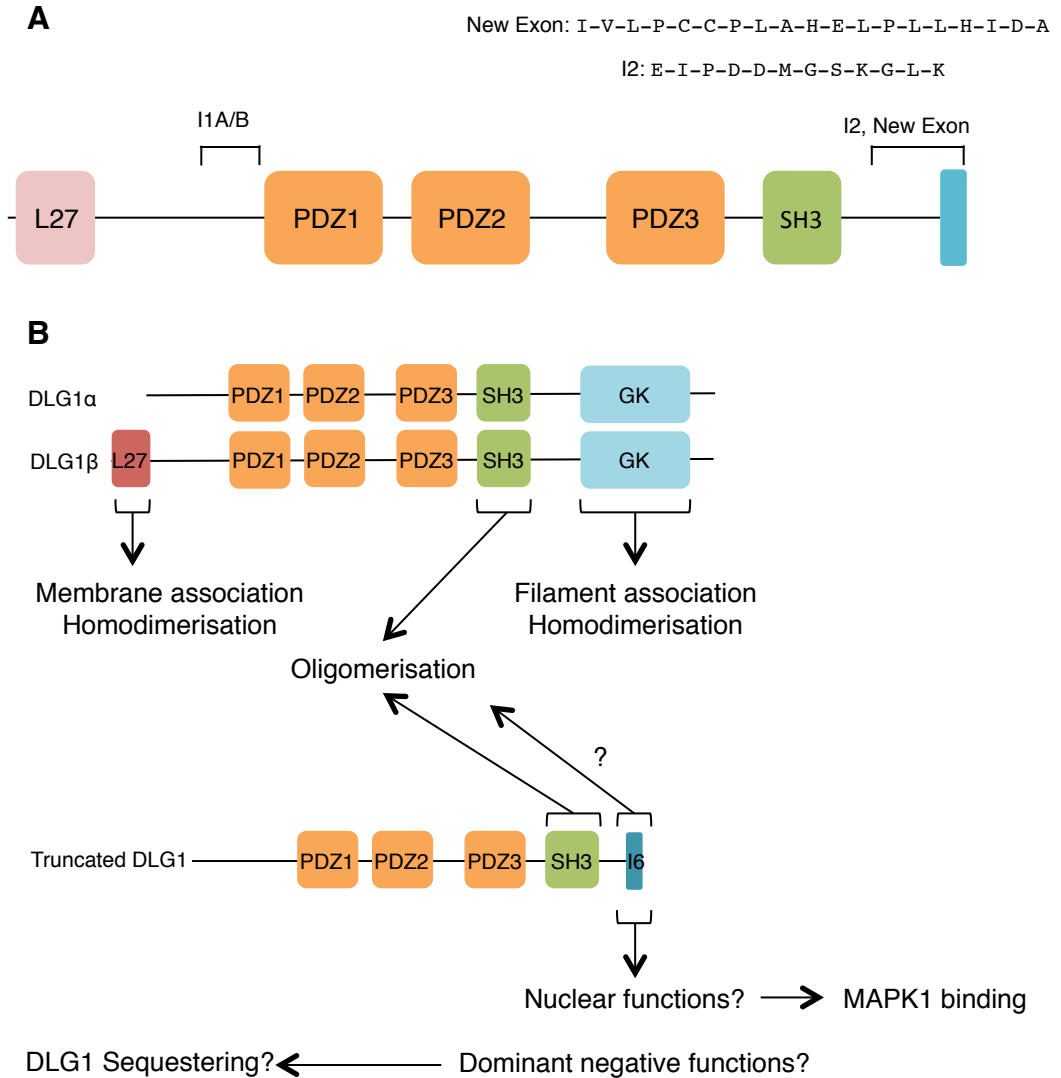


**Figure 4.18: Predicted protein structure of I6-containing DLG1**

(A) Translation of the new exon would produce a C terminal truncation, removing the DLG1 GK domain. We also suggest that this isoform lacks the N-terminal L27 domain.

(B) The absence of the GK domain may remove the ability of DLG1 to associate with cytoskeletal filaments, although homodimerisation is still possible with an intact SH3 domain. The presence of the PDZ and SH3 domains, as well as I2, may still influence DLG1 localisation and cellular interactions. Question marks imply suggested consequences of I6 inclusion.

not affect epithelial polarity (Bellaïche *et al.*, 2001); mouse models expressing a truncated form of DLG1 lacking the SH3, GK and HOOK region display growth retardation, severe craniofacial abnormalities and perinatal death (Caruana and Bernstein, 2001; Klocker *et al.*, 2002). Although no effect was observed by Caruana and Bernstein (2001) on synaptic clustering of the protein, the domain obviously facilitates important interactions during mammalian development. Interestingly studies in mice showed that, in the absence of the GK domain, DLG1 was restricted to adherens junctions (Naim *et al.*, 2005). This may be due to the presence of the I3 insertion, which has been shown to direct membrane localisation of the protein (Naim *et al.*, 2005; Roberts *et al.*, 2007; McLaughlin *et al.*, 2002). Altogether, *in vivo* studies indicate that the GK truncated form of DLG1 does not perform functions in cell division or development, eliminating a role for I6-containing variants in these functions.

As the I2 insertion has been identified as predominantly nuclear, and the GK nuclear export signal is predicted to be absent in this truncated variant, there is an expectation that the I6-containing protein resides in the nucleus (Roberts *et al.*, 2007; Kohu *et al.*, 2002). However, the precise role of nuclear DLG1 has not yet been elucidated; it is known to be important in the growth of undifferentiated epithelial cells (Roberts *et al.*, 2007). Notably, I2 has been implicated in chromatin-association (Kohu *et al.*, 2002; McLaughlin *et al.*, 2002); as the I6 isoform was identified downstream of I2, the insertion may contribute to DLG1 interactions with cellular chromatin. The nuclear protein NET1 has been shown to interact with DLG1 to promote translocation of the complex to the nucleus and, based on its function at the plasma membrane, the PDZ protein may act as a scaffold protein, organising protein complexes and nuclear filaments (Garcia-Mata *et al.*, 2007; Sabio *et al.*, 2010). The related MAGUK proteins CASK and ZO-1, which are involved in organisation of protein complexes at cell-cell junctions and synapses, are able to translocate to the

nucleus and contribute to the transcriptional regulation of specific genes; the truncated form of DLG1 may function similarly. Moreover, DLG1 has been shown to interact with the nuclear RNA-binding protein PSF (protein-associated splicing factor, Sabio *et al.*, 2010). *Via* the PSF interaction, DLG1 binds to various RNAs (Sabio *et al.*, 2010). Although the domain of DLG1 responsible has not been identified, this is another indication that nuclear DLG1 is involved in the regulation of gene transcription. This, with the observation that the GK domain forms interactions with a number of cytoskeletal filaments, could suggest that a nuclear form of GK-truncated DLG1 performs nuclear-specific functions.

Alternatively, the truncated form of DLG1 may act in a regulatory fashion and modify full-length protein function in a dominant negative manner. A number of PDZ proteins have been shown to act in this fashion. For example dynamin-2 sequesters GOPC at the cell periphery to block clathrin-mediated endocytosis (Cheng *et al.*, 2004) and overexpression of the PDZ containing chromatin organiser SATB1 exerts a dominant negative effect upon itself, completely removing the transcriptional repressor functions (Notani *et al.*, 2011). Indeed, overexpression of a dominant-negative isoform of CASK results in the mislocalisation of endogenous DLG1 (Lee *et al.*, 2002). The I1A and I1B insertions, as well as the DLG1 SH3 domain have all been shown to facilitate DLG1 homodimerisation (McLaughlin *et al.*, 2002; Hanada *et al.*, 1997) and these are likely present in the I6-containing form. Interestingly, in *Drosophila*, the expression of a DlgA isoform lacking the GK domain bound endogenous Dlg1 to enable trafficking of the truncated protein, acting as a 'hitchhiker' (Mendoza *et al.*, 2003; Mendoza-Topaz *et al.*, 2008; Asaba *et al.*, 2003). Such a mechanism may also be employed by truncated I6-containing forms of DLG1. Moreover, functional screening of the I6 protein sequence hypothesised an SH3 binding site, which has the potential to interact with the full-length DLG1 SH3 domain. Altogether, it is possible that the full-length and truncated forms of DLG1 are able to bind each other,

forcing other cellular proteins compete for binding to full-length protein and thus control DLG1 interactions.

Screening indicated that inclusion of I6 introduces a MAPK1 binding site to DLG1. Upon activation, MAPK1 phosphorylates nuclear proteins to activate or repress transcription of genes involved in proliferation, differentiation and apoptosis. The interaction with I6-containing DLG1 may facilitate interactions with, and thus phosphorylation of, specific transcription factors, and thus direct transcription of viral life cycle promoting genes. Interaction with MAPK1 may also facilitate phosphorylation of DLG; the PDZ protein is a known target of the MAPK cascade proteins ERK5, p38 $\gamma$  and cell cycle regulators CDK1 and CDK2 and the interaction with I6 may regulate the location and stability of the isoform in a similar fashion (Sabio *et al.*, 2005; Narayan *et al.*, 2008; Iñesta-Vaquera *et al.*, 2010).

Likewise, screening has suggested an SH3 binding site within the insertion, which may allow binding of the kinases Src or PI3K to enable DLG1 phosphorylation or interaction with the membrane located proteins phospholipase C, cortactin or SORBS1 to facilitate the formation of protein complexes at the cell periphery.

It is interesting to speculate whether the inclusion of I6 affects DLG1 mRNA stability. Cavatorta *et al.* (2011) have identified two alternative 5'UTRs of DLG1 which are likely to affect the stability of transcribed mRNA and efficiency of translation. Elements within mRNA have been shown to effect the stability of  $\beta$ -catenin transcripts and isoforms of ZO-1 exhibit different mRNA stabilities (Reichert *et al.*, 2000; Bachurski *et al.*, 1994). Alternatively, I6 transcripts may act at an mRNA level to regulate other DLG1 transcripts. For example, genes encode long non-coding RNAs (lncRNA) or microRNAs (miRNA), which partially anneal with their target protein coding mRNAs, which can trigger degradation and regulate expression (Hannon *et al.*, 2006; Ponting *et al.*, 2009; Wilusz *et al.*,

2009; Wu and Brewer, 2012). In this manner, the I6-containing transcripts may act as a dominant-negative regulatory element. Although we hypothesize that this novel DLG1 spliced variant is expressed as protein, the precise function will be characterized in more detail in future studies (see Section 4.4.4).

#### 4.5.3 Differential expression of DLG1 isoforms

DLG1 isoforms are differentially expressed in human tissues and deregulated in cancers (Godreau *et al.*, 2003; Fuja *et al.*, 2004). Thus, the expression of DLG1  $\alpha$  and  $\beta$  isoforms was investigated in various stages of HPV-associated malignant disease. Previous studies from the Roberts lab have shown that DLG1 protein is overexpressed and mislocalised at early stages and then disappears in late stages of cervical cancer (Watson *et al.*, 2002). In this study, DLG1 $\alpha$ , but not  $\beta$ , transcripts were increased by the presence of high-risk HPV genomes in primary keratinocytes and upon integration of HPV genome, the abundance of  $\beta$  transcripts decreased. However, in the cervical epithelial cells analysed, only the  $\alpha$  form was upregulated in Caski cells, other cell lines indicated no change in expression of either of the DLG1 isoforms investigated. Cells containing HPV16 (Caski and SiHa) or HPV18 (HeLa) and HPV negative (C33A) cells were included in the analysis, which indicates that the effect upon *DLG1* expression is not HPV specific. Both Caski and SiHa are HPV16 positive, but differ in the number of integrated genomes; more than 600 have been detected in Caski and one in SiHa (Raybould *et al.*, 2014). The difference in DLG1 expression between the two HPV16-driven cancer cells may be attributed to the vast difference in copy number, but it is more likely that there are other mutational changes that have occurred in the different malignancies from which the cells are derived. It has been noted that *DLG1* expression in C33A cells is low and, as the PDZ protein is deregulated at either the gene or protein level in a number of cancers, it is likely that the cancers from

which these cell lines were generated had developed mechanisms other than via HPV to disrupt DLG1 expression (Fuja *et al.*, 2004; Watson *et al.*, 2002; Cavatorta *et al.*, 2004; Frese *et al.*, 2006).

Although the presence of HPV in HNSCC cells lines correlated with effects upon the expression of DLG1 isoforms, it varied amongst the cell lines as to whether the levels decreased or increased. Both SCC154 and Vu147 are HPV16 positive; the former indicated a decrease in all DLG isoforms whereas there was a trend towards an increase in  $\alpha$ -DLG1 transcripts in Vu147 cells. The disparity between cell lines may be due to a difference in cell background; SCC154 and SCC040 are derived from tongue, whereas Vu40 and Vu147 are both from floor of mouth cancers (Steenbergen *et al.*, 1995; Rampias *et al.*, 2009). This implies that *DLG1* expression is context specific, but needs to be confirmed experimentally by further repeats, and could be extended by analysis of further HNSCC derived lines.

This expression analysis included differentiated cells and healthy tissue, where DLG1 $\beta$  was more abundant than the  $\alpha$  form. As keratinocytes were stratified in culture, the abundance of both DLG1 isoforms increased, which correlates with the established knowledge that DLG1 is upregulated during differentiation of epithelium (Rivera *et al.*, 2009). The combinations of insertions included in DLG1 are known to depend upon the tissue in which they are expressed (Godreau *et al.*, 2003; McLaughlin *et al.*, 2002; Roberts *et al.*, 2007). The presence of an L27 domain is important in targeting the  $\beta$  isoform to the membrane, *via* DLG2, and specifically to the baso-lateral membrane of epithelia *via* CASK (Lozovatsky *et al.*, 2009; Hanada *et al.*, 2003). The DLG1-mediated formation and maintenance of cell-cell contacts is a crucial function of the PDZ protein in cells and the abundance of the DLG1 $\beta$  isoform may therefore be unsurprising.

The specific functions of the  $\alpha$  isoform have not been extensively studied, although it is known that the  $\alpha$  and  $\beta$  forms differentially traffic AMPA receptors at the synapse (Waites *et al.*, 2009). The specific upregulation of the  $\alpha$ -isoform during episomal HPV genome replication may reflect the viral requirement for increased nuclear functions of the protein. In the nucleus, DLG1 has been implicated in chromatin reorganization, in the regulation of transcription, splicing and as a scaffolding protein (Kohu *et al.*, 2002; Lue *et al.*, 1994; Huang *et al.*, 2000). Upregulation of DLG1 $\alpha$  in epithelia may therefore promote the transcription of growth-promoting genes and/or promote viral genome replication in order to create an environment beneficial to viral propagation. In addition, DLG1, specifically I2-containing isoforms, is known to be important in the growth of undifferentiated epithelial cells (Roberts *et al.*, 2007) and thus HPV upregulation of DLG1 $\alpha$  may be a viral mechanism to promote the growth of keratinocytes.

#### 4.5.4 Future directions

Although protein analysis using a range of DLG1 antibodies revealed a number of lower molecular species, none were obviously suggestive of a truncated isoform. However, this is limited by the absence of an untransfected keratinocyte control, which would enable a comparison of expression levels and thus the identification of the expected truncated protein expressed to a lesser degree. Design and use of an  $\alpha$ -specific antibody did not identify a smaller form that would be expected if the upregulated I6 form were detected. Thus, further work aims to dissect the downstream consequences of I6 inclusion in DLG1 mRNA and/or protein. In the short term, as the I2 sequenced has been identified upstream of I6, antibodies specific to I2 could be applied to protein extracted from primary cells and from cancer cell lines.

Further characterisation of I6 expression will be carried out; production of an I6-specific antibody has not yet been successful, but expression of the sequence can be achieved by cloning techniques. In this way, an investigation into the consequences of endogenous expression of this novel variant in cells could clarify the effect upon full-length DLG1 subcellular localisation, identify interacting proteins and infer function, as well as assess the phenotype of cells where this protein is overexpressed. Furthermore, it would be of interest to identify the presence of I6-containing isoforms in a larger range of tissue than was investigated here, including primary cancer tissue.

Having generated an antibody specific to the  $\alpha$  isoform of DLG1, future work could investigate whether the ratio of  $\alpha$  and  $\beta$  isoforms mRNA corresponds to protein levels and could more specifically identify the localisation of the isoforms in epithelia. Moreover, immunoprecipitation experiments with this antibody will enable the identification of cellular interactors and refine our knowledge of the functions of DLG1 isoforms.

There is also further characterisation of spliced variants of DLG1 to be carried out. An I3 and I6 containing isoform was identified but not studied in this thesis. Work by McLaughlin *et al.* suggests that transcripts containing both I3 and I2 produced a protein truncated after the I3 region *in vitro*, but the presence and consequence of combinations of insertions can be additional investigated. The spliced insertions present in DLG1 HOOK region are likely to exist in a range of combinations (there are more than 500 mathematical possibilities), the investigation of which across different tissues and cells would greatly expand current knowledge of DLG1 isoform expression.

## CHAPTER 5: REGULATION OF THE HUMAN PAPILLOMAVIRUS E6 PDZ BINDING MOTIF DURING THE VIRUS LIFE CYCLE

### 5.1 Introduction

#### 5.1.1 Cellular PDZ interactions

*In vivo* many cellular PDZ-PBM interactions occur, acting to orientate cells, receptors and organise signalling scaffolds (Fan and Zhang, 2002). The PDZ domain is composed of six  $\beta$ -sheets and two  $\alpha$ -helices; a groove between the second  $\beta$ -strand and the second  $\alpha$ -helix forms the hydrophobic pocket where the PBM peptide binds, serving as an extra  $\beta$ -strand (Doyle *et al.*, 1996; Songyang *et al.*, 1997; Niethammer *et al.*, 1998). Further interactions between main chain residues stabilise and add specificity to the binding, for example a loop at the end of the binding groove is involved in positioning the PBM peptide and the terminal COOH of the PBM is coordinated by a network of hydrogen bonds to main-chain amide groups (Doyle *et al.*, 1996). When bound within the PDZ groove, the side chain of the terminal and -3 residues of the PBM peptide point towards the base of the peptide-binding groove (Songyang *et al.*, 1997; Doyle *et al.*, 1996). In some cases, recognition of the PBM involves residues outside of the four amino acid consensus motif, enabling specificity of interactions unique to individual PDZ domains (Figure 1.11, Niethammer *et al.*, 1998).

The specificity of PDZ:PBM must be regulated in order to coordinate interactions spatially and temporally. As such, many PDZ:PBM interactions are regulated by phosphorylation of the PDZ-binding peptide (Table 5.1 and Table 5.2). Due to the charge and size of a phospho group, its introduction can prevent the PBM sterically from binding within the PDZ pocket (Akiva *et al.*, 2012, Figure 1.11). For example, phosphorylation of the PBM

serine residue of the glutamate receptor subunit GluR2 (SVKI) prevents its interaction with PICK (protein that interacts with C kinase 1) and reduces affinity for GRIP (glutamate receptor interacting protein, Shao *et al.*, 2010; Matsuda *et al.*, 1999). Interaction with PICK1 and GRIP modulates the location of the receptor and influences AMPAR clustering at the cell membrane, which in turn controls the transmission of synaptic impulses (Matsuda *et al.*, 1999). Thus, phosphorylation of the GluR2 C-terminus may regulate postsynaptic clustering in neurons and downstream transmission of impulses (Matsuda *et al.*, 1999; Shao *et al.*, 2010).

**Table 5.1: Examples of PBM phosphorylation**

<b>PDZ containing protein</b>	<b>Binding partner</b>	<b>PBM</b>	<b>Kinase</b>	<b>Reference</b>
DLG4 and TIP-1	Kir 2.3	RREESRI	PKA	Tanemoto <i>et al.</i> , 2002
DLG4	Stargazin	RR <b>T</b> <u>TPV</u>	PKA/MA PK	Choi <i>et al.</i> , 2002
DLG4 and DLG3	NR2B subunit of NMDAR	SSI <b>E</b> <u>SDV</u>	CK2	Chung <i>et al.</i> , 2004
GRIP1	GluR2 subunit of AMPAR	GIES <b>V</b> KI	PKC	Matsuda <i>et al.</i> , 1999
DLG4 and DLG1	NR2B subunit of NMDAR	SS <b>L</b> E <u>SEV</u>	PKA/PK C	Chung <i>et al.</i> , 2004
DLG4	LRP4	SS <b>E</b> S <u>QV</u>	CaMKII	Tian <i>et al.</i> , 2006
GRID2IP	GluR2 subunit of AMPAR	DPDR <b>G</b> <u>TSI</u>	PKA	Sonoda <i>et al.</i> , 2006
DLG1	HTLV-1 Tax-1	SPGGLEPP <b>S</b> E <b>K</b> H <b>F</b> <u>R</u> <b>E</b> <b>T</b> <b>E</b> <b>V</b>	CK2	Bidoia <i>et al.</i> , 2010

Phosphorylated residue highlighted in bold, PBM underlined.

Conversely, phosphorylation of a residue adjacent to the PBM of the mutated in colorectal cancer (MCC) protein increases the affinity of MCC for the polarity protein SCRIB, indicating that phosphorylation can also promote interactions (Pangon *et al.*, 2012). The binding affinity is thought to increase due to the availability of additional interactions between MCC and the SCRIB PDZ domain upon PBM phosphorylation (Pangon *et al.*, 2012). It has been suggested that the interaction between SCRIB and MCC regulates the

formation of lamellipodia in migrating cells, and that this is regulated by MCC phosphorylation (Pangon *et al.*, 2012).

In the case of the membrane protein apactin, phosphorylation of the PBM decreases affinity for the second PDZ domain of NHERF1 but increases binding affinity for the first PDZ domain and for fellow PDZ protein PDZK1 (Tandon *et al.*, 2007). PBM phosphorylation also increases apactin association with the cytoskeleton, implying that the switch in interaction promotes the function of apactin in maintaining actin filament bundles at the apical surface (Tandon and De Lisle, 2004). Moreover, it has been suggested that, as apactin and NHERF1 function together in exocytosis, switching the PDZ binding preference allows NHERF1 to act as a scaffold and bring together an alternative combination of proteins *via* their PBMs (Tandon *et al.*, 2007; Tandon and De Lisle, 2004).

Interestingly, regulatory phosphorylation outside of the PBM can affect PDZ binding, leading to a change in protein structure that affects the availability of the PBM for cognate binding. For example, regions of the pleckstrin homology (PH) domain of Kalirin-7 are heavily phosphorylated in neuronal cells and this is predicted to affect the interaction with a number of PDZ substrates, including DLG4, at the synapse (Kiraly *et al.*, 2011). Furthermore, different patterns of phosphorylation depend upon cellular context; Kalirin-7 sites at the N terminus were phosphorylated in mouse brain by PKA, PKC and CaMKII but phosphorylation was not identified in non-neuronal cells (Kiraly *et al.*, 2011). Thus, phosphorylation of PDZ-binding proteins both within and outside of the PBM can have varying effects upon PBM:PDZ interactions, and is likely to depend upon the cellular context and the proteins in question (Table 5.2).

### 5.1.2 Viral PBM regulation

Post-translational modifications of HTLV-1 Tax have been suggested to regulate the activity of the viral PBM (Bidoia *et al.*, 2010; Lodewick *et al.*, 2013). HTLV-1 Tax is

phosphorylated within the PBM at threonine 351 by CK2 and is acetylated proximal to the PBM at lysine 346 by p300 (Bidoia *et al.*, 2010; Lodewick *et al.*, 2009). Phosphorylation of the Tax PBM interrupts the proteins ability to interact with DLG1 and disrupts viral activation of the NFκB pathway, whilst acetylation promotes activation of the NFκB pathway (Suzuki *et al.*, 1999; Bidoia *et al.*, 2010). The NFκB family of transcription factors regulate the expression of a number of cellular genes associated with cell growth, apoptosis, embryonic development, immune responses, stress responses and oncogenesis (Pahl, 1999). HTLV-1 mediated activation of these genes is likely to promote viral replication, indeed the PBM is crucial to Tax-induced T-cell proliferation (Xie *et al.*, 2006). Phosphorylation of the Tax PBM may be a mechanism to impair PBM binding when NFκB activation is not required (Bidoia *et al.*, 2010). Furthermore, as Tax binding to MAGI-1 alters the localization of both proteins, interruption of this by phosphorylation may act to regulate Tax location and thus control the interactions that the viral protein is able to make spatially during stages of viral replication (Ohashi *et al.*, 2004). However, the functional consequences of Tax PBM phosphorylation during HTLV-1 replication have yet to be fully characterized.

Crystal structures have revealed that, as well as the four residue class I PBM, residues upstream are also involved in recognition by DLG1 and MAGI-1 PDZ domain recognition (Zhang *et al.*, 2007; Charbonnier *et al.*, 2011; Mischo *et al.*, 2013). Moreover, a peptide-binding loop of the PDZ domain specifically interacts with an arginine residue at the -5 position the HPV18 E6 peptide which, when mutated, was demonstrated to be crucial in HPV-mediated degradation of DLG1 and MAGI-1 (Zhang *et al.*, 2007). The presence of the binding loop and the interaction with six of the E6 PBM residues may explain the specificity of high-risk HPV E6 proteins in their ability to target cellular PDZ domain containing proteins (Zhang *et al.*, 2007; Charbonnier *et al.*, 2011).

As phosphorylation is an established mechanism by which binding to PBMs is controlled, cellular kinases may also regulate the E6 PDZ binding function during the HPV life cycle. As with cellular proteins, phosphorylation within the PBM of E6 has been predicted to affect binding activity. Recognition sites of the serine/threonine kinases protein kinase A (PKA) and AKT have been identified proximal to the PBM (Figure 5.1). Structural analysis of the E6 PBM bound to PDZ proteins DLG1 and MAGI-1 indicates that a phosphate group would not fit in the interacting groove and would therefore disrupt E6-PBM binding to cellular PDZ proteins (Zhang *et al.*, 2007; Charbonnier *et al.*, 2011).

*In vitro* kinase assays have shown that the HPV18 E6 PBM is phosphorylated by PKA and studies have identified phosphorylated E6 in human epithelial cells (Kühne *et al.*, 2000). Furthermore, stimulation of PKA activity inhibits the degradation of DLG1 induced by HPV18 E6, indicating that phosphorylation inhibits E6-PDZ interactions (Kühne *et al.*, 2000). Moreover, mutating the PKA recognition site proximal to the PBM, by substituting an arginine residue for a leucine residue at position 153, removes the sensitivity of HPV-mediated DLG1 degradation to PKA activity, indicating that regulation of PBM activity is removed once the PKA recognition site is mutated (Kühne *et al.*, 2000). It is suggested that this substitution enables E6 to degrade DLG1, and other PDZ targets constitutively, regardless of PKA activity (Kühne *et al.*, 2000). Thus phosphorylation of the E6 PBM is able affect E6 PDZ interactions.

Different HPV E6 proteins exhibit different susceptibilities to PKA phosphorylation; HPV18 E6 shows a higher susceptibility to PKA phosphorylation than HPV16, and HPV31 was shown to be a weak PKA substrate (Kühne *et al.*, 2000; Boon *et al.*, 2014). The kinase AKT (also known as protein kinase B) is another candidate for recognizing and phosphorylating high-risk HPV E6 PBMs (Figure 5.1). Conservation of a kinase recognition site in high-risk HPV types suggests that phosphorylation of the PBM is

### Group 1

HPV 16 CMSCC RSSR**T**R**R**E**T**Q**L**  
HPV 18 CHSCCN**R**A**R**Q**E** R**L**Q**R**R**R**E**T**Q**V**  
HPV 31 CIVCW R**R**P**R**T**E**T**Q**V  
HPV 33 CAACW RS R**R**R**E**T**A**L  
HPV 35 CMSCW K**P**T**R**R**E**T**E**V  
HPV 39 CRRCW**T**T**K**R**E**D R**R**L**T**R**R**E**T**Q**V**  
HPV 45 CNTCCDQ**A**R**Q**E R**L**R**R**R**R**E**T**Q**V**  
HPV 51 CANCW Q R**T**R**O**R**N**A**T**Q**V**  
HPV 52 CSECW R**P**R**P**V**T**Q**V**  
HPV 56 CLGCW R**Q** T**S**R**E**P**R**E**S**T**V**  
HPV 58 CAVCW R**P**R**R**O**T**Q**V**  
HPV 59 CRGCR**T**R**A**R**H**L**R**Q**O**R**A**R**S**E**T**V

### Group 2A

HPV 68 CRHCW**T**S**K**R**E**D R**R**R**T**R**O**E**T**Q**V**

### Group 2B

HPV 26 CTNCW R**P**R**R**O**T**E**T**Q**V**  
HPV 30 CLQCW R**H**T**T**S**T**E**T**A**V**  
HPV 34 CRQCW R**P**S**A**T**V**V  
HPV 53 CLTCW R**H**T**T**A**T**E**S**A**V**  
HPV 66 CLQCW R**H**T**S**R**O**A**T**E**S**T**V**  
HPV 67 CSVCW R**P**O**R**T**O**T**Q**V  
HPV 69 CTNCW R**P**R**R**E**A**T**E**T**Q**V  
HPV 70 CRHCW**T**S**N**R**E**D R**R**R**I**R**R**E**T**Q**V**  
HPV 73 CTRCW R**P**S**A**T**V**V  
HPV 82 CANCR**T**A**A** R**O**R**S**E**T**Q**V**  
HPV 85 CRRCM**T**R**A** Q**E** Q**O**G**S**R**R**E**T**Q**V**  
HPV 97 CNSC**Y**N**Q**S**R**Q**E** R**L**S**R**R**R**E**T**Q**V**

### Group 3

HPV 6 CLHCW**T**T**C**M**E**D MLP  
HPV 11 CLHCW**T**T**C**M**E**D LLP

Key:

PDZ binding motif (PBM)

Bold and arrow indicates residue targeted

PKA recognition sequence (R-R-S/T-Y)

Akt recognition motif (R-X-R-X-X-S/T)

Consensus PBM:  $RX^S_TX^L_V$

**Figure 5.1: Alignment of E6 C-terminal sequences**

Alignment of the C terminus of the E6 protein from HPV types belonging to IARC Groups 1, 2A, 2B and 3. PBM shaded in grey, PKA recognition site boxed and AKT recognition site underlined, target residue for phosphorylation indicated in bold.

The consensus PBM sequence is shown. Number above PBM indicates residue nomenclature, numbered in reverse from the C-terminal amino acid.

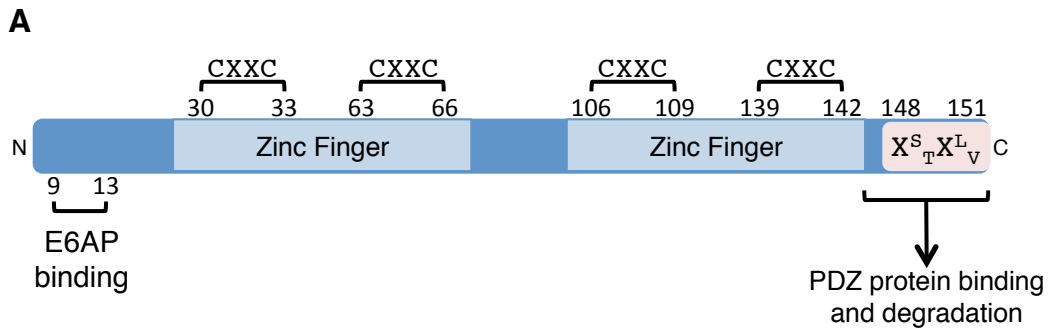
important during the viral life cycle, and that it may be an important feature in viral oncogenesis.

**Table 5.2: Consequences of cellular PBM Phosphorylation**

<b>PBM-containing protein</b>	<b>Protein function</b>	<b>Consequences of phosphorylation</b>	<b>Kinase</b>	<b>Reference</b>
MCC protein	Cell cycle regulator	Increase binding affinity with SCRIB	PAK1	Pangon <i>et al.</i> , 2012
GluR2	Glutamate receptor subunit	Disrupted interaction with PICK1 Disrupted binding to glutamate receptor interacting protein	CK2	Shao <i>et al.</i> , 2010; Matsuda <i>et al.</i> , 1999
Kir2.3	Potassium ion channel	Interruption of colocalisation with DLG4 at postsynaptic membrane TIP-1 interaction through its PDZ domain is abolished	PKA	Yan <i>et al.</i> , 2009a; Cohen <i>et al.</i> , 1996
MMAC1/P TEN	Membrane tethered phosphatase	Promotes binding with DLG1 and hMAST205	Unknown	Adey <i>et al.</i> , 2000
Ephrin B	Receptor tyrosine kinase	Syntenin binding hindered PTPN13 binding unchanged RGS3 binding unchanged Par6 interaction disrupted	PKA	Lu <i>et al.</i> , 2001; Lee <i>et al.</i> , 2008
Jagged-1	Membrane bound ligand	Binding to AF-6 disrupted	Unknown	Popovic <i>et al.</i> , 2012; Chetkovich <i>et al.</i> , 2002; Stein and Chetkovich, 2010
Stargazin	Calcium ion channel	Binding to DLG4 inhibited	PKA	Chetkovich:2002 wg, Stein:2010gb}
NR2B	Subunit of NMDA receptor	Affects binding to DLG4 and DLG2	CaMKII	Chung <i>et al.</i> , 2004
Apactin	Membrane glycoprotein	Decreased affinity for NHERF1 PDZ2. Increased affinity for PDZK1 and NHERF1 PDZ1	Unknown	Tandon <i>et al.</i> , 2007
Kalirin-7	RhoGEF kinase	Decreased affinity for DLG4 suggested	Fyn, PKA, PKC, CK2, CaMKII	Kiraly <i>et al.</i> , 2011
$\beta$ 2-adrenergic receptor	GPCR	NHERF1 interaction disrupted, leading to mis-sorting of receptor	GRK5	Cao <i>et al.</i> , 1999
LRP4	Wnt signalling regulator	Suppressed its interaction with DLG1 and DLG4	CaMKII	Tian <i>et al.</i> , 2006
Syndecan-1	GPCR coreceptor	Interaction with syntenin-1 promoted by dephosphorylation Impair binding to DLG1	Unknown	Sulka <i>et al.</i> , 2009
HTLV-1 Tax	Viral oncoprotein	Affects NF $\kappa$ B pathway interaction	CK2	Bidoia <i>et al.</i> , 2010

As well as interrupting PDZ interactions, phosphorylation of the E6 PBM enables alternative protein interactions (Figure 5.2). Phosphorylation of exogenously expressed HPV18 E6 by PKA promotes an interaction with the adapter protein 14-3-3 $\zeta$  (Boon and Banks, 2012a; Boon *et al.*, 2014). This suggests that phosphorylation of the PBM can act as a switch, changing the binding profile of the PBM. The same study demonstrated that binding of 14-3-3 $\zeta$  increased the stability of the viral oncoprotein (Boon and Banks, 2012b).

Thus, the PBMs of high-risk  $\alpha$ -HPV E6 proteins are highly likely to be phosphorylated during the viral life cycle. However, the affect of PBM phosphorylation upon E6 interactions during the viral life cycle is largely unknown.



**B**

HPV18 E6 C terminus:

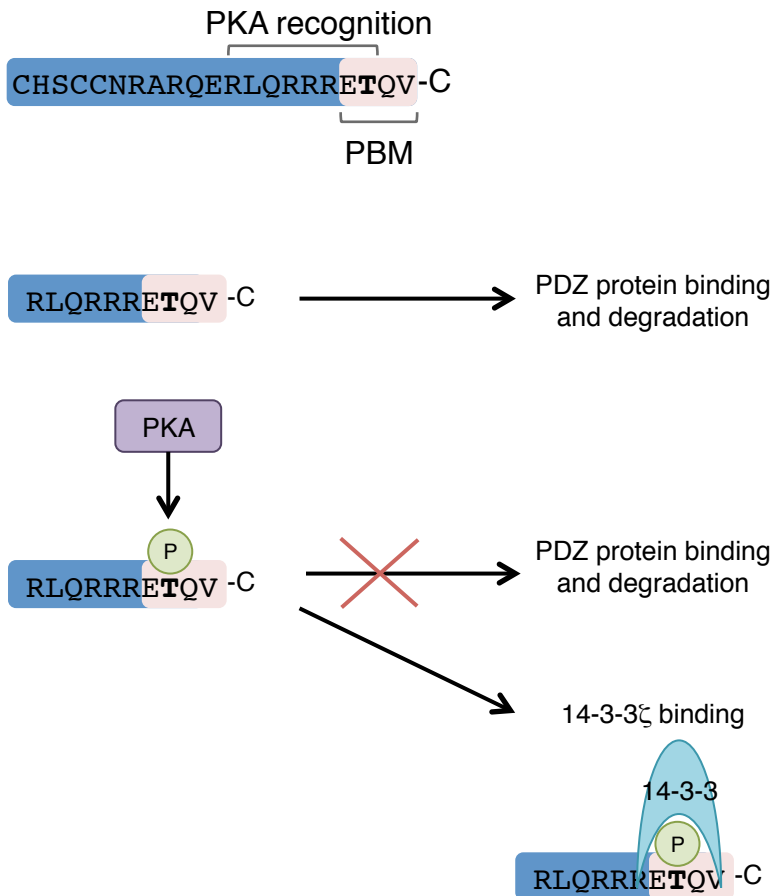


**Figure 5.2: The HPV18 E6 PDZ binding motif**

(A) The amino acid sequence of the HPV18 E6

(B) The HPV18 E6 PBM sequence and current binding models: A number of E6 oncoproteins have been shown to bind cellular PDZ proteins via a C-terminal PBM, leading to their proteasome mediated degradation. The PBM overlaps with a PKA recognition site, phosphorylation of which sterically hinders PDZ protein binding. Boon *et al.* have shown that the phosphorylated PBM can bind to 14-3-3ζ.

### 5.3 Hypothesis and objectives

Studies to date have shown that the PBM of HPV18 E6 is phosphorylated by PKA, and that this alters the interactions that E6 is able to form with cellular factors. The experiments described in this chapter aimed to study phosphorylation of the PBM within a model of the HPV18 life cycle: Specific objectives were to:

- i. Identify kinase recognition sites overlapping the PBMs of high-risk  $\alpha$ -HPV E6 oncoproteins
- ii. Determine whether the HPV18 E6-PBM is phosphorylated by PKA in the HPV18 life cycle model
- iii. Determine whether phosphorylation affects HPV18 E6 protein levels in viral genome containing cells
- iv. Determine whether E6 PBM phosphorylation affects PBM-PDZ interactions during the HPV life cycle.

## 5.4 Results

### 5.4.1 Computational screening predicts phosphorylation of $\alpha$ -HPV E6 PBMs

To date, twelve HPV types have been defined by the International Agency for Research on Cancer (IARC), a department of the WHO, as 'high-risk' with respect to causing cancer (group 1), and a further ten types are recognised as 'probably and 'possibly' cancer-causing (group 2A and 2B, Table 1.3, Bouvard *et al.*, 2009). To initially assess the susceptibility of high-risk HPV E6 proteins to phosphorylation, a Scansite motif screen was performed on the amino acid sequences of HPV E6 proteins from the IARC groups 1, 2A and 2B (Figure 5.3). The screen assessed the likelihood of peptide phosphorylation to produce a probability score within the range of 0 to 1. All of the group 1 HPV types are predicted in this screen to be targeted by a kinase within, or proximal to the PBM, with a probability score of 0.49 or more (Figure 5.3). Furthermore, the cellular kinases predicted to perform this phosphorylation included the AGC kinase family members PKA, AKT, protein kinase C (PKC) and AMPK (AMP-activated protein kinase) (Figure 5.3). Both PKA and AKT were predicted to phosphorylate the HPV16 PBM with scores of 0.49 and 0.52, whereas the PBM of HPV18 E6 was a predicted target of PKA alone, with a score of 0.46 (Figure 5.3). Phosphorylation of HPV16 by AKT produced a higher probability score than for PKA (0.53 *cf.* 0.49). During this study, it was confirmed *in vitro* that AKT is able to phosphorylate purified HPV16 E6 at the PBM and that PKA is able to target the PBM of both HPV16 and HPV18 E6 proteins (Boon *et al.*, 2014; Boon and Banks, 2012b). Boon *et al.* confirmed that  $\alpha$ -HPV E6 proteins are susceptible to phosphorylation at the PBM and further investigations in this study focussed on this in the context of whole genome replication in primary cells. In contrast to the group 1 viruses, not all members of group 2

Virus	Kinase	Scansite Score
HPV 16	Protein Kinase A	0.4969
	Akt Kinase	0.5272
HPV 18	Protein Kinase A	0.4626
HPV 31	Akt Kinase	0.5565
HPV 33	Protein Kinase A	0.4939
HPV 35	Protein Kinase A	0.5472
HPV 39	Protein Kinase A	0.5054
	Protein Kinase C	0.5663
HPV 45	Protein Kinase A	0.4207
	Akt Kinase	0.5451
HPV 51	Akt Kinase	0.6631
HPV 52	Akt Kinase	0.6997
HPV 56	Akt Kinase	0.5733
HPV 58	Protein Kinase	0.4892
HPV 59	Akt Kinase	0.616
HPV 68	Akt Kinase	0.6313
HPV 26	Protein Kinase A	0.6086
	Akt Kinase	0.6564
	AMP Kinase	0.661
HPV 34	AMP kinase	0.7454
HPV 66	PKC	0.4996
HPV 67	AMP kinase	0.6841
HPV 69	AMP kinase	0.7299
HPV 70	PKA	0.4931
	Akt	0.62
HPV 82	Akt	0.5272
	AMP kinase	0.6779
HPV 85	Protein Kinase A	0.5563

**Figure 5.3: Computational screen of E6 C-terminal sequences**

A screen of the peptide sequence of E6 proteins from HPV types classified by the IARC as cancer causing (Group 1) and probably (2A) and possibly (2B) cancer causing was carried out using Scansite software (<http://scansite.mit.edu/>). The probability score for each kinase targeting the E6 C-terminus is indicated by green bar and number.

had predicted kinase sites within the C-terminus of E6. These included HPV types 53, 73 and 97 (Figure 5.3).

#### 5.4.2 Investigation into the effect of PBM phosphorylation upon E6

##### *5.4.2.1 E6 is phosphorylated in primary keratinocytes harbouring HPV genomes*

In order to assess whether phosphorylation of the PBM occurs during the HPV life cycle, primary keratinocytes containing HPV18 genomes were grown in monolayer and treated with the PKA activator forskolin (FK), or with vehicle (DMSO) for 6 hours. The HPV18 DNA positive HeLa cells were included in the assay since the E6:PDZ protein interactions in these cells can be modulated by PKA activation (Kühne *et al.*, 2000). Total protein was extracted from the cells in urea buffer and then subjected to western blot analysis using an antibody that recognises the phosphorylated form of the HPV18 E6 PBM (E6P, a kind gift from L. Banks). Under conditions of PKA activation, phospho E6 was detected in both HeLa and genome containing cells; the levels of phosphorylated E6 (E6P) detected were higher in cells exposed to PKA activator, whereas it was barely detectable in vehicle-treated cells (Figure 5.4 A). Furthermore, when the same treatment was applied to wild-type genome containing cells alongside cells containing  $\Delta$ PKA genomes (the mutation abrogates the PKA recognition site), the levels of phosphorylated E6 (E6P) were again higher in cells harbouring the wild type genomes exposed to PKA activator (Figure 5.4 B). In this analysis, there was no significant detection of the mutated protein ( $\Delta$ PKA) (Figure 5.4 B). Untransfected HFKs were included to show that neither the E6 nor the E6P antibodies detected proteins in these cells (Figure 5.4 B). An increase in E6 levels in HeLa and WT genome containing cells was observed in many, but not all studies, where cells were treated with PKA activator (Figure 5.4 A). This suggested an effect of the kinase upon E6 protein stability.

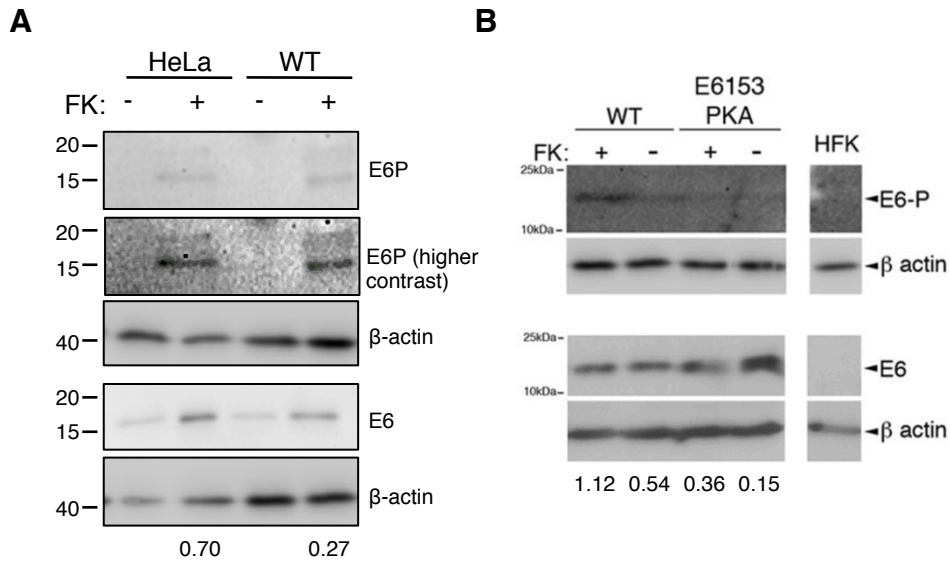


**Figure 5.4: Phosphorylation of E6 in HPV18 positive cells**

- (A) HeLa and HPV18 genome containing keratinocytes, grown in monolayer, were treated with the PKA activator forskolin (FK,+) or the vehicle DMSO (-) in serum-free media. After 6 hours, protein was harvested and separated by SDS-PAGE. Membranes were blotted with mouse anti-HPV18 E6 (Santa-Cruz) or rabbit anti-HPV18 E6P, alongside β-actin as a loading control. Molecular weight markers indicated in kDa
- (B) From Delury *et al.* 2013. HPV18 genome containing keratinocytes were grown in monolayer alongside ΔPKA genome containing cells and were treated with the PKA activator forskolin (FK) or the vehicle DMSO (-) in serum-free media. After 6 hours, protein was harvested and separated by SDS-PAGE. Membranes were blotted with mouse anti-HPV18 E6 (Santa-Cruz) or rabbit anti-HPV18 E6P, alongside β-actin as a loading control. HFK was included as a negative control.

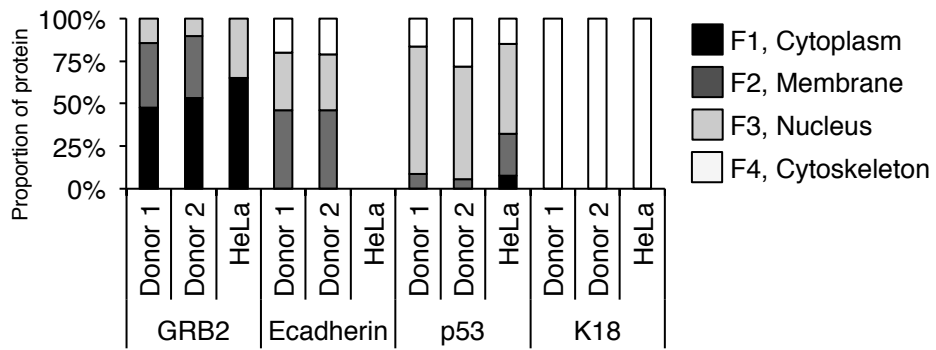
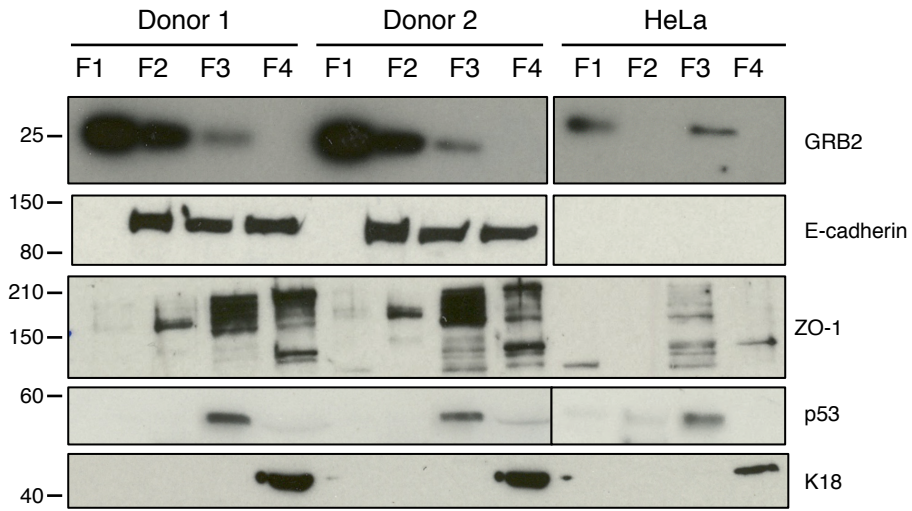
Numbers indicate fold change in E6P relative to E6, following normalisation of each to the respective loading control.

In order to assess whether specific cellular pools of E6 were phosphorylated by PKA, HPV18 genome-containing cells were grown in monolayer culture and subjected to subcellular fractionation, alongside the HPV18 positive cancer cell line HeLa. Housekeeping gene analysis confirmed enrichment of four subcellular compartments; cytoplasmic (F1), membrane (F2), nuclear (F3) and cytoskeletal (F4). As E-cadherin was not detectable in HeLa cells, ZO-1 was included to demonstrate enrichment of the membrane fraction in these cells (Figure 5.5 A).

The E6 oncoprotein was predominantly nuclear with a small amount of protein detected in the cytoplasmic, membrane and cytoskeletal fractions (Figure 5.5 B). Immunoblotting with the phospho-specific E6 PBM antibody detected protein primarily in the nuclear fraction of the HPV18 containing cells. Similarly, in HeLa cells the nuclear fraction of E6 was detected with the phospho E6 antibody, and this was consistent across three experiments (Figure 5.5 B and C).

Whilst the profile of E6 distribution is similar between genome containing cells and HeLa cells, where the viral DNA is integrated into the host genomes, a very small increase in E6 present in the cytoplasm was observed in the cancer cells (Figure 5.5). This modest change did not appear to relate to phosphorylation of E6, but this may be unclear due to the sensitivity of the E6P antibody. To establish whether localisation of the other viral oncoprotein E7 was altered upon disease progression, the fractionation lysates were immunoblotted with an anti-E7 antibody. The HPV18 protein E7 was detected in all subcellular fractions of primary keratinocytes harbouring the HPV18 genomes (Figure 5.5). E7 was detected primarily in the membrane fraction, with less protein observed in the cytoplasm and nucleus and a small amount in cytoskeletal fraction (Figure 5.5 B). In HeLa cells, E7 was predominantly detected in the cytoplasm, with small amounts of the protein

**A**



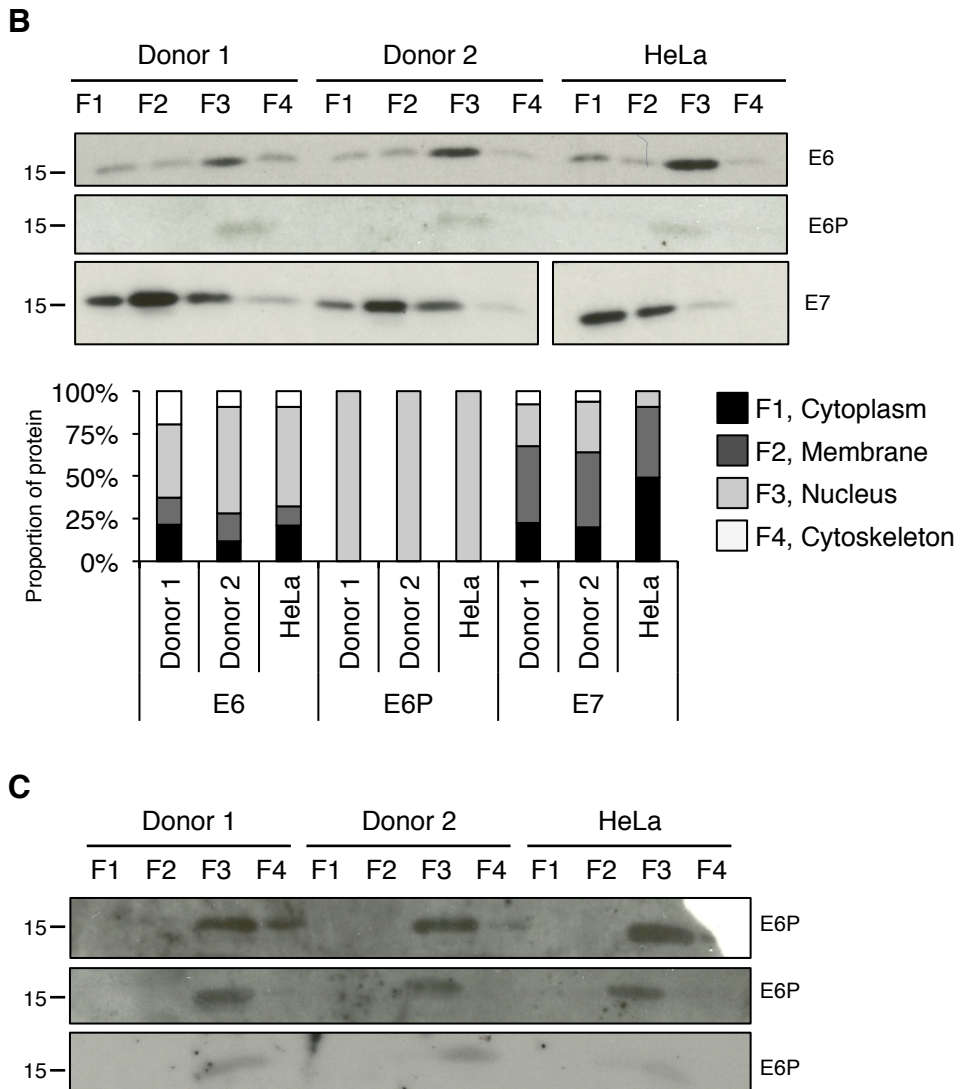


**Figure 5.5: Distribution of phosphorylated E6 in monolayer-grown cells**

HeLa and HPV18 genome containing keratinocytes, from two donor backgrounds, were grown in monolayer to approximately 70% confluency before subjection to subcellular fractionation. Western blots were quantified by densitometry and are representative of three repeats.

- (A) Housekeeping gene analysis indicated sufficient enrichment of the cytoplasmic, membrane, nuclear and cytoskeletal fractions (F1-F4), as described in Section 3.
- (B) HPV protein distribution was analysed by subcellular fractionation followed by western blot using mouse anti-HPV18 E6 (Santa Cruz), rabbit anti-HPV18 E6P or mouse anti-HPV18 E7.
- (C) Three subcellular fractionation repeats with detection of E6P.

in the membrane and in the nucleus (Figure 5.5 B). These data indicate that the subcellular localization of both oncoproteins changes upon disease progression.

#### *5.4.2.2 E6 protein levels are affected by PKA activity*

In some experiments, treatment of the HPV18 genome containing cells with a PKA activator led to an increase in E6 protein suggesting that PKA mediated phosphorylation of the E6 PBM regulates E6 stability (Figure 5.4 A). Indeed, it has been suggested by knockdown of 14-3-3 $\zeta$  expression in HeLa cells that the association between the viral oncoprotein and the cellular adapter protein regulates E6 protein stability (Boon and Banks, 2012b). Thus, to investigate the relationship between PKA activity and E6 protein stability in the viral genome containing cells, monolayer-grown cells were treated with the PKA inhibitor dihydrochloride (H89). The cells were harvested after 4 and 6 hours incubation with H89 and E6 protein levels assessed by western blot. Following both 4 and 6 hours of treatment with H-89 led to a marked decrease in E6 protein in two different donor backgrounds (Figure 5.6).

Because the inhibitor H89 is not a selective inhibitor of PKA but has been shown to inhibit at least 8 other kinases, including AKT, ribosomal S6 kinase (RSK) and Rho-associated protein kinase II (ROCKII, Lochner and Moolman, 2006), the effect of PKA on E6 stability was also examined by transfecting the cells with a plasmid expressing the PKA inhibitor peptide (mPKI). This plasmid (a kind gift from M. Diskar) expresses a GFP fusion of protein kinase inhibitor peptide (PKI), which has been identified as an endogenous specific inhibitor of PKA (Dalton and Dewey, 2006). Transfection efficiency was estimated via observation of the GFP reporter, typically 50-60% in HeLa and 30-40% in HFKs following incubation for 48 hours. In genome containing cells and in HeLa cells transfected with the specific inhibitor, the levels of the E6 protein were decreased

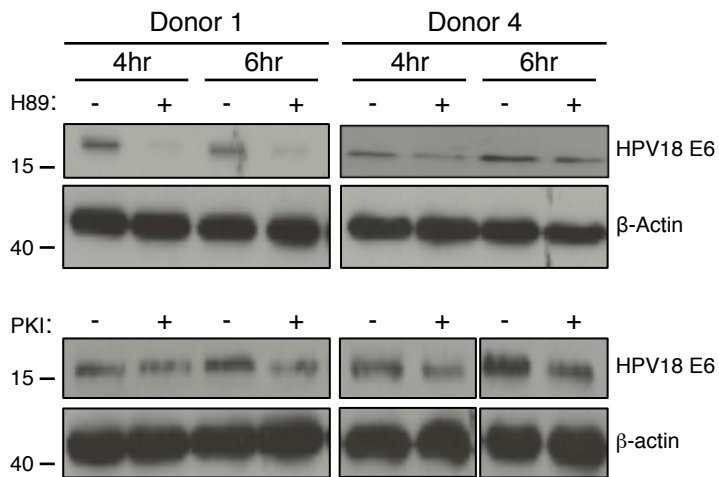


**Figure 5.6: The effect of PKA inhibition upon HPV18 E6 protein**

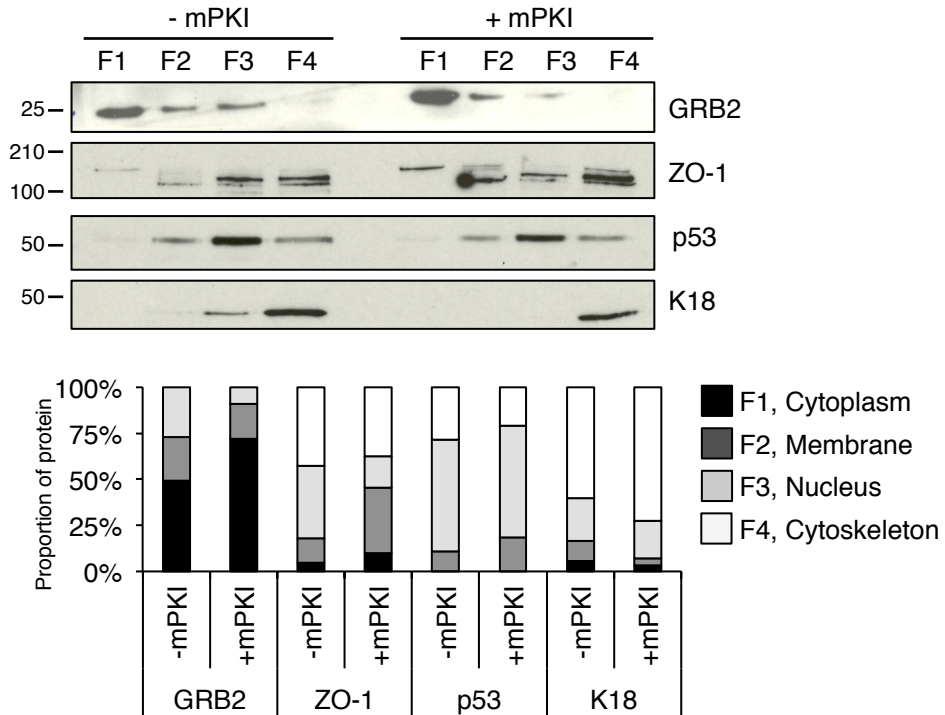
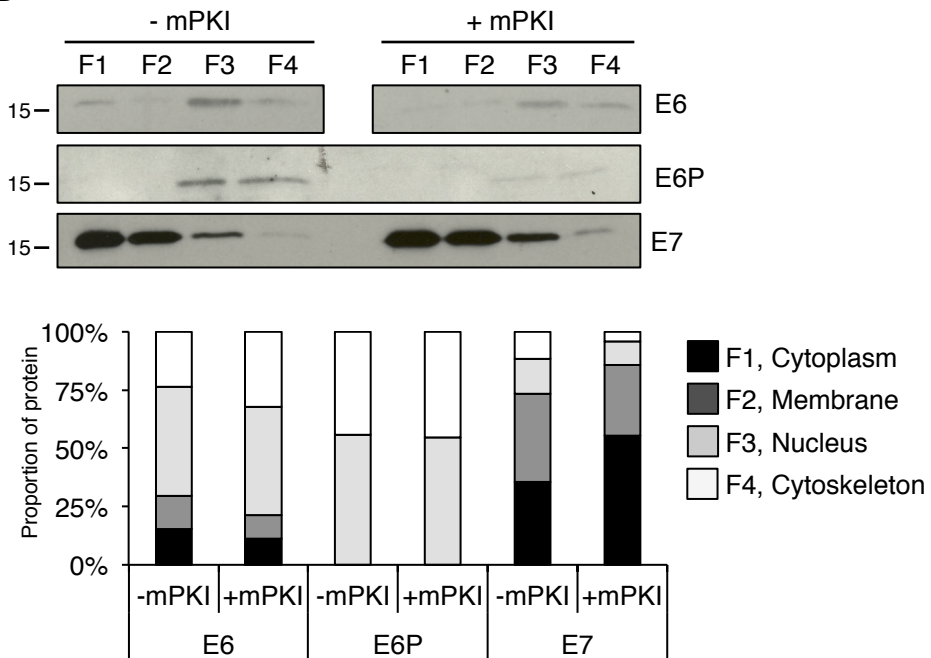
Keratinocytes containing HPV18 genomes were treated with the PKA inhibitors H89 or PKI for 4 and 6 hours. Control cells were treated with the vehicle DMSO alongside H89 or 1% BSA alongside PKI. Protein extracted in urea buffer from cells derived from 2 donor backgrounds. Western blot analysis was applied using antibodies specific to HPV18 E6 protein and  $\beta$ -actin loading control. Representative of two repeats.

compared to the untransfected cells (Figure 5.6). Together these data suggest that PKA phosphorylation regulates E6 steady state stability.

The next step aimed to examine whether the observed change in E6 levels reflected a change in a specific cellular pool of E6. Firstly, HeLa cells were transfected with the mPKI plasmid, incubated for 48 hours and then equal numbers of treated and untreated cells were subjected to subcellular fractionation. Firstly, housekeeping gene analysis confirmed that the enrichment of the cytoplasmic, membrane, nuclear and cytoskeletal compartments was successful (Figure 5.8). As noted previously (Figure 5.4) HPV18 E6 was present in all four fractions analysed and was detected predominantly in the nucleus of HeLa cells (Figure 5.7). Where PKA was inhibited (+mPKI), less E6 was detected in the cytoplasmic fraction along with a subtle shift from the membrane to the nucleus compared to untransfected cells (-mPKI) (Figure 5.7). The distribution of the phosphorylated form remained nuclear and cytoskeletal in the presence and absence of mPKI, although less E6P was detected where PKI was expressed, indicating that phosphorylation of E6 was inhibited (Figure 5.8). As an equal number of cells were subjected to fractionation and less total E6 was detected where PKA was inhibited, this supports the earlier data where PKA phosphorylation stabilised E6 protein levels (Figure 5.6).

To determine whether these changes in distribution and abundance were specific to E6, the distribution of the viral protein E7 was included in the analysis and was shown to reside predominantly in the cytoplasmic and membrane fractions, with lower levels detected in the nuclear and cytoskeletal fractions, irrespective of mPKI expression (Figure 5.7).

Next, the sensitivity of E6 localization to changes in PKA signalling was examined in HPV18 genome-containing cells. Keratinocytes were transfected with the GFP-mPKI expressing plasmid and fractionated as described. Detection of GRB2, E-cadherin, p53 and K18 confirmed successful enrichment of the subcellular compartments (Figure 5.8 A). As

**A****B**

**Figure 5.7: HPV oncoprotein expression in HeLa expressing mPKI**

HeLa were transfected with plasmid expressing peptide inhibitor of PKA (+PKI) or vehicle (-PKI), quenched with serum-containing media after 8 hours and protein harvested subcellular fractionation after a further 40 hours. Left-hand key describes each fraction number corresponding to a subcellular compartment.

(A) Lysates probed for GRB2, ZO-1, p53 and K18 to show enrichment of the cytoplasmic, membrane, nuclear and cytoskeletal fractions, respectively.

(B) Fractions probed for analysis of HPV protein distribution.

Densitometry was performed on scanned film using ImageJ. Representative of three repeats.

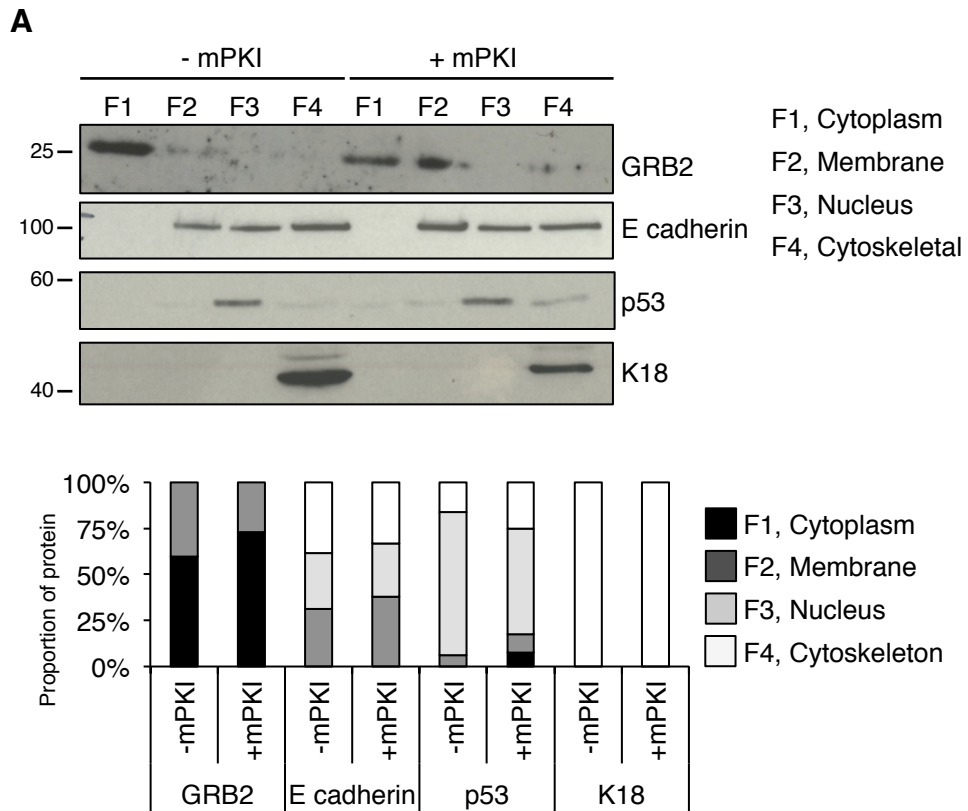


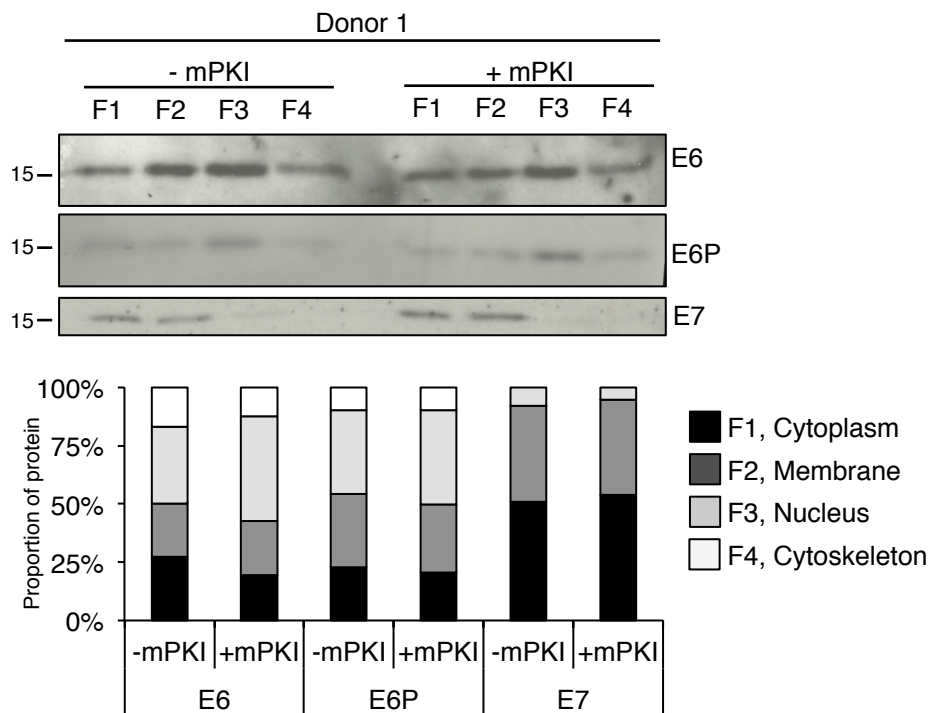
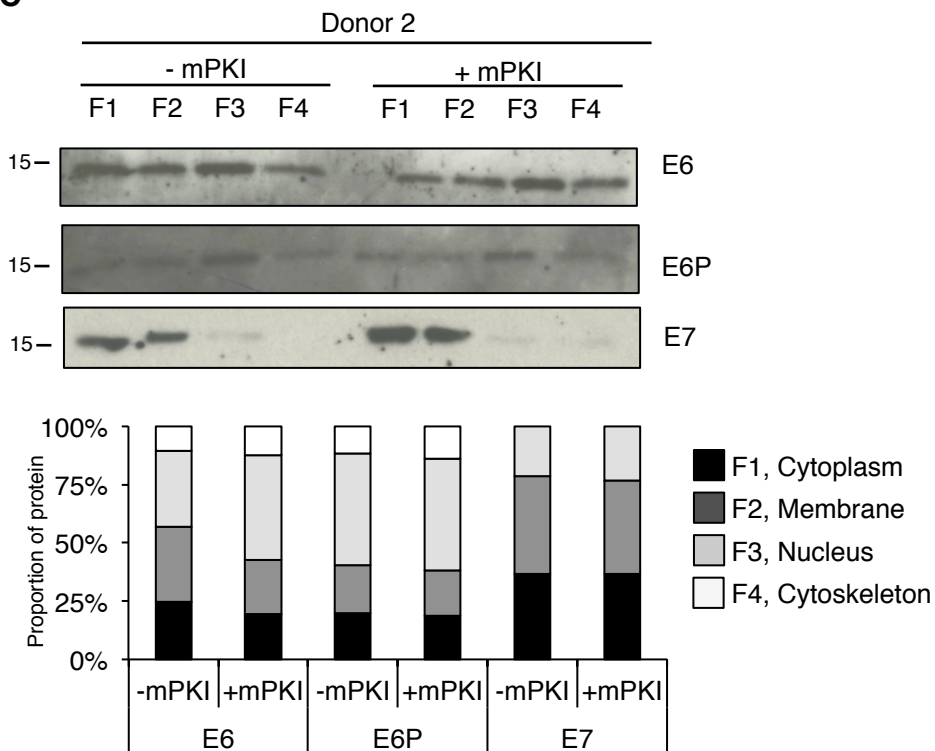
**Figure 5.8: HPV oncoprotein expression in primary cells expressing mPKI**

HPV18 genome containing keratinocytes derived from two donor backgrounds were treated with transfection vehicle (-mPKI) or plasmid expressing peptide inhibitor of PKA (+mPKI). Following 48 hours, cytoplasmic (F1), membrane (F2), nuclear (F3) and cytoskeletal (F4) fractions were sequentially extracted and subject to western blot analysis. The top panel (A) shows an example of housekeeping gene analysis to confirm enrichment of each fraction. The lower panels (B and C, on next page) shows detection of HPV18 E6, E6P and E7 in lysates. Densitometry analysis perform using ImageJ software. Representative of 2 repeats per donor background.

in HeLa cells, E6 was predominantly localized to the nucleus of keratinocytes, with the remaining protein distributed across the other three cellular compartments (Figure 5.8 B and C). This fractionation also agrees with previous detection of E6 in fractions of genome containing cells (Figure 5.5). In cells derived from two donor backgrounds, no major change in E6 distribution was observed where PKA was inhibited (Figure 5.8 B and C). Phospho-E6 was primarily detected in the nucleus of HPV18 positive keratinocytes, with some protein detected in the cytoskeletal fraction of keratinocytes, and this was not significantly affected by the expression of mPKI (Figure 5.8 B and C). The E7 protein remained within the cytoplasmic and membrane fractions in the presence and absence of mPKI (Figure 5.8). Together these data suggest that phosphorylation by PKA does not alter the stability of a specific subcellular pool of viral oncoproteins.

#### *5.4.2.3 E6 levels are affected by PDZ binding activity*

If phosphorylation of the E6 PBM mediates interactions with cellular factors that stabilize E6, then mutations of the E6 domain that prevent phosphorylation would be expected to affect E6 protein levels. To test this hypothesis, E6 protein levels were examined in keratinocytes harbouring the HPV18 mutant genomes that either lack the E6 PBM ( $\Delta$ PDZ), or genomes that express a mutant form of E6 that is not sensitive to PKA phosphorylation ( $\Delta$ PKA). Interestingly, comparison of levels of the E6 oncoprotein to wild type genome containing cells showed decreased levels of E6 where the PBM was removed and this was consistent between two donors. However, there was no consistent change in E6 levels in the presence of the  $\Delta$ PKA genomes; in one donor E6 protein levels were comparable to WT genome containing cells and in the second donor E6 levels were decreased (Figure 5.9). This indicates that the PDZ binding activity of E6 is influential in the protein's stability. Moreover, the alteration in viral protein levels was not restricted to

**B****C**

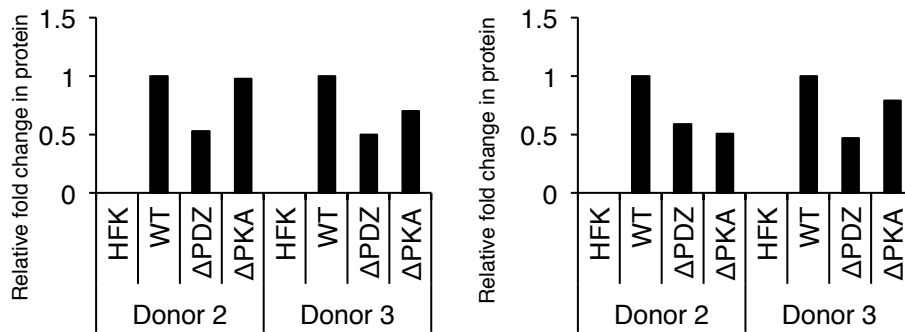
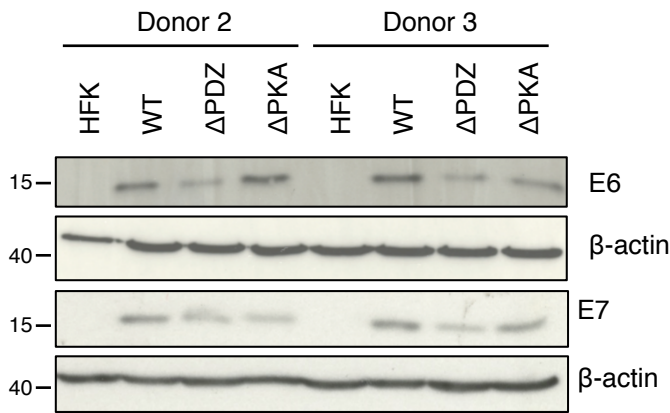


### Figure 5.9: E6 protein in HPV18 genome containing HFKs

Protein was extracted from HFKs containing WT HPV18, ΔPDZ or ΔPKA genomes, from two donor backgrounds, and subject to western blot analysis to assess HPV18 E6 and E7 oncoprotein levels. Untransfected keratinocytes (HFK) included as a control. Densitometry performed in ImageJ, values first normalised to β-actin and then to levels of protein in WT genome containing cells to calculate a relative fold change. Representative of two repeats.

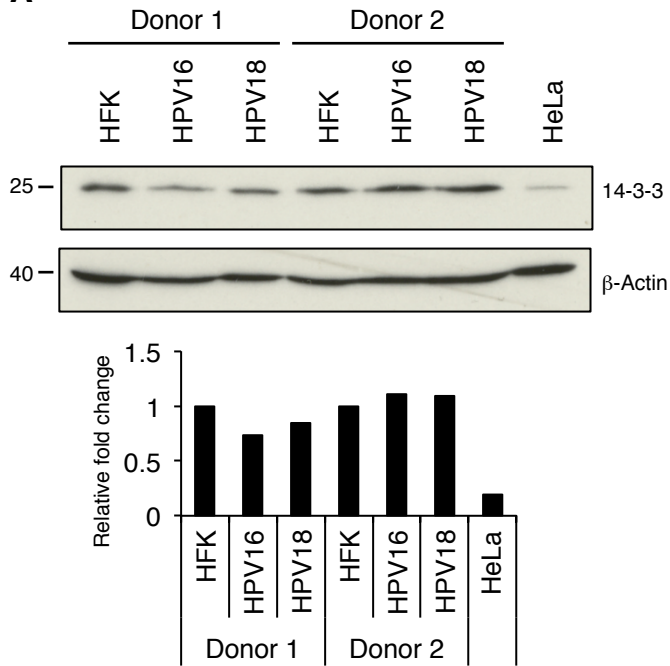
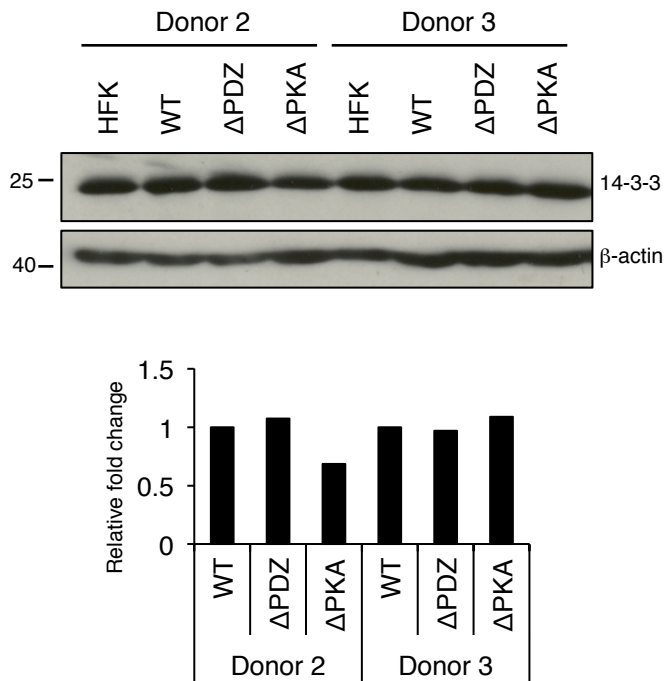
E6, analysis of E7 protein levels also revealed a decrease in protein levels in cells containing  $\Delta$ PDZ genomes (Figure 5.9). This decrease was sustained in the presence of  $\Delta$ PKA genomes, albeit to a larger extent in donor 1 (0.5-fold) than donor 2 (0.7-fold, Figure 5.9).

#### 5.4.3 14-3-3 $\zeta$

Phosphorylation of the HPV18 PBM allows an alternative interaction with 14-3-3 $\zeta$  (Boon and Banks, 2012b). To investigate whether interaction with the viral protein alters 14-3-3 $\zeta$  levels and/or localization in the life cycle, the overall abundance of the scaffold protein was assessed in primary keratinocytes containing high-risk  $\alpha$ -HPV types 16 and 18 and in the cervical cancer cell line HeLa. Although 14-3-3 $\zeta$  levels decreased in HeLa compared to untransfected HFKS, there was no change in abundance of the scaffold protein where intact  $\alpha$ -HPV genomes were present (Figure 5.10 A). Furthermore, perturbing the activity of the HPV18 E6 PBM activity had no effect upon the abundance of 14-3-3 $\zeta$  (Figure 5.10 B).

To determine if PKA activity was inhibited *via* the expression of mPKI in HeLa or HPV18 genome containing cells. There was no effect upon the distribution of the scaffold protein in monolayer cells, where the majority of the protein was in the cytoplasmic and membrane fractions, with some protein detected in the nucleus and a little at the cytoskeleton (Figure 5.10 C).

The distribution of 14-3-3 $\zeta$  was further investigated in differentiated keratinocytes by immunofluorescence of cells stratified in raft culture. Together, these data indicate that the expression levels or the localization of cellular factor is not affected by changes in E6 PBM activity.

**A****B**

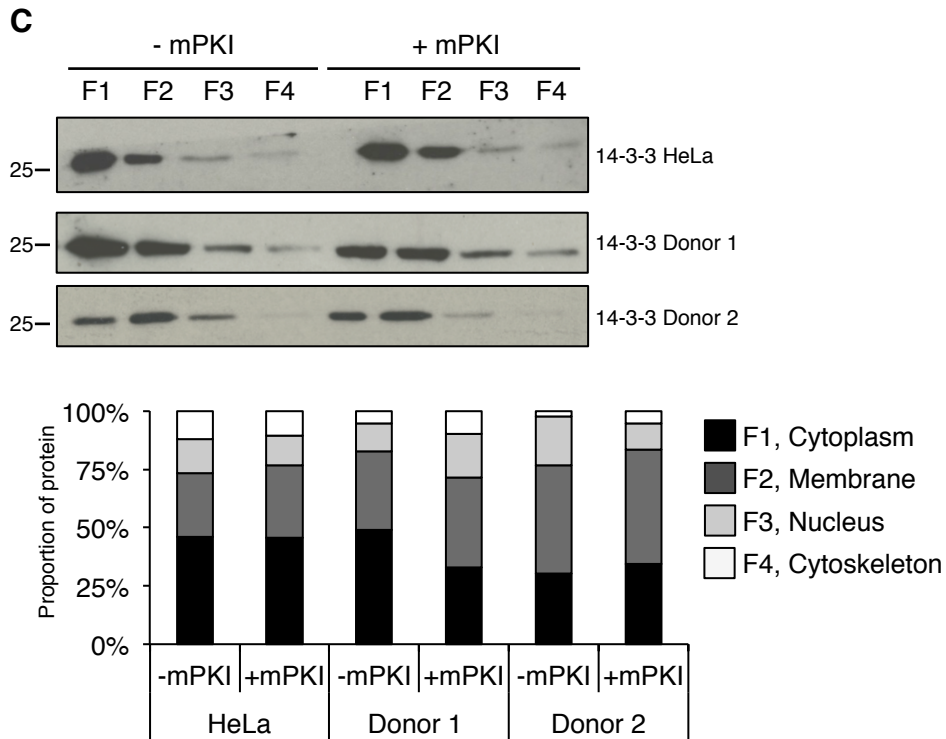


**Figure 5.10: 14-3-3 $\zeta$  protein expression in HPV genome containing keratinocytes**

- (A) Total protein was extracted from primary keratinocytes and from HPV16 or HPV18 genome containing cells from two donor backgrounds and subject to western blot analysis. Representative of two repeats. Fold change calculated relative to levels in HFKs of the same donor background, following normalisation to  $\beta$ -actin loading control.
- (B) Total protein was extracted from HFKs and from HPV18 WT,  $\Delta$ PDZ and  $\Delta$ PKA genome containing cells from two donor backgrounds and subject to western blot analysis. Representative of two repeats. Fold change calculated relative to levels in WT genome containing cells of the same donor background, following normalisation to  $\beta$ -actin loading control.
- (C) Analysis of 14-3-3 $\zeta$  distribution in monolayer-grown HeLa cells and keratinocytes containing HPV18 genomes, from two donor backgrounds. Cells were transfected with vehicle (-mPKI) or mPKI plasmid and subjected to subcellular fractionation. Representative two repeats.

Densitometry analysis perform using ImageJ software.

## 5.5 Discussion

This study showed for the first time that the E6 PBM is phosphorylated during the life cycle of the high-risk virus HPV18. The data suggests that phosphorylation occurs principally to the nuclear pool of E6. The nuclear localization of E6 observed in monolayer grown keratinocytes agrees with established knowledge; three nuclear localisation signals have been identified in HPV16 E6 and exogenous expression of the oncoprotein in cervical cells leads to a predominantly nuclear subcellular location (Masson *et al.*, 2003; Tao *et al.*, 2003; Liang *et al.*, 1993). However, as the E6P antibody detected the phospho form weakly, it is possible that the phosphorylated protein was only detected in nuclear fractions because this is where the majority of the E6 protein resides. If E6 phosphorylation occurs mainly to protein in the nucleus, then activation of PKA could be expected to lead to an increase in nuclear DLG1, and inhibition of PKA to a decrease of the cellular protein. Due to time constraints, this study was unable to investigate the distribution of DLG1, and other PDZ targets, during the expression of mPKI, and so this requires further characterisation, perhaps with additional investigation including small molecule inhibitors and activators of PKA.

Activation of PKA using forskolin led to an increase in E6 abundance and correspondingly inhibition of PKA by both specific and less-specific inhibitors led to a decrease in oncoprotein levels. Although no change in a specific pool of phosphorylated E6 was observed upon PKA inhibition of keratinocytes, there may be an alteration in E6 distribution in mPKI treated cancer cells. The differences observed between cancer cells and primary cells may be attributable to differences in mPKI transfection efficiency, which could be overcome using small molecule inhibitors in combination with the subcellular distribution analysis.

It has been demonstrated that E6 binding to the PDZ protein SCRIB stabilizes the oncoprotein (Nicolaidis *et al.*, 2011). Phosphorylation of the PBM is likely to disrupt this interaction and thus destabilize the protein. However, since phosphorylation presents novel interactions for E6, it is feasible that this compensates for any interruption in the stability provided by PDZ interactions (Figure 1.12). In this study, lower levels of E6 were observed where the PBM was removed, indicating that an interaction 14-3-3 $\zeta$  may stabilise E6 in primary cells. However, if this were the case E6 levels where the PKA recognition site is altered would exhibit the same decrease in protein levels, and this was not consistently observed. As the  $\Delta$ PKA mutation allows constitutive binding to PDZ proteins and interaction between E6 and SCRIB has been shown to promote the stability of both proteins (Nicolaidis *et al.*, 2011), perhaps the inability of the  $\Delta$ PDZ mutant to interact with either PDZ proteins or 14-3-3 $\zeta$  has negative consequences on protein stability (Figure 5.11).

It should also be noted that other sites within the E6 protein may be recognised by PKA, for example HPV18 threonine 86 was identified in the Scansite screen as a potential target for basophilic kinases (data not shown), phosphorylation of which may have an effect upon E6 stability. In addition deletion of the E6 PBM was associated with a moderate decrease E7 oncoprotein levels (Figure 5.9) and so an effect of the mutation upon E6E7 mRNA transcription cannot be ruled out completely.

It may also be that binding to either PDZs or 14-3-3 $\zeta$  functions to control the stability of E6 at different times during the viral life cycle. The aforementioned analysis of the effect of phosphorylation on PDZ protein expression levels and distribution could aid this investigation. Further work could also include the analysis of PDZ protein levels and/or 14-3-3 isoforms in differentiated keratinocytes, perhaps in the presence of PKA inhibitors

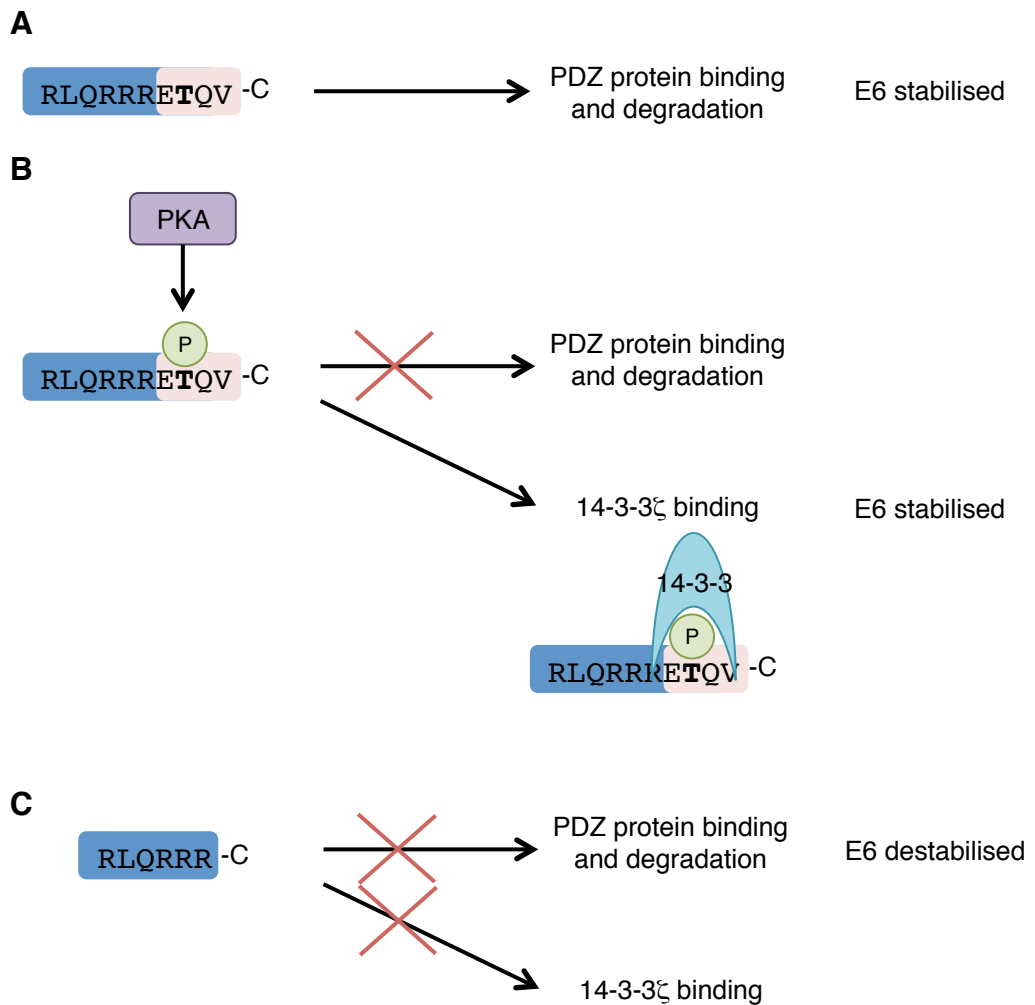


**Figure 5.11: The consequences of E6 phosphorylation**

A number of E6 oncoproteins have been shown to bind cellular PDZ proteins via a C-terminal PBM.

- (A) Work by Nicolaides *et al.* has shown that the interaction with SCRIB stabilises the viral protein.
- (B) Phosphorylation of the PBM sterically hinders PDZ protein binding and Boon *et al.* have shown that the ability of 14-3-3 $\zeta$  to bind the phosphorylated PBM promotes the stability of HPV18 E6.
- (C) Removal of the PBM removes the ability of E6 to interact with both cellular PDZ proteins and 14-3-3 $\zeta$ , and may therefore be the cause of the observed E6 destabilisation.

or activators. In this study, investigation into the degree of E6 phosphorylation in differentiated cells was investigated by applying western blot analysis to protein extracted from keratinocytes grown in organotypic raft culture. However, the results from multiple experiments were inconsistent and thus inconclusive. Due to this, and the challenging nature of immuno staining for E6, calcium-induced and/or methylcellulose differentiation may present a more practical option to observe E6 interactions during productive viral life cycle.

It seems that the steady state stability of E6 is affected by PKA phosphorylation. This may be due to the increased ability to interact with 14-3-3 $\zeta$ , which has been previously shown to stabilise E6 (Boon and Banks, 2012b). To examine this further and identify whether an interaction between E6 and 14-3-3 $\zeta$  occurs in primary keratinocytes, attempts were made to co-immunoprecipitate E6 and 14-3-3 $\zeta$  in cells were treated with vehicle (DMSO) or with PKA activators. These were unsuccessful, but with further optimisation pose an interesting avenue of investigation.

As E6 exists in more than one subcellular compartment, it is likely that the different pools perform different functions during viral replication. Phosphorylation of E6 may affect pools of protein differently, depending on the proteins available for interactions. For example, the interaction with 14-3-3  $\zeta$  has been shown to stabilise E6 protein and this may be specific to E6 located at the membrane (Boon and Banks, 2012b). Such phosphorylation of the PBM may promote 14-3-3  $\zeta$  binding to the PBM and thus organise E6 with other junctional proteins at the nuclear membrane. Equally, in the nucleus, PBM phosphorylation may prevent binding to cellular PDZ proteins where (or when) the interaction is not required, thereby allowing spatial and temporal regulation of E6 PBM

interactions. This speculation requires further investigation, perhaps in stratified cells for better observation of E6 distribution during differentiation.

Work by Delury *et al.* showed that loss of the PKA recognition site proximal to the E6 PBM was associated with an increased cell growth rate, whilst WT genome containing cells treated with PKA activators exhibited a slowed growth rate. Here, no difference was observed in E6 levels between  $\Delta$ PKA and HPV18 WT genome containing cells, which may indicate that the difference in growth rate phenotypes are due to the regulation of E6 interactions. The absence of PBM phosphorylation confers constitutive PDZ binding and an increased capacity of E6 to promote cell growth, whereas, in WT cells, PKA phosphorylation regulates E6:PDZ interactions to prevent uncontrolled growth. This could be further investigated using specific kinase inhibitors such as mPKI. In conditions of PKA inhibition, it is expected that growth levels of WT genome containing cells increase as PDZ protein interactions would no longer be sterically hindered by a phosphate group, resembling the constitutive binding conditions of the  $\Delta$ PKA mutant. The PBM function is linked to the maintenance of episomal genomes and thus observation of the state of HPV genomes under conditions of PKA activation and inhibition may also be of interest (Delury *et al.*, 2013).

A kinase screen of high-risk HPV E6 proteins revealed that the group 1 proteins are targeted at a common site within the PBM by either PKA or AKT. Less of the group 2 E6 proteins were predicted to be phosphorylated by PKA or other kinases, and in some cases (e.g. HPV 34 and 53) this phosphorylation is predicted to occur outside of PBM. The conservation of this site in these high-risk viruses may reflect a role for the modification in HPV-mediated cancer development. Indeed, both kinases have been implicated in growth factor-induced proliferative pathways (Jang *et al.*, 2012). However, the recognition sites of these kinases differ by an extra amino acid between the double arginine and target

serine/threonine residues (PKA, RRR<sup>T</sup>/<sub>S</sub> and AKT, RRRX<sup>T</sup>/<sub>S</sub>) and both HPV16 and HPV58 are phosphorylated by both *in vitro* (Boon *et al.*, 2014). Furthermore, HPV31 has been shown to be phosphorylated by PKA within the core of the E6 protein with no effect on PDZ interactions (Boon *et al.*, 2014). Thus, the Scansite screen is limited and unable to recapitulate *in vivo* interactions, it is important to confirm PBM phosphorylation *via in vitro* assays and to test the role of phosphorylation in the primary keratinocyte model of HPV propagation.

It has been demonstrated that HPV16 is phosphorylated by the kinase AKT and that expression of HPV16 E6 in HFKs causes accumulation of the active phosphorylated form of AKT (Spangle and Münger, 2010; Boon *et al.*, 2014). Furthermore, deletion of the HPV16 E6 PBM was unable to activate AKT and degradation of NHERF-1 mediated by HPV16 E6 correlates with the activation of the AKT signalling pathway (Accardi *et al.*, 2011; Spangle and Münger, 2010). This indicates a strong relationship between the HPV16 PBM function and cellular kinase activity, and has been suggested to be important during the differentiation dependent stage of the virus life cycle. While analysis of the PKA pathway in the life cycle of HPV18 is currently under investigation in the Roberts lab, it may also be of interest to the field to investigate the phosphorylation of the HPV16 PBM, perhaps using mutations in the PBM analogous to those used in the context of HPV18 during this thesis.

## CHAPTER 6: FINAL DISCUSSION

### 6.1 Overview of findings

High-risk HPV types 16 and 18 encode a C-terminal PDZ-binding motif in the E6 oncoprotein. Although this motif has been shown to direct the degradation of a number of cellular PDZ domain containing proteins, is known to influence the maintenance of viral genomes and is essential to the productive viral life cycle, the precise function of the interactions in the context of the virus life cycle has not been fully characterized. More recently, HPV16 studies demonstrated that expression of the E6 and E7 oncoproteins had no effect upon degradation nor altered cellular localization of endogenous PDZ proteins in primary keratinocytes (Choi *et al.*, 2013). The study described in this thesis investigated the expression of known and suggested PDZ targets of E6 in the presence of whole HPV genomes. In the main, results in this thesis agree with Choi *et al.*, 2013; the major known targets of HPV genomes were unaffected by the replicating virus at a protein level. Unexpectedly, the tight junction proteins ZO-1 and ZO-2 were affected by HPV18 and HPV16 respectively; ZO-2 protein was decreased whilst ZO-1 protein increased in keratinocytes. Both ZO-1 and ZO-2 proteins have been suggested to interact with E6, although this has yet to be confirmed in primary cells (Hernandez-Monge *et al.*, 2013; Belotti *et al.*, 2013). Thus, the next step would be to identify an interaction with the E6 PBM and utilize transcriptional analysis to identify whether HPV is exerting an effect at a gene level.

A number of microarray studies have identified changes in protein expression in the presence of HPV genomes, and when expressing HPV oncoproteins alone (Duffy *et al.*,

2003; Chang and Laimins, 2000; 2001; Karstensen *et al.*, 2006; Reiser *et al.*, 2011). The deregulated genes identified in these studies are mostly downstream of the p53, pRb/E2F or interferon-responsive pathways, and thus changes are likely due to the effect of the E6 and E7 oncoproteins upon pathway components (Chang and Laimins, 2001; 2000; Nees *et al.*, 2001; Karstensen *et al.*, 2006). Work in this thesis demonstrates that HPV genomes exert an influence over the transcription of specific PDZ-domain containing protein genes, including *DLG1*, *PTPN13*, *NHERF1* and *PATJ*. HPV-mediated upregulation of these genes may occur indirectly, *via* p53, pRb etc. or directly *via* a virally encoded factor.

Moreover, HPV differentially affects the transcription of DLG1 isoforms, with the DLG1 $\beta$  form largely unaffected by viral genomes and upregulation of an isoform containing a previously unidentified exon. In this study, an exon was identified in the DLG1 HOOK region, which exists in DLG1 $\alpha$  transcripts. This insertion (I6) is predicted to include a 20-amino acid sequence and produce a truncated form of the DLG1 protein. However, it is also possible that I6 acts at an mRNA level.

Finally, studies described in this thesis investigated the role of PBM phosphorylation in the context of genome replication. The phosphorylation of the HPV18 E6 PBM in primary cells was confirmed. Although this did not affect E6:PDZ interactions in monolayer grown cells, much of this preliminary work forms some foundation for ongoing investigations in the Roberts lab which focuses upon the influence and importance of PKA in the HPV life cycle. As the motif is conserved amongst high-risk  $\alpha$ -HPV types, these data suggest that phosphorylation of the PBM performs a crucial role in regulating E6 interactions during the virus life cycle.

As tight junctions regulate epithelial integrity and polarity, viral targeting of these proteins may be advantageous to HPV by interrupting differentiation of the infected basal

keratinocytes that would otherwise cause exit from the cell cycle. The PDZ proteins are multifunctional and thus there are likely to be functions, including the control of proliferation and pro-proliferative transcription factors, which are required at different stages of viral propagation. Especially since HPV targets subsets of PDZ proteins depending upon post-translational modifications, cellular localization or differential splicing of cellular proteins. As there is such specific PDZ targeting by E6 during the HPV life cycle, it can be assumed that the deregulation of the viral protein observed in transformed cells, and the ensuing disruption of polarity complexes, enhances HPV-mediated malignant progression.

## 6.2 Future directions

Despite the increase in transcript levels, no change was observed in the abundance or distribution of major known E6:PDZ targets, DLG1 and SCRIB during the early stages of the HPV life cycle. Although no changes in the protein abundance of PDZ targets (DLG1, PTPN13, NHERF1, PATJ) was observed in monolayer grown cells, some changes in protein distribution were observed in differentiated cells. However, more thorough investigation of degradation pathways may identify an increase in transcript correlates with translation, but also with an increase in protein turnover. Alternatively, the transcripts may be unstable or again turned over by infected cells more quickly to counter the detrimental effects of increased PDZ mRNA. Studies by Watson *et al.*, 2002 revealed an increase in cytoplasmic DLG1 in CIN1. Further investigation of DLG1, SCRIB and of other PDZ protein gene expression during neoplastic progression, for example following viral genome integration and in increasing CIN stages, would provide an insight into these interactions during the development of HPV-mediated cancers.

As well as the consequences of PDZ gene upregulation, it is also of interest to identify the viral mechanisms promoting upregulation of PDZ genes in such a selective fashion. This is

especially interesting in the case of DLG1 isoform expression; the ability of HPV to promote the inclusion of exons and the transcription of certain isoforms merits further exploration.

Replication of high-risk  $\alpha$ -HPV genomes led to an increase in transcription of selected PDZ domain containing targets, and affected proteins ZO-1 and ZO-2. The effect of HPV appears to concentrate upon the tight junctions and their protein partners, which may aid viral propagation by promoting growth factor signalling or the release of proliferatory transcription factors (Balda and Matter, 2000; Betanzos *et al.*, 2004). These proteins warrant further study in the HPV life cycle model and it may be of interest to investigate the consequences of kinase activation or inhibition on the tight-junction proteins.

Analysis of PDZ gene expression during the HPV life cycle identified the upregulation of a novel variant of DLG1. Expression of this form identified differential expression in HPV genome containing cell but not in cancers, suggesting that the form is not required during carcinogenesis but may be important in viral propagation. This work provides an exciting foundation for further investigation into the expression of this variant, and indeed of DLG1 isoforms, during HPV replication, in carcinogenesis and across tissue and cell contexts.

Although challenging to study, E6 PBM phosphorylation is likely a key influence in PDZ interactions. Thus, future studies investigating the effect of phosphorylation in differentiating cells, following genome integration and during the progression of HPV-driven cancers will further our understanding of E6:PDZ interactions.

### 6.3 Final statement

Overall, this study has contributed to current knowledge of HPV interactions with cellular PDZ proteins by performing a systematic analysis of PDZ proteins in the context of viral

replication. Although a number of major targets were unaffected by  $\alpha$ -HPV types at a protein level, it was shown the virus acts on DLG1, PATJ, NHERF1 and PTPN13 at a gene transcription level and on ZO-1 and ZO-2 at a protein level. Furthermore, it was observed that HPV genomes promoted inclusion of a novel insertion of DLG1.

Together, data from this study offers a new perspective on the interactions between oncogenic HPV types and PDZ domain-containing targets, indicating that deregulation of PDZ protein function by the virus occurs *via* multiple mechanisms.

Disruption of cell-cell junctions contributes to invasive growth and, ultimately, metastases. A thorough knowledge of E6:PDZ interactions and their regulation may aid their manipulation during HPV-mediated cancers and thus the development of therapeutic strategies targeting the PDZ:PBM interaction.

## REFERENCES

- Accardi, R., Rubino, R., Scalise, M., *et al.* (2011) E6 and E7 from Human Papillomavirus Type 16 Cooperate To Target the PDZ Protein Na/H Exchange Regulatory Factor 1. **Journal of Virology**, 85 (16): 8208–8216
- Adey, N.B., Huang, L., Ormonde, P.A., *et al.* (2000) Threonine phosphorylation of the MMAC1/PTEN PDZ binding domain both inhibits and stimulates PDZ binding. **Cancer research**, 60 (1): 35–37
- Ainsworth, J., Thomas, M., Banks, L., *et al.* (2008) Comparison of p53 and the PDZ domain containing protein MAGI-3 regulation by the E6 protein from high-risk human papillomaviruses. **Virology Journal**, 5: –
- Akagi, K., Li, J., Broutian, T.R., *et al.* (2014) Genome-wide analysis of HPV integration in human cancers reveals recurrent, focal genomic instability. **Genome research**, 24 (2): 185–199
- Akgül, B., Cooke, J.C. and Storey, A. (2006) HPV-associated skin disease. **The Journal of pathology**, 208 (2): 165–175
- Akgül, B., Garcia-Escudero, R., Ghali, L., *et al.* (2005) The E7 Protein of Cutaneous Human Papillomavirus Type 8 Causes Invasion of Human Keratinocytes into the Dermis in Organotypic Cultures of Skin. **Cancer research**, 65 (6): 2216–2223
- Akiva, E., Friedlander, G., Itzhaki, Z., *et al.* (2012) A dynamic view of domain-motif interactions. **PLoS Computational Biology**, 8 (1): e1002341
- Alam, M. and Ratner, D. (2001) Primary care: Cutaneous squamous-cell carcinoma. **New England Journal of Medicine**, 344 (13): 975–983
- Albornoz, V., Mendoza-Topaz, C., Oliva, C., *et al.* (2008) Temporal and spatial expression of Drosophila DLGS97 during neural development. **Gene Expression Patterns**, 8 (6): 443–451
- Alfandari, J., Magal, S.S., Jackman, A., *et al.* (1999) HPV16 E6 oncoprotein inhibits apoptosis induced during serum-calcium differentiation of foreskin human keratinocytes. **Virology**, 257 (2): 383–396
- Altschul, S.F., GISH, W., MILLER, W., *et al.* (1990) Basic Local Alignment Search Tool. **Journal of Molecular Biology**, 215 (3): 403–410
- Andersson, S., Safari, H., Mints, M., *et al.* (2005) **Type distribution, viral load and integration status of high-risk human papillomaviruses in pre-stages of cervical cancer (CIN).**, 92 (12): 2195–2200
- Ang, K.K. and Sturgis, E.M. (2012) Human Papillomavirus as a Marker of the Natural History and Response to Therapy of Head and Neck Squamous Cell Carcinoma. **Seminars**

in **Radiation Oncology**, 22 (2): 128–142

Ang, K.K., Harris, J., Wheeler, R., *et al.* (2010) Human Papillomavirus and Survival of Patients with Oropharyngeal Cancer. **New England Journal of Medicine**, 363 (1): 24–35

Aoyagi, T., Takahashi, M., Higuchi, M., *et al.* (2010) The PDZ domain binding motif (PBM) of human T-cell leukemia virus type 1 Tax can be substituted by heterologous PBMs from viral oncoproteins during T-cell transformation. **Virus Genes**, 40 (2): 193–199

Applebaum, K.M., Furniss, C.S., Zeka, A., *et al.* (2007) Lack of association of alcohol and tobacco with HPV16-associated head and neck cancer. **Journal of the National Cancer Institute**, 99 (23): 1801–1810

Aranda, V., Nolan, M.E. and Muthuswamy, S.K. (2008) Par complex in cancer: a regulator of normal cell polarity joins the dark side. **Oncogene**, 27 (55): 6878–6887

Arbeit, J.M., Howley, P.M. and Hanahan, D. (1996) Chronic estrogen-induced cervical and vaginal squamous carcinogenesis in human papillomavirus type 16 transgenic mice. **Proceedings of the National Academy of Sciences of the United States of America**, 93 (7): 2930–2935

Arpin-Andre, C. and Mesnard, J.-M. (2007) The PDZ domain-binding motif of the human T cell leukemia virus type 1 tax protein induces mislocalization of the tumor suppressor hScrib in T cells. **Journal of Biological Chemistry**, 282 (45): 33132–33141

Asaba, N., Hanada, T., Takeuchi, A., *et al.* (2003) Direct interaction with a kinesin-related motor mediates transport of mammalian discs large tumor suppressor homologue in epithelial cells. **Journal of Biological Chemistry**, 278 (10): 8395–8400

Assémat, E., Bazellères, E., Pallesi-Pocachard, E., *et al.* (2008) Polarity complex proteins. **Biochimica Et Biophysica Acta-Molecular Cell Research**, 1778 (3): 614–630

Assémat, E., Crost, E., Ponsérre, M., *et al.* (2013) The Multi-Pdz Domain Protein-1 (Mupp-1) Expression Regulates Cellular Levels Of The Pals-1/Patj Polarity Complex. **Experimental Cell Research**

Attner, P., Nasman, A., Marklund, L., *et al.* (2009) Frequency of HPV-associated tonsillar cancer in Sweden. **Journal of clinical oncology : official journal of the American Society of Clinical Oncology**, 27 (15)

Awad, A., Sar, S., Barré, R., *et al.* (2013) SHIP2 regulates epithelial cell polarity through its lipid product, which binds to Dlg1, a pathway subverted by hepatitis C virus core protein. **Molecular Biology of the Cell**, 24 (14): 2171–2185

Baadsgaard, O., Fisher, G.J., Voorhees, J.J., *et al.* (1990) Interactions of epidermal cells and T cells in inflammatory skin diseases. **Journal of the American Academy of Dermatology**, 23 (6 Pt 2): 1312–6– discussion 1316–7

Bachurski, C.J., Theodorakis, N.G., Coulson, R.M., *et al.* (1994) An amino-terminal tetrapeptide specifies cotranslational degradation of beta-tubulin but not alpha-tubulin mRNAs. **Molecular and Cellular Biology**, 14 (6): 4076–4086

- Balda, M.S. and Anderson, J.M. (1993) Two classes of tight junctions are revealed by ZO-1 isoforms. **The American journal of physiology**, 264 (4 Pt 1): C918–24
- Balda, M.S. and Matter, K. (2000) The tight junction protein ZO-1 and an interacting transcription factor regulate ErbB-2 expression. **Embo Journal**, 19 (9): 2024–2033
- Balda, M.S. and Matter, K. (2003) Epithelial cell adhesion and the regulation of gene expression. **Trends in cell biology**, 13 (6): 310–318
- Banks, L., Pim, D. and Thomas, M. (2012) Human tumour viruses and the deregulation of cell polarity in cancer. **Nature Reviews Cancer**, 12 (12): 877–886
- Barbosa, M.S., Lowy, D.R. and Schiller, J.T. (1989) Papillomavirus Polypeptide-E6 and Polypeptide-E7 Are Zinc-Binding Proteins. **Journal of Virology**, 63 (3): 1404–1407
- Barnard, A.L., Igakura, T., Tanaka, Y., *et al.* (2005) Engagement of specific T-cell surface molecules regulates cytoskeletal polarization in HTLV-1-infected lymphocytes. **Blood**, 106 (3): 988–995
- Baseman, J.G. and Koutsky, L.A. (2005) The epidemiology of human papillomavirus infections. **Journal of Clinical Virology**, 32 Suppl 1: S16–24
- Basile, J.R., Zacny, V. and Münger, K. (2001) The cytokines tumor necrosis factor-alpha (TNF-alpha) and TNF-related apoptosis-inducing ligand differentially modulate proliferation and apoptotic pathways in human keratinocytes expressing the human papillomavirus-16 E7 oncoprotein. **Journal of Biological Chemistry**, 276 (25): 22522–22528
- Bedell, M.A., Hudson, J.B., Golub, T.R., *et al.* (1991) Amplification of human papillomavirus genomes in vitro is dependent on epithelial differentiation. **Journal of Virology**, 65 (5): 2254–2260
- Bekkers, R.L.M., Massuger, L.F.A.G., Bulten, J., *et al.* (2004) Epidemiological and clinical aspects of human papillomavirus detection in the prevention of cervical cancer. **Reviews in Medical Virology**, 14 (2): 95–105
- Bell, D.A. and DeMarini, D.M. (1991) Excessive cycling converts PCR products to random-length higher molecular weight fragments. **Nucleic acids research**, 19 (18): 5079
- Bellaïche, Y., Radovic, A., Woods, D.F., *et al.* (2001) The Partner of Inscuteable/Disc-large complex is required to establish planar polarity during asymmetric cell division in *Drosophila*. **Cell**, 106 (3): 355–366
- Belleudi, F., Leone, L., Purpura, V., *et al.* (2011) HPV16 E5 affects the KGFR/FGFR2b-mediated epithelial growth through alteration of the receptor expression, signaling and endocytic traffic. **Oncogene**, 30 (50): 4963–4976
- Belotti, E., Polanowska, J., Daulat, A.M., *et al.* (2013) The Human PDZome: A Gateway to PSD95-Disc Large-Zonula Occludens (PDZ)-mediated Functions. **Molecular & Cellular Proteomics**, 12 (9): 2587–2603

- Berkhout, R.J., Tieben, L.M., Smits, H.L., *et al.* (1995) Nested PCR approach for detection and typing of epidermodysplasia verruciformis-associated human papillomavirus types in cutaneous cancers from renal transplant recipients. **Journal of clinical microbiology**, 33 (3): 690–695
- Bernard, B.A., Bailly, C., Lenoir, M.C., *et al.* (1989) The Human Papillomavirus Type-18 (Hpv18) E2 Gene-Product Is a Repressor of the Hpv18 Regulatory Region in Human Keratinocytes. **Journal of Virology**, 63 (10): 4317–4324
- Bernard, H.-U., Burk, R.D., Chen, Z., *et al.* (2010) Classification of papillomaviruses (PVs) based on 189 PV types and proposal of taxonomic amendments. **Virology**, 401 (1): 70–79
- Berumen, J., Unger, E.R., Casas, L., *et al.* (1995) **Amplification of human papillomavirus types 16 and 18 in invasive cervical cancer.**, 26 (6): 676–681
- Betanzos, A., Huerta, M., Lopez-Bayghen, E., *et al.* (2004) The tight junction protein ZO-2 associates with Jun, Fos and C/EBP transcription factors in epithelial cells. **Experimental Cell Research**, 292 (1): 51–66
- Betschinger, J., Mechtler, K. and Knoblich, J.A. (2003) The Par complex directs asymmetric cell division by phosphorylating the cytoskeletal protein Lgl. **Nature**, 422 (6929): 326–330
- Bidoia, C., Mazzorana, M., Pagano, M.A., *et al.* (2010) The pleiotropic protein kinase CK2 phosphorylates HTLV-1 Tax protein in vitro, targeting its PDZ-binding motif. **Virus Genes**, 41 (2): 149–157
- Bilder, D., Schober, M. and Perrimon, N. (2003) Integrated activity of PDZ protein complexes regulates epithelial polarity. **Nature cell biology**, 5 (1): 53–58
- Blot, W.J., McLaughlin, J.K., Winn, D.M., *et al.* (1988) Smoking and drinking in relation to oral and pharyngeal cancer. **Cancer research**, 48 (11): 3282–3287
- Boccardo, E., Manzini Baldi, C.V., Carvalho, A.F., *et al.* (2010) Expression of human papillomavirus type 16 E7 oncoprotein alters keratinocytes expression profile in response to tumor necrosis factor-alpha. **Carcinogenesis**, 31 (3): 521–531
- Bodily, J. and Laimins, L.A. (2011) Persistence of human papillomavirus infection: keys to malignant progression. **Trends in Microbiology**, 19 (1): 33–39
- Bonanni, P., Boccalini, S. and Bechini, A. (2009) **Progress in the research on HPV vaccination: updates from the 25th International Papillomavirus Conference in Malmo, Sweden, 2009.** In **September 2009**. pp. 131–134
- Bonilla-Delgado, J., Bulut, G., Liu, X., *et al.* (2012) The E6 oncoprotein from HPV16 enhances the canonical Wnt/ $\beta$ -catenin pathway in skin epidermis in vivo. **Molecular cancer research : MCR**, 10 (2): 250–258
- Boon, S.S. and Banks, L. (2012a) **High Risk HPV E6 oncoproteins interact with 14-3-3z in a PDZ binding Motif (PBM)-dependant manner.** pp. 1–25

Boon, S.S. and Banks, L. (2012b) High Risk HPV E6 Oncoproteins Interact with 14-3-3 $\zeta$  in a PDZ Binding Motif (PBM)-Dependent Manner. **Journal of Virology**

Boon, S.S., Tomaić, V., Thomas, M., *et al.* (2014) Cancer-Causing Human Papillomavirus E6 Proteins Display Major Differences in the Phospho-Regulation of their PDZ Interactions. **Journal of Virology**, pp. JVI.01961–14

Borrell-Pagès, M., Fernández-Larrea, J., Borroto, A., *et al.* (2000) The carboxy-terminal cysteine of the tetraspanin L6 antigen is required for its interaction with SITAC, a novel PDZ protein. **Molecular Biology of the Cell**, 11 (12): 4217–4225

Bouvard, V., Baan, R., Straif, K., *et al.* (2009) A review of human carcinogens—Part B: biological agents. **Lancet Oncology**, 10 (4): 321–322

Bouvard, V., Matlashewski, G., Gu, Z.M., *et al.* (1994a) The human papillomavirus type 16 E5 gene cooperates with the E7 gene to stimulate proliferation of primary cells and increases viral gene expression. **Virology**, 203 (1): 73–80

Bouvard, V., Storey, A., Pim, D., *et al.* (1994b) Characterization of the Human Papillomavirus E2 Protein - Evidence of Transactivation and Transrepression in Cervical Keratinocytes. **Embo Journal**, 13 (22): 5451–5459

Brehm, A., Miska, E.A., McCance, D.J., *et al.* (1998) Retinoblastoma protein recruits histone deacetylase to repress transcription. **Nature**, 391 (6667): 597–601

Brehm, A., Nielsen, S.J., Miska, E.A., *et al.* (1999) The E7 oncoprotein associates with Mi2 and histone deacetylase activity to promote cell growth. **Embo Journal**, 18 (9): 2449–2458

Brenman, J.E., Topinka, J.R., Cooper, E.C., *et al.* (1998) Localization of postsynaptic density-93 to dendritic microtubules and interaction with microtubule-associated protein 1A. **The Journal of neuroscience : the official journal of the Society for Neuroscience**, 18 (21): 8805–8813

Brimer, N. and Vande Pol, S.B. (2014) Papillomavirus E6 PDZ interactions can be replaced by repression of p53 to promote episomal human papillomavirus genome maintenance. **Journal of Virology**, 88 (5): 3027–3030

Brimer, N., Lyons, C. and Vande Pol, S.B. (2007) Association of E6AP (UBE3A) with human papillomavirus type 11 E6 protein. **Virology**, 358 (2): 303–310

Brimer, N., Lyons, C., Wallberg, A.E., *et al.* (2012) Cutaneous papillomavirus E6 oncoproteins associate with MAML1 to repress transactivation and NOTCH signaling. **Oncogene**, 31 (43): 4639–4646

Brown, D.R., Schroeder, J.M., Bryan, J.T., *et al.* (1999) Detection of multiple human papillomavirus types in Condylomata acuminata lesions from otherwise healthy and immunosuppressed patients. **Journal of clinical microbiology**, 37 (10): 3316–3322

Buck, C.B., Cheng, N., Thompson, C.D., *et al.* (2008) Arrangement of L2 within the papillomavirus capsid. **Journal of Virology**, 82 (11): 5190–5197

- Buck, C.B., Day, P.M. and Trus, B.L. (2013) The papillomavirus major capsid protein L1. **Virology**, 445 (1-2): 169–174
- Bustin, S.A. and Nolan, T. (2004) Pitfalls of quantitative real-time reverse-transcription polymerase chain reaction. **Journal of biomolecular techniques : JBT**, 15 (3): 155–166
- Cai, C., Coleman, S.K., Niemi, K., *et al.* (2002) Selective binding of synapse-associated protein 97 to GluR-A alpha-amino-5-hydroxy-3-methyl-4-isoxazole propionate receptor subunit is determined by a novel sequence motif. **Journal of Biological Chemistry**, 277 (35): 31484–31490
- Camus, S., Higgins, M., Lane, D.P., *et al.* (2003) Differences in the ubiquitination of p53 by Mdm2 and the HPV protein E6. **FEBS letters**, 536 (1-3): 220–224
- Canova, C., Richiardi, L., Merletti, F., *et al.* (2010) Alcohol, tobacco and genetic susceptibility in relation to cancers of the upper aerodigestive tract in northern Italy. **Tumori**, 96 (1): 1–10
- Cao, T.T., Deacon, H.W., Reczek, D., *et al.* (1999) A kinase-regulated PDZ-domain interaction controls endocytic sorting of the beta2-adrenergic receptor. **Nature**, 401 (6750): 286–290
- Carr, H.S., Cai, C., Keinänen, K., *et al.* (2009) Interaction of the RhoA Exchange Factor Net1 with Discs Large Homolog 1 Protects It from Proteasome-mediated Degradation and Potentiates Net1 Activity. **Journal of Biological Chemistry**, 284 (36): 24269–24280
- Caruana, G. and Bernstein, A. (2001) Craniofacial dysmorphogenesis including cleft palate in mice with an insertional mutation in the discs large gene. **Molecular and Cellular Biology**, 21 (5): 1475–1483
- Castellani, S., Guerra, L., Favia, M., *et al.* (2012) NHERF1 and CFTR restore tight junction organisation and function in cystic fibrosis airway epithelial cells: role of ezrin and the RhoA/ROCK pathway. **Laboratory Investigation**, 92 (11): 1527–1540
- Castellsagué, X. and Muñoz, N. (2003) Chapter 3: Cofactors in human papillomavirus carcinogenesis--role of parity, oral contraceptives, and tobacco smoking. **Journal of the National Cancer Institute. Monographs**, (31): 20–28
- Castillo, A., Wang, L., Koriyama, C., *et al.* (2014) A systems biology analysis of the changes in gene expression via silencing of HPV-18 E1 expression in HeLa cells. **Open biology**, 4 (10): 130119–130119
- Cauthen, A.N., Swayne, D.E., Sekellick, M.J., *et al.* (2007) Amelioration of influenza virus pathogenesis in chickens attributed to the enhanced interferon-inducing capacity of a virus with a truncated NS1 gene. **Journal of Virology**, 81 (4): 1838–1847
- Cavatorta, A.L., Facciuto, F., Valdano, M.B., *et al.* (2011) Regulation of translational efficiency by different splice variants of the Disc large 1 oncosuppressor 5'-UTR. **The FEBS journal**, 278 (14): 2596–2608
- Cavatorta, A.L., Fumero, G.N., Chouhy, D., *et al.* (2004) Differential expression of the

human homologue of drosophila discs large oncosuppressor in histologic samples from human papillomavirus-associated lesions as a marker for progression to malignancy. **International Journal of Cancer**, 111 (3): 373–380

Cavatorta, A.L., Giri, A.A., Banks, L., *et al.* (2008) Cloning and functional analysis of the promoter region of the human Disc large gene. **Gene**, 424 (1-2): 87–95

Chan, S.Y., Delius, H., Halpern, A.L., *et al.* (1995) Analysis of Genomic Sequences of 95 Papillomavirus Types - Uniting Typing, Phylogeny, and Taxonomy. **Journal of Virology**, 69 (5): 3074–3083

Chang, Y. and Laimins, L.A. (2001) Interferon-inducible genes are major targets of human papillomavirus type 31: Insights from microarray analysis. **Disease Markers**, 17 (3): 139–142

Chang, Y.E. and Laimins, L.A. (2000) Microarray analysis identifies interferon-inducible genes and Stat-1 as major transcriptional targets of human papillomavirus type 31. **Journal of Virology**, 74 (9): 4174–4182

Charbonnier, S., Nominé, Y., Ramirez, J., *et al.* (2011) The Structural and Dynamic Response of MAGI-1 PDZ1 with Noncanonical Domain Boundaries to the Binding of Human Papillomavirus E6. **Journal of Molecular Biology**, 406 (5): 745–763

Chaturvedi, A.K., Engels, E.A., Anderson, W.F., *et al.* (2008) Incidence trends for human papillomavirus-related and -unrelated oral squamous cell carcinomas in the United States. **Journal of clinical oncology : official journal of the American Society of Clinical Oncology**, 26 (4): 612–619

Chellappan, S., Kraus, V.B., Kroger, B., *et al.* (1992) Adenovirus E1A, simian virus 40 tumor antigen, and human papillomavirus E7 protein share the capacity to disrupt the interaction between transcription factor E2F and the retinoblastoma gene product. **Proceedings of the National Academy of Sciences of the United States of America**, 89 (10): 4549–4553

Chen, E.Y., Howley, P.M., Levinson, A.D., *et al.* (1982) The primary structure and genetic organization of the bovine papillomavirus type 1 genome. **Nature**, 299 (5883): 529–534

Chen, Z., Schiffman, M., Herrero, R., *et al.* (2011) Evolution and Taxonomic Classification of Human Papillomavirus 16 (HPV16)-Related Variant Genomes: HPV31, HPV33, HPV35, HPV52, HPV58 and HPV67 Chan, K.Y.K. (ed.). **PLoS ONE**, 6 (5)

Cheng, J., Wang, H. and Guggino, W.B. (2004) Modulation of mature cystic fibrosis transmembrane regulator protein by the PDZ domain protein CAL. **Journal of Biological Chemistry**, 279 (3): 1892–1898

Cheng, S., Schmidt-Grimminger, D.C., Murant, T., *et al.* (1995) Differentiation-dependent up-regulation of the human papillomavirus E7 gene reactivates cellular DNA replication in suprabasal differentiated keratinocytes. **Genes & development**, 9 (19): 2335–2349

Chetkovich, D.M., Chen, L., Stocker, T.J., *et al.* (2002) Phosphorylation of the postsynaptic density-95 (PSD-95)/discs large/zona occludens-1 binding site of stargazin regulates

binding to PSD-95 and synaptic targeting of AMPA receptors. **The Journal of neuroscience : the official journal of the Society for Neuroscience**, 22 (14): 5791–5796

Choi, J., Ko, J., Park, E., *et al.* (2002) Phosphorylation of stargazin by protein kinase A regulates its interaction with PSD-95. **Journal of Biological Chemistry**, 277 (14): 12359–12363

Choi, M., Lee, S., Choi, T., *et al.* (2013) Roles of the PDZ domain-binding motif of the human papillomavirus type 16 E6 on the immortalization and differentiation of primary human foreskin keratinocytes. **Virus Genes**, 57 (4): 447–451

Chomczynski, P. and Sacchi, N. (1987) Single-step method of RNA isolation by acid guanidinium thiocyanate-phenol-chloroform extraction. **Analytical Biochemistry**, 162 (1): 156–159

Chow, L.T., Reilly, S.S., Broker, T.R., *et al.* (1987) Identification and mapping of human papillomavirus type 1 RNA transcripts recovered from plantar warts and infected epithelial cell cultures. **Journal of Virology**, 61 (6): 1913–1918

Chung, H.J., Huang, Y.H., Lau, L.-F., *et al.* (2004) Regulation of the NMDA receptor complex and trafficking by activity-dependent phosphorylation of the NR2B subunit PDZ ligand. **The Journal of neuroscience : the official journal of the Society for Neuroscience**, 24 (45): 10248–10259

Chung, S.-H., Weiss, R.S., Frese, K.K., *et al.* (2008) Functionally distinct monomers and trimers produced by a viral oncoprotein. **Oncogene**, 27 (10): 1412–1420

Ciuffo G. (1907). Innesto positivo con filtrato di verruca volgare. *Giorn Ital Mal Veneree*; **48**:12–7

Clifford, G.M., Gonçalves, M.A.G. and Franceschi, S. (2006) Human papillomavirus types among women infected with HIV: a meta-analysis. **AIDS (London, England)**, 20 (18): 2337–2344

Clifford, G.M., Smith, J.S., Plummer, M., *et al.* (2003) Human papillomavirus types in invasive cervical cancer worldwide: a meta-analysis. **British journal of cancer**, 88 (1): 63–73

Cohen, N.A., Brenman, J.E., Snyder, S.H., *et al.* (1996) Binding of the inward rectifier K<sup>+</sup> channel Kir 2.3 to PSD-95 is regulated by protein kinase A phosphorylation. **Neuron**, 17 (4): 759–767

Collins, S., Rollason, T.P., Young, L.S., *et al.* (2010) Cigarette smoking is an independent risk factor for cervical intraepithelial neoplasia in young women: a longitudinal study. **European journal of cancer (Oxford, England : 1990)**, 46 (2): 405–411

Collins, S.I., Constandinou-Williams, C., Wen, K., *et al.* (2009) Disruption of the E2 gene is a common and early event in the natural history of cervical human papillomavirus infection: a longitudinal cohort study. **Cancer research**, 69 (9): 3828–3832

Combita, A.L., Touze, A., Bousarghin, L., *et al.* (2001) **Gene transfer using human papillomavirus pseudovirions varies according to virus genotype and requires cell**

**surface heparan sulfate.** 204 (1): 183–188

Comerford, S.A., Maika, S.D., Laimins, L.A., *et al.* (1995) E6 and E7 expression from the HPV 18 LCR: development of genital hyperplasia and neoplasia in transgenic mice. **Oncogene**, 10 (3): 587–597

Cooper, K.D. and McGee, J. (1992) **HPV genotypes in cervical neoplasia in South Africa.**, 45 (1): 90–90. Available from: <http://eutils.ncbi.nlm.nih.gov/entrez/eutils/elink.fcgi?dbfrom=pubmed&id=1311003&retmode=ref&cmd=prlinks>

Cornet, I., Bouvard, V., Campo, M.S., *et al.* (2012) Comparative analysis of transforming properties of E6 and E7 from different beta human papillomavirus types. **Journal of Virology**, 86 (4): 2366–2370

Coutlee, F., de Pokomandy, A. and Franco, E.L. (2012) Epidemiology, natural history and risk factors for anal intraepithelial neoplasia. **Sexual health**, 9 (6): 547–555

Cricca, M., Venturoli, S., Morselli-Labate, A.M., *et al.* (2006) **HPV DNA patterns and disease implications in the follow-up of patients treated for HPV16 high-grade carcinoma in situ.**, 78 (4): 494–500

Crocetti, J., Silva, O., Humphries, L.A., *et al.* (2014) Selective Phosphorylation of the Dlg1AB Variant Is Critical for TCR-Induced p38 Activation and Induction of Proinflammatory Cytokines in CD8+ T Cells. **The Journal of Immunology**, 193 (6): 2651–2660

Crook, T., Tidy, J.A. and Vousden, K.H. (1991) Degradation of p53 can be targeted by HPV E6 sequences distinct from those required for p53 binding and trans-activation. **Cell**, 67 (3): 547–556

Crusius, K., Auvinen, E., Steuer, B., *et al.* (1998) The human papillomavirus type 16 E5-protein modulates ligand-dependent activation of the EGF receptor family in the human epithelial cell line HaCaT. **Experimental Cell Research**, 241 (1): 76–83

Cubie, H.A. (2013) Diseases associated with human papillomavirus infection. **Virology**, 445 (1-2): 21–34

Cullinan, P., Sperling, A.I. and Burkhardt, J.K. (2002) The distal pole complex: a novel membrane domain distal to the immunological synapse. **Immunological Reviews**, 189: 111–122

Culp, T.D., Budgeon, L.R., Marinkovich, M.P., *et al.* (2006) Keratinocyte-secreted laminin 5 can function as a transient receptor for human papillomaviruses by binding virions and transferring them to adjacent cells. **Journal of Virology**, 80 (18): 8940–8950

D'Costa, Z.J., Jolly, C., Androphy, E.J., *et al.* (2012) Transcriptional repression of E-cadherin by human papillomavirus type 16 E6. Hotchin, N.A. (ed.). **PLoS ONE**, 7 (11): e48954

D'Souza, G., Kreimer, A.R., Viscidi, R., *et al.* (2007) Case-control study of human

papillomavirus and oropharyngeal cancer. **The New England journal of medicine**, 356 (19): 1944–1956

Dalton, G.D. and Dewey, W.L. (2006) Protein kinase inhibitor peptide (PKI): A family of endogenous neuropeptides that modulate neuronal cAMP-dependent protein kinase function. **Neuropeptides**, 40 (1): 23–34

Daniels, D.L., Cohen, A.R., Anderson, J.M., *et al.* (1998a) Crystal structure of the hCASK PDZ domain reveals the structural basis of class II PDZ domain target recognition. **Nature Structural Biology**, 5 (4): 317–325

Daniels, P.R., Sanders, C.M. and Maitland, N.J. (1998b) Characterization of the interactions of human papillomavirus type 16 E6 with p53 and E6-associated protein in insect and human cells. **Journal of General Virology**, 79 ( Pt 3): 489–499

Das, B.C., Sharma, J.K., Gopalakrishna, V., *et al.* (1992) **Analysis by Polymerase Chain-Reaction of the Physical State of Human Papillomavirus Type-16 Dna in Cervical Preneoplastic and Neoplastic Lesions.** 73: 2327–2336

Davy, C., McIntosh, P., Jackson, D.J., *et al.* (2009) A novel interaction between the human papillomavirus type 16 E2 and E1--E4 proteins leads to stabilization of E2. **Virology**, 394 (2): 266–275

Day, P.M., Lowy, D.R. and Schiller, J.T. (2003) Papillomaviruses infect cells via a clathrin-dependent pathway. **Virology**, 307 (1): 1–11

de Jong, A., van Poelgeest, M.I., van der Hulst, J.M., *et al.* (2004) Human papillomavirus type 16-positive cervical cancer is associated with impaired CD4+T-cell immunity against early antigens E2 and E6. **Cancer research**, 64 (15): 5449–5455

de Martel, C., Ferlay, J., Franceschi, S., *et al.* (2012) Global burden of cancers attributable to infections in 2008: a review and synthetic analysis. **The lancet oncology**

de Sanjose, S., Quint, W.G., Alemany, L., *et al.* (2010) Human papillomavirus genotype attribution in invasive cervical cancer: a retrospective cross-sectional worldwide study. **The lancet oncology**, 11 (11): 1048–1056

de Villiers, E.-M. (2013) Cross-roads in the classification of papillomaviruses. **Virology**

de Villiers, E.-M., Fauquet, C., Broker, T.R., *et al.* (2004) Classification of papillomaviruses. **Virology**, 324 (1): 17–27

DeDiego, M.L., Alvarez, E., Almazan, F., *et al.* (2007) A severe acute respiratory syndrome coronavirus that lacks the E gene is attenuated in vitro and in vivo. **Journal of Virology**, 81 (4): 1701–1713

DeDiego, M.L., Pewe, L., Alvarez, E., *et al.* (2008) Pathogenicity of severe acute respiratory coronavirus deletion mutants in hACE-2 transgenic mice. **Virology**, 376 (2): 379–389

DeFilippis, R.A., Goodwin, E.C., Wu, L., *et al.* (2003) Endogenous human papillomavirus E6 and E7 proteins differentially regulate proliferation, senescence, and apoptosis in HeLa

cervical carcinoma cells. **Journal of Virology**, 77 (2): 1551–1563

DeGregori, J. and Johnson, D.G. (2006) Distinct and Overlapping Roles for E2F Family Members in Transcription, Proliferation and Apoptosis. **Current molecular medicine**, 6 (7): 739–748

Deguchi, M., Hata, Y., Takeuchi, M., *et al.* (1998) BEGAIN (brain-enriched guanylate kinase-associated protein), a novel neuronal PSD-95/SAP90-binding protein. **Journal of Biological Chemistry**, 273 (41): 26269–26272

Delury, C.P., Marsh, E., James, C.D., *et al.* (2013) The role of protein kinase A regulation of the E6 PDZ-binding domain during the differentiation-dependent life cycle of human papillomavirus type 18. **Journal of Virology**, 87 (15)

DeMarco, S.J. and Strehler, E.E. (2001) Plasma membrane Ca<sup>2+</sup>-atpase isoforms 2b and 4b interact promiscuously and selectively with members of the membrane-associated guanylate kinase family of PDZ (PSD95/Dlg/ZO-1) domain-containing proteins. **Journal of Biological Chemistry**, 276 (24): 21594–21600

Demers, G.W., Halbert, C.L. and Galloway, D.A. (1994) Elevated wild-type p53 protein levels in human epithelial cell lines immortalized by the human papillomavirus type 16 E7 gene. **Virology**, 198 (1): 169–174

Desaintes, C., Hallez, S., Van Alphen, P., *et al.* (1992) Transcriptional activation of several heterologous promoters by the E6 protein of human papillomavirus type 16. **Journal of Virology**, 66 (1): 325–333

Desmet, F.-O., Hamroun, D., Lalande, M., *et al.* (2009) Human Splicing Finder: an online bioinformatics tool to predict splicing signals. **Nucleic acids research**, 37 (9)

Dobrosotskaya, I., Guy, R.K. and James, G.L. (1997) MAGI-1, a membrane-associated guanylate kinase with a unique arrangement of protein-protein interaction domains. **The Journal of Biological Chemistry**, 272 (50): 31589–31597

Doerks, T., Bork, P., Kamberov, E., *et al.* (2000) L27, a novel heterodimerization domain in receptor targeting proteins Lin-2 and Lin-7. **Trends in Biochemical Sciences**, 25 (7): 317–318

Dong, G., Broker, T.R. and Chow, L.T. (1994) Human Papillomavirus Type-11 E2 Proteins Repress the Homologous E6 Promoter by Interfering with the Binding of Host Transcription Factors to Adjacent Elements. **Journal of Virology**, 68 (2): 1115–1127

Doorbar, J., Ely, S., Sterling, J., *et al.* (1991) Specific interaction between HPV-16 E1-E4 and cytokeratins results in collapse of the epithelial cell intermediate filament network. **Nature**, 352 (6338): 824–827

Doorbar, J., Quint, W., Banks, L., *et al.* (2012) The Biology and Life-Cycle of Human Papillomaviruses. **Vaccine**, 30: F55–F70

Dostatni, N., Lambert, P.F., Sousa, R., *et al.* (1991) The Functional Bpv-1 E2 Trans-Activating Protein Can Act as a Repressor by Preventing Formation of the Initiation

Complex. **Genes & development**, 5 (9): 1657–1671

Doyle, D.A., Lee, A., Lewis, J., *et al.* (1996) Crystal structures of a complexed and peptide-free membrane protein-binding domain: molecular basis of peptide recognition by PDZ. **Cell**, 85 (7): 1067–1076

Du, J., Näsman, A., Carlson, J.W., *et al.* (2011) Prevalence of Human Papillomavirus (HPV) types in cervical cancer 2003-2008 in Stockholm, Sweden, before public HPV vaccination. **Acta oncologica (Stockholm, Sweden)**, 50 (8): 1215–1219

Du, M.J., Fan, X.L., Hanada, T., *et al.* (2005) Association of cottontail rabbit papillomavirus E6 oncoproteins with the hDlg/SAP97 tumor suppressor. **Journal of cellular biochemistry**, 94 (5): 1038–1045

Duffy, C.L., Phillips, S.L. and Klingelhutz, A.J. (2003) Microarray analysis identifies differentiation-associated genes regulated by human papillomavirus type 16 E6. **Virology**, 314 (1): 196–205

Durst, M., Gallahan, D., Jay, G., *et al.* (1989) Glucocorticoid-enhanced neoplastic transformation of human keratinocytes by human papillomavirus type 16 and an activated ras oncogene. **Virology**, 173 (2): 767–771

Dyson, N., Howley, P.M., Münger, K., *et al.* (1989) The human papilloma virus-16 E7 oncoprotein is able to bind to the retinoblastoma gene product. **Science**, 243 (4893): 934–937

Ellencrona, K., Syed, A. and Johansson, M. (2009) Flavivirus NS5 associates with host-cell proteins zonula occludens-1 (ZO-1) and regulating synaptic membrane exocytosis-2 (RIMS2) via an internal PDZ binding mechanism. **Biological chemistry**, 390 (4): 319–323

Facciuto, F., Bugnon Valdano, M., Marziali, F., *et al.* (2014) Human papillomavirus (HPV)-18 E6 oncoprotein interferes with the epithelial cell polarity Par3 protein. **Molecular oncology**, 8 (3): 533–543

Facciuto, F., Cavatorta, A.L., Valdano, M.B., *et al.* (2012) Differential expression of PDZ domain-containing proteins in human diseases - challenging topics and novel issues. **The FEBS journal**, 279 (19): 3538–3548

Fakhry, C., Westra, W.H., Li, S., *et al.* (2008) Improved survival of patients with human papillomavirus-positive head and neck squamous cell carcinoma in a prospective clinical trial. **Journal of the National Cancer Institute**, 100 (4): 261–269

Fan, J.-S. and Zhang, M. (2002) Signaling complex organization by PDZ domain proteins. **Neuro-Signals**, 11 (6): 315–321

Favre, B., Fontao, L., Koster, J., *et al.* (2001) The Hemidesmosomal Protein Bullous Pemphigoid Antigen 1 and the Integrin beta 4 Subunit Bind to ERBIN. **Journal of Biological Chemistry**, 276 (35): 32427–32436

Favre-Bonvin, A., Reynaud, C., Kretz-Remy, C., *et al.* (2005) Human papillomavirus type 18 E6 protein binds the cellular PDZ protein TIP-2/GIPC, which is involved in

transforming growth factor beta signaling and triggers its degradation by the proteasome. **Journal of Virology**, 79 (7): 4229–4237

Feldman, S. (2014) Human papillomavirus testing for primary cervical cancer screening: is it time to abandon Papanicolaou testing? **JAMA internal medicine**, 174 (10): 1539–1540

Feng, W., Wu, H., Chan, L.-N., *et al.* (2008) Par-3-mediated junctional localization of the lipid phosphatase PTEN is required for cell polarity establishment. **Journal of Biological Chemistry**, 283 (34): 23440–23449

Ferber, M.J., Thorland, E.C., Brink, A.A.T.P., *et al.* (2003) Preferential integration of human papillomavirus type 18 near the c-myc locus in cervical carcinoma. **Oncogene**, 22 (46): 7233–7242

Ferlay, J., Forman, D., Mathers, C.D., *et al.* (2012) Breast and cervical cancer in 187 countries between 1980 and 2010. **Lancet**, 379 (9824): 1390–1391

Fernandes, N. and Allbritton, N.L. (2009) Effect of the DEF motif on phosphorylation of peptide substrates by ERK. **Biochemical and Biophysical Research Communications**, 387 (2): 414–418

Filippova, M., Johnson, M.M., Bautista, M., *et al.* (2007) The large and small isoforms of human papillomavirus type 16 E6 bind to and differentially affect procaspase 8 stability and activity. **Journal of Virology**, 81 (8): 4116–4129

Filippova, M., Parkhurst, L. and Duerksen-Hughes, P.J. (2004) The human papillomavirus 16 E6 protein binds to Fas-associated death domain and protects cells from Fas-triggered apoptosis. **Journal of Biological Chemistry**, 279 (24): 25729–25744

Finnen, R.L., Erickson, K.D., Chen, X.S., *et al.* (2003) **Interactions between Papillomavirus L1 and L2 Capsid Proteins**. 77 (8): 4818–4826. Available from: <http://jvi.asm.org/content/77/8/4818.full>

Flicek, P., Amode, M.R., Barrell, D., *et al.* (2014) Ensembl 2014. **Nucleic acids research**, 42 (D1): D749–D755

Forman, D., de Martel, C., Lacey, C.J., *et al.* (2012) Global burden of human papillomavirus and related diseases. **Vaccine**, 30 Suppl 5: F12–23

Forouzanfar, M.H., Foreman, K.J., Delossantos, A.M., *et al.* (2011) Breast and cervical cancer in 187 countries between 1980 and 2010: a systematic analysis. **Lancet**, 378 (9801): 1461–1484

Fournane, S., Charbonnier, S., Chapelle, A., *et al.* (2011) Surface plasmon resonance analysis of the binding of high-risk mucosal HPV E6 oncoproteins to the PDZ1 domain of the tight junction protein MAGI-1. **Journal of molecular recognition : JMR**, 24 (4): 511–523

Francis, D.A., Schmid, S.I. and Howley, P.M. (2000) Repression of the integrated papillomavirus E6/E7 promoter is required for growth suppression of cervical cancer cells. **Journal of Virology**, 74 (6): 2679–2686

Frese, K., Latorre, I., Chung, S., *et al.* (2006) Oncogenic function for the Dlg1 mammalian homolog of the *Drosophila* discs-large tumor suppressor. **Embo Journal**, 25 (6): 1406–1417

Frese, K.K., Lee, S.S., Thomas, D.L., *et al.* (2003) Selective PDZ protein-dependent stimulation of phosphatidylinositol 3-kinase by the adenovirus E4-ORF1 oncoprotein. **Oncogene**, 22 (5): 710–721

Fu, J., Yan, P., Li, S., *et al.* (2010) Molecular determinants of PDLIM2 in suppressing HTLV-I Tax-mediated tumorigenesis. **Oncogene**, 29 (49): 6499–6507

Fuchs, P.G., Giradi, F. and Pfister, H. (1989) **Human Papillomavirus 16 Dna in Cervical Cancers and in Lymph-Nodes of Cervical-Cancer Patients - a Diagnostic Marker for Early Metastases**. 43 (1): 41–44

Fuja, T.J., Lin, F., Osann, K.E., *et al.* (2004) Somatic mutations and altered expression of the candidate tumor suppressors CSNK1 epsilon, DLG1, and EDD/hHYD in mammary ductal carcinoma. **Cancer research**, 64 (3): 942–951

Funk, J.O., Waga, S., Harry, J.B., *et al.* (1997) Inhibition of CDK activity and PCNA-dependent DNA replication by p21 is blocked by interaction with the HPV-16 E7 oncoprotein. **Genes & development**, 11 (16): 2090–2100

Gammoh, N., Isaacson, E., Tomaic, V., *et al.* (2009) Inhibition of HPV-16 E7 oncogenic activity by HPV-16 E2. **Oncogene**, 28 (23): 2299–2304

Ganzenmueller, T., Matthaei, M., Muench, P., *et al.* (2008) The E7 protein of the cottontail rabbit papillomavirus immortalizes normal rabbit keratinocytes and reduces pRb levels, while E6 cooperates in immortalization but neither degrades p53 nor binds E6AP. **Virology**, 372 (2): 313–324

Gao, L., Macara, I.G. and Joberty, G. (2002) Multiple splice variants of Par3 and of a novel related gene, Par3L, produce proteins with different binding properties. **Gene**, 294 (1-2): 99–107

Garcia-Mata, R., Dubash, A.D., Sharek, L., *et al.* (2007) The nuclear RhoA exchange factor Net1 interacts with proteins of the Dlg family, affects their localization, and influences their tumor suppressor activity. **Molecular and Cellular Biology**, 27 (24): 8683–8697

Gardiol, D., Kühne, C., Glaunsinger, B., *et al.* (1999) Oncogenic human papillomavirus E6 proteins target the discs large tumour suppressor for proteasome-mediated degradation. **Oncogene** [online], 18 (40): 5487–5496. Available from: <http://gateway.webofknowledge.com/gateway/Gateway.cgi?GWVersion=2&SrcAuth=me kentosj&SrcApp=Papers&DestLinkType=FullRecord&DestApp=WOS&KeyUT=000082894700001>

Gardiol, D., Zacchi, A., Petrer, F., *et al.* (2006) Human discs large and scrib are localized at the same regions in colon mucosa and changes in their expression patterns are correlated with loss of tissue architecture during malignant progression. **International Journal of Cancer**, 119 (6): 1285–1290

Gardner, L.A., Naren, A.P. and Bahouth, S.W. (2007) Assembly of an SAP97-AKAP79-cAMP-dependent protein kinase scaffold at the type 1 PSD-95/DLG/ZO1 motif of the human beta(1)-adrenergic receptor generates a receptosome involved in receptor recycling and networking. **Journal of Biological Chemistry**, 282 (7): 5085–5099

Gardoni, F., Mauceri, D., Fiorentini, C., *et al.* (2003) CaMKII-dependent phosphorylation regulates SAP97/NR2A interaction. **The Journal of Biological Chemistry**, 278 (45): 44745–44752

Gariglio, P., Gutierrez, J., Cortes, E., *et al.* (2009) The Role of Retinoid Deficiency and Estrogens as Cofactors in Cervical Cancer. **Archives of Medical Research**, 40 (6): 449–465

Gaudet, S., Branton, D. and Lue, R.A. (2000) Characterization of PDZ-binding kinase, a mitotic kinase. **Proceedings of the National Academy of Sciences of the United States of America**, 97 (10): 5167–5172

Gauson, E.J., Windle, B., Donaldson, M.M., *et al.* (2014) Regulation of human genome expression and RNA splicing by human papillomavirus 16 E2 protein. **Virology**, 468-470 (C): 10–18

Gee, S.H., Sekely, S.A., Lombardo, C., *et al.* (1998) Cyclic peptides as non-carboxyl-terminal ligands of syntrophin PDZ domains. **Journal of Biological Chemistry**, 273 (34): 21980–21987

Ghigna, C., Valacca, C. and Biamonti, G. (2008) Alternative Splicing and Tumor Progression. **Current Genomics**, 9 (8): 556–570

Giallourakis, C., Cao, Z., Green, T., *et al.* (2006) A molecular-properties-based approach to understanding PDZ domain proteins and PDZ ligands. **Genome research**, 16 (8): 1056–1072

Gillespie, K.A., Mehta, K.P., Laimins, L.A., *et al.* (2012) Human papillomaviruses recruit cellular DNA repair and homologous recombination factors to viral replication centers. **Journal of Virology**, 86 (17): 9520–9526

Gillison, M.L. and Shah, K.V. (2001) Human papillomavirus-associated head and neck squamous cell carcinoma: mounting evidence for an etiologic role for human papillomavirus in a subset of head and neck cancers. **Current Opinion in Oncology**, 13 (3): 183–188

Giroglou, T., Florin, L., Schäfer, F., *et al.* (2001) Human papillomavirus infection requires cell surface heparan sulfate. **Journal of Virology**, 75 (3): 1565–1570

Git, A., Dvinge, H., Salmon-Divon, M., *et al.* (2010) Systematic comparison of microarray profiling, real-time PCR, and next-generation sequencing technologies for measuring differential microRNA expression. **Rna-a Publication of the Rna Society**, 16 (5): 991–1006

Glaunsinger, B.A., Lee, S.S., Thomas, M., *et al.* (2000) Interactions of the PDZ-protein MAGI-1 with adenovirus E4-ORF1 and high-risk papillomavirus E6 oncoproteins.

**Oncogene**, 19 (46): 5270–5280

Glaunsinger, B.A., Weiss, R.S., Lee, S.S., *et al.* (2001) Link of the unique oncogenic properties of adenovirus type 9 E4-ORF1 to a select interaction with the candidate tumor suppressor protein ZO-2. **Embo Journal**, 20 (20): 5578–5586

Glondou-Lassis, M., Dromard, M., Lacroix-Triki, M., *et al.* (2010) PTPL1/PTPN13 regulates breast cancer cell aggressiveness through direct inactivation of Src kinase. **Cancer research**, 70 (12): 5116–5126

Godreau, D., Vranckx, R., Maguy, A., *et al.* (2003) Different isoforms of synapse-associated protein, SAP97, are expressed in the heart and have distinct effects on the voltage-gated K<sup>+</sup> channel Kv1.5. **The Journal of Biological Chemistry**, 278 (47): 47046–47052

Golebiewski, L., Liu, H., Javier, R.T., *et al.* (2011) The Avian Influenza Virus NS1 ESEV PDZ Binding Motif Associates with Dlg1 and Scribble To Disrupt Cellular Tight Junctions. **Journal of Virology**, 85 (20): 10639–10648

González-Mariscal, L., Tapia, R., Huerta, M., *et al.* (2009) The Tight Junction Protein ZO-2 Blocks Cell Cycle Progression and Inhibits Cyclin D1 Expression. **Annals of the New York Academy of Sciences**, 1165 (1): 121–125

Goodwin, E.C. and DiMaio, D. (2000) Repression of human papillomavirus oncogenes in HeLa cervical carcinoma cells causes the orderly reactivation of dormant tumor suppressor pathways. **Proceedings of the National Academy of Sciences of the United States of America**, 97 (23): 12513–12518

Gordón-Alonso, M., Rocha-Perugini, V., Álvarez, S., *et al.* (2012) The PDZ-adaptor protein syntenin-1 regulates HIV-1 entry. **Molecular Biology of the Cell**, 23 (12): 2253–2263

Graham, F.L., Rowe, D.T., McKinnon, R., *et al.* (1984) Transformation by human adenoviruses. **Journal of cellular physiology. Supplement**, 3: 151–163

Green, J., Berrington de Gonzalez, A., Sweetland, S., *et al.* (2003) Risk factors for adenocarcinoma and squamous cell carcinoma of the cervix in women aged 20-44 years: the UK National Case-Control Study of Cervical Cancer. **British journal of cancer**, 89 (11): 2078–2086

Greer, C.E., Wheeler, C.M., Ladner, M.B., *et al.* (1995) Human papillomavirus (HPV) type distribution and serological response to HPV type 6 virus-like particles in patients with genital warts. **Journal of clinical microbiology**, 33 (8): 2058–2063

Griep, A.E., Herber, R., Jeon, S., *et al.* (1993) Tumorigenicity by human papillomavirus type 16 E6 and E7 in transgenic mice correlates with alterations in epithelial cell growth and differentiation. **Journal of Virology**, 67 (3): 1373–1384

Grm, H.S. and Banks, L. (2004) Degradation of hDIg and MAGIs by human papillomavirus E6 is E6-AP-independent. **Journal of General Virology**, 85 (10): 2815–2819

Grossman, S.R. and Laimins, L.A. (1989) E6 protein of human papillomavirus type 18

binds zinc. **Oncogene**, 4 (9): 1089–1093

Guth, C.A. and Sodroski, J. (2014) Contribution of PDZD8 to stabilization of the human immunodeficiency virus type 1 capsid. **Journal of Virology**, 88 (9): 4612–4623

Gyongyosi, E., Szalmas, A., Ferenczi, A., *et al.* (2012) Effects of human papillomavirus (HPV) type 16 oncoproteins on the expression of involucrin in human keratinocytes. **Virol Journal**, 9 (1): 36

Hampson, L., Li, C., Oliver, A.W., *et al.* (2004) The PDZ protein Tip-1 is a gain of function target of the HPV16 E6 oncoprotein. **International journal of oncology**, 25 (5): 1249–1256

Hanada, N., Makino, K., Koga, H., *et al.* (2000) NE-dlg, a mammalian homolog of Drosophila dlg tumor suppressor, induces growth suppression and impairment of cell adhesion: possible involvement of down-regulation of beta-catenin by NE-dlg expression. **International Journal of Cancer**, 86 (4): 480–488

Hanada, T., Lin, L., Chandy, K.G., *et al.* (1997) Human homologue of the Drosophila discs large tumor suppressor binds to p56lck tyrosine kinase and Shaker type Kv1.3 potassium channel in T lymphocytes. **Journal of Biological Chemistry**, 272 (43): 26899–26904

Hanada, T., Takeuchi, A., Sondarva, G., *et al.* (2003) Protein 4.1-mediated membrane targeting of human discs large in epithelial cells. **The Journal of Biological Chemistry**, 278 (36): 34445–34450

Hanahan, D. and Weinberg, R.A. (2011) Hallmarks of cancer: the next generation. **Cell**, 144 (5): 646–674

Handa, K., Yugawa, T., Narisawa-Saito, M., *et al.* (2007) E6AP-dependent degradation of DLG4/PSD95 by high-risk human papillomavirus type 18 E6 protein. **Journal of Virology**, 81 (3): 1379–1389

Handa, Y., Durkin, C.H., Dodding, M.P., *et al.* (2013) Vaccinia Virus F11 Promotes Viral Spread by Acting as a PDZ-Containing Scaffolding Protein to Bind Myosin-9A and Inhibit RhoA Signaling. **Cell Host and Microbe**, 14 (1): 51–62

Hannon, G.J., Rivas, F.V., Murchison, E.P., *et al.* (2006) The expanding universe of noncoding RNAs. **Cold Spring Harbor symposia on quantitative biology**, 71 (0): 551–564

Hansson, B.G., Rosenquist, K., Antonsson, A., *et al.* (2005) Strong association between infection with human papillomavirus and oral and oropharyngeal squamous cell carcinoma: A population-based case-control study in southern Sweden. **Acta Oto-Laryngologica**, 125 (12): 1337–1344

Harper, D.M., Groner, J.A., Griffith, R.S., *et al.* (2013) RE: Annual Report to the Nation on the Status of Cancer, 1975-2009, Featuring the Burden and Trends in Human Papillomavirus (HPV)-Associated Cancers and HPV Vaccination Coverage Levels and RE: Inequalities in Human Papillomavirus (HPV)-Associated Cancers: Implications for the Success of HPV Vaccination. **Journal of the National Cancer Institute**, 105 (10): 749–

- Harper, J.M., Levine, A.J., Rosenthal, D.L., *et al.* (1994) Erythrocyte folate levels, oral contraceptive use and abnormal cervical cytology. **Acta cytologica**, 38 (3): 324–330
- Harper, J.W., Adami, G.R., Wei, N., *et al.* (1993) The p21 Cdk-interacting protein Cip1 is a potent inhibitor of G1 cyclin-dependent kinases. **Cell**, 75 (4): 805–816
- Harris, B.Z. and Lim, W.A. (2001) Mechanism and role of PDZ domains in signaling complex assembly. **Journal of Cell Science**, 114 (18): 3219–3231
- Harris, B.Z. and Senapathy, P. (1990) Distribution and Consensus of Branch Point Signals in Eukaryotic Genes - a Computerized Statistical-Analysis. **Nucleic acids research**, 18 (10): 3015–3019
- Harwood, C.A. and Proby, C.M. (2002) Human papillomaviruses and non-melanoma skin cancer. **Current opinion in infectious diseases**, 15 (2): 101–114
- Hausen, zur, H. (1999) Immortalization of human cells and their malignant conversion by high risk human papillomavirus genotypes. **Seminars in cancer biology**, 9 (6): 405–411
- Hausen, zur, H. (2002) Papillomaviruses and cancer: from basic studies to clinical application. **Nature Reviews Cancer**, 2 (5): 342–350
- Hausen, zur, H., Meinhof, W., Scheiber, W., *et al.* (1974) Attempts to detect virus-specific DNA in human tumors. I. Nucleic acid hybridizations with complementary RNA of human wart virus. **International Journal of Cancer**, 13 (5): 650–656
- Havard, L., Rahmouni, S., Boniver, J., *et al.* (2005) High levels of p105 (NFkB1) and p100 (NFkB2) proteins in HPV16-transformed keratinocytes: role of E6 and E7 oncoproteins. **Virology**, 331 (2): 357–366
- Hawley-Nelson, P., Vousden, K.H., Hubbert, N.L., *et al.* (1989) HPV16 E6 and E7 proteins cooperate to immortalize human foreskin keratinocytes. **Embo Journal**, 8 (12): 3905–3910
- He, J.Q., Lau, A.G., Yaffe, M.B., *et al.* (2001) Phosphorylation and cell cycle-dependent regulation of Na<sup>+</sup>/H<sup>+</sup> exchanger regulatory factor-1 by Cdc2 kinase. **Journal of Biological Chemistry**, 276 (45): 41559–41565
- Henken, F.E., De-Castro Arce, J., Rösl, F., *et al.* (2012) The functional role of Notch signaling in HPV-mediated transformation is dose-dependent and linked to AP-1 alterations. **Cellular Oncology**, 35 (2): 77–84
- Henning, M.S., Morham, S.G., Goff, S.P., *et al.* (2010) PDZD8 Is a Novel Gag-Interacting Factor That Promotes Retroviral Infection. **Journal of Virology**, 84 (17): 8990–8995
- Henning, M.S., Stiedl, P., Barry, D.S., *et al.* (2011) PDZD8 is a novel moesin-interacting cytoskeletal regulatory protein that suppresses infection by herpes simplex virus type 1. **Virology**, 415 (2): 114–121

Herber, R., Liem, A., Pitot, H., *et al.* (1996) Squamous epithelial hyperplasia and carcinoma in mice transgenic for the human papillomavirus type 16 E7 oncogene. **Journal of Virology**, 70 (3): 1873–1881

Herbst, L.H., Lenz, J., van Doorslaer, K., *et al.* (2009) Genomic characterization of two novel reptilian papillomaviruses, *Chelonia mydas* papillomavirus 1 and *Caretta caretta* papillomavirus 1. **Virology**, 383 (1): 131–135

Herfs, M., Yamamoto, Y., Laury, A., *et al.* (2012) A discrete population of squamocolumnar junction cells implicated in the pathogenesis of cervical cancer. **Proceedings of the National Academy of Sciences U.S.A.**, 109 (26): 10516–10521

Hernandez-Monge, J., Garay, E., Raya-Sandino, A., *et al.* (2013) Papillomavirus E6 oncoprotein up-regulates occludin and ZO-2 expression in ovariectomized mice epidermis. **Experimental Cell Research**, 319 (17): 2588–2603

Herrero, R., Castellsagué, X., Pawlita, M., *et al.* (2003) Human papillomavirus and oral cancer: the International Agency for Research on Cancer multicenter study. **Journal of the National Cancer Institute**, 95 (23): 1772–1783

Hibino, H., Inanobe, A., Tanemoto, M., *et al.* (2000) Anchoring proteins confer G protein sensitivity to an inward-rectifier K(+) channel through the GK domain. **Embo Journal**, 19 (1): 78–83

Hiebert, S.W., Chellappan, S.P., Horowitz, J.M., *et al.* (1992) The interaction of RB with E2F coincides with an inhibition of the transcriptional activity of E2F. **Genes & development**, 6 (2): 177–185

Higuchi, M., Tsubata, C., Kondo, R., *et al.* (2007) Cooperation of NF-kappaB2/p100 activation and the PDZ domain binding motif signal in human T-cell leukemia virus type 1 (HTLV-1) Tax1 but not HTLV-2 Tax2 is crucial for interleukin-2-independent growth transformation of a T-cell line. **Journal of Virology**, 81 (21): 11900–11907

Hildesheim, A., Reeves, W.C., Brinton, L.A., *et al.* (1990) Association of oral contraceptive use and human papillomaviruses in invasive cervical cancers. **International Journal of Cancer**, 45 (5): 860–864

Hillier, B.J., Christopherson, K.S., Prehoda, K.E., *et al.* (1999) Unexpected modes of PDZ domain scaffolding revealed by structure of nNOS-syntrophin complex. **Science**, 284 (5415): 812–815

Hirao, K., Hata, Y., Yao, I., *et al.* (2000) Three isoforms of synaptic scaffolding molecule and their characterization. Multimerization between the isoforms and their interaction with N-methyl-D-aspartate receptors and SAP90/PSD-95-associated protein. **Journal of Biological Chemistry**, 275 (4): 2966–2972

Hirata, A., Higuchi, M., Niinuma, A., *et al.* (2004) PDZ domain-binding motif of human T-cell leukemia virus type 1 Tax oncoprotein augments the transforming activity in a rat fibroblast cell line. **Virology**, 318 (1): 327–336

Holloway, A., Simmonds, M., Azad, A., *et al.* (2014) Resistance to UV-induced apoptosis by

$\beta$ -HPV5 E6 involves targeting of activated BAK for proteolysis by recruitment of the HERC1 ubiquitin ligase. **International Journal of Cancer**, pp. n/a–n/a

Horwitz, M.S. (2001) Adenovirus immunoregulatory genes and their cellular targets. **Virology**, 279 (1): 1–8

Hough, C.D., Woods, D.F., Park, S., *et al.* (1997) Organizing a functional junctional complex requires specific domains of the Drosophila MAGUK Discs large. **Genes & development**, 11 (23): 3242–3253

Howes, K.A., Ransom, N., Papermaster, D.S., *et al.* (1994) Apoptosis or retinoblastoma: alternative fates of photoreceptors expressing the HPV-16 E7 gene in the presence or absence of p53. **Genes & development**, 8 (11): 1300–1310

Howie, H.L., Katzenellenbogen, R.A. and Galloway, D.A. (2009) Papillomavirus E6 proteins. **Virology**, 384 (2): 324–334

Huang, Y.Z., Won, S., Ali, D.W., *et al.* (2000) Regulation of neuregulin signaling by PSD-95 interacting with ErbB4 at CNS synapses. **Neuron**, 26 (2): 443–455

Huber, M.A., Kraut, N. and Beug, H. (2005) Molecular requirements for epithelial-mesenchymal transition during tumor progression. **Current opinion in cell biology**, 17 (5): 548–558

Hudson, J.B., Bedell, M.A., McCance, D.J., *et al.* (1990) immortalization and altered differentiation of human keratinocytes in vitro by the E6 and E7 open reading frames of human papillomavirus type 18. **Journal of Virology**, 64 (2): 519–526

Huerta, M., Muñoz, R., Tapia, R., *et al.* (2007) Cyclin D1 is transcriptionally down-regulated by ZO-2 via an E box and the transcription factor c-Myc. **Molecular Biology of the Cell**, 18 (12): 4826–4836

Huh, K., Zhou, X., Hayakawa, H., *et al.* (2007) Human papillomavirus type 16 E7 oncoprotein associates with the cullin 2 ubiquitin ligase complex, which contributes to degradation of the retinoblastoma tumor suppressor. **Journal of Virology**, 81 (18): 9737–9747

Hui, S., Xing, X. and Bader, G.D. (2013) Predicting PDZ domain mediated protein interactions from structure. **Bmc Bioinformatics**, 14 (1)

Huibregtse, J.M., Scheffner, M. and Howley, P.M. (1993a) Cloning and expression of the cDNA for E6-AP, a protein that mediates the interaction of the human papillomavirus E6 oncoprotein with p53. **Molecular and Cellular Biology**, 13 (2): 775–784

Huibregtse, J.M., Scheffner, M. and Howley, P.M. (1993b) Localization of the E6-AP regions that direct human papillomavirus E6 binding, association with p53, and ubiquitination of associated proteins. **Molecular and Cellular Biology**, 13 (8): 4918–4927

Humbert, P., Russell, S. and Richardson, H. (2003) Dlg, Scribble and Lgl in cell polarity, cell proliferation and cancer. **BioEssays**, 25 (6): 542–553

Humbert, P.O., Grzeschik, N.A., Brumby, A.M., *et al.* (2012) The Scribble-Dlg-Lgl polarity module in development and cancer: from flies to man. **Cell Polarity and Cancer** [online], 53 (55): 6888–6907. Available from: <http://gateway.webofknowledge.com/gateway/Gateway.cgi?GWVersion=2&SrcAuth=me kentosj&SrcApp=Papers&DestLinkType=FullRecord&DestApp=WOS&KeyUT=000261108200003>

Hummel, M., Hudson, J.B. and Laimins, L.A. (1992) Differentiation-induced and constitutive transcription of human papillomavirus type 31b in cell lines containing viral episomes. **Journal of Virology**, 66 (10): 6070–6080

Hurlin, P.J., Kaur, P., Smith, P.P., *et al.* (1991) Progression of human papillomavirus type 18-immortalized human keratinocytes to a malignant phenotype. **Proceedings of the National Academy of Sciences of the United States of America**, 88 (2): 570–574

Hwang, S.G., Lee, D., Kim, J., *et al.* (2002) Human papillomavirus type 16 E7 binds to E2F1 and activates E2F1-driven transcription in a retinoblastoma protein-independent manner. **Journal of Biological Chemistry**, 277 (4): 2923–2930

Iñesta-Vaquera, F.A., Campbell, D.G., Arthur, J.S.C., *et al.* (2010) ERK5 pathway regulates the phosphorylation of tumour suppressor hDlg during mitosis. **Biochemical and Biophysical Research Communications**, 399 (1): 84–90

Ishidate, T., Matsumine, A., Toyoshima, K., *et al.* (2000) The APC-hDLG complex negatively regulates cell cycle progression from the G0/G1 to S phase. **Oncogene**, 19 (3): 365–372

Ishioka, K., Higuchi, M., Takahashi, M., *et al.* (2006) Inactivation of tumor suppressor Dlg1 augments transformation of a T-cell line induced by human T-cell leukemia virus type 1 Tax protein. **Retrovirology**, 3 (1)

Jackson, D., Hossain, M.J., Hickman, D., *et al.* (2008) A new influenza virus virulence determinant: The NS1 protein four C-terminal residues modulate pathogenicity. **Proceedings of the National Academy of Sciences of the United States of America**, 105 (11): 4381–4386

Jackson, S. and Storey, A. (2000) E6 proteins from diverse cutaneous HPV types inhibit apoptosis in response to UV damage. **Oncogene**, 19 (4): 592–598

James, M.A., Lee, J.H. and Klingelutz, A.J. (2006) Human papillomavirus type 16 E6 activates NF-kappa B, induces cIAP-2 expression, and protects against apoptosis in a PDZ binding motif-dependent manner. **Journal of Virology**, 80 (11): 5301–5307

Jan, Y.-J., Ko, B.-S., Liu, T.-A., *et al.* (2013) Expression of Partitioning Defective 3 (Par-3) for Predicting Extrahepatic Metastasis and Survival with Hepatocellular Carcinoma. **International Journal of Molecular Sciences**, 14 (1): 1684–1697

Jang, M.W., Yun, S.P., Park, J.H., *et al.* (2012) Cooperation of Epac1/Rap1/Akt and PKA in prostaglandin E(2) -induced proliferation of human umbilical cord blood derived mesenchymal stem cells: involvement of c-Myc and VEGF expression. **Journal of cellular**

**physiology**, 227 (12): 3756–3767

Javier, R.T. (2008) Cell polarity proteins: common targets for tumorigenic human viruses. **Oncogene**, 27 (55): 7031–7046

Javier, R.T. and Rice, A.P. (2011) Emerging Theme: Cellular PDZ Proteins as Common Targets of Pathogenic Viruses. **Journal of Virology**, 85 (22): 11544–11556

Jeckel, S., Huber, E., Stubenrauch, F., *et al.* (2002) A transactivator function of cottontail rabbit papillomavirus e2 is essential for tumor induction in rabbits. **Journal of Virology**, 76 (22): 11209–11215

Jeffrey, P.D., Russo, A.A., Polyak, K., *et al.* (1995) Mechanism of Cdk Activation Revealed by the Structure of a Cyclin-Cdk2 Complex. **Nature**, 376 (6538): 313–320

Jemal, A., Simard, E.P., Dorell, C., *et al.* (2013) Annual Report to the Nation on the Status of Cancer, 1975-2009, featuring the burden and trends in human papillomavirus(HPV)-associated cancers and HPV vaccination coverage levels. **Journal of the National Cancer Institute**, 105 (3): 175–201

Jeon, S. and Lambert, P.F. (1995) Integration of human papillomavirus type 16 DNA into the human genome leads to increased stability of E6 and E7 mRNAs: implications for cervical carcinogenesis. **Proceedings of the National Academy of Sciences of the United States of America**, 92 (5): 1654–1658

Jeon, S., Allen-Hoffmann, B.L. and Lambert, P.F. (1995) Integration of human papillomavirus type 16 into the human genome correlates with a selective growth advantage of cells. **Journal of Virology**, 69 (5): 2989–2997

Jeong, K.W., Kim, H.-Z., Kim, S., *et al.* (2007) Human papillomavirus type 16 E6 protein interacts with cystic fibrosis transmembrane regulator-associated ligand and promotes E6-associated protein-mediated ubiquitination and proteasomal degradation. **Oncogene**, 26 (4): 487–499

Jeyifous, O., LWaites, C., Specht, C.G., *et al.* (2009) SAP97 and CASK mediate sorting of NMDA receptors through a previously unknown secretory pathway. **Nature Neuroscience**, 12 (8): 1011–U81

Jha, S., Pol, S.V., Banerjee, N.S., *et al.* (2010) Destabilization of TIP60 by Human Papillomavirus E6 Results in Attenuation of TIP60-Dependent Transcriptional Regulation and Apoptotic Pathway. **Molecular Cell**, 38 (5): 700–711

Jimenez-Guardeño, J.M., Nieto-Torres, J.L., DeDiego, M.L., *et al.* (2014) The PDZ-Binding Motif of Severe Acute Respiratory Syndrome Coronavirus Envelope Protein Is a Determinant of Viral Pathogenesis. **PLoS Pathogens**, 10 (8): e1004320

Jing, M., Bohl, J., Brimer, N., *et al.* (2007) Degradation of tyrosine phosphatase PTPN3 (PTPH1) by association with oncogenic human papillomavirus E6 proteins. **Journal of Virology**, 81 (5): 2231–2239

Johansson, C., Somberg, M., Li, X., *et al.* (2012) HPV-16 E2 contributes to induction of

HPV-16 late gene expression by inhibiting early polyadenylation. **Embo Journal**

Johnson, K.M., Kines, R.C., Roberts, J.N., *et al.* (2009) **Role of Heparan Sulfate in Attachment to and Infection of the Murine Female Genital Tract by Human Papillomavirus.** 83 (5): 2067–2074. Available from: <http://jvi.asm.org/content/83/5/2067.full>

Johnson, M., Zaretskaya, I., Raytselis, Y., *et al.* (2008) NCBIBLAST: a better web interface. **Nucleic acids research**, 36 (Web Server issue): W5–W9

Jones, D.L. and Münger, K. (1997) Analysis of the p53-mediated G1 growth arrest pathway in cells expressing the human papillomavirus type 16 E7 oncoprotein. **Journal of Virology**, 71 (4): 2905–2912

Jones, S.J., Dicker, A.J., Dahler, A.L., *et al.* (1997) E2F as a regulator of keratinocyte proliferation: implications for skin tumor development. **The Journal of investigative dermatology**, 109 (2): 187–193

Joyce, J.G., Tung, J.S., Przysiecki, C.T., *et al.* (1999) The L1 major capsid protein of human papillomavirus type 11 recombinant virus-like particles interacts with heparin and cell-surface glycosaminoglycans on human keratinocytes. **The Journal of Biological Chemistry**, 274 (9): 5810–5822

Kadaja, M., Isok-Paas, H., Laos, T., *et al.* (2009) Mechanism of genomic instability in cells infected with the high-risk human papillomaviruses. **PLoS Pathogens**, 5 (4): e1000397

Kajitani, N., Satsuka, A., Kawate, A., *et al.* (2012) Productive lifecycle of human papillomaviruses that depends upon squamous epithelial differentiation. **Frontiers in Microbiology**, 3

Kanda, T., Furuno, A. and Yoshiike, K. (1988) Human papillomavirus type 16 open reading frame E7 encodes a transforming gene for rat 3Y1 cells. **Journal of Virology**, 62 (2): 610–613

Karstensen, B., Poppelreuther, S., Bonin, M., *et al.* (2006) Gene expression profiles reveal an upregulation of E2F and downregulation of interferon targets by HPV18 but no changes between keratinocytes with integrated or episomal viral genomes. **Virology**, 353 (1): 200–209

Karthikeyan, S., Leung, T., Birrane, G., *et al.* (2001) Crystal structure of the PDZ1 domain of human Na(+)/H(+) exchanger regulatory factor provides insights into the mechanism of carboxyl-terminal leucine recognition by class I PDZ domains. **Journal of Molecular Biology**, 308 (5): 963–973

Kaur, P. and McDougall, J.K. (1988) Characterization of primary human keratinocytes transformed by human papillomavirus type 18. **Journal of Virology**, 62 (6): 1917–1924

Kemphues, K.J., Priess, J.R., Morton, D.G., *et al.* (1988) Identification of genes required for cytoplasmic localization in early *C. elegans* embryos. **Cell**, 52 (3): 311–320

Kho, E.-Y., Wang, H.-K., Banerjee, N.S., *et al.* (2013) HPV-18 E6 mutants reveal p53

modulation of viral DNA amplification in organotypic cultures. **Proceedings of the National Academy of Sciences U.S.A.**

Kim, E., Naisbitt, S., Hsueh, Y.P., *et al.* (1997) GKAP, a novel synaptic protein that interacts with the guanylate kinase-like domain of the PSD-95/SAP90 family of channel clustering molecules. **Journal of Cell Biology**, 136 (3): 669–678

Kim, E., Niethammer, M., Rothschild, A., *et al.* (1995) Clustering of Shaker-type K<sup>+</sup> channels by interaction with a family of membrane-associated guanylate kinases. **Nature**, 378 (6552): 85–88

Kim, H., Abd Elmageed, Z.Y., Davis, C., *et al.* (2014) Correlation between PDZK1, Cdc37, Akt and Breast Cancer Malignancy: The Role of PDZK1 in Cell Growth through Akt Stabilization by Increasing and Interacting with Cdc37. **Molecular medicine (Cambridge, Mass.)**, 20 (1): 270–279

Kim, J.-H., Kushihiro, K., Graham, N.A., *et al.* (2009) Tunable interplay between epidermal growth factor and cell-cell contact governs the spatial dynamics of epithelial growth. **Proceedings of the National Academy of Sciences U.S.A.**, 106 (27): 11149–11153

Kines, R.C., Thompson, C.D., Lowy, D.R., *et al.* (2009) The initial steps leading to papillomavirus infection occur on the basement membrane prior to cell surface binding. **Proceedings of the National Academy of Sciences of the United States of America**, 106 (48): 20458–20463

Kiraly, D.D., Stone, K.L., Colangelo, C.M., *et al.* (2011) Identification of kalirin-7 as a potential post-synaptic density signaling hub. **Journal of proteome research**, 10 (6): 2828–2841

Kirnbauer, R., TAUB, J., GREENSTONE, H., *et al.* (1993) Efficient Self-Assembly of Human Papillomavirus Type-16 L1 and L1-L2 Into Virus-Like Particles. **Journal of Virology**, 67 (12): 6929–6936

Kiyono, T., Foster, S.A., Koop, J.I., *et al.* (1998) Both Rb/p16INK4a inactivation and telomerase activity are required to immortalize human epithelial cells. **Nature**, 396 (6706): 84–88

Kiyono, T., Hiraiwa, A., Fujita, M., *et al.* (1997) Binding of high-risk human papillomavirus E6 oncoproteins to the human homologue of the Drosophila discs large tumor suppressor protein. **Proceedings of the National Academy of Sciences of the United States of America**, 94 (21): 11612–11616

Kjellberg, L., Hallmans, G., Ahren, A.M., *et al.* (2000) Smoking, diet, pregnancy and oral contraceptive use as risk factors for cervical intra-epithelial neoplasia in relation to human papillomavirus infection. **British journal of cancer**, 82 (7): 1332–1338

Klocker, N., Bunn, R.C., Schnell, E., *et al.* (2002) Synaptic glutamate receptor clustering in mice lacking the SH3 and GK domains of SAP97. **The European journal of neuroscience**, 16 (8): 1517–1522

Knight, G.L., Grainger, J.R., Gallimore, P.H., *et al.* (2004) Cooperation between different

forms of the human papillomavirus type 1 E4 protein to block cell cycle progression and cellular DNA synthesis. **Journal of Virology**, 78 (24): 13920–13933

Knight, G.L., Pugh, A.G., Yates, E., *et al.* (2011) A cyclin-binding motif in human papillomavirus type 18 (HPV18) E1<sup>E4</sup> is necessary for association with CDK-cyclin complexes and G2/M cell cycle arrest of keratinocytes, but is not required for differentiation-dependent viral genome amplification or L1 capsid protein expression. **Virology**, 412 (1): 196–210

Knust, E. and Bossinger, O. (2002) Composition and formation of intercellular junctions in epithelial cells. **Science**, 298 (5600): 1955–1959

Koh, Y.H., Popova, E., Thomas, U., *et al.* (1999) Regulation of DLG localization at synapses by CaMKII-dependent phosphorylation. **Cell**, 98 (3): 353–363

Kohu, K., Ogawa, F. and Akiyama, T. (2002) The SH3, HOOK and guanylate kinase-like domains of hDLG are important for its cytoplasmic localization. **Genes to Cells**, 7 (7): 707–715

Kong, K., Kumar, M., Taruishi, M., *et al.* (2014) The Human Adenovirus E4-ORF1 Protein Subverts Discs Large 1 to Mediate Membrane Recruitment and Dysregulation of Phosphatidylinositol 3-Kinase. **PLoS Pathogens**, 10 (5): e1004102

Kornau, H.C., Schenker, L.T., Kennedy, M.B., *et al.* (1995) Domain interaction between NMDA receptor subunits and the postsynaptic density protein PSD-95. **Science**, 269 (5231): 1737–1740

Kotelevets, L., van Hengel, J., Bruyneel, E., *et al.* (2005) Implication of the MAGI-1b/PTEN signalosome in stabilization of adherens junctions and suppression of invasiveness. **FASEB journal : official publication of the Federation of American Societies for Experimental Biology**, 19 (1): 115–117

Kranjec, C. and Banks, L. (2011) A Systematic Analysis of Human Papillomavirus (HPV) E6 PDZ Substrates Identifies MAGI-1 as a Major Target of HPV Type 16 (HPV-16) and HPV-18 Whose Loss Accompanies Disruption of Tight Junctions. **Journal of Virology**, 85 (4): 1757–1764

Kranjec, C., Massimi, P. and Banks, L. (2014) Restoration of MAGI-1 Expression in HPV Positive Tumour Cells Induces Cell Growth Arrest and Apoptosis. **Journal of Virology**, 88 (13): 7155–7169

Kreimer, A.R., Clifford, G.M., Boyle, P., *et al.* (2005a) Human papillomavirus types in head and neck squamous cell carcinomas worldwide: a systematic review. **Cancer epidemiology, biomarkers & prevention : a publication of the American Association for Cancer Research, cosponsored by the American Society of Preventive Oncology**, 14 (2): 467–475

Kreimer, A.R., Clifford, G.M., Snijders, P.J.F., *et al.* (2005b) HPV16 semiquantitative viral load and serologic biomarkers in oral and oropharyngeal squamous cell carcinomas. **International Journal of Cancer**, 115 (2): 329–332

- Kuhlendahl, S., Spangenberg, O., Konrad, M., *et al.* (1998) Functional analysis of the guanylate kinase-like domain in the synapse-associated protein SAP97. **European journal of biochemistry / FEBS**, 252 (2): 305–313
- Kumar, A., Zhao, Y., Meng, G., *et al.* (2002) Human papillomavirus oncoprotein E6 inactivates the transcriptional coactivator human ADA3. **Molecular and Cellular Biology**, 22 (16): 5801–5812
- Kumar, M., Kong, K. and Javier, R.T. (2014) Hijacking Discs Large 1 for Oncogenic Phosphatidylinositol 3-Kinase Activation in Human Epithelial Cells Is a Conserved Mechanism of Human Adenovirus E4-ORF1 Proteins. **Journal of Virology**, 88 (24): 14268–14277
- Kumar, M., Liu, H. and Rice, A.P. (2012) Regulation of interferon- $\beta$  by MAGI-1 and its interaction with influenza A virus NS1 protein with ESEV PBM. **PLoS ONE**, 7 (7): e41251
- Kühne, C., Gardiol, D., Guarnaccia, C., *et al.* (2000) Differential regulation of human papillomavirus E6 by protein kinase A: conditional degradation of human discs large protein by oncogenic E6. **Oncogene**, 19 (51): 5884–5891
- Lacey, C.J.N. (2005) Therapy for genital human papillomavirus-related disease. **Journal of clinical virology : the official publication of the Pan American Society for Clinical Virology**, 32 Suppl 1: S82–90
- Lambert, P.F. (1991) Papillomavirus Dna-Replication. **Journal of Virology**, 65 (7): 3417–3420
- Laprise, P., Viel, A. and Rivard, N. (2004) Human homolog of disc-large is required for adherens junction assembly and differentiation of human intestinal epithelial cells. **Journal of Biological Chemistry**, 279 (11): 10157–10166
- Larkin, M.A., Blackshields, G., Brown, N.P., *et al.* (2007) Clustal W and clustal X version 2.0. **Bioinformatics**, 23 (21): 2947–2948
- Lassen, P., Eriksen, J.G., Krogdahl, A., *et al.* (2011) The influence of HPV-associated p16-expression on accelerated fractionated radiotherapy in head and neck cancer: Evaluation of the randomised DAHANCA 6&7 trial. **Radiotherapy and oncology : journal of the European Society for Therapeutic Radiology and Oncology**, 100 (1): 49–55
- Latorre, I.J., Roh, M.H., Frese, K.K., *et al.* (2005) Viral oncoprotein-induced mislocalization of select PDZ proteins disrupts tight junctions and causes polarity defects in epithelial cells. **Journal of Cell Science**, 118 (Pt 18): 4283–4293
- Laura, R.P., Ross, S., Koeppen, H., *et al.* (2002) MAGI-1: a widely expressed, alternatively spliced tight junction protein. **Experimental Cell Research**, 275 (2): 155–170
- Lavezzari, G., McCallum, J., Lee, R., *et al.* (2003) Differential binding of the AP-2 adaptor complex and PSD-95 to the C-terminus of the NMDA receptor subunit NR2B regulates surface expression. **Neuropharmacology**, 45 (6): 729–737

- Lazarczyk, M., Dalard, C., Hayder, M., *et al.* (2012) EVER proteins, key elements of the natural anti-human papillomavirus barrier, are regulated upon T-cell activation. **PLoS ONE**, 7 (6): e39995
- Lazarczyk, M., Pons, C., Mendoza, J.-A., *et al.* (2008) Regulation of cellular zinc balance as a potential mechanism of EVER-mediated protection against pathogenesis by cutaneous oncogenic human papillomaviruses. **Journal of Experimental Medicine**, 205 (1): 35–42
- Lazic, D., Hufbauer, M., Zigrino, P., *et al.* (2012) Human Papillomavirus Type 8 E6 Oncogene Inhibits Transcription of the PDZ-Protein Syntenin-2. **Journal of Virology**
- Le Buanec, H., D'Anna, R., Lachgar, A., *et al.* (1999) HPV-16 E7 but not E6 oncogenic protein triggers both cellular immunosuppression and angiogenic processes. **Biomedicine & pharmacotherapy = Biomédecine & pharmacothérapie**, 53 (9): 424–431
- Lechler, T. and Fuchs, E. (2005) Asymmetric cell divisions promote stratification and differentiation of mammalian skin. **Nature**, 437 (7056): 275–280
- Lechner, M.S. and Laimins, L.A. (1994) Inhibition of p53 DNA binding by human papillomavirus E6 proteins. **Journal of Virology**, 68 (7): 4262–4273
- Lee, C. and Laimins, L.A. (2004) Role of the PDZ domain-binding motif of the oncoprotein E6 in the pathogenesis of human papillomavirus type 31. **Journal of Virology**, 78 (22): 12366–12377
- Lee, H.-S., Nishanian, T.G., Mood, K., *et al.* (2008) EphrinB1 controls cell-cell junctions through the Par polarity complex. **Nature cell biology**, 10 (8): 979–986
- Lee, S., Fan, S.L., Makarova, Y., *et al.* (2002) A novel and conserved protein-protein interaction domain of mammalian Lin-2/CASK binds and recruits SAP97 to the lateral surface of epithelia. **Molecular and Cellular Biology**, 22 (6): 1778–1791
- Lee, S., Glaunsinger, B., Mantovani, F., *et al.* (2000) Multi-PDZ domain protein MUPP1 is a cellular target for both adenovirus E4-ORF1 and high-risk papillomavirus type 18 E6 oncoproteins. **Journal of Virology**, 74 (20): 9680–9693
- Lee, S.S., Weiss, R.S. and Javier, R.T. (1997) Binding of human virus oncoproteins to hDlg/SAP97, a mammalian homolog of the Drosophila discs large tumor suppressor protein. **Proceedings of the National Academy of Sciences of the United States of America**, 94 (13): 6670–6675
- Lehman, C.W. and Botchan, M.R. (1998) Segregation of viral plasmids depends on tethering to chromosomes and is regulated by phosphorylation. **Proceedings of the National Academy of Sciences of the United States of America**, 95 (8): 4338–4343
- Lemmers, C. (2002) hINAD1/PATJ, a Homolog of Discs Lost, Interacts with Crumbs and Localizes to Tight Junctions in Human Epithelial Cells. **Journal of Biological Chemistry**, 277 (28): 25408–25415
- Leonard, A.S., Davare, M.A., Horne, M.C., *et al.* (1998) SAP97 is associated with the alpha-amino-3-hydroxy-5-methylisoxazole-4-propionic acid receptor GluR1 subunit. **Journal of**

**Biological Chemistry**, 273 (31): 19518–19524

Leverrier, S., Bergamaschi, D., Ghali, L., *et al.* (2007) Role of HPV E6 proteins in preventing UVB-induced release of pro-apoptotic factors from the mitochondria. **Apoptosis : an international journal on programmed cell death**, 12 (3): 549–560

Li, N., Franceschi, S., Howell-Jones, R., *et al.* (2011) Human papillomavirus type distribution in 30,848 invasive cervical cancers worldwide: Variation by geographical region, histological type and year of publication. **International Journal of Cancer**, 128 (4): 927–935

Li, Z., Jiang, Y., Jiao, P., *et al.* (2006) The NSI gene contributes to the virulence of H5N1 avian influenza viruses. **Journal of Virology**, 80 (22): 11115–11123

Liang, X.H., Volkman, M., Klein, R., *et al.* (1993) Colocalization of the Tumor-Suppressor Protein P53 and Human Papillomavirus-E6 Protein in Human Cervical-Carcinoma Cell-Lines. **Oncogene**, 8 (10): 2645–2652

Liaw, K.L., Glass, A.G., Manos, M.M., *et al.* (1999) Detection of human papillomavirus DNA in cytologically normal women and subsequent cervical squamous intraepithelial lesions. **Journal of the National Cancer Institute**, 91 (11): 954–960

Lichtig, H., Gilboa, D.A., Jackman, A., *et al.* (2010) HPV16 E6 augments Wnt signaling in an E6AP-dependent manner. **Virology**, 396 (1): 47–58

Lin, E.I., Jeyifous, O. and Green, W.N. (2013) CASK Regulates SAP97 Conformation and Its Interactions with AMPA and NMDA Receptors. **The Journal of neuroscience : the official journal of the Society for Neuroscience**, 33 (29): 12067–12076

Lin, H.-T., Steller, M.A., Aish, L., *et al.* (2004) Differential expression of human Dlg in cervical intraepithelial neoplasias. **Gynecologic oncology**, 93 (2): 422–428

Lipari, F., McGibbon, G.A., Wardrop, E., *et al.* (2001) Purification and biophysical characterization of a minimal functional domain and of an N-terminal Zn<sup>2+</sup>-binding fragment from the human papillomavirus type 16 E6 protein. **Biochemistry**, 40 (5): 1196–1204

Liu, H., Golebiewski, L., Dow, E.C., *et al.* (2010) The ESEV PDZ-Binding Motif of the Avian Influenza A Virus NS1 Protein Protects Infected Cells from Apoptosis by Directly Targeting Scribble. **Journal of Virology**, 84 (21): 11164–11174

Liu, Y., Henry, G.D., Hegde, R.S., *et al.* (2007) Solution Structure of the hDlg/SAP97 PDZ2 Domain and Its Mechanism of Interaction with HPV-18 Papillomavirus E6 Protein †,‡. **Biochemistry**, 46 (38): 10864–10874

Livak, K.J. and Schmittgen, T.D. (2001) Analysis of relative gene expression data using real-time quantitative PCR and the 2<sup>-</sup>(-Delta Delta C(T)) Method. **Methods (San Diego, Calif.)**, 25 (4): 402–408

Lochner, A. and Moolman, J.A. (2006) The many faces of H89: a review. **Cardiovascular drug reviews**, 24 (3-4): 261–274

- Lockwood, C.A., Lynch, A.M. and Hardin, J. (2008) Dynamic analysis identifies novel roles for DLG-1 subdomains in AJM-1 recruitment and LET-413-dependent apical focusing. **Journal of Cell Science**, 121 (Pt 9): 1477–1487
- Lodewick, J., Lamsoul, I., Polania, A., *et al.* (2009) Acetylation of the human T-cell leukemia virus type 1 Tax oncoprotein by p300 promotes activation of the NF-kappaB pathway. **Virology**, 386 (1): 68–78
- Lodewick, J., Sampaio, C., Boxus, M., *et al.* (2013) Acetylation at lysine 346 controls the transforming activity of the HTLV-1 Tax oncoprotein in the Rat-1 fibroblast model. **Retrovirology**, 10 (1): 75
- Longworth, M.S. and Laimins, L.A. (2004a) Pathogenesis of human papillomaviruses in differentiating epithelia. **Microbiology and molecular biology reviews : MMBR**, 68 (2): 362–372
- Longworth, M.S. and Laimins, L.A. (2004b) The binding of histone deacetylases and the integrity of zinc finger-like motifs of the E7 protein are essential for the life cycle of human papillomavirus type 31. **Journal of Virology**, 78 (7): 3533–3541
- Longworth, M.S., Wilson, R. and Laimins, L.A. (2005) HPV31 E7 facilitates replication by activating E2F2 transcription through its interaction with HDACs. **Embo Journal**, 24 (10): 1821–1830
- Lowy, D.R. and Schiller, J.T. (2012) Reducing HPV-Associated Cancer Globally. **Cancer Prevention Research**, 5 (1): 18–23
- Lozovatsky, L., Abayasekara, N., Piawah, S., *et al.* (2009) CASK deletion in intestinal epithelia causes mislocalization of LIN7C and the DLG1/Scrib polarity complex without affecting cell polarity. **Molecular Biology of the Cell**, 20 (21): 4489–4499
- Lu, Q., Sun, E.E., Klein, R.S., *et al.* (2001) Ephrin-B reverse signaling is mediated by a novel PDZ-RGS protein and selectively inhibits G protein-coupled chemoattraction. **Cell**, 105 (1): 69–79
- Ludford-Menting, M.J., Oliaro, J., Sacirbegovic, F., *et al.* (2005) A network of PDZ-containing proteins regulates T cell polarity and morphology during migration and immunological synapse formation. **Immunity**, 22 (6): 737–748
- Lue, R.A., Brandin, E., Chan, E.P., *et al.* (1996) Two independent domains of hDlg are sufficient for subcellular targeting: the PDZ1-2 conformational unit and an alternatively spliced domain. **Journal of Cell Biology**, 135 (4): 1125–1137
- Lue, R.A., Marfatia, S.M., Branton, D., *et al.* (1994) Cloning and characterization of hdlg: the human homologue of the Drosophila discs large tumor suppressor binds to protein 4.1. **Proceedings of the National Academy of Sciences of the United States of America**, 91 (21): 9818–9822
- Majewski, S. and Jablonska, S. (2002) Human papillomavirus and oncogenesis: critical evaluation of recent findings. **International journal of dermatology**, 41 (6): 319–320

- Majewski, S. and Jabłońska, S. (1995) Epidermodysplasia verruciformis as a model of human papillomavirus-induced genetic cancer of the skin. **Archives of dermatology**, 131 (11): 1312–1318
- Makino, K., Kuwahara, H., Masuko, N., *et al.* (1997) Cloning and characterization of NE-dlg: a novel human homolog of the Drosophila discs large (dlg) tumor suppressor protein interacts with the APC protein. **Oncogene**, 14 (20): 2425–2433
- Manneville, J.-B., Jehanno, M. and Etienne-Manneville, S. (2010) Dlg1 binds GKAP to control dynein association with microtubules, centrosome positioning, and cell polarity. **The Journal of Cell Biology**, 191 (3): 585–598
- Mantovani, F. and Banks, L. (2001) The human papillomavirus E6 protein and its contribution to malignant progression. **Oncogene**, 20 (54): 7874–7887
- Mantovani, F., Massimi, P. and Banks, L. (2001) Proteasome-mediated regulation of the hDIg tumour suppressor protein. **Journal of Cell Science**, 114 (23): 4285–4292
- Martinez, I., Gardiner, A.S., Board, K.F., *et al.* (2008) Human papillomavirus type 16 reduces the expression of microRNA-218 in cervical carcinoma cells. **Oncogene**, 27 (18): 2575–2582
- Marur, S., D'Souza, G., Westra, W.H., *et al.* (2010) HPV-associated head and neck cancer: a virus-related cancer epidemic. **The lancet oncology**, 11 (8): 781–789
- Massimi, P., Gammoh, N., Thomas, M., *et al.* (2004) HPV E6 specifically targets different cellular pools of its PDZ domain-containing tumour suppressor substrates for proteasome-mediated degradation. **Oncogene**, 23 (49): 8033–8039
- Massimi, P., Narayan, N., Cuenda, A., *et al.* (2006) Phosphorylation of the discs large tumour suppressor protein controls its membrane localisation and enhances its susceptibility to HPV E6-induced degradation. **Oncogene**, 25 (31): 4276–4285
- Massimi, P., Shai, A., Lambert, P., *et al.* (2008) HPV E6 degradation of p53 and PDZ containing substrates in an E6AP null background. **Oncogene**, 27 (12): 1800–1804
- Masson, M., Hindelang, C., Sibler, A.P., *et al.* (2003) Preferential nuclear localization of the human papillomavirus type 16 E6 oncoprotein in cervical carcinoma cells. **Journal of General Virology**, 84 (Pt 8): 2099–2104
- Matsuda, S., Mikawa, S. and Hirai, H. (1999) Phosphorylation of serine-880 in GluR2 by protein kinase C prevents its C terminus from binding with glutamate receptor-interacting protein. **Journal of Neurochemistry**, 73 (4): 1765–1768
- Matsumine, A., Ogai, A., Senda, T., *et al.* (1996) Binding of APC to the human homolog of the Drosophila discs large tumor suppressor protein. **Science**, 272 (5264): 1020–1023
- Mauceri, D., Gardoni, F., Marcello, E., *et al.* (2007) Dual role of CaMKII-dependent SAP97 phosphorylation in mediating trafficking and insertion of NMDA receptor subunit NR2A. **Journal of Neurochemistry**, 100 (4): 1032–1046

- Maufort, J.P., Shai, A., Pitot, H.C., *et al.* (2010) A role for HPV16 E5 in cervical carcinogenesis. **Cancer research**, 70 (7): 2924–2931
- Maufort, J.P., Williams, S.M.G., Pitot, H.C., *et al.* (2007) Human papillomavirus 16 E5 oncogene contributes to two stages of skin carcinogenesis. **Cancer research**, 67 (13): 6106–6112
- McBride, A.A. (2008) Replication and Partitioning of Papillomavirus Genomes. **Advances in Virus Research**, Vol 72, 72: 155–205
- McCance, D.J., Kopan, R., Fuchs, E., *et al.* (1988) Human papillomavirus type 16 alters human epithelial cell differentiation in vitro. **Proceedings of the National Academy of Sciences of the United States of America**, 85 (19): 7169–7173
- McKenna, D.J., Patel, D. and McCance, D.J. (2014) miR-24 and miR-205 expression is dependent on HPV onco-protein expression in keratinocytes. **Virology**, 448: 210–216
- McLaughlin, M., Hale, R., Ellston, D., *et al.* (2002) The Distribution and Function of Alternatively Spliced Insertions in hDlg. **Journal of Biological Chemistry**, 277 (8): 6406–6412
- McLaughlin-Drubin, M.E. and Meyers, C. (2004) Evidence for the coexistence of two genital HPV types within the same host cell in vitro. **Virology**, 321 (2): 173–180
- Mee, C.J., Farquhar, M.J., Harris, H.J., *et al.* (2010) Hepatitis C virus infection reduces hepatocellular polarity in a vascular endothelial growth factor-dependent manner. **Gastroenterology**, 138 (3): 1134–1142
- Mehanna, H., Beech, T., Nicholson, T., *et al.* (2012) Prevalence of human papillomavirus in oropharyngeal and nonoropharyngeal head and neck cancer-systematic review and meta-analysis of trends by time and region Eisele, D.W. (ed.). **Head & Neck**, 35 (5): n/a–n/a
- Melik, W., Ellenrona, K., Wigerius, M., *et al.* (2012) Two PDZ binding motifs within NS5 have roles in Tick-borne encephalitis virus replication. **Virus Research**, 169 (1): 54–62
- Mendoza, C., Olguin, P., Lafferte, G., *et al.* (2003) Novel isoforms of Dlg are fundamental for neuronal development in *Drosophila*. **The Journal of neuroscience : the official journal of the Society for Neuroscience**, 23 (6): 2093–2101
- Mendoza-Topaz, C., Urra, F., Barria, R., *et al.* (2008) DLGS97/SAP97 is developmentally upregulated and is required for complex adult behaviors and synapse morphology and function. **The Journal of neuroscience : the official journal of the Society for Neuroscience**, 28 (1): 304–314
- Meyer, T., Arndt, R., Christophers, E., *et al.* (2001) Importance of human papillomaviruses for the development of skin cancer. **Cancer detection and prevention**, 25 (6): 533–547
- Meyers, C. and Laimins, L.A. (1994) In vitro systems for the study and propagation of human papillomaviruses. **Current topics in microbiology and immunology**, 186: 199–215

- Meyers, J.M., Spangle, J.M. and Münger, K. (2013) The human papillomavirus type 8 E6 protein interferes with NOTCH activation during keratinocyte differentiation. **Journal of Virology**, 87 (8): 4762–4767
- Mischo, A., Ohlenschläger, O., Hortschansky, P., *et al.* (2013) Structural insights into a wildtype domain of the oncoprotein E6 and its interaction with a PDZ domain. **PLoS ONE**, 8 (4): e62584
- Mohr, I.J., Clark, R., Sun, S., *et al.* (1990) Targeting the E1 replication protein to the papillomavirus origin of replication by complex formation with the E2 transactivator. **Science**, 250 (4988): 1694–1699
- Mole, S., Milligan, S.G. and Graham, S.V. (2009) Human papillomavirus type 16 E2 protein transcriptionally activates the promoter of a key cellular splicing factor, SF2/ASF. **Journal of Virology**, 83 (1): 357–367
- Moody, C.A. and Laimins, L.A. (2009) Human papillomaviruses activate the ATM DNA damage pathway for viral genome amplification upon differentiation. Galloway, D. (ed.). **PLoS Pathogens**, 5 (10): e1000605
- Moody, C.A. and Laimins, L.A. (2010) Human papillomavirus oncoproteins: pathways to transformation. **Nature Reviews Cancer**, 10 (8): 550–560
- Moody, C.A., Fradet-Turcotte, A., Archambault, J., *et al.* (2007) Human papillomaviruses activate caspases upon epithelial differentiation to induce viral genome amplification. **Proceedings of the National Academy of Sciences U.S.A.**, 104 (49): 19541–19546
- Moreno-Bueno, G., Portillo, F. and Cano, A. (2008) Transcriptional regulation of cell polarity in EMT and cancer. **Oncogene**, 27 (55): 6958–6969
- Mori, K., Iwao, K., Miyoshi, Y., *et al.* (1998) Identification of brain-specific splicing variants of the hDLG1 gene and altered splicing in neuroblastoma cell lines. **Journal of human genetics**, 43 (2): 123–127
- Morkel, M., Wenkel, J., Bannister, A.J., *et al.* (1997) An E2F-like repressor of transcription. **Nature**, 390 (6660): 567–568
- Muench, P., Hiller, T., Probst, S., *et al.* (2009) Binding of PDZ proteins to HPV E6 proteins does neither correlate with epidemiological risk classification nor with the immortalization of foreskin keratinocytes. **Virology**, 387 (2): 380–387
- Muench, P., Probst, S., Schuetz, J., *et al.* (2010) Cutaneous Papillomavirus E6 Proteins Must Interact with p300 and Block p53-Mediated Apoptosis for Cellular Immortalization and Tumorigenesis. **Cancer research**, 70 (17): 6913–6924
- Münger, K., Phelps, W.C., Bubb, V., *et al.* (1989a) The E6 and E7 genes of the human papillomavirus type 16 together are necessary and sufficient for transformation of primary human keratinocytes. **Journal of Virology**, 63 (10): 4417–4421
- Münger, K., Werness, B.A., Dyson, N., *et al.* (1989b) Complex formation of human papillomavirus E7 proteins with the retinoblastoma tumor suppressor gene product.

**Embo Journal**, 8 (13): 4099–4105

Muñoz, N., Bosch, F.X., de Sanjose, S., *et al.* (2003) Epidemiologic classification of human papillomavirus types associated with cervical cancer. **The New England journal of medicine**, 348 (6): 518–527

Muschik, D., Braspenning-Wesch, I., Stockfleth, E., *et al.* (2011) Cutaneous HPV23 E6 prevents p53 phosphorylation through interaction with HIPK2. **PLoS ONE**, 6 (11): e27655

Naim, E., Bernstein, A., Bertram, J.F., *et al.* (2005) Mutagenesis of the epithelial polarity gene, discs large 1, perturbs nephrogenesis in the developing mouse kidney. **Kidney international**, 68 (3): 955–965

Nakagawa, S. and Huibregtse, J.M. (2000) Human scribble (Vartul) is targeted for ubiquitin-mediated degradation by the high-risk papillomavirus E6 proteins and the E6AP ubiquitin-protein ligase. **Molecular and Cellular Biology**, 20 (21): 8244–8253

Nakahara, T., Peh, W.L., Doorbar, J., *et al.* (2005) Human papillomavirus type 16 E1 approximate to E4 contributes to multiple facets of the papillomavirus life cycle. **Journal of Virology**, 79 (20): 13150–13165

Narayan, N., Massimi, P. and Banks, L. (2008) CDK phosphorylation of the discs large tumour suppressor controls its localisation and stability. **Journal of Cell Science**, 122 (1): 65–74

Narayan, N., Subbaiah, V.K. and Banks, L. (2009) The high-risk HPV E6 oncoprotein preferentially targets phosphorylated nuclear forms of hDlg. **Virology**, 387 (1): 1–4

Nava, P., López, S., Arias, C.F., *et al.* (2004) The rotavirus surface protein VP8 modulates the gate and fence function of tight junctions in epithelial cells. **Journal of Cell Science**, 117 (Pt 23): 5509–5519

Navarro, C., Nola, S., Audebert, S., *et al.* (2005) Junctional recruitment of mammalian Scribble relies on E-cadherin engagement. **Oncogene**, 24 (27): 4330–4339

Nazli, A., Chan, O., Dobson-Belaire, W.N., *et al.* (2010) Exposure to HIV-1 Directly Impairs Mucosal Epithelial Barrier Integrity Allowing Microbial Translocation. **PLoS Pathogens**, 6 (4)

Nees, M., Geoghegan, J.M., Hyman, T., *et al.* (2001) Papillomavirus type 16 oncogenes downregulate expression of interferon-responsive genes and upregulate proliferation-associated and NF-kappaB-responsive genes in cervical keratinocytes. **Journal of Virology**, 75 (9): 4283–4296

Neuman, E., Flemington, E.K., Sellers, W.R., *et al.* (1994) Transcription of the E2F-1 gene is rendered cell cycle dependent by E2F DNA-binding sites within its promoter. **Molecular and Cellular Biology**, 14 (10): 6607–6615

Newman, R.A. and Prehoda, K.E. (2009) Intramolecular Interactions Between the Src Homology 3 and Guanylate Kinase Domains of Discs Large Regulate Its Function in

- Asymmetric Cell Division. **Journal of Biological Chemistry**, 284 (19): 12924–12932
- Nguyen, D.X., Westbrook, T.F. and McCance, D.J. (2002) Human papillomavirus type 16 E7 maintains elevated levels of the cdc25A tyrosine phosphatase during deregulation of cell cycle arrest. **Journal of Virology**, 76 (2): 619–632
- Nguyen, M.M., Nguyen, M.L., Caruana, G., *et al.* (2003) Requirement of PDZ-containing proteins for cell cycle regulation and differentiation in the mouse lens epithelium. **Molecular and Cellular Biology**, 23 (24): 8970–8981
- Nguyen, M.M., Rivera, C. and Griep, A.E. (2005) Localization of PDZ domain containing proteins discs large-1 and scribble in the mouse eye. **Molecular Vision**, 11 (136-38): 1183–1199
- Nicolaidis, L., Davy, C., Raj, K., *et al.* (2011) Stabilization of HPV16 E6 protein by PDZ proteins, and potential implications for genome maintenance. **Virology**, 414 (2): 137–145
- Niethammer, M., Valtschanoff, J.G., Kapoor, T.M., *et al.* (1998) CRIPT, a novel postsynaptic protein that binds to the third PDZ domain of PSD-95/SAP90. **Neuron**, 20 (4): 693–707
- Nikandrova, Y.A., Jiao, Y., Baucum, A.J., *et al.* (2010) Ca<sup>2+</sup>/calmodulin-dependent protein kinase II binds to and phosphorylates a specific SAP97 splice variant to disrupt association with AKAP79/150 and modulate alpha-amino-3-hydroxy-5-methyl-4-isoxazolepropionic acid-type glutamate receptor (AMPA) activity. **The Journal of Biological Chemistry**, 285 (2): 923–934
- Nix, S.L., Chishti, A.H., Anderson, J.M., *et al.* (2000) hCASK and hDlg associate in epithelia, and their Src homology 3 and guanylate kinase domains participate in both intramolecular and intermolecular interactions. **Journal of Biological Chemistry**, 275 (52): 41192–41200
- Nolan, M.E., Aranda, V., Lee, S., *et al.* (2008) The Polarity Protein Par6 Induces Cell Proliferation and Is Overexpressed in Breast Cancer. **Cancer research**, 68 (20): 8201–8209
- Nooh, M.M., Naren, A.P., Kim, S.-J., *et al.* (2013) SAP97 Controls the Trafficking and Resensitization of the Beta-1-Adrenergic Receptor through Its PDZ2 and I3 Domains. **PLoS ONE**, 8 (5): e63379
- Notani, D., Ramanujam, P.L., Kumar, P.P., *et al.* (2011) N-terminal PDZ-like domain of chromatin organizer SATB1 contributes towards its function as transcription regulator. **Journal of biosciences**, 36 (3): 461–469
- O'Neill, A.K., Gallegos, L.L., Justilien, V., *et al.* (2011) Protein Kinase C Promotes Cell Migration through a PDZ-Dependent Interaction with its Novel Substrate Discs Large Homolog 1 (DLG1). **The Journal of Biological Chemistry**, 286 (50): 43559–43568
- Obenauer, J.C., Cantley, L.C. and Yaffe, M.B. (2003) Scansite 2.0: Proteome-wide prediction of cell signaling interactions using short sequence motifs. **Nucleic acids research**, 31 (13): 3635–3641

- Obenauer, J.C., Denson, J., Mehta, P.K., *et al.* (2006) Large-scale sequence analysis of avian influenza isolates. **Science**, 311 (5767): 1576–1580
- Oh, J.-E., Kim, J.-O., Shin, J.-Y., *et al.* (2013) Molecular genetic characterization of p53 mutated oropharyngeal squamous cell carcinoma cells transformed with human papillomavirus E6 and E7 oncogenes. **International journal of oncology**
- Oh, S.T., Kyo, S. and Laimins, L.A. (2001) Telomerase activation by human papillomavirus type 16 E6 protein: induction of human telomerase reverse transcriptase expression through Myc and GC-rich Sp1 binding sites. **Journal of Virology**, 75 (12): 5559–5566
- Oh, S.T., Longworth, M.S. and Laimins, L.A. (2004) Roles of the E6 and E7 proteins in the life cycle of low-risk human papillomavirus type 11. **Journal of Virology**, 78 (5): 2620–2626
- Ohashi, M., Sakurai, M., Higuchi, M., *et al.* (2004) Human T-cell leukemia virus type 1 Tax oncoprotein induces and interacts with a multi-PDZ domain protein, MAGI-3. **Virology**, 320 (1): 52–62
- Olsen, O. and Brecht, D.S. (2003) Functional analysis of the nucleotide binding domain of membrane-associated guanylate kinases. **Journal of Biological Chemistry**, 278 (9): 6873–6878
- Oriel, J.D. (1971) Natural history of genital warts. **The British journal of venereal diseases**, 47 (1): 1–13
- Ozburn, M.A. and Meyers, C. (1997) Characterization of late gene transcripts expressed during vegetative replication of human papillomavirus type 31b. **Journal of Virology**, 71 (7): 5161–5172
- Ozburn, M.A. and Meyers, C. (1998) Human papillomavirus type 31b E1 and E2 transcript expression correlates with vegetative viral genome amplification. **Virology**, 248 (2): 218–230
- Paarmann, I., Spangenberg, O., Lavie, A., *et al.* (2002) Formation of complexes between Ca<sup>2+</sup>-calmodulin and the synapse-associated protein SAP97 requires the SH3 domain-guanylate kinase domain-connecting HOOK region. **The Journal of Biological Chemistry**, 277 (43): 40832–40838
- Pahl, H.L. (1999) Activators and target genes of Rel/NF-kappaB transcription factors. **Oncogene**, 18 (49): 6853–6866
- Pan, H. and Griep, A.E. (1995) Temporally distinct patterns of p53-dependent and p53-independent apoptosis during mouse lens development. **Genes & development**, 9 (17): 2157–2169
- Pan, H.C. and Griep, A.E. (1994) Altered Cell-Cycle Regulation in the Lens of HPV-16 E6 or E7 Transgenic Mice - Implications for Tumor-Suppressor Gene-Function in Development. **Genes & development**, 8 (11): 1285–1299
- Pangon, L., Van Kralingen, C., Abas, M., *et al.* (2012) The PDZ-binding motif of MCC is

phosphorylated at position -1 and controls lamellipodia formation in colon epithelial cells. **Biochimica Et Biophysica Acta-Molecular Cell Research**, 1823 (6): 1058–1067

Parish, J.L., Bean, A.M., Park, R.B., *et al.* (2006) ChIR1 is required for loading papillomavirus E2 onto mitotic chromosomes and viral genome maintenance. **Molecular Cell**, 24 (6): 867–876

Park, R.B. and Androphy, E.J. (2002) Genetic analysis of high-risk e6 in episomal maintenance of human papillomavirus genomes in primary human keratinocytes. **Journal of Virology**, 76 (22): 11359–11364

Parkin, D.M. and Bray, F. (2006) Chapter 2: The burden of HPV-related cancers. **Vaccine**, 24 Suppl 3: S3–11–25

Parkin, D.M., Bray, F., Ferlay, J., *et al.* (2001) Estimating the world cancer burden: Globocan 2000. **International Journal of Cancer**, 94 (2): 153–156

Patel, D., Huang, S.M., Baglia, L.A., *et al.* (1999) The E6 protein of human papillomavirus type 16 binds to and inhibits co-activation by CBP and p300. **Embo Journal**, 18 (18): 5061–5072

Peh, W.L., Brandsma, J.L., Christensen, N.D., *et al.* (2004) The viral E4 protein is required for the completion of the cottontail rabbit papillomavirus productive cycle in vivo. **Journal of Virology**, 78 (4): 2142–2151

Pei, X.F., Sherman, L., Sun, Y.H., *et al.* (1998) HPV-16 E7 protein bypasses keratinocyte growth inhibition by serum and calcium. **Carcinogenesis**, 19 (8): 1481–1486

Peitsaro, P., Johansson, B. and Syrjanen, S. (2002) Integrated human papillomavirus type 16 is frequently found in cervical cancer precursors as demonstrated by a novel quantitative real-time PCR technique. **Journal of clinical microbiology**, 40 (3): 886–891

Penkert, R.R., DiVittorio, H.M. and Prehoda, K.E. (2004) Internal recognition through PDZ domain plasticity in the Par-6-Pals1 complex. **Nature Structural & Molecular Biology**, 11 (11): 1122–1127

Peto, J., Gilham, C., Fletcher, O., *et al.* (2004) The cervical cancer epidemic that screening has prevented in the UK. **Lancet**, 364 (9430): 249–256

Pett, M. and Coleman, N. (2007) Integration of high-risk human papillomavirus: a key event in cervical carcinogenesis? **The Journal of pathology**, 212 (4): 356–367

Petti, L., Nilson, L.A. and DiMaio, D. (1991) Activation of the Platelet-Derived Growth-Factor Receptor by the Bovine Papillomavirus-E5 Transforming Protein. **Embo Journal**, 10 (4): 845–855

Pfister, H. (2003) Chapter 8: Human papillomavirus and skin cancer. **Journal of the National Cancer Institute. Monographs**, (31): 52–56

Philipp, S. and Flockerzi, V. (1997) Molecular characterization of a novel human PDZ domain protein with homology to INAD from *Drosophila melanogaster*. **FEBS letters**,

413 (2): 243–248

Pim, D. and Banks, L. (1999) HPV-18 E6\**I* protein modulates the E6-directed degradation of p53 by binding to full-length HPV-18 E6. **Oncogene**, 18 (52): 7403–7408

Pim, D., COLLINS, M. and Banks, L. (1992) Human Papillomavirus Type-16 E5 Gene Stimulates the Transforming Activity of the Epidermal Growth-Factor Receptor. **Oncogene**, 7 (1): 27–32

Pim, D., Massimi, P. and Banks, L. (1997) Alternatively spliced HPV-18 E6\* protein inhibits E6 mediated degradation of p53 and suppresses transformed cell growth. **Oncogene**, 15 (3): 257–264

Pim, D., Thomas, M., Javier, R., *et al.* (2000) HPV E6 targeted degradation of the disc large protein: evidence for the involvement of a novel ubiquitin ligase. **Oncogene**, 19 (6): 719–725

Pim, D., Tomaic, V. and Banks, L. (2009) The Human Papillomavirus (HPV) E6\* Proteins from High-Risk, Mucosal HPVs Can Direct Degradation of Cellular Proteins in the Absence of Full-Length E6 Protein. **Journal of Virology**, 83 (19): 9863–9874

Pintos, J., Black, M.J., Sadeghi, N., *et al.* (2008) Human papillomavirus infection and oral cancer: A case-control study in Montreal, Canada. **Oral oncology**, 44 (3): 242–250

Ponting, C.P., Oliver, P.L. and Reik, W. (2009) Evolution and functions of long noncoding RNAs. **Cell**, 136 (4): 629–641

Popovic, M., Zlatev, V., Hodnik, V., *et al.* (2012) Flexibility of the PDZ-binding motif in the micelle-bound form of Jagged-1 cytoplasmic tail. **BBA - Biomembranes**, pp. 1–11

Posner, M.R., Lorch, J.H., Goloubeva, O., *et al.* (2011) Survival and human papillomavirus in oropharynx cancer in TAX 324: a subset analysis from an international phase III trial. **Annals of Oncology**, 22 (5): 1071–1077

Prehaud, C., Wolff, N., Terrien, E., *et al.* (2010) Attenuation of Rabies Virulence: Takeover by the Cytoplasmic Domain of Its Envelope Protein. **Science Signaling**, 3 (105): –ra5

Prescott, E.L., Brimacombe, C.L., Hartley, M., *et al.* (2014) Human papillomavirus type 1 (HPV1) E1<sup>E4</sup> protein is a potent inhibitor of the serine-arginine (SR) protein kinase SRPK1 and inhibits phosphorylation of host SR proteins and of the viral transcription and replication regulator E2. **Journal of Virology**, 88 (21): 12599–12611

Pyeon, D., Pearce, S.M., Lank, S.M., *et al.* (2009) Establishment of Human Papillomavirus Infection Requires Cell Cycle Progression Munger, K. (ed.). **PLoS Pathogens**, 5 (2)

Ramoz, N., Rueda, L.-A., Bouadjar, B., *et al.* (2002) Mutations in two adjacent novel genes are associated with epidermodysplasia verruciformis. **Nature Genetics**, 32 (4): 579–581

Ramoz, N., Rueda, L.A., Bouadjar, B., *et al.* (1999) A susceptibility locus for epidermodysplasia verruciformis, an abnormal predisposition to infection with the oncogenic human papillomavirus type 5, maps to chromosome 17qter in a region

- containing a psoriasis locus. **The Journal of investigative dermatology**, 112 (3): 259–263
- Ramoz, N., Taieb, A., Rueda, L.A., *et al.* (2000) Evidence for a nonallelic heterogeneity of epidermodysplasia verruciformis with two susceptibility loci mapped to chromosome regions 2p21-p24 and 17q25. **The Journal of investigative dermatology**, 114 (6): 1148–1153
- Rampias, T., Sasaki, C., Weinberger, P., *et al.* (2009) E6 and E7 Gene Silencing and Transformed Phenotype of Human Papillomavirus 16-Positive Oropharyngeal Cancer Cells. **Journal of the National Cancer Institute**, 101 (6): 412–423
- Raybould, R., Fiander, A., Wilkinson, G.W.G., *et al.* (2014) HPV Integration detection in CaSki and SiHa using Detection of Integrated Papillomavirus Sequences and Restriction-site PCR. **Journal of virological methods**
- Razanskas, R. and Sasnauskas, K. (2010) Interaction of hepatitis B virus core protein with human GIPC1. **Archives of virology**, 155 (2): 247–250
- Rebeaud, F., Hailfinger, S. and Thome, M. (2007) Dlg1 and Carma1 MAGUK proteins contribute to signal specificity downstream of TCR activation. **Trends in Immunology**, 28 (5): 196–200
- Reichert, M., Müller, T. and Hunziker, W. (2000) The PDZ domains of zonula occludens-1 induce an epithelial to mesenchymal transition of Madin-Darby canine kidney I cells. Evidence for a role of beta-catenin/Tcf/Lef signaling. **Journal of Biological Chemistry**, 275 (13): 9492–9500
- Reiser, J., Hurst, J., Voges, M., *et al.* (2011) High-Risk Human Papillomaviruses Repress Constitutive Kappa Interferon Transcription via E6 To Prevent Pathogen Recognition Receptor and Antiviral-Gene Expression. **Journal of Virology**, 85 (21): 11372–11380
- Ress, A. and Moelling, K. (2006) Interaction partners of the PDZ domain of Erbin. **Protein and Peptide Letters**, 13 (9): 877–879
- Reuver, S.M. and Garner, C.C. (1997) The association of SAP97 with cell adhesion sites in epithelial cells requires the actin-based cortical cytoskeleton. **Molecular Biology of the Cell**, 8: 1014–1014
- Reuver, S.M. and Garner, C.C. (1998) E-cadherin mediated cell adhesion recruits SAP97 into the cortical cytoskeleton. **Journal of Cell Science**, 111: 1071–1080
- Richards, K.H., Doble, R., Wasson, C.W., *et al.* (2014) Human papillomavirus E7 oncoprotein increases production of the anti-inflammatory interleukin-18 binding protein in keratinocytes. **Journal of Virology**, 88 (8): 4173–4179
- Richards, R.M., Lowy, D.R., Schiller, J.T., *et al.* (2006) Cleavage of the papillomavirus minor capsid protein, L2, at a furin consensus site is necessary for infection. **Proceedings of the National Academy of Sciences of the United States of America**, 103 (5): 1522–1527
- Riley, R.R., Duensing, S., Brake, T., *et al.* (2003) Dissection of human papillomavirus E6

and E7 function in transgenic mouse models of cervical carcinogenesis. **Cancer research**, 63 (16): 4862–4871

Rincon, M. and Davis, R.J. (2007) Choreography of MAGUKs during T cell activation. **Nature Immunology**, 8 (2): 126–127

Rischin, D., Young, R.J., Fisher, R., *et al.* (2010) Prognostic Significance of p16(INK4A) and Human Papillomavirus in Patients With Oropharyngeal Cancer Treated on TROG 02.02 Phase III Trial. **Journal of clinical oncology : official journal of the American Society of Clinical Oncology**, 28 (27): 4142–4148

Rivera, C., Yamben, I.F., Shatadal, S., *et al.* (2009) Cell-autonomous requirements for Dlg-1 for lens epithelial cell structure and fiber cell morphogenesis. Dyer, M.A., Kumar, J.P., Link, B.A., *et al.* (eds.). **Developmental dynamics : an official publication of the American Association of Anatomists**, 238 (9): 2292–2308

Roberts, S., Ashmole, I., Rookes, S.M., *et al.* (1997) Mutational analysis of the human papillomavirus type 16 E1--E4 protein shows that the C terminus is dispensable for keratin cytoskeleton association but is involved in inducing disruption of the keratin filaments. **Journal of Virology**, 71 (5): 3554–3562

Roberts, S., Calautti, E., Vanderweil, S., *et al.* (2007) Changes in localization of human discs large (hDlg) during keratinocyte differentiation is associated with expression of alternatively spliced hDlg variants. **Experimental Cell Research**, 313 (12): 2521–2530

Roberts, S., Delury, C. and Marsh, E. (2012) The PDZ protein discs-large (DLG): the Jekyll and Hyde' of the epithelial polarity proteins. **The FEBS journal**, 279 (19): 3549–3558

Roden, R.B., Greenstone, H.L., Kirnbauer, R., *et al.* (1996) In vitro generation and type-specific neutralization of a human papillomavirus type 16 virion pseudotype. **Journal of Virology**, 70 (9): 5875–5883

Roh, M.H., Makarova, O., Liu, C.-J., *et al.* (2002) The Maguk protein, Pals1, functions as an adapter, linking mammalian homologues of Crumbs and Discs Lost. **Journal of Cell Biology**, 157 (1): 161–172

Ronco, L.V., Karpova, A.Y., Vidal, M., *et al.* (1998) Human papillomavirus 16 E6 oncoprotein binds to interferon regulatory factor-3 and inhibits its transcriptional activity. **Genes & development**, 12 (13): 2061–2072

Rothenberg, S.M., Mohapatra, G., Rivera, M.N., *et al.* (2010) A Genome-Wide Screen for Microdeletions Reveals Disruption of Polarity Complex Genes in Diverse Human Cancers. **Cancer research**, 70 (6): 2158–2164

Round, J.L., Humphries, L.A., Tomassian, T., *et al.* (2007a) Scaffold protein Dlg1 coordinates alternative p38 kinase activation, directing T cell receptor signals toward NFAT but not NF-kappa B transcription factors. **Nature Immunology**, 8 (2): 154–161

Round, J.L., Humphries, L.A., Tommasian, T., *et al.* (2007b) MAGUK family member Dlg1 coordinates TCR-dependent p38 activation, specifically linking TCR engagement to

activation of NFAT but not NF-kappa B. **Cytokine**, 39 (1): 36–36

Round, J.L., Tomassian, T., Zhang, M., *et al.* (2005) Dlg1 coordinates actin polymerization, synaptic T cell receptor and lipid raft aggregation, and effector function in T cells. **The Journal of experimental medicine**, 201 (3): 419–430

Rous, P. and Beard, J.W. (1935) THE PROGRESSION TO CARCINOMA OF VIRUS-INDUCED RABBIT PAPILOMAS (SHOPE). **The Journal of experimental medicine**, 62 (4): 523–548

Rousset, R., Fabre, S., Desbois, C., *et al.* (1998) The C-terminus of the HTLV-1 Tax oncoprotein mediates interaction with the PDZ domain of cellular proteins. **Oncogene**, 16 (5): 643–654

Rubin, A.I., Chen, E.H. and Ratner, D. (2005) Basal-cell carcinoma. **The New England journal of medicine**, 353 (21): 2262–2269

Rumbaugh, G., Sia, G.M., Garner, C.C., *et al.* (2003) Synapse-associated protein-97 isoform-specific regulation of surface AMPA receptors and synaptic function in cultured neurons. **The Journal of neuroscience : the official journal of the Society for Neuroscience**, 23 (11): 4567–4576

Saadaoui, M., Machicoane, M., di Pietro, F., *et al.* (2014) Dlg1 controls planar spindle orientation in the neuroepithelium through direct interaction with LGN. **Journal of Cell Biology**, 206 (6): 707–717

Sabio, G., Arthur, J.S.C., Kuma, Y., *et al.* (2005) p38gamma regulates the localisation of SAP97 in the cytoskeleton by modulating its interaction with GKAP. **Embo Journal**, 24 (6): 1134–1145

Sabio, G., Cerezo-Guisado, M.I., Del Reino, P., *et al.* (2010) p38gamma regulates interaction of nuclear PSF and RNA with the tumour-suppressor hDlg in response to osmotic shock. **Journal of Cell Science**, 123 (Pt 15): 2596–2604

Sajjan, U., Wang, Q., Zhao, Y., *et al.* (2008) Rhinovirus Disrupts the Barrier Function of Polarized Airway Epithelial Cells. **American Journal of Respiratory and Critical Care Medicine**, 178 (12): 1271–1281

Sanders, C.M. and Stenlund, A. (2000) Transcription factor-dependent loading of the E1 initiator reveals modular assembly of the papillomavirus origin melting complex. **Journal of Biological Chemistry**, 275 (5): 3522–3534

Sans, N., Wang, P.Y., Du, Q., *et al.* (2005) mPins modulates PSD-95 and SAP102 trafficking and influences NMDA receptor surface expression. **Nature cell biology**, 7 (12): 1179–1190

Scheffner, M., Werness, B.A., Huibregtse, J.M., *et al.* (1990) The E6 oncoprotein encoded by human papillomavirus types 16 and 18 promotes the degradation of p53. **Cell**, 63 (6): 1129–1136

Schlueter, O.M., Xu, W. and Malenka, R.C. (2006) Alternative N-terminal domains of

PSD-95 and SAP97 govern activity-dependent regulation of synaptic AMPA receptor function. **Neuron**, 51 (1): 99–111

Schmittgen, T.D. and Zakrajsek, B.A. (2000) Effect of experimental treatment on housekeeping gene expression: validation by real-time, quantitative RT-PCR. **Journal of biochemical and biophysical methods**, 46 (1-2): 69–81

Schneider, C.A., Rasband, W.S. and Eliceiri, K.W. (2012) NIH Image to ImageJ: 25 years of image analysis. **Nature methods**, 9 (7): 671–675

Schulz, E., Gottschling, M., Bravo, I.G., *et al.* (2009) Genomic characterization of the first insectivoran papillomavirus reveals an unusually long, second non-coding region and indicates a close relationship to Betapapillomavirus. **Journal of General Virology**, 90 (Pt 3): 626–633

Schwartz, S. (2013) Papillomavirus transcripts and posttranscriptional regulation. **Virology**

Sedman, S.A., Barbosa, M.S., Vass, W.C., *et al.* (1991) The full-length E6 protein of human papillomavirus type 16 has transforming and trans-activating activities and cooperates with E7 to immortalize keratinocytes in culture. **Journal of Virology**, 65 (9): 4860–4866

Shai, A., Pitot, H.C. and Lambert, P.F. (2010) E6-associated protein is required for human papillomavirus type 16 E6 to cause cervical cancer in mice. **Cancer research**, 70 (12): 5064–5073

Shao, X., Zhu, L., Wang, Y., *et al.* (2010) Threonine 82 at the PDZ domain of PICK1 is critical for AMPA receptor interaction and localization. **Neurochemistry international**, 56 (8): 962–970

Sheridan, D.L., Kong, Y., Parker, S.A., *et al.* (2008) Substrate discrimination among mitogen-activated protein kinases through distinct docking sequence motifs. **Journal of Biological Chemistry**, 283 (28): 19511–19520

Sherman, L., Jackman, A., Itzhaki, H., *et al.* (1997) Inhibition of serum- and calcium-induced differentiation of human keratinocytes by HPV16 E6 oncoprotein: Role of p53 inactivation. **Virology**, 237 (2): 296–306

Shope, R.E. and Hurst, E.W. (1933) INFECTIOUS PAPILLOMATOSIS OF RABBITS : WITH A NOTE ON THE HISTOPATHOLOGY. **The Journal of experimental medicine**, 58 (5): 607–624

Sierralta, J. and Mendoza, C. (2004) PDZ-containing proteins: alternative splicing as a source of functional diversity. **Brain research. Brain research reviews**, 47 (1-3): 105–115

Sigrist, C.J.A., Cerutti, L., de Castro, E., *et al.* (2010) PROSITE, a protein domain database for functional characterization and annotation. **Nucleic acids research**, 38: D161–D166

Simmonds, M. and Storey, A. (2008) Identification of the regions of the HPV 5 E6 protein involved in Bak degradation and inhibition of apoptosis. **International Journal of Cancer**, 123 (10): 2260–2266

- Simonson, S.J.S., Difilippantonio, M.J. and Lambert, P.F. (2005) Two distinct activities contribute to human papillomavirus 16 E6's oncogenic potential. **Cancer research**, 65 (18): 8266–8273
- Smith, E.M., Ritchie, J.M., Summersgill, K.F., *et al.* (2004) Human papillomavirus in oral exfoliated cells and risk of head and neck cancer. **Journal of the National Cancer Institute**, 96 (6): 449–455
- Smotkin, D. and Wettstein, F.O. (1986) Expression of Hpv-16 Early Genes. **Journal of cellular biochemistry**, pp. 221–221
- Soejima, H., Kawamoto, S., Akai, J., *et al.* (2001) Isolation of novel heart-specific genes using the BodyMap database. **Genomics**, 74 (1): 115–120
- Song, C., Wang, W., Li, M., *et al.* (2009) Tax1 Enhances Cancer Cell Proliferation via Ras-Raf-MEK-ERK Signaling Pathway Chang, Z., Wang, C.-C. and Wang, Z.-X. (eds.). **Iubmb Life**, 61 (6): 685–692
- Song, S. and Pitot, H.C. (1999) The Human Papillomavirus Type 16 E6 Gene Alone Is Sufficient To Induce Carcinomas in Transgenic Animals. **Journal of Virology**, 73 (7): 887–893
- Song, S., Liem, A., Miller, J.A., *et al.* (2000) Human papillomavirus types 16 E6 and E7 contribute differently to carcinogenesis. **Virology**, 267 (2): 141–150
- Songyang, Z., Fanning, A.S., Fu, C., *et al.* (1997) Recognition of unique carboxyl-terminal motifs by distinct PDZ domains. **Science**, 275 (5296): 73–77
- Sonoda, T., Mochizuki, C., Yamashita, T., *et al.* (2006) Binding of glutamate receptor delta 2 to its scaffold protein, Delphilin, is regulated by PKA. **Biochemical and Biophysical Research Communications**, 350 (3): 748–752
- Sotelo, N.S., Schepens, J.T.G., Valiente, M., *et al.* (2014) PTEN-PDZ domain interactions: Binding of PTEN to PDZ domains of PTPN13. **Methods (San Diego, Calif.)**
- Sotillos, S., Diaz-Meco, M.T., Caminero, E., *et al.* (2004) DaPKC-dependent phosphorylation of Crumbs is required for epithelial cell polarity in Drosophila. **Journal of Cell Biology**, 166 (4): 549–557
- Soubies, S.M., Hoffmann, T.W., Croville, G., *et al.* (2013) Deletion of the C-terminal ESEV domain of NS1 does not affect the replication of a low-pathogenic avian influenza virus H7N1 in ducks and chickens. **The Journal of general virology**, 94 (Pt 1): 50–58
- Soubies, S.M., Volmer, C., Croville, G., *et al.* (2010a) Species-specific contribution of the four C-terminal amino acids of influenza A virus NS1 protein to virulence. **Journal of Virology**, 84 (13): 6733–6747
- Soubies, S.M., Volmer, C., Guérin, J.-L., *et al.* (2010b) Truncation of the NS1 protein converts a low pathogenic avian influenza virus into a strong interferon inducer in duck cells. **Avian diseases**, 54 (1 Suppl): 527–531

Spangle, J., Ghosh-Choudhury, N. and Münger, K. (2012) Activation of cap dependent translation by mucosal Human Papillomavirus E6 proteins is dependent on the integrity of the LXXLL binding motif. **Journal of Virology**

Spangle, J.M. and Münger, K. (2010) The human papillomavirus type 16 E6 oncoprotein activates mTORC1 signaling and increases protein synthesis. **Journal of Virology**, 84 (18): 9398–9407

Spanos, W.C., Geiger, J., Anderson, M.E., *et al.* (2008a) Deletion of the PDZ motif of HPV16 E6 preventing immortalization and anchorage-independent growth in human tonsil epithelial cells. **Head & Neck**, 30 (2): 139–147

Spanos, W.C., Hoover, A., Harris, G.F., *et al.* (2008b) The PDZ Binding Motif of Human Papillomavirus Type 16 E6 Induces PTPN13 Loss, Which Allows Anchorage-Independent Growth and Synergizes with Ras for Invasive Growth. **Journal of Virology**, 82 (5): 2493–2500

Spoden, G., Kühling, L., Cordes, N., *et al.* (2013) The Human Papillomaviruses Type 16, 18, and 31 share similar endocytic requirements for entry. **Journal of Virology**

Srebrow, A. and Kornblihtt, A.R. (2006) The connection between splicing and cancer. **Journal of Cell Science**, 119 (13): 2635–2641

St Johnston, D. and Ahringer, J. (2010) Cell polarity in eggs and epithelia: parallels and diversity. **Cell**, 141 (5): 757–774

Stanley, M.A. (2001) Human papillomavirus and cervical carcinogenesis. **Best practice & research. Clinical obstetrics & gynaecology**, 15 (5): 663–676

Stanley, M.A. (2010) Pathology and epidemiology of HPV infection in females. **Gynecologic oncology**, 117 (2 Suppl): S5–10

Stanley, M.A. (2012) Epithelial cell responses to infection with human papillomavirus. **Clinical microbiology reviews**, 25 (2): 215–222

Steenbergen, R.D.M., Hermsen, M., Walboomers, J.M.M., *et al.* (1995) Integrated Human Papillomavirus Type-16 and Loss of Heterozygosity at 11q22 and 18q21 in an Oral-Carcinoma and Its Derivative Cell-Line. **Cancer research**, 55 (22): 5465–5471

Stein, E.L.A. and Chetkovich, D.M. (2010) Regulation of stargazin synaptic trafficking by C-terminal PDZ ligand phosphorylation in bidirectional synaptic plasticity. **Journal of Neurochemistry**, 113 (1): 42–53

Sterling, J.C., Handfield-Jones, S. and Hudson, P.M. (2001) Guidelines for the management of cutaneous warts. **The British journal of dermatology**. 144 (1) pp. 4–11

Storrs, C.H. and Silverstein, S.J. (2007) PATJ, a Tight Junction-Associated PDZ Protein, Is a Novel Degradation Target of High-Risk Human Papillomavirus E6 and the Alternatively Spliced Isoform 18 E6. **Journal of Virology**, 81 (8): 4080–4090

Stöppler, M.C., Straight, S.W., Tsao, G., *et al.* (1996) The E5 gene of HPV-16 enhances

keratinocyte immortalization by full-length DNA. **Virology**, 223 (1): 251–254

Straight, S.W., Hinkle, P.M., Jewers, R.J., *et al.* (1993) The E5 oncoprotein of human papillomavirus type 16 transforms fibroblasts and effects the downregulation of the epidermal growth factor receptor in keratinocytes. **Journal of Virology**, 67 (8): 4521–4532

Strausberg, R.L., Feingold, E.A., Grouse, L.H., *et al.* (2002) Generation and initial analysis of more than 15,000 full-length human and mouse cDNA sequences. **Proceedings of the National Academy of Sciences of the United States of America**, 99 (26): 16899–16903

Stubenrauch, F., Leigh, I.M. and Pfister, H. (1996) E2 represses the late gene promoter of human papillomavirus type 8 at high concentrations by interfering with cellular factors. **Journal of Virology**, 70 (1): 119–126

Stucke, V.M., Timmerman, E., Vandekerckhove, J., *et al.* (2007) The MAGUK protein MPP7 binds to the polarity protein hDlg1 and facilitates epithelial tight junction formation. **Molecular Biology of the Cell**, 18 (5): 1744–1755

Subbaiah, V.K., Kranjec, C., Thomas, M., *et al.* (2011) PDZ domains: the building blocks regulating tumorigenesis. **The Biochemical journal**, 439 (2): 195–205

Sulka, B., Lortat-Jacob, H., Terreux, R., *et al.* (2009) Tyrosine dephosphorylation of the syndecan-1 PDZ binding domain regulates syntenin-1 recruitment. **The Journal of Biological Chemistry**, 284 (16): 10659–10671

Surviladze, Z., Dziduszko, A. and Ozbun, M.A. (2012) Essential Roles for Soluble Virion-Associated Heparan Sulfonated Proteoglycans and Growth Factors in Human Papillomavirus Infections Imperiale, M. (ed.). **PLoS Pathogens**, 8 (2): e1002519

Suzuki, T., Ohsugi, Y., Uchida-Toita, M., *et al.* (1999) Tax oncoprotein of HTLV-1 binds to the human homologue of Drosophila discs large tumor suppressor protein, hDLG, and perturbs its function in cell growth control. **Oncogene**, 18 (44): 5967–5972

Tachezy, R., Klozar, J., Rubenstein, L., *et al.* (2009) Demographic and Risk Factors in Patients With Head and Neck Tumors. **Journal of medical virology**, 81 (5): 878–887

Tafazoli, F., Zeng, C.Q., Estes, M.K., *et al.* (2001) NSP4 enterotoxin of rotavirus induces paracellular leakage in polarized epithelial cells. **Journal of Virology**, 75 (3): 1540–1546

Tan, M.J.A., White, E.A., Sowa, M.E., *et al.* (2012) Cutaneous  $\beta$ -human papillomavirus E6 proteins bind Mastermind-like coactivators and repress Notch signaling. **Proceedings of the National Academy of Sciences U.S.A.**, 109 (23): E1473–80

Tandon, C. and De Lisle, R.C. (2004) Apatin is involved in remodeling of the actin cytoskeleton during regulated exocytosis. **European journal of cell biology**, 83 (2): 79–89

Tandon, C., De Lisle, R.C., Boulatnikov, I., *et al.* (2007) Interaction of carboxyl-terminal peptides of cytosolic-tail of apatin with PDZ domains of NHERF/EBP50 and PDZK-1/CAP70. **Molecular and cellular biochemistry**, 302 (1-2): 157–167

Tanemoto, M., Fujita, A., Higashi, K., *et al.* (2002) PSD-95 mediates formation of a

- functional homomeric Kir5.1 channel in the brain. **Neuron**, 34 (3): 387–397
- Tang, S., Tao, M., McCoy, J.P., *et al.* (2006) The E7 oncoprotein is translated from spliced E6\*I transcripts in high-risk human papillomavirus type 16- or type 18-positive cervical cancer cell lines via translation reinitiation. **Journal of Virology**, 80 (9): 4249–4263
- Tanos, B. and Rodriguez-Boulan, E. (2008) The epithelial polarity program: machineries involved and their hijacking by cancer. **Oncogene**, 27 (55): 6939–6957
- Tao, M., Kruhlak, M., Xia, S., *et al.* (2003) Signals that dictate nuclear localization of human papillomavirus type 16 oncoprotein E6 in living cells. **Journal of Virology**, 77 (24): 13232–13247
- Tapia, R., Huerta, M., Islas, S., *et al.* (2009) Zona Occludens-2 Inhibits Cyclin D1 Expression and Cell Proliferation and Exhibits Changes in Localization along the Cell Cycle. **Molecular Biology of the Cell**, 20 (3): 1102–1117
- Teoh, K.-T., Siu, Y.-L., Chan, W.-L., *et al.* (2010) The SARS Coronavirus E Protein Interacts with PALS1 and Alters Tight Junction Formation and Epithelial Morphogenesis. **Molecular Biology of the Cell**, 21 (22): 3838–3852
- Termine, N., Panzarella, V., Falaschini, S., *et al.* (2008) HPV in oral squamous cell carcinoma vs head and neck squamous cell carcinoma biopsies: a meta-analysis (1988-2007). **Annals of Oncology**, 19 (10): 1681–1690
- Terrien, E., Chaffotte, A., Lafage, M., *et al.* (2012) Interference with the PTEN-MAST2 Interaction by a Viral Protein Leads to Cellular Relocalization of PTEN. **Science Signaling**, 5 (237): –ra58
- Thierry-Mieg, D. and Thierry-Mieg, J. (2006) AceView: a comprehensive cDNA-supported gene and transcripts annotation. **Genome biology**, 7 (Suppl 1)
- Thomas, M. and Banks, L. (1998) Inhibition of Bak-induced apoptosis by HPV-18 E6. **Oncogene**, 17 (23): 2943–2954
- Thomas, M. and Banks, L. (1999) Human papillomavirus (HPV) E6 interactions with Bak are conserved amongst E6 proteins from high and low risk HPV types. **Journal of General Virology** [online], 80: 1513–1517. Available from: <http://gateway.webofknowledge.com/gateway/Gateway.cgi?GWVersion=2&SrcAuth=me kentosj&SrcApp=Papers&DestLinkType=FullRecord&DestApp=WOS&KeyUT=000080542600022>
- Thomas, M. and Banks, L. (2005) In vitro assays of substrate degradation induced by high-risk HPV E6 oncoproteins. **Methods in molecular medicine**, 119: 411–417
- Thomas, M. and Banks, L. (2014) PDZRN3/LNX3 is a Novel Target of HPV 16 and HPV-18 E6. **Journal of Virology**, pp. JVI.01743–14
- Thomas, M., Glaunsinger, B., Pim, D., *et al.* (2001) HPV E6 and MAGUK protein interactions: determination of the molecular basis for specific protein recognition and degradation. **Oncogene**, 20 (39): 5431–5439

- Thomas, M., Kranjec, C., Nagasaka, K., *et al.* (2011) Analysis of the PDZ binding specificities of Influenza A Virus NS1 proteins. **Virology Journal**, 8 (1)
- Thomas, M., Laura, R., Hepner, K., *et al.* (2002) Oncogenic human papillomavirus E6 proteins target the MAGI-2 and MAGI-3 proteins for degradation. **Oncogene**, 21 (33): 5088–5096
- Thomas, M., Massimi, P., Navarro, C., *et al.* (2005) The hScrib/Dlg apico-basal control complex is differentially targeted by HPV-16 and HPV-18 E6 proteins. **Oncogene**, 24 (41): 6222–6230
- Thomas, U., Ebitsch, S., Gorczyca, M., *et al.* (2000) Synaptic targeting and localization of discs-large is a stepwise process controlled by different domains of the protein. **Current biology : CB**, 10 (18): 1108–1117
- Thompson, D.A., Zacny, V., Belinsky, G.S., *et al.* (2001) The HPV E7 oncoprotein inhibits tumor necrosis factor alpha-mediated apoptosis in normal human fibroblasts. **Oncogene**, 20 (28): 3629–3640
- Tian, Q.-B., Suzuki, T., Yamauchi, T., *et al.* (2006) Interaction of LDL receptor-related protein 4 (LRP4) with postsynaptic scaffold proteins via its C-terminal PDZ domain-binding motif, and its regulation by Ca/calmodulin-dependent protein kinase II. **The European journal of neuroscience**, 23 (11): 2864–2876
- Tochio, H., Zhang, Q., Mandal, P., *et al.* (1999) Solution structure of the extended neuronal nitric oxide synthase PDZ domain complexed with an associated peptide. **Nature Structural Biology**, 6 (5): 417–421
- Toft, L., Tolstrup, M., Mueller, M., *et al.* (2014) Comparison of the immunogenicity of Cervarix (R) and Gardasil (R) human papillomavirus vaccines for oncogenic non-vaccine serotypes HPV-31, HPV-33, and HPV-45 in HIV-infected adults. **Human Vaccines & Immunotherapeutics**, 10 (5): 1147–1154
- Tokes, A.-M., Szasz, A.M., Juhasz, E., *et al.* (2012) Expression of Tight Junction Molecules in Breast Carcinomas Analysed by Array PCR and Immunohistochemistry. **Pathology & Oncology Research**, 18 (3): 593–606
- Tomaic, V., Gardiol, D., Massimi, P., *et al.* (2009) Human and primate tumour viruses use PDZ binding as an evolutionarily conserved mechanism of targeting cell polarity regulators. **Oncogene**, 28 (1): 1–8
- Tomaić, V., Pim, D. and Banks, L. (2009) The stability of the human papillomavirus E6 oncoprotein is E6AP dependent. **Virology**, 393 (1): 7–10
- Töpffer, S., Müller-Schiffmann, A., Matentzoglou, K., *et al.* (2007) Protein tyrosine phosphatase H1 is a target of the E6 oncoprotein of high-risk genital human papillomaviruses. **Journal of General Virology**, 88 (Pt 11): 2956–2965
- Tsubata, C., Higuchi, M., Takahashi, M., *et al.* (2005) PDZ domain-binding motif of human T-cell leukemia virus type I Tax oncoprotein is essential for the interleukin 2 independent growth induction of a T-cell line. **Retrovirology**, 2 (1)

Tungteakkhun, S.S. and Duerksen-Hughes, P.J. (2008) Cellular binding partners of the human papillomavirus E6 protein. **Archives of virology**, 153 (3): 397–408

Tungteakkhun, S.S., Filippova, M., Fodor, N., *et al.* (2010) The full-length isoform of human papillomavirus 16 E6 and its splice variant E6\* bind to different sites on the procaspase 8 death effector domain. **Journal of Virology**, 84 (3): 1453–1463

Underbrink, M.P., Howie, H.L., Bedard, K.M., *et al.* (2008) E6 proteins from multiple human betapapillomavirus types degrade Bak and protect keratinocytes from apoptosis after UVB irradiation. **Journal of Virology**, 82 (21): 10408–10417

Valle, G.F. and Banks, L. (1995) The human papillomavirus (HPV)-6 and HPV-16 E5 proteins co-operate with HPV-16 E7 in the transformation of primary rodent cells. **Journal of General Virology**, 76 ( Pt 5): 1239–1245

van Doorslaer, K. and Burk, R.D. (2012) Association between hTERT activation by HPV E6 proteins and oncogenic risk. **Virology**, 433 (1): 216–219

van Doorslaer, K., Tan, Q., Xirasagar, S., *et al.* (2013) The Papillomavirus Episteme: a central resource for papillomavirus sequence data and analysis. **Nucleic acids research**, 41 (Database issue): D571–8

Vande Pol, S.B. and Klingelhutz, A.J. (2013) Papillomavirus E6 oncoproteins. **Virology**

Vandermark, E.R., Deluca, K.A., Gardner, C.R., *et al.* (2012) Human papillomavirus type 16 E6 and E 7 proteins alter NF-κB in cultured cervical epithelial cells and inhibition of NF-κB promotes cell growth and immortalization. **Virology**, 425 (1): 53–60

Vermeer, P.D., Bell, M., Lee, K., *et al.* (2012) ErbB2, EphrinB1, Src kinase and PTPN13 signaling complex regulates MAP kinase signaling in human cancers. **PLoS ONE**, 7 (1): e30447

Vermeer, P.D., Einwalter, L.A., Moniger, T.O., *et al.* (2003) Segregation of receptor and ligand regulates activation of epithelial growth factor receptor. **Nature**, 422 (6929): 322–326

Viarisio, D., Mueller-Decker, K., Kloz, U., *et al.* (2011) E6 and E7 from beta HPV38 cooperate with ultraviolet light in the development of actinic keratosis-like lesions and squamous cell carcinoma in mice. **PLoS Pathogens**, 7 (7): e1002125

Vieira, V.C., Leonard, B., White, E.A., *et al.* (2014) Human Papillomavirus E6 Triggers Upregulation of the Antiviral and Cancer Genomic DNA Deaminase APOBEC3B. **mBio**, 5 (6): e02234–14–e02234–14

Villa, L.L. (2011) HPV prophylactic vaccination: The first years and what to expect from now. **Cancer Letters**, 305 (2): 106–112

Vliet-Gregg, P.A., Hamilton, J.R. and Katzenellenbogen, R.A. (2013) NFX1-123 and Human Papillomavirus 16E6 Increase Notch Expression in Keratinocytes. **Journal of Virology**

Vliet-Gregg, P.A., Hamilton, J.R. and Katzenellenbogen, R.A. (2015) Human papillomavirus 16E6 and NFX1-123 potentiate notch signaling and differentiation without activating cellular arrest. **Virology**, 478C: 50–60

Waites, C.L., Specht, C.G., Haertel, K., *et al.* (2009) Synaptic SAP97 Isoforms Regulate AMPA Receptor Dynamics and Access to Presynaptic Glutamate. **The Journal of neuroscience : the official journal of the Society for Neuroscience**, 29 (14): 4332–4345

Walboomers, J.M., Jacobs, M.V., Manos, M.M., *et al.* (1999) Human papillomavirus is a necessary cause of invasive cervical cancer worldwide. **The Journal of pathology**, 189 (1): 12–19

Wald, A.I., Hoskins, E.E., Wells, S.I., *et al.* (2011) ALTERATION OF microRNA PROFILES IN SQUAMOUS CELL CARCINOMA OF THE HEAD AND NECK CELL LINES BY HUMAN PAPILLOMAVIRUS Sturgis, E.M. (ed.). **Head & Neck**, 33 (4): 504–512

Walker, J., Smiley, L.C., Ingram, D., *et al.* (2011) Expression of human papillomavirus type 16 E7 is sufficient to significantly increase expression of angiogenic factors but is not sufficient to induce endothelial cell migration. **Virology**, 410 (2): 283–290

Wallin, K.L., Wiklund, F., Angström, T., *et al.* (1999) Type-specific persistence of human papillomavirus DNA before the development of invasive cervical cancer. **New England Journal of Medicine**, 341 (22): 1633–1638

Wang, H.-K., Duffy, A.A., Broker, T.R., *et al.* (2009a) Robust production and passaging of infectious HPV in squamous epithelium of primary human keratinocytes. **Genes & development**, 23 (2): 181–194

Wang, L., Piserchio, A. and Mierke, D.F. (2005) Structural characterization of the intermolecular interactions of synapse-associated protein-97 with the NR2B subunit of N-methyl-D-aspartate receptors. **Journal of Biological Chemistry**, 280 (29): 26992–26996

Wang, S.S., Concepcion Bratti, M., Rodriguez, A.C., *et al.* (2009b) Common Variants in Immune and DNA Repair Genes and Risk for Human Papillomavirus Persistence and Progression to Cervical Cancer. **Journal of Infectious Diseases**, 199 (1): 20–30

Wang, T.L., Ling, M., Shih, I.M., *et al.* (2000) Intramuscular administration of E7-transfected dendritic cells generates the most potent E7-specific anti-tumor immunity. **Gene therapy**, 7 (9): 726–733

Wang, W.-L., Yeh, S.-F., Chang, Y.-I., *et al.* (2003) PICK1, an anchoring protein that specifically targets protein kinase Calpha to mitochondria selectively upon serum stimulation in NIH 3T3 cells. **The Journal of Biological Chemistry**, 278 (39): 37705–37712

Wang, X., Wang, H.-K., McCoy, J.P., *et al.* (2009c) Oncogenic HPV infection interrupts the expression of tumor-suppressive miR-34a through viral oncoprotein E6. **Rna-a Publication of the Rna Society**, 15 (4): 637–647

Wang, Z., Shen, D., Parsons, D.W., *et al.* (2004) Mutational analysis of the tyrosine

phosphatome in colorectal cancers. **Science**, 304 (5674): 1164–1166

Watson, R.A., Rollason, T.P., Reynolds, G.M., *et al.* (2002) Changes in expression of the human homologue of the *Drosophila* discs large tumour suppressor protein in high-grade premalignant cervical neoplasias. **Carcinogenesis**, 23 (11): 1791–1796

Watson, R.A., Thomas, M., Banks, L., *et al.* (2003) Activity of the human papillomavirus E6 PDZ-binding motif correlates with an enhanced morphological transformation of immortalized human keratinocytes. **Journal of Cell Science**, 116 (24): 4925–4934

Weiss, R.S. and Javier, R.T. (1997) A carboxy-terminal region required by the adenovirus type 9 E4 ORF1 oncoprotein for transformation mediates direct binding to cellular polypeptides. **Journal of Virology**, 71 (10): 7873–7880

Weiss, R.S., Lee, S.S., Prasad, B.V., *et al.* (1997) Human adenovirus early region 4 open reading frame 1 genes encode growth-transforming proteins that may be distantly related to dUTP pyrophosphatase enzymes. **Journal of Virology**, 71 (3): 1857–1870

Weissenborn, S.J., Nindl, I., Purdie, K., *et al.* (2005) Human papillomavirus-DNA loads in actinic keratoses exceed those in non-melanoma skin cancers. **The Journal of investigative dermatology**, 125 (1): 93–97

Wentzensen, N., Vinokurova, S. and Knebel Doeberitz, von, M. (2004) Systematic review of genomic integration sites of human papillomavirus genomes in epithelial dysplasia and invasive cancer of the female lower genital tract. **Cancer research**, 64 (11): 3878–3884

Werme, K., Wigerius, M. and Johansson, M. (2008) Tick-borne encephalitis virus NS5 associates with membrane protein scribble and impairs interferon-stimulated JAK-STAT signalling. **Cellular Microbiology**, 10 (3): 696–712

Werness, B.A., Levine, A.J. and Howley, P.M. (1990) Association of human papillomavirus types 16 and 18 E6 proteins with p53. **Science**, 248 (4951): 76–79

Wetherill, L.F., Holmes, K.K., Verow, M., *et al.* (2012) High-risk human papillomavirus E5 oncoprotein displays channel-forming activity sensitive to small-molecule inhibitors. **Journal of Virology**, 86 (9): 5341–5351

Wicking, B.G., Vermeer, D.W., Spanos, W.C., *et al.* (2012) A non-oncogenic HPV 16 E6/E7 vaccine enhances treatment of HPV expressing tumors. **Cancer gene therapy**, 19 (10): 667–674

Wiemann, S., Bechtel, S., Bannasch, D., *et al.* (2003) The German cDNA network: cDNAs, functional genomics and proteomics. **Journal of structural and functional genomics**, 4 (2-3): 87–96

Williams, H.C., Pottier, A. and Strachan, D. (1993) The descriptive epidemiology of warts in British schoolchildren. **The British journal of dermatology**, 128 (5): 504–511

Williams, S.J. (2002) 5'-Adenosinephosphosulfate Lies at a Metabolic Branch Point in Mycobacteria. **Journal of Biological Chemistry**, 277 (36): 32606–32615

Wilson, K.C., Center, D.M., Cruikshank, W.W., *et al.* (2003) Binding of HTLV-1 tax oncoprotein to the precursor of interleukin-16, a T cell PDZ domain-containing protein. **Virology**, 306 (1): 60–67

Wilson, R. and Laimins, L.A. (2005) Differentiation of HPV-containing cells using organotypic “raft” culture or methylcellulose. **Methods in molecular medicine**, 119: 157–169

Wilson, R., Ryan, G.B., Knight, G.L., *et al.* (2007) The full-length E1<sup>E4</sup> protein of human papillomavirus type 18 modulates differentiation-dependent viral DNA amplification and late gene expression. **Virology**, 362 (2): 453–460

Wilson, R., Wilson, R., Fehrman, F., *et al.* (2005) Role of the E1 E4 Protein in the Differentiation-Dependent Life Cycle of Human Papillomavirus Type 31. **Journal of Virology** [online], 79 (11): 6732–6740. Available from: <http://eutils.ncbi.nlm.nih.gov/entrez/eutils/elink.fcgi?dbfrom=pubmed&id=15890911&retmode=ref&cmd=prlinks>

Wilusz, J.E., Sunwoo, H. and Spector, D.L. (2009) Long noncoding RNAs: functional surprises from the RNA world. **Genes & development**, 23 (13): 1494–1504

Wise-Draper, T.M., Allen, H.V., Thobe, M.N., *et al.* (2005) The human DEK proto-oncogene is a senescence inhibitor and an upregulated target of high-risk human papillomavirus E7. **Journal of Virology**, 79 (22): 14309–14317

Wodarz, A. and Näthke, I. (2007) Cell polarity in development and cancer. **Nature cell biology**, 9 (9): 1016–1024

Wong, H.C., Bourdelas, A., Krauss, A., *et al.* (2003) Direct binding of the PDZ domain of Dishevelled to a conserved internal sequence in the C-terminal region of frizzled. **Molecular Cell**, 12 (5): 1251–1260

Woodman, C.B., Collins, S., Winter, H., *et al.* (2001) Natural history of cervical human papillomavirus infection in young women: a longitudinal cohort study. **Lancet**, 357 (9271): 1831–1836

Woodman, C.B.J., Collins, S.I. and Young, L.S. (2007) The natural history of cervical HPV infection: unresolved issues. **Nature Reviews Cancer**, 7 (1): 11–22

Woods, D.F., Hough, C., Peel, D., *et al.* (1996) Dig Protein Is Required for Junction Structure, Cell Polarity, and Proliferation Control in *Drosophila* Epithelia. **Journal of Cell Biology**, 134 (6): 1469–1482

Woodworth, C.D., Doniger, J. and DiPaolo, J.A. (1989) Immortalization of human foreskin keratinocytes by various human papillomavirus DNAs corresponds to their association with cervical carcinoma. **Journal of Virology**, 63 (1): 159–164

Wu, H., Reuver, S.M., Kuhlendahl, S., *et al.* (1998) Subcellular targeting and cytoskeletal attachment of SAP97 to the epithelial lateral membrane. **Journal of Cell Science**, 111 ( Pt 16): 2365–2376

- Wu, H.J., Reissner, C., Kuhlendahl, S., *et al.* (2000) Intramolecular interactions regulate SAP97 binding to GKAP. **Embo Journal**, 19 (21): 5740–5751
- Wu, X. and Brewer, G. (2012) The regulation of mRNA stability in mammalian cells: 2.0. **Gene**, 500 (1): 10–21
- Xavier, R., Rabizadeh, S., Ishiguro, K., *et al.* (2004) Discs large (Dlg1) complexes in lymphocyte activation. **Journal of Cell Biology**, 166 (2): 173–178
- Xiang, Y., Xiang, Y., Devic, E., *et al.* (2002) The PDZ binding motif of the beta 1 adrenergic receptor modulates receptor trafficking and signaling in cardiac myocytes. **Journal of Biological Chemistry**, 277 (37): 33783–33790
- Xie, L., Yamamoto, B., Haoudi, A., *et al.* (2006) PDZ binding motif of HTLV-1 Tax promotes virus-mediated T-cell proliferation in vitro and persistence in vivo. **Blood**, 107 (5): 1980–1988
- Xu, B., Chotewutmontri, S., Wolf, S., *et al.* (2013) Multiplex Identification of Human Papillomavirus 16 DNA Integration Sites in Cervical Carcinomas. Ramqvist, T. (ed.). **PLoS ONE**, 8 (6): e66693
- Yablonska, S., Hoskins, E.E., Wells, S.I., *et al.* (2013) Identification of miRNAs Dysregulated in Human Foreskin Keratinocytes (HFKs) Expressing the Human Papillomavirus (HPV) Type 16 E6 and E7 Oncoproteins. **MicroRNA**, 2 (1): 2–13
- Yamada, K.H., Hanada, T. and Chishti, A.H. (2007) The Effector Domain of Human Dlg Tumor Suppressor Acts as a Switch That Relieves Autoinhibition of Kinesin-3 Motor GAKIN/KIF13B †. **Biochemistry**, 46 (35): 10039–10045
- Yamanaka, T. and Ohno, S. (2008) Role of Lgl/Dlg/Scribble in the regulation of epithelial junction, polarity and growth. **Frontiers in Bioscience**, 13: 6693–6707
- Yamazaki, T., Walchli, S., Fujita, T., *et al.* (2010) Splice variants of Enigma homolog, differentially expressed during heart development, promote or prevent hypertrophy. **Cardiovascular Research**, 86 (3): 374–382
- Yan, J., Sun, L., Wu, G., *et al.* (2009a) Rational design and synthesis of highly potent anti-acetylcholinesterase activity huperzine A derivatives. **Bioorganic & Medicinal Chemistry**, 17 (19): 6937–6941
- Yan, P., Fu, J., Qu, Z., *et al.* (2009b) PDLIM2 suppresses human T-cell leukemia virus type I Tax-mediated tumorigenesis by targeting Tax into the nuclear matrix for proteasomal degradation. **Blood**, 113 (18): 4370–4380
- Yates, L.L., Schnatwinkel, C., Hazelwood, L., *et al.* (2013) Scribble is required for normal epithelial cell-cell contacts and lumen morphogenesis in the mammalian lung. **Developmental biology**, 373 (2): 267–280
- Yeo, G. and Burge, C.B. (2004) Maximum entropy modeling of short sequence motifs with applications to RNA splicing signals. **Journal of Computational Biology**, 11 (2-3): 377–394

Yeo, N.-K. and Jang, Y.J. (2010) Rhinovirus Infection-Induced Alteration of Tight Junction and Adherens Junction Components in Human Nasal Epithelial Cells. **Laryngoscope**, 120 (2): 346–352

You, J., JL, C., A, N., *et al.* (2004) **Interaction of the bovine papillomavirus E2 protein with Brd4 tethers the viral DNA to host mitotic chromosomes.**, 117 (3): 349–360. Available from: <http://eutils.ncbi.nlm.nih.gov/entrez/eutils/elink.fcgi?dbfrom=pubmed&id=15109495&retmode=ref&cmd=prlinks>

Yuan, H., Fu, F., Zhuo, J., *et al.* (2005) Human papillomavirus type 16 E6 and E7 oncoproteins upregulate c-IAP2 gene expression and confer resistance to apoptosis. **Oncogene**, 24 (32): 5069–5078

Yugawa, T. and Kiyono, T. (2009) Molecular mechanisms of cervical carcinogenesis by high-risk human papillomaviruses: novel functions of E6 and E7 oncoproteins. **Reviews Medical Virology**, 19 (2): 97–113

Zanier, K., Charbonnier, S., Sidi, A.O.M.O., *et al.* (2013) Structural Basis for Hijacking of Cellular LxxLL Motifs by Papillomavirus E6 Oncoproteins. **Science**, 339 (6120): 694–698

Zen, K., Yasui, K., Gen, Y., *et al.* (2009) Defective expression of polarity protein PAR-3 gene (PARD3) in esophageal squamous cell carcinoma. **Oncogene**, 28 (32): 2910–2918

Zerfass-Thome, K., Zwerschke, W., Mannhardt, B., *et al.* (1996) Inactivation of the cdk inhibitor p27KIP1 by the human papillomavirus type 16 E7 oncoprotein. **Oncogene**, 13 (11): 2323–2330

Zhang, Y., Appleton, B.A., Wiesmann, C., *et al.* (2009) Inhibition of Wnt signaling by Dishevelled PDZ peptides. **Nature Chemical Biology**, 5 (4): 217–219

Zhang, Y., Dasgupta, J., Ma, R.Z., *et al.* (2007) Structures of a Human Papillomavirus (HPV) E6 Polypeptide Bound to MAGUK Proteins: Mechanisms of Targeting Tumor Suppressors by a High-Risk HPV Oncoprotein. **Journal of Virology**, 81 (7): 3618–3626

Zhang, Z., Li, H., Chen, L., *et al.* (2011) Molecular basis for the recognition of adenomatous polyposis coli by the Discs Large 1 protein. Driscoll, P.C. (ed.). **PLoS ONE**, 6 (8): e23507

Zhou, Y., Fang, L., Du, D., *et al.* (2008) Proteome identification of binding-partners interacting with cell polarity protein Par3 in Jurkat cells. **Acta biochimica et biophysica Sinica**, 40 (8): 729–739

Zhu, J., Shang, Y., Wan, Q., *et al.* (2014) Phosphorylation-dependent interaction between tumor suppressors Dlg and Lgl. **Cell research**

Zhu, J., Shang, Y., Xia, C., *et al.* (2011) Guanylate kinase domains of the MAGUK family scaffold proteins as specific phospho-protein-binding modules. **Embo Journal**, 30 (24): 4986–4997

Ziegert, C., Wentzensen, N., Vinokurova, S., *et al.* (2003) A comprehensive analysis of HPV

integration loci in anogenital lesions combining transcript and genome-based amplification techniques. **Oncogene**, 22 (25): 3977–3984

Zielecki, F., Semmler, I., Kalthoff, D., *et al.* (2010) Virulence Determinants of Avian H5N1 Influenza A Virus in Mammalian and Avian Hosts: Role of the C-Terminal ESEV Motif in the Viral NS1 Protein. **Journal of Virology**, 84 (20): 10708–10718

Zimmermann, H., Degenkolbe, R., Bernard, H.U., *et al.* (1999) The human papillomavirus type 16 E6 oncoprotein can down-regulate p53 activity by targeting the transcriptional coactivator CBP/p300. **Journal of Virology**, 73 (8): 6209–6219

Zimmermann, P., Meerschaert, K., Reekmans, G., *et al.* (2002) PIP(2)-PDZ domain binding controls the association of syntenin with the plasma membrane. **Molecular Cell**, 9 (6): 1215–1225

Zipper, H., Brunner, H., Bernhagen, J., *et al.* (2004) Investigations on DNA intercalation and surface binding by SYBR Green I, its structure determination and methodological implications. **Nucleic acids research**, 32 (12): e103

Zubakov, D., Stupar, Z. and Kovacs, G. (2006) Differential expression of a new isoform of DLG2 in renal oncocytoma. **BMC cancer**, 6: 106

Zwicker, J., Liu, N.S., Engeland, K., *et al.* (1996) Cell cycle regulation of E2F site occupation in vivo. **Science**, 271 (5255): 1595–1597

Websites:

<http://www.cancerscreening.nhs.uk/cervical/about-cervical-screening.html#cost>

Copyright Public Health England 2013 [Accessed 02/06/13]

<http://pave.niaid.nih.gov/> [Accessed 22/12/14]